

University of Florence

Pharmaceutical Sciences Department

PhD thesis in Chemistry and Pharmaceutical Technology

Curriculum: design, synthesis and molecular modelling of drugs

education field CHIM-08

Design, synthesis and pharmacological evaluation
of new heterocyclic ligands of
Formyl Peptide Receptors, potentially useful as
analgesic and anti-inflammatory agents

Dr. Agostino Cilibrizzi

Supervisor : Prof. Vittorio Dal Piaz

Coordinator : Prof. Elisabetta Teodori

COURSE XXIII (2008-2010)

DECLARATION:

This dissertation is submitted in partial fulfilment of the requirements for the Certificate of Postgraduate Studies. It describes work carried out in the Pharmaceutical Sciences Department, University of Florence, between January 2008 and December 2010 under the supervision of Prof. Vittorio Dal Piaz. During the PhD course, a 7-months period was spent at the Chemistry Department, University of Cambridge, under the supervision of Dr. David R. Spring. Unless otherwise indicated, the research described is my own and not the product of collaboration.

Signed..... Date.....

TABLE OF CONTENTS

Abbreviations	VII
Table of the amino acids and their abbreviations	IX
Index of figures	X
Index of tables	XI
Index of schemes	XII
1. Introduction	1
1.1 Inflammation and infection: an overview	3
1.2 White blood cells or leukocytes	3
1.2.1 Neutrophils	4
1.2.2 Basophils	5
1.2.3 Eosinophils	5
1.2.4 Lymphocytes	6
1.2.5 Monocytes	7
1.2.6 Macrophages	7
1.2.7 Dendritic cells	7
1.3 Leukocytes: involvement in inflammation and infection	8
1.4 Formyl Peptide Receptors (FPRs) role in inflammation and infection	8
1.5 Formyl Peptide Receptors (FPRs) localization and classification	9
1.5.1 Formyl Peptide Receptor 1 (FPR1)	10
1.5.2 Formyl Peptide Receptor 2 (FPR2 or FPR2/ALX)	11
1.5.3 Formyl Peptide Receptor 3 (FPR3)	12
1.6 FPRs activation and cell functions	12
1.6.1 Chemotaxis	14
1.6.2 Superoxide generation	14
1.6.3 Degranulation	15
1.6.4 Transcriptional regulation and anti-inflammatory functions	15
1.6.5 Neutrophil apoptosis	16
1.7 FPRs involvement in several diseases	16
1.8 FPRs ligands	17
1.8.1 FPRs natural agonists	18
1.8.2 Agonists from peptide library	24

1.8.3 Agonists from nonpeptide library: synthetic small molecules	25
1.8.4 FPRs antagonists	26
1.9 FPRs: future	28
2. Background and Aims of the Project	29
3. Chemistry	35
3.1 Investigating different heterocyclic scaffolds	37
3.1.1 Synthesis of indole and indazole derivatives	37
3.1.2 Synthesis of quinoline derivatives	38
3.1.3 Synthesis of naphthyridone derivatives	38
3.1.4 Synthesis of phthalazinone derivative	40
3.1.5 Synthesis of phthalhydrazide derivatives	40
3.1.6 Synthesis of 2-benzyl pyridazinone derivatives	41
3.1.7 Synthesis of 2-phenyl pyridazinone derivatives	42
3.2 6-Methyl-2,4-Disubstituted Pyridazin-3(2 <i>H</i>)-ones: synthesis of the lead compound 46a	43
3.2.1 Synthesis of dihydropyridazinone scaffolds	43
3.2.2 Synthesis of substituted <i>N</i> -arylacetamide pyridazinones	44
3.3 Optimization of the lead: 2,3,4,5,6-substituted pyridazinones	44
3.3.1 Synthesis of C-6 modified <i>N</i> -arylacetamide pyridazinones	44
3.3.2 Synthesis of C-4 modified <i>N</i> -arylacetamide pyridazinones	45
3.3.3 Synthesis of <i>N</i> -arylacetamide modified pyridazinone derivatives	51
3.3.4 Synthesis of <i>N</i> -2/C-4 inverted pyridazinone analogues	53
3.3.5 Synthesis of C-3 substituted pyridazine analogue	54
3.3.6 Synthesis of chiral pyridazinone analogues	54
3.3.6.1 Enantioselective synthesis of the <i>N</i> -arylpropanamide analogue	55
3.3.6.2 Synthesis of the homologous series of <i>N</i> -aryl-(alkyl)-amide derivatives	55
3.3.6.3 Chiral Chromatographic resolution of racemates (±)-95b and (±)-117a-f	56
3.3.6.4 Assignment of the absolute configurations	60
4. Results and Conclusions	65
4.1 Results	67
4.1.1 Screening different nitrogen heterocyclic derivatives as FPRs agonists	67
4.1.2 EC ₅₀ and efficacy of <i>N</i> -arylacetamide pyridazinones	68
4.1.3 EC ₅₀ and efficacy of C-6 modified <i>N</i> -arylacetamide pyridazinones	69

4.1.4 EC ₅₀ and efficacy of C-4 modified <i>N</i> -arylacetamide pyridazinones	70
4.1.5 EC ₅₀ and efficacy of <i>N</i> -arylacetamide modified pyridazinones, <i>N</i> -2/ <i>C</i> -4 inverted pyridazinones and <i>C</i> -3 substituted pyridazine analogue	74
4.1.6 EC ₅₀ and efficacy of chiral pyridazinone analogues	75
4.1.7 Evaluation of chemotactic activity and Ca ²⁺ mobilization	77
4.2 Conclusions	78
5. Experimental Chemistry	81
5.1 Materials and Methods	83
5.2 Experimental	84
6. Biological Methods	191
6.1 Cell Culture	193
6.2 Isolation of Human Neutrophils	193
6.3 Ca ²⁺ Mobilization Assay	193
6.4 Chemotaxis Assay	194
7. Bibliographic References	195
8. Supplement: Solid-Phase Synthesis of Transition State Mimetics in the Quorum Sensing System of <i>Staphylococcus Aureus</i> to Develop Catalytic Antibodies	215
8.1 Introduction	217
8.1.1 Antibiotics today: an overview	217
8.1.2 Quorum sensing (QS)	218
8.1.3 Catalytic antibodies through Transition State (TS) mimetics	219
8.1.4 Transition state mimetics and <i>quorum quenching</i>	220
8.1.5 Quorum sensing in <i>Staphylococcus aureus</i>	220
8.1.6 Autoinducing (oligo)peptides (AIPs)	221
8.2 Background and Aims of the Project	222
8.3 Chemistry	223
8.3.1 Synthesis of the “ <i>serine building blocks</i> ”	223
8.3.1.1 Protection of the starting amino acids and amino alcohols	224
8.3.1.2 Phosphorus couplings	224
8.3.2 Synthesis of the phosphorus cyclic peptides	225
8.3.2.1 Fmoc/ <i>t</i> -Bu solid-phase synthesis of the branched peptides	226
8.3.2.2 Macrocyclization	228
8.3.3 Total synthesis of the AIP-III	229

8.4 Results and Conclusions	231
8.5 Experimental Chemistry	233
8.5.1 Materials and Methods	233
8.5.2 Protection of amino acids and amino alcohols	234
8.5.3 Phosphorus couplings	237
8.5.4 Total synthesis of the TS mimetic	241
8.5.5 Total synthesis of the AIP-III	243
8.6 Bibliographic References	255

ABBREVIATIONS

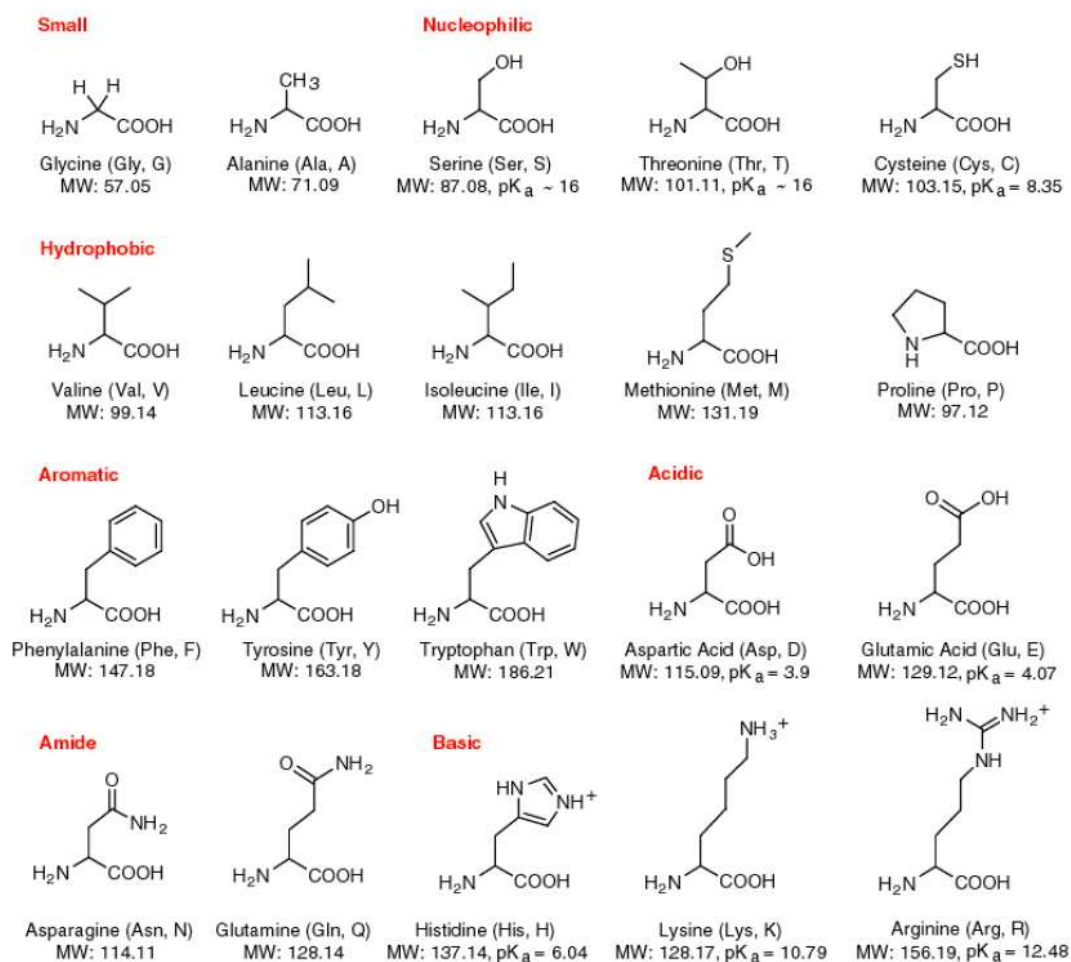
- $[\alpha]_D^{20}$ = optical specific rotation
 $\Delta\Delta G^*$ = quantity of the transition state stabilization
 δ = chemical shifts
& = cyclic peptides
 λ = wavelength
 λ_{em} = emission wavelength
 λ_{ex} = excitation wavelength
 λ_{max} = maximum wavelength
7TM = seven-trans membrane
 $A\beta$ = β -amyloid peptide
 $A\beta Ac$ = Alzheimer's β -amyloidogenic conformer
aa = amino acid
Ab = antibody
Ab.TS = antibody-bound transition state
Ac = annexin-1-derived peptide(s)
AcOH = acetic acid
Agr = agr = accessory gene regulator(s)
AIP(s) = autoinducing (oligo)peptide(s)
Alloc = allyloxycarbonyl group
ALX = lipoxin A4 receptor
an. = anhydrous
ANXA1 = annexin A1
aq. = aqueous
Ar = aromatic ring
Asu = aspartimide (aminosuccinimide, 3-amino-pyrrolidine-2,5-dione)
Bn = benzyl
Boc = tert-butoxycarbonyl group
c = concentration
C5a = complement component 5a
calcd. = calculated
cAMP = cyclic adenosine monophosphate
CAN = ceric ammonium nitrate
CD = circular dichroism
CD4+ = T helper cells
CD8+ = cytotoxic T cells
CDCA = chenodeoxycholic acid
cDNA = complementary deoxyribonucleic acid
CHIPS = chemotaxis inhibitory protein of *S. aureus*
CHX = cyclohexane
CI = chemical ionisation
CM = complex mixture
CSP(s) = chiral stationary phase(s)
CsH = cyclosporin H
c-suPAR = cleaved soluble uPAR
CTC = chlorotriyl chloride polystyrene resin
d = day(s)
DCA = deoxycholic acid
DCC = dicyclohexylcarbodiimide
DCP = diethyl cyanophosphonate
DC(s) = dendritic cell(s)
DIC = diisopropylcarbodiimide
DIPEA = DIEA = *N,N*-Diisopropylethylamine or Hünig's base
DKP = diketopiperazine
DMAP = 4-dimethylaminopyridine
DMF = dimethylformamide
DMSO = dimethyl sulfoxide
EC₅₀ = half maximal effective concentration
E. coli = escherichia coli
EDC = 1-ethyl-3-(3'-dimethylaminopropyl) carbodiimide hydrochloride
EDTA = ethylenediaminetetraacetic acid
ee = enantiomeric excess
EI = electron ionisation
equiv = equivalent(s)
EMRSA-16 = Epidemic methicillin-resistant *Staphylococcus aureus* 16
ERK = extracellular regulated kinase
ESI = electrospray ionisation
EtOAc = ethyl acetate
F2L = peptide derived from heme-binding protein
FAB (LSIMIS) = fast atom bombardment (liquid secondary ion mass spectrometry)
FBS = fetal bovine serum
Fe(acac)₃ = iron(III) acetylacetonate
FLIPR = fluorometric imaging plate reader
FLIPr = FPRL1 inhibitory protein
fMLF = *N*-formyl-methionine-leucine-phenylalanine
FMLPR(s) = formil-metinine-leucine-phenilalanine receptor(s)
Fmoc = Fluorenylmethyloxycarbonyl group
FPR(s) = formyl peptide receptor(s)
FPRH1 = formyl peptide receptor-homolog 1
FPRH2 = formyl peptide receptor-homolog 2
FPRL1 = formyl peptide receptor like 1
FPRL2 = formyl peptide receptor-like 2
FT-IR = Fourier Transform Infrared Spectroscopy
G-CSF = granulocyte macrophage-colony-stimulating factor
gp41 = envelope glycoprotein 41 of HIV-1

GPCR(s) = G-protein-coupled receptor(s)
 GTPase(s) = enzymes that bind GTP (guanine triphosphate)
 h = hour(s)
 HATU = 1-[bis(dimethylamino)methylene]-1H-1,2,3-triazolo-[4,5-b]pyridinium hexafluoro-phosphate 3-oxide
 HBA= hydrogen bond acceptor
 HBD= hydrogen bond donor
 HBSS = Hanks' Balanced Salt Solution
 HEPES = 4-(2-hydroxyethyl)-1-piperazine ethanesulfonic acid
 Hex = hexane
 HIV = Human immunodeficiency virus
 HIV-1 = Human immunodeficiency virus type 1
 HK= histidine kinase
 HL-60= Human promyelocytic leukemia 60 cell line
 HM63 = FPR2 antibody
¹H NMR = proton nuclear magnetic resonance
 HOAt = 7-aza-1-hydroxybenzotriazole
 HOBt = 1-hydroxybenzotriazole
 HPLC = high-performance liquid chromatography
 HSV-2= herpes simplex virus type 2
 IC₅₀ = half maximal inhibitory concentration
 I.D. = internal diameter
 IFN- γ = interferon gamma
 IgE = immunoglobulin E
 IL = interleukin
 IPA = isopropanol
 IR = Infrared spectroscopy
 IUPAC = International Union of Pure and Applied Chemistry
J = coupling constants
 K_d = dissociation constant
 kDa = kilodalton
 K_i = inhibition constant
 KTS = transition state (TS) dissociation constant
 LC-MS = LCMS = liquid chromatography-mass spectrometry
 LL-37 = a Cathelicidin-derived peptide
 LPS = lipopolysaccharide
 LTB₄ = leucotriene B₄
 LXA₄, LXB₄ = lipoxin A₄, lipoxin B₄
 LXA₄R= lipoxine A₄ receptor
 MALDI = matrix-assisted laser desorption /ionisation
 MAPK = mitogen-activated protein kinase
 TBHP = tert-butyl hydroperoxide
 m-CPBA = meta-chloroperbenzoic acid
 mdeg = millidegrees (for the angle of polarization in CD spectra)
 MHC= major histocompatibility complex
 min = minute(s)
 mp = melting point
 MRSA = Methicillin-resistant strains of *Staphylococcus aureus*
m/z = mass to charge ratio
 MS = mass spectrometry
 N.A.= no activity
 NADPH = nicotinamide adenine dinucleotide phosphate-oxidase
 NBS = *N*-bromosuccinimide
 N.D. = non determined
 NF- κ B = eukaryotic transcription factor
 NK= natural killer cells
 NMR = nuclear magnetic resonance spectroscopy
 NO = nitric oxide
 o/n = overnight
 P = product
 PAF = platelet-activating factor
 PGE₂ = prostaglandin E₂
 pK_a = -log(acidity constant)
 PKC(s) = protein kinase C(s)
 PMN(s) = polymorphonuclear leukocyte(s)
 ppm = part(s) per milion
 PPA = Polyphosphoric Acid
 PrP = prion protein
 PyAOP = (7-azabenzotriazol-1-yloxy)-tris(pyrrolidino)phosphonium hexafluoro-phosphate
 QS = quorum sensing
 QQ = quorum quenching
 Q-ToF = Quadrupole-Time of Flight
 RBL-2H3 = Rat basophilic leukemia 2H3 cell line
 RPMI 1640 = a medium used for the culture of human normal and neoplastic leukocytes
 rt = room temperature
 S = substrate
 SAA = serum amyloid A
 SAR(s) = structure-activity relationship(s)
S. aureus = *Staphylococcus aureus*
 S.D. = standard deviation
 SM = starting material
 SN₂ = bimolecular nucleophilic substitution
 SPPS = solid-phase peptide synthesis
^tBu = *t*-Bu = *tert*-butyl group

TFA = trifluoroacetic acid
 THF = tetrahydrofuran
 TLC = thin layer chromatography
 TLR(s) = toll-like receptor(s)
 TNF- α = tumor necrosis factor alpha
 t_R = retention time (in min)
 TS = Transition-State
 uPA = urokinase-type plasminogen activator

uPAR = urokinase-type plasminogen activator receptor
 UV = ultraviolet spectroscopy
 UV-VIS = ultraviolet-visible spectroscopy
 v/v = volume/volume
 V3 = vasopressin receptor
 WBC(s) = white blood cell(s)
 WT = wild-type cells
 w/v = weight/volume

Table of the amino acids and their abbreviations.



INDEX OF FIGURES

Figure 1.1. The different types of WBCs and hematopoietic cells from which they derive.	4
Figure 1.2. Sequence homology between the FPR family members and their tissue distribution.	10
Figure 1.3. Schematic signaling pathways of an activated FPR.	13
Figure 1.4. Leukocyte migration cascade via the FPRs family.	13
Figure 1.5. Chemical structures of fMLF, a FPR1 selective agonist.	18
Figure 1.6. Chemical structures of LXA4, a highly selective agonist for FPR2/ALX.	23
Figure 1.7. Chemical structures of selected small-molecule ligands for the FPRs.	25
Figure 1.8. Chemical structures of Quin-C7 and Quin-C1.	27
Figure 2.1. The key reference molecules used as leads in ligand-based drug design approach for the synthesis of FPRs agonists.	31
Figure 2.2. Some examples of compounds designed and synthesized using different nitrogen heterocyclic scaffold.	31
Figure 2.3. Modification performed on the lead compound.	32
Figure 2.4. Homologue series of chiral derivatives.	32
Figure 3.1. Chiral semi-preparative HPLC resolution of racemates (\pm)- 95b and (\pm)- 117a .	57
Figure 3.2. Chiral semi-preparative HPLC resolution of racemates (\pm)- 117b-f .	58
Figure 3.3. Chiral analytical HPLC analysis of the chromatographically resolved enantiomers (+)- 95b /(-)- 95b and (+)- 117a-f /(-)- 117a .	59
Figure 3.4. Experimental Circular dichroism (CD) spectra of the pure enantiomeric pairs synthesized and the reference compounds.	62
Figure 4.1. Analysis of Ca^{2+} mobilization in phagocytes treated with compound 46a .	77
Figure 8.1. Energy diagram for an antibody-catalyzed and uncatalyzed transformation of a substrate S to a product P.	219
Figure 8.2. Proposed mechanism of the two-component <i>agr</i> autoinduction system in <i>S. aureus</i> .	221
Figure 8.3. Chemical structure of AIP-I and peptide sequences of AIPs I through IV.	221
Figure 8.4. Structure of the natural autoinducing (oligo)peptide AIP-III .	222
Figure 8.5. Structures of the “ <i>serine building blocks</i> ” and the two AIP-III analogues designed.	223
Figure 8.6. The biotinylated variants of the AIP-III analogue designed.	223
Figure 8.7. A frequent fragment detected by mass spectrometry due to the instability of the phosphate group and two possible side products that could occur during the cyclization.	232

INDEX OF TABLES

Table 1.1. FPR1 and FPR2/ALX receptor associations with human disease.	17
Table 1.2. FPR2/ALX ligand association with human disease.	17
Table 1.3. Agonists for the human FPRs.	18
Table 1.4. Binding affinity and potency of bacterial and mitochondrial formyl peptides.	19
Table 1.5. Antagonists for the human formyl peptide receptors.	27
Table 3.1. Data of the chiral HPLC separations for the racemates (\pm)- 95b and (\pm)- 117a-f .	58
Table 3.2. Data for the different racemates (\pm)- 95b and (\pm)- 117a-f of ($[\alpha]_D^{20}$) and ee.	60
Table 4.1. Activity of the compounds 46a-s (scheme 12) in HL-60 cells.	68
Table 4.2. Activity of the compounds 50a-v (scheme 13) in HL-60 cells.	70
Table 4.3. Activity of compounds 53a-d and 57a-f (schemes 14,15) in HL-60 cells.	71
Table 4.4. Activity of compounds 61a-p , 62a-c and 66a-c (schemes 16-18) in HL-60 cells.	72
Table 4.5. Activity of compounds 69 , 71 , 77 , 83 , 87-89a,b and 92 (schemes 18-21) in HL-60 cells.	74
Table 4.6. Activity of compounds 95-97a,b , 100-102 , 103a,b , 104a-c , 105 , 108 , 109 and 111 (schemes 22-27) in HL-60 cells.	76
Table 4.7. Activity of racemates and pure enantiomers (\pm)- 95b , (\pm)- 117a-f and non chiral homologue 118 (schemes 22, 29, 30) in HL-60 cells.	76
Table 4.8. Ca ²⁺ mobilization and chemotactic activity in human neutrophils treated with selected FPR1/FPRL1 agonists.	78
Table 8.1. Macrocyclization conditions screened for the synthesis of transition state mimetic 23 .	228
Table 8.2. Coupling methods screened to carry out the cyclization for the synthesis of the AIP-III (28) .	230

INDEX OF SCHEMES

Scheme 1. Synthesis of indazoles (2a,b , 3a-d) and indoles (2b,c , 3e-h) derivatives.	37
Scheme 2. Synthetic pathway for “indomethacin-like” analogue 5 .	38
Scheme 3. Synthetic pathway for “indomethacin-like” analogue 6 .	38
Scheme 4. Synthesis of quinoline derivatives 8a-d .	38
Scheme 5. Synthesis of naphthyridone derivatives 14a,b , 16a,b and 19a-c .	39
Scheme 6. Synthetic pathways for “nalidixic acid-like” analogues 20 and 21 .	40
Scheme 7. Synthetic pathway for phthalazinone final compound 23 .	40
Scheme 8. Synthesis of diidrophthalazindione derivatives 25a-c and 26 .	40
Scheme 9. Synthesis of <i>N</i> -2-benzyl pyridazinone derivatives 29a,b and 30a,b .	41
Scheme 10. Synthesis of <i>N</i> -2-phenyl pyridazinone derivatives 35-37 and 38a-c .	42
Scheme 11. Synthetic pathways for γ -keto acids 41 a-c and dihydropyridazinones 42a-m .	43
Scheme 12. Synthesis of the lead compound 46a and <i>N</i> -arylacetamide analogues 46b-s .	44
Scheme 13. Synthesis of C-6 modified <i>N</i> -arylacetamide pyridazinones 50a-v .	45
Scheme 14. Synthetic pathway for C-4 modified final compounds 53a and (\pm)- 53b-d .	46
Scheme 15. Synthetic pathway for C-4 modified final compounds 57a-f .	46
Scheme 16. Synthesis of the final compounds 61a-p .	47
Scheme 17. Synthesis of the final compounds 62a-c .	47
Scheme 18. Synthetic pathways for final compounds 66a-c and 69 .	48
Scheme 19. Synthesis of 4-arylketone derivative 71 .	49
Scheme 20. Synthesis of 4-methoxyphenyl pyridazinone 77 .	49
Scheme 21. Synthetic pathways for final compounds 83 , 87 , 88 , 89a-b and 92 .	50
Scheme 22. Synthesis of <i>N</i> -arylacetamide modified pyridazinones 95-97a,b .	51
Scheme 23. Synthesis of <i>N</i> -arylacetamide modified pyridazinones 100 , 101 and 103a,b .	52
Scheme 24. Synthetic pathway for final compounds 104a-c .	53
Scheme 25. Synthesis of the thioamide analogue 105 .	53
Scheme 26. Synthesis of <i>N</i> -2/ <i>C</i> -4 inverted pyridazinone analogues 108 and 109 .	54
Scheme 27. Synthesis of <i>C</i> -3 substituted pyridazine analogue 111 .	54
Scheme 28. Unsuccessful asymmetrical synthesis for final compounds (+)- 113 and (-)- 113 .	55
Scheme 29. Synthetic pathway for final racemates (\pm)- 117a-f and compound 118 .	56
Scheme 30. Chromatographic resolution for racemates (\pm)- 95b and (\pm)- 117a-f .	57
Scheme 31. Acetyl derivatives used as reference compounds in CD experiments.	61

Scheme S.1. Synthesis of <i>N</i> - α -Fmoc-serine- <i>t</i> -butyl ester 1 .	224
Scheme S.2. Synthetic pathways for Alloc protected ethanolamine (2) and L-leucinol (3)	224
Scheme S.3. Synthetic pathway for “ <i>serine building blocks</i> ” 12 and 13 .	225
Scheme S.4. Fmoc/ <i>t</i> -Bu solid-phase synthesis of the branched phosphopeptide 21 .	226
Scheme S.5. Macrocyclization reaction for phosphopeptide 23 .	229
Scheme S.6. Total synthesis of the AIP-III (28) .	229

1. INTRODUCTION

1.1 Inflammation and infection: an overview

Inflammation is the first response of the immune system to infection or irritation. Through this process the white blood cells and chemicals released from them protect human organism against exogenous substances and pathogenic microorganisms such as bacteria and viruses.¹ Nevertheless, if the injurious agent continues or the control of cellular recruitment breaks down, both acute and chronic inflammatory disorders will ensue.²

Innate immunity is a very important mechanism in defending humans against infectious microbes but in some diseases the immune system inappropriately triggers an inflammatory response when there are no foreign substances to fight off.³ In these cases, the decompensations are called “autoimmune diseases” and the body responds as if normal tissues are infected or somehow abnormal: as result of this response, the normal protective immune system of the body causes damage to its own tissues. Thus, immune dysregulation exposes patients to life-threatening risks. As known, infection and inappropriate inflammatory processes play a central role in many diseases such as asthma, rheumatoid arthritis and multiple sclerosis. Moreover, as consequence of the increasing aging of the population, in more developed countries it was observed that older people exhibit a natural immune function dysregulation, which may be exacerbated in chronic stress conditions.⁴ In addition, the ongoing emergence of resistant bacterial and viral strains to multiple classes of chemotherapeutics increases morbidity, mortality, and costs associated with nosocomial infections.⁵

Nowadays there is a large number of treatments for inflammatory diseases and many anti-inflammatory therapeutic agents have been developed. Unluckily, the most part of currently used anti-inflammatory drugs has some limitations due to their interference with pro-inflammatory mediators, whereas less is understood about the biochemical processes that resolve inflammation. Principally, selective activation of such a pathway might lead to an alternative treatment for inflammation.⁶ Moreover, identification of immunomodulatory agents enhancing innate immune responses represents a promising strategy for combating inflammation and infectious diseases and development of bioactive molecules that selectively stimulate the innate immune response is an important challenge both for biologists and chemists.⁷

1.2 White blood cells or leukocytes

White blood cells (WBCs), or leukocytes, are immune system cells delegated to defend the body against both infectious disease and foreign materials.⁸ There are several different types of white blood cells and they all derive from a multipotent cell in the bone marrow, known as a hematopoietic stem cell. Leukocytes are found throughout the body, including the blood and lymphatic system (**figure 1.1**).⁹ A major distinguishing feature of some leukocytes is the presence of granules, so that white blood cells are often characterized as granulocytes or agranulocytes. Granulocytes (neutrophils, basophils, eosinophils)

1. Introduction

are polymorphonuclear leukocytes and they are characterised by the presence in their cytoplasm of differently staining granules visible under light microscopy. These granules are membrane-bound enzymes which primarily act in the digestion of endocytosed particles through the action of lysosomes.

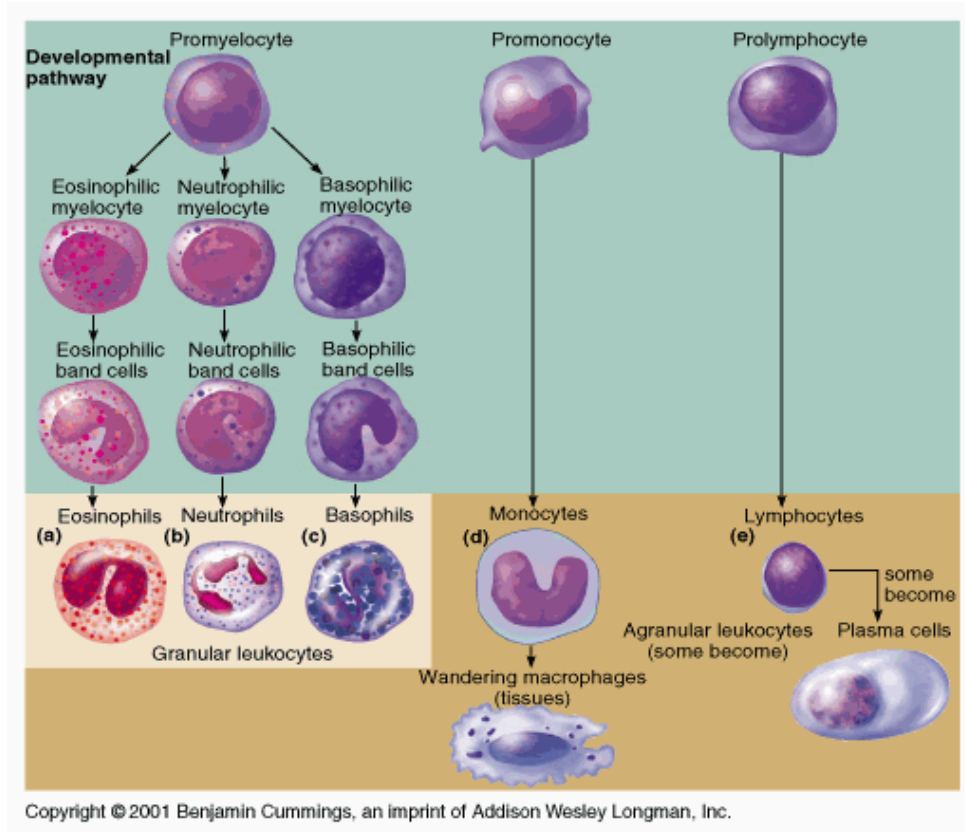


Figure 1.1. The different types of white blood cells and hematopoietic cells from which they derive.

Agranulocytes (lymphocytes, monocytes, macrophages) are mononuclear leucocytes and they are characterized by the apparent absence of granules in their cytoplasm. Although the name implies a lack of granules, these cells contain lysosomes.¹⁰ Some leukocytes migrate into the tissues of the body to take up a permanent residence at that location rather than remaining in the blood. Often these cells have specific names depending on the tissue in which they settle in but, generically, they are well-known as “fixed macrophages” and dendritic cells.

1.2.1 Neutrophils

Neutrophils are the most abundant type of white blood cells in mammals and form an essential part of the innate immune system. They belong to polymorphonuclear leukocytes (PMNs) together with basophils and eosinophils (in fact, technically, PMN refers to all granulocytes). Normally found in the blood, neutrophils are usually the first responders to microbial infection, defending against bacteria, fungi and other inflammatory process.¹¹ Being highly motile, they quickly congregate at the focus of inflammation.

Thus, neutrophils are the most common cells recruited in acute phase of inflammation, coming in and destroying foreign organisms or substances.^{12,13,14} Considering their ability to migrate toward the site of inflammation, through the blood vessels and the interstitial tissue, following “chemical signals” in the process of chemotaxis, neutrophils are recruited in the site of injury within few minutes from trauma and they should be considered as the hallmark of acute inflammation.¹⁵ Cell surface receptors allow neutrophils to detect chemical gradients of molecules such as interleukin-8 (IL-8), interferon gamma (IFN-gamma) and complement component 5a (C5a,) which these cells use to direct the path of their migration. They are very active in phagocytosing bacteria and are able to release soluble anti-microbial proteins.^{16,17} As a consequence of their activity and death usually they determine pus formation. Moreover, neutrophils express and release cytokines,¹⁸ which, in turn, amplify inflammatory reactions through several other cell types.

1.2.2 Basophils

Basophils appear in many specific kinds of inflammatory reactions, particularly those that cause allergic symptoms. They can be found in unusually high numbers at sites of infection and play a crucial role in both parasitic infections and allergies.¹⁹ Basophils are usually chiefly responsible for allergic and antigenic response by releasing histamine, proteoglycans (e.g. heparin and chondroitin), proteolytic enzymes (e.g. elastase and lysophospholipase), causing inflammation and contributing in this manner to the severity of the allergic response. When activated, they also secrete lipid mediators like leukotrienes and several cytokines. Histamine and proteoglycans are pre-stored in the cell's granules while the other secreted substances are newly generated. Each of these substances contributes to inflammation.²⁰ A specific receptor on basophilic cell surface is involved in the IgE binding and the interaction with this immunoglobulin involved in parasite defense and allergy confers to the basophils a selective response to environmental substances, such as pollen proteins or helminth antigens. Recent studies in mice suggest that basophils may also regulate the behavior of T cells and mediate the magnitude of the secondary immune response.²¹

1.2.3 Eosinophils

Among the immune system components, eosinophils are white blood cells responsible for combating multicellular parasites and certain infections.²² Usually they fight viral infections and helminth colonization, being slightly elevated in the presence of certain parasites. Eosinophils are also important mediators involved in the control of allergy and asthma and are closely associated with the severity of disease. In addition, they are frequently involved in many other biological processes, including allograft rejection and neoplasia.²³ After maturation in bone marrow, eosinophils circulate in blood and migrate to

1. Introduction

inflamed tissues in response to chemokines and certain leukotrienes (e.g. leukotriene B₄).²⁴ Following activation by an immune stimulus, eosinophils degranulate and release an array of cytotoxic granule cationic proteins that are capable to induce tissue damage and dysfunction.^{25,26} Their effector functions include also production of reactive oxygen species (such as superoxide, peroxide, and hypobromite), lipid mediators like the eicosanoids (leukotrienes and prostaglandins),²⁷ growth factors,^{28,29} cytokines and TNF- α .²³

1.2.4 Lymphocytes

Also lymphocytes are white blood cells of the vertebrate immune system and they are much more common in the lymphatic system. All lymphocytes originate during haematopoiesis process and, after maturation, enter in the circulation and peripheral lymphoid organs (e.g. the spleen and lymph nodes) where they survey for invading pathogens and/or tumor cells. The three major types of lymphocyte are natural killer (NK) cells, T cells and B cells.³⁰

NK cells are a part of the innate immune system and play a fundamental role in defending the host from both tumors and viral infected cells. They distinguish infected cells and tumors from normal and uninfected cells by recognizing changes of the level of a surface molecule called MHC (major histocompatibility complex) class I. NK cells are activated in response to a family of cytokines called interferons and they release cytotoxic granules which are able to destroy the altered cells.²⁰

T and B cells are the major cellular components of the adaptive immune response. T cells are involved in cell-mediated immunity whereas B cells are primarily responsible for humoral immunity (relating to antibodies). B cells mature into B lymphocytes at the level of the bone marrow, while T cells migrate to and mature in a distinct organ, called thymus.³¹ The function of T cells and B cells is to recognize specific “non-self” antigens, during a process known as “antigen presentation”. Once these cells have identified an invader, they generate specific responses that are tailored to maximally eliminate specific pathogens or pathogen infected cells. B cells respond to pathogens by producing large quantities of antibodies which neutralize foreign organism like bacteria and viruses. Always in response to pathogens, some T cells, called T helper cells (CD4+), produce cytokines that direct the immune response,³² while other T cells, called cytotoxic T cells (CD8+), produce toxic granules which induce the death of pathogen infected and tumor cells. Following activation, B cells and T cells leave a lasting legacy of the antigens they have encountered, in the form of “memory cells”. During all the host life, these memory cells will “remember” each specific pathogen encountered, and will be able to determine a strong response if the pathogen will be detected again.³¹

1.2.5 Monocytes

Monocytes are white blood cells that develop in the bone marrow and then go into blood, where they circulate for few days to finally migrate into tissues. In response to inflammation signals, they can move quickly to the sites of infection and differentiate into resident macrophages and dendritic cells to elicit an immune response.³³ Monocytes are responsible for phagocytosis of foreign substances in the body and this action is performed by using intermediary proteins such as antibodies or complement factors. In addition, they are able to directly bind the microbes via pattern-recognition receptors which recognize pathogens. Finally, monocytes are also capable to kill infected host cells through antibody recognition in a process called “antibody-mediated cellular cytotoxicity”.^{34,35}

1.2.6 Macrophages

Macrophages are mononuclear leucocytes responsible to protect tissues from foreign substances. When a leukocyte enters injured tissues attracted by a range of various stimuli in the process of chemotaxis, it undergoes a series of changes to become a macrophage. The majority of macrophages migrate into the tissues of the body to take up a permanent residence at that location (“fixed macrophages”), rather than remain in the blood. Each type of macrophage has a specific name determined by its location. Some examples of this differentiation are the Kupffer cells (in the liver), the histiocytes (in the connective tissue), the microglia (in the neural tissue), the mesangial cells (in the kidney), sinusoidal lining cells (in the spleen), the osteoclasts (in the bone) and the dust cells (in the lung).²⁰ As a consequence of their different fixed location, macrophages are versatile cells that play many roles. They act as phagocytes in both non-specific defense (innate immunity) and specific adaptive immunity. Their main roles consist to phagocytize necrotic tissues and pathogens, either as stationary or as mobile cells, and to stimulate lymphocytes and other immune cells to respond to the pathogen.

1.2.7 Dendritic cells

Dendritic cells (DCs) are immune cells that, as well as macrophages do, migrate into the tissues of the body to take up a permanent residence at that location. As mentioned above, these cells always arise from monocytes that depending on the specific signal, can become either dendritic cells or macrophages respectively. Dendritic cells can also be found as immature form in the blood,³⁶ but they are usually found in lung, stomach, intestine and, in small amount, in tissues that are in contact with the external environment, such as the skin. Langerhans cells are indeed a specialized kind of dendritic cells. Their main function is to process antigen material and to present it on the surface to other cells of the immune system.³⁷ They are the most potent of all the “antigen-presenting cells” and, once activated, they migrate

1. Introduction

to the lymphoid tissues where they interact with T cells and B cells to initiate and shape the adaptive immune response.³⁸

1.3 Leukocytes: involvement in inflammation and infection

The host defense response of humans is complex and multileveled, involving many cell types with distinct but overlapping roles. Leukocyte infiltration is an important feature in host response and defense to invading potentially pathogenic organisms and to fight a variety of inflammation processes. Phagocytic leukocytes are one of the earliest cell types responding to an inflammatory stimulus and they are key participants in innate immune response.³⁹ Leukocytes accumulate at sites of inflammation and microbial infection as response to locally produced “chemical signals”.⁴⁰ In fact their recruitment is strictly dependent on the presence of a gradient of chemotactic factors.⁴¹ In response to inflammatory challenges, phagocytes such as neutrophils, monocytes and macrophages migrate to the site of infection in a process of adhesion and transmigration through blood-vessel walls, where they engulf and destroy bacteria or other damage stimuli.⁴² They are usually activated by a wide variety of inflammatory stimuli, including cytokines and other endogenous chemical messengers, pathogen-associated molecular structures and oligopeptides derived from various pathogens or endogenously produced.^{43,44} After phagocytosis of microorganisms or other particulate substances, leukocytes secrete a variety of mediators that possess potent proinflammatory and antimicrobial activities. These mediators include antibiotic peptides and proteases which are sometimes stored in granules and are released during the process of degranulation.⁴⁵ Leukocytes perform as well a variety of other complex microbicidal functions, including chemotaxis (migration to site of inflammation), margination (rolling and adhesion to vessel walls), diapedesis (transmigration across the endothelial barrier),⁴⁶⁻⁴⁷ phagocytosis of foreign particles, destruction of targeted organisms and reactive free radicals production.¹⁶

In this scenario, more detailed signalling studies in leukocytes may help to identify new targets for potential therapeutic interventions. In addition, future combinatorial therapies with higher selectivity for certain leukocyte subsets promise improved approaches for treating acute and chronic inflammatory disorders.

1.4 Formyl Peptide Receptors (FPRs) role in inflammation and infection

Formyl peptide receptors (FPRs) are a small family of chemoattractant receptors and they play an essential role in host defense mechanisms against pathogen infection and trauma. In addition, they are involved at different levels in the regulation of inflammatory reactions and sensing cellular dysfunction.⁴⁸ These receptors belong to the seven transmembrane domain G-protein-coupled receptor (GPCR) family which are expressed in the majority of white blood cells and are known to be important

in host defense and inflammation.⁴⁹ All major neutrophil functions stimulated towards FPRs can be inhibited by treatment of the cells with pertussis toxin,^{42,50} indicating that the G proteins coupled to them belong to the Gi family of heterotrimeric proteins.⁵¹ Several studies conducted throughout the 1980s led to the identification of the formyl peptide receptors as highly promiscuous receptors that can be activated by a wide range of structurally unrelated non-peptide and peptide agonists, including synthetic, or both host-derived and pathogen-derived agents.^{42,48,50,52,53} Further investigations resulted in the identification of different chemotactic factors derived from bacteria as low-molecular weight peptides having a blocked amino terminus group, which were able to bond and activate FPRs. Because prokaryotes initiate protein synthesis with *N*-formyl methionine, short peptides starting with *N*-formyl methionine (CHOMet) were chemically synthesized and tested.⁵⁴ It was found a potent chemotactic activity for neutrophils in many of the synthetic *N*-formyl peptides tested, especially peptides containing *N*-formyl-methionyl-leucine and *N*-formyl-methionyl-phenylalanine.⁵⁵ The above findings led Freer et al.⁵⁶ to propose that the *N*-formyl group is essential for the bioactivity of these chemotactic peptides through interaction with FPRs. These studies resulted in identification of *N*-formyl-methionine-leucine-phenylalanine (fMet-Leu-Phe, or fMLF) as the most potent agonist among 24 synthetic peptides tested in neutrophil chemotaxis assays.⁵⁷

Owing to its ability to bind and activate the G protein-coupled formyl peptide receptors (FPRs), the tripeptide fMLF became a prototype of formylated chemotactic peptides for neutrophils able to act through FPRs activation. At subnanomolar to nanomolar concentrations, this binding event translates into directional movement of neutrophils, while at higher concentrations (> 100 nM), the same peptide also stimulates bactericidal functions including lysosomal enzyme release,⁵⁶ degranulation and production of superoxide.^{40,58,59} Because these peptides are derived from bacterial or mitochondrial proteins,^{1,55} it has been proposed that a primary FPR function is to promote trafficking of phagocytic myeloid cells to sites of infection and tissue damage, where they exert antibacterial effector functions and clear cell debris. In support of this hypothesis, mice lacking a known murine FPR variant were more susceptible to bacterial infections.⁶⁰ Intriguingly, the bactericidal activities triggered by these chemotactic peptides contribute to tissue damage when neutrophils are activated in certain different pathological conditions. Therefore, an understanding of the pharmacological basis of FPR binding and signaling has the potential to enhance anti infective activity as well as to reduce unwanted neutrophil activation and the resulting tissue damage.⁶¹

1.5 Formyl Peptide Receptors (FPRs) localization and classification

Three FPR subtypes have been identified till now in humans (FPR1, FPR2/ALX, FPR3), whereas eight FPR-related receptors have been discovered in mice (**figure 1.2**).⁴⁸ Activation of FPRs induces a variety

1. Introduction

of responses, which depend on the agonist, cell type, receptor subtype and species involved. The receptors of the FPR gene family are primarily found in myeloid cells, but the distribution changes within myeloid cell subsets. Indeed, the three different FPRs display a quite different expression profile on phagocytic leukocytes (**figure 1.2**). For example, neutrophils express functional FPR1 and FPR2/ALX, while monocytes express all the three receptors at their surface. Differently, monocyte-derived DCs express FPR1 and FPR3 when immature and only retain FPR3 after maturation.^{62,63} Many studies also indicate the presence of formyl peptide receptors in non-myeloid cells. In this context, there is evidence that FPRs might play different key roles in the activation of the immune system cells and functions in different body districts.

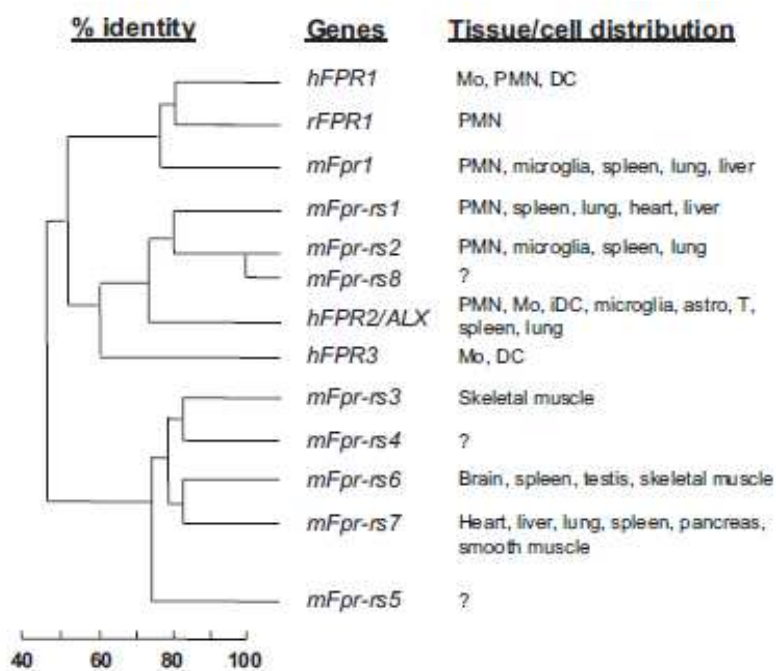


Figure 1.2. Sequence homology between the FPR family members and their tissue distribution. The predicted protein sequences of the three human (h) FPR genes, the eight mouse (m) Fpr genes, and the rabbit (r) FPR1 gene were compared. Based on sequence homology, the hFPR1, mFpr1, and rFPR1 are in the same cluster. Note that some of these genes are not expressed in neutrophils and monocytes. The tissue expression profiles for mFpr-rs4, mFpr-rs5, and mFpr-rs8 have not been determined. Mo, monocytes; PMN, polymorphnuclear leukocytes; iDC, immature dendritic cells; astro, astrocytes; T, T lymphocytes. Adapted from Ye et al. (2009).⁴⁹

1.5.1 Formyl Peptide Receptor 1 (FPR1)

Human FPR1 is a relatively abundant chemoattractant receptor on phagocytic cells and it was first defined biochemically in 1976,⁴⁰ as a high affinity binding site on the surface of neutrophils for the prototypic peptide fMLF. Other names used in the literature to define FPR1 include FPR (“classic FPR”) and FMLPR (formil-metinine-leucine-phenilalanine receptor).⁴⁹ Biochemical studies indicated that the receptor is a glycoprotein of 55-70 kDa that functionally couples to G proteins for transmembrane signalling.⁶⁴ It was then cloned in 1990 by Boulay *et al.*^{65,66} from a differentiated HL-60 myeloid

leukemia-cell cDNA library. Cloning of the cDNA for FPR1 identified the receptor to be a single polypeptide of 350 amino acids with a typical hydropathy plot pattern for a seven transmembrane domain structure.⁶⁵⁻⁶⁸ In transfected cell lines, FPR1 binds fMLF with high affinity ($K_d < 1$ nM) and it is activated by picomolar to low nanomolar concentrations of fMLF in chemotaxis assays.⁴⁰ Besides being expressed on phagocytes (e.g. neutrophils and monocytes) and a small number of non-phagocytic cells (e.g. hepatocytes, immature dendritic cells, astrocytes, microglial cells),⁶⁹ FPR1 has been identified also in the tunica media of coronary arteries.⁴⁰ Using an antibody recognizing the carboxyl terminal 11 amino acids of FPR1, Becker et al.⁷⁰ found immunoreactivity for this subtype of receptor in multiple organs and tissues, including epithelial cells in organs with secretory functions, endocrine cells (including follicular cells of the thyroid and cortical cells of the adrenal gland), liver hepatocytes and Kupffer cells, smooth muscle cells and endothelial cells, brain, spinal cord and both motor and sensory neurons.⁴⁹

1.5.2 Formyl Peptide Receptor 2 (FPR2 or FPR2/ALX)

In 1990s several laboratories reported the identification of a cDNA and a gene,⁷¹⁻⁷⁴ coding for a putative seven transmembrane receptor that shares significant sequence homology to human FPR1. Different names were given to the gene product, including FPR2/ALX for its low-affinity binding of fMLF,⁷³ FPRL1 (formyl peptide receptor like1),⁷¹ FPRH1 (formyl peptide receptor-homolog 1),⁷⁴ and “receptor related to formyl peptide receptor” based on its sequence homology to the human FPR1.⁷² Other names used in the literature include HM63,⁷⁵ and FMLF-related receptor II.⁴⁹ Pharmacological characterization has led to the identification of the eicosanoid lipoxin A4 (LXA4),^{76,77} of aspirin-triggered lipoxins,^{78,79} and of a variety of peptides,⁸⁰ as ligands for this receptor.^{40,48} Therefore, in addition to FPRL1, which frequently appears in the literature, the name ALX (or LXA4R, “Lipoxine A4 receptor”) has been introduced to convey the ability of the receptor to interact with LXA4 and aspirin-triggered lipoxins.⁸¹ FPR2/ALX is a 7TM receptor with 351 amino acids and shares 69% of amino acid identity with human FPR1. Despite the relatively high level of sequence homology with FPR1, FPR2/ALX is a low-affinity receptor for fMLF, with a K_d of 430 nM.^{67,71,73} It has been reported that mitochondria-derived formyl peptides are more potent agonists for FPR2/ALX than fMLF,⁸² suggesting that its primary function may be to recognize host-driven mitochondrial peptides or possibly other bacterially derived formyl peptides. Human FPR2/ALX has a tissue distribution similar to that of FPR1, but FPR2/ALX is expressed also in other cell types, including phagocytic leukocytes, hepatocytes, epithelial cells, T lymphocytes, neuroblastoma cells, astrocytoma cells and microvascular endothelial cells.⁶⁹ These patterns of tissue expression suggest that FPR1/FPR2/ALX may also participate in a number of functions other than host defense. In addition to formyl peptides and LXA4, FPR2/ALX is also able to interact with non formylated peptides. Compared with FPR1, FPR2/ALX exhibits a high level of ligand promiscuity and it

1. Introduction

is activated by numerous and chemically unrelated ligands, including synthetic peptides, pathogen derived peptides, host-derived peptides, lipids⁴⁹ and small synthetic compounds.

1.5.3 Formyl Peptide Receptor 3 (FPR3)

A second gene with significant sequence homology to human FPR1 was identified using a similar cloning strategy used to discover FPR2/ALX. This gene encodes for FPR3,⁴⁹ a putative 7TM receptor of 352 amino acids initially named FPRL2,⁷¹ (formyl peptide receptor-like 2) and FPRH2 (formyl peptide receptor-homolog 2),⁷⁴ taking into account the sequence homology to FPR1. FPR3 shares 56% and 83% sequence identity with human FPR1 and FPR2/ALX respectively. FPR3 does not bind N-formyl peptides,⁸³ such as fMLF, but it responds to some non formylated chemotactic peptides identified for FPR2/ALX.^{84,85} Migeotte et al.⁸⁶ recently reported that a naturally occurring endogenous acylated peptide, derived from the N-terminal sequence of heme-binding protein, is a potent agonist for FPR3. Unlike FPR1 and FPR2/ALX, FPR3 had been not found in neutrophils.⁷¹ This receptor is characterized by its specific expression on monocytes and DCs.⁸⁶ As already seen, monocytes express the three receptors at their surface, whereas monocyte-derived DCs express FPR1 and FPR3 when immature and only retain FPR3 after maturation.^{62,63} In particular, in the process of monocyte differentiation into immature dendritic cells (DCs), the cellular expression of FPR2/ALX progressively declines,⁶³ whereas FPR2/ALX expression remains unchanged during monocyte differentiation into macrophages. There is also a progressive loss of FPR1 during differentiation of immature DC to mature DC, such that FPR3 becomes the predominant human formyl peptide receptor in mature DC.^{62,86} The biological significance of differential expression of formyl peptide receptors in monocytes, macrophages and DCs has not yet been clearly defined, but it seems that the three receptors might play key role in the differential migration pattern of these antigen presenting cells.⁸⁶

1.6 FPRs activation and cell functions

The stimulation of FPRs is regulated at the levels of receptor by G protein activation, transduction and amplification of signals through various effectors, including kinases and small GTPases (**figure 1.3**), and integration of effector signals leading to phagocyte functions such as chemotaxis, degranulation, and superoxide generation. Regulation of FPRs at the receptor level concern mainly three different processes: desensitization, phosphorylation and interaction with β -arrestins, which in turn involve the following uncoupling of G proteins and internalization of the receptors (**figure 1.4**). It is noteworthy that, although there are many similarities between FPR1 and FPR2/ALX (and, perhaps, also FPR3),⁸⁸ major differences exist between these receptors in signalling.

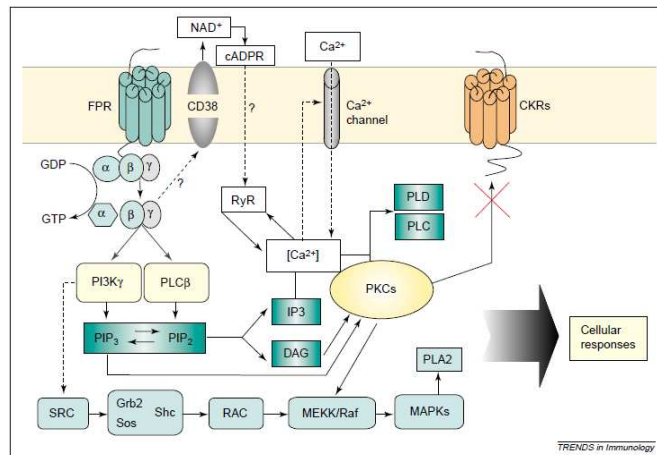


Figure 1.3. Signaling pathways of an activated FPR. On agonist binding, trimeric Gi-proteins are uncoupled and a series of signal transduction events ensue that result in cell activation and protein kinase C (PKC)-dependent desensitization of unrelated chemotactic receptors. CD38 induces the conversion of NAD^+ to cyclic ADP-ribose (cADPR), which acts at ryanodine receptors to release calcium ions (Ca^{2+}) from intracellular stores. This results in a sustained influx of extracellular Ca^{2+} required for fMLF-induced neutrophil migration. CKR, chemokine receptor; DAG, diacylglycerol; IP, inositol phosphate; MAPK, mitogen-activated protein kinase; PI3K, phosphatidylinositol 3-kinase; PIP_2 , phosphatidylinositol diphosphate; PIP_3 , phosphatidylinositol triphosphate; PKC, protein kinase C; PLA, phospholipase A; PLC, phospholipase C; PLD, phospholipase D; RAC, Rac guanine triphosphatase family; SRC, Src-like tyrosine kinases. Adapted from Le et al. (2002).⁴⁰

Evidence also suggests that the basic mechanism by which these receptors trigger a transient increase in intracellular Ca^{2+} may be different (figure 1.4).⁸⁹

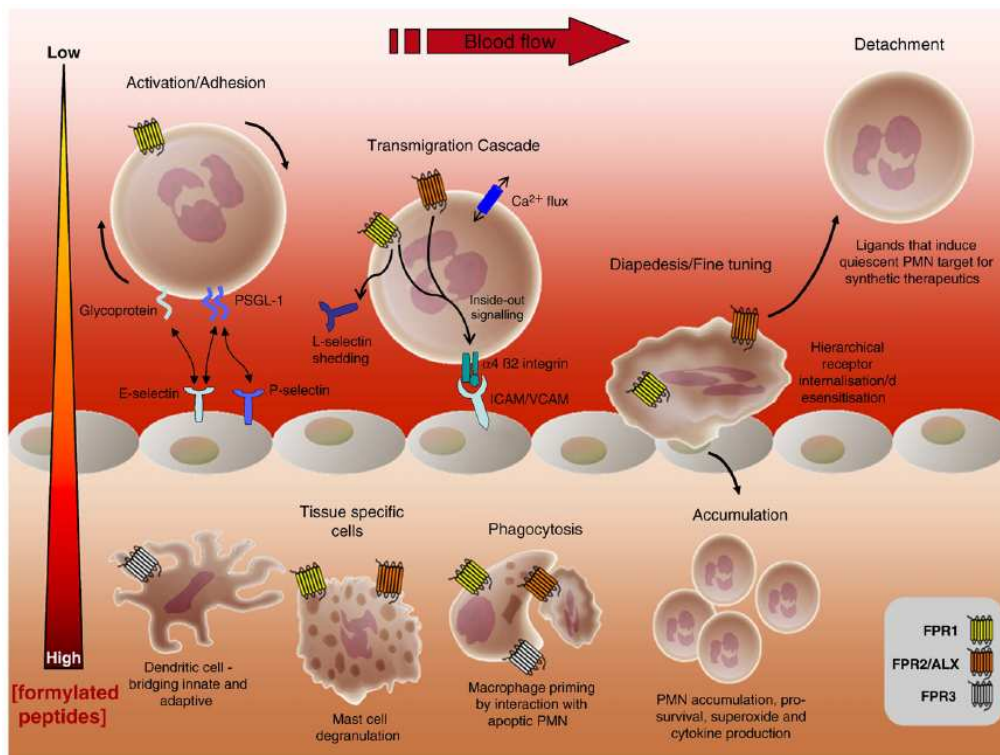


Figure 1.4. Leukocyte migration cascade via the FPRs family. FPR1 is activated at low concentration of formyl peptide (yellow). With increasing concentration of formyl peptide (orange) can also instigate FPR2 signalling. FPR activation of leukocytes, results in integrin expression and activation. Adherent leukocytes are an interesting therapeutic target for FPR2: interaction with endogenous ligands can lead to either leukocyte detachment (AnxA1/LXA4) or tissue accumulation (SAA). High concentration (red) or repeated stimulation by formyl peptide can lead to receptor desensitisation. FPRs play distinct role in myeloid cell priming and macrophage phagocytosis, mast cell membrane stabilisation. Adapted from Dufton and Perretti (2010).⁸⁷

1. Introduction

1.6.1 Chemotaxis

FPR1, along with the receptor for C5a, was the first identified phagocyte chemoattractant receptor.⁹⁰ Chemotaxis is a multistep process, induced by various chemoattractants such as PAF,⁹¹ LTB₄,⁹² C5a anaphylotoxin,⁹³ and different chemokines such as the IL8.⁹⁴ In comparison with “classic chemoattractants”, fMLF has predominant properties in cross-desensitization of other receptors,⁹⁵ and it is a potent agonist for stimulating bactericidal functions such as superoxide generation. Once established that its responses are induced by activation of specific G-protein-coupled receptors (FPRs) which are expressed on target cells, several N-formyl peptides have been extensively studied due to their abilities to induce directional migration of neutrophils.^{96,97} Indeed, human neutrophils are able to detect a chemotactic gradient of subnanomolar concentrations of fMLF.^{56,57} Therefore, exposure of neutrophils to a chemotactic agent creates an intracellular gradient of signalling molecules that defines the leading edge as well as the direction of cell migration. In addition, several exogenously and endogenously produced leukocyte chemoattractants that initiate leukocyte migration and activation have been identified. Migrating neutrophils in tissues are then exposed to multiple chemoattractants so that different and sometimes conflicting signals can sort out. In this scenario, that “navigation” of neutrophils is considered as a multistep process, and a migrating cell not only detects multiple chemoattractants but also integrates these different signals.⁹⁸⁻¹⁰⁰

A hierarchy in chemotactic signalling, determining the direction of migrating cells in opposing chemotactic gradients, have been identified and new insights into the molecular mechanisms that allow neutrophils to prioritize chemotactic signals have been provided.¹⁰¹ It resulted evident that “end-target chemoattractants” such as fMLF, dominate over the “intermediary chemoattractants” as IL-8 and LTB₄. The ability of neutrophils to distinguish between these chemoattractants is crucial for their optimal migration toward bacteria with minimal interference by the “intermediary chemoattractants” which are also present in the inflammatory site.¹⁰² Considering all these evidences, it stands to reason to assume that net result of cell migration is determined by the type of orienting signals, the strength of the signals and the time sequence in which they appear.

1.6.2 Superoxide generation

Stimulation of neutrophils with fMLF, at concentrations higher than those required for chemotaxis, leads to generation of superoxide. In most published studies, fMLF concentrations of 50 to 100 nM are required for the induction of superoxide production by human neutrophils in suspension.^{103,104} Superoxide production in neutrophils results from membrane assembly and activation of NADPH oxidase, which is a multicomponent enzyme complex for electron transfer, leading to one-electron reduction of molecular oxygen.¹⁰⁵ The different concentrations required for chemotaxis and superoxide generation, effectively

prevent oxidant-mediated tissue injury that may be caused by migrating neutrophils. It is not entirely clear why neutrophils require a 50- to 100-fold higher concentration of fMLF for superoxide production with respect to chemotaxis, but a high signalling strength is probably necessary for simultaneous activation of multiple pathways leading to NADPH oxidase activation in phagocytes. However, several studies reported in literature suggest that there are multiple mechanisms for the potentiation of the same enzyme.⁴⁹ It is noteworthy that, when used at low concentrations (e.g., 5 nM), fMLF is unable to stimulate neutrophil superoxide production but it can synergize with other neutrophils activators for a more robust response and.¹⁰⁶

1.6.3 Degranulation

In addition to the induction of superoxide generation, at higher concentrations (usually 10-50 times higher than the optimal concentration for chemotaxis) formyl peptides stimulate the release of granule constituents from neutrophils.^{57,107} The fMLF-induced mobilization of granules produces a variety of effects, including proteolytic cleavage of membrane-localized adhesion molecules such as L-selectin, cell surface expression of new adhesion molecules and release of proinflammatory proteins and enzymes that can cause tissue degradation and killing of bacteria. For instance, neutrophil myeloperoxidases, released from the azurophil granules, help to convert hydrogen peroxide to hypochlorous acid,¹⁰⁸ a metabolite important both for killing invading microbes and for the resolution of inflammation. Moreover, most of the membrane associated with NADPH oxidase components are localized on mobilizable granules which, if activated, become more available for the assembly of NADPH oxidase itself. Last but not the least, there are intracellular pools of FPR1 as well as of FPR2/ALX that are up-regulated to the cell surface when cells are stimulated with inflammatory mediators that mobilize the granules.^{109,110} Degranulation in fMLF-stimulated neutrophils involves the second messenger diacylglycerol and PKCs which are activated by diacylglycerol and Ca^{2+} .¹¹¹ However, fMLF is still able to induce secretory granule release when extracellular and intracellular Ca^{2+} is chelated, suggesting the presence of Ca^{2+} independent pathways for degranulation.¹¹² Further investigations will be necessary to determine the cross-talk between FPRs and other components taking place in process and their roles in regulating vesicular fusion during degranulation.

1.6.4 Transcriptional regulation and anti-inflammatory functions

Although neutrophils are terminally differentiated myeloid cells with special bactericidal functions, these cells retain the ability to synthesize selected proteins, including certain cytokines.¹¹³ fMLF has been found to stimulate neutrophil transcriptional regulation and cytokine production.¹¹⁴ fMLF-induced IL-8 secretion is accompanied by the activation of NF- κ B, a nuclear factor for transcription of a large number

1. Introduction

of proinflammatory genes.¹¹⁵ In addition NF- κ B activation is also mediated by FPR2/ALX, in response to SAA (serum amyloid A) stimulation, which leads to IL-8 secretion.¹¹⁶ These results are consistent with the ability of certain GPCRs to regulate transcriptional activation that contributes to the proinflammatory activities of the respective ligands.¹¹⁷ In contrast, FPR2/ALX ligands such as LXA4 (lipoxin A4) and ANXA1 (annexin A1) exhibit anti-inflammatory activities.^{76,79} ANXA1 has been shown to cause detachment of leukocytes and prevent transendothelial migration (diapedesis).¹¹⁸ In comparison, the anti-inflammatory effect of LXA4 is shown to involve suppression of proinflammatory gene expression.¹¹⁹ It is not entirely clear if this action of LXA4 is mediated through FPR2/ALX-dependent negative signalling or blockade of FPR2/ALX binding and activation by an endogenous, proinflammatory agonist for this receptor,⁴⁹ even if it is known that LXA4 can compete off the binding of FPR2/ALX agonists.¹²⁰ However, LXA4 stimulation does not lead to calcium mobilization in several types of transfected cells neither induce neutrophil degranulation and superoxide generation.¹²¹⁻¹²³ In contrast, LXA4 has been shown to activate monocytes.¹²⁴ The discrepancy suggests that signaling molecules essential for certain LXA4-induced functions might be missing in neutrophils and epithelial cells. It also reflects that LXA4 lacks full agonistic activities at FPR2/ALX.

1.6.5 Neutrophil apoptosis

Neutrophils released to blood circulation have a half-life of 8 to 10 h. If not activated, these cells are destined for apoptosis.¹²⁵ Stimulation of neutrophils with proinflammatory cytokines such as G-CSF (granulocyte macrophage-colony-stimulating factor) and IL-1 β , but not with fMLF, C5a, or IL-8, prolongs the lifespan of neutrophils.¹²⁶ Other reports have shown that stimulation of neutrophils with fMLF can induce apoptosis and this process requires superoxide generation.¹²⁷ Neutrophil apoptosis and phagocytosis of apoptotic neutrophils are related to resolution of inflammation. Several ligands for the formyl peptide receptors are found to play different roles in neutrophil apoptosis. The underlying mechanism has not been fully identified, however these results suggest a potential role of FPRs, mainly of FPR2/ALX,⁴⁹ in the regulation of neutrophil apoptosis, but other receptors may be involved as well and in the future it will be important to determine how a single class of receptors mediates different functions in cell survival and apoptosis when stimulated with different ligands.

1.7 FPRs involvement in several diseases

Till now, a part from the clear involvement of FPRs in inflammation, host defense against bacterial infection and as well as in the clearance of damaged cells, additional and more complex physiological functions have been proposed for FPRs.

Receptor	Disease pathology	Mechanism
FPR1	Periodontitis	Functional polymorphisms
FPR2/ALX	Alzheimer's disease	Cellular infiltration and amyloidosis
	Asthma	Decreased expression in BALF samples and on peripheral blood granulocytes Increase FPR2/ALX expression
	Rheumatoid arthritis	Regulating extracellular matrix turnover Increased expression in synovial tissues
	Acute ischemic stroke	Increased expression in peripheral blood mononuclear cells

Table 1.1. FPR1 and FPR2/ALX receptor associations with human disease. Adapted from Dufton and Perretti (2010).⁸⁷

Indeed these receptors have been found to interact with a menagerie of structurally different pro- and anti-inflammatory ligands associated with different diseases (**table 1.1** and **1.2**), including amyloidosis and Alzheimer's disease,¹²⁸ some kinds of cancers and related alopecia induced by most anticancer agents,^{129,130} prion disease,¹³¹ HIV,¹³²⁻¹³⁵ and stomach ulcer.^{136,137} In addition, it has been demonstrated that exogenously administered fMLF as well as other FPRs agonists can peripherally and centrally inhibit the nociceptive transmission associated with inflammatory processes through a mechanism that involves formyl peptide receptors.¹³⁸

Ligand	Disease pathology	Mechanism
AnxA1	Alzheimer's disease	Decreased expression following proteomic analysis of peripheral leukocytes.
	Coronary artery disease	Augmented levels in circulating neutrophils.
	Cystic fibrosis	Higher proteolysis in BAL Absence in epithelial cells (proteomic study)
LXA ₄	Rheumatoid arthritis	Higher expression in circulating T cells upon GC treatment
	Severe asthma	Decreased levels in BALF samples
SAA	Rheumatoid arthritis	Elevated levels in synovial fluid
	Coronary artery disease	Increased systemic levels as a diagnostic marker of prevalent Promotes monocyte tissue factor and TNF induction from mononuclear cells
	Crohn's disease	Close correlation with IL-6 production
	Rheumatoid arthritis	Systemic disease progression and secondary amyloidosis Inducing IL-6 in synoviocytes

Table 1.2. FPR2/ALX ligand association with human disease. Adapted from Dufton and Perretti (2010).⁸⁷

Moreover, these receptors have been proposed as prospective targets for therapeutic intervention against malignant gliomas.¹³⁹ How these receptors recognize so different ligands and how they contribute to disease pathogenesis and host defense, are basic questions currently under investigation.

1.8 FPRs ligands

Ligand diversity is a prominent and unusual feature of the FPRs (**table 1.3**). With the exception of the eicosanoid LXA₄, all known FPR family ligands are peptides. More recently, small synthetic molecules have emerged from a number of compound library screens as ligands for the formyl peptide receptors.^{40,48,80} Whereas many of the natural agonists and antagonists for FPRs are identified and purified from living organisms, a lot of peptides are synthesized based on the sequences of known

1. Introduction

proteins of microbe and host origins (**table 1.3**). Whether these peptides are present in vivo and have physiological functions has yet to be determined for the most part of them.

Ligand	Origin/Description	Potency	Selectivity
<i>N</i> -formyl peptides			
fMLF and other bacterial formyl peptides*	Bacteria		FPR1 > FPR2/ALX
Mitochondrial formyl peptides*	Mitochondria		FPR1 ≈ FPR2/ALX
<i>N</i> -formyl-Nle-Leu-Phe-Nle-Tyr-Lys	Synthetic	$pK_d = 9.22$	FPR1 ≫ FPR2/ALX
Microbe-derived nonformyl peptides			
T20 (DP178)	HIV-1 gp41 aa. 643–678	$pEC_{50} = 8.30$	FPR1
Hp (2–20)	<i>H. pylori</i>	$pEC_{50} = 6.52$	FPR2/ALX ≫ FPR3
T21 (DP107)	HIV-1 gp41 aa. 558–595	$pEC_{50} = 6.30$	FPR2/ALX
V3 peptide	HIV-1 gp120, V3 loop	$pEC_{50} = 5.82$	FPR2/ALX
N36 peptide	HIV-1 gp41 aa. 546–581	$pEC_{50} = 5.00$	FPR2/ALX
F peptide	HIV-1 gp120 aa. 414–434	$pEC_{50} = 5.00$	FPR2/ALX
Host-derived peptides			
CKβ8–1 (human CCL23)*	Chemokine	$pEC_{50} = 9.00–7.82$	FPR2/ALX ≈ CCR1
SHAAGtide*	CCL23 <i>N</i> -terminal 18 aa.	$pEC_{50} = 7.72$	FPR2/ALX > CCR1
Humanin*	Neuroprotective peptide	$pEC_{50} = 8.46$	FPR2/ALX
F2L*	Heme binding protein	$pEC_{50} = 8.00$	FPR3 ≫ FPR2/ALX
SAA*	Acute-phase protein	$pEC_{50} = 7.35$	FPR2/ALX, others
Annexin 1 / lipocortin 1*		$pIC_{50} = 6.82$	FPR1
Ac2–26*	Annexin 1	$pEC_{50} = 6.05–5.77$	FPR1, FPR2/ALX
Ac9–25	Annexin 1	$pEC_{50} = 4.70$	FPR1, FPR2/ALX
Aβ (1–42)*	Amyloid precursor	$pEC_{50} = 7.00$	FPR2/ALX
D2D3*	uPAR (88–274)	$pEC_{50} = 7.08$	FPR2/ALX
LL-37*	Cathelicidin	$pEC_{50} = 6.00$	FPR2/ALX
PrP (106–126)*	Prion protein	$pEC_{50} = 4.60$	FPR2/ALX
Temporin (from <i>Rana temporaria</i>)*	Anti-microbial peptide	$pEC_{50} = 6.60$	FPR2/ALX
	Pituitary adenylate cyclase activating polypeptide	$pEC_{50} = 6.00$	FPR2/ALX
Host-derived nonpeptide agonists			
Lipoxin A4 and aspirin-triggered lipoxins*	Eicosanoids	$pK_d = 8.77$	FPR2/ALX, AhR
Agonists from peptide library			
WKYMVm	Peptide library	$pEC_{50} = 10.13$	FPR2/ALX > FPR ≫ FPR3
WKYMVM	Peptide library	$pEC_{50} = 8.70$	FPR2/ALX ≫ FPR3
MMK-1	Peptide library	$pEC_{50} = 8.70$	FPR2/ALX
MMWLL, formyl-MMWLL	Peptide library	$pEC_{50} = 8.96$	FPR1
Agonists from nonpeptide library			
Quinazolinone derivative (Quin-C1)	Combinatorial library	$pEC_{50} = 5.72$	FPR2/ALX ≫ FPR1
Pyrazolone, 4-iodo-substituted, no. 43	Combinatorial library	$pIC_{50} = 7.36$	FPR2/ALX ≫ FPR1
AG-14	Drug-like molecule library	$pEC_{50} = 7.38$	FPR1

Table 1.3. Agonists for the human FPRs. The agonists are listed in the order of their potency within each group. The mitochondrial *N*-formylated peptides, listed in the first group, are also host-derived peptides and their potency is expressed in **table 1.4**, as well as the potency of other bacterial *N*-formylated peptides. Ligands that have been isolated from living organisms in the forms listed, and those generated by the actions of physiologically relevant enzymes, are indicated with an asterisk (*). aa., amino acid; pIC_{50} , negative logarithm of the IC_{50} ; pEC_{50} , negative logarithm of the EC_{50} ; pK_d , negative logarithm of K_d . Adapted from Ye et al. (2009).⁴⁹

1.8.1 FPRs natural agonists

A) *N*-Formyl Peptides. The *E. coli*-derived tripeptide fMLF (**figure 1.5, table 1.4**) is the most widely used chemotactic peptide for several reasons. It was one of the first characterized synthetic chemotactic peptides and has been extensively studied because it is the smallest formyl peptide that displays full agonistic activities. Its potency and efficacy in activating major bactericidal functions of neutrophils equals that of C5a. Whereas fMLF is by far the most frequently used chemotactic peptide in studies of neutrophil functions, this prototypic formyl peptide should not be taken as the sole standard in judging the presence of functional formyl peptide receptors.⁴⁹

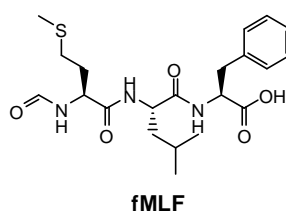


Figure 1.5. Chemical structures of fMLF, a FPR1 selective agonist.

Because bacterial protein synthesis starts with an *N*-formyl methionine, formyl peptides released from bacteria can be considered a type of microbe-associated molecular pattern, recognizable by specialized receptors in the innate immune cells of the host, such as the Toll-like receptors (TLRs). These non rearranging innate receptors have evolved to aid the host in detecting nonself such as bacterial products.¹⁴⁰ Ample evidence shows that the formyl peptide receptors can detect not only the *E. coli*-derived fMLF but also formyl peptides from other bacteria strains and from mitochondria of the host cells. **Table 1.4** lists selected bacterial and mitochondrial Formyl peptides that have been characterized for their bioactivities. Given the variety of formyl peptides from both bacteria and mitochondria (**table 1.4**), it is worthwhile to revisit some previous studies conducted with the use of fMLF and determine whether the receptors of interest are, at the present, more selective for formyl peptides of different sequences. For example, differently to FPR1, FPR2/ALX was first identified as a low affinity receptor for fMLF,⁸² but it is always able to detect and respond to several different formyl peptides. Moreover FPR2/ALX is able to discriminate between *N*-formyl peptides of different sizes, hydrophobicities, and charges.¹⁴¹ The biological relevance of this property of the receptor is not yet entirely understood but it is evident that several *N*-formyl peptides other than fMLF should demonstrate more selective for certain receptors (**table 1.4**). Indeed, although *N*-formyl peptides are a class of ligands representing a pattern recognized by the FPRs,⁵⁵ there are important differences in potency and receptor selectivity among the individual peptides.

Ligand	Origin	Assay	Potency
<i>N</i> -formyl-Met-Leu-Phe	<i>E. coli</i>	Chemotaxis	pEC ₅₀ = 10.15
		Lysozyme release	pEC ₅₀ = 7.49
		O ₂ ⁻ production	pEC ₅₀ = 7.00
		Binding	pK _d = 9.28–7.61 pK _d = 6.37
<i>N</i> -formyl-Met-Ile-Phe-Leu	<i>S. aureus</i>	Chemotaxis	pEC ₅₀ = 7.51
<i>N</i> -formyl-Met-Ile-Val-Ile-Leu	<i>L. monocytogenes</i>	Competitive binding	pIC ₅₀ = 8.01
		O ₂ ⁻ production	pEC ₅₀ = 8.00
		Ca ²⁺ flux	pEC ₅₀ = 8.66 pEC ₅₀ = 6.80
<i>N</i> -formyl-Met-Ile-Gly-Trp-Ile	<i>L. monocytogenes</i>	O ₂ ⁻ production	pEC ₅₀ = 7.82
		Ca ²⁺ flux	pEC ₅₀ = 7.70 pEC ₅₀ = 6.68
<i>N</i> -formyl-Met-Ile-Val-Thr-Leu-Phe	<i>L. monocytogenes</i>	Ca ²⁺ flux	pEC ₅₀ = 8.57 pEC ₅₀ = 6.70
<i>N</i> -formyl-Met-Ile-Gly-Trp-Ile-Ile	<i>L. monocytogenes</i>	Ca ²⁺ flux	pEC ₅₀ = 7.40
<i>N</i> -formyl-Met-Phe-Glu-Asp-Ala-Val-Ala-Trp-Phe	<i>M. avium</i>	Chemotaxis	pEC ₅₀ = 6.00
<i>N</i> -formyl-Met-Met-Tyr-Ala-Leu-Phe	Mitochondria, ND6	Ca ²⁺ flux	pEC ₅₀ = 7.92 pEC ₅₀ = 7.82
			pEC ₅₀ = 7.82
<i>N</i> -formyl-Met-Leu-Lys-Leu-Ile-Val	Mitochondria, ND4	Ca ²⁺ flux	pEC ₅₀ = 7.92 pEC ₅₀ = 7.26
<i>N</i> -formyl-Met-Tyr-Phe-Ile-Asn-Ile-Leu-Thr-Leu	Mitochondria, ND1	Binding	pK _d = 9.00
<i>N</i> -formyl-Met-Phe-Ala-Asp-Arg-Trp	Cytochrome <i>c</i> oxidase subunit	Ca ²⁺ flux	pEC ₅₀ = 6.80 pEC ₅₀ = 6.68

Table 1.4. Binding affinity and potency of bacterial and mitochondrial formyl peptides. pEC₅₀ is defined as the negative logarithm of the EC₅₀ and pIC₅₀ as the negative logarithm of the IC₅₀. HL-60 cells transfected to express FPR1 or FPR2/ALX, and Chinese hamster ovary cells transfected to express FPR1 were used in some studies. Adapted from Ye et al. (2009).⁴⁹

1. Introduction

Furthermore, there are several examples in which addition of an N-formyl group increases agonistic activity of the peptides.¹⁴² Humanin is an endogenous peptide with neuroprotective activity that also binds to FPR2/ALX and FPR3.^{143,144} For example, when humanin is N-formylated became a more potent agonist for these receptors,¹⁴⁵ in comparison to its non formylated form. In the latter example, although the primary sequences of FPR2/ALX and FPR3 differ considerably from those of FPR1, especially in the ligand binding domains,¹⁴⁶ these two receptors seem to retain the ability to preferentially interact with formylated peptides. Despite their evident importance in FPRs binding, it is not yet known whether these peptides are produced in vivo and whether they modulate inflammation.

B) Microbe-derived non-formyl peptides. Despite the absence of an *N*-formyl group, several different peptides have been found as FPRs full agonists (**table 1.3**).^{85,137} In this context, it is well known that HIV-1 envelope proteins, such as several fragments derived from gp41, contain peptide sequences capable of interacting with either or both FPR1 and FPR2/ALX.¹⁴⁷⁻¹⁵⁰ V3 peptide is another peptide derived from HIV-1 strain that showed to interact with FPRs.¹⁵¹ The existence of these peptides in vivo and their biological significance are not known at present. In addition to HIV-1 proteins, other viral proteins contain sequences that can work as ligands for FPRs when tested in the form of synthetic peptides. gG-2p20, is a peptide present in Herpes simplex virus type 2 (HSV-2), activates neutrophils and monocytes via FPR1.¹⁵² In addition, the same peptide activates phagocytes to release reactive oxygen species that inhibit NK cell cytotoxicity and accelerate apoptotic cell death. Recently, additional peptides from coronavirus have been identified as FPR1 ligands.¹⁵³

It will be interesting to understand whether and how these peptides are generated during viral infection and as well the functional consequences of phagocyte response to these peptides.

C) Host-derived peptides. In addition to mitochondrial formyl peptides discussed above, a large number of endogenous peptides of various compositions (**table 1.3**), often without an *N*-formyl group, have been identified as agonists for the formyl peptide receptors, especially FPR2/ALX. Of particular interest are peptides associated with amyloidogenic diseases, peptides associated with inflammatory and antibacterial responses, and a peptide derived from heme-binding protein which acts as a potent endogenous FPR3 agonist.⁴⁹

At least three amyloidogenic polypeptides, associated with chronic inflammation and amyloidosis, have been identified as FPR2/ALX agonists. Serum amyloid A (SAA) is an acute-phase protein whose serum concentration is increased by as much as 1000-fold in response to trauma, acute infection and other environmental stress causing acute-phase responses.¹⁵⁴ Studies with recombinant human SAA identified it as the first mammalian host-derived chemotactic peptide ligand for FPR2/ALX.¹²¹ SAA, acting through

FPR2/ALX, is chemotactic for monocytes, neutrophils, mast cells, and T lymphocytes. In addition this protein stimulates production of metalloproteases and cytokines and increases expression of cytokine receptors. In neutrophils, SAA activates FPR2/ALX and induces IL-8 secretion.¹¹⁶ In monocytes, SAA shows a peculiar pattern of cytokine induction via FPR2/ALX. Moreover, the cells respond to low concentrations of SAA by producing TNF- α while releasing IL-10 in response to high concentrations of SAA.¹⁵⁵ The synovial tissues of patients with inflammatory arthritis express high levels of SAA and FPR2/ALX and the protein induces the expression of matrix metalloproteinase-1 and -3 in fibroblast-like synoviocytes.^{156,157} Furthermore, SAA promotes synovial hyperplasia and angiogenesis through activation of FPR2/ALX and,¹⁵⁸ in addition to using the formyl peptide receptors, SAA activates neutrophil NADPH oxidase through a different receptor.¹⁵⁹

Another peptide, the 42-amino acid form of β -amyloid peptide ($A\beta_{42}$), which is a cleavage product of the amyloid precursor protein in the brain and a pathologic protein in Alzheimer's disease, was also found to activate FPR2/ALX.^{160,161} An additional amyloidogenic disease-associated FPR2/ALX agonist is represented by the prion protein fragment PrP(106–126), which is produced in human brains with prion disease.¹⁶² FPR2/ALX mediates the migration and activation of monocytic phagocytes, including macrophages and brain microglia, induced by β -amyloid ($A\beta$).^{160,163} Moreover, prolonged exposure of FPR2/ALX to this fragment peptide results in accumulation of the $A\beta_{42}$ and culminates in progressive fibrillary aggregation of $A\beta_{42}$ and macrophage death.¹⁶⁴ Therefore, FPR2/ALX not only mediates the proinflammatory activity of the peptide agonists associated with amyloidogenic diseases, but it also participates to the regulation of fibrillary peptide formation and deposition, which contribute to tissue and organ destruction.¹²⁸ The in vivo significance of this action for the pathogenesis of Alzheimer's disease is not yet known.

Humanin is a peptide encoded by a cDNA cloned from a relatively healthy region of an Alzheimer's disease brain.¹⁶⁵ Both secreted and synthetic humanin peptides protect neuronal cells from damage by $A\beta_{42}$. Humanin uses human FPR2/ALX and FPR3 as functional receptors to induce chemotaxis of mononuclear phagocytes.^{166,167} In addition, humanin reduces aggregation and fibrillary formation by suppressing the interaction of $A\beta_{42}$ with mononuclear phagocytes through FPR2/ALX. Moreover, human neuroblastoma cell lines express functional FPR2/ALX but not FPR1. In these cells, although humanin and $A\beta_{42}$ both activate FPR2/ALX, only $A\beta_{42}$ causes apoptotic death of the cells, a process blocked by humanin. These observations suggest that humanin may exert its neuroprotective effects by competitively inhibiting the access of $A\beta_{42}$.¹⁶⁷

Urokinase-type plasminogen activator (uPA) is a serine protease known for its ability to regulate fibrinolysis binding to a specific high affinity surface receptor (uPAR). In addition to this action, the uPA-uPAR system is crucial for cell adhesion, migration and tissue repair. A cleaved soluble uPAR

1. Introduction

fragment (D2D388–274) binds and activates FPR2/ALX in monocytes, inducing cell migration.⁷⁷ The ability of cleaved soluble uPAR (c-suPAR) to activate other members of the FPR family has been reported. For instance, a peptide corresponding to residues 88 to 92 of uPAR, binds to and activates FPR1.¹⁶⁸ Another fragment induces basophil migration by activating both FPR2/ALX and FPR3.¹³⁶ Recent studies showed that pretreatment of monocytes with the FPR2/ALX agonist D2D388–274 strongly decreases chemokine-induced integrin-dependent rapid cell adhesion,¹⁶⁹ indicating that FPRs regulate leukocyte chemotaxis at multiple levels and other than mediate cell migration, they may suppress cell responses to chemokines by desensitizing chemokine receptors.

Furthermore, FPRs interact with several bactericidal peptides contained in human neutrophil granules. LL-37, an enzymatic cleavage fragment of the neutrophil granule protein cathelicidin, is an agonist for FPR2/ALX.¹⁷⁰ LL-37 is expressed by leukocytes and epithelial cells and secreted into wounds and into the airway surface. In addition to its microbicidal activity, LL-37 induces directional migration of human monocytes, neutrophils, and T lymphocytes, a function mediated by FPR2/ALX. Recent studies showed that LL-37-induced angiogenesis is mediated by FPR2/ALX in vascular endothelial cells.¹⁷¹ LL-37 seems to be a multifunctional peptide with a central role in innate immunity against bacterial infection and in the induction of arteriogenesis.

Another antibacterial granule protein, cathepsin G, which is a serine protease and participates in wound healing, is identified as a specific FPR1 agonist and it is considered responsible for chemotactic activity in phagocytes.¹⁷²

Annexin A1 (ANXA1) and its N-terminal peptides have interesting properties in activating formyl peptide receptors by playing a dual role in inflammatory host responses. ANXA1 (also termed lipocortin I) is a glucocorticoid-regulated, phospholipid-binding protein of 37 kDa that possesses both pro- and anti-inflammatory activity, in part mediated by FPR1.¹⁷³ Expressed in a variety of cell types, ANXA1 is particularly abundant in neutrophils. The protein is primarily cytosolic, but it may also be secreted through a non classic secretory process and found on the outer cell surface, causing leukocyte detachment and thereby inhibiting their transendothelial migration. At low concentrations, both ANXA1 holoprotein and its N-terminal peptides (Ac2–26 and Ac9–25) elicit Ca²⁺ transients through FPR1 without fully activating the MAPK pathway, causing neutrophil desensitization and inhibition of transendothelial migration induced by other chemoattractants such as the chemokine IL-8. In contrast, at high concentrations, the ANXA1 peptides fully activate neutrophils *in vitro* and they become potent proinflammatory stimulants. The antimigratory activity of exogenous and endogenous ANXA1 has been shown in both acute and chronic models of inflammation.¹¹⁸ Other studies have shown that the ANXA1 N-terminal peptides use FPR2/ALX for its anti-inflammatory actions.⁷⁶ These peptides are also ligands for FPR3.¹⁷³ The utilization of the FPRs by ANXA1 and its amino terminal peptides for their various

function is a complex issue. To this end, one published report demonstrates that Ac9–25 stimulates neutrophil NADPH oxidase activation through FPR1, but its inhibitory effect is mediated through a receptor other than FPR1 or FPR2/ALX,¹⁷⁴ suggesting the presence of additional receptors for ANXA1 and its peptides.

F2L is a highly potent and efficacious human FPR3 agonist peptide.⁸⁶ It is an amino-terminally acetylated peptide resulting from the natural cleavage of human heme-binding protein, an intracellular tetrapyrrole-binding protein. The peptide binds and activates FPR3 in the low nanomolar range, triggering typical G protein-mediated intracellular calcium release, inhibition of cAMP accumulation and phosphorylation of the ERK 1/2MAPKs. F2L also chemoattracts and activates monocyte-derived DCs. Thus, F2L seems to be a novel and unique natural chemotactic peptide for FPR3 in DCs and monocytes, in agreement with the selective expression of FPR3 in these cells.⁶² F2L may play a role in linking innate and adaptive immune responses by activating antigen-presenting DCs, which express little FPR1 and FPR2/ALX.

D) Host-derived nonpeptide agonists. LXA4 (5*S*,6*R*,15*S*-trihydroxy-7,9,13-*trans*-11-eicosatetraenoic acid, **figure 1.6**) is a potent mediator biosynthesized from arachidonic acid. It is a small molecule with physical and chemical properties that differ from the most part of lipids: it has a unique structure and belongs to a class of conjugated tetraene containing eicosanoids that display stereoselective and highly potent anti-inflammatory effects *in vivo*, together with pro-resolving activities in many mammalian systems.¹⁷⁵

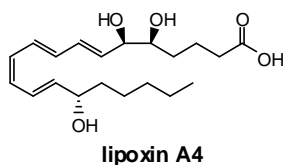


Figure 1.6. Chemical structures of LXA4, a highly selective agonist for FPR2/ALX.

This aspect is unusual since the most part of eicosanoids are pro-inflammatory. As an endogenous mediator, LXA4 displays multilevel control of relevant processes in acute inflammation through specific and selective actions on multiple cell types via specific receptors.¹⁷⁶ In particular, LXA4 has been reported to directly interact with human FPR2/ALX and in addition it is the first identified endogenous ligand for this receptor (**table 1.3**). LXA4 has showed to be responsible for the specific LXA4 functions in neutrophils.¹⁷⁷ In fact, it stimulates rapid (within seconds) phospholipase activation in these cells and this event directly correlates with the induction time course of specific LXA4 binding.^{178,179} In cell line HL-60, when differentiated into neutrophils, LXA4 gives high-affinity binding with FPR2/ALX as well as ligand selectivity, compared with other eicosanoids including LXB4, leukotriene B4, leukotriene D4, and PGE2. Each of the actions of LXA4 proved to be stereoselective, because double bond isomerization

1. Introduction

and alcohol chirality (*R* or *S*), as well as dehydrogenation of alcohols and reduction of double bonds, are associated with changes in potency. Elimination of the carbon 15 position alcohol from LXA4, denoted 15-deoxy-LXA4, is essentially inactive *in vivo* and does not stop either neutrophil transmigration or reduce adhesion.¹⁷⁵ Moreover, several *in vivo* studies have shown that nanogram amounts of LXA4 stops neutrophil infiltration and blocks human neutrophil transmigration across mucosal epithelial cells and vascular endothelial cells.^{79,180-186} One of the mechanisms by which it inhibits neutrophil infiltration is the induction of NO production, which suppresses leukocyte-endothelial cell interaction.¹⁸⁷ LXA4 inhibits as well TNF α -induced production of cytokines (IL-1 β and IL-6),¹⁸⁸ chemokines (IL-8),¹⁸⁹ and consequently decreases LPS induced secretion of IL-1 β , IL-6, and IL-8.¹⁹⁰ Dendritic cell production of the immunomodulatory cytokine IL-12 is also regulated by LXA4.^{191,192} In addition to its inhibition of proinflammatory cytokine production, LXA4 plays a role in regulating inflammation-induced pain.¹⁹³ This function is probably mediated through alteration of spinal nociceptive processing via astrocyte activation. LXA4 also stimulates non phlogistic phagocytosis of apoptotic neutrophils, which accelerates the clearance of neutrophils and promotes resolution of inflammation.¹⁹⁴ These examples show that, in general terms, LXA4 actively inhibits many endogenous processes which can amplify local acute inflammation, leading to potent anti-inflammatory as well as pro-resolving actions *in vivo*. The multilevel control by LXA4 on relevant processes of acute inflammation raises the intriguing question of how LXA4, binding to FPR2/ALX, might translate into the anti-inflammatory and pro-resolving activities and whether other receptors contribute to these activities.⁴⁹

1.8.2 Agonists from peptide library

Using combinatorial peptide library screens, a number of peptides have been identified as potent agonists for the formyl peptide receptors (**table 1.3**). WKYMVm, a hexapeptide representing a modified sequence isolated from a random peptide library, was found to be a highly efficacious stimulant for human B lymphocytes, monocytic cell lines and blood neutrophils.¹⁹⁵ WKYMVm binds to FPR1, FPR2/ALX, and FPR3 for activation of human phagocytic cells.^{196,197} WKYMVm is by far the most potent peptide agonist for FPR2/ALX, with an EC₅₀ well within the picomolar range in chemotaxis assays. WKYMVM, a derivative of WKYMVm with a L-methionine at the carboxyl terminus, is a highly selective agonist for FPR2/ALX and it is also a weaker activator of FPR3.⁸⁴ A recent study investigated the relationship between FPR1 and FPR2/ALX, both found in neutrophils, in mediating the WKYMVm-stimulated cellular functions. It was found that WKMYVm activates neutrophils through FPR1 only when the signal through FPR2/ALX is blocked,¹⁹⁸ suggesting its affinity for one type of receptor despite the presence of two different types of receptors in neutrophils. WKYMVm also inhibits LPS-induced maturation of human monocyte-derived dendritic cells via FPR1 and FPR3.¹⁹⁷

The peptide MMK-1 was identified from a library screen and it was found to be a highly selective FPR2/ALX chemotactic agonist.¹⁹⁹⁻²⁰⁰ Furthermore, an additional peptide FPR1 agonist was identified from a library based on the activation mechanism of the thrombin receptor PAR-1.²⁰¹ This peptide becomes 1000 times more potent when N-formylated, confirming the preferential recognition of *N*-formylmethionine-containing peptides by FPR1.

1.8.3 Agonists from nonpeptide library: synthetic small molecules

Several laboratories have recently identified ligands for the FPRs through the screening of combinatorial libraries consisting of synthetic, non-peptide compounds. These synthetic small molecules belong to different chemical classes (**figure 1.7**) and are highly selective for either FPR1 or FPR2/ALX, providing useful tools for the characterization of formyl peptide receptors. A small molecule named Quin-C1 (**figure 1.7**) with a quinazolinone scaffold was the first reported as a highly selective FPR2/ALX agonist.⁶¹ Quin-C1 (4-butoxy- *N*-[2-(4-methoxy-phenyl)-4-oxo-1,4-dihydro-2*H*quinazolin-3-yl]-benzamide) induces chemotaxis and secretion of β -glucuronidase in peripheral blood neutrophils with a potency approximately 1000 fold lower in comparison with WKYMVm, which is the most potent FPR2/ALX agonist identified till now. However, unlike most FPR2/ALX peptidic agonists, Quin-C1 did not induce substantial neutrophil superoxide generation, even at high concentrations (up to 100 μ M). The structural basis for this particular agonistic activity is still unknown but it appeared attractive for its potential use as a therapeutic agent.

A series of pyrazolone compounds were initially identified from a cell-based assay for high-throughput screening and subsequently modified.^{202,203} These ligands are also highly selective for FPR2/ALX and exhibit anti-inflammatory properties in mouse. Some pyrazolones belonging to this series were able to stimulate calcium flux in transfected cells expressing FPR2/ALX and the most interesting term, compound 43 (**table 1.3** and **figure 1.7**), was formulated for oral administration and was found to significantly reduce inflammation in a mice model assay.

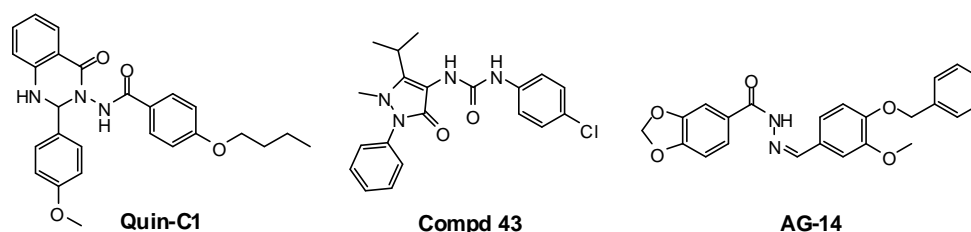


Figure 1.7. Chemical structures of selected small-molecule ligands for the formyl peptide receptors. Despite their abilities to bind to FPR1 and/or FPR2/ALX, these ligands have quite different structures. Quin-C1, and compound 43 are highly selective agonists for FPR2/ALX, whereas AG-14 is selective for FPR1.

Using a strategy combining computer model-based virtual screening and high-throughput no-wash cytometry screening, from an initial pool of 480,000 compounds, 30 leads were identified as FPR1 partial

1. Introduction

agonists or antagonists.¹³⁹ The pharmacophore model for FPR1 developed in this study may be useful in future identification of agonists and antagonists for this class of receptors.

Starting from a neutrophil superoxide production assay, combined with substructure screen, fragment focusing and structure-activity relationship analyses, *t*-butyl benzene and thiophene-2-amide-3-carboxylic ester derivatives were identified as potential agonists for neutrophil chemoattractant receptors.²⁰⁴ Among these compounds it emerged AG-14 (**figure 1.7** and **table 1.3**) which was found to be able to activate neutrophils at nanomolar concentrations. Based on desensitization and antagonist inhibition data, the investigators concluded that AG-14 is a FPR1 agonist.

Arylcarboxylic acid hydrazide derivatives were identified by the same investigators as agonists for FPR2/ALX that induce de novo production of TNF- α through activation of macrophages.²⁰⁵

All these studies further demonstrate that agonists of FPR1/FPR2 include compounds with wide chemical diversity. The computational studies regarding both the pharmacophore models of FRRs and the structure-activity relationships analysis,²⁰⁶⁻²⁰⁷ widely confirm the hypothesis that analysis of such diverse compounds can help to better understand the ligand/receptor interaction features.

1.8.4 FPRs antagonists

Early studies showed that replacing the formyl group of fMLF with tertiary butyloxycarbonyl group (*t*-Boc) renders the peptide of antagonistic activity (**table 1.5**). *t*-Boc-Met-Leu-Phe (Boc1) and *t*-Boc-Phe-D-Leu-Phe-DLeu-Phe (Boc2) are two frequently used antagonists for FPR1, with pIC₅₀ values of 6.19 and 6.59 respectively.⁵⁶ In several recent studies, Boc2 was used at high concentrations (e.g., 100 μ M) for inhibition of FPR2/ALX.^{208,209} A different study has shown that, when used at low micromolar concentrations, both Boc1 and Boc2 are selective FPR1 antagonists; at high micromolar concentrations, Boc2 partially inhibits FPR2/ALX in addition to FPR1.²¹⁰ Therefore, the antagonistic effect of Boc2 at high concentrations is not specific for FPR2/ALX.

Cyclosporin H (CsH) is a cyclic undecapeptide produced by fungi and it displays selective antagonistic activity at human FPR1.²¹¹ Studies have shown that CsH is 14-fold more potent than the tertiary butyloxycarbonyl analogs of formyl peptides such as Boc2 in FPR1 binding assays, and approximately 5-fold more potent than Boc2 in the inhibition of fMLF-induced calcium flux and enzyme release.²¹² CsH is an inverse agonist (negative antagonist) that suppresses the constitutive activity of FPR1.²¹³ The biological significance of constitutive activity for FPR is not established. Both Boc2 and CsH competitively displace FPR1-bound fMLF, indicating that its antagonistic activity is mediated through inhibition of fMLF binding. CsH did not displays any detectable inhibitory effect on FPR2/ALX-mediated cellular functions.

Ligand	Assay	Potency	Selectivity
Chemotaxis inhibitory protein of <i>S. aureus</i> (CHIPS)	Binding	$pK_d = 7.46$	FPR1
FPRL1-inhibitor protein (FLIPr)	Binding, Ca^{2+} flux	N.D.	FPR2/ALX \gg FPR1
Trp-Arg-Trp-Trp-Trp-Trp (WRW ⁴)	Ca^{2+} flux	$pIC_{50} = 6.64$	FPR2/ALX \gg FPR1 \approx FPR3
CsH	Binding	$pK_i = 7.00$	FPR1
CsA	Enzyme release	$pK_i = 6.22$	FPR1
<i>i</i> -Boc-Met-Leu-Phe	O ₂ generation	$pIC_{50} = 6.60$	FPR1
<i>t</i> -Boc-Met-Leu-Phe	Enzyme release	$pIC_{50} = 6.19$	FPR1
<i>t</i> -Boc-Phe-Leu-Phe-Leu-Phe	Enzyme release	$pIC_{50} = 6.59$	FPR1 \gg FPR2/ALX
Quin-C7	Binding	$pK_i = 5.19$	FPR2/ALX
CDCA	Binding	$pK_i = 4.76-4.52$	FPR1 > FPR2/ALX
DCA	Binding	$pK_i = 4.00$	FPR1
Spinorphin	O ₂ generation	$pIC_{50} = 4.30$	FPR1

Table 1.5. Antagonists for the human formyl peptide receptors. Antagonists for the FPRs are listed in the order of their approximate potency, except that antagonists of same types are listed together. *t*-Boc, *N*-tert-butoxycarbonyl group; *i*-Boc, -butoxycarbonyl group; pIC_{50} , negative logarithm of the IC_{50} ; pK_i , negative logarithm of K_i ; N.D., binding affinity or potency was not determined. Adapted from Ye et al. (2009).⁴⁹

Endogenous FPR1 antagonists have been as well identified. Spinorphin, an opioid, is an endogenous peptide antagonist for FPR1 with a pIC_{50} of 4.30.^{214,215} The bile acids deoxycholic acid (DCA) and chenodeoxycholic acid (CDCA) are two other identified FPR1 antagonists.^{216,217} Chemotaxis inhibitory protein of *S. aureus* (CHIPS) is a bacteria-derived protein of 14.1 kDa found in more than half of the clinical strains of *S. aureus*. CHIPS showed antagonistic activity for FPR1.²¹⁸ The identification of a bacteria-derived FPR1 antagonist suggests a mechanism used by microorganisms to thwart host defenses. Indeed, the same researchers in a subsequent study reported the identification from *S. aureus* of a 105-amino acid protein, termed FPRL1 inhibitory protein (FLIPr), that selectively inhibits the binding of and activation by FPR2/ALX agonists including MMK-1, WKYMVM, the prion fragment PrP106–126, and amyloid peptide A β 1–42.¹²³ At higher concentrations, FLIPr also inhibits fMLF binding to FPR1. FLIPr was found to bind directly FPR2/ALX and FPR1, but not FPR3. The biological function of this inhibition has not been identified.

Quin-C7 (table 1.5 and figure 1.8) is a synthetic, nonpeptide FPR2/ALX antagonist, developed through chemical modification of the FPR2/ALX agonist Quin-C1.²¹⁹

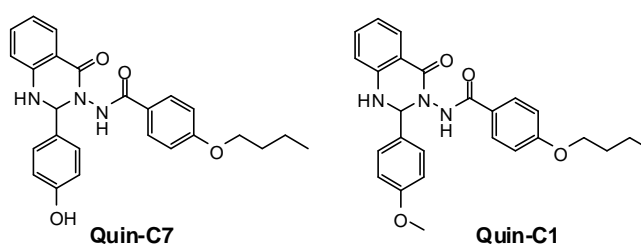


Figure 1.8. Chemical structures of Quin-C7 and Quin-C1, a synthetic pair of antagonist/agonist ligands for FPR2/ALX.

1. Introduction

In binding assays, Quin-C7 inhibited iodinated WKYMVm binding to FPR2/ALX. This antagonist showed to be highly selective for FPR2/ALX. In summary, several FPR1 and FPR2/ALX antagonists have been identified and characterized. It is noteworthy that, in most cases, these antagonists differ considerably from the identified FPR1 and FPR2/ALX agonists. The observation that *t*-Boc peptides are antagonists while *N*-formyl peptides of the same or similar composition are agonists may be helpful to define the binding pocket of these peptides in FPR1. For the same reason, the synthetic nonpeptide antagonist Quin-C7 (**figure 1.8**), differing from the agonist Quin-C1 (**figure 1.7**) only in the *para* position of the phenyl ring,²¹⁹ provides a potentially useful tool in study the binding properties of FPR2/ALX.

1.9 FPRs: future

It is clear that FPR family can convey a large variety of signals, thereby affecting an ever-increasing number of biological functions. The study of endogenous ligands for FPRs provides evidence of both activatory and inhibitory responses in experimental settings and validate endogenous anti-inflammation for successful drug discovery programs. However, the characterisation of the pharmacological properties of synthetic agonists for these receptors strongly suggests a prominent role in inflammation and in general in host defence context. The overarching hypothesis is that compounds that are able to mime specific pathways operative in the host to down-regulate inflammation could present beneficial reductions in side effects of potential therapeutics.

In this scenario, the identification and development of small-molecules represent an ideal strategy to clarify FPR structures and functions, since such molecules are well defined and can be easily modified for structure-activity relationships (SAR) analysis. Moreover, this approach may provide a basis for construction of useful pharmacophore models of FPR ligands and contribute to the development of an innovative approach to modulate host defence in inflammatory pathologies.

2. BACKGROUND AND AIMS OF THE PROJECT

The overall aim of this project is to exploit the versatility and usefulness of heterocyclic chemistry to generate a library of compounds able to act as FPRs agonists. Over the past thirty years, Prof. Dal Piaz and co-workers have shown that heterocyclic compounds such as isoxazoles, pyridazines, pyridazinones, pyrimidines, phtalazinones and pyrazoles, are good candidates to develop small molecules which achieve a high interaction with different biological systems.²²⁰⁻²³² Taking advantage of these previous experiences acquired in these researches, a similar approach was undertaken to generate a number of FPRs agonists. To achieve this goal, it was initially necessary to identify in literature a lead compound working as FPRs agonist, and then to synthesize some different series of heterocyclic compounds.

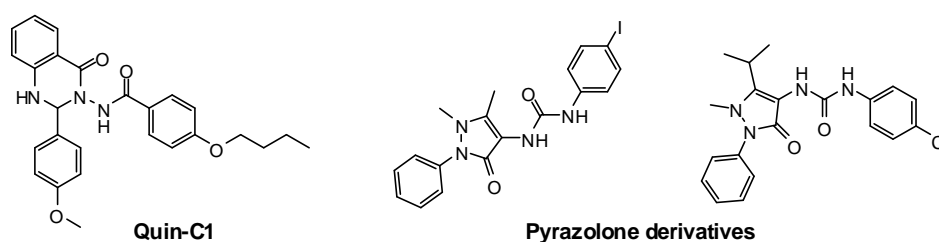


Figure 2.1. The key reference molecules used as leads in ligand-based drug design approach for the synthesis of FPRs agonists.

Thus, in the first instance, our project was based on the structural analysis of “Quin-C1” (**figure 2.1**),^{61,219} the first synthetic compound reported in literature as FPR2 selective ligand; moreover, we took into account also some pyrazolone derivatives, which were among the most potent small molecules discovered as FPRs agonists (**figure 2.1**).^{202,203}

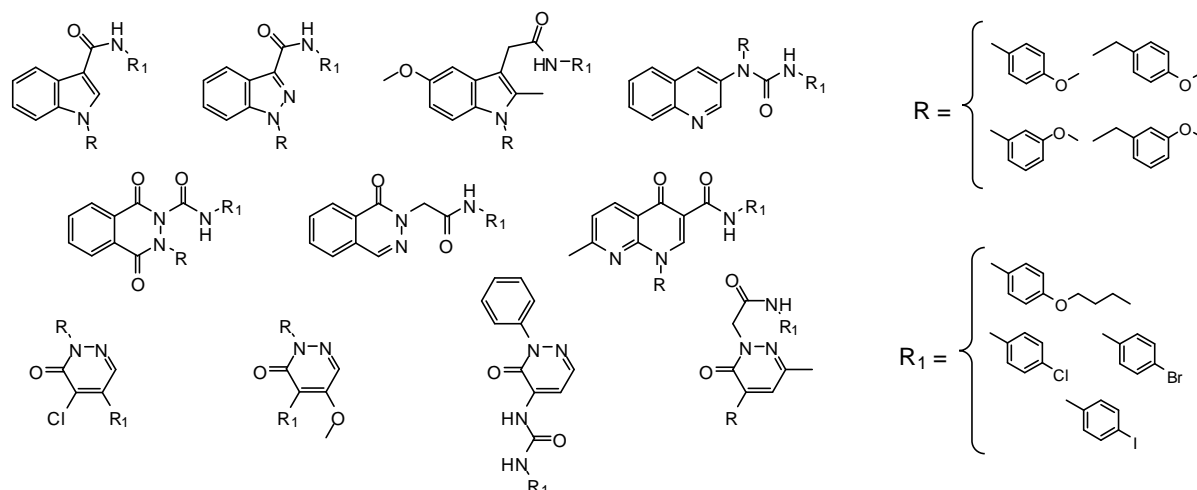


Figure 2.2. Some examples of compounds designed and synthesized using different nitrogen heterocyclic scaffold and bearing the functional groups strictly required for the activity of the reference molecules.

Thus, following a ligand-based drug design approach, we synthesized several series of nitrogen heterocyclic derivatives (**figure 2.2**) characterized by geometric, electronic, steric and lipophilic properties similar to that of the reference compounds. The aim of this approach was to allow the rapid

2. Background and Aims of the Project

identification of the appropriate scaffold bearing the suitable substituents able to interact with the FPRs system. Thus the activity of the synthesized compounds was tested on HL-60 cells transfected with FPR1, FPR2 and FPR3 respectively. The biological tests were performed by Prof. Quinn and co-workers of Veterinary Molecular Biology Department, Montana State University. In this initial screening we luckily were able to identify compound **46a** (scheme 12 in section 3 and table 4.1 in section 4), a potent mixed FPR1/FPR2 agonist.²³³ Thus, **46a** became our lead compound, on which we planned to perform extensive structure-activity relationship (SAR) studies by modifying the nature and the length of the functionalized side chain and by changing as well the substituents and their position on the pyridazinone ring (figure 2.3). Moreover, several groups were introduced to replace Br and OCH₃ on both the aromatic systems of the lead compound.

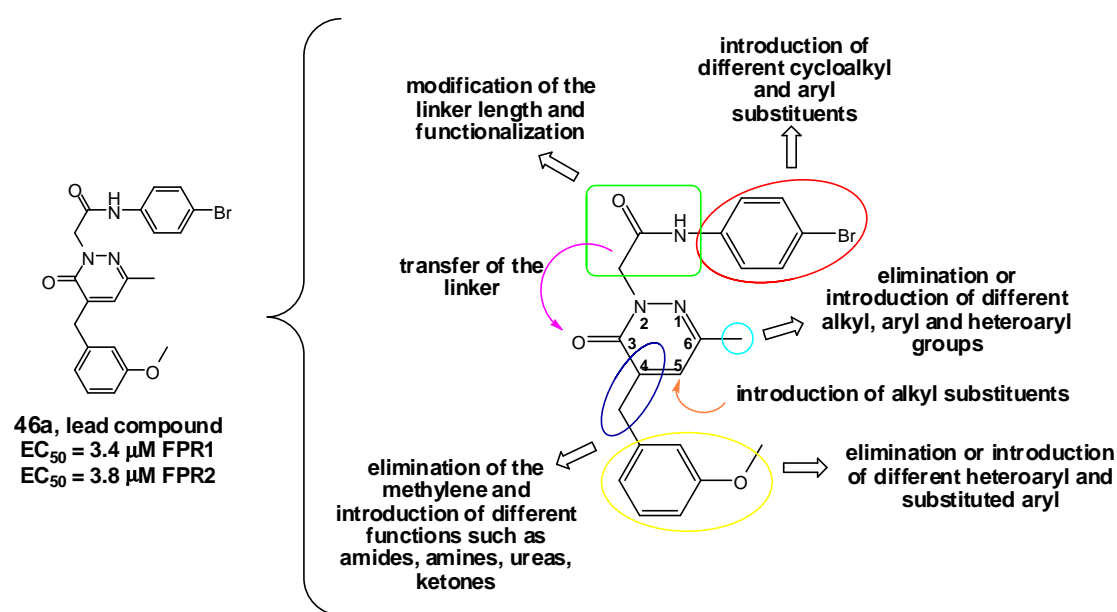


Figure 2.3. Modification performed on the lead compound (**46a**, scheme 12, table 4.1).

Once the reactions on the pyridazinone ring have been optimized, a small library of analogues was designed and synthesized in order to achieve a convenient chemical diversity on this scaffold (figure 2.3). The introduction of a chiral center on the phenylacetamide linker at N-2 position of the lead compound (figure 2.4), represent an additional project which led to the development of a new series of chiral and branched derivatives.

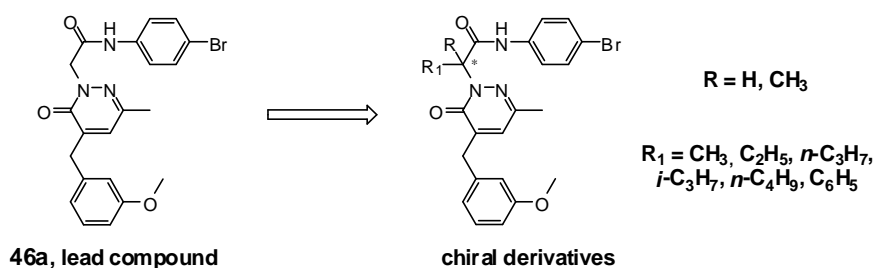


Figure 2.4. Homologue series of chiral derivatives.

During this research, the preliminary biological results prompted us to prepare and test as well the pure enantiomers in order to see if the enantioselectivity could produce an increase of the activity and/or selectivity. Since asymmetric synthesis did not allow us to obtain the pure enantiomers, chiral HPLC purification was performed to obtain both enantiomerically pure compounds. The analytical work was carried out in collaboration with Dr. Bartolucci and co-workers of Pharmaceutical Sciences Department, University of Florence.

In the present thesis are reported the results of these chemical efforts as well as the biological activity of the novel synthesized molecules.

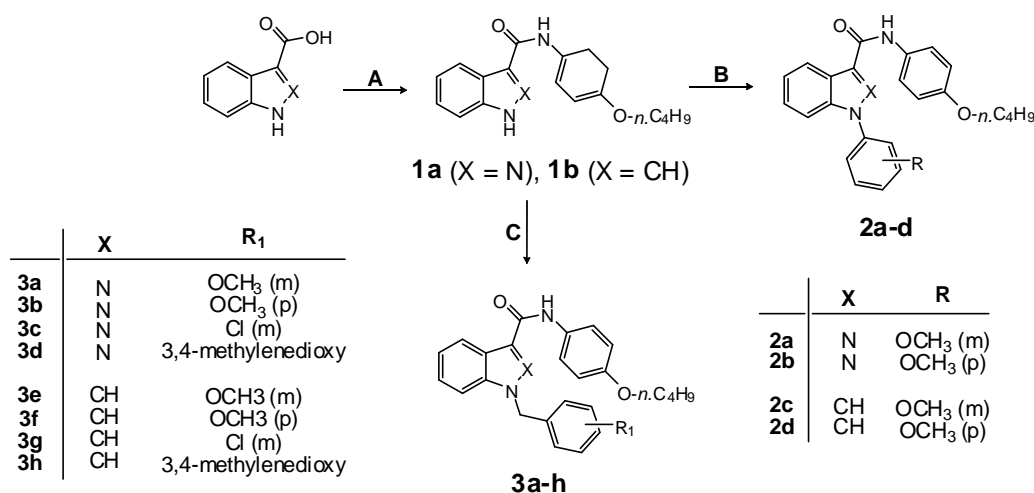
3. CHEMISTRY

Initial investigations in the FPRs agonists field have been focused on the synthesis of small molecules based on different heterocyclic scaffolds, such as indole, indazole, quinoline, naphthyridone, phthalazinone, phthalhydrazide and pyridazinone (**section 3.1**). Using this approach a relevant number of functionalised aryl-substituted heterocycles were prepared in moderate to good yields. Among them a pyridazinone derivative (**46a**, **scheme 12**) was found to be an interesting FPR1/FPR2 mixed agonist (**section 3.2**).²³³ Therefore, the next progress of the project, concerned the optimization of the selected lead compound by modifying the position of the substituents on the pyridazinone ring and the nature and the length of the functionalized side chain (**section 3.3**).

3.1 Investigating different heterocyclic scaffolds

3.1.1 Synthesis of indole and indazole derivatives

Indoles and indazoles **2a-d** and **3a-h** can be easily prepared in two steps using respectively the commercially available indole-3-carboxylic acid and indazole-3-carboxylic acid as starting material (**scheme 1**). These compounds were first treated with SOCl_2 , in presence of Et_3N , to afford the intermediate acid chlorides. Addition of 4-butoxyaniline generated the corresponding amides **1a,b** which in turn were transformed into the final compounds **2a-d**, under coupling conditions with the appropriate phenylboronic acid in presence of $\text{Cu}(\text{OAc})_2$. Finally, the target compounds **3a-h** were prepared by classical alkylation with the opportune benzyl halide.

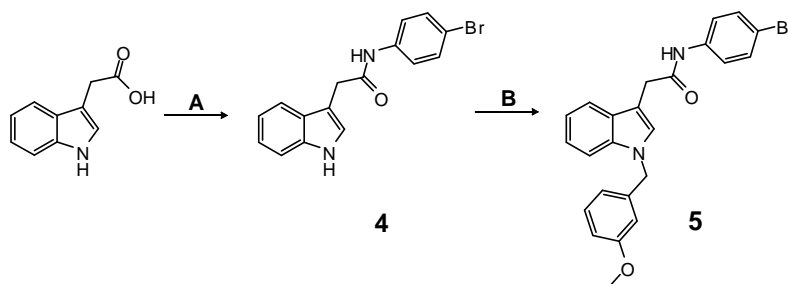


Scheme 1. Reagents and conditions: A) SOCl_2 (27 equiv), Et_3N (catalytic), 1 h, 60 °C, then 4-*n*.butoxyaniline (2 equiv), anhydrous THF, 12 h, rt; B) 3- or 4-methoxy-phenylboronic acid (2 equiv), $\text{Cu}(\text{OAc})_2$ (1.5 equiv), Et_3N (2 equiv), CH_2Cl_2 , 5-12 h, rt; C) substituted benzyl halide (1.1 equiv), K_2CO_3 (2 equiv), anhydrous acetone, 2-10 h, reflux.

In **schemes 2** and **3** are depicted the synthetic pathways to prepare two “indomethacin-like” analogues. The amide intermediate **4** was obtained by coupling the 3-indoleacetic acid with 4-bromoaniline,²³⁴ both

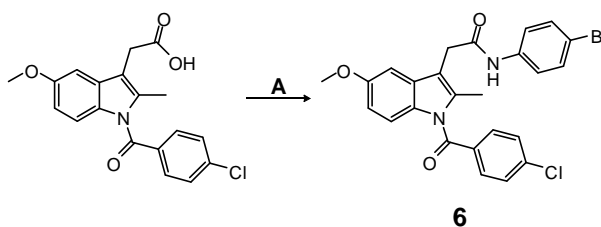
3. Chemistry

commercially available, using DCC to activate the carboxylic group. The following alkylation with 3-methoxybenzyl chloride gave the final compound **5**.



Scheme 2. Reagents and conditions: A) 4-bromoaniline (1 equiv), DCC (1 equiv), anhydrous CH₂Cl₂, 24 h, rt; B) 3-methoxybenzyl chloride (1.5 equiv), K₂CO₃ (2 equiv), anhydrous acetone, 4 h, reflux.

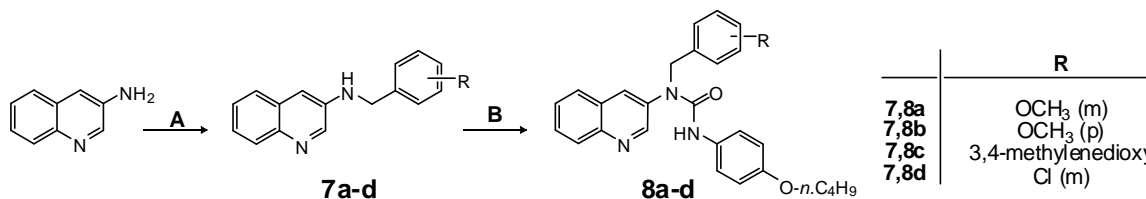
The same coupling reaction with 4-bromoaniline was also carried out on indomethacin to give the final compound **6**.



Scheme 3. Reagents and conditions: A) 4-Bromoaniline (1 equiv), DCC (1 equiv), anhydrous CH₂Cl₂, 24 h, rt.

3.1.2 Synthesis of quinoline derivatives

Final compounds **8a-d** with quinoline scaffold were prepared in two steps (**scheme 4**): the commercially available 3-aminoquinoline was firstly alkylated with the suitable substituted benzyl halide in standard conditions to give intermediates **7a-d** which, in turn, by treatment with the 4-*n*.butoxyphenyl isocyanate afforded the desired urea derivatives **8a-d**.

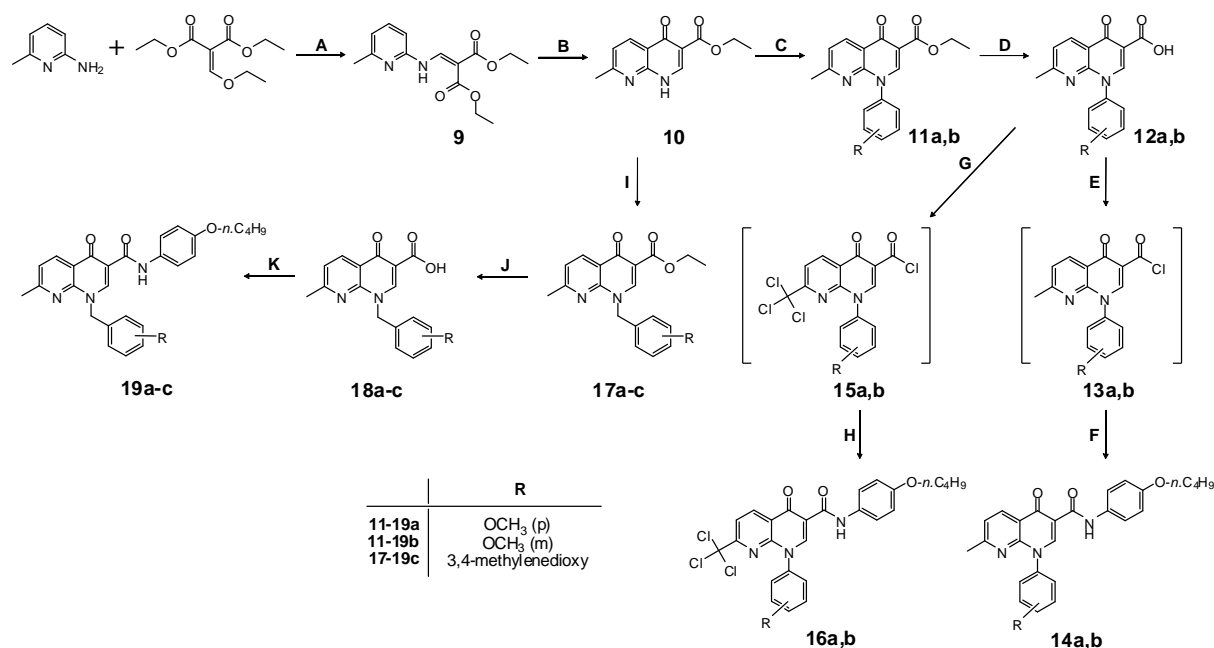


Scheme 4. Reagents and conditions: A) substituted benzyl halide (2 equiv), K₂CO₃ (2 equiv), anhydrous acetone, 3-7 h, 60 °C; B) 4-*n*.butoxyphenyl isocyanate (1.1 equiv), anhydrous CH₂Cl₂, 3-8 h, rt.

3.1.3 Synthesis of naphtrydione derivatives

The synthesis of naphtrydione scaffold **10** (**scheme 5**),²³⁵ was performed starting from commercially available 2-amino-6-methylpyridine and diethyl-2-(ethoxymethylene)malonate, followed by thermal ring closure of the diethyl-(6-methyl-2-pyridylaminomethylene)malonate **9**.²³⁶ To prepare the final compounds **14a,b** and **16a,b**, the intermediate **10** was coupled with the appropriate phenylboronic acid in presence of

$\text{Cu}(\text{OAc})_2$. An alkaline hydrolysis of the ester group afforded the carboxylic acids **12a,b** which were converted in the acid chlorides using SOCl_2 . 4-Butoxyaniline was then added to intermediates **13a,b** to give the final amides **14a,b**.



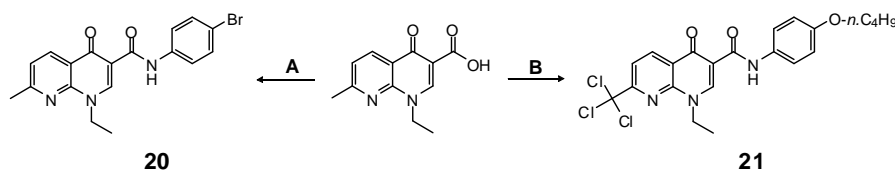
Scheme 5. Reagents and conditions: **A**) 6 h, 100 °C; **B**) diphenyl ether, 0.5 h, 270 °C; **C**) 3- or 4-methoxyphenylboronic acid (2 equiv), $\text{Cu}(\text{OAc})_2$ (1.5 equiv), Et_3N (2 equiv), CH_2Cl_2 , 15-20 h, rt; **D**) NaOH 6N, EtOH , 0.5-1 h, rt; **E**) SOCl_2 (27 equiv), Et_3N (catalytic), 2-3 h, rt; **F**) 4-*n*-butoxyaniline (2 equiv), anhydrous THF, 2 h, rt; **G**) SOCl_2 (27 equiv), Et_3N (catalytic), 2-3 h, 60 °C; **H**) see F; **I**) substituted benzyl halide (1.1 equiv), K_2CO_3 (2 equiv), anhydrous acetone, 5-7 h, 60 °C; **J**) see D; **K**) 4-*n*-butoxyaniline (1 equiv), DCP (4 equiv), Et_3N (catalytic), anhydrous DMF, 15 h, rt.

It is worth noting that treatment of the acids **12a,b** with SOCl_2 , followed by heating at 60 °C afforded the corresponding trichloromethyl acid chlorides **15a,b**. Indeed, it is well known in the literature that compounds such as 2-methylpyridines,²³⁷ 2-methylquinolines,²³⁸ 2-methyl-4(1*H*)-quinolones,²³⁹ react with different chlorinating agents to give the corresponding trichloromethyl derivatives.²⁴⁰ In our case, **15a,b**, were transformed into the final **16a,b** (scheme 5) in moderate yields, monitoring the reactions by TLC, and the products were characterized by ¹H NMR and MS spectroscopy. The synthesis of the final compounds **19a-c** was performed in standard condition starting from the intermediate **10**, through alkylation and alkaline hydrolysis, to give the carboxylic acids **18a-c**. In the last step **18a-c** were treated with the appropriate amine at room temperature in anhydrous DMF, using a catalytic amount of Et_3N and *diethyl cyanophosphonate* (DCP) to activate the carboxylic group (scheme 5).

In scheme 6 it is showed the synthetic pathway to prepare two nalidixic acid derivatives. The treatment of nalidixic acid with ethyl chloroformate, in THF and in presence of triethylamine, afforded the intermediate mixed anhydride, which was transformed into the final amide **20**. On the contrary,

3. Chemistry

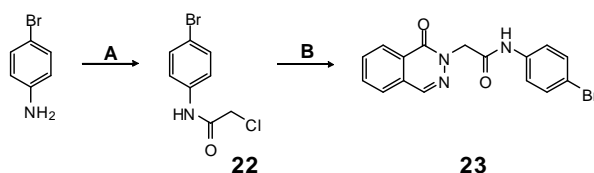
compound **21** was obtained using the same reaction sequence performed for the trichloromethyl analogues **16a,b** (scheme 5).



Scheme 6. Reagents and conditions: **A)** ethyl chloroformate (1.1 equiv), Et₃N (3.5 equiv), 4-bromoaniline (2 equiv), anhydrous THF, 12 h, -5 °C → rt; **B)** SOCl₂ (27 equiv), Et₃N (catalytic), 2 h, 60 °C, then 4-*n*-butoxyaniline (2 equiv), anhydrous THF, 2 h, rt.

3.1.4 Synthesis of phthalazinone derivative

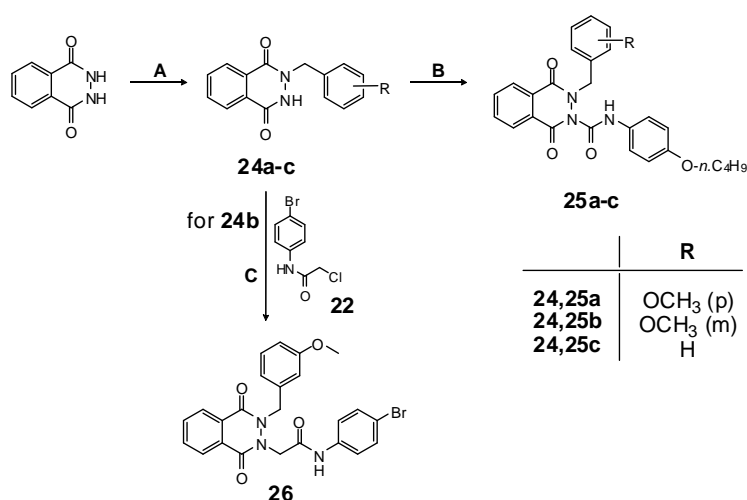
The synthetic route employed to obtain the phthalazinone derivative **23** is depicted in **scheme 7**. The 4-bromoaniline was converted in good yield to the known phenylamide intermediate **22** following a procedure reported in literature.²⁴¹ Alkylation in standard conditions of the phthalazin-1(2*H*)-one with compound **22** gave rise the final compound **23**.



Scheme 7. Reagents and conditions: **A)** *chloroacetyl chloride* (1.2 equiv), K₂CO₃ (1.2 equiv), anhydrous CH₂Cl₂, 2 h, reflux; **B)** 1-(2*H*)-*phthalazinone* (0.9 equiv), K₂CO₃ (1.8 equiv), anhydrous CH₃CN, 3 h, reflux.

3.1.5 Synthesis of phthalhydrazide derivatives

Scheme 8 outlines the synthetic procedure performed to get the final compounds **25a-c** and **26**.

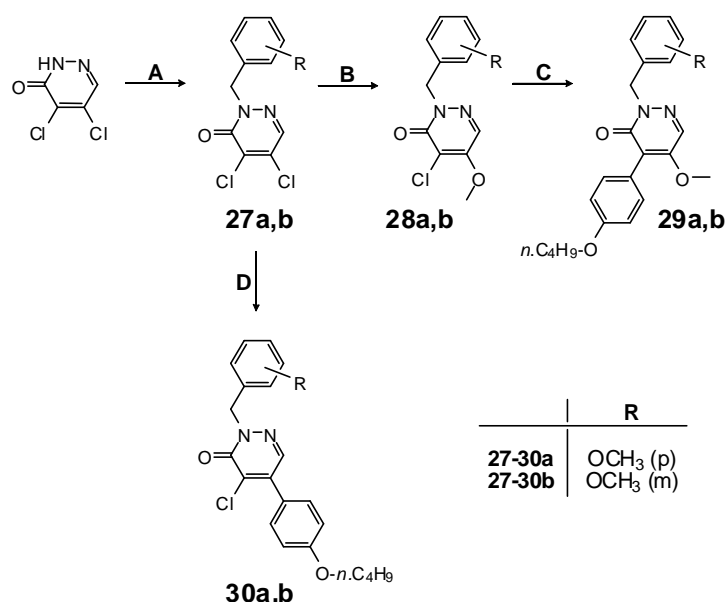


Scheme 8. Reagents and conditions: **A)** substituted benzyl halide (1.1 equiv), K₂CO₃ (2 equiv), anhydrous DMF, 2-4 h, 80 °C; **B)** 4-*n*-butoxyphenyl isocyanate (2 equiv), anhydrous CH₂Cl₂, 14 h, 0 °C → rt; **C)** **22** (1.5 equiv), K₂CO₃ (2 equiv), anhydrous CH₃CN, 3 h, reflux.

The first step is the alkylation in standard conditions of the commercially available 2,3-diidrophthalazin-1,4-dione with the suitable benzyl halide. For this reaction, anhydrous DMF gave the best results in terms of mono- and bi-alkylated ratio, although traces of product alkylated at both nitrogens were recovered in all reactions, as showed by chromatographic and ^1H NMR analysis. The previously described intermediate **24c**,²⁴² and the new **24a,b** were converted in the final urea derivatives **25a-c** using 4-*n*-butoxyphenyl isocyanate in anhydrous CH_2Cl_2 . The final compound **26** was instead synthesized through the further alkylation of compound **24b**, using the previously described intermediate **22** (scheme 7).

3.1.6 Synthesis of *N*-2-benzyl pyridazinone derivatives

In scheme 9 is depicted the synthesis of final compounds **29a,b** and **30a,b** starting from the cheap and commercially available 4,5-dichloro-3(2*H*)-pyridazinone. Following a procedure of *N*-benzylation at 2-position of the pyridazinone ring reported in the literature,²⁴³ *N*-2-benzyl derivatives **27a,b** were prepared in good yields by treatment with 3- or 4-methoxybenzyl bromide in anhydrous acetonitrile in the presence of potassium carbonate and tetrabutylammonium bromide.²⁴⁴ To synthesize final compounds **30a,b** starting from the 4,5-dichloro-3(2*H*)-pyridazinone, it was not possible to obtain selective monoarylation under Suzuki conditions. Interestingly, selective C-5 coupling with 4-butoxyphenylboronic acid was achieved using *trans*-dichlorobis(triethylphosphine)palladium (II) as catalyst and 1M Na_2CO_3 as base in DMF at room temperature, as reported in the literature.²⁴⁵ An important strategy to achieve high mono- (versus di-) substitution is the use of a two fold excess of pyridazin-3(2*H*)-one versus boronic acid.



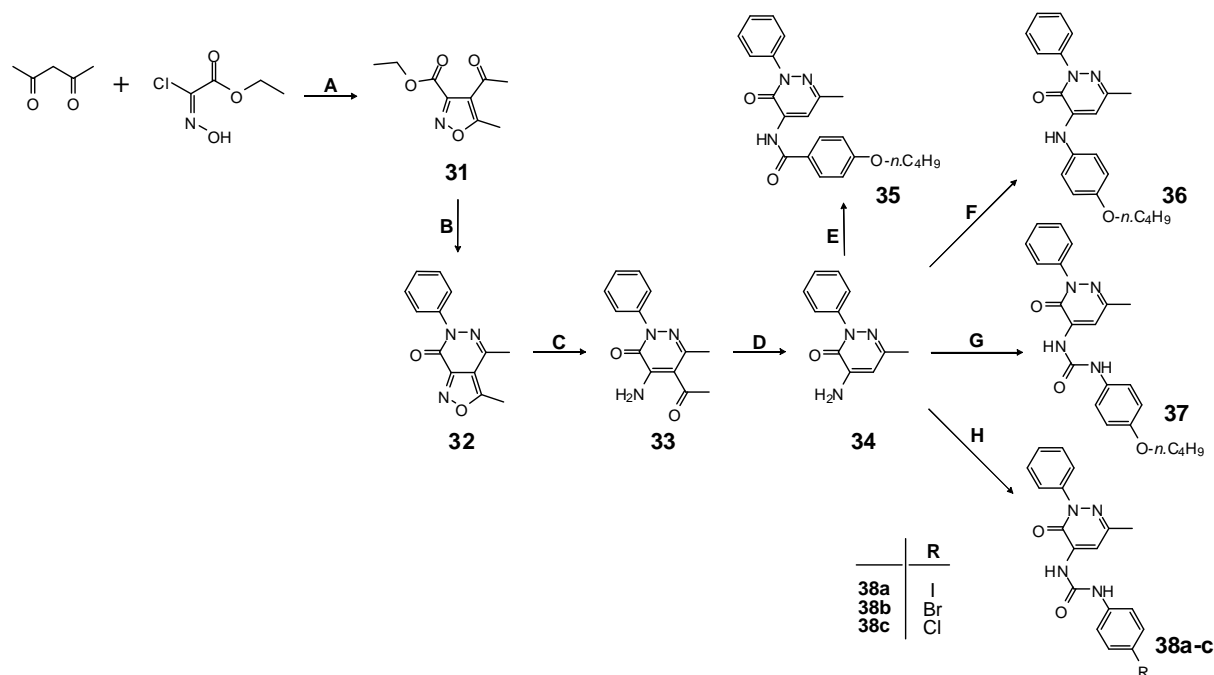
Scheme 9. Reagents and conditions: **A)** 3 or 4-methoxybenzyl chloride (1.5 equiv), K_2CO_3 (2 equiv), Bu_4NBr (0.1 equiv), anhydrous CH_3CN , 5-7 h, reflux; **B)** NaOCH_3 (2 equiv), anhydrous CH_3OH , 1 h, rt; **C)** 4-*n*-butoxyphenylboronic acid (3 equiv), $\text{Pd}(\text{PPh}_3)_4$ (0.03 equiv), Na_2CO_3 2M in H_2O (1 equiv), toluene, 5-8 h, reflux; **D)** 4-*n*-butoxyphenylboronic acid (0.5 equiv), $\text{PdCl}_2[(\text{C}_2\text{H}_5)_3\text{P}]_2$ (0.1 equiv), Na_2CO_3 1M in H_2O (1 equiv), DMF, 6-12 h, rt.

3. Chemistry

The final compounds **29a,b** were instead obtained in two steps starting from **27a,b** (**scheme 9**) where the first nucleophilic reaction involved a selective displacement of the chlorine at C-5 of the pyridazinone ring,²⁴⁶ using sodium methoxide in anhydrous methanol; the second step was an oxidative addition to tetrakis(triphenylphosphine)palladium(0) catalyst to give, in good yields, the final 4-arylated-5-methoxypyridazinones using the 4-butoxyphenylboronic acid under classical Suzuki conditions.²⁴⁷

3.1.7 Synthesis of *N*-2-phenyl pyridazinone derivatives²³³

The synthetic pathway affording the final compounds **35-37** and **38a-c** is depicted in **scheme 10**. The isoxazole **31**, the isoxazolo[3,4-*d*]-pyridazinone **32** and the pyridazinones **33,34** were synthesized following the procedures previously described.²⁴⁸⁻²⁵¹ Subsequently, the amide **35** was obtained from the primary amine **34** by treatment with the opportune arylchloride in toluene at reflux, while coupling of **34** with 4-butoxyphenylboronic acid in CH₂Cl₂ in presence of Cu(Ac)₂ gave derivative **36**.



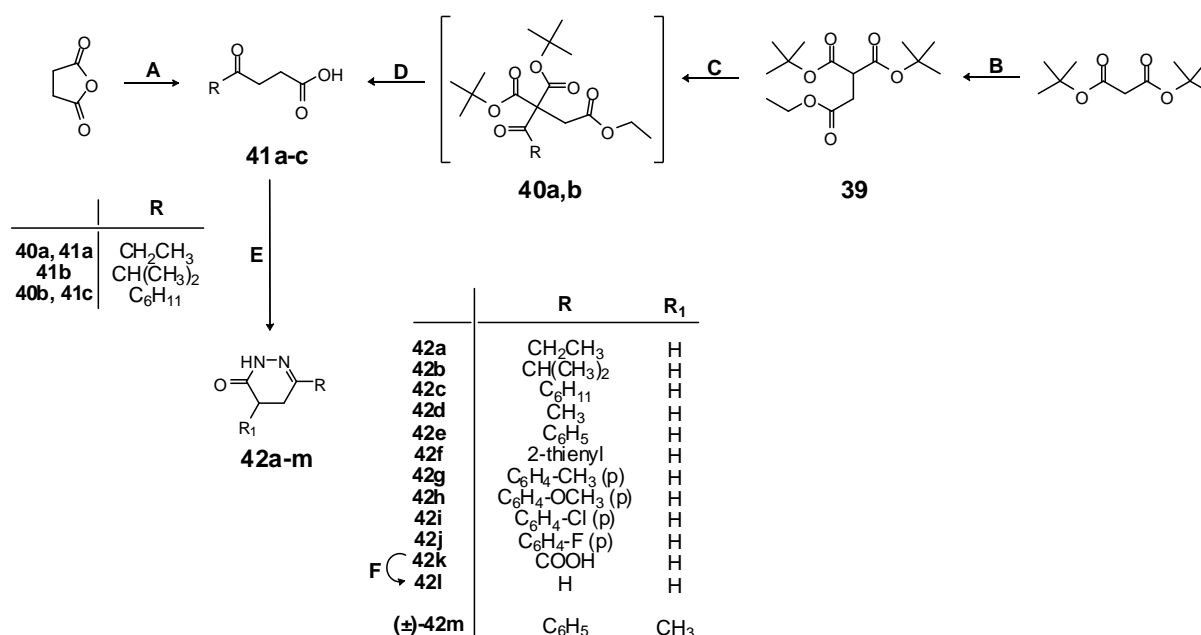
Scheme 10. Reagents and conditions: **A**) NaOEt (1 equiv), anhydrous EtOH, 2 h, -5 °C → rt; **B**) NH₂-NH-C₆H₅ (2 equiv), PPA, anhydrous EtOH, 3.5 h, reflux; **C**) HCOONH₄ (2.5 equiv), Pd/C 10% (catalytic), anhydrous EtOH, 1.5 h, reflux; **D**) HBr 48%, 1 h, 140 °C; **E**) 4-*n*.butoxybenzoyl chloride (0.9 equiv), Et₃N (4.1 equiv), anhydrous toluene, 4 h, reflux; **F**) 4-*n*.butoxyphenylboronic acid (2 equiv), Cu(OAc)₂ (1.5 equiv), Et₃N (2 equiv), CH₂Cl₂, 12 h, rt; **G**) NaOAc (2.4 equiv), CO(OCCl₃)₂ (3.5 equiv), anhydrous THF, 2 h, reflux, then 4-*n*.butoxyaniline (2.4 equiv), 12 h, rt; **H**) substituted aryl isocyanate (1.1 equiv), anhydrous toluene, 4-7 h, reflux.

Compound **34** in anhydrous toluene was refluxed with the appropriate aryl isocyanate to afford the urea derivatives **38a-c**. The 4-butoxy analogue **37** was synthesized with an alternative procedure,² starting from the same precursor **34** and using triphosgene in anhydrous THF, followed by treatment with the appropriate aniline.

3.2 6-Methyl-2,4-Disubstituted Pyridazin-3(2H)-ones: synthesis of the lead compound **46a**²³³

3.2.1 Synthesis of dihydropyridazinone scaffolds

The dihydropyridazinones **42a-m** (scheme 11) are the key building blocks for the synthesis of the pyridazinone class of compounds examined in the sections 3.2 and 3.3. As extensively reported in the literature, the γ -keto acids are the common starting material to easily achieve them.²⁵²⁻²⁵⁴ Some of the γ -keto acids useful for the synthesis of the dihydropyridazinone scaffold are not commercially available. Thus, the first goal for this second part of the project was the development of an efficient synthetic route to obtain this starting material.



Scheme 11. Reagents and conditions: **A**) Fe(acac)₃ (3 equiv), *i*PrMgCl (for compound **41b**) 2M in diethyl ether (3 equiv), anhydrous THF, 12 h, rt; **B**) NaH 60% in mineral oil (1.3 equiv), ethyl bromoacetate (1 equiv), anhydrous THF, 15 h, rt; **C**) propionyl chloride (for compound **41a**) or cyclohexylcarbonyl chloride (for compound **41c**) (1 equiv), NaH 60% in mineral oil (1.05 equiv), anhydrous THF, 3 h, rt; **D**) *p*-toluenesulfonic acid • H₂O (0.1 equiv), anhydrous toluene, 2.5 h, reflux, then EtOH, NaOH 1N, 4 h, rt; **E**) NH₂NH₂ • H₂O (1 equiv), EtOH, 1-3 h, 60 °C; **F**) 0.5 h, 160 °C.

The synthesis of the γ -keto acid **41b** was achieved following a procedure reported in the literature (**A** in scheme 11) starting from the cheap and commercially available succinic anhydride which was reacted with isopropyl magnesium chloride in anhydrous THF at 0 °C in presence of iron(III) acetylacetonate.²⁵⁵ Since the obtained yields were lower compared to that reported in literature, to prepare quickly and efficiently the key starting materials another route was explored, in which the di-tert-butyl malonate was firstly alkylated with ethyl bromoacetate in the presence of NaH and the following acylation of **39** with the appropriate acid chlorides gave intermediates **40a,b**. These intermediates were not isolated and were directly decarboxylated in presence of *p*-toluenesulfonic acid as catalyst. Hydrolysis of the ethyl esters under basic conditions afforded the previously described γ -keto acids **41a,c** in good yields.²⁵⁶⁻²⁵⁷ This

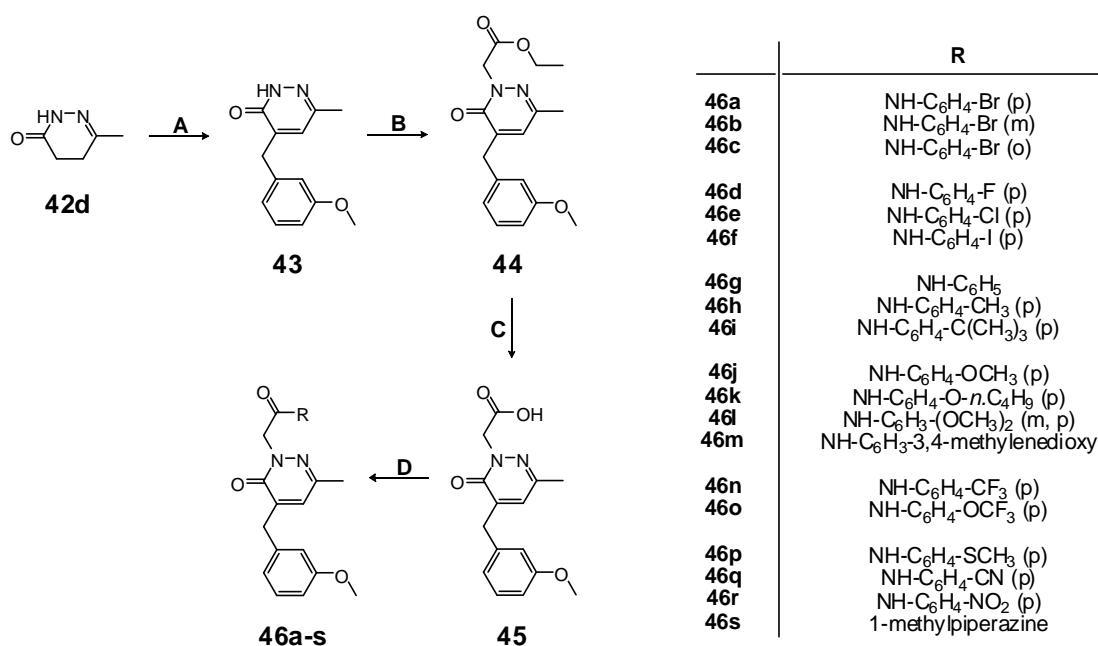
3. Chemistry

route resulted amenable for the synthesis of a large number of γ -keto acid analogues, using a wide range of cheap and commercially available acid chlorides.

The following condensation of both commercially available and synthesized γ -keto acids with *hydrazine hydrate* afforded the previously described C-6 substituted dihydropyridazinones **42a-i,k,m**,^{252,258-264} and the new **42j** in good yields. A further synthetic step was required to obtain the compound **42l** generated by melting and spontaneous decarboxylation of the carboxylic acid **42k** at 160° C.²⁶⁵

3.2.2 Synthesis of substituted *N*-arylacetamide pyridazinones²³³

In **scheme 12** is depicted the synthesis of compounds **46a-s**. The dihydropyridazinone **42d** was firstly converted into the 4-benzyl derivative **43** by Knoevenagel condensation using the appropriate aromatic aldehyde in the presence of KOH and then alkylated with ethyl bromoacetate to give **44**. Alkaline hydrolysis of the ester afforded the carboxylic acid **45**, which is the key intermediate for the synthesis of a range of substituted *N*-phenylacetamide pyridazinones. Indeed treatment with ethyl chloroformate in THF in presence of triethylamine, afforded the intermediate mixed anhydrous, which was transformed in good yields into the final amides by treatment with the appropriate aryl (**46a-r**) or cycloalkyl amine (**46s**).



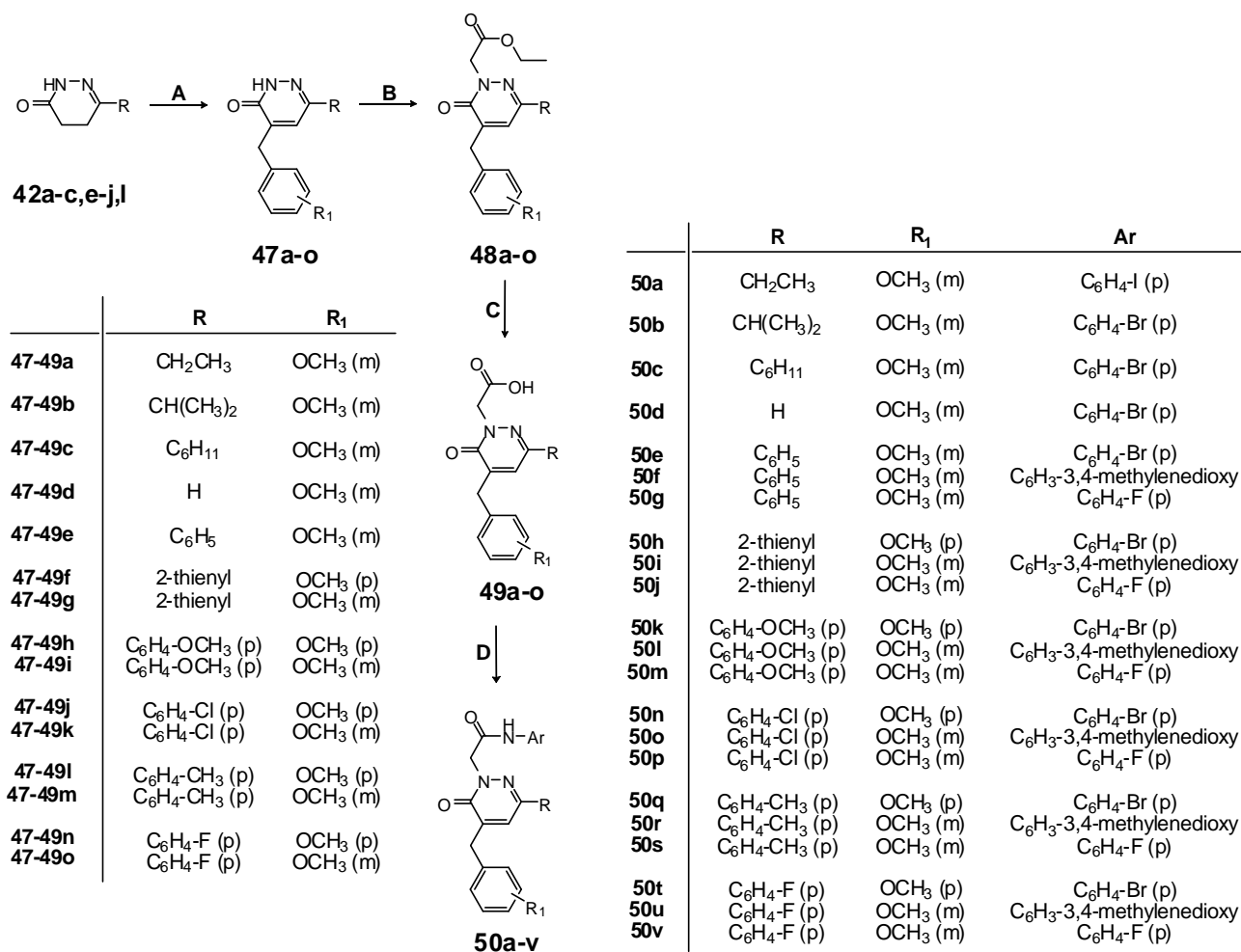
Scheme 12. Reagents and conditions: A) 3-methoxybenzaldehyde (1 equiv), KOH 5% (w/v) in anhydrous EtOH, 3 h, reflux; B) ethyl bromoacetate (3 equiv), K₂CO₃ (2 equiv), anhydrous CH₃CN, 6 h, reflux; C) NaOH 6N, EtOH, 1 h, reflux; D) ethyl chloroformate (1.1 equiv), Et₃N (3.5 equiv), substituted aryl(cycloalkyl)-amine (2 equiv), anhydrous THF, 12 h, -5 °C → rt.

3.3 Optimization of the lead: 2,3,4,5,6-substituted pyridazinones

3.3.1 Synthesis of C-6 modified *N*-arylacetamide pyridazinones

The C-6 modified pyridazinones **50a-v** (**scheme 13**) were prepared in four steps starting from the dihydropyridazinones **42a-c,e-j,l** synthesized as shown in **scheme 11** and using the same procedure

already described to get the final compounds **46a-s** (scheme 12). Through Knoevenagel condensation with the commercially available 3- or 4-methoxybenzaldehyde, the previously described derivatives **47h,j,l**,²⁶⁶ and the new **47a-g,i,k,m-o** were obtained in good yields. The following alkylation and alkaline hydrolysis were performed in standard conditions. The reaction of the carboxylic acids **49a-o** with ethyl chloroformate, to give the anhydride intermediate, and then with the appropriate aryl amines, furnished the final compounds **50a-v**.

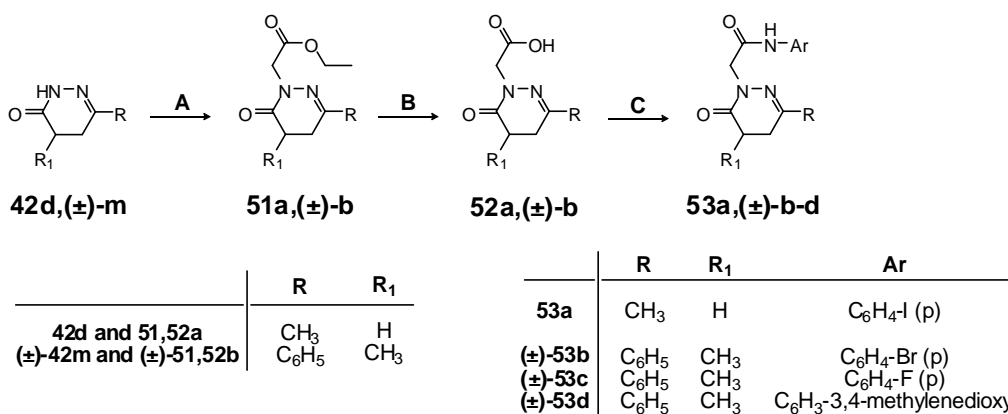


Scheme 13. Reagents and conditions: **A**) 3 or 4-methoxybenzaldehyde (1 equiv), KOH 5% (w/v) in anhydrous EtOH, 1-3 h, reflux; **B**) ethyl bromoacetate (1.5 equiv), K₂CO₃ (2 equiv), anhydrous CH₃CN, 1-3 h, reflux; **C**) NaOH 6N, 1-2 h, 60-80 °C; **D**) ethyl chloroformate (1.1 equiv), Et₃N (3.5 equiv), substituted aniline (2 equiv), anhydrous THF, 12 h, -5 °C → rt.

3.3.2 Synthesis of C-4 modified N-arylacetamide pyridazinones

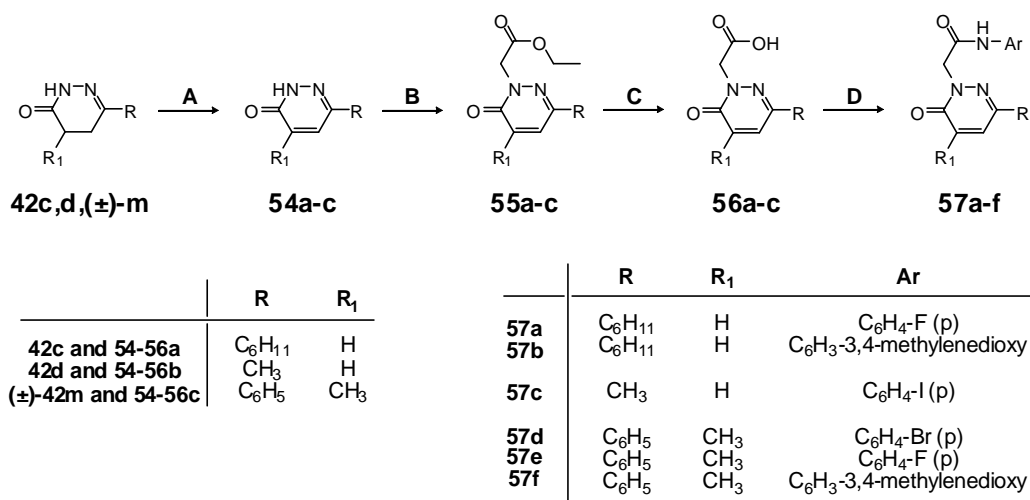
The C-4 modified dihydropyridazinones **53a-d** (scheme 14) were obtained in good yields carrying out the same reaction sequence (alkylation/hydrolysis/amide bond formation) shown in schemes 12 and 13 starting from compounds **42d-m** whose synthesis is reported in scheme 11.

3. Chemistry



Scheme 14. Reagents and conditions: **A**) ethyl bromoacetate (1.5 equiv), K₂CO₃ (2 equiv), anhydrous CH₃CN, 2-3 h, reflux; **B**) NaOH 6N, 3-5 h, 80 °C; **C**) ethyl chloroformate (1.1 equiv), Et₃N (3.5 equiv), substituted aniline (2 equiv), anhydrous THF, 12 h, -5 °C → rt.

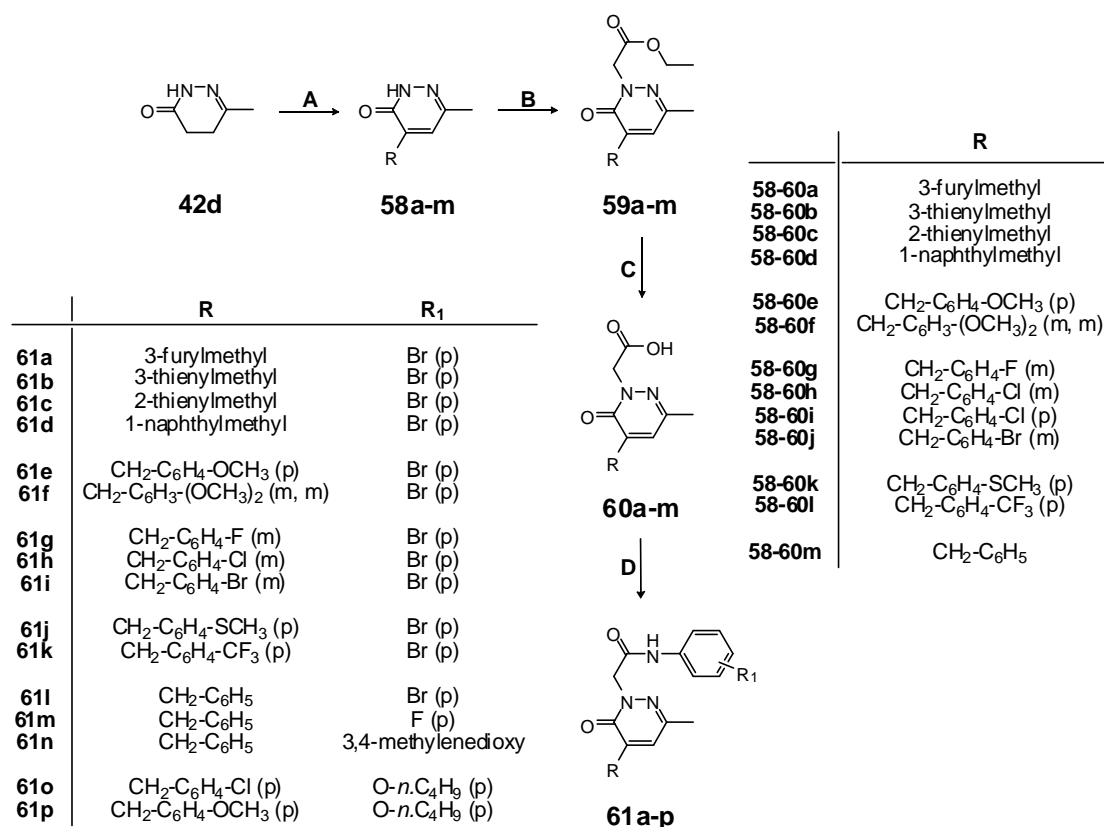
In **scheme 15** is depicted the synthesis of compounds **57a-f**, where the starting dihydropyridazinines **42c,d,(±)-m** (**scheme 11**) were, as first step, converted in the previously described pyridazinones **54a-c**. The reaction was carried out using selenium dioxide or bromine in acetic acid as oxidizing agents.^{263,267,268} Then, the alkylation in standard condition with ethyl bromoacetate afforded the known **55c**,²⁶⁹ and the new **55a,b** which were subjected to the usual hydrolysis and amide bond formation steps, performed as already described (**schemes 12,13**).



Scheme 15. Reagents and conditions: **A**) for compound **54c**: Br₂ (4 equiv), CH₃COOH 100%, 4-5 h, reflux; for compounds **54a,b**: SeO₂ (3 equiv), anhydrous EtOH, 5-7 h, reflux; **B**) ethyl bromoacetate (1.5 equiv), K₂CO₃ (2 equiv), anhydrous CH₃CN, 2-3 h, reflux; **C**) NaOH 6N, 2 h, 80 °C; **D**) ethyl chloroformate (1.1 equiv), Et₃N (3.5 equiv), substituted aniline (2 equiv), anhydrous THF, 12 h, -5 °C → rt.

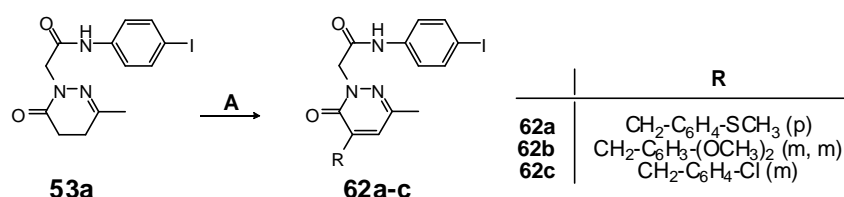
The synthesis of final compounds **61a-p**, where the 4-methoxybenzyl at the C-4 position of the pyridazinone ring was replaced with several heterocyclic or substituted benzyl moieties, is shown in **scheme 16**. The dihydropyridazinone **42d** (**scheme 11**) was converted into the previously described derivatives **58b-e,i**,²⁷⁰⁻²⁷³ and the new **58a,f,h,j-m** by Knoevenagel condensation with the appropriate

aromatic aldehyde in the presence of KOH. Compounds **58a-m**, in turn, were alkylated with ethyl bromoacetate to give the esters **59a-m**, whose **59d,e,i** were previously reported.^{271,272,274} Alkaline hydrolysis of compounds **59a-m** gave the known **60i**,²⁷⁰ and the new carboxylic acid derivatives **60a-h,j-m**. These compounds were treated with ethyl chloroformate in THF in presence of triethylamine, affording the mixed anhydrides, which in turn were transformed into the final amides **61a-p** by treatment with the appropriate aryl amine.



Scheme 16. Reagents and conditions: **A)** substituted benzaldehyde (1 equiv), KOH 5% (w/v) in anhydrous EtOH, 3-5 h, reflux; **B)** ethyl bromoacetate (1.5 equiv), K₂CO₃ (2 equiv), anhydrous CH₃CN, 2-4 h, reflux; **C)** NaOH 6N, 1-2 h, 80 °C; **D)** ethyl chloroformate (1.1 equiv), Et₃N (3.5 equiv), substituted aniline (2 equiv), anhydrous THF, 12 h, -5 °C → rt.

In **scheme 17** is shown the synthesis of final compounds **62a-c** modified at the C-4 of the pyridazinone ring and bearing a 4-iodophenylacetamide chain at position 2. To get this compounds, the Koenenagel condensation with the appropriate aromatic aldehyde was performed on the intermediate **53a** (**scheme 14**).

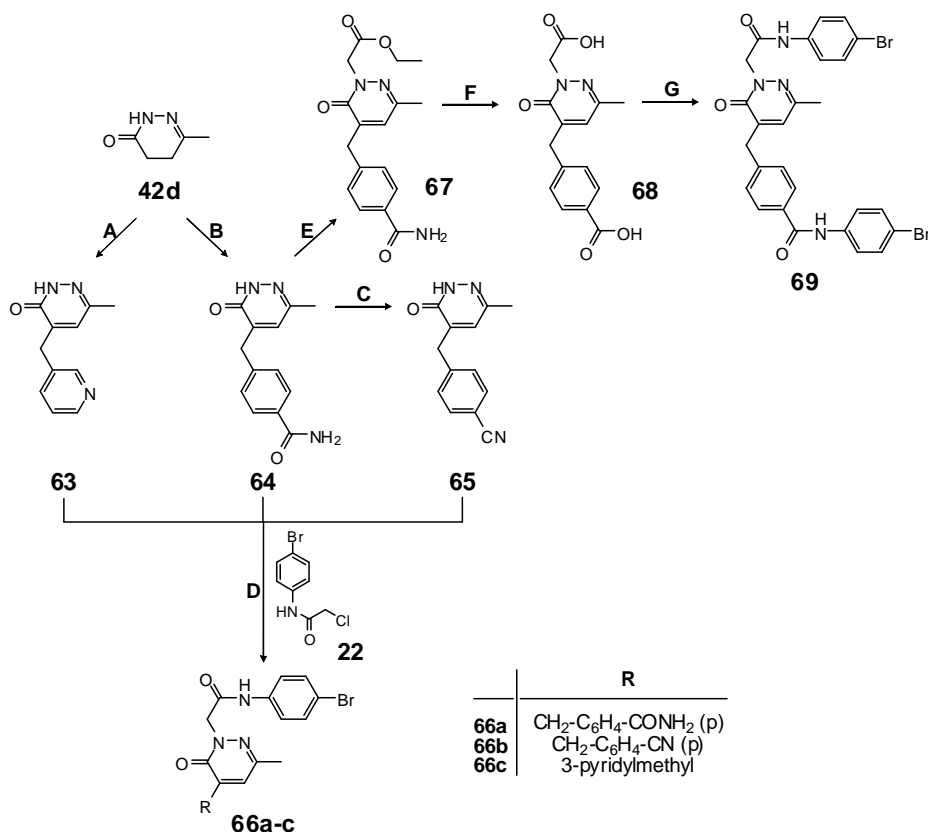


Scheme 17. Reagents and conditions: **A)** substituted benzaldehyde (1 equiv), KOH 5% (w/v) in anhydrous EtOH, 1-5 h, reflux.

3. Chemistry

This alternative methodology was chosen over the previous synthetic pathway (**scheme 12**) due to the exciting possibility to synthesize the suitable building block (**53a**, **scheme 14**) and then to condensate it with the convenient aromatic aldehyde. Despite the fact that Knoevenagel condensation appeared relatively simple and high-yielding on the C-4 of the pyridazinone ring (**schemes 12** and **13**), the *N*-(phenylacetamido)pyridazinone **53a** didn't result suitable for the synthesis of a various range of compounds, probably due to the instability of the phenylacetamido moiety. Indeed, in this conditions, a mixture of products resulted and just three aromatic aldehydes were able to react in low to moderate yields. For these reasons the alternative route was not efficient for the preparation of analogues as we supposed.

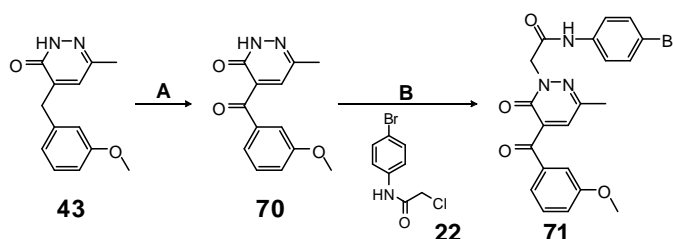
Moreover, a further procedure was required to get the final compounds **66a-c** (**scheme 18**). Intermediates **63** and **64** were obtained by Knoevenagel condensation in the same conditions already described (**scheme 12**), using the commercially available 3-pyridinecarboxaldehyde and 4-cyanobenzaldehyde respectively. Compound **65** was instead prepared from **64** by dehydration of the amide with phosphorus oxychloride. Due to their instability to strong base treatment, the intermediates **63-65** were directly converted in the final compounds **66a-c** by alkylation in standard condition with compound **22** (**scheme 7**).



Scheme 18. Reagents and conditions: **A)** 3-pyridinecarboxaldehyde (1 equiv), KOH 5% (w/v) in anhydrous EtOH, 5 h, reflux; **B)** 4-cyanobenzaldehyde (2 equiv), KOH 5% (w/v) in anhydrous EtOH, 4 h, reflux; **C)** POCl₃, 3 h, 60 °C; **D)** **22** (1.5 equiv), K₂CO₃ (2 equiv), anhydrous CH₃CN, 2-3 h, reflux; **E)** ethyl bromoacetate (1.5 equiv), K₂CO₃ (2 equiv), anhydrous CH₃CN, 2 h, reflux; **F)** NaOH 6N, 2 h, 60 °C; **G)** ethyl chloroformate (1.1 equiv), Et₃N (3.5 equiv), 4-bromoaniline (2 equiv), anhydrous THF, 12 h, -5 °C → rt.

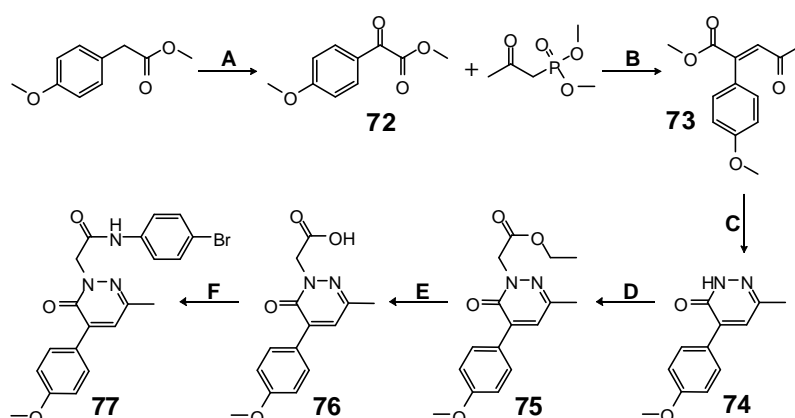
To get the pyridazinone **69** (scheme 18), the intermediate **64** was alkylated with ethyl bromoacetate to give **67** which, after alkaline hydrolysis of the ester moiety afforded the bicarboxylic acid **68**. Treating **68** firstly with ethyl chloroformate and then with 4-bromoaniline, in the usual conditions (scheme 12), it was possible to obtain in good yields compound **69**, bearing two amide functions.

In scheme 19 is depicted the synthesis of the 4-arylketone derivative **71** prepared from **44** (scheme 12) by oxidation of the benzylic methylene (**70**) with cerium ammonium nitrate (CAN) and subsequent alkylation in standard conditions with the previously described intermediate **22** (scheme 7).



Scheme 19. Reagents and conditions: A) CAN (3 equiv), CH₃COOH 50%, 1.5 h, 60 °C; B) **22** (1.5 equiv), K₂CO₃ (2 equiv), anhydrous CH₃CN, 6 h, reflux.

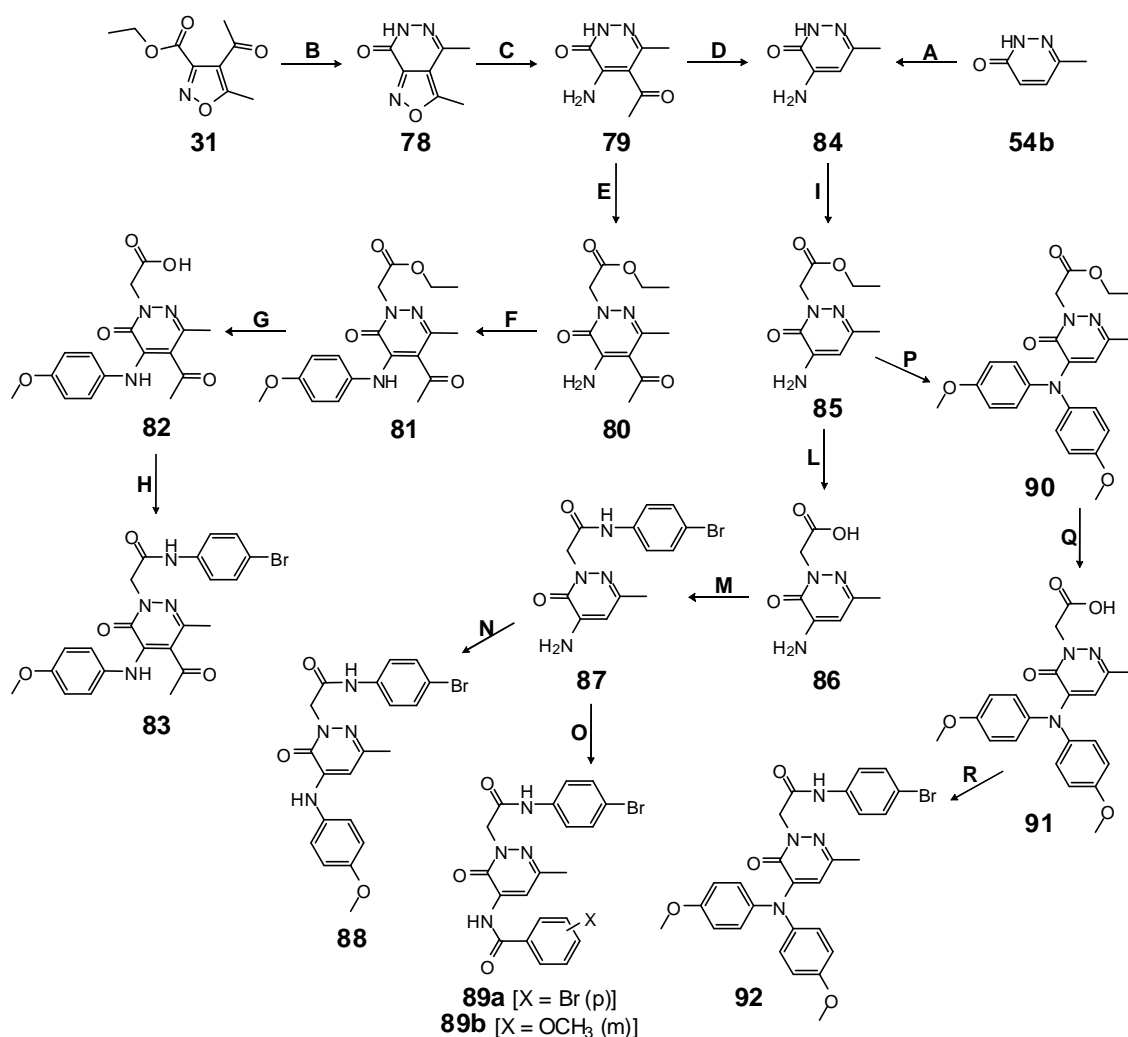
The synthesis of compound **77** with the 4-methoxyphenyl group directly bonded to the C-4 of the pyridazinone ring is shown in scheme 20. As reported in literature,²⁷⁵ the commercially available methyl 4-methoxyphenylacetate can be easily converted in the previously described keto ester **72**,²⁷⁶ by oxidation with tert-butyl hydroperoxide (TBHP) and a catalytic amount of iron trichloride in pyridine at 85 °C. The intermediate **72** was then processed to Wittig reaction,^{277,278} using dimethyl acetylmethylphosphonate as phosphonium ylide source and sodium methoxyde in methanol at 0 °C, to afford the known γ -keto ester **73**.²⁷⁹ Condensation with hydrazine hydrate afforded the intermediate **74**, which as usual, was subjected to alkylation with ethyl bromoacetate, alkaline hydrolysis and finally coupling with 4-bromoaniline, through the intermediate mixed anhydride to give the final amide **77** in good yield.



Scheme 20. Reagents and conditions: A) TBHP (3 equiv), FeCl₃ • 6 H₂O, pyridine, 8 h, 85 °C; B) NaOCH₃ (2 equiv), anhydrous CH₃OH, 3.5 h, 0 °C → rt; C) NH₂NH₂ • H₂O (2 equiv), anhydrous toluene, 2 h, reflux; D) ethyl bromoacetate (1.5 equiv), K₂CO₃ (2 equiv), anhydrous CH₃CN, 1.5 h, reflux; E) NaOH 6N, 0.5 h, 60 °C; F) ethyl chloroformate (1.1 equiv), Et₃N (3.5 equiv), 4-Bromoaniline (2 equiv), anhydrous THF, 12 h, -5 °C → rt.

3. Chemistry

The synthetic pathway affording the final compounds **83**, **87-89** and **92** is depicted in **scheme 21**. The isoxazoles **31** (**scheme 10**) and the isoxazolo[3,4-*d*]pyridazinones **78** were previously described.^{227, 280} Reductive opening of the isoxazole ring carried out on the intermediate **78** with ammonium formate and a catalytic amount of carbon-supported palladium catalyst (Pd/C) in anhydrous ethanol at reflux, afforded the known 4-amino-5-acetyl pyridazinone derivative **79**.²²³ Performing the usual alkylation/alkaline hydrolysis/amide bond formation reaction sequence (**schemes 12** and **13**) the final amide **83** was synthesized in good yields. The already described intermediate **84** was obtained by deacetylation of **79** using 48% hydrobromic acid under pressure at high temperature (140 °C).²³¹

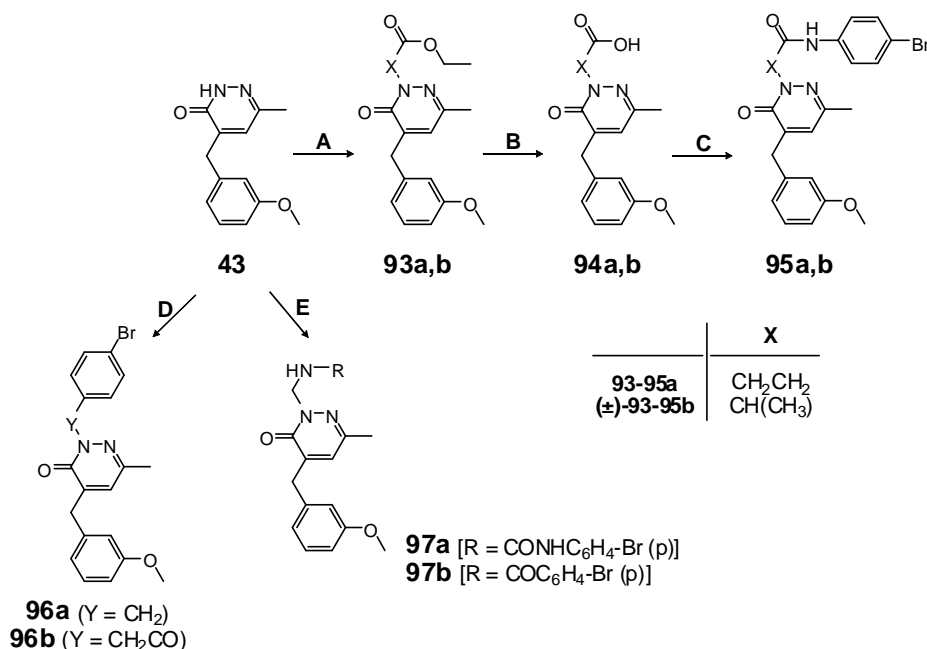


Scheme 21. Reagents and conditions: **A**) NH₂NH₂ • H₂O, 4 h, 180 °C; **B**) NH₂-NH₂ • H₂O (2 equiv), EtOH, 10 min, rt; **C**) HCOONH₄ (2.5 equiv), Pd/C 10% (catalytic), anhydrous EtOH, 1.5 h, reflux; **D**) HBr 48%, 1 h, 140 °C; **E**) ethyl bromoacetate (1.5 equiv), K₂CO₃ (2 equiv), anhydrous CH₃CN, 3 h, reflux; **F**) 4-methoxyphenylboronic acid (2 equiv), Cu(OAc)₂ (1.5 equiv), Et₃N (2 equiv), CH₂Cl₂, 12 h, rt; **G**) NaOH 6N, 1.5 h, 80 °C; **H**) ethyl chloroformate (1.1 equiv), Et₃N (3.5 equiv), 4-bromoaniline (2 equiv), anhydrous THF, 12 h, -5 °C → rt; **I**) see E; **L**) see G; **M**) see H; **N**) 4-methoxyphenylboronic acid (1 equiv), Cu(OAc)₂ (1.5 equiv), Et₃N (2 equiv), CH₂Cl₂, 12 h, rt; **O**) substituted benzoyl chloride (2.4 equiv), Et₃N (catalytic), anhydrous CH₂Cl₂, 16 h, 0 °C → rt; **P**) see F; **Q**) see G; **R**) see H.

To get **84** in high yields, a previously described procedure starting from **54b** (scheme 15) and using hydrazine hydrate at 180 °C was as well tried.²⁸¹ The high temperature of reaction afforded a mixture difficult to purify and the resulting yield was lower than that stated in the literature. Thus, the previous methodology based on deacetylation of **79** was elected to get the intermediate **84**. This compound was processed to standard alkylation, hydrolysis and amidation reactions to generate the final 4-amino pyridazinone **87**. Subsequently, the coupling of the amine group of **87** with 4-methoxyphenylboronic acid in presence of $\text{Cu}(\text{Ac})_2$ in CH_2Cl_2 gave the 4-arylamine **88**, while the 4-arylamide analogues **89a,b** were obtained from **87** by treatment with the opportune aroylchloride and triethylamine in CH_2Cl_2 at 0 °C. To synthesize the biarylamine **90** the intermediate **85** was coupled with a two-fold amount of 4-methoxyphenylboronic acid in usual conditions and then, after hydrolysis of the ester group and following usual amidation, the final compound **92** was obtained in good yields.

3.3.3 Synthesis of *N*-arylamide modified pyridazinone derivatives

Scheme 22 depict the synthetic procedure for compounds **95-97**. The precursor **43** was alkylated with the appropriate bromo ester to give compounds **93a,b**, which, in turn, were converted in the corresponding acids **94a,b**. The final step was the transformation of these compounds into the final amides **95a,b** using the same procedure extensively described in the present section of the thesis.

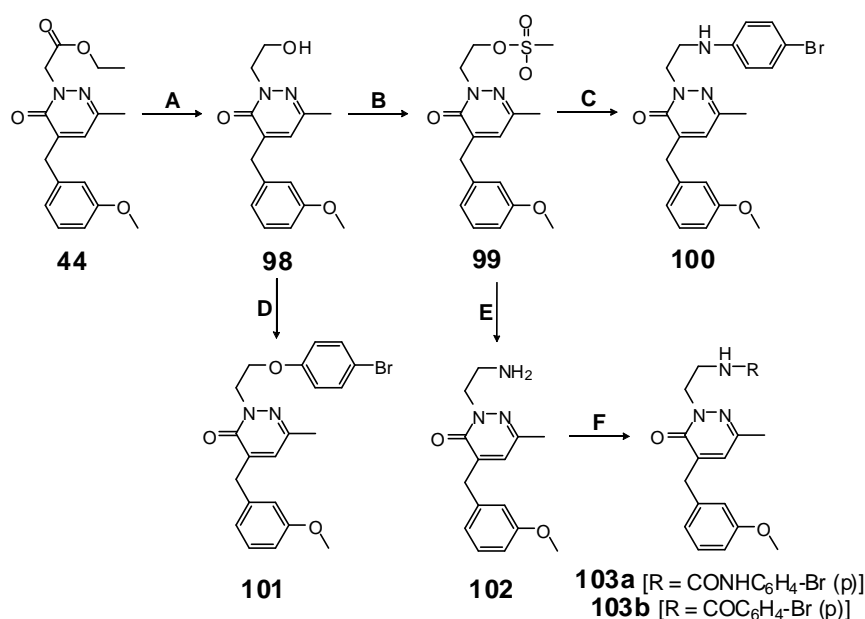


Scheme 22. Reagents and conditions: **A**) ethyl 3-bromopropionate (for compound **93a**) or (±)-ethyl-2-bromopropionate (for compound **93b**) (1.5 equiv), K_2CO_3 (2 equiv), anhydrous CH_3CN , 6 h, reflux; **B**) NaOH 6N, 1 h, 80 °C; **C**) ethyl chloroformate (1.1 equiv), Et_3N (3.5 equiv), 4-Bromoaniline (2 equiv), anhydrous THF, 12 h, -5 °C → rt; **D**) alkyl halide (1.5 equiv), K_2CO_3 (2 equiv), anhydrous CH_3CN , 6 h, reflux; **E**) CH_2O 40%, NH_3 33%, dioxane, 1 h, 50 °C, then 4-bromophenyl isocyanate (for compound **97a**) (1.1 equiv) or 4-bromobenzoyl chloride (for compound **97b**) (1.5 equiv), CH_2Cl_2 , 6-12 h, rt (**97a**), 0 °C (**97b**).

3. Chemistry

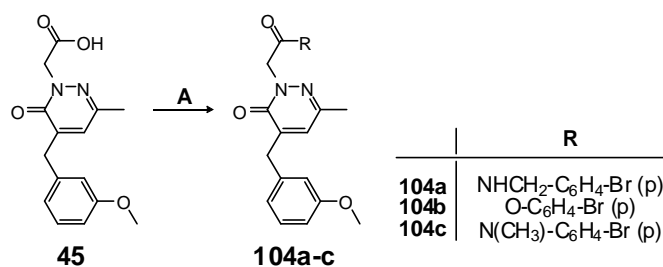
On the other hand, compounds **96a,b** were obtained by alkylation of **43** with the appropriate halide in standard conditions (**scheme 22**). Moreover the precursor **43** was converted into the final **97a,b** through a multicomponent Mannich reaction ($\text{CH}_2\text{O} + \text{NH}_3$).²⁸² The intermediate amine was not isolated and it was converted one-pot into the urea **97a** by treatment with 4-bromophenyl isocyanate and into the amide **97b** with 4-bromobenzoyl chloride.

The final compounds **100**, **101** and **103a,b** were synthesized as shown in **scheme 23**. The intermediate **44** was reduced with sodium borohydride in THF/MeOH to generate the primary alcohol **98**. This compound was the starting material for the synthesis both of the ether **101**, through a coupling reaction with the 4-bromophenylboronic acid in presence of $\text{Cu}(\text{Ac})_2$, and of compound **100**, through the mesylate **99**,²⁸³ which, in turn, was then converted into the final compound **100** by nucleophilic replacement with 4-bromo aniline. Treatment of **99** with ammonia gave the intermediate **102**, from which the urea **103a** and the amide **103b** were obtained using 4-bromophenyl isocyanate or 4-bromobenzoyl chloride respectively in CH_2Cl_2 .



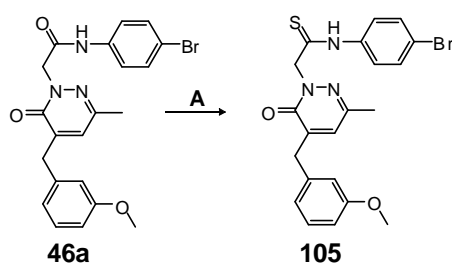
Scheme 23. Reagents and conditions: **A**) NaBH_4 (5.6 equiv), anhydrous THF, anhydrous CH_3OH , 1 h, 60°C ; **B**) methanesulfonyl chloride (1.5 equiv), pyridine (1.1 equiv), anhydrous CH_2Cl_2 , 4 h, $0^\circ\text{C} \rightarrow \text{rt}$; **C**) 4-bromoaniline (2 equiv), 2-propanol, 6 h, 60°C ; **D**) 4-bromophenylboronic acid (2 equiv), $\text{Cu}(\text{OAc})_2$ (1.5 equiv), Et_3N (2 equiv), CH_2Cl_2 , 12 h, rt; **E**) NH_3 33%, 2-propanol, 3 h, 60°C ; **F**) 4-bromophenyl isocyanate (for compound **103a**) (1.1 equiv) or 4-bromobenzoyl chloride (for compound **103b**) (1.1 equiv), Et_3N (2 equiv), anhydrous CH_2Cl_2 , 6 h, 0°C .

To obtain the analogues **104a-c** (**scheme 24**), the mixed anhydride generated as usual by treatment of the intermediate **45** (**scheme 12**) with ethyl chloroformate was transformed in good yields into the final compounds by treatment respectively with commercially available 4-bromobenzylamine (for **104a**), 4-bromophenol (for **104b**) and *N*-methyl-4-bromobenzylamine (for **104c**).



Scheme 24. Reagents and conditions: A) ethyl chloroformate (1.1 equiv), Et₃N (3.5 equiv), 4-bromobenzylamine or 4-bromo-*N*-methylaniline or 4-bromophenol (2 equiv), anhydrous THF, 12 h, -5 °C → rt.

In **scheme 25** is shown the synthesis of the thioamide analogue **105** directly generated from **46a** (**scheme 12**) using Lawesson's reagent in toluene at 80 °C.²⁸⁴



Scheme 25. Reagents and conditions: A) Lawesson's Reagent (2 equiv), anhydrous toluene, 3 h, 80 °C.

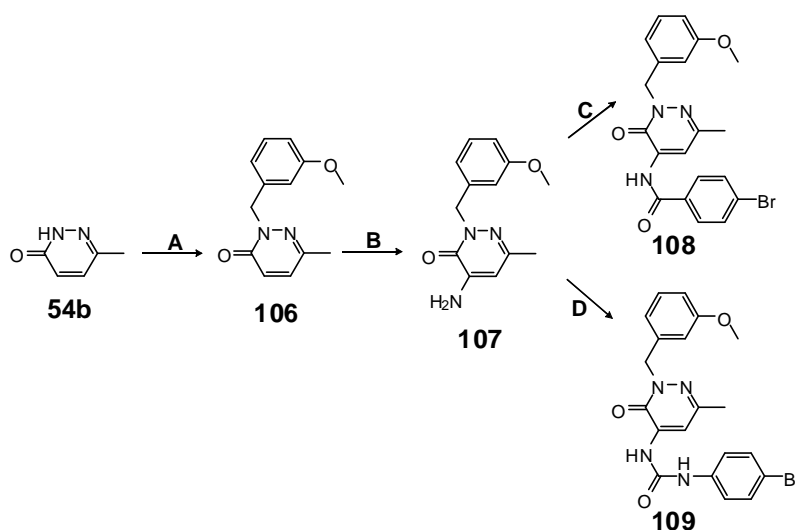
There are two possible achievable mono-tioderivatives from this reaction: the first one, where the sulphur replace the oxygen of carbonyl group at C-3 of the pyridazinone ring, and the second, where the sulphur replaced the oxygen of CO in the exocyclic amide side chain (**105**). Thus, the relative position of tionation needed to be attributed, and the structure of **105** was confirmed by both ¹H NMR and MS(ESI) analysis. ¹H NMR experiments showed a clear difference in the chemical shift between the methylene bonded to the carbonyl group in **46a** and that bonded to the thiocarbonyl group in **105**. In addition, LCMS experiments showed that it is evident a correlation between the fragments generated during the analysis and the structure **105**. Indeed, leaving aside the fact that the exact mass was exactly the one expected for **105**, it resulted evident the presence of the pyridazinone fragment without the *N*-phenylacetamide or the *N*-phenylethanethioamide moiety. This result was a proof that the pyridazinone ring was unchanged and the sulphur is on the side chain as drawn (**scheme 25**). Thus, it is reasonable to presume that reaction via sulphur substitution by Lawesson's reagent is favoured on the carbonyl group of the side chain.

3.3.4 Synthesis of N-2/C-4 inverted pyridazinone analogues

In **scheme 26** is depicted the synthesis of compounds **108** and **109**. Alkylation in standard condition of the 6-methylpyridazinone **54b** (**scheme 15**) with 3-methoxybenzyl chloride in acetonitrile resulted in compound **106** which gave the corresponding 4-amino derivative **107** by heating with N₂H₄ · H₂O in hard

3. Chemistry

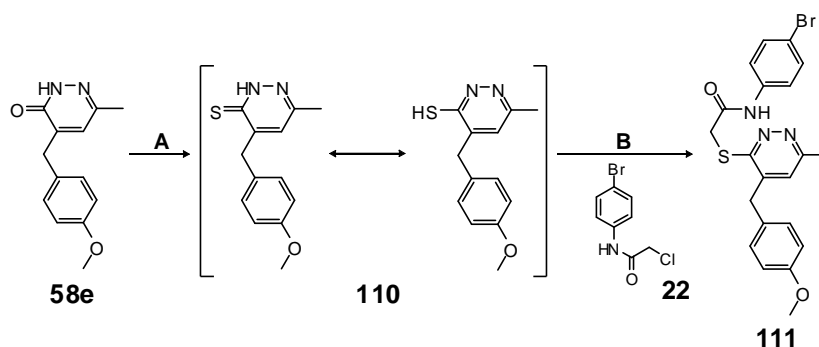
conditions. The amide **108** and the urea **109** were obtained from **107** by treatment with the opportune aryl chloride or the aryl isocyanate following the same conditions reported for **89a,b** (scheme 21) and **38a-c** (scheme 10).



Scheme 26. Reagents and conditions: **A**) 3-methoxybenzyl chloride (1.5 equiv), K_2CO_3 (2 equiv), anhydrous CH_3CN , 6 h, reflux; **B**) $NH_2NH_2 \cdot H_2O$, 12 h, 180 °C; **C**) 4-bromobenzoyl chloride (2.4 equiv), Et_3N (catalytic), anhydrous CH_2Cl_2 , 10 h, 0 °C; **D**) 4-bromophenyl isocyanate (2.2 equiv), anhydrous toluene, 7 h, reflux.

3.3.5 Synthesis of C-3 substituted pyridazine analogue

Scheme 27 outlines the synthetic procedure for compound **111**. Using Lawesson's reagent, as previously described, the precursor **58e** (scheme 16) was transformed into intermediate **110** (scheme 25) which, in turn, was alkylated in standard condition using **22** (scheme 7) to afford the corresponding analogue **111**, having the phenylacetamide moiety at the C-3 of the pyridazinone ring.



Scheme 27. Reagents and conditions: **A**) Lawesson's Reagent (1 equiv), anhydrous toluene, 2 h, 80 °C; **B**) **22** (1.5 equiv), K_2CO_3 (2 equiv), anhydrous CH_3CN , 3 h, reflux.

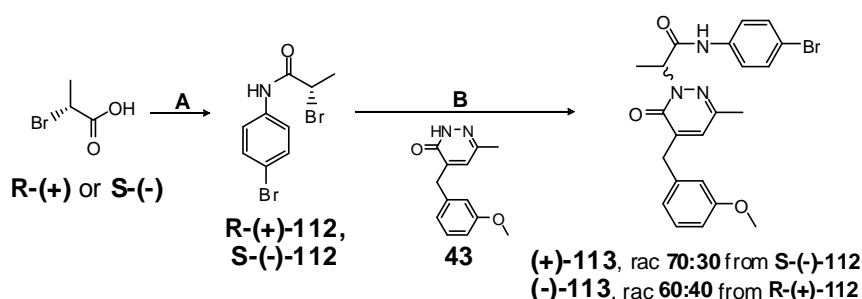
3.3.6 Synthesis of chiral pyridazinone analogues

A further development of the project was the introduction of stereogenic center on the *N*-phenylacetamide linker of the lead compound **46a** (scheme 12). The modification introduces stereochemical complexity into the products and, at the same time, it should be interesting to see the effect of the presence of a

stereogenic center on the biological activity, maintaining however the essential conformational shape of the molecules. The development of an homologous series of chiral compounds, possibly through enantioselective reaction, would be particularly desirable in the case of the synthesis of a group of biologically-useful small molecules due to the well known advantages of chirality when considering the interactions of small-molecules with biological systems.

3.3.6.1 Enantioselective synthesis of the *N*-arylpropanamide analogue

In the first instance, the asymmetric synthesis of enantiomers (+)-**113** and (-)-**113** had been tried (**scheme 28**). Commercially available *R*-(+)- and *S*-(-)-bromopropionic acids were firstly treated with SOCl₂ affording the intermediate acid chlorides which in turn were transformed in the amides *R*-(+)-**112** and *S*-(-)-**112** using 4-bromoaniline.²⁸⁵ As expected and as confirmed by chiral HPLC and polarographic analysis, the amide bond formation occurred by retention of the relative configuration of the starting carboxylic acids due to the missing participation of the chiral center in the reaction and to the not basic reaction conditions.²⁸⁶⁻²⁸⁷ The amides *R*-(+)-**112** and *S*-(-)-**112** were then used to alkylate in standard conditions the intermediate **43** (**scheme 12**) to give respectively the two pure enantiomers. Precedent literature described the alkylation on the N-2 of the pyridazinone ring as a classical S_N2 reaction,²⁸⁸ so that this methodology could be theoretically applied to the synthesis of both enantiomers (+)-**113** and (-)-**113**, with complete inversion of the configuration of starting amides. Despite the fact that this reaction is simple and well known,²⁸⁹⁻²⁹² it was found that it is not suitable for asymmetrical synthesis because the inversion of configuration was not complete and consequent racemization occurred. Inspection by chiral HPLC analysis of the chromatographically pure compounds showed the achievement of a mixture 70:30 starting from *S*-(-)-**112** and a mixture 60:40 from *R*-(+)-**112**. All attempts at doing this stereoselective alkylation reaction proved unsuccessful.



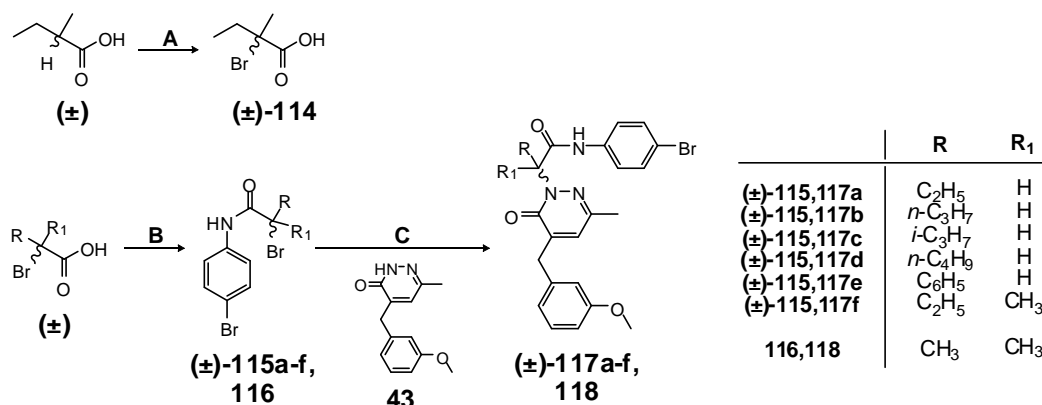
Scheme 28. Reagents and conditions: A) SOCl₂ (6 equiv), anhydrous CH₂Cl₂, 4 h, reflux, then 4-bromoaniline (2 equiv), anhydrous THF, 4 h, rt; B) **43** (0.9 equiv), K₂CO₃ (1.8 equiv), anhydrous CH₃CN, 2 h, reflux.

3.3.6.2 Synthesis of the homologous series of *N*-aryl-(alkyl)-amide derivatives

To get the chiral compounds (±)-**117a-f** as racemates and the dimethyl analogue **118**, not optically active, the same synthetic pathway used for (+)-**113**/(-)-**113** (**scheme 28**) has been performed as shown

3. Chemistry

in **scheme 29**. For the synthesis of the compound (\pm)-**117f** it was previously required the preparation of the starting bromo-derivative (\pm)-**114**, not commercially available and obtained as reported in literature by treatment with *N*-bromosuccinimide in CCl_4 at reflux.²⁹³ After treatment with SOCl_2 of the appropriate chiral carboxylic acids (**scheme 29**) the commercially available 4-bromophenyl amides (\pm)-**115a,c**, the already described (\pm)-**115e,f**, **116**,²⁹⁴⁻²⁹⁸ and the new (\pm)-**115b,d** were obtained in low yields as useful intermediates for the synthesis of the final compounds (\pm)-**117a-f** and **118**.

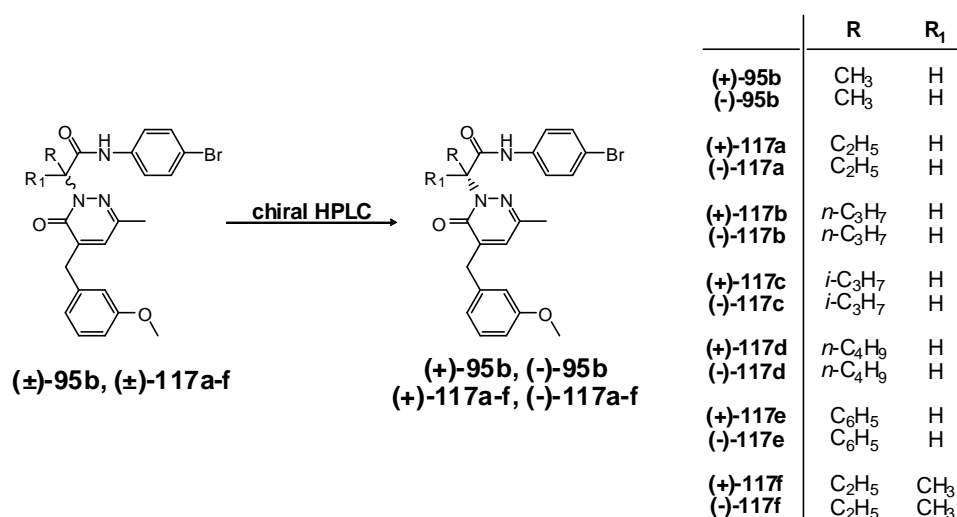


Scheme 29. Reagents and conditions: **A**) NBS (1.05 equiv), CCl_4 , N_2 , 8 h, reflux; **B**) SOCl_2 (6 equiv), anhydrous CH_2Cl_2 , 4 h, reflux, then 4-bromoaniline (2 equiv), anhydrous THF, 4 h, rt; **C**) **43** (0.9 equiv), K_2CO_3 (1.8 equiv), anhydrous CH_3CN , 4-5 h, reflux.

3.3.6.3 Chiral Chromatographic resolution of racemates (\pm)-**95b** and (\pm)-**117a-f**

Due to the significant racemization during nucleophilic displacement of bromide with the pyridazinone intermediate **43** (**scheme 28**, section 3.3.6.2), an alternative strategy was required to get the pure enantiomers of (\pm)-**95b** and (\pm)-**117a-f** (**schemes 29** and **30**). Chiral HPLC is one of the most valid and efficient methods for obtaining both enantiomers of a chiral compound in high optical purity [$> 97\%$ enantiomeric excess (ee)]. This approach has now become an established procedure for *in vitro* comparative biological testing, where few milligrams of both enantiomers are required. In addition, the isolation of single enantiomers represents a strategy for rational drug design due to the role of stereochemistry in molecular interactions involving biological macromolecules.

Compounds (\pm)-**95b** and (\pm)-**117a-f** (**scheme 30**) were then isolated as pure (ee = 97.4-99.9%) by semi-preparative chiral HPLC (**scheme 30**) and two distinct polysaccharide based chiral stationary phases (CSPs) had to be employed to separate the different racemates. Indeed in the early stage of the chromatographic resolution a Chiralcel OD[®] column [cellulose tris(3,5-dimethylphenylcarbamate)] was used to separate racemates (\pm)-**95b** and (\pm)-**117a** (**table 3.1**), according to the literature for a series of pyridazinone like compounds.²²¹ An isocratic elution mode was employed and detection by UV was carried out at 250 nm.



Scheme 30. Chromatographic resolution using Chiralcel OD[®] column for (±)-95b and (±)-117a (eluent: *n*-hexane/2-propanol 95:5); Lux Amylose-2[®] column for (±)-117b-f (eluent: *n*-hexane/2-propanol 60:40).

Unexpectedly, during the analytical work resulted a lack of selectivity of the Chiralcel OD[®] column by increasing the steric hindrance on the chiral center. Indeed, already the resolution of racemate (±)-117b, having a propyl group on the chiral center, resulted not possible due to poor resolution between two enantiomers (figure 3.1).

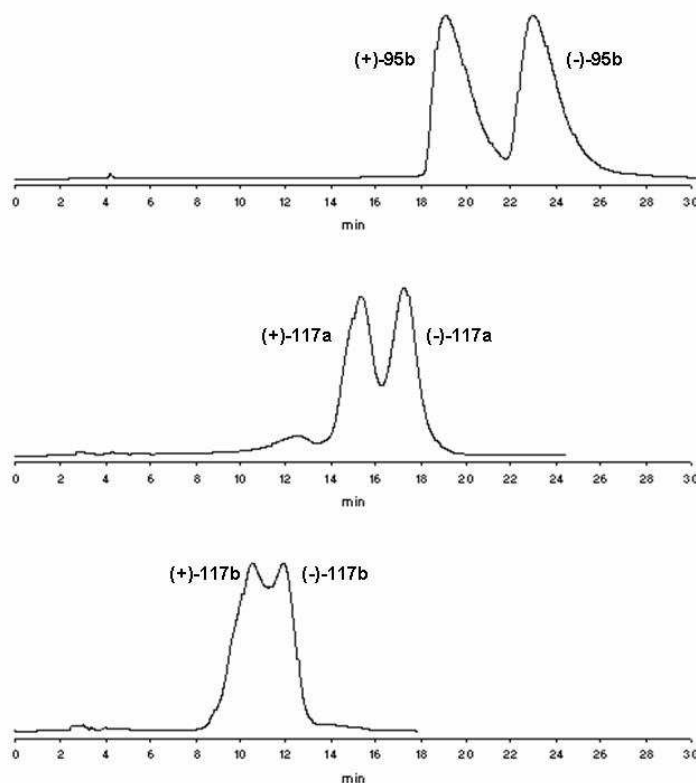


Figure 3.1. Chiral semi-preparative HPLC resolution of racemates (±)-95b and (±)-117a. **Conditions:** Chiralcel OD column (10 μm, 4.6 mm I.D. x 250 mm), *n*-hexane/IPA 95:5 (v/v) as eluent, flow rate 1.2 mL/min, detection by UV at 250 nm, temperature 25 °C. At the bottom it is shown the lack of selectivity resulted using Chiralcel OD column in the same conditions to separate racemate (±)-117b.

3. Chemistry

Enantiomer	Stationary Phase	Eluent (<i>n</i> -hexane/IPA)	Flow rate (mL/min)	Temperature (°C)	Retention Time (t_R , min)
(+)- 95b	Chiralcel OD	95:5	1.2	25	19.2
(-)- 95b					23.2
(+)- 117a	Chiralcel OD	95:5	1.2	25	15.9
(-)- 117a					17.9
(+)- 117b	Amylose-2	60:40	1.5	40	5.1
(-)- 117b					9.4
(+)- 117c	Amylose-2	60:40	1.5	40	3.9
(-)- 117c					10.1
(+)- 117d	Amylose-2	60:40	1.5	40	5.4
(-)- 117d					9.7
(+)- 117e	Amylose-2	60:40	1.5	40	12.3
(-)- 117e					7.6
(+)- 117f	Amylose-2	60:40	1.5	40	8.6
(-)- 117f					6.7

Table 3.1. Data of the chiral HPLC separations for the different racemates (\pm)-**95b** and (\pm)-**117a-f** related to semi-preparative conditions, column types (250 mm x 4.6 mm I.D.), mobile phases, flow rates, temperature and retention times (t_R) detected by UV at 250 nm.

In order to develop the semi-preparative resolution it was required to find another chiral stationary phase. As it shown in **table 3.1** and in **figure 3.2** a very good separation of the (+) and (-) enantiomers of **117b-f** was achieved using Lux Amylose-2[®] column [amylose tris(5-chloro-2-methylphenyl-carbamate)] and the optically pure compounds were obtained as required. In all cases, an isocratic elution mode was employed and detection by UV was carried out at 250 nm.

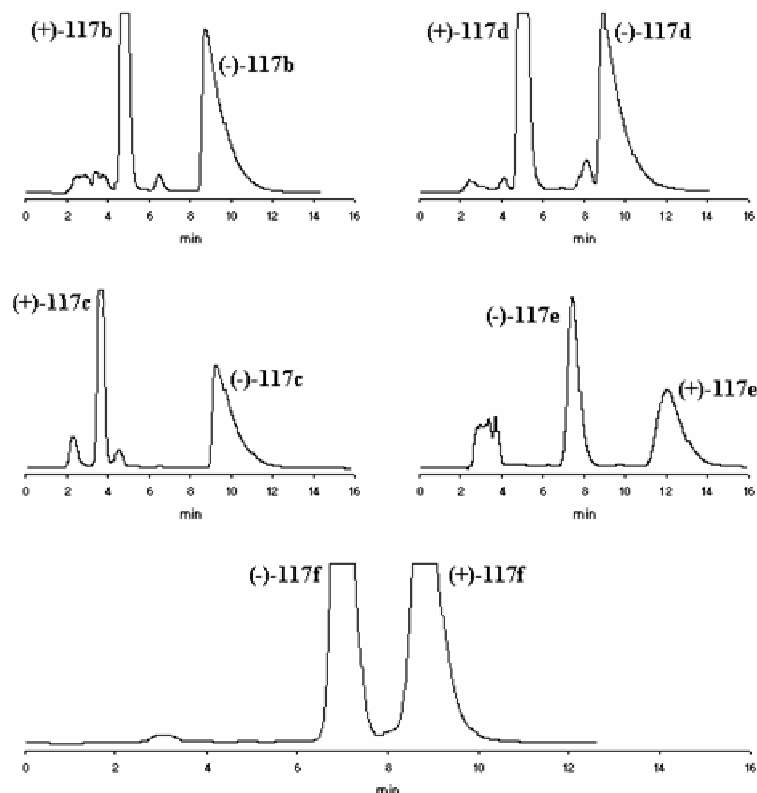


Figure 3.2. Chiral semi-preparative HPLC resolution of racemates (\pm)-**117b-f**. **Conditions:** Lux Amylose-2 column (5 μ m, 4.6 mm I.D. x 250 mm), *n*-hexane/IPA 60:40 (v/v) as eluent, flow rate 1.5 mL/min, detection by UV at 250 nm, temperature 40 °C.

After semipreparative HPLC the fractions collected were dried under nitrogen and analyzed on chiral analytical Lux Amylose-2[®] (3 μ m, 4.6 mm I.D. x 50 mm) column to determine their enantiomeric excess (ee) (**figure 3.3** and **table 3.2**).

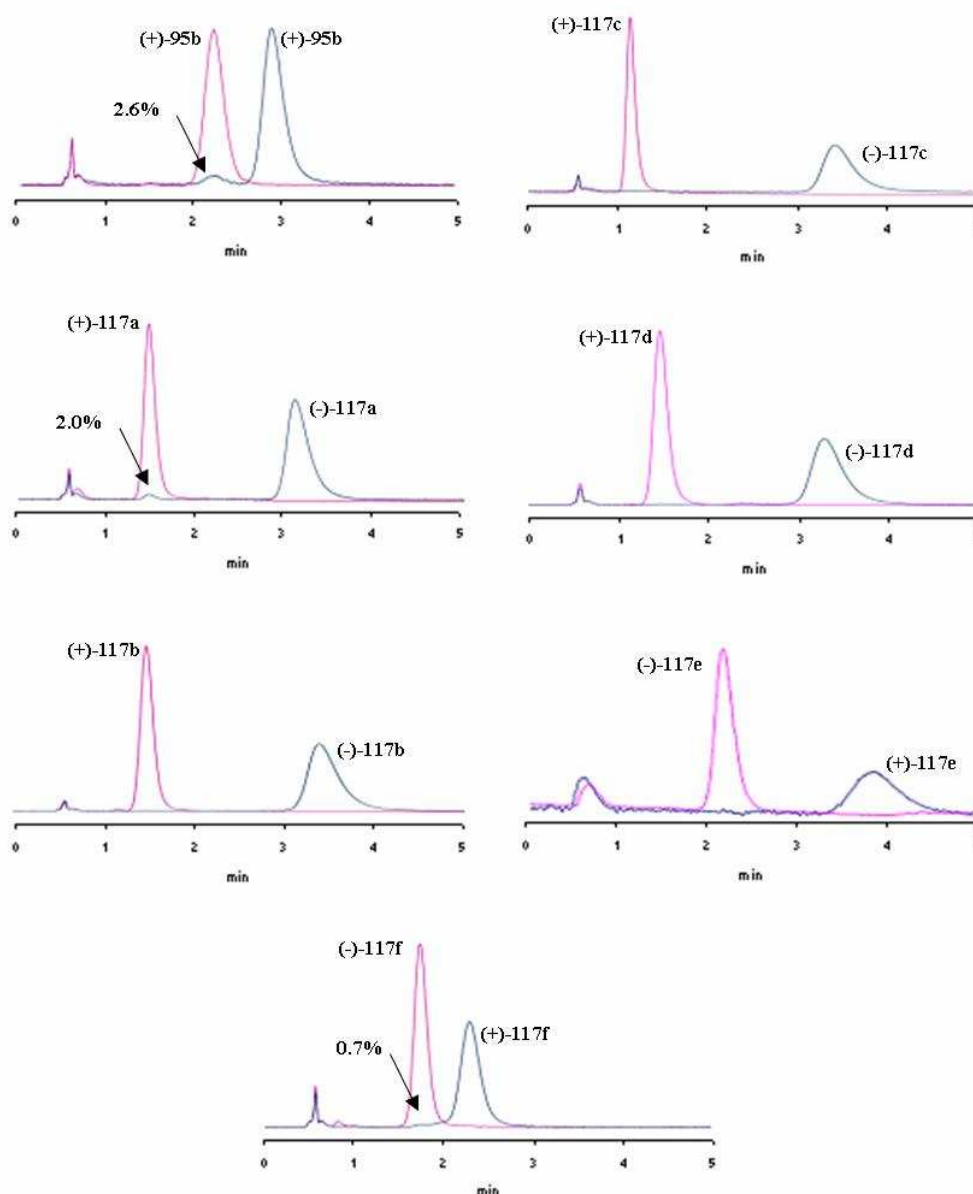


Figure 3.3. Chiral analytical HPLC analysis of the chromatographically resolved enantiomers (+)-**95b**/(-)-**95b** and (+)-**117a-f**/(-)-**117a**. **Conditions:** Lux Amylose-2 column (3 μ m, 4.6 mm I.D. x 50 mm), *n*-hexane/IPA 60:40 (v/v) as eluent, flow rate 1.0 mL/min, detection by UV at 250 nm, temperature 40 °C, injection volume of 10 μ L. For analytical enantioseparations a standard solution was prepared by dissolving 0.1 mg of each enantiomer into 1 mL of ethanol. The ee values were calculated from relative peak areas (**table 3.2**). Arrows indicate the percentage of the enantiomeric impurities for (+)-**95b**, (-)-**117a**, (+)-**117f** whereas all the other enantiomers were obtained with a purity > 99.9%.

Polarimetric analysis were as well performed by dissolving 20 mg of pure compounds into 2 mL of chloroform ($c = 1$) to establish the specific rotations ($[\alpha]_{D}^{20}$) of enantiomers (**table 3.2**). The signal was measured at 589 nm using a polarimeter equipped with a Na lamp.

Enantiomer	$[\alpha]_D^{20}$ (CHCl ₃ , <i>c</i> = 1)	Enantiomeric excess (ee, %)
(+)- 95b	+ 80°	> 99.9
(-)- 95b	- 78°	97.4
(+)- 117a	+ 129°	> 99.9
(-)- 117a	- 129°	98.0
(+)- 117b	+ 139°	> 99.9
(-)- 117b	- 137°	> 99.9
(+)- 117c	+ 99°	> 99.9
(-)- 117c	- 97°	> 99.9
(+)- 117d	+ 111°	> 99.9
(-)- 117d	- 110°	> 99.9
(+)- 117e	+ 16°	> 99.9
(-)- 117e	- 17°	> 99.9
(+)- 117f	+ 17°	99.3
(-)- 117f	- 18°	> 99.9

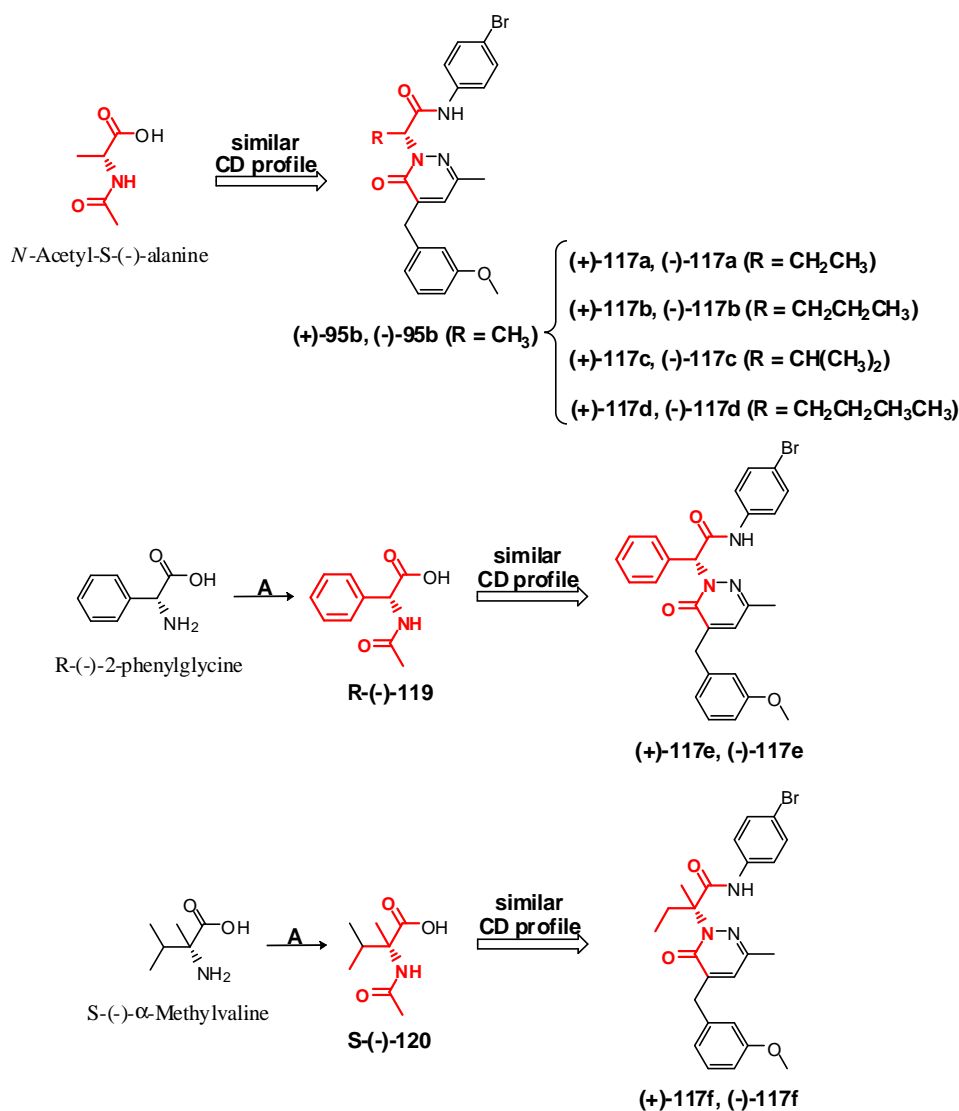
Table 3.2. Data for the different racemates (\pm)-**95b** and (\pm)-**117a-f** of specific rotation factor ($[\alpha]_D^{20}$), determined by polarimeter in CHCl₃ (*c* = 1 mg/1 mL), and enantiomeric excess, determined by chiral analytical HPLC separations.

Chiral HPLC and polarimetric analysis indicated that for racemates (\pm)-**95b** and (\pm)-**117a-d** the first eluted enantiomers using both Chiralcel OD or Lux Amylose-2 columns rotated polarized light in the positive direction, accordingly to the comparable nature of substituents on the stereogenic center (R = alkyl, R₁ = H, **schemes 29** and **30**). Oppositely, the elution sequence was reversed in the case of racemates (\pm)-**117e,f** where the enantiomers (-)-**117e,f** eluted faster than the corresponding (+)-forms during the separating process. Enantiomer elution order is a very important topic in the determination of enantiomeric purity of chiral compounds as well as in the study of enantioselective mechanism.²⁹⁹ The polysaccharide-type CSPs are based on natural materials and are available only in one configuration. Although it is difficult to control the enantiomer elution order with these CSPs, examples of inversion enantiomer retention order have been reported by alteration of the mobile phase composition or enantioseparation temperature.³⁰⁰ In our case, these results appear to be consistent with the assumption that structural differences on the chiral center between the analytes determined the reversal of the enantiomer elution order. Probably the bigger hindrance of the phenyl group in (\pm)-**117e** and the absence of H on the chiral center in (\pm)-**117f** are the key determinants in this inversion of chromatographic elution. Thus, from seven separated compounds five [(\pm)-**95b** and (\pm)-**117a-d**] exhibited higher affinity of the (-)-form for the stationary phase over the (+)-form and for the remaining two [(\pm)-**117e,f**] it was the opposite. It is as well interesting to note that enantiomer elution order was not influenced by changing the amount of alcohol (2-propanol) used in the mobile phase in both columns.

3.3.6.4 Assignment of the absolute configurations

To assign the absolute configuration to the pure enantiomers (+)-**95b**, (-)-**95b**, (+)-**117a-f** and (-)-**117a-f**, we made several attempts to get crystals suitable for single crystal X-ray analysis but, unluckily, none of

these analogues were amenable for configurational analysis by crystallization. Since this approach failed, for the configurational assignment we took into account the methodology based on the comparison of CD curve analysis of the unknown enantiomers and the CD profile of commercially available molecules or well known compounds whose absolute configuration was already been established. Examples of assignment of the absolute configuration using this approach have been extensively reported in the literature.³⁰¹⁻³⁰⁸



Scheme 31. *N*-Acetyl-*S*(-)-alanine and acetyl derivatives of *R*(-)-2-phenylglycine [*R*(-)-119] and *S*(-)- α -Methylvaline [*S*(-)-120] used as reference compounds in CD experiments in comparison to enantiomeric pairs (+)-95b/(-)-95b, (+)-117e/(-)-117e, (+)-117f/(-)-117f due to their comparable substituents on the stereogenic center. The result obtained for (+)-95b/(-)-95b can be extended as well for enantiomers (+)-117a-d/(-)-117a-d.

Reagents and conditions: A) acetic anhydride (7.5 equiv), H₂O, 0.5 h, 70 °C.

Commercially available *N*-acetyl-*S*(-)-alanine, *R*(-)-2-phenylglycine and *S*(-)- α -methylvaline were chosen as reference molecules considering that they are characterized by comparable substituents on the stereogenic centre. Indeed, as it shown in **scheme 31**, *N*-acetyl-*S*(-)-alanine bearing a methyl group on the chiral center, an hydrogen, a carboxylic CO and an amidic NH can be used in CD analysis as

3. Chemistry

reference for (+)-**95b**/(-)-**95b** and the result can be extended as well for (+)-**117a-d**/(-)-**117a-d** enantiomeric pairs. R(-)-**2-phenylglycine** and S(-)- α -methylvaline were instead firstly converted into their acetyl derivatives **R(-)-119** [commercially available, *N*-acetyl-R(-)-phenylglycine] and **S(-)-120** [*N*-acetyl-S(-)- α -methylvaline] to make the chiral center more similar to that of (+)-**117e**/(-)-**117e** and (+)-**117f**/(-)-**117f** respectively (**scheme 31**). The acetylation reaction was performed in H₂O using acetic anhydride at 70 °C and it occurred by complete retention of the absolute configuration as reported in literature.³⁰⁹ Both enantiomers of (\pm)-**95b** were analyzed in comparison with *N*-acetyl-S(-)-alanine ($[\alpha]_D^{23} - 62^\circ$ ($c = 1$, H₂O)) (**scheme 31** and **figure 3.4**). The solutions of (+)-**95b** and (-)-**95b** in methanol (concentration about 0.25 mg/mL, optical pathway 0.1 cm) and of *N*-acetyl-S(-)-alanine (concentration about 1 mg/mL, optical pathway 0.1 cm) were analyzed in nitrogen atmosphere. CD spectra were scanned at 50nm/min with a spectral band width of 1 nm and data resolution of 0.2 nm. The spectra were averaged over five instrumental scans and the intensities are presented in terms of ellipticity values (mdeg) (**figure 3.4**). The CD spectrum of the (+)-**95b** enantiomer (**figure 3.4**) displays a broad positive Cotton effect around 300 nm. The (-)-**95b** enantiomer exhibited the corresponding mirror-image CD. In comparison, the positive Cotton effect of the *N*-acetyl-S(-)-alanine is in the range of wavelength between 215 and 250 nm. Therefore, (S)-absolute configuration of the reference compound may also be assigned to (+)-**95b** and (R)-absolute configuration to (-)-**95b** that oppositely showed a negative Cotton effect around 300 nm. The differences in the profile of the curves could depend on the different type of chromophore between (+)-**95b**/(-)-**95b** and the *N*-acetyl-S(-)-alanine without any aromatic substituent.

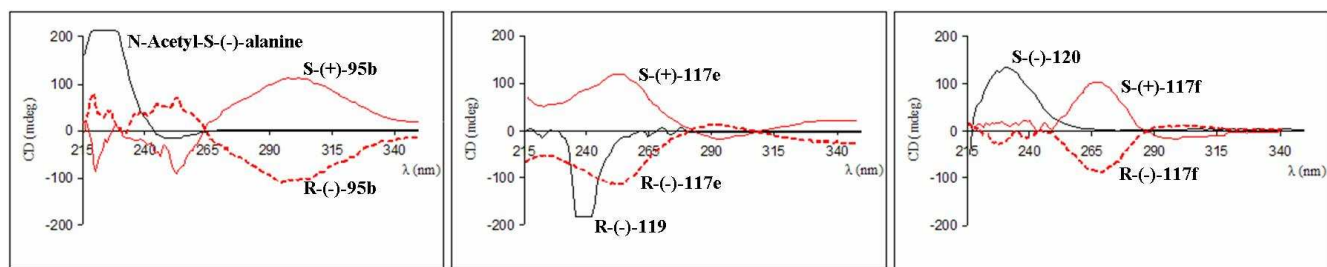


Figure 3.4. Experimental Circular dichroism (CD) spectra recorded in methanol at 25 °C of the pure enantiomeric pairs (+)-**95b**/(-)-**95b**, (+)-**117e**/(-)-**117e**, (+)-**117f**/(-)-**117f** and the reference compounds *N*-acetyl-S(-)-alanine, **R(-)-119**, **S(-)-120** (**scheme 31**). In each spectra black traces refers to the reference compounds, whereas solid and dashed red traces correspond respectively to the (S)- and (R)-enantiomers analyzed.

Due to the similarity on the chiral center between compounds **S-(+)-95b**/**R(-)-95b** and enantiomeric pairs (+)-**117a-d**/(-)-**117a-d** (**scheme 31**), it seems then possible that enantiomers of the same sign of optical rotation may have the same absolute configuration. Some support for such a reasoning is in the fact that a correlation between the absolute configuration of these optically active analogues could be deduced as well from the same elution order showed during chiral HPLC analysis (**section 3.3.6.3**, **figure 3.2** and **3.3**). Indeed analogues (+)-**117a-d**/(-)-**117a-d** exhibited same-sense chiral recognition mechanism

and, consequently, the same enantiomer elution order on both stationary phases used (Chiralcel OD and Lux Amylose-2) with preferential retention of the (-)-enantiomer. These data support the presumption that all the enantiomers (+)-**117a-d** possess the same absolute (S)-configuration and, obviously, the absolute (R)-configuration is for levorotatory isomers (-)-**117a-d**.

Similarity of CD spectra of reference molecule (R)-(-)-**119** and (-)-**117e** (**figure 3.4**) is certainly in line with the rule that enantiomers with the same sign of Cotton effect may have the same absolute configuration. Enantiomers (-)-**117e**/(+)-**117e** display the Cotton effects between 230 and 270 nm and a maximum around 250 nm. Also in this case, it is noteworthy that differences in the profile of the curves could depend from different type of chromophore between (-)-**117e**/(+)-**117e** and the (R)-(-)-**119**. CD spectra of (-)-**117e** and (+)-**117e**, recorded in methanol, clearly are mirror images (**figure 3.4**), demonstrating again the enantiomeric relationship. The negative Cotton effect of (-)-**117e** is in agreement with negative Cotton effects of the previously described (R)-(-)-**119**,³¹⁰⁻³¹² supporting the absolute R-(-)-configuration assigned to this enantiomer (**scheme 31**).

The configurational assignment for the last enantiomeric pair (-)-**117f**/(+)-**117f** was performed by comparing their circular dichroism spectra with that of S-(-)-**120** (**scheme 31**), always characterized by similar substituents on the stereogenic centers (two alkyl groups, a carboxylic CO and an amidic NH), whose configuration was already established. The spectra showed once more analogous profiles and comparable Cotton effects between S-(-)-**120** and (+)-**117f** in the spectral region between 215 and 300 nm (**figure 3.4**). The bathochromic shift of the S-(-)-**120** curve could depend on the differences between the different chromophores. Therefore the absolute configurations of S-(-)-**120** may be proposed also for (+)-**117f** and, consequently, the absolute R-configuration was assigned to (-)-**117f** (**scheme 31**).

In conclusion, on the basis of combined chromatographic and chiroptical studies, the absolute configuration assignment was unambiguously completed, and configurations were assigned as follow to the seven enantiomeric pairs synthesized: S-(+)-**95b**/R-(-)-**95b** and S-(+)-**117a-f**/R-(-)-**117a-f**. Due to the comparable chiral centers in this group of homologue molecules, the results showed as well that (S)-absolute configuration is for all dextrorotatory enantiomers of the series and (R)-absolute configuration is for the corresponding levorotatory isomers.

4. RESULTS AND CONCLUSIONS

4.1 Results

In the present study, we synthesized a library of 162 heterocyclic compounds which were screened in order to identify novel molecules able to activate human neutrophil through FPRs interaction. Thus the final compounds were evaluated for their ability to induce intracellular Ca^{2+} flux in HL-60 (Human promyelocytic leukemia) cells transfected with FPR1, FPR2, or FPR3. In fact it is well known that it is possible to estimate FPRs affinity by means of evaluation in Ca^{2+} flux changing.³¹³⁻³¹⁴ All compounds were also evaluated in WT (wild-type non-transfected HL-60 cells) and they were inactive. Moreover, both EC_{50} values and relative efficacy, compared to the peptide agonists fMLF and WKYMVm, were determined. Finally, the compounds that showed the best activity profile were selected to evaluate the activity as chemotactic agents and the capacity to mobilize Ca^{2+} in human neutrophils.

4.1.1 Screening different nitrogen heterocyclic derivatives as FPRs agonists

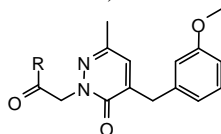
In the early phase of our project, we synthesized several compounds where functionalized side chains similar to that of the reference compounds (Quin-C1 and pyrazolone derivatives in **figure 2.1**) are bonded to different heterocyclic scaffolds such as indazole, indole, quinoline, naphthyridone, phthalazinone and phthalhydrazide (**schemes 1-8, section 3.1**). Any activity was found for these compounds towards the three FPR subtypes. Some of them showed low activity as chemotactic agent (data not shown) probably due to the interaction with a different biological system or other receptors in the neutrophils. Likewise pyridazin-3(2H)-ones bearing a methoxybenzyl or a phenyl group at position 2 and a functionalized side chain at positions 4 or 5 (**schemes 9,10, section 3.1**) were inactive as FPRs agonists. Performing further modifications on the same scaffold as the insertion of substituted benzyl at position 4 together with a functionalized chain at N-2 (**scheme 12, section 3.1**), we identified compound **46a (table 4.1)**, as a potent mixed FPR1 and FPR2 agonist.²³³ Thus, this first active compound **46a** was selected as lead and extensive structure-activity relationship (SAR) studies on this prototype were performed.

During the development of the project, it became necessary to replace the initial cell line RBL-2H3 (Rat basophilic leukemia) cells, used to test agonistic activity of the compounds, with HL-60 cells, having higher expression of FPRs and as well higher response to reference molecule fMLF. In the meantime some modifications of the lead compound had been already performed, such as the introduction of a phenyl group in the position C-6 of the pyridazinone and a iodine on the phenyl of the acetamidic spacer. The biological tests carried out on the first cell line (RBL-2H3) showed for these compounds a very interesting activity and, thus, several analogues were designed and synthesized on the basis of this evidence. Unluckily, the same results were not confirmed by testing the same molecules in HL-60 cell.

4.1.2 EC₅₀ and efficacy of *N*-arylacetamide pyridazinones

The nature and the position of the substituent on the phenyl group of the side chain proved to play a crucial role in ligand activity as it is shown in **table 4.1**. Moving Br of lead compound **46a** from position para to meta (**46b**) and ortho (**46c**) resulted in a complete loss of FPR1/FPR2 activity. Among halo-derivatives, the 4-chloro analogue **46e** exhibited the same profile as **46a**, while the corresponding 4-iodo derivative **46f** was two times less potent for FPR2. For this compound, a weak effect at FPR3 was also observed. The 4-fluoro analogue **46d** was less potent compared to **46a**, but specificity for FPR1 was demonstrated.

Table 4.1. Activity of the compounds **46a-s** (scheme 12) in HL-60 cells expressing human FPR1, FPR2, or FPR3.



compd	R	Ca ²⁺ Mobilization EC ₅₀ (μM) and Efficacy (%) ^a		
		FPR1	FPR2	FPR3
46a	NH-C ₆ H ₄ -Br (p)	3.4 ± 1.6 (75)	3.8 ± 1.5 (70)	N.A.
46b	NH-C ₆ H ₄ -Br (m)	N.A.	N.A.	N.A.
46c	NH-C ₆ H ₄ -Br (o)	N.A.	N.A.	N.A.
46d	NH-C ₆ H ₄ -F (p)	7.6 ± 0.2 (40)	N.A.	N.A.
46e	NH-C ₆ H ₄ -Cl (p)	2.6 ± 0.3 (110)	4.0 ± 1.6 (35)	N.A.
46f	NH-C ₆ H ₄ -I (p)	2.8 ± 0.2 (90)	6.8 ± 2.2 (40)	13.0 ± 3.1 (30)
46g	NH-C ₆ H ₅	N.A.	N.A.	N.A.
46h	NH-C ₆ H ₄ -CH ₃ (p)	7.2 ± 2.2 (120)	10.9 ± 3.4 (50)	N.A.
46i	NH-C ₆ H ₄ -tC ₄ H ₉ (p)	N.A.	N.A.	N.A.
46j	NH-C ₆ H ₄ -OCH ₃ (p)	7.7 ± 2.5 (65)	14.4 ± 2.0 (35)	N.A.
46k	NH-C ₆ H ₄ -OC ₄ H ₉ (p)	N.A.	N.A.	N.A.
46l	NH-C ₆ H ₃ -(OCH ₃) ₂ (3, 4)	15.5 ± 2.9 (25)	16.8 ± 3.2 (25)	N.A.
46m	NH-C ₆ H ₃ -3,4-methylenedioxy	2.3 ± 1.1 (50)	N.A.	N.A.
46n	NH-C ₆ H ₄ -CF ₃ (p)	5.7 ± 1.8 (50)	8.8 ± 2.3 (95)	N.A.
46o	NH-C ₆ H ₄ -OCF ₃ (p)	N.A.	N.A.	N.A.
46p	NH-C ₆ H ₄ -SCH ₃ (p)	26.4	14.7	N.A.
46q	NH-C ₆ H ₄ -CN (p)	N.A.	N.A.	N.A.
46r	NH-C ₆ H ₄ -NO ₂ (p)	10.5 ± 2.9 (60)	12.3 ± 2.5 (55)	N.A.
46s	1-methylpiperazine	N.A.	N.A.	N.A.
fMLF		0.01	20.4	1.9
WKYMVm		0.5	0.001	0.01

^aN.A., no activity was observed (no response was observed during first 2 min after addition of compounds under investigation) considering the limits of efficacy > 20 % and EC₅₀ < 50 μM. The EC₅₀ values are presented as the mean ± S.D. of three independent experiments, in which median effective concentration values (EC₅₀) were determined by nonlinear regression analysis of the dose-response curves (5-6 points) generated using GraphPad Prism 5 with 95% confidential interval (*p* < 0.05). Efficacy (in bracket) is expressed as percent of the response induced by 5 nM fMLF (FPR1) or 5 nM WKYMVm (FPR2 and FPR3).

The elimination of Br (compound **46g**) was associated with a complete loss of activity. Replacement of Br in **46a** with substituents having similar steric properties, such as *t*-But (**46i**), OCF₃ (**46o**), and CN (**46q**), led to loss of activity at both FPR1 and FPR2. The 4-trifluoromethyl and the 4-nitro analogues (**46n** and **46r**, respectively) as well as compound **46h**, bearing a methyl group at position 4, had relatively low activity. Introduction of alkoxy groups gave interesting results: the 4-methoxy derivative **46j** and the 3,4-dimethoxy derivative **46l** had low activity at both receptors, whereas of the 3,4-methylenedioxy derivative **46m** showed specificity for FPR1. Differently compound **46p**, with a methylthio group in the para position of the phenyl group showed a drastic decrease of activity. It is worth noting that compounds **46k**, where Br in the para position is substituted with a butoxy, and **46s**, where the amidic nitrogen is included in a piperazine nucleus, were found to be completely devoid of activity.

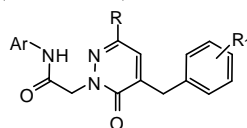
4.1.3 EC₅₀ and efficacy of C-6 modified *N*-arylacetamide pyridazinones

SAR studies at position 6 of the pyridazinone ring were planned by modifying the methyl group of the lead compound **46a** (table 4.1) as follow: elimination or replacement with superior homologues, cyclohexyl group, thiophene and (substituted)aryls (table 4.2).

As it is possible to see from the biological results, the ethyl analogue (**50b**) displayed a very similar behaviour with respect to the lead compound (**46a**), whereas the isopropyl derivative (**50a**) resulted a mixed agonist for FPR1, FPR2 and FPR3. On the contrary, the introduction of a cyclohexyl at position C-6 (**50c**) was associated with FPR1 selectivity. The elimination of the methyl group (**50d**) led to a quite potent but not selective compound, since it was able to activate all the three receptor subtypes. Among compounds having a phenyl group at C-6 only **50e**, bearing Br in the phenylacetamide chain showed a relevant activity, mainly at FPR1 level. The 2-thienyl derivatives **50h-j** were completely inactive, as well as all compounds bearing OCH₃ (**50k-m**), Cl (**50n-p**), CH₃ (**50q-s**), F (**50t-v**), in para position of the phenyl at C-6 of pyridazinone nucleous. It is worth nothing the inactivity of 4-F analogue **50t**, in comparison with the above seen **50e** unsubstituted analogue. This finding suggest that for these compounds electronic features play a more important role than steric properties.

4. Results and Conclusions

Table 4.2. Activity of the compounds **50a-v** (scheme 13) in HL-60 cells expressing human FPR1, FPR2, or FPR3.



compd	R	R ₁	Ar	Ca ²⁺ Mobilization EC ₅₀ (μM) and Efficacy (%) ^a		
				FPR1	FPR2	FPR3
50a	CH ₂ CH ₃	OCH ₃ (m)	NH-C ₆ H ₄ -I (p)	5.0 (95)	7.2 (75)	N.A.
50b	CH(CH ₃) ₂	OCH ₃ (m)	NH-C ₆ H ₄ -Br (p)	4.5 (135)	7.2 (90)	17.4 (30)
50c	C ₆ H ₁₁	OCH ₃ (m)	NH-C ₆ H ₄ -Br (p)	10.8 (80)	N.A.	N.A.
50d	H	OCH ₃ (m)	NH-C ₆ H ₄ -Br (p)	6.1 (125)	7.7 (60)	14.6 (25)
50e	C ₆ H ₅	OCH ₃ (m)	NH-C ₆ H ₄ -Br (p)	9.0 (110)	4.3 (25)	N.A.
50f	C ₆ H ₅	OCH ₃ (m)	NH-C ₆ H ₃ -3,4-methylenedioxy	N.A.	N.A.	N.A.
50g	C ₆ H ₅	OCH ₃ (m)	NH-C ₆ H ₄ -F (p)	N.A.	N.A.	N.A.
50h	2-thienyl	OCH ₃ (p)	NH-C ₆ H ₄ -Br (p)	N.A.	N.A.	N.A.
50i	2-thienyl	OCH ₃ (m)	NH-C ₆ H ₃ -3,4-methylenedioxy	N.A.	N.A.	N.A.
50j	2-thienyl	OCH ₃ (m)	NH-C ₆ H ₄ -F (p)	N.A.	N.A.	N.A.
50k	C ₆ H ₄ -OCH ₃	OCH ₃ (p)	NH-C ₆ H ₄ -Br (p)	N.A.	N.A.	N.A.
50l	C ₆ H ₄ -OCH ₃	OCH ₃ (m)	NH-C ₆ H ₃ -3,4-methylenedioxy	N.A.	N.A.	N.A.
50m	C ₆ H ₄ -OCH ₃	OCH ₃ (m)	NH-C ₆ H ₄ -F (p)	N.A.	N.A.	N.A.
50n	C ₆ H ₄ -Cl	OCH ₃ (p)	NH-C ₆ H ₄ -Br (p)	N.A.	N.A.	N.A.
50o	C ₆ H ₄ -Cl	OCH ₃ (m)	NH-C ₆ H ₃ -3,4-methylenedioxy	N.A.	N.A.	N.A.
50p	C ₆ H ₄ -Cl	OCH ₃ (m)	NH-C ₆ H ₄ -F (p)	N.A.	N.A.	N.A.
50q	C ₆ H ₄ -CH ₃	OCH ₃ (p)	NH-C ₆ H ₄ -Br (p)	N.A.	N.A.	N.A.
50r	C ₆ H ₄ -CH ₃	OCH ₃ (m)	NH-C ₆ H ₃ -3,4-methylenedioxy	N.A.	N.A.	N.A.
50s	C ₆ H ₄ -CH ₃	OCH ₃ (m)	NH-C ₆ H ₄ -F (p)	N.A.	N.A.	N.A.
50t	C ₆ H ₄ -F	OCH ₃ (p)	NH-C ₆ H ₄ -Br (p)	N.A.	N.A.	N.A.
50u	C ₆ H ₄ -F	OCH ₃ (m)	NH-C ₆ H ₃ -3,4-methylenedioxy	N.A.	N.A.	N.A.
50v	C ₆ H ₄ -F	OCH ₃ (m)	NH-C ₆ H ₄ -F (p)	N.A.	N.A.	N.A.
46a				3.4 (75)	3.8 (70)	N.A.
fMLF				0.01	20.4	1.9
WKYMVm				0.5	0.001	0.01

^aN.A., no activity was observed (no response was observed during first 2 min after addition of compounds under investigation) considering the limits of efficacy > 20 % and EC₅₀ < 50 μM. The EC₅₀ values are presented as the mean of three independent experiments, in which median effective concentration values (EC₅₀) were determined by nonlinear regression analysis of the dose-response curves (5-6 points) generated using GraphPad Prism 5 with 95% confidential interval (*p* < 0.05). Efficacy (in bracket) is expressed as percent of the response induced by 5 nM fMLF (FPR1) or 5 nM WKYMVm (FPR2 and FPR3).

4.1.4 EC₅₀ and efficacy of C-4 modified N-arylacetylamide pyridazinones

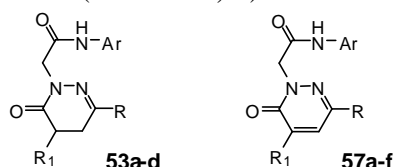
SAR studies at position 4 were performed on the lead compound **46a** (table 4.1) as function of the following criteria:

- complete elimination of the substituents of the benzyl or replacement with a methyl group (table 4.3);

- b) replacement of the methoxyphenyl in benzyl group with heterocycles or different aromatic groups (**table 4.4**);
- c) introduction of different substituents in meta position of the benzyl group (**table 4.4**);
- d) introduction of substituents in para position of the benzyl group (**table 4.4**);
- e) elimination of OCH₃ on the benzyl group (**table 4.4**);
- f) elimination of the CH₂-spacer of the benzyl group or introduction of different functionalized linkers (**table 4.5**).

a) With the exception of low active agonists (\pm)-**53b** and **57c,d** (**table 4.3**), the derivatives in which the methoxybenzyl is eliminated or replaced by a methyl group were completely devoid of activity and this behaviour is evident in both series of 4,5-dihydropyridazinones (**53a-d**) and pyridazinones (**57a-f**).

Table 4.3. Activity of compounds **53a-d** and **57a-f** (schemes 14,15) in HL-60 cells expressing human FPR1, FPR2, or FPR3.



compd	R	R ₁	Ar	Ca ²⁺ Mobilization EC ₅₀ (μM) and Efficacy (%) ^a		
				FPR1	FPR2	FPR3
53a	CH ₃	H	NH-C ₆ H ₄ -I (p)	N.A.	N.A.	N.A.
(±)- 53b	C ₆ H ₅	CH ₃	NH-C ₆ H ₄ -Br (p)	23.5 (55)	7.0 (65)	N.A.
(±)- 53c	C ₆ H ₅	CH ₃	NH-C ₆ H ₄ -F (p)	N.A.	N.A.	N.A.
(±)- 53d	C ₆ H ₅	CH ₃	NH-C ₆ H ₃ -3,4-methylenedioxy	N.A.	N.A.	N.A.
57a	C ₆ H ₁₁	H	NH-C ₆ H ₄ -F (p)	N.A.	N.A.	N.A.
57b	C ₆ H ₁₁	H	NH-C ₆ H ₃ -3,4-methylenedioxy	N.A.	N.A.	N.A.
57c	CH ₃	H	NH-C ₆ H ₄ -I (p)	30.4 (45)	19.7	N.A.
57d	C ₆ H ₅	CH ₃	NH-C ₆ H ₄ -Br (p)	21.5 (50)	10.1 (45)	N.A.
57e	C ₆ H ₅	CH ₃	NH-C ₆ H ₄ -F (p)	N.A.	N.A.	N.A.
57f	C ₆ H ₅	CH ₃	NH-C ₆ H ₃ -3,4-methylenedioxy	N.A.	N.A.	N.A.
46a				3.4 (75)	3.8 (70)	N.A.
fMLF				0.01	20.4	1.9
WKYMVm				0.5	0.001	0.01

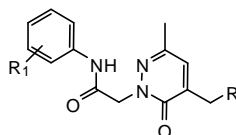
^aN.A., no activity was observed (no response was observed during first 2 min after addition of compounds under investigation) considering the limits of efficacy > 20 % and EC₅₀ < 50 μM. The EC₅₀ values are presented as the mean of three independent experiments, in which median effective concentration values (EC₅₀) were determined by nonlinear regression analysis of the dose-response curves (5-6 points) generated using GraphPad Prism 5 with 95% confidential interval (*p* < 0.05). Efficacy (in bracket) is expressed as percent of the response induced by 5 nM fMLF (FPR1) or 5 nM WKYMVm (FPR2 and FPR3).

b) Useful informations originated by replacement of methoxyphenyl group with 5- and 6-membered heterocycles (**table 4.4**). Indeed, both thienyl derivatives (**61b,c**) showed an interesting level of potency

4. Results and Conclusions

but a weak selectivity for FPR1, as well as furyl (**61a**) and piridyl (**66c**) analogues which had a similar profile of activity without relevant subtype-selectivity. On the contrary, the insertion of a naphthylmethyl (**61d**) and a 3,5 dimethoxybenzyl (**61f**, **62b**) groups in the position 4 was associated with decrease or complete loss of the activity.

Table 4.4. Activity of compounds **61a-p**, **62a-c** and **66a-c** (schemes 16-18) in HL-60 cells expressing human FPR1, FPR2, or FPR3.



compd	R	R ₁	Ca ²⁺ Mobilization EC ₅₀ (μM) and Efficacy (%) ^a		
			FPR1	FPR2	FPR3
61a	3-furyl	Br (p)	5.8 (100)	6.3 (75)	N.A.
61b	3-thienyl	Br (p)	4.5 (100)	14.1 (65)	N.A.
61c	2-thienyl	Br (p)	8.1 (140)	11.4 (60)	10.2 (25)
61d	1-naphthyl	Br (p)	13.8 (20)	N.A.	N.A.
66c	3-pyridyl	Br (p)	9.3 (85)	2.8 (90)	N.A.
61e	C ₆ H ₄ -OCH ₃ (p)	Br (p)	N.A.	2.4 ± 0.9 (70)	N.A.
61f	C ₆ H ₃ -(OCH ₃) ₂ (3,5)	Br (p)	N.A.	N.A.	N.A.
62b	C ₆ H ₃ -(OCH ₃) ₂ (3,5)	I (p)	11.1 (90)	9.7	N.A.
61g	C ₆ H ₄ -F (m)	Br (p)	6.6 (110)	N.A.	N.A.
61h	C ₆ H ₄ -Cl (m)	Br (p)	10.5 (100)	N.A.	N.A.
62c	C ₆ H ₄ -Cl (m)	I (p)	6.8 (65)	10.6 (30)	N.A.
61i	C ₆ H ₄ -Br (m)	Br (p)	N.A.	N.A.	N.A.
61j	C ₆ H ₄ -SCH ₃ (p)	Br (p)	N.A.	N.A.	N.A.
62a	C ₆ H ₄ -SCH ₃ (p)	I (p)	19.7 (60)	15.9 (90)	30.1
61k	C ₆ H ₄ -CF ₃ (p)	Br (p)	N.A.	N.A.	N.A.
66a	C ₆ H ₄ -CN (p)	Br (p)	N.A.	N.A.	N.A.
66b	C ₆ H ₄ -CONH ₂ (p)	Br (p)	29.3 (40)	27.2 (80)	N.A.
61l	C ₆ H ₅	Br (p)	5.5 (50)	11.6 (20)	N.A.
61m	C ₆ H ₅	F (p)	N.A.	N.A.	N.A.
61n	C ₆ H ₅	3,4-methylenedioxy	6.9 (55)	N.A.	N.A.
61o	C ₆ H ₄ -Cl (p)	O-C ₄ H ₉ -n (p)	N.A.	N.A.	N.A.
61p	C ₆ H ₄ -OCH ₃ (p)	O-C ₄ H ₉ -n (p)	N.A.	N.A.	N.A.
46a			3.4 ± 1.6 (75)	3.8 ± 1.5 (70)	N.A.
fMLF			0.01	20.4	1.9
WKYMVm			0.5	0.001	0.01

^aN.A., no activity was observed (no response was observed during first 2 min after addition of compounds under investigation) considering the limits of efficacy > 20 % and EC₅₀ < 50 μM. The EC₅₀ values are presented as the mean ± S.D. of three independent experiments, in which median effective concentration values (EC₅₀) were determined by nonlinear regression analysis of the dose-response curves (5-6 points) generated using GraphPad Prism 5 with 95% confidential interval (*p* < 0.05). Efficacy (in bracket) is expressed as percent of the response induced by 5 nM fMLF (FPR1) or 5 nM WKYMVm (FPR2 and FPR3).

c) Replacement of 3-methoxy group, on the benzyl at position 4 of the pyridazinone nucleus of the lead compound **46a**, with different substituents showed as well attractive results (**table 4.4**). In fact,

introduction of F in meta position gave compound **61g** which is a selective FPR1 agonist and a similar behaviour was evident for compound with Cl (**61h**). Differently, analogue **62c** bearing a 4-iodophenyl in the acetamidic spacer was a mixed FPR1/FPR2 agonist. Introduction of a Br (**61i**) in the place of OCH₃ group of lead compound **46a** was associated with loss of activity. All these data suggest that the presence of a substituents of limited hindrance in the meta position is an essential requirement for binding at FPR1 and FPR2.

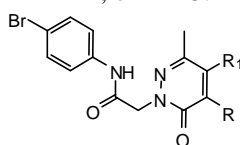
d) Moving OCH₃ from the meta to the para position (**61e**) surprisingly resulted in high activity (EC₅₀ = 2.4 μM) and selectivity for FPR2 (**table 4.4**). Oppositely, introduction of SCH₃ (**61j**, **62a**), CF₃ (**61k**), CN (**66a**) and CONH₂ (**66b**) in the para position was generally detrimental. However compound **62a**, bearing a 4-iodophenyl moiety on the acetamidic linker, and the benzamide derivative **66b** showed a weak mixed agonistic activity. These data confirmed that the methoxy group is the optimum for steric and electronic properties in the aromatic moiety at position 4 of the pyridazinone nucleus, as both biological results of old (**46a**, **table 4.1**) and new (**61e**, **table 4.4**) lead compounds showed. On the contrary, compounds **61o** and **61p** where a 4-Cl or a 4-OCH₃ were introduced in the benzyl group and bearing a butoxy group on the phenylacetamide spacer were completely devoid of activity.

e) In comparison to lead compound **46a** (**table 4.1**), when OCH₃ group was eliminated from the benzyl fragment at position 4 of the pyridazinone scaffold (**61 l**) the activity lowered particularly as FPR2 agonist (**table 4.4**), while the concomitant presence of an unsubstituted benzyl at C-4 and F (**61m**) or methylenedioxy (**61n**) in the aryl acetamide side chain was associated in the first case with a complete loss of activity and in the second with a weak agonistic FPR1 activity.

f) Introduction of carbonyl group as spacer in the place of CH₂ of the benzyl group at position 4 of the pyridazinone ring resulted in compound **71** which is a potent mixed agonist of both FPR1 and FPR2 (**table 4.5**), while elimination of the methylenic linker originated a very selective ligand (**77**) at FPR1. When CH₂ was replaced by NH (**88**) an interesting activity was found mainly at FPR2 and the same behaviour was shown by the 5-acetyl analogue (**83**), whereas the synthetic precursor **87** resulted less potent as FPR2 ligand. Substitution of CH₂ with an amidic group was detrimental for activity, since compound **89a** was totally inactive and the 3-methoxy analogue **89b** showed low activity as FPR1/FPR2 agonist. Lastly, when more hindered substituents were introduced in the position 4, the activity disappeared completely, being compound **69** and the biaryl derivative **92** completely devoid of activity.

4. Results and Conclusions

Table 4.5. Activity of compounds **69**, **71**, **77**, **83**, **87-89a,b** and **92** (schemes 18-21) in HL-60 cells expressing human FPR1, FPR2, or FPR3.



compd	R	R ₁	Ca ²⁺ Mobilization EC ₅₀ (μM) and Efficacy (%) ^a		
			FPR1	FPR2	FPR3
69	CH ₂ -C ₆ H ₄ -CONH(p)-C ₆ H ₄ -Br (p)	H	N.A.	N.A.	N.A.
71	CO-C ₆ H ₄ -OCH ₃ (m)	H	3.0 (140)	1.4 (100)	N.A.
77	C ₆ H ₄ -OCH ₃ (p)	H	11.2 (55)	N.A.	N.A.
83	NH-C ₆ H ₄ -OCH ₃ (p)	COCH ₃	13.5 (75)	2.3 (80)	N.A.
87	NH ₂	H	8.1 (115)	29.4 (85)	N.A.
88	NH-C ₆ H ₄ -OCH ₃ (p)	H	12.8 (100)	3.8 (85)	N.A.
89a	NHCO-C ₆ H ₄ -Br (p)	H	N.A.	N.A.	N.A.
89b	NHCO-C ₆ H ₄ -OCH ₃ (m)	H	9.3 (120)	6.4 (70)	N.A.
92	N-(C ₆ H ₄ -OCH ₃ (p)) ₂	H	N.A.	N.A.	N.A.
46a			3.4 (75)	3.8 (70)	N.A.
fMLF			0.01	20.4	1.9
WKYMVm			0.5	0.001	0.01

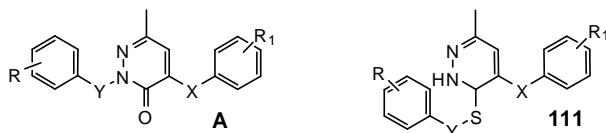
^aN.A., no activity was observed (no response was observed during first 2 min after addition of compounds under investigation) considering the limits of efficacy > 20 % and EC₅₀ < 50 μM. The EC₅₀ values are presented as the mean of three independent experiments, in which median effective concentration values (EC₅₀) were determined by nonlinear regression analysis of the dose-response curves (5-6 points) generated using GraphPad Prism 5 with 95% confidential interval (*p* < 0.05). Efficacy (in bracket) is expressed as percent of the response induced by 5 nM fMLF (FPR1) or 5 nM WKYMVm (FPR2 and FPR3).

4.1.5 EC₅₀ and efficacy of *N*-arylacetamide modified pyridazinones, *N*-2/*C*-4 inverted pyridazinones and *C*-3 substituted pyridazine analogue

Elongation of carbon chain from one to two methylene groups, at the level of aryl acetamide side chain of lead compound **46a**, gave **95a** which resulted less potent of the lead compound as FPR1/FPR2 ligand (table 4.6). More substantial modifications of the functionalized chain were obtained with compounds **96a,b** and were completely detrimental. Further inactive compounds were the urea derivative **97a**, the inverse amide **97b**, as well as their superior homologues **103a,b**. Replacement of CH₂CONH of the lead compound **46a** with a secondary amine and an ether group gave compounds **100** and **101** respectively, which also resulted inactive. Other unproductive modifications of the functionalized chain were performed with the synthesis of compounds **104a,c**, and replacement of CONH with COO (**104b**) gave the same effect. Differently when the amidic group of the lead compound **46a** was changed into the corresponding thioamide (**105**) a low activity toward FPR2 is retained. Moreover, compounds **108** and **109**, in which the substituents at position 2 and 4 were interchanged, were inactive. Finally, moving the 4-

bromo phenylacetamide moiety from the N-2 to the C-3 of the pyridazinone led to a decrease of activity, being the pyridazine derivative **111** a selective but weak FPR2 agonist.

Table 4.6. Activity of compounds **95-97a,b**, **100-102**, **103a,b**, **104a-c**, **105**, **108**, **109** (structure **A**) and **111** (schemes 22-27) in HL-60 cells expressing human FPR1, FPR2, or FPR3.



Compd	Y	R	X	R ₁	Ca ²⁺ Mobilization EC ₅₀ (μM) and Efficacy (%) ^a		
					FPR1	FPR2	FPR3
95a	(CH ₂) ₂ CONH	Br (p)	CH ₂	OCH ₃ (m)	9.7 ± 2.7 (30)	5.4 ± 1.2 (25)	N.A.
96a	CH ₂	Br (p)	CH ₂	OCH ₃ (m)	N.A.	N.A.	N.A.
96b	CH ₂ CO	Br (p)	CH ₂	OCH ₃ (m)	N.A.	N.A.	N.A.
97a	CH ₂ NHCONH	Br (p)	CH ₂	OCH ₃ (m)	N.A.	N.A.	N.A.
97b	CH ₂ NHCO	Br (p)	CH ₂	OCH ₃ (m)	N.A.	N.A.	N.A.
103a	(CH ₂) ₂ NHCONH	Br (p)	CH ₂	OCH ₃ (m)	N.A.	N.A.	N.A.
103b	(CH ₂) ₂ NHCO	Br (p)	CH ₂	OCH ₃ (m)	N.A.	N.A.	N.A.
100	(CH ₂) ₂ NH	Br (p)	CH ₂	OCH ₃ (m)	N.A.	N.A.	N.A.
101	(CH ₂) ₂ ^o	Br (p)	CH ₂	OCH ₃ (m)	N.A.	N.A.	N.A.
104a	CH ₂ CONHCH ₂	Br (p)	CH ₂	OCH ₃ (m)	N.A.	N.A.	N.A.
104b	CH ₂ COO	Br (p)	CH ₂	OCH ₃ (m)	N.A.	N.A.	N.A.
104c	CH ₂ CON(CH ₃)	Br (p)	CH ₂	OCH ₃ (m)	N.A.	N.A.	N.A.
105	CH ₂ CSNH	Br (p)	CH ₂	OCH ₃ (m)	N.A.	8.3 (< 25)	N.A.
108	CH ₂	OCH ₃ (m)	NHCO	Br (p)	N.A.	N.A.	N.A.
109	CH ₂	OCH ₃ (m)	NHCONH	Br (p)	N.A.	N.A.	N.A.
111	CH ₂ CONH	Br (p)	CH ₂	OCH ₃ (p)	N.A.	14.7 (< 25)	N.A.
46a					3.4 (75)	3.8 (70)	N.A.
fMLF					0.01	20.4	1.9
WKYMVm					0.5	0.001	0.01

^aN.A., no activity was observed (no response was observed during first 2 min after addition of compounds under investigation) considering the limits of efficacy > 20 % and EC₅₀ < 50 μM. The EC₅₀ values are presented as the mean ± S.D. of three independent experiments, in which median effective concentration values (EC₅₀) were determined by nonlinear regression analysis of the dose-response curves (5-6 points) generated using GraphPad Prism 5 with 95% confidential interval (*p* < 0.05). Efficacy (in bracket) is expressed as percent of the response induced by 5 nM fMLF (FPR1) or 5 nM WKYMVm (FPR2 and FPR3).

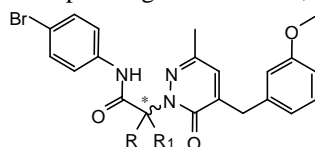
4.1.6 EC₅₀ and efficacy of chiral pyridazinone analogues

The insertion of alkyl or aryl groups at the level of the methylene spacer in the acetamide side chain of the lead compound **46a** (table 4.1, scheme 12) led to series of branched and chiral compounds which were tested both as racemates and as pure enantiomers. Starting from compound (±)-**95b**, data showed that the racemate did not activate FPR2 but retained activity for FPR1 similar to that of **46a** (table 4.7). As soon as the biological tests on the pure enantiomers were ongoing, the higher activity of the R(-)-

4. Results and Conclusions

forms of the alkyl derivatives was evident from the beginning. Indeed, the first tested enantiomers **R(-)-95b** and **R(-)-117a** showed to be more active at both FPR1 and FPR2 compared to the corresponding **S(+)-forms** [**S(+)-95b** and **S(+)-117a**].

Table 4.7. Activity of racemates and pure enantiomers (\pm)-**95b**, (\pm)-**117a-f** and non chiral homologue **118** (schemes 22, 29, 30) in HL-60 cells expressing human FPR1, FPR2, or FPR3.



compd	R	R ₁	Ca ²⁺ Mobilization EC ₅₀ (μM) and Efficacy (%) ^a		
			FPR1	FPR2	FPR3
(±)- 95b	H	CH ₃	3.2 ± 1.5 (90)	N.A.	N.A.
S(+)-95b	H	CH ₃	17.9 (35)	N.A.	N.A.
R(-)-95b	H	CH ₃	8.4 (80)	14.4 (70)	N.A.
(±)- 117a	H	C ₂ H ₅	1.4 (160)	1.2 (100)	N.A.
S(+)-117a	H	C ₂ H ₅	15.7 (130)	23.1 (55)	N.A.
R(-)-117a	H	C ₂ H ₅	2.8 (135)	3.0 (70)	N.A.
(±)- 117b	H	<i>n</i> -C ₃ H ₇	2.8 (75)	2.3 (60)	N.A.
S(+)-117b	H	<i>n</i> -C ₃ H ₇	N.A.	N.A.	N.A.
R(-)-117b	H	<i>n</i> -C ₃ H ₇	0.5 (90)	0.6 (90)	N.A.
(±)- 117c	H	<i>i</i> -C ₃ H ₇	2.0 (75)	13.5 (30)	N.A.
S(+)-117c	H	<i>i</i> -C ₃ H ₇	N.A.	N.A.	N.A.
R(-)-117c	H	<i>i</i> -C ₃ H ₇	1.9 (95)	3.9 (70)	N.A.
(±)- 117d	H	<i>n</i> -C ₄ H ₉	1.1 (110)	0.20 (110)	N.A.
S(+)-117d	H	<i>n</i> -C ₄ H ₉	21.8 (40)	15.2 (45)	N.A.
R(-)-117d	H	<i>n</i> -C ₄ H ₉	0.7 (120)	0.10 (110)	N.A.
(±)- 117e	H	C ₆ H ₅	0.26 (80)	0.24 (45)	N.A.
S(+)-117e	H	C ₆ H ₅	0.16 (120)	0.18 (50)	N.A.
R(-)-117e	H	C ₆ H ₅	N.A.	N.A.	N.A.
(±)- 117f	CH ₃	C ₂ H ₅	1.5 (70)	N.A.	N.A.
S(+)-117f	CH ₃	C ₂ H ₅	2.1 (80)	N.A.	N.A.
R(-)-117f	CH ₃	C ₂ H ₅	4.8 (50)	N.A.	N.A.
118	CH ₃	CH ₃	3.7 (50)	N.A.	N.A.
46a			3.4 ± 1.6 (75)	3.8 ± 1.5 (70)	N.A.
fMLF			0.01	20.4	1.9
WKYMVm			0.5	0.001	0.01

^aN.A., no activity was observed (no response was observed during first 2 min after addition of compounds under investigation) considering the limits of efficacy > 20 % and EC₅₀ < 50 μM. The EC₅₀ values are presented as the mean ± S.D. of three independent experiments, in which median effective concentration values (EC₅₀) were determined by nonlinear regression analysis of the dose-response curves (5-6 points) generated using GraphPad Prism 5 with 95% confidential interval (*p* < 0.05). Efficacy (in bracket) is expressed as percent of the response induced by 5 nM fMLF (FPR1) or 5 nM WKYMVm (FPR2 and FPR3).

This behaviour was mainly confirmed by testing *n*-propyl and *i*-propyl derivatives (\pm)-**117b** and (\pm)-**117c**. In this case the (+)-forms were completely inactive, while enantiomers **R(-)-117b** and **R(-)-117c**

showed an increase of activity being their EC_{50} in the sub-micromolar and low micromolar range respectively (**table 4.7**). Elongation of carbon chain on the chiral center gave *n*-butyl derivative (\pm)-**117d** which, even if it showed less stereoselectivity, in his (-)-form resulted the most potent FPR1/FPR2 mixed agonist of the series ($EC_{50} = 100$ nM for FPR2). Introduction of a phenyl group in the chiral center gave racemate (\pm)-**117e** having an activity in the sub-micromolar range. In this case, enantiomer **S-(+)-117e** is more potent of its racemate, while **R-(-)-117e** is completely devoid of activity. This is a surprising result in terms of stereoselectivity, also taking into account that the previously discussed alkyl derivatives have always in their R-(-)-forms the most potent compounds of each pair (see enantiomers (-)-**95b** and (-)-**117a-d**, **table 4.7**). Introduction of an additional alkyl group on the chiral center raised a complete loss of stereoselectivity and a total shift of activity toward FPR1. Indeed compounds (+)-**117f** and (-)-**117f**, bearing on the chiral center a methyl and an ethyl group, are selective agonists of FPR1 and their racemate (\pm)-**117f** resulted more potent than the pure enantiomers on the same receptor. In this case the sterical hindrance on the chiral center seemed to be the main determinant for the activity and the selectivity, and this result was confirmed again by testing the non chiral analogue **118**, which is as well a selective and relatively potent FPR1 agonist.

4.1.7 Evaluation of chemotactic activity and Ca^{2+} mobilization

Compounds that showed the best agonistic profiles were as well selected to evaluate their activity as chemotactic agents and their ability to produce Ca^{2+} mobilization in human neutrophils.

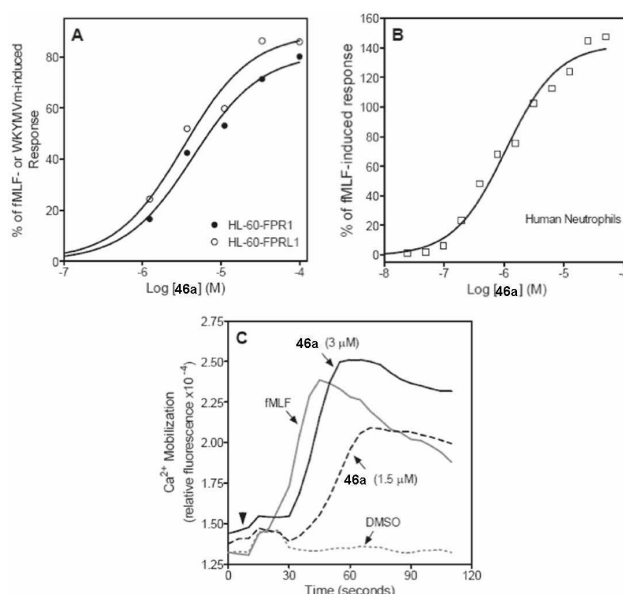


Figure 4.1. Analysis of Ca^{2+} mobilization in phagocytes treated with compound **46a**. HL-60-FPR1 and HL-60-FPR2 cells (A) or human neutrophils (B) were loaded with FLIPR calcium 3 dye, and Ca^{2+} flux was analyzed, as described in **section 6**. Responses were normalized to the response induced by 5 nM fMLF for HL-60-FPR1 cells and neutrophils, or 5 nM WKYMVm for HL-60-FPR2 cells, which were assigned a value of 100%. (C) Representative kinetics of Ca^{2+} mobilization after treatment with compound **46a** or fMLF. Human neutrophils were treated with the compound **46a** (1.5 and 3 μ M), 5 nM fMLF (positive control), or 1% DMSO (negative control), and Ca^{2+} flux was monitored for the indicated times. The data are from one experiment that is representative of three independent experiments.

4. Results and Conclusions

Table 4.8. Ca²⁺ mobilization and chemotactic activity in human neutrophils treated with selected FPR1/FPRL1 agonists.

Compd	EC ₅₀ (μM)	
	Ca ²⁺ mobilization	Chemotaxis
46a	2.6 ± 0.3	2.1 ± 0.8
46d	3.9 ± 0.6	8.2 ± 1.4
46e	6.7 ± 1.1	1.6 ± 0.2
46f	3.2 ± 1.2	1.8 ± 0.3
46h	3.2 ± 0.3	0.6 ± 0.3
46j	1.6 ± 0.8	0.9 ± 0.2
46l	1.1 ± 0.6	1.1 ± 0.6
46m	3.6 ± 1.0	1.2 ± 0.6
46n	3.6 ± 0.8	4.5 ± 2.5
46r	21.7 ± 4.2	1.9 ± 0.6
61e	4.3 ± 1.1	13.1 ± 2.3
95a	11.3 ± 2.8	11.8 ± 2.6
(±)-95b	0.8 ± 0.2	0.6 ± 0.4

The data are presented as the mean ± S.D. of three independent experiments with cells from different donors, in which median effective concentration values (EC₅₀) were determined by nonlinear regression analysis of the dose-response curves (5-6 points) generated using GraphPad Prism 5 with 95% confidential interval ($p < 0.05$).

Some of these FPRs agonists proved to be able to stimulate chemotaxis at sub-micromolar concentrations (**table 4.8**). Furthermore, the effect of selected agonists on Ca²⁺ flux in human neutrophils was also determined to verify if the results coming from HL-60 tests were confirmed in primary phagocytes (**table 4.8**). We usually found that both selective and nonselective agonists identified in HL-60 cell assays also induced Ca²⁺ flux in human neutrophils, with EC₅₀ values in the range 0.8-21.7 μM. Among compounds tested to evaluate the chemotactic activity, the most potent resulted **46h** (EC₅₀ = 0.6 μM) and **46j** (EC₅₀ = 0.9 μM), which were both FPR1/FPR2 nonselective agonists. It is noteworthy that the FPR2-selective agonist (**61e**) showed lower potency (EC₅₀ = 13.1 μM) as chemotactic agent.

For lead compound **46a** were also calculated dose-response curves as shown in **figure 4.1**.

4.2 Conclusions

In conclusion, the data acquired and processed till now showed that we have identified a novel chemotype endowed with interesting selective or mixed FPR1/FPR2 agonistic activity in human neutrophils. From biological tests it resulted evident that, by manipulating the chemical structure of a series of *N*-arylacetamide pyridazinones (**46a-s**, **scheme 12**, **table 4.1**), it is possible to achieve potency and selectivity towards FPR1 and FPR2 subtype receptors.

Going to analyse the data in our hands, we can observe that regarding the aromatic system at the end of the functionalized chain in position 2 (**scheme 12**, **table 4.1**), the presence of a lipophilic and/or electronegative substituent, such as F, Br, I or CH₃, in position para is an essential requirement for potency and/or selectivity.

The position 6 (**table 4.2**) of the pyridazinone ring resulted poorly tolerant to modifications. A methyl group is the substituent that gives the best results regarding the activity as agonist, while its elimination or substitution with more hindered moiety produce a deep loss of activity.

Likewise, the presence of an acetamide spacer at N-2 of the pyridazinone ring also plays a crucial role in specificity and potency (**table 4.6**). The role of both CO and NH in the side chain seems to indicate that a hydrogen bond donor (HBD) neighbouring an acceptor (HBA) system is also an essential requirement for binding at FPRs. Moreover, this HBD\HBA system must be placed at an appropriate distance from both the aromatic and the heterocyclic scaffold. The very low activity of the thioamide analogue **105** (**table 4.6**) further support this hypothesis.

Differently, the position 4 (**tables 4.3-4.5**) resulted more amenable to chemical manipulation, indeed heterocycles (e.g. thienyl, piridyl, furyl) or substituted benzyl groups and functionalised spacers (e.g. CO, NH) can be productively introduced at this level, retaining a good agonistic activity.

Lastly, the chiral compounds reported in this work (**table 4.7**) represent a series of homologues differently hindered at stereocenter level and all of them show a different affinity for the three FPR isoforms. Enantioselectivity showed from the R-(-)-enantiomers, among the alkyl derivatives, may be related to the ability of these compounds to establish a better interaction with the receptors, compared to the respective S-(+)-forms. On the other hand, for enantiomers S-(+)-**117e** and R-(-)-**117e** the activity of the pure enantiomers resulted exactly the opposite, probably due to the high hindrance and lipophilicity of the phenyl group. Furthermore, in contrast with compounds having just one alkyl group on the chiral center, dialkylated enantiomers of (\pm)-**117f** did not show enantioselectivity and in addition, chirality doesn't seem crucial for the activity. This result was evident testing non chiral dimethyl analogue **118**; however both dimethyl and chiral ethyl-methyl derivatives showed selectivity for FPR1.

Work is underway and further modification have been planned to develop new FPRs agonists hoping they may be useful to gain further structure-activity relationships in this class of compounds in order to optimize the potency and selectivity and to increase the knowledge of the pharmacological basis of FPRs binding and signalling.

5. EXPERIMENTAL CHEMISTRY

5.1 Materials and Methods

Reagents and starting materials were obtained from commercial sources. Extracts were dried over Na_2SO_4 , and the solvents were removed under reduced pressure. All reactions were monitored by thin layer chromatography (TLC) using commercial plates precoated with Merck silica gel 60 F-254. Visualization was performed by UV fluorescence ($\lambda_{\text{max}} = 254 \text{ nm}$) or by staining with iodine or potassium permanganate. Chromatographic separations were performed on a silica gel column by gravity chromatography (Kieselgel 40, 0.063-0.200 mm; Merck), flash chromatography (Kieselgel 40, 0.040-0.063 mm; Merck), silica gel preparative TLC (Kieselgel 60 F₂₅₄, 20 x 20 cm, 2 mm), or CombiFlash[®] Rf System (using RediSep[®] Rf Silica Columns, Teledyne Isco, Lincoln, Nebraska, USA). Yields refer to chromatographically and spectroscopically pure compounds, unless otherwise stated. When reactions were performed in anhydrous conditions, the mixtures were maintained under nitrogen atmosphere. Compounds were named following IUPAC rules as applied by Beilstein-Institut AutoNom 2000 (4.01.305) or CA Index Name.

The identity and purity of intermediates and final compounds was ascertained through NMR and TLC chromatography. All melting points were determined on a microscope hot stage Büchi apparatus and are uncorrected.

¹H NMR spectra were recorded with Avance 400 instruments (Bruker Biospin Version 002 with SGU). Chemical shifts (δ) are reported in ppm to the nearest 0.01 ppm, using the solvent as internal standard. Coupling constants (J values) are given in Hz and were calculated using 'TopSpin 1.3' software rounded to the nearest 0.1 Hz. Data are reported as follows: chemical shift, multiplicity [exch, exchange; br, broad; s, singlet; d, doublet; t, triplet; q, quartet; quin, quintet; sext, sextet; sept, septet; m, multiplet; or as a combination of these (e.g. dd, dt *etc.*)], integration, assignment and coupling constant(s). Diastereotopic protons are assigned as CH-*H*. Mass spectra (m/z) were recorded on a ESI-TOF mass spectrometer (Bruker Micro TOF) and reported mass values are within the error limits of ± 5 ppm mass units. IR spectra were measured as Nujol mulls for solids and neat for liquids with a PerkinElmer Spectrum (RX I FT-IR, Spectrum 1000) spectrometer. Absorption maxima (λ_{max}) are reported in wavenumbers (cm^{-1}).

Semi-preparative HPLC enantioseparations were performed using stainless-steel Chiralcel OD[®] (250 mm x 4.6 mm I.D., 10 μm particle size, Chiral Technologies Europe, Illkirch, France) and Lux Amylose-2[®] (250 mm x 4.6 mm I.D., 5 μm particle size, Phenomenex, Bologna, Italy) columns. The HPLC apparatus consisted of a Perkin-Elmer (Norwalk, CT) series 200 composed by quaternary pump, autosampler, Peltier column oven and UV-VIS detector coupled with a Biologic BioFrac fraction collector (from Bio-Rad, Milan, Italy). UV detector wavelength was fixed at 250 nm. HPLC-grade solvents were supplied by Sigma-Aldrich (Milan, Italy). The mobile phases were a mixtures of *n*-hexane/IPA and they were degassed by sonication just before use. The signal was acquired and processed by Totalchrom 6.3.1.0504

5. Experimental Chemistry

software. The values of retention time (t_R) are given in minutes. After semipreparative separation, the collected fractions were analyzed on the same HPLC instrument by chiral Lux Amylose-2[®] (50 mm x 4.6 mm I.D., 3 μ m particle size, Phenomenex, Bologna, Italy) column to determine their enantiomeric excess (ee). The ee values were calculated from relative peak areas of enantiomeric pairs. The mobile phase was *n*-hexane/IPA 60:40. In analytical enantioseparations, a standard solution was prepared by diluting 0.1 mg of compounds into 1 mL of ethanol. The injection volume was 10 μ L, the flow rate 1.0 mL/min, the temperature of column was 40 °C and UV detector wavelength was fixed at 250 nm.

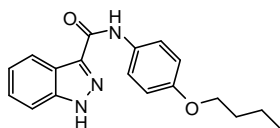
Specific rotations of enantiomers were measured at 589 nm with a Perkin-Elmer polarimeter model 241 equipped with a Na lamp. The volume of the cell was 2 mL, and the optical path was 10 cm. A standard solution was prepared by dissolving 20 mg of compounds into 2 mL of CHCl₃ ($c = 1$). The system was set at a temperature of 20 °C using a Neslab RTE 740 cryostat.

The circular dichroism (CD) spectra of enantiomers, dissolved in methanol (concentrations are about 0.25 mg/mL for analytes and 1 mg/mL for reference molecules) in a quartz cell (0.1 cm-path length) at 25 °C were measured using a Jasco model J-810 spectropolarimeter (Jasco, Ishikawa-cho, Hachioji City, Tokyo, Japan). The spectra were averaged over five instrumental scans from 350 to 215 nm at 50nm/min scanning speed, acquired and processed with Spectra Analysis software and the intensities are presented in terms of ellipticity values (mdeg).

5.2 Experimental

General Procedure for 1a,b. To a cooled (0 °C) and stirred suspension of commercially available indazole-3-carboxylic or indole-3-carboxylic acid (1.55 mmol) in SOCl₂ (3 mL), Et₃N (0.2 mL) was added. After 1 h at 60 °C, the mixture was cooled and the excess of SOCl₂ was removed in vacuo. The residue was then dissolved in anhydrous THF (1.5 mL) and cooled at 0 °C. A solution of 4-*n*-butoxyaniline (3.10 mmol) in anhydrous THF (1 mL) was added dropwise and the reaction was carried out at room temperature for 12 h. The mixture was concentrated in vacuo, diluted with ice-cold water (10 mL) and kept under stirring at 0 °C for 0.5 h; then the precipitate was filtered off and purified by crystallization from ethanol to afford intermediate compounds **1a,b**.

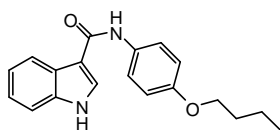
5.2.1 *N*-(4-Butoxyphenyl)-1*H*-indazole-3-carboxamide (**1a**)



Yield = 97 %; mp = 157-159 °C (EtOH). ¹H NMR (CDCl₃) δ 1.01 (t, 3H, CH₂CH₃, $J = 6.7$ Hz), 1.52 (sext, 2H, CH₂CH₃, $J = 7.4$ Hz), 1.80 (quin, 2H, CH₂CH₂CH₂, $J = 6.9$ Hz), 4.00 (t, 2H, OCH₂, $J = 6.6$ Hz), 6.94 (d, 2H, Ar, $J = 8.3$ Hz), 7.36 (t, 1H, Ar, $J = 8.0$ Hz), 7.50 (t, 1H, Ar, $J = 8.4$ Hz), 7.57 (d, 1H,

Ar, $J = 8.4$ Hz), 7.67 (d, 2H, Ar, $J = 8.3$ Hz), 8.49 (d, 1H, Ar, $J = 8.2$ Hz), 8.85 (exch br s, 1H, NH), 10.42 (exch br s, 1H, NH).

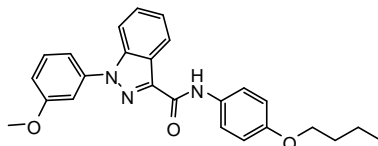
5.2.2 *N*-(4-Butoxyphenyl)-1*H*-indole-3-carboxamide (**1b**)



Yield = 94 %; mp = 181-182 °C (EtOH). $^1\text{H NMR}$ (CDCl_3) δ 1.01 (t, 3H, CH_2CH_3 , $J = 7.3$ Hz), 1.52 (sext, 2H, CH_2CH_3 , $J = 7.5$ Hz), 1.79 (quin, 2H, $\text{CH}_2\text{CH}_2\text{CH}_2$, $J = 6.7$ Hz), 3.97 (t, 2H, OCH_2 , $J = 6.4$ Hz), 6.93 (d, 2H, Ar, $J = 8.4$ Hz), 7.31 (t, 2H, Ar, $J = 3.2$ Hz), 7.48 (d, 1H, Ar, $J = 5.9$ Hz), 7.56 (d, 2H, Ar, $J = 8.5$ Hz), 7.86 (s, 1H, Ar), 8.06 (d, 1H, Ar, $J = 3.7$ Hz), 8.78 (exch br s, 1H, NH), 9.21 (exch br s, 1H, NH).

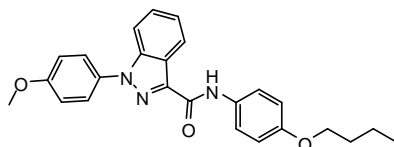
General Procedure for 2a-d. To the suspension of **1a** or **1b** (0.32 mmol), copper acetate (0.48 mmol) and 3- or 4-methoxyphenylboronic acid (0.64 mmol) in CH_2Cl_2 (2 mL), Et_3N (0.96 mmol) was added and the mixture was stirred at room temperature for 5-12 h. The suspension was extracted with 15% aqueous ammonia (10 mL), and the organic layer was washed with 10 mL of water and dried over Na_2SO_4 . After removal of the solvent under reduced pressure, the residue was purified by flash column chromatography using as eluents CH_2Cl_2 for **2a,b** and $\text{CH}_2\text{Cl}_2/\text{MeOH}$ 99:1 for **2c,d**.

5.2.3 *N*-(4-Butoxyphenyl)-1-(3-methoxyphenyl)-1*H*-indazole-3-carboxamide (**2a**)



Yield = 46 %; colorless-yellowish oil. $^1\text{H NMR}$ (CDCl_3) δ 1.01 (t, 3H, CH_2CH_3 , $J = 7.4$ Hz), 1.53 (sext, 2H, CH_2CH_3 , $J = 7.4$ Hz), 1.80 (quin, 2H, $\text{CH}_2\text{CH}_2\text{CH}_2$, $J = 8.1$ Hz), 3.94 (s, 3H, OCH_3), 4.00 (t, 2H, OCH_2 , $J = 6.5$ Hz), 6.95 (d, 2H, Ar, $J = 7.9$ Hz), 7.03 (dd, 1H, Ar, $J = 6.1$ Hz, $J = 2.2$ Hz), 7.36 (s, 1H, Ar), 7.38 (dd, 1H, Ar, $J = 1.0$ Hz, $J = 1.0$ Hz), 7.42 (d, 1H, Ar, $J = 7.9$ Hz), 7.52 (t, 2H, Ar, $J = 8.2$ Hz), 7.68 (d, 2H, Ar, $J = 8.9$ Hz), 7.77 (d, 1H, Ar, $J = 8.6$ Hz), 8.56 (d, 1H, Ar, $J = 8.1$ Hz), 8.86 (exch br s, 1H, NH).

5.2.4 *N*-(4-Butoxyphenyl)-1-(4-methoxyphenyl)-1*H*-indazole-3-carboxamide (**2b**)

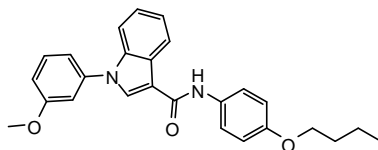


Yield = 60 %; colorless-yellowish oil. $^1\text{H NMR}$ (CDCl_3) δ 1.01 (t, 3H, CH_2CH_3 , $J = 7.5$ Hz), 1.53 (sext, 2H, CH_2CH_3 , $J = 7.4$ Hz), 1.80 (quin, 2H, $\text{CH}_2\text{CH}_2\text{CH}_2$, $J = 8.0$ Hz), 3.94 (s, 3H, OCH_3), 4.00 (t, 2H,

5. Experimental Chemistry

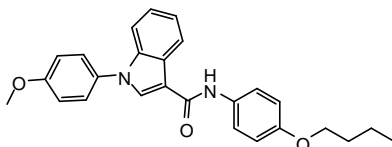
OCH₂, $J = 6.6$ Hz), 6.94 (d, 2H, Ar, $J = 8.8$ Hz), 7.13 (d, 2H, Ar, $J = 9.0$ Hz), 7.39 (t, 1H, Ar, $J = 7.0$ Hz), 7.49 (t, 1H, Ar, $J = 8.4$ Hz), 7.63-7.70 (m, 5H, Ar), 8.55 (d, 1H, Ar, $J = 8.1$ Hz), 8.85 (exch br s, 1H, NH).

5.2.5 *N*-(4-Butoxyphenyl)-1-(3-methoxyphenyl)-1*H*-indole-3-carboxamide (**2c**)



Yield = 23 %; colorless-yellowish oil. ¹H NMR (CDCl₃) δ 1.01 (t, 3H, CH₂CH₃, $J = 7.4$ Hz), 1.53 (sext, 2H, CH₂CH₃, $J = 7.4$ Hz), 1.80 (quin, 2H, CH₂CH₂CH₂, $J = 7.8$ Hz), 3.90 (s, 3H, OCH₃), 4.00 (t, 2H, OCH₂, $J = 6.6$ Hz), 6.94 (d, 2H, Ar, $J = 6.5$ Hz), 7.01 (d, 1H, Ar, $J = 8.2$ Hz), 7.06 (s, 1H, Ar), 7.12 (d, 1H, Ar, $J = 7.4$ Hz), 7.36 (quin, 2H, Ar, $J = 7.3$ Hz), 7.48 (t, 1H, Ar, $J = 8.0$ Hz), 7.56-1.62 (m, 3H, Ar), 7.94 (br s, 1H, Ar), 8.15 (d, 2H, Ar, $J = 7.2$ Hz), 9.72 (exch br s, 1H, NH).

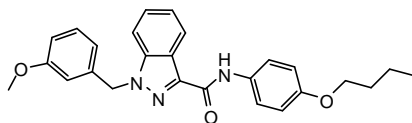
5.2.6 *N*-(4-Butoxyphenyl)-1-(4-methoxyphenyl)-1*H*-indole-3-carboxamide (**2d**)



Yield = 15 %; colorless-yellowish oil. ¹H NMR (CDCl₃) δ 1.01 (t, 3H, CH₂CH₃, $J = 7.4$ Hz), 1.48 (sext, 2H, CH₂CH₃, $J = 7.4$ Hz), 1.80 (quin, 2H, CH₂CH₂CH₂, $J = 7.8$ Hz), 3.92 (s, 3H, OCH₃), 4.00 (t, 2H, OCH₂, $J = 6.5$ Hz), 6.94 (d, 2H, Ar, $J = 8.9$ Hz), 7.08 (d, 2H, Ar, $J = 8.8$ Hz), 7.33 (quin, 2H, Ar, $J = 8.1$ Hz), 7.42 (d, 2H, Ar, $J = 8.7$ Hz), 7.47 (d, 1H, Ar, $J = 8.3$ Hz), 7.57 (d, 2H, Ar, $J = 8.9$ Hz), 7.88 (br s, 1H, Ar), 8.14 (d, 1H, Ar, $J = 7.2$ Hz).

General Procedure for 3a-h. Compounds **3a-h** were obtained starting from **1a** for **3a-d** and from **1b** for **3e-h** respectively. A mixture of **1a** or **1b** (0.32 mmol), K₂CO₃ (0.65 mmol), and the appropriate substituted benzyl halide (0.36 mmol) in anhydrous acetone (2 mL) was refluxed under stirring for 2-10 h. The mixture was then concentrated in vacuo, diluted with cold water, and extracted with CH₂Cl₂ (3 x 15 mL). The organic layer was dried with Na₂SO₄, evaporated in vacuo, and compounds **3a-h** were purified by column chromatography using alternatively CH₂Cl₂ (for **3a-d,g**) or CH₂Cl₂/MeOH 99:1 (for **3e,f,h**) as eluent.

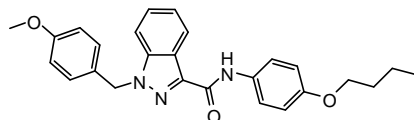
5.2.7 *N*-(4-Butoxyphenyl)-1-(3-methoxybenzyl)-1*H*-indazole-3-carboxamide (**3a**)



Yield = 65 %; colorless-yellowish oil. ¹H NMR (CDCl₃) δ 1.00 (t, 3H, CH₂CH₃, $J = 7.4$ Hz), 1.52 (sext, 2H, CH₂CH₃, $J = 5.4$ Hz), 1.79 (quin, 2H, CH₂CH₂CH₂, $J = 6.4$ Hz), 3.63 (s, 3H, OCH₃), 4.00 (t, 2H,

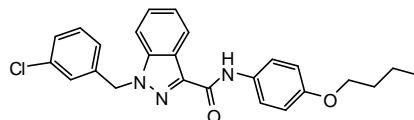
OCH₂, $J = 6.5$ Hz), 5.74 (s, 2H, CH₂N), 6.29 (s, 1H, Ar), 6.80 (d, 1H, Ar, $J = 8.8$ Hz), 6.94 (d, 2H, Ar, $J = 9.0$ Hz), 7.29 (s, 1H, Ar), 7.36 (d, 2H, Ar, $J = 8.8$ Hz), 7.44 (t, 2H, Ar, $J = 8.2$ Hz), 7.66 (d, 2H, Ar, $J = 9.0$ Hz), 8.49 (d, 1H, Ar, $J = 8.2$ Hz), 8.77 (exch br s, 1H, NH).

5.2.8 *N*-(4-Butoxyphenyl)-1-(4-methoxybenzyl)-1*H*-indazole-3-carboxamide (3b)



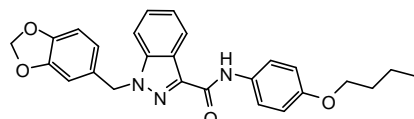
Yield = 73 %; mp = 115-16 °C (EtOH). ¹H NMR (CDCl₃) δ 1.01 (t, 3H, CH₂CH₃, $J = 7.4$ Hz), 1.53 (sext, 2H, CH₂CH₃, $J = 7.4$ Hz), 1.78 (quin, 2H, CH₂CH₂CH₂, $J = 8.0$ Hz), 3.79 (s, 3H, OCH₃), 3.99 (t, 2H, OCH₂, $J = 6.5$ Hz), 5.60 (s, 2H, CH₂N), 6.87 (d, 2H, Ar, $J = 8.5$ Hz), 6.94 (d, 2H, Ar, $J = 8.9$ Hz), 7.19 (d, 2H, Ar, $J = 8.6$ Hz), 7.30-7.34 (m, 1H, Ar), 7.40 (s, 2H, Ar), 7.67 (d, 2H, Ar, $J = 8.9$ Hz), 8.47 (d, 1H, Ar, $J = 8.2$ Hz), 8.80 (exch br s, 1H, NH).

5.2.9 *N*-(4-Butoxyphenyl)-1-(3-chlorobenzyl)-1*H*-indazole-3-carboxamide (3c)



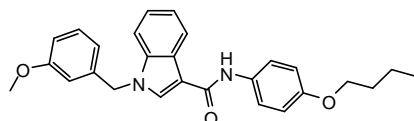
Yield = 86 %; mp = 119-20 °C (EtOH). ¹H NMR (CDCl₃) δ 1.01 (t, 3H, CH₂CH₃, $J = 7.4$ Hz), 1.52 (sext, 2H, CH₂CH₃, $J = 7.6$ Hz), 1.81 (quin, 2H, CH₂CH₂CH₂, $J = 6.6$ Hz), 4.00 (t, 2H, OCH₂, $J = 6.5$ Hz), 5.63 (s, 2H, CH₂N), 6.94 (d, 2H, Ar, $J = 9.0$ Hz), 7.08 (d, 2H, Ar, $J = 6.7$ Hz), 7.24 (s, 1H, Ar), 7.30-7.27 (m, 1H, Ar), 7.33-7.39 (m, 2H, Ar), 7.43-7.47 (m, 1H, Ar), 7.67 (d, 2H, Ar, $J = 9.0$ Hz), 8.49 (d, 1H, Ar, $J = 8.1$ Hz), 8.76 (exch br s, 1H, NH).

5.2.10 1-(1,3-Benzodioxol-5-ylmethyl)-*N*-(4-butoxyphenyl)-1*H*-indazole-3-carboxamide (3d)



Yield = 78 %; mp = 134-35 °C (EtOH). ¹H NMR (CDCl₃) δ 1.01 (t, 3H, CH₂CH₃, $J = 7.3$ Hz), 1.53 (sext, 2H, CH₂CH₃, $J = 7.4$ Hz), 1.76-1.83 (m, 2H, CH₂CH₂CH₂), 4.00 (t, 2H, OCH₂, $J = 6.5$ Hz), 5.56 (s, 2H, CH₂N), 5.95 (s, 2H, OCH₂O), 6.72 (s, 1H, Ar), 6.78 (s, 2H, Ar), 6.94 (d, 2H, Ar, $J = 8.9$ Hz), 7.30-7.34 (m, 1H, Ar), 7.42 (s, 2H, Ar), 7.67 (d, 2H, Ar, $J = 8.9$ Hz), 8.47 (d, 1H, Ar, $J = 8.1$ Hz), 8.78 (exch br s, 1H, NH).

5.2.11 *N*-(4-Butoxyphenyl)-1-(3-methoxybenzyl)-1*H*-indole-3-carboxamide (3e)

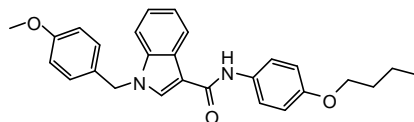


Yield = 58 %; mp = 166-67 °C (EtOH). ¹H NMR (CDCl₃) δ 1.01 (t, 3H, CH₂CH₃, $J = 7.3$ Hz), 1.52 (sext, 2H, CH₂CH₃, $J = 7.6$ Hz), 1.80 (quin, 2H, CH₂CH₂CH₂, $J = 7.0$ Hz), 3.77 (s, 3H, OCH₃), 3.99 (t, 2H,

5. Experimental Chemistry

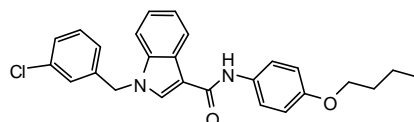
OCH₂, $J = 6.5$ Hz), 5.31 (s, 2H, CH₂N), 6.71 (s, 1H, Ar), 6.75 (d, 1H, Ar, $J = 7.5$ Hz), 6.85 (d, 1H, Ar, $J = 8.3$ Hz), 6.92 (d, 2H, Ar, $J = 8.8$ Hz), 7.25 (d, 1H, Ar, $J = 7.8$ Hz), 7.29-7.33 (m, 2H, Ar), 7.38 (d, 1H, Ar, $J = 8.0$ Hz), 7.53 (d, 2H, Ar, $J = 8.3$ Hz), 7.73 (br s, 1H, Ar), 8.10 (d, 1H, Ar, $J = 7.1$ Hz).

5.2.12 *N*-(4-Butoxyphenyl)-1-(4-methoxybenzyl)-1*H*-indole-3-carboxamide (3f)



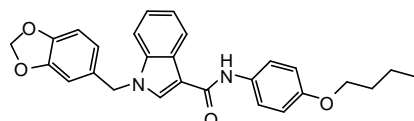
Yield = 29 %; mp = 160-62 °C (EtOH). ¹H NMR (CDCl₃) δ 1.01 (t, 3H, CH₂CH₃, $J = 7.4$ Hz), 1.52 (sext, 2H, CH₂CH₃, $J = 7.6$ Hz), 1.79 (quin, 2H, CH₂CH₂CH₂, $J = 7.1$ Hz), 3.81 (s, 3H, OCH₃), 3.98 (t, 2H, OCH₂, $J = 6.6$ Hz), 5.28 (s, 2H, CH₂N), 6.89 (q, 4H, Ar, $J = 8.4$ Hz), 7.13 (d, 2H, Ar, $J = 8.7$ Hz), 7.29-7.34 (m, 2H, Ar), 7.40 (d, 1H, Ar, $J = 8.8$ Hz), 7.53 (d, 2H, Ar, $J = 8.9$ Hz), 7.73 (br s, 1H, Ar), 8.10 (d, 1H, Ar, $J = 12.1$ Hz).

5.2.13 *N*-(4-Butoxyphenyl)-1-(3-chlorobenzyl)-1*H*-indole-3-carboxamide (3g)



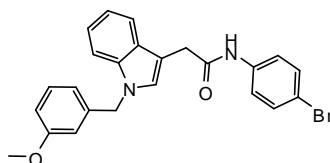
Yield = 51 %; mp = 136-37 °C (EtOH). ¹H NMR (CDCl₃) δ 1.01 (t, 3H, CH₂CH₃, $J = 7.3$ Hz), 1.52 (sext, 2H, CH₂CH₃, $J = 7.6$ Hz), 1.80 (quin, 2H, CH₂CH₂CH₂, $J = 7.0$ Hz), 3.99 (t, 2H, OCH₂, $J = 6.5$ Hz), 5.32 (s, 2H, CH₂N), 6.92 (d, 2H, Ar, $J = 8.9$ Hz), 7.02 (d, 1H, Ar, $J = 7.1$ Hz), 7.17 (s, 1H, Ar), 7.25-7.34 (m, 5H, Ar), 7.53 (d, 2H, Ar, $J = 8.3$ Hz), 7.75 (br s, 1H, Ar), 8.10 (d, 1H, Ar, $J = 8.4$ Hz).

5.2.14 1-(1,3-Benzodioxol-5-ylmethyl)-*N*-(4-butoxyphenyl)-1*H*-indole-3-carboxamide (3h)



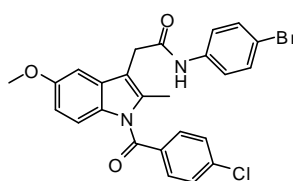
Yield = 42 %; mp = 165-67 °C (EtOH). ¹H NMR (CDCl₃) δ 1.01 (t, 3H, CH₂CH₃, $J = 7.4$ Hz), 1.52 (sext, 2H, CH₂CH₃, $J = 7.4$ Hz), 1.80 (quin, 2H, CH₂CH₂CH₂, $J = 6.8$ Hz), 3.99 (t, 2H, OCH₂, $J = 6.6$ Hz), 5.23 (s, 2H, CH₂N), 5.96 (s, 2H, OCH₂O), 6.64 (s, 1H, Ar, $J = 8.4$ Hz), 6.71 (d, 1H, Ar, $J = 7.9$ Hz), 6.78 (d, 1H, Ar, $J = 7.9$ Hz), 6.92 (d, 2H, Ar, $J = 8.9$ Hz), 7.31-7.33 (m, 2H, Ar), 7.40 (m, 1H, Ar), 7.53 (d, 2H, Ar, $J = 8.2$ Hz), 7.71 (br s, 1H, Ar), 8.09 (d, 1H, Ar, $J = 7.7$ Hz).

5.2.15 *N*-(4-Bromophenyl)-2-(1-(3-methoxybenzyl)-1*H*-indol-3-yl)acetamide (5)



A mixture of **4** (0.46 mmol), K_2CO_3 (0.92 mmol) and 3-methoxybenzyl chloride (0.69 mmol) in anhydrous acetone (3 mL) was refluxed under stirring for 4 h and then concentrated in vacuo. After dilution with cold water, it was extracted with CH_2Cl_2 (3 x 15 mL) and the solvent was evaporated in vacuo to afford the crude **5**, which was purified by column chromatography using toluene/ethyl acetate 7:3 as eluent. Yield = 29 %; mp = 153-55 °C (EtOH). 1H NMR ($CDCl_3$) δ 3,77 (s, 3H, OCH_3); 3,90 (s, 2H, $COCH_2$); 5,33 (s, 2H, CH_2N); 6,68 (s, 1H, CH); 6,76 (d, 1H, Ar, $J = 7.1$ Hz); 7,84 (dd, 1H, Ar, $J = 8.5$ Hz, $J = 1.9$ Hz); 7,17-7,30 (m, 5H, Ar); 7,36-7,41 (m, 4H, Ar); 7,63 (d, 1H, Ar, $J = 8.2$ Hz).

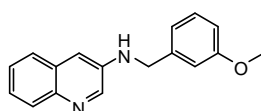
5.2.16 *N*-(4-Bromophenyl)-2-[1-(4-chlorobenzoyl)-5-methoxy-2-methyl-1*H*-indol-3-yl]acetamide (**6**)



To a solution of indomethacin (0.28 mmol) in anhydrous CH_2Cl_2 (5 ml) were added DCC (0.28 mmol) and 4-Bromoaniline (0.28 mmol). The reaction mixture was stirred at room temperature for 24 h. The solid residue was filtered off in vacuo and the solution was washed with HCl 2 N (2 x 10 mL) and with H_2O (10 mL). The organic phase was dried over $NaSO_4$ and concentrated under reduce pressure. The resulting residue was purified by flash column chromatography using $CH_2Cl_2/MeOH$ 99:1 as eluent to furnish **6** as a white solid. Yield = 35 %; mp = 200-01 °C (EtOH). 1H NMR ($CDCl_3$) δ 2,48 (s, 3H, CH_3); 3,83 (s, 5H, $OCH_3 + COCH_2$); 6,74 (dd, 1H, Ar, $J = 6.6$ Hz, $J = 2.5$ Hz); 6,88 (d, 1H, Ar, $J = 9.1$ Hz); 6,94 (d, 1H, Ar, $J = 2.3$ Hz); 7,25 (exch, br, s, 1H, NH); 7,31 (d, 2H, Ar, $J = 8.8$ Hz); 7,41 (d, 2H, Ar, $J = 8.7$ Hz); 7,52 (d, 2H, Ar, $J = 8.4$ Hz); 7,71 (d, 2H, Ar, $J = 8.4$ Hz).

General Procedure for 7a-d. A mixture of 3-aminoquinoline (0.69 mmol), K_2CO_3 (1.38 mmol) and the appropriate substituted benzyl halide (0.69 mmol) in anhydrous acetone (3 mL) was refluxed under stirring for 1-3 h. Extra benzyl halide (0.69 mmol) was added and the reaction was kept refluxing for additional 2-4 h. The mixture was then concentrated in vacuo, diluted with cold water and extracted with CH_2Cl_2 (3 x 15 mL). The organic layer was dried over Na_2SO_4 and evaporated in vacuo to afford the crude compounds **7a-d** which were purified by column chromatography using cyclohexane/ethyl acetate 1:2 (for **7a,b,d**) or 2:1 (for **7c**) respectively as eluent.

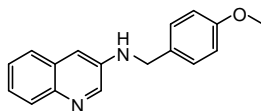
5.2.17 *N*-(3-Methoxybenzyl)quinolin-3-amine (**7a**)



5. Experimental Chemistry

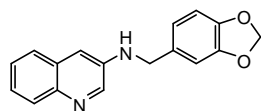
Yield = 49 %; clear oil. $^1\text{H NMR}$ (CDCl_3) δ 3.82 (s, 3H, OCH_3), 4.44 (s, 2H, CH_2N), 4.67 (exch br s, 1H, NH), 6.86 (dd, 1H, Ar, $J = 8.2$ Hz, $J = 2.5$ Hz), 6.98 (s, 1H, Ar), 7.02 (d, 1H, Ar, $J = 7.6$ Hz), 7.07 (d, 1H, Ar, $J = 2.7$ Hz), 7.31 (t, 1H, Ar, $J = 7.9$ Hz), 7.43-7.45 (m, 2H, Ar), 7.59-7.61 (m, 2H, Ar), 7.98-8.01 (m, 1H, Ar), 8.59 (d, 1H, Ar, $J = 2.8$ Hz).

5.2.18 *N*-(4-Methoxybenzyl)quinolin-3-amine (7b)



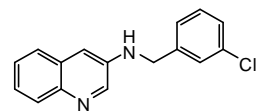
Yield = 60 %; mp = 80-82 °C (EtOH). $^1\text{H NMR}$ (CDCl_3) δ 3.83 (s, 3H, OCH_3), 4.37 (s, 2H, CH_2N), 4.43 (exch br s, 1H, NH), 6.92 (d, 2H, Ar, $J = 8.7$ Hz), 7.05 (d, 1H, Ar, $J = 2.7$ Hz), 7.34 (d, 2H, Ar, $J = 8.6$ Hz), 7.42-7.44 (m, 2H, Ar), 7.59-7.63 (m, 1H, Ar), 7.95-7.98 (m, 1H, Ar), 8.50 (d, 1H, Ar, $J = 2.8$ Hz).

5.2.19 *N*-(1,3-Benzodioxol-5-ylmethyl)quinolin-3-amine (7c)



Yield = 26 %; brown oil. $^1\text{H NMR}$ (CDCl_3) δ 4.40 (s, 2H, CH_2N), 5.21 (exch br s, 1H, NH), 5.97 (s, 3H, OCH_2O), 6.81 (d, 1H, Ar, $J = 7.8$ Hz), 6.91 (d, 1H, Ar, $J = 11.2$ Hz), 7.13 (s, 1H, Ar), 7.46-7.49 (m, 2H, Ar), 7.62-7.65 (m, 1H, Ar), 8.06-8.09 (m, 1H, Ar), 8.78 (s, 1H, Ar).

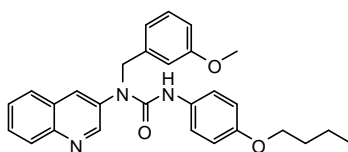
5.2.20 *N*-(3-Chlorobenzyl)quinolin-3-amine (7d)



Yield = 22 %; clear oil. $^1\text{H NMR}$ (CDCl_3) δ 4.51 (d, 2H, CH_2N , $J = 4.5$ Hz), 5.73 (exch br s, 1H, NH), 7.13 (d, 1H, Ar, $J = 2.6$ Hz), 7.29-7.34 (m, 3H, Ar), 7.44 (s, 1H, Ar), 7.49-7.52 (m, 2H, Ar), 7.63-7.65 (m, 1H, Ar), 8.13 (t, 1H, Ar, $J = 6.3$ Hz), 8.94 (s, 1H, Ar).

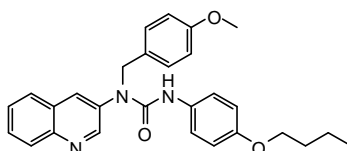
General Procedure for 8a-d. The appropriate amine of type **7** (**7a-d**) (0.34 mmol) was dissolved in 2 mL of anhydrous CH_2Cl_2 and 4-*n*-butoxyphenyl isocyanate (0.37 mmol) was added under stirring. The reaction was carried out at room temperature for 3-8 h, then the solid residue was filtered off and the solution was evaporated in vacuo to afford compounds **8a-d**, which were purified by flash column chromatography using cyclohexane/ethyl acetate 1:1 (for **7a,b**) or 2:1 (for **7c,d**) respectively as eluent.

5.2.21 3-(4-Butoxyphenyl)-1-(3-methoxybenzyl)-1-(quinolin-3-yl)urea (8a)



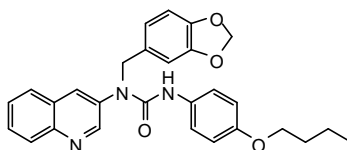
Yield = 58 %; clear oil. $^1\text{H NMR}$ (CDCl_3) δ 0.98 (t, 3H, CH_2CH_3 , $J = 7.4$ Hz), 1.48 (sext, 2H, CH_2CH_3 , $J = 7.6$ Hz), 1.75 (quin, 2H, $\text{CH}_2\text{CH}_2\text{CH}_2$, $J = 7.0$ Hz), 3.77 (s, 3H, OCH_3), 3.93 (t, 2H, OCH_2 , $J = 6.5$ Hz), 5.04 (s, 2H, CH_2N), 6.10 (exch br s, 1H, NH), 6.81-6.84 (m, 3H, Ar), 6.88 (d, 2H, Ar, $J = 7.4$ Hz), 7.19-7.25 (m, 3H, Ar), 7.63 (t, 1H, Ar, $J = 8.2$ Hz), 7.78-7.82 (m, 2H, Ar), 8.01 (s, 1H, Ar), 8.18 (d, 1H, Ar, $J = 8.7$ Hz), 8.79 (d, 1H, Ar, $J = 2.4$ Hz).

5.2.22 3-(4-Butoxyphenyl)-1-(4-methoxybenzyl)-1-(quinolin-3-yl)urea (8b)



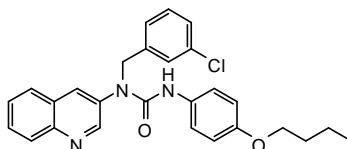
Yield = 47 %; clear oil. $^1\text{H NMR}$ (CDCl_3) δ 0.97 (t, 3H, CH_2CH_3 , $J = 7.4$ Hz), 1.48 (sext, 2H, CH_2CH_3 , $J = 7.6$ Hz), 1.74 (quin, 2H, $\text{CH}_2\text{CH}_2\text{CH}_2$, $J = 7.0$ Hz), 3.79 (s, 3H, OCH_3), 3.92 (t, 2H, OCH_2 , $J = 6.5$ Hz), 4.97 (s, 2H, CH_2N), 6.18 (exch br s, 1H, NH), 6.81 (dd, 4H, Ar, $J = 2.0$ Hz, $J = 6.6$ Hz), 7.21 (dd, 4H, Ar, $J = 6.4$ Hz, $J = 2.1$ Hz), 7.62 (t, 1H, Ar, $J = 7.0$ Hz), 7.78 (t, 2H, Ar, $J = 7.2$ Hz), 7.97 (s, 1H, Ar), 8.14 (d, 1H, Ar, $J = 8.0$ Hz), 8.71 (d, 1H, Ar, $J = 2.3$ Hz).

5.2.23 1-(1,3-Benzodioxol-5-ylmethyl)-3-(4-butoxyphenyl)-1-(quinolin-3-yl)urea (8c)



Yield = 36 %; brown oil. $^1\text{H NMR}$ (CDCl_3) δ 0.97 (t, 3H, CH_2CH_3 , $J = 7.4$ Hz), 1.48 (sext, 2H, CH_2CH_3 , $J = 7.6$ Hz), 1.75 (quin, 2H, $\text{CH}_2\text{CH}_2\text{CH}_2$, $J = 7.0$ Hz), 3.92 (t, 2H, OCH_2 , $J = 6.6$ Hz), 4.96 (s, 2H, CH_2N), 5.96 (s, 3H, OCH_3), 6.20 (exch br s, 1H, NH), 6.65-6.71 (m, 2H, Ar), 6.81 (d, 2H, Ar, $J = 9.0$ Hz), 6.91 (s, 1H, Ar), 7.21 (d, 2H, Ar, $J = 9.0$ Hz), 7.66 (t, 1H, Ar, $J = 7.2$ Hz), 7.82 (q, 2H, Ar, $J = 6.7$ Hz), 8.06 (s, 1H, Ar), 8.21 (d, 1H, Ar, $J = 8.5$ Hz), 8.75 (d, 1H, Ar, $J = 2.4$ Hz).

5.2.24 3-(4-Butoxyphenyl)-1-(3-chlorobenzyl)-1-(quinolin-3-yl)urea (8d)

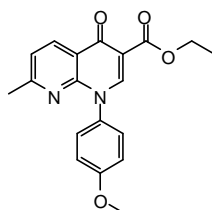


Yield = 44 %; colorless oil. $^1\text{H NMR}$ (CDCl_3) δ 0.98 (t, 3H, CH_2CH_3 , $J = 7.4$ Hz), 1.48 (sext, 2H, CH_2CH_3 , $J = 7.6$ Hz), 1.75 (quin, 2H, $\text{CH}_2\text{CH}_2\text{CH}_2$, $J = 7.1$ Hz), 3.93 (t, 2H, OCH_2 , $J = 6.6$ Hz), 5.03 (s, 2H, CH_2N), 6.33 (exch br s, 1H, NH), 6.82 (d, 2H, Ar, $J = 9.0$ Hz), 7.17-7.26 (m, 5H, Ar), 7.35 (s, 1H, Ar), 7.67 (t, 1H, Ar, $J = 7.8$ Hz), 7.79-7.85 (m, 2H, Ar), 8.06 (s, 1H, Ar), 8.19 (d, 1H, Ar, $J = 8.4$ Hz), 8.77 (d, 1H, Ar, $J = 2.4$ Hz).

5. Experimental Chemistry

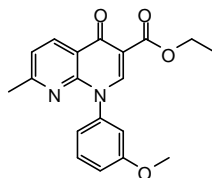
General Procedure for 11a,b. To a suspension of **10** (0.86 mmol), copper acetate (1.29 mmol) and the appropriate butoxyphenylboronic acid (1.72 mmol) in CH₂Cl₂ (2 mL), Et₃N (1.72 mmol) was added. The mixture was stirred at room temperature for 15-20 h. The suspension was extracted with 33% aqueous ammonia/saturated aqueous EDTA 1:1 solution (3 x 10 mL) and the organic layer was washed with 10 mL of water and dried over Na₂SO₄. After removal of the solvent, the residue was purified by flash column chromatography using as eluent cyclohexane/ethyl acetate 1:3.

5.2.25 Ethyl-1-(4-methoxyphenyl)-7-methyl-4-oxo-1,4-dihydro-1,8-naphthyridine-3-carboxylate (**11a**)



Yield = 34 %; mp = 146-47 °C (EtOH). ¹H NMR (CDCl₃) δ 1.42 (t, 3H, CH₂CH₃, *J* = 7.1 Hz), 2.52 (s, 3H, CH₃C=N), 3.92 (s, 3H, OCH₃), 4.41 (q, 2H, OCH₂, *J* = 7.1 Hz), 7.06 (d, 2H, Ar, *J* = 9.0 Hz), 7.25 (d, 1H, Ar, *J* = 8.1 Hz), 7.35 (d, 2H, Ar, *J* = 8.9 Hz), 8.67 (s, 1H, Ar), 8.69 (d, 1H, Ar, *J* = 8.1 Hz).

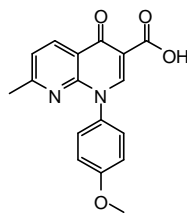
5.2.26 Ethyl-1-(3-methoxyphenyl)-7-methyl-4-oxo-1,4-dihydro-1,8-naphthyridine-3-carboxylate (**11b**)



Yield = 14 %; mp = 165-66 °C (EtOH). ¹H NMR (CDCl₃) δ 1.43 (t, 3H, CH₂CH₃, *J* = 7.1 Hz), 2.54 (s, 3H, CH₃C=N), 3.89 (s, 3H, OCH₃), 4.42 (q, 2H, OCH₂, *J* = 7.1 Hz), 6.99 (t, 1H, Ar, *J* = 2.2 Hz), 7.03 (d, 1H, Ar, *J* = 7.8 Hz), 7.08 (d, 1H, Ar, *J* = 7.7 Hz), 7.27 (d, 1H, Ar, *J* = 8.5 Hz), 7.48 (t, 1H, Ar, *J* = 8.1 Hz), 8.69 (s, 1H, Ar), 8.70 (d, 1H, Ar, *J* = 8.1 Hz).

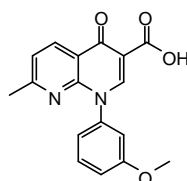
General Procedure for 12a,b. A suspension of the appropriate derivative **11a** or **11b** respectively (0.29 mmol), and 6 N NaOH (3 mL) in ethanol (3 mL) was stirred at rt for 0.5-1 h. The mixture was then concentrated in vacuo, diluted with cold water and acidified with 6 N HCl. The final product was filtered off by suction and recrystallized from ethanol.

5.2.27 1-(4-Methoxyphenyl)-7-methyl-4-oxo-1,4-dihydro-1,8-naphthyridine-3-carboxylic acid (12a)



Yield = ~ 100 %; mp = 268-70 °C (EtOH). ¹H NMR (CDCl₃) δ 2.61 (s, 3H, CH₃C=N), 3.94 (s, 3H, OCH₃), 7.08 (d, 2H, Ar, *J* = 9.0 Hz), 7.35 (d, 2H, Ar, *J* = 9.0 Hz), 7.41 (d, 1H, Ar, *J* = 8.2 Hz), 8.73 (d, 1H, Ar, *J* = 8.2 Hz), 8.97 (s, 1H, Ar), 14.60 (exch br s, 1H, COOH).

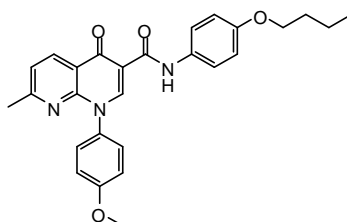
5.2.28 1-(3-Methoxyphenyl)-7-methyl-4-oxo-1,4-dihydro-1,8-naphthyridine-3-carboxylic acid (12b)



Yield = 80 %; mp = 217-19 °C (EtOH). ¹H NMR (CDCl₃) δ 2.61 (s, 3H, CH₃C=N), 3.90 (s, 3H, OCH₃), 6.97 (t, 1H, Ar, *J* = 2.2 Hz), 7.01 (d, 1H, Ar, *J* = 7.8 Hz), 7.12 (d, 1H, Ar, *J* = 6.0 Hz), 7.42 (d, 1H, Ar, *J* = 8.2 Hz), 7.50 (t, 1H, Ar, *J* = 8.1 Hz), 8.74 (d, 1H, Ar, *J* = 8.2 Hz), 8.98 (s, 1H, Ar), 14.58 (exch br s, 1H, COOH).

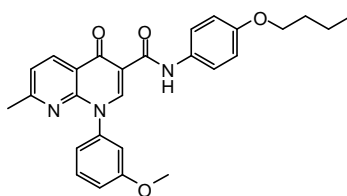
General Procedure for 14a,b. To cooled (0 °C) and stirred suspension of **12a** or **12b** (0.19 mmol) in SOCl₂ (1.5 mL), Et₃N (0.2 mL) was added. After 2-3 h at room temperature the excess of SOCl₂ was removed in vacuo. Due to their instability, the intermediates **13a,b** obtained were not isolated and characterized. Thus, the residue was dissolved in anhydrous THF (2 mL) and cooled to 0 °C. A solution of 4-*n*-butoxyaniline (0.38 mmol) in anhydrous THF (1 mL) was added dropwise to the mixture and the reaction was carried out at room temperature for 2 h. The mixture was concentrated under reduced pressure and, after dilution with ice-cold water (10 mL), the precipitate was then filtered and purified by flash column chromatography using cyclohexane/ethyl acetate 2:1 (for **14a**) or cyclohexane/ethyl acetate 1:1 (for **14b**) as eluent.

5.2.29 *N*-(4-Butoxyphenyl)-1-(4-methoxyphenyl)-7-methyl-4-oxo-1,4-dihydro-1,8-naphthyridine-3-carboxamide (**14a**)



Yield = 35 %; mp = 154-55 °C (EtOH). ¹H NMR (CDCl₃) δ 1.00 (t, 3H, CH₂CH₃, *J* = 7.4 Hz), 1.52 (sext, 2H, CH₂CH₃, *J* = 7.6 Hz), 1.79 (quin, 2H, CH₂CH₂CH₂, *J* = 7.9 Hz), 2.58 (s, 3H, CH₃C=N), 3.94 (s, 3H, OCH₃), 3.99 (t, 2H, OCH₂, *J* = 6.5 Hz), 6.92 (d, 2H, Ar, *J* = 9.0 Hz), 7.07 (d, 2H, Ar, *J* = 8.9 Hz), 7.35 (d, 1H, Ar, *J* = 8.2 Hz), 7.38 (d, 2H, Ar, *J* = 8.9 Hz), 7.70 (d, 2H, Ar, *J* = 9.0 Hz), 8.74 (d, 1H, Ar, *J* = 8.2 Hz), 9.08 (s, 1H, Ar), 11.97 (exch br s, 1H, NH).

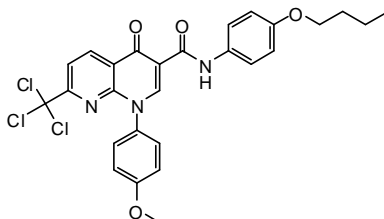
5.2.30 *N*-(4-Butoxyphenyl)-1-(3-methoxyphenyl)-7-methyl-4-oxo-1,4-dihydro-1,8-naphthyridine-3-carboxamide (**14b**)



Yield = 44 %; mp = 203-05 °C (EtOH). ¹H NMR (CDCl₃) δ 1.00 (t, 3H, CH₂CH₃, *J* = 7.4 Hz), 1.52 (sext, 2H, CH₂CH₃, *J* = 7.6 Hz), 1.79 (quin, 2H, CH₂CH₂CH₂, *J* = 7.1 Hz), 2.59 (s, 3H, CH₃C=N), 3.89 (s, 3H, OCH₃), 3.99 (t, 2H, OCH₂, *J* = 6.5 Hz), 6.92 (d, 2H, Ar, *J* = 9.0 Hz), 7.01 (s, 1H, Ar), 7.05 (d, 1H, Ar, *J* = 7.8 Hz), 7.10 (d, 1H, Ar, *J* = 7.7 Hz), 7.35 (d, 1H, Ar, *J* = 8.2 Hz), 7.48 (t, 1H, Ar, *J* = 8.1 Hz), 7.70 (d, 2H, Ar, *J* = 9.0 Hz), 8.74 (d, 1H, Ar, *J* = 8.2 Hz), 9.09 (s, 1H, Ar), 11.95 (exch br s, 1H, NH).

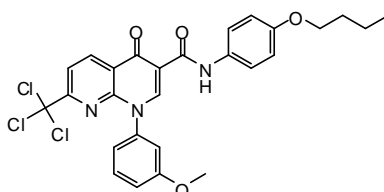
General Procedure for 16a,b. To cooled (0 °C) and stirred suspensions of **12a** or **12b** (0.29 mmol) in SOCl₂ (1.5 mL), Et₃N (0.2 mL) was added. After 2-3 h at 60 °C, the mixture was allowed to cool down and the excess of SOCl₂ was removed in vacuo. Due to their instability, the intermediates **15a,b** obtained were not isolated and characterized. Thus, the residue was dissolved in anhydrous THF (1 mL) and cooled to 0 °C. A solution of 4-*n*-Butoxyaniline (0.58 mmol) in anhydrous THF (1 mL) was added dropwise to the mixture and the reaction was carried out at room temperature for 2 h. The mixture was then concentrated in vacuo and diluted with ice-cold water (10 mL). The precipitate was filtered off and purified by flash column chromatography using CH₂Cl₂ (for **15a**) or CH₂Cl₂/MeOH 99:1 (for **15b**) as eluent.

5.2.31 *N*-(4-Butoxyphenyl)-1-(4-methoxyphenyl)-4-oxo-7-trichloromethyl-1,4-dihydro-1,8-naphthyridine-3-carboxamide (**16a**)



Yield = 49 %; mp = 289-91 °C (EtOH). ^1H NMR (CDCl_3) δ 1.01 (t, 3H, CH_2CH_3 , $J = 7.4$ Hz), 1.52 (sext, 2H, CH_2CH_3 , $J = 7.6$ Hz), 1.81 (quin, 2H, $\text{CH}_2\text{CH}_2\text{CH}_2$, $J = 6.6$ Hz), 3.94 (s, 3H, OCH_3), 4.00 (t, 2H, OCH_2 , $J = 6.5$ Hz), 6.93 (d, 2H, Ar, $J = 9.0$ Hz), 7.07 (d, 2H, Ar, $J = 8.9$ Hz), 7.44 (d, 2H, Ar, $J = 8.9$ Hz), 7.70 (d, 2H, Ar, $J = 9.00$ Hz), 8.15 (d, 1H, Ar, $J = 8.4$ Hz), 9.02 (d, 1H, Ar, $J = 8.4$ Hz), 9.20 (s, 1H, Ar), 11.75 (exch br s, 1H, NH). MS (ESI), calcd. For $\text{C}_{27}\text{H}_{24}\text{Cl}_3\text{N}_3\text{O}_4$, 560,86. Found: m/z 560.36 $[\text{M}]^+$, 562.36 $[\text{M} + \text{H}]^+$.

5.2.32 *N*-(4-Butoxyphenyl)-1-(3-methoxyphenyl)-4-oxo-7-trichloromethyl-1,4-dihydro-1,8-naphthyridine-3-carboxamide (**16b**)

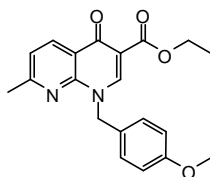


Yield = 54 %; mp = 148-50 °C (EtOH). ^1H NMR (CDCl_3) δ 1.01 (t, 3H, CH_2CH_3 , $J = 7.4$ Hz), 1.52 (sext, 2H, CH_2CH_3 , $J = 7.6$ Hz), 1.80 (quin, 2H, $\text{CH}_2\text{CH}_2\text{CH}_2$, $J = 6.8$ Hz), 3.88 (s, 3H, OCH_3), 3.99 (t, 2H, OCH_2 , $J = 6.5$ Hz), 6.93 (d, 2H, Ar, $J = 8.9$ Hz), 7.08 (s, 1H, Ar), 7.10 (d, 2H, Ar, $J = 8.1$ Hz), 7.49 (t, 1H, Ar, $J = 8.1$ Hz), 7.70 (d, 2H, Ar, $J = 8.9$ Hz), 8.15 (d, 1H, Ar, $J = 8.4$ Hz), 9.02 (d, 1H, Ar, $J = 8.4$ Hz), 9.23 (s, 1H, Ar), 11.73 (exch br s, 1H, NH). MS (ESI), calcd. For $\text{C}_{27}\text{H}_{24}\text{Cl}_3\text{N}_3\text{O}_4$, 560,86. Found: m/z 560.36 $[\text{M}]^+$, 562.36 $[\text{M} + \text{H}]^+$, 584.18 $[\text{M} + \text{Na}]^+$.

General Procedure for 17a-c. A mixture of **10** (0.65 mmol), K_2CO_3 (1.30 mmol), and the appropriate substituted benzyl halide (0.71 mmol) in anhydrous acetone (3 mL) was refluxed under stirring for 5-7 h. The mixture was then concentrated in vacuo, diluted with cold water and extracted with CH_2Cl_2 (3 x 15 mL). The organic layer was dried over Na_2SO_4 , evaporated in vacuo and compounds **17a-c** were purified by column chromatography using alternatively cyclohexane/ethyl acetate 1:6 (for **17a,b**) or cyclohexane/ethyl acetate 1:9 (for **17c**) as eluent.

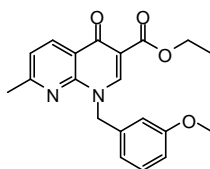
5. Experimental Chemistry

5.2.33 Ethyl-1-(4-methoxybenzyl)-7-methyl-4-oxo-1,4-dihydro-1,8-naphthyridine-3-carboxylate (17a)



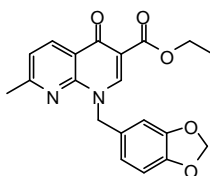
Yield = 35 %; mp = 107-09 °C (EtOH). $^1\text{H NMR}$ (CDCl_3) δ 1.41 (t, 3H, CH_2CH_3 , $J = 7.1$ Hz), 2.69 (s, 3H, $\text{CH}_3\text{C}=\text{N}$), 3.80 (s, 3H, OCH_3), 4.40 (q, 2H, OCH_2 , $J = 7.1$ Hz), 5.59 (s, 2H, NCH_2), 6.88 (d, 2H, Ar, $J = 8.6$ Hz), 7.26 (d, 1H, Ar, $J = 8.1$ Hz), 7.32 (d, 2H, Ar, $J = 8.1$ Hz), 8.66 (d, 1H, Ar, $J = 8.1$ Hz), 8.71 (s, 1H, Ar).

5.2.34 Ethyl-1-(3-methoxybenzyl)-7-methyl-4-oxo-1,4-dihydro-1,8-naphthyridine-3-carboxylate (17b)



Yield = 18 %; colorless oil. $^1\text{H NMR}$ (CDCl_3) δ 1.43 (t, 3H, CH_2CH_3 , $J = 7.0$ Hz), 2.69 (s, 3H, $\text{CH}_3\text{C}=\text{N}$), 3.80 (s, 3H, OCH_3), 4.43 (q, 2H, OCH_2 , $J = 7.1$ Hz), 5.69 (s, 2H, NCH_2), 6.87 (d, 1H, Ar, $J = 8.5$ Hz), 6.92 (s, 1H, Ar), 6.93 (d, 1H, Ar, $J = 8.2$ Hz), 7.26-7.31 (m, 2H, Ar), 8.68 (d, 1H, Ar, $J = 8.0$ Hz), 8.71 (s, 1H, Ar).

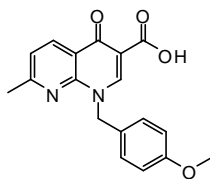
5.2.35 Ethyl-1-(1,3-benzodioxol-5-ylmethyl)-7-methyl-4-oxo-1,4-dihydro-1,8-naphthyridine-3-carboxylate (17c)



Yield = 70 %; mp = 152-54 °C (EtOH). $^1\text{H NMR}$ (CDCl_3) δ 1.42 (t, 3H, CH_2CH_3 , $J = 7.1$ Hz), 2.69 (s, 3H, $\text{CH}_3\text{C}=\text{N}$), 4.40 (q, 2H, OCH_2 , $J = 7.1$ Hz), 5.54 (s, 2H, NCH_2), 5.96 (s, 2H, OCH_2O), 6.78 (d, 1H, Ar, $J = 7.7$ Hz), 6.87 (d, 2H, Ar, $J = 8.2$ Hz), 7.28 (d, 1H, Ar, $J = 3.0$ Hz), 8.66 (d, 2H, Ar, $J = 7.3$ Hz).

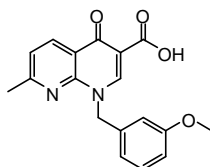
General Procedure for 18a-c. A suspension of the appropriate derivative **17a-c** (0.65 mmol), and 6 N NaOH (6 mL) in ethanol (5 mL) was stirred at rt 2 h. The mixture was then concentrated in vacuo, diluted with cold water and acidified with 6 N HCl. The pure final compound of type **18** was filtered off by suction and recrystallized from ethanol.

5.2.36 1-(4-Methoxybenzyl)-7-methyl-4-oxo-1,4-dihydro-1,8-naphthyridine-3-carboxylic acid (18a)



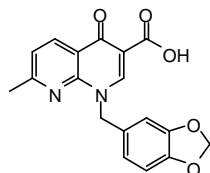
Yield = 67 %; mp = 215-17 °C (EtOH). ¹H NMR (CDCl₃) δ 2.79 (s, 3H, CH₃C=N), 3.81 (s, 3H, OCH₃), 5.69 (s, 2H, NCH₂), 6.89 (d, 2H, Ar, *J* = 8.5 Hz), 7.36 (d, 2H, Ar, *J* = 8.5 Hz), 7.42 (d, 1H, Ar, *J* = 8.2 Hz), 8.70 (d, 1H, Ar, *J* = 8.2 Hz), 8.97 (s, 1H, Ar), 14.63 (exch br s, 1H, OH).

5.2.37 1-(3-Methoxybenzyl)-7-methyl-4-oxo-1,4-dihydro-1,8-naphthyridine-3-carboxylic acid (18b)



Yield = 77 %; mp = 244-46 °C (EtOH). ¹H NMR (CDCl₃) δ 2.77 (s, 3H, CH₃C=N), 3.80 (s, 3H, OCH₃), 5.73 (s, 2H, NCH₂), 6.87-6.91 (m, 2H, Ar), 6.93 (d, 1H, Ar, *J* = 7.7 Hz), 7.29 (t, 2H, Ar, *J* = 8.1 Hz), 7.42 (d, 1H, Ar, *J* = 8.2 Hz), 8.71 (d, 1H, Ar, *J* = 8.2 Hz), 8.97 (s, 1H, Ar), 14.60 (exch br s, 1H, OH).

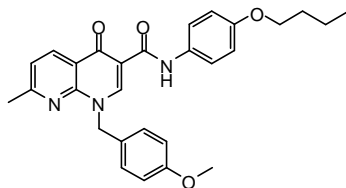
5.2.38 1-(1,3-Benzodioxol-5-ylmethyl)-7-methyl-4-oxo-1,4-dihydro-1,8-naphthyridine-3-carboxylic acid (18c)



Yield = 68 %; mp = 237-39 °C (EtOH). ¹H NMR (CDCl₃) δ 2.79 (s, 3H, CH₃C=N), 5.66 (s, 2H, NCH₃), 5.98 (s, 2H, OCH₂O), 6.80 (d, 1H, Ar, *J* = 7.9 Hz), 6.88 (s, 1H, Ar), 6.90 (d, 1H, Ar, *J* = 7.9 Hz), 7.43 (d, 1H, Ar, *J* = 8.2 Hz), 8.70 (d, 1H, Ar, *J* = 8.2 Hz), 8.95 (s, 1H, Ar).

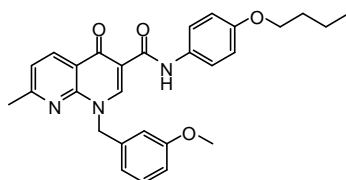
General Procedure for 19a-c. To a cooled (0 °C) and stirred solution of compound of type **18** (**18a-c**) (0.17 mmol) in anhydrous DMF (1 mL), Et₃N (5 drops), *diethyl cyanophosphate* (0.68 mmol) and 4-*n*-Butoxyaniline (0.17 mmol) were added. After 0.5 h at 0 °C, the reaction was kept at room temperature for 15 h. The mixture was then diluted with ice-cold water (10 mL) and kept under stirring for 0.5 h at 0 °C. The precipitate was filtered off and purified by flash column chromatography using cyclohexane/ethyl acetate 2:1 as eluent.

5.2.39 *N*-(4-Butoxyphenyl)-1-(4-methoxybenzyl)-7-methyl-4-oxo-1,4-dihydro-1,8-naphthyridine-3-carboxamide (19a)



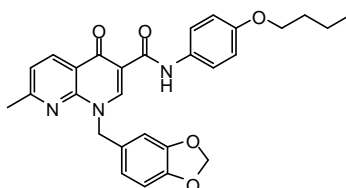
Yield = 75 %; mp = 190-91 °C (EtOH). ¹H NMR (CDCl₃) δ 1.00 (t, 3H, CH₂CH₃, *J* = 7.4 Hz), 1.51 (sext, 2H, CH₂CH₃, *J* = 7.6 Hz), 1.79 (quin, 2H, CH₂CH₂CH₂, *J* = 7.0 Hz), 2.75 (s, 3H, CH₃C=N), 3.80 (s, 3H, OCH₃), 3.98 (t, 2H, OCH₂, *J* = 6.5 Hz), 5.68 (s, 2H, NCH₂), 6.89 (qd, 4H, Ar, *J* = 3.5 Hz, *J* = 9.0 Hz), 7.34-7.37 (m, 3H, Ar), 7.68 (d, 2H, Ar, *J* = 7.9 Hz), 8.69 (d, 1H, Ar, *J* = 8.1 Hz), 9.08 (s, 1H, Ar), 11.97 (exch br s, 1H, NH).

5.2.40 *N*-(4-Butoxyphenyl)-1-(3-methoxybenzyl)-7-methyl-4-oxo-1,4-dihydro-1,8-naphthyridine-3-carboxamide (19b)



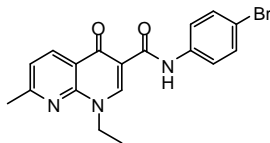
Yield = 71 %; mp = 145-47 °C (EtOH). ¹H NMR (CDCl₃) δ 1.00 (t, 3H, CH₂CH₃, *J* = 7.4 Hz), 1.51 (sext, 2H, CH₂CH₃, *J* = 7.6 Hz), 1.79 (quin, 2H, CH₂CH₂CH₂, *J* = 6.9 Hz), 2.74 (s, 3H, CH₃C=N), 3.80 (s, 3H, OCH₃), 3.98 (t, 2H, OCH₂, *J* = 6.5 Hz), 5.72 (s, 2H, NCH₂), 6.86 (d, 1H, Ar, *J* = 8.5 Hz), 6.91 (d, 2H, Ar, *J* = 8.9 Hz), 6.95-7.02 (m, 2H, Ar), 7.27 (t, 1H, Ar, *J* = 7.9 Hz), 7.37 (d, 1H, Ar, *J* = 7.0 Hz), 7.69 (d, 2H, Ar, *J* = 8.2 Hz), 8.71 (d, 1H, Ar, *J* = 8.2 Hz), 9.08 (s, 1H, Ar), 11.97 (exch br s, 1H, NH).

5.2.41 1-(1,3-Benzodioxol-5-ylmethyl)-*N*-(4-butoxyphenyl)-7-methyl-4-oxo-1,4-dihydro-1,8-naphthyridine-3-carboxamide (19c)



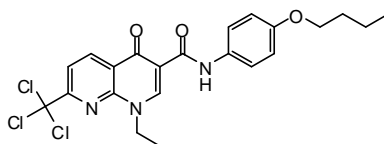
Yield = 62 %; mp = 181-83 °C (EtOH). ¹H NMR (CDCl₃) δ 1.00 (t, 3H, CH₂CH₃, *J* = 7.3 Hz), 1.51 (sext, 2H, CH₂CH₃, *J* = 7.8 Hz), 1.79 (quin, 2H, CH₂CH₂CH₂, *J* = 6.8 Hz), 2.77 (s, 3H, CH₃C=N), 3.98 (t, 2H, OCH₂, *J* = 6.4 Hz), 5.65 (s, 2H, NCH₂), 5.96 (s, 2H, OCH₂O), 6.79 (d, 1H, Ar, *J* = 7.8 Hz), 6.91 (d, 4H, Ar, *J* = 8.5 Hz), 7.38 (d, 1H, Ar, *J* = 6.7 Hz), 7.69 (d, 2H, Ar, *J* = 5.6 Hz), 8.71 (d, 1H, Ar, *J* = 8.0 Hz), 9.06 (s, 1H, Ar), 11.97 (exch br s, 1H, NH).

5.2.42 *N*-(4-Bromophenyl)-1-ethyl-7-methyl-4-oxo-1,4-dihydro-1,8-naphthyridine-3-carboxamide (**20**)



To a cooled (-5 °C) and stirred solution of nalidixic acid (0.43 mmol) in anhydrous tetrahydrofuran (3 mL), Et₃N (1.50 mmol) was added. After 30 min, the mixture was allowed to warm up to 0 °C, and ethyl chloroformate (0.47 mmol) was added. After 1 h 4-bromo aniline was added and the reaction was carried out at room temperature for 12 h. The mixture was then concentrated in vacuo, diluted with cold water (20 mL) and extracted with CH₂Cl₂ (3 x 15 mL). The solvent was evaporated to afford final compound **20**, which was purified by two consecutive flash chromatography using firstly cyclohexane/ethyl acetate 2:1 and then CH₂Cl₂ as eluents. Yield = 18 %; mp = 290-92 °C (EtOH). ¹H NMR (CDCl₃) δ 1.56 (t, 3H, CH₂CH₃, *J* = 7.2 Hz), 2.74 (s, 3H, CH₃C=N), 4.62 (q, 2H, NCH₂, *J* = 7.2 Hz), 7.97 (d, 1H, Ar, *J* = 8.2 Hz), 7.48 (d, 2H, Ar, *J* = 8.7 Hz), 7.70 (d, 2H, Ar, *J* = 8.8 Hz), 8.70 (d, 1H, Ar, *J* = 8.1 Hz), 9.00 (s, 1H, Ar), 12.24 (exch br s, 1H, NH).

5.2.43 *N*-(4-Butoxyphenyl)-1-ethyl-4-oxo-7-trichloromethyl-1,4-dihydro-1,8-naphthyridine-3-carboxamide (**21**)

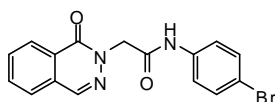


To a cooled (0 °C) and stirred suspension of nalidixic acid (0.43 mmol) in SOCl₂ (1.5 mL), Et₃N (0.2 mL) was added. After 2 h at 60 °C, the mixture was allowed to cool down and the excess of SOCl₂ was removed in vacuo. The residue was dissolved in anhydrous THF (3 mL) and cooled again to 0 °C. A solution of 4-*n*.butoxyaniline (0.86 mmol) in anhydrous THF (2 mL) was then added dropwise to the mixture. Finally, the reaction was carried out at room temperature for 2 h. The mixture was concentrated under reduced pressure and diluted with ice-cold water (10 mL). The precipitate was then filtered off and purified by flash column chromatography using CH₂Cl₂/MeOH/CH₃COOH 99:1:0.1 as eluent.

Yield = 15 %; mp = 162-63 °C (EtOH). ¹H NMR (CDCl₃) δ 1.01 (t, 3H, CH₂CH₂CH₃, *J* = 7.4 Hz), 1.52 (sext, 2H, CH₂CH₂CH₃, *J* = 7.6 Hz), 1.62 (t, 3H, NCH₂CH₃, *J* = 7.2 Hz), 1.80 (quin, 2H, CH₂CH₂CH₂, *J* = 7.1 Hz), 4.00 (t, 2H, OCH₂, *J* = 6.6 Hz), 4.64 (q, 2H, NCH₂, *J* = 7.2 Hz), 6.93 (d, 2H, Ar, *J* = 9.0 Hz), 7.69 (d, 2H, Ar, *J* = 9.0 Hz), 8.15 (d, 1H, Ar, *J* = 8.4 Hz), 8.99 (d, 1H, Ar, *J* = 8.4 Hz), 9.12 (s, 1H, Ar), 11.76 (exch br s, 1H, NH).

5. Experimental Chemistry

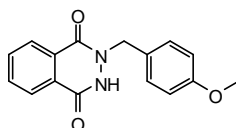
5.2.44 *N*-(4-Bromophenyl)-2-(1-oxophthalazin-2(1*H*)-yl)acetamide (**23**)



A solution of **22** (1.54 mmol) in anhydrous acetonitrile (1 ml) was added dropwise to a stirred solution of commercially available 1-(2*H*)-phthalazinone (1.03 mmol) in anhydrous acetonitrile (3 mL). K_2CO_3 (2.06 mmol) was added and the reaction was carried out for 3 h at reflux. Removal of the solvent gave a residue which was poured into ice-cold water and after 1 h stirring in ice-bath the final product was filtered off by suction and recrystallized from ethanol. Yield = 45 %; mp = 245-46 °C (EtOH). 1H NMR ($CDCl_3$) δ 4.97 (s, 2H, NCH_2CO), 7.53 (qd, 4H, Ar, $J = 13.9$ Hz, $J = 8.3$ Hz), 7.91 (m, 1H, Ar), 7.99 (d, 2H, Ar, $J = 5.8$ Hz), 8.26 (d, 1H, Ar, $J = 8.0$ Hz), 8.48 (s, 1H, Ar), 10.46 (exch br s, 1H, NH).

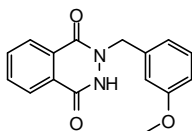
General Procedure for 24a-c. Commercially available 2,3-dihydrophthalazin-1,4-dione (4.93 mmol), K_2CO_3 (9.80 mmol) and the suitable benzyl halide (5.43 mmol) were stirred in anhydrous DMF (5 mL) for 2-4 h at 80 °C. The mixture was then diluted with ice-cold water and extracted with CH_2Cl_2 (3 x 15 mL). The organic layer was dried over Na_2SO_4 and evaporated in vacuo. Compounds **24a-c** were then purified by flash column chromatography using cyclohexane/ethyl acetate 1:1 as eluent.

5.2.45 2-(4-Methoxybenzyl)-2,3-dihydrophthalazine-1,4-dione (**24a**)



Yield = 23 %; mp = 150-52 °C (EtOH). 1H NMR ($CDCl_3$) δ 3.86 (s, 3H, OCH_3), 5.31 (s, 2H, NCH_2), 6.96 (d, 2H, Ar, $J = 8.6$ Hz), 7.44 (d, 2H, Ar, $J = 8.5$ Hz), 7.83 (quin, 2H, Ar, $J = 3.7$ Hz), 8.07 (dd, 1H, Ar, $J = 3.1$ Hz, $J = 3.5$ Hz), 8.41 (dd, 1H, Ar, $J = 2.4$ Hz, $J = 2.8$ Hz), 9.98 (exch br s, 1H, NH).

5.2.46 2-(3-Methoxybenzyl)-2,3-dihydrophthalazine-1,4-dione (**24b**)

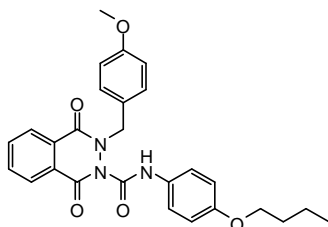


Yield = 18 %; mp = 184-86 °C (EtOH). 1H NMR ($CDCl_3$) δ 3.87 (s, 3H, OCH_3), 5.36 (s, 2H, NCH_2), 6.93 (dd, 1H, Ar, $J = 5.8$ Hz, $J = 2.4$ Hz), 7.06 (s, 1H, Ar), 7.09 (d, 1H, Ar, $J = 7.6$ Hz), 7.36 (t, 1H, Ar, $J = 7.9$ Hz), 7.82-7.89 (m, 2H, Ar), 8.09 (dd, 1H, Ar, $J = 6.9$ Hz, $J = 1.9$ Hz), 8.44 (dd, 1H, Ar, $J = 4.0$ Hz, $J = 2.1$ Hz), 9.94 (exch br s, 1H, NH).

General Procedure for 25a-c. The appropriate derivative of type **24** (**24a-c**) (1.10 mmol) was dissolved in 3 mL of anhydrous CH_2Cl_2 and 4-butoxyphenyl isocyanate (2.20 mmol) was added under

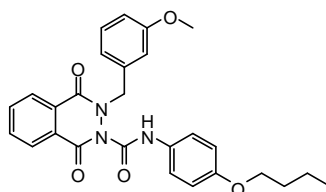
stirring at 0 °C. The reaction was carried out at 0 °C for 2 h and subsequently at room temperature for 12 h. The solid residue was filtered off and the solution was evaporated in vacuo to afford compounds **25a-c**, which were purified by flash column chromatography using CH₂Cl₂ as eluent.

5.2.47 *N*-(4-Butoxyphenyl)-3-(4-methoxybenzyl)-1,4-dioxo-3,4-dihydro-phthalazine-2(1*H*)-carboxamide (**25a**)



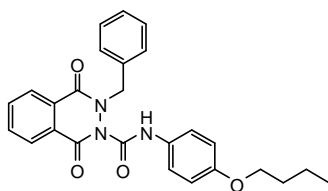
Yield = 53 %; mp = 117-19 °C (EtOH). ¹H NMR (CDCl₃) δ 1.01 (t, 3H, CH₂CH₃, *J* = 7.4 Hz), 1.52 (sext, 2H, CH₂CH₃, *J* = 7.5 Hz), 1.80 (quin, 2H, CH₂CH₂CH₂, *J* = 6.8 Hz), 3.84 (s, 3H, OCH₃), 3.99 (t, 2H, OCH₂, *J* = 6.5 Hz), 5.51 (s, 2H, NCH₂), 6.95 (t, 4H, Ar, *J* = 8.7 Hz), 7.56 (d, 2H, Ar, *J* = 8.5 Hz), 7.62 (d, 2H, Ar, *J* = 8.9 Hz), 7.86 (quin, 2H, Ar, *J* = 7.8 Hz), 8.06 (d, 1H, Ar, *J* = 7.8 Hz), 8.47 (d, 1H, Ar, *J* = 7.6 Hz), 11.86 (exch br s, 1H, NH).

5.2.48 *N*-(4-Butoxyphenyl)-3-(3-methoxybenzyl)-1,4-dioxo-3,4-dihydro-phthalazine-2(1*H*)-carboxamide (**25b**)



Yield = 75 %; mp = 104-06 °C (EtOH). ¹H NMR (CDCl₃) δ 1.01 (t, 3H, CH₂CH₃, *J* = 7.4 Hz), 1.52 (sext, 2H, CH₂CH₃, *J* = 7.6 Hz), 1.80 (quin, 2H, CH₂CH₂CH₂, *J* = 7.0 Hz), 3.87 (s, 3H, OCH₃), 3.99 (t, 2H, OCH₂, *J* = 6.5 Hz), 5.56 (s, 2H, NCH₂), 6.93 (dd, 3H, Ar, *J* = 4.6 Hz, *J* = 3.2 Hz), 7.18 (d, 1H, Ar, *J* = 7.0 Hz), 7.19 (s, 1H, Ar), 7.35 (t, 1H, Ar, *J* = 7.7 Hz), 7.61 (d, 2H, Ar, *J* = 9.0 Hz), 7.84-7.92 (m, 2H, Ar), 8.10 (d, 1H, Ar, *J* = 7.1 Hz), 8.49 (d, 1H, Ar, *J* = 7.2 Hz), 11.84 (exch br s, 1H, NH).

5.2.49 3-Benzyl-*N*-(4-butoxyphenyl)-1,4-dioxo-3,4-dihydrophthalazine-2(1*H*)-carboxamide (**25c**)

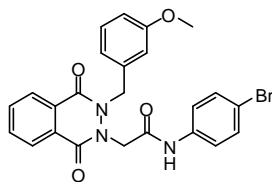


Yield = 86 %; mp = 117-19 °C (EtOH). ¹H NMR (CDCl₃) δ 1.01 (t, 3H, CH₂CH₃, *J* = 7.4 Hz), 1.52 (sext, 2H, CH₂CH₃, *J* = 7.6 Hz), 1.80 (quin, 2H, CH₂CH₂CH₂, *J* = 6.9 Hz), 3.99 (t, 2H, OCH₂, *J* = 6.5 Hz), 5.59 (s, 2H, NCH₂), 6.94 (d, 2H, Ar, *J* = 8.9 Hz), 7.37-7.46 (m, 3H, Ar), 7.62 (dd, 4H, Ar, *J* = 1.3 Hz, *J* = 5.3

5. Experimental Chemistry

Hz), 7.84-7.92 (m, 2H, Ar), 8.09 (d, 1H, Ar, $J = 7.8$ Hz), 8.49 (d, 1H, Ar, $J = 7.5$ Hz), 11.85 (exch br s, 1H, NH).

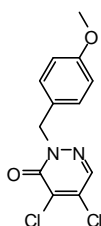
5.2.50 *N*-(4-Bromophenyl)-2-(3-(3-methoxybenzyl)-1,4-dioxo-3,4-dihydro-phthalazin-2(1*H*)-yl)acetamide (26)



A suspension of the intermediate **24b** (0.18 mmol), K_2CO_3 (0.36 mmol) and amide **22** (0.27 mmol) in anhydrous acetonitrile (1 mL) was stirred at reflux for 3 h. The solvent was then evaporated in vacuo and the mixture was poured into ice-cold water. After 1 h stirring in ice-bath, the precipitate was filtered off and purified through two consecutive crystallization from ethanol. Yield = 45 %; mp = 178-80 °C (EtOH). 1H NMR ($CDCl_3$) δ 3.85 (s, 3H, OCH_3), 4.95 (s, 2H, $NCH_2-C_6H_5$), 5.39 (s, 2H, NCH_2CO), 6.91 (d, 1H, Ar, $J = 8.5$ Hz), 7.06 (s, 1H, Ar), 7.09 (d, 1H, Ar, $J = 6.7$ Hz), 7.34 (t, 1H, Ar, $J = 7.6$ Hz), 7.43 (s, 4H, Ar), 7.78 (t, 2H, Ar, $J = 4.8$ Hz), 8.09-8.12 (m, 1H, Ar), 8.45-8.48 (m, 1H, Ar), 8.80 (exch br s, 1H, NH).

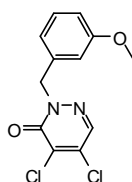
General Procedure for 27a,b. K_2CO_3 (6.06 mmol) and tetrabutylammonium bromide (0.30 mmol) were added to a stirred solution of *4,5-dichloro-3(2H)-pyridazinone* (3.03 mmol) in anhydrous acetonitrile (3 mL). The appropriate benzyl chloride (3- or 4-methoxybenzyl chloride) (4.54 mmol) was added and the reaction was carried out at reflux for 5-7 h. The mixture was then allowed to cool down and the solvent was evaporated in vacuo. Ice-cold water was added to the residue and after 1 h stirring in ice-bath, compounds **27a,b** were filtered off and recrystallized from ethanol.

5.2.51 *4,5-Dichloro-2-(4-methoxybenzyl)pyridazin-3(2H)-one (27a)*



Yield = 81 %; mp = 116-17 °C (EtOH). 1H NMR ($CDCl_3$) δ 3.81 (s, 3H, OCH_3), 5.28 (s, 2H, NCH_2), 6.88 (d, 2H, Ar, $J = 8.6$ Hz), 7.42 (d, 2H, Ar, $J = 8.5$ Hz), 7.79 (s, 1H, Ar).

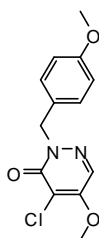
5.2.52 *4,5-Dichloro-2-(3-methoxybenzyl)pyridazin-3(2H)-one (27b)*



Yield = 60 %; mp = 80-82 °C (EtOH). $^1\text{H NMR}$ (CDCl_3) δ 3.82 (s, 3H, OCH_3), 5.31 (s, 2H, NCH_2), 6.87 (dd, 1H, Ar, $J = 5.6$ Hz, $J = 2.6$ Hz), 6.99-7.05 (m, 2H, Ar), 7.27 (t, 1H, Ar, $J = 3.6$ Hz), 7.80 (s, 1H, Ar).

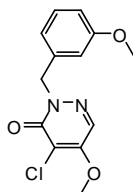
General Procedure for 28a,b. Compound **27a** or **27b** (0.88 mmol) was added to a stirred solution of Na° (1.76 mmol) in 3 mL of anhydrous methanol. The reaction mixture was stirred for 1 h at room temperature. After removal of the solvent in vacuo, ice-cold water was added to the residue and the precipitate was filtered off by suction and purified by crystallization from ethanol.

5.2.53 4-Chloro-5-methoxy-2-(4-methoxybenzyl)pyridazin-3(2H)-one (28a)



Yield = 53 %; mp = 135-37 °C (EtOH). $^1\text{H NMR}$ (CDCl_3) δ 3.80 (s, 3H, $\text{C}_6\text{H}_4\text{-OCH}_3$), 4.06 (s, 3H, OCH_3 pyridaz.), 5.31 (s, 2H, NCH_2), 6.87 (d, 2H, Ar, $J = 8.6$ Hz), 7.42 (d, 2H, Ar, $J = 8.6$ Hz), 7.80 (s, 1H, Ar).

5.2.54 4-Chloro-5-methoxy-2-(3-methoxybenzyl)pyridazin-3(2H)-one (28b)

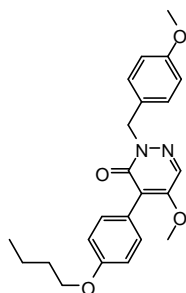


Yield = 60 %; mp = 80-82 °C (EtOH). $^1\text{H NMR}$ (CDCl_3) δ 3.81 (s, 3H, $\text{C}_6\text{H}_4\text{-OCH}_3$), 4.07 (s, 3H, OCH_3 pyridaz.), 5.34 (s, 2H, NCH_2), 6.85 (dd, 1H, Ar, $J = 6.2$ Hz, $J = 1.89$ Hz), 6.99 (s, 1H, Ar), 7.03 (d, 1H, Ar, $J = 7.3$ Hz), 7.26 (t, 1H, Ar, $J = 7.9$ Hz), 7.83 (s, 1H, Ar).

General Procedure for 29a,b. To the suspension of **28a** or **28b** (0.71 mmol), $\text{Pd}(\text{PPh}_3)_4$ [tetrakis(triphenylphosphine)palladium(0), 0.02 mmol] and 4-butoxyphenylboronic acid (1.07 mmol) in toluene (2 mL), Na_2CO_3 (1.42 mmol, 2 M in H_2O) was added and the mixture was stirred at reflux for 2 h. Extra 4-butoxyphenylboronic acid (1.07 mmol) was added and the reaction was refluxed for additional 3-6 h. The solvent was evaporated under vacuo, then the suspension was diluted with ice-cold water and extracted with CH_2Cl_2 . The organic layer was dried over Na_2SO_4 and the residue was purified by flash column chromatography using cyclohexane/ethyl acetate 3:1 as eluent.

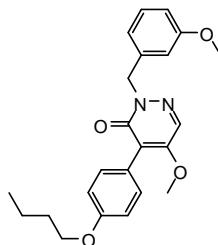
5. Experimental Chemistry

5.2.55 4-(4-Butoxyphenyl)-5-methoxy-2-(4-methoxybenzyl)pyridazin-3(2H)-one (29a)



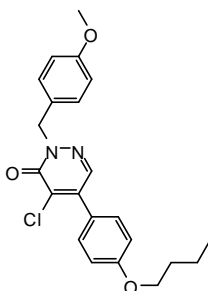
Yield = 82 %; colorless oil. ^1H NMR (CDCl_3) δ 0.99 (t, 2H, CH_2CH_3 , $J = 7.4$ Hz), 1.51 (sext, 2H, CH_2CH_3 , $J = 7.6$ Hz), 1.79 (quin, 2H, $\text{CH}_2\text{CH}_2\text{CH}_2$, $J = 6.9$ Hz), 3.80 (s, 3H, $\text{C}_6\text{H}_4\text{-OCH}_3$), 3.89 (s, 3H, OCH_3 pyridaz.), 4.01 (t, 2H, OCH_2 , $J = 6.5$ Hz), 5.31 (s, 2H, NCH_2), 6.87 (d, 2H, Ar, $J = 8.6$ Hz), 6.94 (d, 2H, Ar, $J = 8.8$ Hz), 7.48 (q, 4H, Ar, $J = 8.0$ Hz), 7.89 (s, 1H, Ar).

5.2.56 4-(4-Butoxyphenyl)-5-methoxy-2-(3-methoxybenzyl)pyridazin-3(2H)-one (29b)

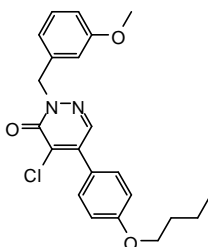


Yield = 28 %; colorless oil. ^1H NMR (CDCl_3) δ 0.99 (t, 2H, CH_2CH_3 , $J = 7.4$ Hz), 1.51 (sext, 2H, CH_2CH_3 , $J = 7.4$ Hz), 1.79 (quin, 2H, $\text{CH}_2\text{CH}_2\text{CH}_2$, $J = 6.9$ Hz), 3.81 (s, 3H, $\text{C}_6\text{H}_4\text{-OCH}_3$), 3.90 (s, 3H, OCH_3 pyridaz.), 4.00 (t, 2H, OCH_2 , $J = 6.5$ Hz), 5.35 (s, 2H, NCH_2), 6.84 (dd, 1H, Ar, $J = 6.0$ Hz, $J = 2.3$ Hz), 6.94 (d, 2H, Ar, $J = 8.7$ Hz), 7.02 (s, 1H, Ar), 7.06 (d, 1H, Ar, $J = 7.6$ Hz), 7.26 (t, 1H, Ar, $J = 8.0$ Hz), 7.51 (d, 2H, Ar, $J = 8.7$ Hz), 7.91 (s, 1H, Ar).

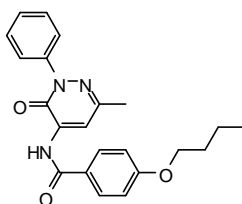
General Procedure for 30a,b. To a suspension of **27a** or **27b** (0.53 mmol), $\text{PdCl}_2[(\text{C}_2\text{H}_5)_3\text{P}]_2$ [trans-dichlorobis(triethylphosphine)palladium(II), 0.05 mmol] and 4-butoxyphenylboronic acid (0.26 mmol) in DMF (2 mL), Na_2CO_3 (0.53 mmol, 1 M in H_2O) was added and the mixture was stirred at room temperature for 6-12 h. The suspension was diluted with ice-cold water and extracted with CH_2Cl_2 . The organic layer was dried over Na_2SO_4 and the residue was purified by flash column chromatography using CH_2Cl_2 (for **30a**) and $\text{CH}_2\text{Cl}_2/\text{MeOH}/\text{NH}_4\text{OH}$ 99:1:0.1 (for **30b**) as eluents.

5.2.57 5-(4-Butoxyphenyl)-4-chloro-2-(4-methoxybenzyl)pyridazin-3(2H)-one (30a)

Yield = 22 %; mp = 84-85 °C (EtOH). ¹H NMR (CDCl₃) δ 1.01 (t, 2H, CH₂CH₃, *J* = 7.4 Hz), 1.53 (sext, 2H, CH₂CH₃, *J* = 7.6 Hz), 1.82 (quin, 2H, CH₂CH₂CH₂, *J* = 6.8 Hz), 3.81 (s, 3H, OCH₃), 4.03 (t, 2H, OCH₂, *J* = 6.5 Hz), 5.34 (s, 2H, NCH₂), 6.90 (d, 2H, Ar, *J* = 8.4 Hz), 7.01 (d, 2H, Ar, *J* = 8.6 Hz), 7.48 (dd, 4H, Ar, *J* = 5.9 Hz, *J* = 8.6 Hz), 7.78 (s, 1H, Ar).

5.2.58 5-(4-Butoxyphenyl)-4-chloro-2-(3-methoxybenzyl)pyridazin-3(2H)-one (30b)

Yield = 14 %; mp = 73-75 °C (EtOH). ¹H NMR (CDCl₃) δ 1.01 (t, 2H, CH₂CH₃, *J* = 7.4 Hz), 1.53 (sext, 2H, CH₂CH₃, *J* = 7.5 Hz), 1.82 (quin, 2H, CH₂CH₂CH₂, *J* = 7.0 Hz), 3.83 (s, 3H, OCH₃), 4.04 (t, 2H, OCH₂, *J* = 6.5 Hz), 5.38 (s, 2H, NCH₂), 6.88 (dd, 1H, Ar, *J* = 5.7 Hz, *J* = 2.6 Hz), 7.02 (d, 2H, Ar, *J* = 8.8 Hz), 7.07 (s, 1H, Ar), 7.10 (d, 1H, Ar, *J* = 7.6 Hz), 7.29 (t, 1H, Ar, *J* = 8.0 Hz), 7.47 (d, 2H, Ar, *J* = 8.7 Hz), 7.79 (s, 1H, Ar).

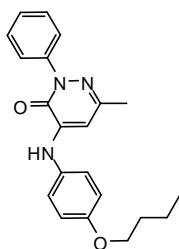
5.2.59 4-Butoxy-N-(6-methyl-3-oxo-2-phenyl-2,3-dihydropyridazin-4-yl)benzamide (35)

4-Butoxybenzoic acid (0.36 mmol) was converted into the corresponding chloride as follows: SOCl₂ (20.7 mmol) was added and the stirred suspension was cooled to 0 °C and treated with Et₃N (0.99 mmol). After 4 h of reflux, the mixture was evaporated in vacuo and the residue was washed with cyclohexane (3 x 5 mL). The residue was dissolved in anhydrous toluene (5 mL), then added of compound **34** (0.40 mmol) dissolved in anhydrous toluene (1 mL) and Et₃N (1.48 mmol). After 4 h of reflux the solvent was removed in vacuo, cold water was added and the aqueous layer was extracted with CH₂Cl₂ (3 x 20 mL).

5. Experimental Chemistry

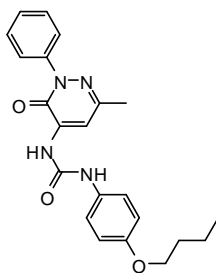
Evaporation of the organic solvent in vacuo gave a residue that was purified by column chromatography (eluent: cyclohexane/ethyl acetate 3:1). Yield = 37 %; mp = 95-97 °C (EtOH). IR (cm⁻¹) 3269 (NH), 1682 (CO), 1644 (CO). ¹H NMR (CDCl₃) δ 1.01 (t, 3H, CH₂CH₃, *J* = 7.4 Hz), 1.53 (sext, 2H, CH₂CH₃, *J* = 7.5 Hz), 1.82 (quin, 2H, CH₂CH₂CH₂, *J* = 7.0 Hz), 2.45 (s, 3H, 6-CH₃), 4.06 (t, 2H, CH₂O, *J* = 6.5 Hz), 6.99 (d, 2H, Ar, *J* = 8.8 Hz), 7.43 (t, 1H, Ar, *J* = 7.4 Hz), 7.52 (t, 2H, Ar, *J* = 7.8 Hz), 7.65 (d, 2H, Ar, *J* = 7.7 Hz), 7.91 (d, 2H, Ar, *J* = 8.8 Hz), 8.24 (s, 1H, Ar), 9.46 (exch br s, 1H, NH). MS (ESI) calcd. For C₂₂H₂₃N₃O₃, 377.44. Found: *m/z* 378.18 [M + H]⁺.

5.2.60 4-(4-Butoxyphenylamino)-6-methyl-2-phenylpyridazin-3(2H)-one (36)



To a suspension of **34** (0.55 mmol), copper acetate (0.82 mmol) and 4-butoxyphenylboronic acid (1.08 mmol) in CH₂Cl₂ (2 mL), Et₃N (1.08 mmol) was added and the mixture was stirred at room temperature for 12 h. The suspension was extracted with 15% aqueous ammonia (10 mL), and the organic layer was washed with 10 mL of water and dried over Na₂SO₄. After removal of the solvent, the residue was purified by column chromatography using as eluent cyclohexane/ethyl acetate 3:1. The analytical sample was obtained through a further purification performed on silica gel preparative TLC (eluent: cyclohexane/ethyl acetate 3:1). Yield = 16 %; mp = 137-139 °C (EtOH). IR (cm⁻¹) 3275 (NH), 1633 (CO). ¹H NMR (CDCl₃) δ 1.02 (t, 3H, CH₂CH₃, *J* = 7.4 Hz), 1.54 (sext, 2H, CH₂CH₃, *J* = 7.0 Hz), 1.81 (quin, 2H, CH₂CH₂CH₂), 2.31 (s, 3H, 6-CH₃), 4.01 (t, 2H, CH₂O, *J* = 6.5 Hz), 6.40 (s, 1H, Ar), 6.97 (d, 2H, Ar, *J* = 8.9 Hz), 7.20 (d, 2H, Ar, *J* = 8.8 Hz), 7.41 (t, 1H, Ar, *J* = 7.4 Hz), 7.51 (t, 3H, Ar, *J* = 7.7 Hz), 7.64 (d, 2H, Ar, *J* = 8.0 Hz). MS (ESI) calcd. For C₂₁H₂₃N₃O₂, 349.43. Found: *m/z* 350.19 [M + H]⁺.

5.2.61 1-(4-Butoxyphenyl)-3-(6-methyl-3-oxo-2-phenyl-2,3-dihydro pyridazin-4-yl)urea (37)

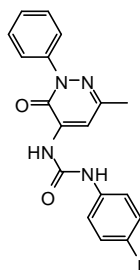


To a cooled and stirred suspension of **34** (0.50 mmol) and anhydrous sodium acetate (1.20 mmol) in anhydrous THF (5 mL), triphosgene (1.75 mmol) was added. The mixture was stirred for additional 10

min at 0 °C and refluxed for 2 h. The solvent was removed in vacuo, and the residue was dissolved in anhydrous THF (2 mL). 4-Butoxyaniline (1.20 mmol) was added and the mixture was stirred at room temperature for 12 h. After dilution with ice-cold water, the suspension was extracted with CH₂Cl₂ (3 x 20 mL). Removal of the solvent in vacuo afforded a crude residue which was purified by column chromatography using absolute EtOH/CH₂Cl₂/petroleum ether/toluene/33% ammonia 3.3:19.7:6.5:70:0.5 as eluent. Yield = 31 %; mp = 189-191 °C (EtOH). IR (cm⁻¹) 3270 (NH), 3255 (NH), 1705 (CO), 1625 (CO). ¹H NMR (CDCl₃) δ 1.01 (t, 3H, CH₂CH₃, *J* = 7.4 Hz), 1.52 (sext, 2H, CH₂CH₃, *J* = 7.4 Hz), 1.79 (quin, 2H, CH₂CH₂CH₂, *J* = 7.0 Hz), 2.40 (s, 3H, 6-CH₃), 3.95 (t, 2H, OCH₂, *J* = 6.6 Hz), 6.70 (s, 4H, Ar), 7.17 (t, 1H, Ar, *J* = 7.5 Hz), 7.32 (t, 2H, Ar, *J* = 7.8 Hz), 7.61 (d, 2H, Ar, *J* = 7.9 Hz), 8.11 (exch br s, 1H, NH), 8.14 (s, 1H, Ar), 9.33 (exch br s, 1H, NH). MS (ESI) calcd. For C₂₂H₂₄N₄O₃, 392.45. Found: *m/z* 393.19 [M + H]⁺.

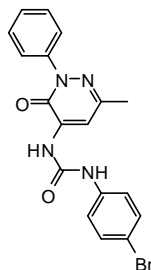
General Procedure for 38a-c. To a stirred solution of compound **34** (0.35 mmol) in anhydrous toluene (2 mL), the proper aryl isocyanate (0.40 mmol) was added. The mixture was refluxed for 4-7 h. After cooling, the precipitate was collected by suction and purified by crystallization from toluene (**38b** and **38c**). In the case of **38a**, after cooling, cold water was added and the mixture was extracted with CH₂Cl₂ (3 x 20 mL). Removal of the solvent gave a residue that was purified by column chromatography using CH₂Cl₂/CH₃OH 9.9:0.1 as eluent.

5.2.62 1-(4-Iodophenyl)-3-(6-methyl-3-oxo-2-phenyl-2,3-dihydropyridazin-4-yl)urea (**38a**)



Yield = 45 %; mp = 264-265 °C (EtOH/toluene). IR (cm⁻¹) 3270 (NH), 3256 (NH), 1708 (CO), 1627 (CO). ¹H NMR (CDCl₃) δ 2.44 (s, 3H, CH₃), 6.50 (d, 2H, Ar, *J* = 8.7 Hz), 7.21 (t, 1H, Ar, *J* = 7.5 Hz), 7.36-7.41 (m, 4H, Ar), 7.68 (d, 2H, Ar, *J* = 7.7 Hz), 8.15 (s, 1H, Ar), 8.41 (exch br s, 1H, NH), 9.38 (exch br s, 1H, NH). MS (ESI) calcd. For C₁₈H₁₅IN₄O₂, 446.24. Found: *m/z* 447.03 [M + H]⁺.

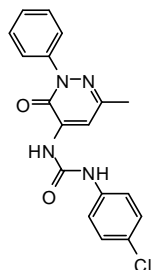
5.2.63 1-(4-Bromophenyl)-3-(6-methyl-3-oxo-2-phenyl-2,3-dihydropyridazin-4-yl)urea (**38b**)



5. Experimental Chemistry

Yield = 50 %; mp = 263-265 °C (toluene). IR (cm⁻¹) 3271 (NH), 3250 (NH), 1704 (CO), 1625 (CO). ¹H NMR (CDCl₃) δ 2.43 (s, 3H, CH₃), 6.60 (d, 2H, Ar, *J* = 8.6 Hz), 7.19-7.22 (m, 3H, Ar), 7.38 (t, 2H, Ar, *J* = 7.8 Hz), 7.69 (d, 2H, Ar, *J* = 7.9 Hz), 8.16 (s, 1H, Ar), 8.44 (exch, br, s, 1H, NH), 9.40 (exch br s, 1H, NH). MS (ESI) calcd. For C₁₈H₁₅BrN₄O₂, 399.24. Found: *m/z* 399.05 [M]⁺.

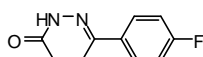
5.2.64 1-(4-Chlorophenyl)-3-(6-methyl-3-oxo-2-phenyl-2,3-dihydropyridazin-4-yl)urea (38c)



Yield = 85 %; mp = 274-276 °C (toluene). IR (cm⁻¹) 3269 (NH), 3255 (NH), 1705 (CO), 1626 (CO). ¹H NMR (CDCl₃) δ 2.44 (s, 3H, CH₃), 6.65 (d, 2H, Ar, *J* = 8.8 Hz), 7.07 (d, 2H, Ar, *J* = 8.8 Hz), 7.21 (t, 1H, Ar, *J* = 7.5 Hz), 7.38 (t, 2H, Ar, *J* = 7.9 Hz), 7.69 (d, 2H, Ar, *J* = 7.6 Hz), 8.16 (s, 1H, Ar), 8.43 (exch br s, 1H, NH), 9.40 (exch br s, 1H, NH). MS (ESI) calcd. For C₁₈H₁₅ClN₄O₂, 354.79. Found: *m/z* 355.10 [M + H]⁺.

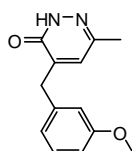
General Procedure for 42a-m. To a stirred solution of the suitable commercially available or synthesized γ -keto acid (1.00 mmol) in EtOH (2 mL), hydrazine hydrate (1.00 mmol) was added dropwise. The mixture was heated at 60 °C for 1-3 h. After cooling, the precipitate was collected by suction and purified by recrystallization alternatively from toluene or ethanol.

5.2.65 6-(4-Fluorophenyl)-4,5-dihydropyridazin-3(2H)-one (42j)



Yield = 95 %; mp = 192-93 °C (EtOH). ¹H NMR (CDCl₃) δ 2.64 (dd, 2H, COCH₂CH₂, *J* = 1.2 Hz, *J* = 7.9 Hz), 3.00 (dd, 2H, COCH₂CH₂, *J* = 1.2 Hz, *J* = 7.3 Hz), 7.13 (qd, 2H, Ar, *J* = 1.8 Hz, *J* = 4.7 Hz), 7.72-7.76 (qd, 2H, Ar, *J* = 0.4 Hz, *J* = 3.1 Hz), 8.51 (exch br s, 1H, NH).

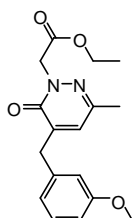
5.2.66 4-(3-Methoxybenzyl)-6-methylpyridazin-3(2H)-one (43)



To 7 mL of KOH in absolute EtOH (5%, w/v), **42d** (1.79 mmol) and 3-methoxybenzaldehyde (1.79 mmol) were added. The reaction was carried out under stirring for 3 h. After cooling, the mixture was concentrated in vacuo, diluted with cold water (10-15 mL) and acidified with 2 N HCl. The suspension

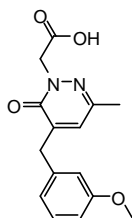
was extracted with CH_2Cl_2 (3 x 15 mL). The organic phase was dried (Na_2SO_4) and evaporated in vacuo to afford compound **43**, which was purified by flash column chromatography using cyclohexane/ethyl acetate 1:1 as eluent. Yield = 61 %; mp = 133-134 °C (EtOH). ^1H NMR (CDCl_3) δ 2.26 (s, 3H, 6- CH_3), 3.82 (s, 3H, OCH_3), 3.90 (s, 2H, CH_2 -Ar), 6.73 (s, 1H, Ar), 6.82-6.86 (m, 3H, Ar), 7.276-7.28 (m, 1H, Ar).

5.2.67 [5-(3-Methoxybenzyl)-3-methyl-6-oxo-6H-pyridazin-1-yl]-acetic acid ethyl ester (**44**)



A mixture of **43** (1.13 mmol), K_2CO_3 (2.26 mmol), and ethyl bromoacetate (3.40 mmol) in CH_3CN (3 mL) was refluxed under stirring for 6 h. The mixture was then concentrated in vacuo, diluted with cold water, and extracted with CH_2Cl_2 (3 x 15 mL). The solvent was evaporated in vacuo and compound **44** was purified by column chromatography using cyclohexane/ethyl acetate 1:1 as eluent. Yield = 98 %; oil. ^1H NMR (CDCl_3) δ 1.29 (t, 3H, CH_2CH_3 , $J = 7.1$ Hz), 2.22 (s, 3H, 3- CH_3), 3.80 (s, 3H, OCH_3), 3.86 (s, 2H, CH_2 -Ar), 4.22-4.25 (m, 2H, OCH_2CH_3), 4.85 (s, 2H, NCH_2CO), 6.67 (s, 1H, Ar), 6.78-6.82 (m, 3H, Ar), 7.26 (t, 1H, Ar, $J = 7.8$ Hz).

5.2.68 [5-(3-Methoxybenzyl)-3-methyl-6-oxo-6H-pyridazin-1-yl]-acetic Acid (**45**)



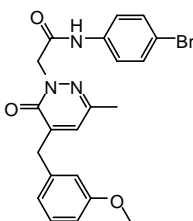
A suspension of **44** (0.5 mmol), 6 N NaOH (6 mL) and ethanol (2 mL) was stirred at rt to 80 °C for 1 h. The mixture was then concentrated in vacuo, diluted with cold water and acidified with 6 N HCl. The final product **45** was filtered off with suction and recrystallized from ethanol. Yield = 97 %; mp = 194-195 °C (EtOH). ^1H NMR (DMSO-d_6) δ 2.21 (s, 3H, 3- CH_3), 3.72 (s, 3H, OCH_3), 3.76 (s, 2H, CH_2 -Ar), 4.69 (s, 2H, NCH_2CO), 6.79-6.85 (m, 3H, Ar), 7.07 (s, 1H, Ar), 7.22 (t, 1H, Ar, $J = 7.8$ Hz).

General Procedure for 46a-s. To a cooled (-5 °C) and stirred solution of compound **45** (0.35 mmol) in anhydrous tetrahydrofuran (3-5 mL), Et_3N (1.22 mmol) was added. After 30 min, the mixture was allowed to warm up to 0 °C and ethyl chloroformate (0.38 mmol) was added. After 1 h, the appropriate substituted aryl(cycloalkyl)amine (0.7 mmol), was added and the reaction was carried out at room temperature for 12 h. The mixture was then concentrated in vacuo, diluted with cold water (20-30

5. Experimental Chemistry

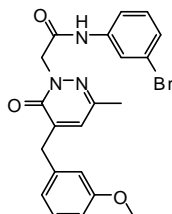
mL) and extracted with CH₂Cl₂ (3 x 15 mL). The solvent was evaporated to afford final compounds **46a-s**, which were purified by column chromatography using cyclohexane/ethyl acetate 1:1 as eluent for compounds **46a,d,e,g-m,p,q**, toluene/NH₄OH/EtOH/CH₂Cl₂/petroleum ether 7:0.05:0.30:2: 0.65 for compounds **46b,c**, cyclohexane/ethyl acetate 1:2 for compounds **46f,n,o,r**, CH₂Cl₂/ CH₃OH 9.5:0.5 for compound **46s**.

5.2.69 *N*-(4-Bromophenyl)-2-[5-(3-methoxybenzyl)-3-methyl-6-oxo-6*H*-pyridazin-1-yl]-acetamide (**46a**)



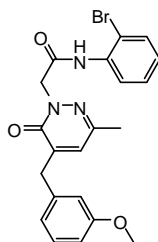
Yield = 86 %; mp = 171-172 °C (EtOH). IR (cm⁻¹) 3300 (NH), 1708 (CO), 1644 (CO). ¹H NMR (CDCl₃) δ 2.20 (s, 3H, 3-CH₃), 3.70 (s, 3H, OCH₃), 3.73 (s, 2H, CH₂-Ar), 4.80 (s, 2H, NCH₂CO), 6.77-6.82 (m, 3H, Ar), 7.13 (s, 1H, Ar), 7.20 (t, 1H, Ar, *J* = 8.0 Hz), 7.47 (s, 4H, Ar). MS (ESI) calcd. For C₂₁H₂₀BrN₃O₃, 442.31. Found: *m/z* 442.08 [M]⁺.

5.2.70 *N*-(3-Bromophenyl)-2-[5-(3-methoxybenzyl)-3-methyl-6-oxo-6*H*-pyridazin-1-yl]-acetamide (**46b**)



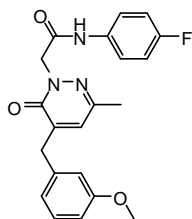
Yield = 85 %; mp = 73-75 °C (EtOH). IR (cm⁻¹) 3295 (NH), 1708 (CO), 1642 (CO). ¹H NMR (CDCl₃) δ 2.30 (s, 3H, 3-CH₃), 3.80 (s, 3H, OCH₃), 3.92 (s, 2H, CH₂-Ar), 4.95 (s, 2H, NCH₂CO), 6.80-6.86 (m, 4H, Ar), 7.14 (t, 1H, Ar, *J* = 8.0 Hz), 7.22 (m, 1H, Ar, *J* = 8.2 Hz), 7.27- 7.31 (m, 1H, Ar), 7.39 (d, 1H, Ar, *J* = 8.0 Hz), 7.77 (s, 1H, Ar), 9.05 (exch br s, 1H, NH). MS (ESI) calcd. For C₂₁H₂₀BrN₃O₃, 442.31. Found: *m/z* 441.11. [M - H]⁺.

5.2.71 *N*-(2-Bromophenyl)-2-[5-(3-methoxybenzyl)-3-methyl-6-oxo-6*H*-pyridazin-1-yl]-acetamide (**46c**)



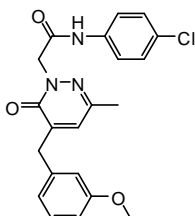
Yield = 80 %; oil. IR (cm⁻¹) 3300 (NH), 1708 (CO), 1644 (CO). ¹H NMR (CDCl₃) δ 2.30 (s, 3H, 3-CH₃), 3.82 (s, 3H, OCH₃), 3.92 (s, 2H, CH₂-Ar), 5.00 (s, 2H, NCH₂CO), 6.76 (s, 1H, Ar), 6.80-6.86 (m, 3H, Ar), 7.00 (t, 1H, Ar, *J* = 7.7 Hz), 7.27-7.34 (m, 2H, Ar), 7.52 (d, 1H, Ar, *J* = 8.0 Hz), 8.36 (d, 1H, Ar, *J* = 8.2 Hz), 8.54 (exch br s, 1H, NH). MS (ESI) calcd. For C₂₁H₂₀BrN₃O₃, 442.31. Found: *m/z* 443.08. [M + H]⁺.

5.2.72 *N*-(4-Fluorophenyl)-2-[5-(3-methoxybenzyl)-3-methyl-6-oxo-6*H*-pyridazin-1-yl]-acetamide (46d)



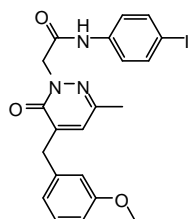
Yield = 97 %; mp = 145-147 °C (EtOH). IR (cm⁻¹) 3300 (NH), 1707 (CO), 1643 (CO). ¹H NMR (CDCl₃) δ 2.30 (s, 3H, 3-CH₃), 3.80 (s, 3H, OCH₃), 3.90 (s, 2H, CH₂-Ar), 4.95 (s, 2H, NCH₂CO), 6.80-6.84 (m, 4H, Ar), 6.90 (t, 2H, Ar, *J* = 8.7 Hz), 7.25-7.29 (m, 1H, Ar), 7.39-7.42 (m, 2H, Ar), 9.21 (exch br s, 1H, NH). MS (ESI) calcd. For C₂₁H₂₀FN₃O₃, 381.40. Found: *m/z* 382.16 [M + H]⁺.

5.2.73 *N*-(4-Chlorophenyl)-2-[5-(3-methoxybenzyl)-3-methyl-6-oxo-6*H*-pyridazin-1-yl]-acetamide (46e)



Yield = 86 %; mp = 170-171 °C (EtOH). IR (cm⁻¹) 3296 (NH), 1705 (CO), 1644 (CO). ¹H NMR (CDCl₃) δ 2.30 (s, 3H, 3-CH₃), 3.80 (s, 3H, OCH₃), 3.90 (s, 2H, CH₂-Ar), 4.95 (s, 2H, NCH₂CO), 6.79 (s, 1H, Ar), 6.80-6.85 (m, 3H, Ar), 7.16 (d, 2H, Ar, *J* = 8.8 Hz), 7.25-7.29 (m, 1H, Ar), 7.38 (d, 2H, Ar, *J* = 8.8 Hz), 9.28 (exch br s, 1H, NH). MS (ESI) calcd. For C₂₁H₂₀ClN₃O₃, 397.85. Found: *m/z* 398.13 [M + H]⁺.

5.2.74 *N*-(4-Iodophenyl)-2-[5-(3-methoxybenzyl)-3-methyl-6-oxo-6*H*-pyridazin-1-yl]-acetamide (46f)

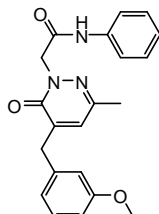


Yield = 99 %; mp = 179-180 °C (EtOH). IR (cm⁻¹) 3300 (NH), 1707 (CO), 1645 (CO). ¹H NMR (CDCl₃) δ 2.30 (s, 3H, 3-CH₃), 3.79 (s, 3H, OCH₃), 3.88 (s, 2H, CH₂-Ar), 4.95 (s, 2H, NCH₂CO), 6.78-6.84 (m,

5. Experimental Chemistry

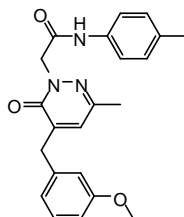
4H, Ar), 7.17 (d, 2H, Ar, $J = 8.7$ Hz), 7.24-7.28 (m, 1H, Ar), 7.45 (d, 2H, Ar, $J = 8.7$ Hz), 9.41 (exch br s, 1H, NH). MS (ESI) calcd. For $C_{21}H_{20}N_3O_3$, 489.31. Found: m/z 490.06 $[M + H]^+$.

5.2.75 2-[5-(3-Methoxybenzyl)-3-methyl-6-oxo-6H-pyridazin-1-yl]-N-phenyl-acetamide (46g)



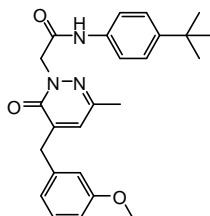
Yield = 97 %; oil. IR (cm^{-1}) 3295 (NH), 1708 (CO), 1644 (CO). 1H NMR ($CDCl_3$) δ 2.28 (s, 3H, 3- CH_3), 3.81 (s, 3H, OCH_3), 3.91 (s, 2H, CH_2 -Ar), 4.96 (s, 2H, NCH_2CO), 6.78-6.86 (m, 4H, Ar), 7.08 (t, 1H, Ar, $J = 7.4$ Hz), 7.26-7.30 (m, 3H, Ar), 7.50 (d, 2H, Ar, $J = 8.0$ Hz), 8.93 (exch br s, 1H, NH). MS (ESI) calcd. For $C_{21}H_{21}N_3O_3$, 363.41. Found: m/z 364.16 $[M + H]^+$.

5.2.76 2-[5-(3-Methoxybenzyl)-3-methyl-6-oxo-6H-pyridazin-1-yl]-N-4-tolyl-acetamide (46h)



Yield = 78 %; mp = 142-144 °C (EtOH). IR (cm^{-1}) 3300 (NH), 1708 (CO), 1644 (CO). 1H NMR ($CDCl_3$) δ 2.28 (s, 3H, 3- CH_3), 2.30 (s, 3H, CH_3 -Ar), 3.81 (s, 3H, OCH_3), 3.90 (s, 2H, CH_2 -Ar), 4.94 (s, 2H, NCH_2CO), 6.76 (s, 1H, Ar), 6.80-6.86 (m, 3H, Ar), 7.08 (d, 2H, Ar, $J = 8.3$ Hz), 7.26-7.30 (m, 1H, Ar), 7.38 (d, 2H, Ar, $J = 8.4$ Hz), 8.82 (exch br s, 1H, NH). MS (ESI) calcd. For $C_{22}H_{23}N_3O_3$, 377.44. Found: m/z 378.18 $[M + H]^+$.

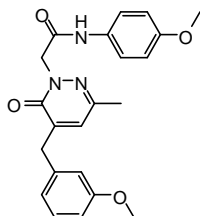
5.2.77 N-(4-tert-Butylphenyl)-2-[5-(3-methoxybenzyl)-3-methyl-6-oxo-6H-pyridazin-1-yl]-acetamide (46i)



Yield = 95 %; mp = 54-56 °C (EtOH). IR (cm^{-1}) 3296 (NH), 1705 (CO), 1644 (CO). 1H NMR ($CDCl_3$) δ 1.30 (s, 9H, C-(CH_3)₃), 2.27 (s, 3H, 3- CH_3), 3.81 (s, 3H, OCH_3), 3.90 (s, 2H, CH_2 -Ar), 4.96 (s, 2H, NCH_2CO), 6.76 (s, 1H, Ar), 6.80 (s, 1H, Ar), 6.81-6.86 (m, 2H, Ar), 7.26-7.30 (m, 3H, Ar), 7.43 (d, 2H,

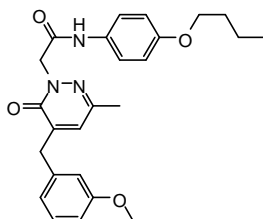
Ar, $J = 8.6$ Hz), 8.88 (exch br s, 1H, NH). MS (ESI) calcd. For $C_{25}H_{29}N_3O_3$, 419.52. Found: m/z 420.22 $[M + H]^+$.

5.2.78 **2-[5-(3-Methoxybenzyl)-3-methyl-6-oxo-6H-pyridazin-1-yl]-N-(4-methoxyphenyl)-acetamide (46j)**



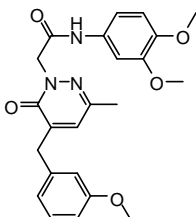
Yield = 75 %; mp = 65-67 °C (EtOH). IR (cm^{-1}) 3300 (NH), 1705 (CO), 1644 (CO). 1H NMR ($CDCl_3$) δ 2.28 (s, 3H, 3- CH_3), 3.80 (s, 3H, OCH_3), 3.81 (s, 3H, OCH_3), 3.91 (s, 2H, CH_2 -Ar), 4.94 (s, 2H, NCH_2CO), 6.77 (s, 1H, Ar), 6.80 (s, 1H, Ar), 6.81-6.86 (m, 4H, Ar), 7.27-7.30 (m, 1H, Ar), 7.42 (d, 2H, Ar, $J = 8.9$ Hz), 8.71 (exch br s, 1H, NH). MS (ESI) calcd. For $C_{22}H_{23}N_3O_4$, 393.44. Found: m/z 394.18 $[M + H]^+$.

5.2.79 **N-(4-Butoxyphenyl)-2-[5-(3-methoxybenzyl)-3-methyl-6-oxo-6H-pyridazin-1-yl]-acetamide (46k)**



Yield = 73 %; oil. IR (cm^{-1}) 3300 (NH), 1708 (CO), 1645 (CO). 1H NMR ($CDCl_3$) δ 0.99 (t, 3H, $O(CH_2)_3CH_3$, $J = 7.5$ Hz), 1.50 (sext, 2H, $OCH_2CH_2CH_2$, $J = 7.5$ Hz), 1.76 (quin, 2H, $OCH_2CH_2CH_2$, $J = 7.0$ Hz), 2.28 (s, 3H, 3- CH_3), 3.81 (s, 3H, OCH_3), 3.90 (s, 2H, CH_2 -Ar), 3.93 (t, 2H, $OCH_2CH_2CH_2$, $J = 6.5$ Hz), 4.94 (s, 2H, NCH_2CO), 6.76 (s, 1H, Ar), 6.80-6.86 (m, 5H, Ar), 7.26-7.30 (m, 1H, Ar), 7.40 (d, 2H, Ar, $J = 8.9$ Hz), 8.76 (exch br s, 1H, NH). MS (ESI) calcd. For $C_{25}H_{29}N_3O_4$, 435.52. Found: m/z 436.23 $[M + H]^+$.

5.2.80 **N-(3,4-Dimethoxyphenyl)-2-[5-(3-methoxybenzyl)-3-methyl-6-oxo-6H-pyridazin-1-yl]-acetamide (46 l)**

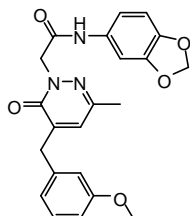


Yield = 74 %; mp = 57-59 °C (EtOH). IR (cm^{-1}) 3298 (NH), 1708 (CO), 1640 (CO). 1H NMR ($CDCl_3$) δ 2.29 (s, 3H, 3- CH_3), 3.80 (s, 3H, OCH_3), 3.83 (s, 3H, OCH_3), 3.84 (s, 3H, OCH_3), 3.90 (s, 2H, CH_2 -Ar),

5. Experimental Chemistry

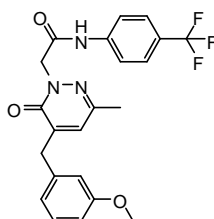
4.95 (s, 2H, NCH₂CO), 6.72 (d, 1H, Ar, *J* = 8.6 Hz), 6.78 (s, 2H, Ar), 6.82-6.88 (m, 3H, Ar), 7.25-7.29 (m, 1H, Ar), 7.32 (d, 1H, Ar, *J* = 2.2 Hz), 8.93 (exch br s, 1H, NH). MS (ESI) calcd. For C₂₃H₂₅N₃O₅, 423.46. Found: *m/z* 424.19 [M + H]⁺.

5.2.81 *N*-Benzo-1,3-dioxol-5-yl-2-[5-(3-methoxybenzyl)-3-methyl-6-oxo-6*H*-pyridazin-1-yl]-acetamide (46m)



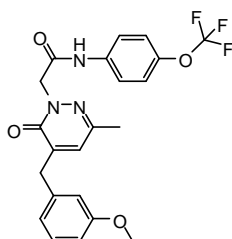
Yield = 98 %; oil. IR (cm⁻¹) 3300 (NH), 1707 (CO), 1643 (CO). ¹H NMR (CDCl₃) δ 2.28 (s, 3H, 3-CH₃), 3.81 (s, 3H, OCH₃), 3.89 (s, 2H, CH₂-Ar), 4.93 (s, 2H, NCH₂CO), 5.92 (s, 2H, O-CH₂-O), 6.65 (d, 1H, Ar, *J* = 8.3 Hz), 6.77-6.85 (m, 5H, Ar), 7.21 (d, 1H, Ar, *J* = 2.0 Hz), 7.25-7.29 (m, 1H, Ar), 9.04 (exch br s, 1H, NH). MS (ESI) calcd. For C₂₂H₂₁N₃O₅, 407.42. Found: *m/z* 408.16 [M + H]⁺.

5.2.82 2-[5-(3-Methoxybenzyl)-3-methyl-6-oxo-6*H*-pyridazin-1-yl]-*N*-(4-trifluoromethylphenyl)-acetamide (46n)



Yield = 80 %; mp = 175-176 °C (EtOH). IR (cm⁻¹) 3297 (NH), 1708 (CO), 1646 (CO). ¹H NMR (CDCl₃) δ 2.33 (s, 3H, 3-CH₃), 3.79 (s, 3H, OCH₃), 3.91 (s, 2H, CH₂-Ar), 5.00 (s, 2H, NCH₂CO), 6.81-6.85 (m, 3H, Ar), 6.89 (s, 1H, Ar), 7.25-7.29 (m, 1H, Ar), 7.38 (d, 2H, Ar, *J* = 8.7 Hz), 7.47 (d, 2H, Ar, *J* = 8.7 Hz), 9.62 (exch br s, 1H, NH). MS (ESI) calcd. For C₂₂H₂₀F₃N₃O₃, 431.41. Found: *m/z* 432.16 [M + H]⁺.

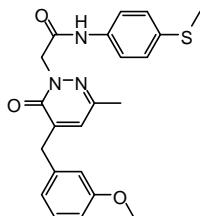
5.2.83 2-[5-(3-Methoxybenzyl)-3-methyl-6-oxo-6*H*-pyridazin-1-yl]-*N*-(4-trifluoromethoxyphenyl)-acetamide (46o)



Yield = 87 %; mp = 168-169 °C (EtOH). IR (cm⁻¹) 3300 (NH), 1708 (CO), 1644 (CO). ¹H NMR (CDCl₃) δ 2.31 (s, 3H, 3-CH₃), 3.78 (s, 3H, OCH₃), 3.89 (s, 2H, CH₂-Ar), 5.00 (s, 2H, NCH₂CO), 6.79-6.83 (m,

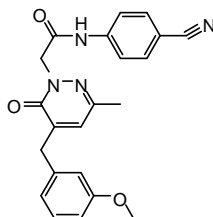
3H, Ar), 6.87 (s, 1H, Ar), 7.00 (d, 2H, Ar, $J = 8.6$ Hz), 7.24- 7.28 (m, 1H, Ar), 7.41 (d, 2H, Ar, $J = 9.0$ Hz), 9.54 (exch br s, 1H, NH). MS (ESI) calcd. For $C_{22}H_{20}F_3N_3O_4$, 447.41. Found: m/z 448.15 $[M + H]^+$.

5.2.84 2-[5-(3-Methoxybenzyl)-3-methyl-6-oxopyridazin-1(6H)-yl]-N-[4-(methylthio)phenyl]acetamide (46p)



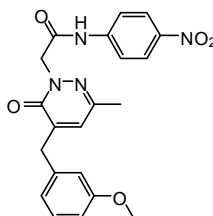
Yield = ~ 100 %; mp = 166-167 °C (EtOH). IR (cm^{-1}) 3285 (NH), 1720 (CO), 1634 (CO). 1H NMR ($CDCl_3$) δ 2.28 (s, 3H, 3- CH_3), 2.45 (s, 3H, SCH_3), 3.80 (s, 3H, OCH_3), 3.89 (s, 2H, CH_2 -Ar), 4.958 (s, 2H, NCH_2CO), 6.79-6.85 (m, 4H, Ar), 7.12-7.15 (m, 1H, Ar), 7.27 (t, 1H, Ar, $J = 7.8$ Hz), 7.39 (dd, 2H, Ar, $J = 5.0$ Hz), 9.13 (exch br s, 1H, NH).

5.2.85 N-(4-Cyanophenyl)-2-[5-(3-methoxybenzyl)-3-methyl-6-oxo-6H-pyridazin-1-yl]-acetamide (46q)



Yield = 55 %; mp = 156-158 °C (EtOH). IR (cm^{-1}) 3285 (NH), 2221 (CN), 1716 (CO), 1644 (CO). 1H NMR ($CDCl_3$) δ 2.32 (s, 3H, 3- CH_3), 3.80 (s, 3H, OCH_3), 3.91 (s, 2H, CH_2 -Ar), 4.98 (s, 2H, NCH_2CO), 6.80-6.88 (m, 4H, Ar), 7.26-7.30 (m, 1H, Ar), 7.50-7.57 (m, 4H, Ar), 9.60 (exch br s, 1H, NH). MS (ESI) calcd. For $C_{22}H_{20}N_4O_3$, 388.42. Found: m/z 389.16 $[M + H]^+$.

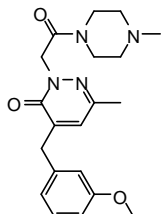
5.2.86 2-[5-(3-Methoxybenzyl)-3-methyl-6-oxo-6H-pyridazin-1-yl]-N-(4-nitrophenyl)-acetamide (46r)



Yield = 49 %; mp = 165-166 °C (EtOH). IR (cm^{-1}) 3298 (NH), 1708 (CO), 1644 (CO). 1H NMR ($CDCl_3$) δ 2.34 (s, 3H, 3- CH_3), 3.79 (s, 3H, OCH_3), 3.92 (s, 2H, CH_2 -Ar), 5.01 (s, 2H, NCH_2CO), 6.80-6.84 (m, 3H, Ar), 6.94 (s, 1H, Ar), 7.25-7.28 (m, 1H, Ar), 7.49 (d, 2H, Ar, $J = 9.2$ Hz), 7.99 (d, 2H, Ar, $J = 9.2$ Hz), 9.92 (exch br s, 1H, NH). MS (ESI) calcd. For $C_{21}H_{20}N_4O_5$, 408.41. Found: m/z 409.15 $[M + H]^+$.

5. Experimental Chemistry

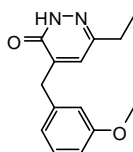
5.2.87 4-(3-Methoxybenzyl)-6-methyl-2-[2-(4-methylpiperazin-1-yl)-2-oxo-ethyl]-pyridazin-3(2H)-one (46s)



Yield = 62 %; oil. IR (cm⁻¹) 1673 (CO), 1644 (CO). ¹H NMR (CDCl₃) δ 2.25 (s, 3H, 3-CH₃), 2.55 (s, 3H, CH₃N), 2.74-2.81 (m, 4H, Ar), 3.77-3.82 (m, 7H (4H, Ar; 3H, OCH₃)), 3.87 (s, 2H, CH₂-Ar), 4.96 (s, 2H, NCH₂CO), 6.69 (s, 1H, Ar), 6.80 (s, 1H, Ar), 6.82-6.85 (m, 2H, Ar), 7.26-7.30 (m, 1H, Ar). MS (ESI) calcd. For C₂₀H₂₆N₄O₃, 370.45. Found: *m/z* 371.21 [M + H]⁺.

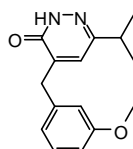
General procedure for 47a-o. To 8 mL of KOH in absolute EtOH (5%, w/v), the appropriate compound of type **42** (**42a-c,e-j,l**) (1.39 mmol) and 3- or 4-methoxybenzaldehyde (1.39 mmol) were added. The mixture was refluxed under stirring for 1-3 h. After cooling, the mixture was concentrated in vacuo, diluted with cold water (10-15 mL) and acidified with 2 N HCl. For compounds **47a-e** the suspension was extracted with CH₂Cl₂ (3 x 15 mL). Removal of the solvent afforded the final compounds, which were purified by column chromatography using respectively cyclohexane/ethyl acetate 1:1 (for **47a,e**), 2:1 (for **47b,c**) and 1:3 (for **47d**) as eluent. On the contrary, compounds **47f-o**, after 1 h stirring in ice-bath, were filtered off by suction from the acidic solutions and recrystallized from ethanol.

5.2.88 6-Ethyl-4-(3-methoxybenzyl)pyridazin-3(2H)-one (47a)

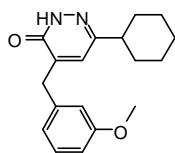


Yield = 20 %; colorless oil. ¹H NMR (CDCl₃) δ 1.18 (t, 3H, CH₂CH₃, *J* = 7.5 Hz), 2.55 (q, 2H, CH₂CH₃, *J* = 7.6 Hz), 3.83 (s, 3H, OCH₃), 3.90 (s, 2H, C₆H₄-CH₂), 6.75 (s, 1H, Ar), 6.82-6.86 (m, 3H, Ar), 7.29 (t, 1H, Ar, *J* = 7.8 Hz), 11.12 (exch br s, 1H, NH).

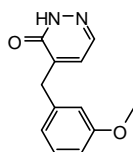
5.2.89 6-Isopropyl-4-(3-methoxybenzyl)pyridazin-3(2H)-one (47b)



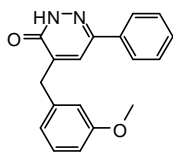
Yield = 44 %; colorless oil. ¹H NMR (CDCl₃) δ 1.19 (d, 6H, CH(CH₃)₂, *J* = 8.3 Hz), 2.83 (sept, 1H, CH(CH₃)₂, *J* = 8.3 Hz), 3.83 (s, 3H, OCH₃), 3.91 (s, 2H, C₆H₄-CH₂), 6.83-6.87 (m, 4H, Ar), 7.29 (t, 1H, Ar, *J* = 8.0 Hz).

5.2.90 6-Cyclohexyl-4-(3-methoxybenzyl)pyridazin-3(2H)-one (47c)

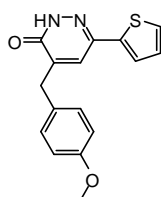
Yield = 96 %; colorless oil. $^1\text{H NMR}$ (CDCl_3) δ 1.28-1.37 (m, 4H, 2 x CH_2 cyclohexyl), 1.62-1.83 (m, 6H, 3 x CH_2 cyclohexyl), 2.35-2.45 (m, 1H, CH cyclohexyl), 3.81 (s, 3H, OCH_3), 3.88 (s, 2H, $\text{C}_6\text{H}_4\text{-CH}_2$), 6.34-6.88 (m, 2H, Ar), 6.97 (d, 2H, Ar, $J = 7.3$ Hz), 7.30 (t, 1H, Ar, $J = 8.0$ Hz).

5.2.91 4-(3-Methoxybenzyl)pyridazin-3(2H)-one (47d)

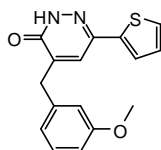
Yield = 27 %; colorless oil. $^1\text{H NMR}$ (CDCl_3) δ 3.83 (s, 3H, OCH_3), 3.92 (s, 2H, $\text{C}_6\text{H}_4\text{-CH}_2$), 6.81-6.89 (m, 4H, Ar), 7.29 (t, 2H, Ar, $J = 8.1$ Hz), 7.77 (d, 1H, Ar, $J = 4.0$ Hz).

5.2.92 4-(3-Methoxybenzyl)-6-phenylpyridazin-3(2H)-one (47e)

Yield = 45 %; mp = 103-05 °C (EtOH). $^1\text{H NMR}$ (CDCl_3) δ 3.84 (s, 3H, OCH_3), 4.00 (s, 2H, $\text{C}_6\text{H}_4\text{-CH}_2$), 6.85-6.92 (m, 3H, Ar), 6.96 (d, 2H, Ar, $J = 8.5$ Hz), 7.28-7.38 (m, 2H, Ar), 7.43-7.45 (m, 2H, Ar), 7.69-7.71 (m, 1H, Ar).

5.2.93 4-(4-Methoxybenzyl)-6-(thiophen-2-yl)pyridazin-3(2H)-one (47f)

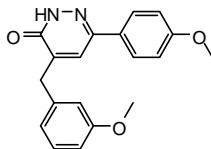
Yield = 97 %; mp = 125-26 °C (EtOH). $^1\text{H NMR}$ (CDCl_3) δ 3.84 (s, 3H, OCH_3), 3.94 (s, 2H, $\text{C}_6\text{H}_4\text{-CH}_2$), 6.91-6.98 (m, 3H, Ar), 7.03-7.08 (m, 1H, Ar), 7.22-7.25 (m, 2H, Ar), 7.31-7.33 (m, 1H, Ar), 7.36 (d, 2H, Ar, $J = 6.5$ Hz).

5.2.94 4-(3-Methoxybenzyl)-6-(thiophen-2-yl)pyridazin-3(2H)-one (47g)

5. Experimental Chemistry

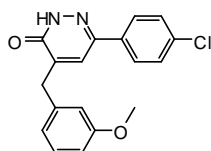
Yield = 97 %; mp = 132-34 °C (EtOH). $^1\text{H NMR}$ (CDCl_3) δ 3.84 (s, 3H, OCH_3), 3.97 (s, 2H, $\text{C}_6\text{H}_4\text{-CH}_2$), 6.86-6.90 (m, 3H, Ar), 7.05 (dd, 1H, Ar, $J = 1.1$ Hz, $J = 3.8$ Hz), 7.24-7.33 (m, 3H, Ar), 7.37 (d, 2H, Ar, $J = 5.1$ Hz).

5.2.95 4-(3-Methoxybenzyl)-6-(4-methoxyphenyl)pyridazin-3(2H)-one (47i)



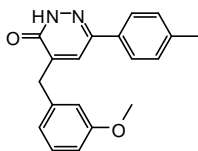
Yield = 99 %; mp = 150-152 °C (EtOH). $^1\text{H NMR}$ (CDCl_3) δ 3.83 (s, 3H, $\text{C}_6\text{H}_4\text{-OCH}_3$), 3.86 (s, 3H, $\text{CH}_2\text{-C}_6\text{H}_4\text{-OCH}_3$), 3.98 (s, 2H, $\text{C}_6\text{H}_4\text{-CH}_2$), 6.86 (d, 1H, Ar, $J = 7.0$ Hz), 6.95 (d, 2H, Ar, $J = 7.6$ Hz), 7.30-7.32 (m, 2H, Ar), 7.62 (d, 2H, Ar, $J = 8.8$ Hz).

5.2.96 6-(4-Chlorophenyl)-4-(3-methoxybenzyl)pyridazin-3(2H)-one (47k)



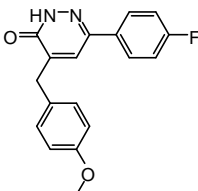
Yield ~ 100 %; mp = 164-166 °C (EtOH). $^1\text{H NMR}$ (CDCl_3) δ 3.83 (s, 3H, OCH_3), 3.98 (s, 2H, $\text{C}_6\text{H}_4\text{-CH}_2$), 6.86-6.90 (m, 3H, Ar), 7.29-7.33 (m, 2H, Ar), 7.40 (d, 2H, Ar, $J = 8.6$ Hz), 7.62 (d, 2H, Ar, $J = 8.8$ Hz).

5.2.97 4-(3-Methoxybenzyl)-6-*p*-tolylpyridazin-3(2H)-one (47m)

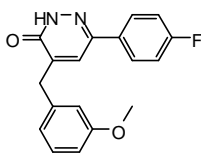


Yield = 98 %; mp = 138-140 °C (EtOH). $^1\text{H NMR}$ (CDCl_3) δ 2.40 (s, 3H, $\text{C}_6\text{H}_4\text{-CH}_3$), 3.83 (s, 3H, OCH_3), 3.98 (s, 2H, $\text{C}_6\text{H}_4\text{-CH}_2$), 6.86 (d, 2H, Ar, $J = 6.7$ Hz), 6.91 (s, 1H, Ar), 7.24 (d, 2H, Ar, $J = 8.0$ Hz), 7.30-7.33 (m, 1H, Ar), 7.35 (s, 1H, Ar), 7.58 (d, 2H, Ar, $J = 8.3$ Hz).

5.2.98 6-(4-Fluorophenyl)-4-(4-methoxybenzyl)pyridazin-3(2H)-one (47n)

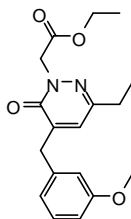


Yield = 70 %; mp = 106-108 °C (EtOH). $^1\text{H NMR}$ (CDCl_3) δ 3.84 (s, 3H, OCH_3), 3.94 (s, 2H, $\text{C}_6\text{H}_4\text{-CH}_2$), 6.92 (d, 2H, Ar, $J = 5.0$ Hz), 7.12 (d, 2H, Ar, $J = 8.4$ Hz), 7.22 (d, 2H, Ar, $J = 8.4$ Hz), 7.65-7.69 (m, 2H, Ar).

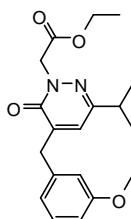
5.2.99 6-(4-Fluorophenyl)-4-(3-methoxybenzyl)pyridazin-3(2H)-one (47o)

Yield = 70 %; mp = 106-108 °C (EtOH). $^1\text{H NMR}$ (CDCl_3) δ 3.83 (s, 3H, OCH_3), 3.98 (s, 2H, $\text{C}_6\text{H}_4\text{-CH}_2$), 6.86-6.91 (m, 3H, Ar), 7.12 (t, 2H, Ar, $J = 8.5$ Hz), 7.29-7.33 (m, 2H, Ar), 7.66-7.69 (m, 2H, Ar).

General procedure for 48a-o. A mixture of the appropriate intermediate **47** (**47a-o**) (1.34 mmol), K_2CO_3 (2.68 mmol), and ethyl bromoacetate (2.01 mmol) in CH_3CN (8 mL) was refluxed under stirring for 1-3 h. The mixture was then concentrated in vacuo, diluted with cold water and extracted with CH_2Cl_2 (3 x 15 mL). The solvent was evaporated in vacuo and compounds **48a-o** were purified by column chromatography using cyclohexane/ethyl acetate 2:1 as eluent.

5.2.100 Ethyl-2-[3-ethyl-5-(3-methoxybenzyl)-6-oxopyridazin-1(6H)-yl]acetate (48a)

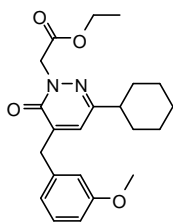
Yield = 98 %; oil. $^1\text{H NMR}$ (CDCl_3) δ 1.15 (t, 3H, CH_2CH_3 , $J = 4.1$ Hz), 1.30 (t, 3H, OCH_2CH_3 , $J = 6.9$ Hz), 2.53 (q, 2H, CH_2CH_3 , $J = 7.6$ Hz), 3.82 (s, 3H, OCH_3), 3.88 (s, 2H, $\text{CH}_2\text{-Ar}$), 4.26 (q, 2H, OCH_2CH_3 , $J = 7.1$ Hz), 4.87 (s, 2H, NCH_2CO), 6.72 (s, 1H, Ar), 6.80-6.85 (m, 3H, Ar), 7.28 (t, 1H, Ar, $J = 6.2$ Hz).

5.2.101 Ethyl-2-[3-isopropyl-5-(3-methoxybenzyl)-6-oxopyridazin-1(6H)-yl]acetate (48b)

Yield = 93 %; oil. $^1\text{H NMR}$ (CDCl_3) δ 1.15 (d, 6H, $\text{CH}(\text{CH}_3)_2$, $J = 6.9$ Hz), 1.28-1.32 (m, 3H, OCH_2CH_3), 2.73-2.83 (m, 1H, $\text{CH}(\text{CH}_3)_2$), 3.81 (s, 3H, OCH_3), 3.89 (s, 2H, $\text{CH}_2\text{-Ar}$), 4.23-4.28 (m, 2H, OCH_2CH_3), 4.86 (s, 2H, NCH_2CO), 6.77 (s, 1H, Ar), 6.80-6.84 (m, 3H, Ar), 7.27 (t, 1H, Ar, $J = 7.8$ Hz).

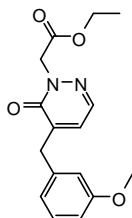
5. Experimental Chemistry

5.2.102 Ethyl-2-[3-cyclohexyl-5-(3-methoxybenzyl)-6-oxopyridazin-1(6H)-yl]acetate (48c)



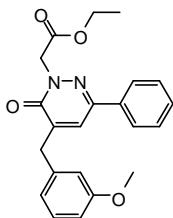
Yield = 58 %; oil. $^1\text{H NMR}$ (CDCl_3) δ 1.28-1.34 (m, 9H, 3 x CH_2 cyclohexyl + OCH_2CH_3), 1.70-1.82 (m, 4H, 2 x CH_2 cyclohexyl), 2.42-2.51 (m, 1H, CH cyclohexyl), 3.83 (s, 3H, OCH_3), 3.89 (s, 2H, CH_2 -Ar), 4.23-4.29 (m, 2H, OCH_2CH_3), 4.87 (s, 2H, NCH_2CO), 6.76 (s, 1H, Ar), 6.80-6.95 (m, 3H, Ar), 7.27 (dt, 1H, Ar, $J = 11.7$ Hz, $J = 2.0$ Hz).

5.2.103 Ethyl-2-[5-(3-methoxybenzyl)-6-oxopyridazin-1(6H)-yl]acetate (48d)



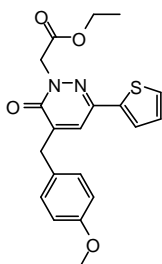
Yield = 47 %; oil. $^1\text{H NMR}$ (CDCl_3) δ 1.31 (t, 3H, CH_2CH_3 , $J = 7.1$ Hz), 3.82 (s, 3H, OCH_3), 3.91 (s, 2H, CH_2 -Ar), 4.27 (q, 2H, OCH_2CH_3 , $J = 7.2$ Hz), 4.92 (s, 2H, NCH_2CO), 6.79-6.80 (m, 2H, Ar), 6.83 (d, 2H, Ar, $J = 7.8$ Hz), 7.28 (t, 1H, Ar, $J = 8.0$ Hz), 7.67 (d, 1H, Ar, $J = 4.1$ Hz).

5.2.104 Ethyl-2-[5-(3-methoxybenzyl)-6-oxo-3-phenylpyridazin-1(6H)-yl]acetate (48e)



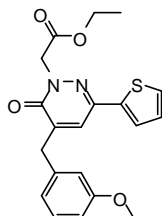
Yield = 47 %; oil. $^1\text{H NMR}$ (CDCl_3) δ 1.29-1.33 (td, 3H, CH_2CH_3 , $J = 6.8$ Hz, $J = 1.9$ Hz), 3.80 (s, 3H, OCH_3), 3.95 (s, 2H, CH_2 -Ar), 4.27 (q, 2H, OCH_2CH_3 , $J = 7.1$ Hz), 4.99 (s, 2H, NCH_2CO), 6.81-6.89 (m, 3H, Ar), 6.92-94 (m, 2H, Ar), 7.24-7.31 (m, 2H, Ar), 7.40-7.42 (m, 2H, Ar), 7.66-7.68 (m, 1H, Ar).

5.2.105 Ethyl-2-[5-(4-methoxybenzyl)-6-oxo-3-(thiophen-2-yl)pyridazin-1(6H)-yl]acetate (48f)



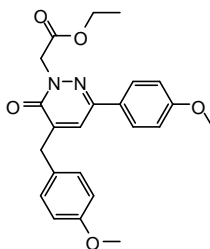
Yield = 91 %; mp = 127-29 °C (EtOH). $^1\text{H NMR}$ (CDCl_3) δ 1.32 (t, 3H, CH_2CH_3 , $J = 6.9$ Hz), 3.84 (s, 3H, OCH_3), 3.93 (s, 2H, $\text{CH}_2\text{-Ar}$), 4.28 (q, 2H, OCH_2CH_3 , $J = 7.1$ Hz), 4.94 (s, 2H, NCH_2CO), 6.92 (d, 2H, Ar, $J = 8.0$ Hz), 7.03 (t, 1H, Ar, $J = 4.0$ Hz), 7.20-7.28 (m, 4H, Ar), 7.35 (d, 1H, Ar, $J = 4.4$ Hz).

5.2.106 Ethyl-2-[5-(3-methoxybenzyl)-6-oxo-3-(thiophen-2-yl)pyridazin-1(6H)-yl]acetate (48g)



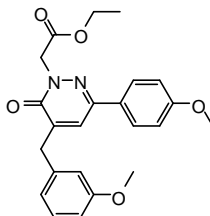
Yield ~ 100 %; mp = 149-51 °C (EtOH). $^1\text{H NMR}$ (CDCl_3) δ 1.32 (t, 3H, CH_2CH_3 , $J = 7.0$ Hz), 3.84 (s, 3H, OCH_3), 3.96 (s, 2H, $\text{CH}_2\text{-Ar}$), 4.28 (q, 2H, OCH_2CH_3 , $J = 7.1$ Hz), 4.94 (s, 2H, NCH_2CO), 6.87 (t, 3H, Ar, $J = 8.4$ Hz), 7.03-7.05 (m, 1H, Ar), 7.23-7.40 (m, 4H, Ar).

5.2.107 Ethyl-2-[5-(4-methoxybenzyl)-3-(4-methoxyphenyl)-6-oxopyridazin-1(6H)-yl]acetate (48h)



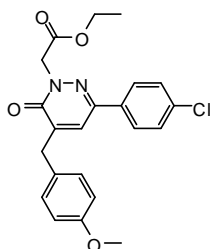
Yield ~ 100 %; oil. $^1\text{H NMR}$ (CDCl_3) δ 1.31 (t, 3H, CH_2CH_3 , $J = 3.9$ Hz), 3.82 (s, 3H, $\text{CH}_2\text{-C}_6\text{H}_4\text{-OCH}_3$), 3.84 (s, 3H, $\text{C}_6\text{H}_4\text{-OCH}_3$), 3.88 (s, 2H, $\text{CH}_2\text{-Ar}$), 4.26 (q, 2H, OCH_2CH_3 , $J = 7.1$ Hz), 4.97 (s, 2H, NCH_2CO), 6.88-6.99 (m, 5H, Ar), 7.21 (q, 2H, Ar, $J = 6.7$ Hz), 7.60 (d, 2H, Ar, $J = 8.8$ Hz).

5.2.108 Ethyl-2-[5-(3-methoxybenzyl)-3-(4-methoxyphenyl)-6-oxopyridazin-1(6H)-yl]acetate (48i)



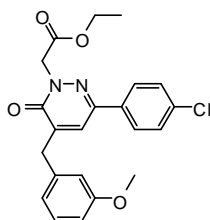
Yield ~ 100 %; oil. $^1\text{H NMR}$ (CDCl_3) δ 1.32 (t, 3H, CH_2CH_3 , $J = 7.2$ Hz), 3.82 (s, 3H, $\text{CH}_2\text{-C}_6\text{H}_4\text{-OCH}_3$), 3.84 (s, 3H, $\text{C}_6\text{H}_4\text{-OCH}_3$), 3.97 (s, 2H, $\text{CH}_2\text{-Ar}$), 4.28 (q, 2H, OCH_2CH_3 , $J = 7.1$ Hz), 4.98 (s, 2H, NCH_2CO), 6.84-6.95 (m, 6H, Ar), 7.27-7.31 (m, 1H, Ar), 7.61 (dd, 2H, Ar, $J = 4.8$ Hz, $J = 2.0$ Hz).

5.2.109 Ethyl-2-[3-(4-chlorophenyl)-5-(4-methoxybenzyl)-6-oxopyridazin-1(6H)-yl]acetate (48j)



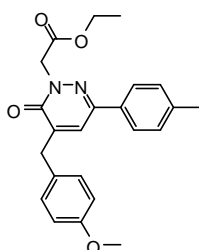
Yield ~ 100 %; oil. $^1\text{H NMR}$ (CDCl_3) δ 1.31 (t, 3H, CH_2CH_3 , $J = 7.1$ Hz), 3.82 (s, 3H, $\text{CH}_2\text{-C}_6\text{H}_4\text{-OCH}_3$), 3.87 (s, 2H, $\text{CH}_2\text{-Ar}$), 4.24 (q, 2H, OCH_2CH_3 , $J = 6.2$ Hz), 4.98 (s, 2H, NCH_2CO), 6.90 (d, 2H, Ar, $J = 8.5$ Hz), 7.21 (t, 2H, Ar, $J = 7.4$ Hz), 7.35-7.39 (m, 3H, Ar), 7.60 (d, 2H, Ar, $J = 8.6$ Hz).

5.2.110 Ethyl-2-[3-(4-chlorophenyl)-5-(3-methoxybenzyl)-6-oxopyridazin-1(6H)-yl]acetate (48k)



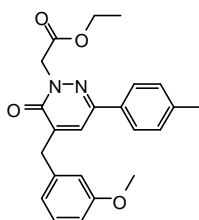
Yield ~ 100 %; oil. $^1\text{H NMR}$ (CDCl_3) δ 1.32 (t, 3H, CH_2CH_3 , $J = 7.2$ Hz), 3.82 (s, 3H, OCH_3), 3.97 (s, 2H, $\text{CH}_2\text{-Ar}$), 4.27 (q, 2H, OCH_2CH_3 , $J = 4.0$ Hz), 4.99 (s, 2H, NCH_2CO), 6.84-6.86 (m, 3H, Ar), 7.26-7.32 (m, 2H, Ar), 7.38 (d, 2H, Ar, $J = 8.6$ Hz), 7.61 (d, 2H, Ar, $J = 8.6$ Hz).

5.2.111 Ethyl-2-[5-(4-methoxybenzyl)-6-oxo-3-(*p*-tolyl)pyridazin-1(6H)-yl]acetate (48l)



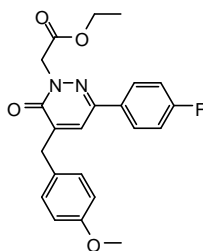
Yield = 98 %; oil. $^1\text{H NMR}$ (CDCl_3) δ 1.31 (t, 3H, CH_2CH_3 , $J = 7.1$ Hz), 2.38 (s, 3H, $\text{C}_6\text{H}_4\text{-CH}_3$), 3.83 (s, 3H, OCH_3), 3.93 (s, 2H, $\text{CH}_2\text{-Ar}$), 4.27 (q, 2H, OCH_2CH_3 , $J = 7.1$ Hz), 4.83 (s, 2H, NCH_2CO), 6.88-6.97 (m, 5H, Ar), 7.27 (d, 2H, Ar, $J = 8.5$ Hz), 8.07 (d, 2H, Ar, $J = 9.0$ Hz).

5.2.112 Ethyl-2-[5-(3-methoxybenzyl)-6-oxo-3-(*p*-tolyl)pyridazin-1(6H)-yl]acetate (48m)



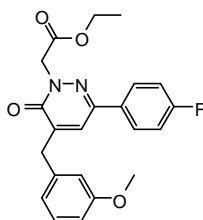
Yield = 97 %; oil. $^1\text{H NMR}$ (CDCl_3) δ 1.31 (t, 3H, CH_2CH_3 , $J = 7.1$ Hz), 2.39 (s, 3H, $\text{C}_6\text{H}_4\text{-CH}_3$), 3.82 (s, 3H, $\text{CH}_2\text{-C}_6\text{H}_4\text{-OCH}_3$), 3.97 (s, 2H, $\text{CH}_2\text{-Ar}$), 4.27 (q, 2H, OCH_2CH_3 , $J = 7.2$ Hz), 4.99 (s, 2H, NCH_2CO), 6.84-6.89 (m, 3H, Ar), 6.95-6.97 (m, 1H, Ar), 7.22 (d, 2H, Ar, $J = 7.9$ Hz), 7.27-7.31 (m, 1H, Ar), 8.07 (d, 2H, Ar, $J = 6.6$ Hz).

5.2.113 Ethyl-2-[3-(4-fluorophenyl)-5-(4-methoxybenzyl)-6-oxopyridazin-1(6H)-yl]acetate (48n)



Yield = 92 %; oil. $^1\text{H NMR}$ (CDCl_3) δ 1.32 (t, 3H, CH_2CH_3 , $J = 7.1$ Hz), 3.84 (s, 3H, OCH_3), 3.94 (s, 2H, $\text{CH}_2\text{-Ar}$), 4.27 (q, 2H, OCH_2CH_3 , $J = 7.1$ Hz), 4.99 (s, 2H, NCH_2CO), 6.92 (d, 3H, Ar, $J = 8.6$ Hz), 7.10 (t, 2H, Ar, $J = 8.5$ Hz), 7.21 (d, 2H, Ar, $J = 9.9$ Hz), 7.63-7.67 (m, 3H, Ar).

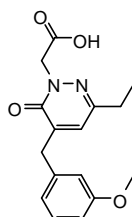
5.2.114 Ethyl-2-[3-(4-fluorophenyl)-5-(3-methoxybenzyl)-6-oxopyridazin-1(6H)-yl]acetate (48o)



Yield = 88 %; oil. $^1\text{H NMR}$ (CDCl_3) δ 1.32 (td, 3H, CH_2CH_3 , $J = 5.9$ Hz, $J = 1.3$ Hz), 3.82 (s, 3H, OCH_3), 3.98 (s, 2H, $\text{CH}_2\text{-Ar}$), 4.27 (q, 2H, OCH_2CH_3 , $J = 7.1$ Hz), 4.99 (s, 2H, NCH_2CO), 6.84-6.89 (m, 3H, Ar), 7.10 (t, 2H, Ar, $J = 8.6$ Hz), 7.25-7.30 (m, 2H, Ar), 7.63-7.67 (m, 3H, Ar).

General procedure for 49a-o. A suspension of the appropriate compound type **48** (**48a-o**) (1.33 mmol) in 6 N NaOH (10 mL) was stirred at rt to 80 °C for 1-2 h. The mixture was diluted with cold water and acidified with 6 N HCl. After 1 h stirring in ice-bath, the products **49a-o** were filtered off by suction and recrystallized from ethanol.

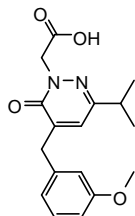
5.2.115 2-[3-Ethyl-5-(3-methoxybenzyl)-6-oxopyridazin-1(6H)-yl]acetic acid (49a)



5. Experimental Chemistry

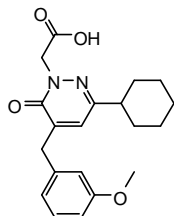
Yield ~ 100 %; mp = 117-19 °C (EtOH). ¹H NMR (CDCl₃) δ 1.17 (t, 3H, CH₂CH₃, *J* = 7.5 Hz), 2.55 (q, 2H, CH₂CH₃, *J* = 7.5 Hz), 3.82 (s, 3H, OCH₃), 3.91 (s, 2H, CH₂-Ar), 4.94 (s, 2H, NCH₂CO), 6.75 (s, 1H, Ar), 6.79 (s, 1H, Ar), 6.82-6.85 (m, 2H, Ar), 7.28 (t, 1H, Ar, *J* = 7.2 Hz).

5.2.116 2-[3-Isopropyl-5-(3-methoxybenzyl)-6-oxopyridazin-1(6*H*)-yl]acetic acid (49b)



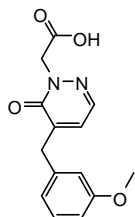
Yield = 69 %; oil. ¹H NMR (CDCl₃) δ 1.16 (d, 6H, CH(CH₃)₂, *J* = 6.9 Hz), 2.75-2.85 (m, 1H, CH(CH₃)₂), 3.81 (s, 3H, OCH₃), 3.91 (s, 2H, CH₂-Ar), 4.93 (s, 2H, NCH₂CO), 6.70 (exch br s, 1H, OH), 6.82 (t, 4H, Ar, *J* = 8.0 Hz), 7.27 (t, 1H, Ar, *J* = 4.2 Hz).

5.2.117 2-[3-Cyclohexyl-5-(3-methoxybenzyl)-6-oxopyridazin-1(6*H*)-yl]acetic acid (49c)



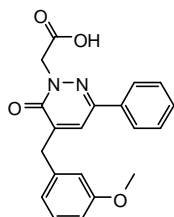
Yield = 70 %; oil. ¹H NMR (CDCl₃) δ 1.21-1.40 (m, 6H, 3 x CH₂ cyclohexyl), 1.70-1.82 (m, 4H, 2 x CH₂ cyclohexyl), 2.41-2.50 (m, 1H, CH cyclohexyl), 3.83 (s, 3H, OCH₃), 3.88 (s, 2H, CH₂-Ar), 4.65 (s, 2H, NCH₂CO), 6.79 (s, 1H, Ar), 6.81-6.98 (m, 3H, Ar), 7.30 (t, 1H, Ar, *J* = 7.1 Hz).

5.2.118 2-[5-(3-Methoxybenzyl)-6-oxopyridazin-1(6*H*)-yl]acetic acid (49d)



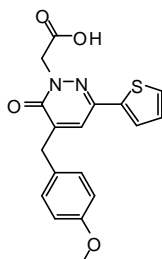
Yield ~ 100 %; oil. ¹H NMR (CDCl₃) δ 3.81 (s, 3H, OCH₃), 3.91 (s, 2H, CH₂-Ar), 4.98 (s, 2H, NCH₂CO), 6.49 (exch br s, 1H, OH), 6.78 (s, 1H, Ar), 6.81-6.85 (m, 3H, Ar), 7.28 (t, 1H, Ar, *J* = 4.6 Hz), 7.72 (d, 1H, Ar, *J* = 4.1 Hz).

5.2.119 2-[5-(3-Methoxybenzyl)-6-oxo-3-phenylpyridazin-1(6*H*)-yl]acetic acid (49e)



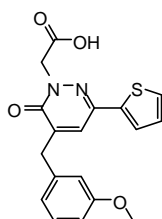
Yield = 60 %; mp = 173-75 °C (EtOH). $^1\text{H NMR}$ (CDCl_3) δ 3.79 (s, 3H, OCH_3), 3.93 (s, 2H, $\text{CH}_2\text{-Ar}$), 5.03 (s, 2H, NCH_2CO), 5.57 (exch br s, 1H, OH), 6.82-6.84 (m, 3H, Ar), 6.93 (t, 2H, Ar, $J = 4.16$ Hz), 7.24-7.31 (m, 2H, Ar), 7.41 (t, 2H, Ar, $J = 3.84$ Hz), 7.66-7.68 (m, 1H, Ar).

5.2.120 2-[5-(4-Methoxybenzyl)-6-oxo-3-(thiophen-2-yl)pyridazin-1(6H)-yl]acetic acid (49f)



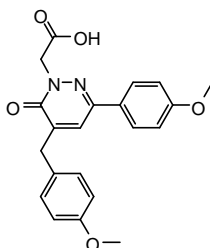
Yield = 89 %; mp = 159-61 °C (EtOH). $^1\text{H NMR}$ (CDCl_3) δ 3.84 (s, 3H, OCH_3), 3.94 (s, 2H, $\text{CH}_2\text{-Ar}$), 5.01 (s, 2H, NCH_2CO), 6.92 (dd, 2H, Ar, $J = 9.2$ Hz, $J = 1.4$ Hz), 7.04 (dd, 1H, Ar, $J = 1.4$ Hz, $J = 6.0$ Hz), 7.20-7.23 (m, 3H, Ar), 7.25 (dd, 1H, $J = 6.4$ Hz, $J = 1.0$ Hz), 7.37 (dd, 1H, Ar, $J = 6.4$ Hz, $J = 1.1$ Hz).

5.2.121 2-[5-(3-Methoxybenzyl)-6-oxo-3-(thiophen-2-yl)pyridazin-1(6H)-yl]acetic acid (49g)



Yield ~ 100 %; mp = 185-87 °C (EtOH). $^1\text{H NMR}$ (CDCl_3) δ 3.82 (s, 3H, OCH_3), 3.97 (s, 2H, $\text{CH}_2\text{-Ar}$), 5.01 (s, 2H, NCH_2CO), 6.84-6.88 (m, 3H, Ar), 7.03 (t, 1H, Ar, $J = 4.8$ Hz), 7.23 (t, 2H, Ar, $J = 3.2$ Hz), 7.28 (t, 1H, Ar, $J = 4.4$ Hz), 7.36 (d, 1H, Ar, $J = 5.0$ Hz).

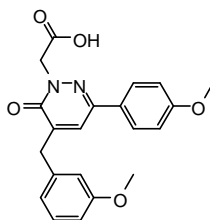
5.2.122 2-[5-(4-Methoxybenzyl)-3-(4-methoxyphenyl)-6-oxopyridazin-1(6H)-yl]acetic acid (49h)



Yield = 99 %; mp = 115-17 °C (EtOH). $^1\text{H NMR}$ (CDCl_3) δ 3.64 (s, 3H, $\text{CH}_2\text{-C}_6\text{H}_4\text{-OCH}_3$), 3.66 (s, 3H, $\text{C}_6\text{H}_4\text{-OCH}_3$), 3.79 (s, 2H, $\text{CH}_2\text{-Ar}$), 4.88 (s, 2H, NCH_2CO), 6.65-6.75 (m, 4H, Ar), 6.90-7.01 (m, 1H, Ar), 7.05-7.15 (m, 1H, Ar), 7.28-7.37 (m, 3H, Ar).

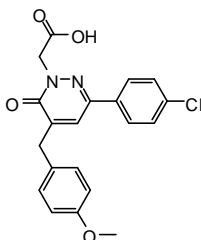
5. Experimental Chemistry

5.2.123 2-[5-(3-Methoxybenzyl)-3-(4-methoxyphenyl)-6-oxopyridazin-1(6H)-yl]acetic acid (49i)



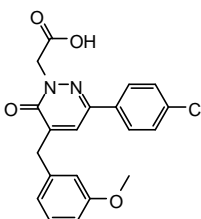
Yield = 98 %; 110-12 °C (EtOH). $^1\text{H NMR}$ (CDCl_3) δ 3.82 (s, 3H, $\text{CH}_2\text{-C}_6\text{H}_4\text{-OCH}_3$), 3.84 (s, 3H, $\text{C}_6\text{H}_4\text{-OCH}_3$), 3.88 (s, 2H, $\text{CH}_2\text{-Ar}$), 5.03 (s, 2H, NCH_2CO), 6.89-6.94 (m, 4H, Ar), 7.19 (d, 2H, Ar, $J = 8.6$ Hz), 7.24 (s, 1H, Ar), 7.60 (d, 2H, Ar, $J = 8.8$ Hz).

5.2.124 2-[3-(4-Chlorophenyl)-5-(4-methoxybenzyl)-6-oxopyridazin-1(6H)-yl]acetic acid (49j)

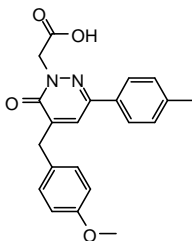


Yield ~ 100 %; mp = 147-49 °C (EtOH). $^1\text{H NMR}$ (CDCl_3) δ 3.83 (s, 3H, $\text{CH}_2\text{-C}_6\text{H}_4\text{-OCH}_3$), 3.92 (s, 2H, $\text{CH}_2\text{-Ar}$), 5.05 (s, 2H, NCH_2CO), 6.92 (d, 2H, Ar, $J = 8.5$ Hz), 7.20 (d, 2H, Ar, $J = 8.5$ Hz), 7.25 (s, 1H, Ar), 7.39 (d, 2H, Ar, $J = 8.5$ Hz), 7.61 (d, 2H, Ar, $J = 8.6$ Hz).

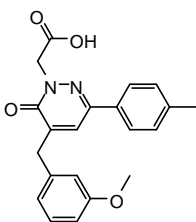
5.2.125 2-[3-(4-Chlorophenyl)-5-(3-methoxybenzyl)-6-oxopyridazin-1(6H)-yl]acetic acid (49k)



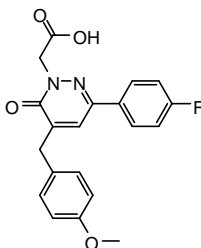
Yield ~ 100 %; mp = 142-44 °C (EtOH). $^1\text{H NMR}$ (CDCl_3) δ 3.81 (s, 3H, OCH_3), 3.97 (s, 2H, $\text{CH}_2\text{-Ar}$), 5.04 (s, 2H, NCH_2CO), 6.83-6.87 (m, 3H, Ar), 7.28 (d, 2H, Ar, $J = 7.8$ Hz), 7.38 (d, 2H, Ar, $J = 8.7$ Hz), 7.60 (d, 2H, Ar, $J = 8.7$ Hz).

5.2.126 2-[5-(4-Methoxybenzyl)-6-oxo-3-(*p*-tolyl)pyridazin-1(6*H*)-yl]acetic acid (49l)

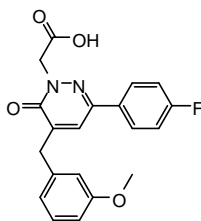
Yield = 98 %; mp = 158-60 °C (EtOH). $^1\text{H NMR}$ (CDCl_3) δ 2.39 (s, 3H, $\text{C}_6\text{H}_4\text{-CH}_3$), 3.83 (s, 3H, OCH_3), 3.95 (s, 2H, $\text{CH}_2\text{-Ar}$), 5.05 (s, 2H, NCH_2CO), 6.89-6.97 (m, 4H, Ar), 7.21 (dd, 2H, Ar, $J = 1.9$ Hz, $J = 6.3$ Hz), 7.29 (s, 1H, Ar), 7.56 (d, 2H, Ar, $J = 8.1$ Hz).

5.2.127 2-[5-(3-Methoxybenzyl)-6-oxo-3-(*p*-tolyl)pyridazin-1(6*H*)-yl]acetic acid (49m)

Yield = 97 %; mp = 150-52 °C (EtOH). $^1\text{H NMR}$ (CDCl_3) δ 2.26 (s, 3H, $\text{C}_6\text{H}_4\text{-CH}_3$), 3.66 (s, 3H, $\text{CH}_2\text{-C}_6\text{H}_4\text{-OCH}_3$), 3.82 (s, 2H, $\text{CH}_2\text{-Ar}$), 4.85 (s, 2H, NCH_2CO), 6.70 (d, 2H, Ar, $J = 5.3$ Hz), 6.95 (s, 1H, Ar), 7.03-7.12 (m, 3H, Ar), 7.28 (t, 1H, Ar, $J = 7.9$ Hz), 7.40 (d, 2H, Ar, $J = 7.8$ Hz).

5.2.128 2-[3-(4-Fluorophenyl)-5-(4-methoxybenzyl)-6-oxopyridazin-1(6*H*)-yl]acetic acid (49n)

Yield = 57 %; mp = 82-84 °C (EtOH). $^1\text{H NMR}$ (CDCl_3) δ 3.83 (s, 3H, OCH_3), 3.93 (s, 2H, $\text{CH}_2\text{-Ar}$), 5.03 (s, 2H, NCH_2CO), 6.91 (d, 2H, Ar, $J = 7.8$ Hz), 7.10 (t, 2H, Ar, $J = 8.4$ Hz), 7.14-7.23 (m, 3H, Ar), 7.65 (t, 2H, Ar, $J = 5.2$ Hz).

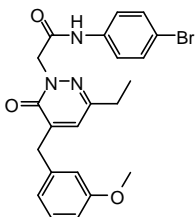
5.2.129 2-[3-(4-Fluorophenyl)-5-(3-methoxybenzyl)-6-oxopyridazin-1(6*H*)-yl]acetic acid (49o)

5. Experimental Chemistry

Yield = 75 %; mp = 103-05 °C (EtOH). ¹H NMR (CDCl₃) δ 3.81 (s, 3H, OCH₃), 3.97 (s, 2H, CH₂-Ar), 5.03 (s, 2H, CH₂CO), 6.83-6.87 (m, 3H, Ar), 7.10 (t, 2H, Ar, *J* = 6.6 Hz), 7.27-7.31 (m, 2H, Ar), 7.63-7.67 (m, 3H, Ar).

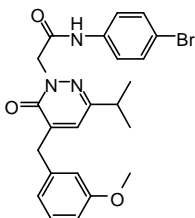
General procedure for 50a-v. To a cooled (-5 °C) and stirred solution of compound type **49** (**49a-o**) (0.60 mmol) in anhydrous tetrahydrofuran (6 mL), Et₃N (2.10 mmol) was added. After 30 min, the mixture was allowed to warm up to 0 °C and ethyl chloroformate (0.66 mmol) was added. After 1 h, the commercially available substituted arylamine (1.20 mmol) was added. The reaction was carried out at room temperature for 12 h, then the mixture was concentrated in vacuo, diluted with cold water (20-30 mL) and extracted with CH₂Cl₂ (3 x 15 mL). The solvent was evaporated to afford final compounds **46a-s**, which were purified by column chromatography using cyclohexane/ethyl acetate 2:1 for compounds **50a,g**, cyclohexane/ethyl acetate 3:1 for compounds **50b,e**, CH₂Cl₂/ CH₃OH/NH₄OH 96:4:0.4 for compound **50c**, cyclohexane/ethyl acetate 1:1 for compounds **50d,f,i,j** and n-hexane/ethyl acetate 3:2 for compound **50h,k-v** as eluents.

5.2.130 *N*-(4-Bromophenyl)-2-[3-ethyl-5-(3-methoxybenzyl)-6-oxopyridazin-1(6*H*)-yl]acetamide (**50a**)



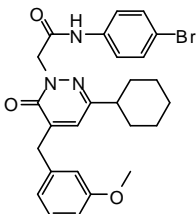
Yield = 61 %; mp = 150-52 °C (EtOH). ¹H NMR (CDCl₃) δ 1.20 (t, 3H, CH₂CH₃, *J* = 7.6 Hz), 2.59 (q, 2H, CH₂CH₃, *J* = 7.6 Hz), 3.81 (s, 3H, OCH₃), 3.91 (s, 2H, CH₂-Ar), 4.95 (s, 2H, NCH₂CO), 6.80-6.86 (m, 4H, Ar), 7.24-7.30 (m, 3H, Ar), 7.55 (d, 2H, Ar, *J* = 8.7 Hz), 9.18 (exch br s, 1H, NH).

5.2.131 *N*-(4-Bromophenyl)-2-[3-isopropyl-5-(3-methoxybenzyl)-6-oxopyridazin-1(6*H*)-yl]acetamide (**50b**)



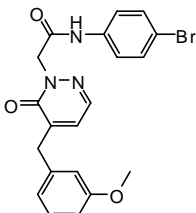
Yield = 67 %; mp = 60-62 °C (EtOH). ¹H NMR (CDCl₃) δ 1.20 (d, 6H, CH(CH₃)₂, *J* = 6.9 Hz), 2.82-2.90 (m, 1H, CH(CH₃)₂), 3.81 (s, 3H, OCH₃), 3.92 (s, 2H, CH₂-Ar), 4.95 (s, 2H, NCH₂CO), 6.82-6.85 (m, 3H, Ar), 6.92 (s, 1H Ar), 7.28 (t, 1H, Ar, *J* = 7.8 Hz), 7.37 (s, 4H, Ar), 9.23 (exch br s, 1H, NH).

5.2.132 *N*-(4-Bromophenyl)-2-[3-cyclohexyl-5-(3-methoxybenzyl)-6-oxopyridazin-1(6*H*)-yl]acetamide (50c)



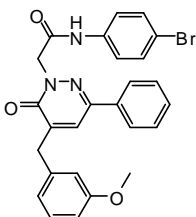
Yield = 36 %; colorless oil. $^1\text{H NMR}$ (CDCl_3) δ 1.30-1.35 (m, 6H, 3 x CH_2 cyclohexyl), 1.70-1.82 (m, 4H, 2 x CH_2 cyclohexyl), 2.45-2.55 (m, 1H, CH cyclohexyl), 3.82 (s, 3H, OCH_3), 3.92 (s, 2H, CH_2 -Ar), 4.95 (s, 2H, NCH_2CO), 6.81-6.88 (m, 4H, Ar), 7.28 (t, 1H, Ar, $J = 9.4$ Hz), 7.41 (s, 4H, Ar), 9.15 (exch br s, 1H, NH).

5.2.133 *N*-(4-Bromophenyl)-2-[5-(3-methoxybenzyl)-6-oxopyridazin-1(6*H*)-yl]acetamide (50d)



Yield = 70 %; mp = 138-40 °C (EtOH). $^1\text{H NMR}$ (DMSO-d_6) δ 3.73 (s, 3H, OCH_3), 3.79 (s, 2H, CH_2 -Ar), 4.90 (s, 2H, NCH_2CO), 6.83 (t, 3H, Ar, $J = 9.5$ Hz), 7.14 (d, 1H, Ar, $J = 3.8$ Hz), 7.23 (t, 1H, Ar, $J = 7.7$ Hz), 7.53 (q, 4H, Ar, $J = 8.2$ Hz), 7.85 (d, 1H, Ar, $J = 3.9$ Hz), 10.47 (exch br s, 1H, NH).

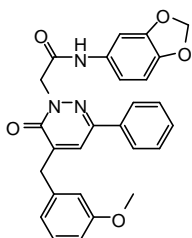
5.2.134 *N*-(4-Bromophenyl)-2-[5-(3-methoxybenzyl)-6-oxo-3-phenylpyridazin-1(6*H*)-yl]acetamide (50e)



Yield = 56 %; mp = 85-87 °C (EtOH). $^1\text{H NMR}$ (DMSO-d_6) δ 3.73 (s, 3H, OCH_3), 3.89 (s, 2H, CH_2 -Ar), 4.99 (s, 2H, NCH_2CO), 6.80 (d, 1H, Ar, $J = 8.0$ Hz), 7.93 (d, 2H, Ar, $J = 9.1$ Hz), 7.23 (t, 1H, Ar, $J = 7.9$ Hz), 7.45-7.51 (m, 5H, Ar), 7.56 (d, 2H, Ar, $J = 8.9$ Hz), 7.83 (d, 2H, Ar, $J = 7.1$ Hz), 7.86 (s, 1H, Ar), 10.51 (exch br s, 1H, NH).

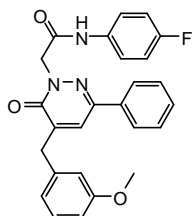
5. Experimental Chemistry

5.2.135 *N*-(1,3-Benzodioxol-5-yl)-2-[5-(3-methoxybenzyl)-6-oxo-3-phenylpyridazin-1(6*H*)-yl]acetamide (50f)



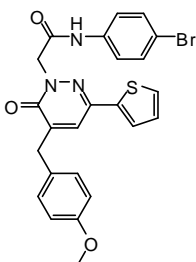
Yield = 41 %; mp = 201-03 °C (EtOH). ¹H NMR (DMSO-d₆) δ 3.73 (s, 3H, OCH₃), 3.88 (s, 2H, CH₂-Ar), 4.95 (s, 2H, NCH₂CO), 5.99 (s, 2H, OCH₂O), 6.80 (d, 1H, Ar, *J* = 6.0 Hz), 6.87 (d, 1H, Ar, *J* = 8.3 Hz), 6.92-6.97 (m, 3H, Ar), 7.23 (t, 1H, Ar, *J* = 7.8 Hz), 7.28 (s, 1H, Ar), 7.44-7.52 (m, 3H, Ar), 7.83 (d, 2H, Ar, *J* = 6.8 Hz), 7.95 (s, 1H, Ar), 10.27 (exch br s, 1H, NH).

5.2.136 *N*-(4-Fluorophenyl)-2-[5-(3-methoxybenzyl)-6-oxo-3-phenyl-pyridazin-1(6*H*)-yl]acetamide (50g)



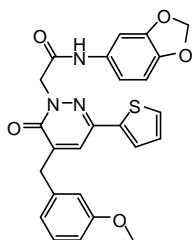
Yield = 78 %; mp = colorless oil. ¹H NMR (CDCl₃) δ 3.81 (s, 3H, OCH₃), 4.01 (s, 2H, CH₂-Ar), 5.10 (s, 2H, NCH₂CO), 6.85-6.90 (m, 3H, Ar), 6.96-7.04 (m, 2H, Ar), 7.29-7.34 (m, 1H, Ar), 7.43-7.49 (m, 6H, Ar), 7.71-7.74 (m, 2H, Ar), 8.95 (exch br s, 1H, NH).

5.2.137 *N*-(4-Bromophenyl)-2-[5-(4-methoxybenzyl)-6-oxo-3-(thiophen-2-yl)pyridazin-1(6*H*)-yl]acetamide (50h)



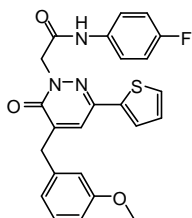
Yield = 77 %; mp = 193-94 °C (EtOH). ¹H NMR (CDCl₃) δ 3.83 (s, 3H, OCH₃), 3.95 (s, 2H, CH₂-Ar), 5.02 (s, 2H, NCH₂CO), 6.91 (dd, 2H, Ar, *J* = 4.6 Hz, *J* = 2.0 Hz), 7.06 (dd, 1H, Ar, *J* = 1.4 Hz, *J* = 3.9 Hz), 7.21 (d, 2H, Ar, *J* = 6.7 Hz), 7.30 (dd, 1H, Ar, *J* = 2.6 Hz, *J* = 1.0 Hz), 7.32-7.38 (m, 5H, Ar), 7.83 (dd, 1H, Ar, *J* = 4.0 Hz, *J* = 1.1 Hz), 9.00 (exch br s, 1H, NH).

5.2.138 *N*-(1,3-Benzodioxol-5-yl)-2-[5-(3-methoxybenzyl)-6-oxo-3-(thiophen-2-yl)pyridazin-1(6*H*)-yl]acetamide (**50i**)



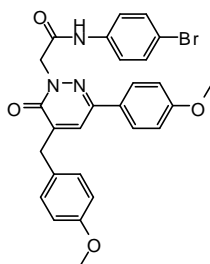
Yield = 41 %; mp = 192-94 °C (EtOH). ¹H NMR (CDCl₃) δ 3.82 (s, 3H, OCH₃), 3.98 (s, 2H, CH₂-Ar), 5.02 (s, 2H, NCH₂CO), 5.94 (s, 2H, OCH₂O), 6.71 (d, 1H, Ar, *J* = 8.3 Hz), 6.81-6.89 (m, 4H, Ar), 7.05 (dd, 1H, Ar, *J* = 1.3 Hz, *J* = 3.7 Hz), 7.23 (d, 1H, Ar, *J* = 1.9 Hz), 7.28-7.32 (m, 3H, Ar), 7.38 (dd, 1H, Ar, *J* = 4.2 Hz, *J* = 0.9 Hz), 8.71 (exch br s, 1H, NH).

5.2.139 *N*-(4-Fluorophenyl)-2-[5-(3-methoxybenzyl)-6-oxo-3-(thiophen-2-yl)pyridazin-1(6*H*)-yl]acetamide (**50j**)



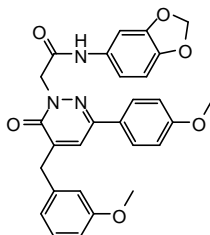
Yield = 37 %; mp = 187-89 °C (EtOH). ¹H NMR (CDCl₃) δ 3.81 (s, 3H, OCH₃), 3.99 (s, 2H, CH₂-Ar), 5.03 (s, 2H, NCH₂CO), 6.85-6.89 (m, 3H, Ar), 6.96 (t, 2H, Ar, *J* = 8.6 Hz), 7.05 (dd, 1H, Ar, *J* = 1.4 Hz, *J* = 3.7 Hz), 7.27-7.30 (m, 2H, Ar), 7.32 (s, 1H, Ar), 7.39 (dd, 1H, Ar, *J* = 4.0 Hz, *J* = 1.1 Hz), 7.43 (m, 2H, Ar), 8.89 (exch br s, 1H, NH).

5.2.140 *N*-(4-Bromophenyl)-2-[5-(4-methoxybenzyl)-3-(4-methoxyphenyl)-6-oxopyridazin-1(6*H*)-yl]acetamide (**50k**)



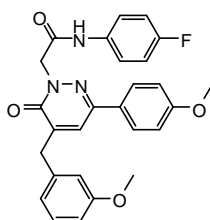
Yield = 32 %; mp = 203-04 °C (EtOH). ¹H NMR (CDCl₃) δ 3.83 (s, 3H, CH₂C₆H₄-OCH₃), 3.86 (s, 3H, C₆H₄-OCH₃), 3.97 (s, 2H, CH₂-Ar), 5.07 (s, 2H, NCH₂CO), 6.90-6.96 (m, 4H, Ar), 7.22 (d, 2H, Ar, *J* = 8.6 Hz), 7.36-7.38 (m, 5H, Ar), 7.67 (d, 1H, Ar, *J* = 8.8 Hz), 9.14 (exch br s, 1H, NH).

5.2.141 *N*-(1,3-Benzodioxol-5-yl)-2-[5-(3-methoxybenzyl)-3-(4-methoxyphenyl)-6-oxopyridazin-1(6*H*)-yl]acetamide (50l)



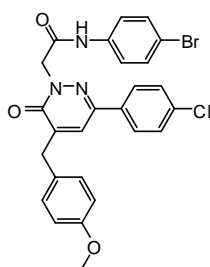
Yield = 89 %; mp = 184-85 °C (EtOH). ¹H NMR (CDCl₃) δ 3.81 (s, 3H, CH₂C₆H₄-OCH₃), 3.85 (s, 3H, C₆H₄-OCH₃), 3.99 (s, 2H, CH₂-Ar), 5.05 (s, 2H, NCH₂CO), 5.93 (s, 2H, OCH₂O), 6.68 (d, 1H, Ar, *J* = 8.3 Hz), 6.79 (dd, 1H, Ar, *J* = 6.2 Hz, *J* = 2.1 Hz), 6.84-6.90 (m, 3H, Ar), 6.94 (dd, 2H, Ar, *J* = 4.9 Hz, *J* = 2.0 Hz), 7.22 (d, 1H, Ar, *J* = 2.0 Hz), 7.27-7.31 (m, 1H, Ar), 7.38 (s, 1H, Ar), 7.66 (d, 2H, Ar, *J* = 1.9 Hz), 8.95 (exch br s, 1H, NH).

5.2.142 *N*-(4-Fluorophenyl)-2-[5-(3-methoxybenzyl)-3-(4-methoxyphenyl)-6-oxopyridazin-1(6*H*)-yl]acetamide (50m)



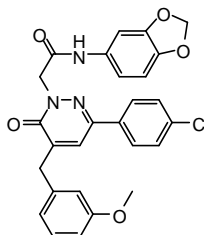
Yield = 84 %; mp = 164-65 °C (EtOH). ¹H NMR (CDCl₃) δ 3.80 (s, 3H, CH₂C₆H₄-OCH₃), 3.86 (s, 3H, C₆H₄-OCH₃), 3.99 (s, 2H, CH₂-Ar), 5.07 (s, 2H, NCH₂CO), 6.83-6.96 (m, 7H, Ar), 7.29 (t, 1H, Ar, *J* = 1.8 Hz), 7.40-7.45 (m, 3H, Ar), 7.67 (d, 2H, Ar, *J* = 7.5 Hz), 9.17 (exch br s, 1H, NH).

5.2.143 *N*-(4-Bromophenyl)-2-[3-(4-chlorophenyl)-5-(4-methoxybenzyl)-6-oxopyridazin-1(6*H*)-yl]acetamide (50n)



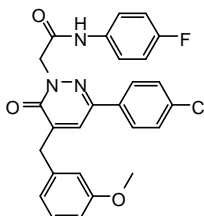
Yield = 27 %; mp = 219-21 °C (EtOH). ¹H NMR (CDCl₃) δ 3.82 (s, 3H, OCH₃), 3.97 (s, 2H, CH₂-Ar), 5.08 (s, 2H, NCH₂CO), 6.91 (d, 2H, Ar, *J* = 8.7 Hz), 7.21 (d, 2H, Ar, *J* = 8.7 Hz), 7.32-7.37 (m, 5H, Ar), 7.41 (d, 2H, Ar, *J* = 8.8 Hz), 7.66 (d, 2H, Ar, *J* = 8.7 Hz), 9.12 (exch br s, 1H, NH).

5.2.144 *N*-(1,3-Benzodioxol-5-yl)-2-[3-(4-chlorophenyl)-5-(3-methoxybenzyl)-6-oxopyridazin-1(6*H*)-yl]acetamide (**50o**)



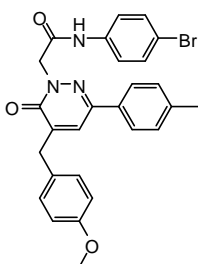
Yield = 99 %; mp = 202-203 °C (EtOH). ¹H NMR (CDCl₃) δ 3.82 (s, 3H, OCH₃), 4.01 (s, 2H, CH₂-Ar), 5.05 (s, 2H, NCH₂CO), 5.95 (s, 2H, OCH₂O), 6.73 (d, 1H, Ar, *J* = 8.4 Hz), 6.80-6.90 (m, 4H, Ar), 7.23 (d, 1H, Ar, *J* = 1.8 Hz), 7.30 (t, 1H, Ar, *J* = 8.2 Hz), 7.36 (s, 1H, Ar), 7.41 (d, 2H, Ar, *J* = 8.5 Hz), 7.66 (d, 2H, Ar, *J* = 8.5 Hz), 8.70 (exch br s, 1H, NH).

5.2.145 *N*-(4-Fluorophenyl)-2-[3-(4-chlorophenyl)-5-(3-methoxybenzyl)-6-oxopyridazin-1(6*H*)-yl]acetamide (**50p**)



Yield = 63 %; mp = 143-45 °C (EtOH). ¹H NMR (CDCl₃) δ 3.80 (s, 3H, OCH₃), 4.00 (s, 2H, CH₂-Ar), 5.08 (s, 2H, NCH₂CO), 6.84-6.95 (m, 5H, Ar), 7.27-7.31 (m, 1H, Ar), 7.39-7.44 (m, 5H, Ar), 7.66 (d, 2H, Ar, *J* = 8.5 Hz), 9.06 (exch br s, 1H, NH).

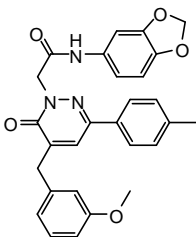
5.2.146 *N*-(4-Bromophenyl)-2-[5-(4-methoxybenzyl)-6-oxo-3-(*p*-tolyl) pyridazin-1(6*H*)-yl]acetamide (**50q**)



Yield = 58 %; mp = 273-274 °C (EtOH). ¹H NMR (CDCl₃) δ 2.40 (s, 3H, C₆H₄-CH₃), 3.81 (s, 3H, OCH₃), 3.95 (s, 2H, CH₂-Ar), 5.09 (s, 2H, NCH₂CO), 6.89 (d, 2H, Ar, *J* = 8.1 Hz), 7.20-7.33 (m, 8H, Ar), 7.41 (s, 1H, Ar), 7.62 (d, 2H, Ar, *J* = 7.7 Hz), 9.38 (exch br s, 1H, NH).

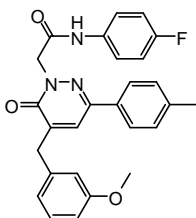
5. Experimental Chemistry

5.2.147 *N*-(1,3-Benzodioxol-5-yl)-2-[5-(3-methoxybenzyl)-6-oxo-3-(*p*-tolyl) pyridazin-1(6*H*)-yl]acetamide (50r)



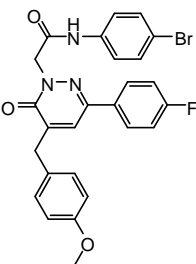
Yield = 66 %; mp = 198-99 °C (EtOH). $^1\text{H NMR}$ (CDCl_3) δ 2.40 (s, 3H, $\text{C}_6\text{H}_4\text{-CH}_3$), 3.81 (s, 3H, OCH_3), 4.00 (s, 2H, $\text{CH}_2\text{-Ar}$), 5.06 (s, 2H, NCH_2CO), 5.94 (s, 2H, OCH_2O), 6.70 (d, 1H, Ar, $J = 8.4$ Hz), 6.79-6.90 (m, 4H, Ar), 7.24 (d, 3H, Ar, $J = 8.0$ Hz), 7.29 (t, 1H, Ar, $J = 7.8$ Hz), 7.40 (s, 1H, Ar), 7.61 (d, 2H, Ar, $J = 8.1$ Hz), 8.84 (exch br s, 1H, NH).

5.2.148 *N*-(4-Fluorophenyl)-2-[5-(3-methoxybenzyl)-6-oxo-3-(*p*-tolyl) pyridazin-1(6*H*)-yl]acetamide (50s)



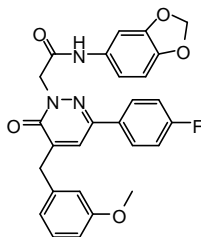
Yield = 54 %; mp = 173-74 °C (EtOH). $^1\text{H NMR}$ (CDCl_3) δ 2.40 (s, 3H, $\text{C}_6\text{H}_4\text{-CH}_3$), 3.80 (s, 3H, OCH_3), 3.99 (s, 2H, $\text{CH}_2\text{-Ar}$), 5.08 (s, 2H, NCH_2CO), 6.83-6.95 (m, 5H, Ar), 7.23-7.26 (m, 2H, Ar), 7.28 (t, 1H, Ar, $J = 5.3$ Hz), 7.42-7.45 (m, 3H, Ar), 7.61 (d, 2H, Ar, $J = 8.2$ Hz), 9.11 (exch br s, 1H, NH).

5.2.149 *N*-(4-Bromophenyl)-2-[3-(4-fluorophenyl)-5-(4-methoxybenzyl)-6-oxopyridazin-1(6*H*)-yl]acetamide (50t)



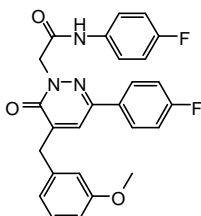
Yield = 75 %; mp = 188-90 °C (EtOH). $^1\text{H NMR}$ (CDCl_3) δ 3.82 (s, 3H, OCH_3), 3.97 (s, 2H, $\text{CH}_2\text{-Ar}$), 5.07 (s, 2H, NCH_2CO), 6.91 (dd, 2H, Ar, $J = 4.6$ Hz, $J = 2.0$ Hz), 7.12 (t, 2H, Ar, $J = 6.7$ Hz), 7.21 (d, 2H, Ar, $J = 8.6$ Hz), 7.30-7.40 (m, 5H, Ar), 7.69-7.73 (m, 2H, Ar), 9.15 (exch br s, 1H, NH).

5.2.150 *N*-(1,3-Benzodioxol-5-yl)-2-[3-(4-fluorophenyl)-5-(3-methoxybenzyl)-6-oxopyridazin-1(6*H*)-yl]acetamide (**50u**)



Yield = 75 %; mp = 188-90 °C (EtOH). ¹H NMR (CDCl₃) δ 3.82 (s, 3H, OCH₃), 4.00 (s, 2H, CH₂-Ar), 5.05 (s, 2H, NCH₂CO), 5.95 (s, 2H, OCH₂O), 6.72 (d, 1H, Ar, *J* = 8.3 Hz), 6.80-6.90 (m, 4H, Ar), 7.12 (t, 2H, Ar, *J* = 8.8 Hz), 7.23 (s, 1H, Ar), 7.30 (t, 1H, Ar, *J* = 8.8 Hz), 7.36 (s, 1H, Ar), 7.71 (dd, 2H, Ar, *J* = 2.4 Hz, *J* = 5.3 Hz), 8.74 (exch br s, 1H, NH).

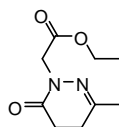
5.2.151 *N*-(4-Fluorophenyl)-2-[3-(4-fluorophenyl)-5-(3-methoxybenzyl)-6-oxopyridazin-1(6*H*)-yl]acetamide (**50v**)



Yield = 58 %; mp = 152-53 °C (EtOH). ¹H NMR (CDCl₃) δ 3.81 (s, 3H, OCH₃), 4.00 (s, 2H, CH₂-Ar), 5.08 (s, 2H, NCH₂CO), 6.85-6.89 (m, 3H, Ar), 6.92-6.96 (m, 2H, Ar), 7.10-7.15 (m, 2H, Ar), 7.28-7.32 (m, 1H, Ar), 7.39 (s, 1H, Ar), 7.42-7.46 (m, 2H, Ar), 7.69-7.73 (m, 2H, Ar), 9.02 (exch br s, 1H, NH).

General procedure for 51a,(±)-51b. A mixture of **42d** or (±)-**42m** (7.41 mmol), K₂CO₃ (14.82 mmol) and ethyl bromoacetate (11.12 mmol) in CH₃CN (5 mL) was refluxed under stirring for 2-3 h. The mixture was then concentrated in vacuo, diluted with cold water, and extracted with CH₂Cl₂ (3 x 15 mL). The organic layer was evaporated in vacuo, and the final compounds **51a,(±)-b** were purified by column chromatography using cyclohexane/ethyl acetate 1:1 as eluent.

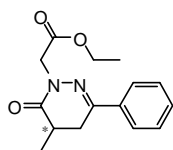
5.2.152 Ethyl-2-[3-Methyl-6-oxo-5,6-dihydropyridazin-1(4*H*)-yl]acetate (**51a**)



Yield = 98 %; oil. ¹H NMR (CDCl₃) δ 1.22 (t, 3H, CH₂CH₃, *J* = 7.1 Hz), 2.01 (s, 3H, 3-CH₃), 2.48 (qd, 2H, CH₂CH₂ pyridaz., *J* = 7.9 Hz, *J* = 5.0 Hz), 4.15 (q, 2H, CH₂CH₃, *J* = 7.1 Hz), 4.40 (s, 2H, NCH₂CO).

5. Experimental Chemistry

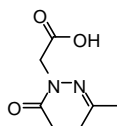
5.2.153 (±)-Ethyl-2-[5-methyl-6-oxo-3-phenyl-5,6-dihydropyridazin-1(4H)-yl]acetate [(±)-51b]



Yield ~ 100 %; oil. $^1\text{H NMR}$ (CDCl_3) δ 1.28 (m, 6H, CH_2CHCH_3 + CH_2CH_3), 2.67-2.79 (m, 2H, CH_2CHCH_3), 3.07-3.14 (m, 1H, CH_2CHCH_3), 4.24 (q, 2H, CH_2CH_3 , $J = 6.9$ Hz), 4.59 (d, 2H, NCH_2CO , $J = 8.0$ Hz), 7.40-7.43 (m, 3H, Ar), 7.72-7.75 (m, 2H, Ar).

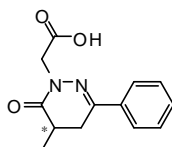
General procedure for 52a,(±)-52b. A suspension of **51a** or (±)-**52b** (7.29 mmol) in 6 N NaOH (10 mL) was stirred at rt to 80 °C for 3-5 h. The mixture was then diluted with cold water and acidified with 6 N HCl. Products **52a** and (±)-**52b** were filtered off by suction and recrystallized from cyclohexane (**52a**) or ethanol [(±)-**52b**].

5.2.154 2-[3-Methyl-6-oxo-5,6-dihydropyridazin-1(4H)-yl]acetic acid (52a)



Yield = 86 %; mp = 171-73 °C (EtOH). $^1\text{H NMR}$ (CDCl_3) δ 1.96 (s, 3H, 3- CH_3), 2.35-2.39 (m, 2H, CH_2 pyridaz.), 2.40-2.49 (m, 2H, CH_2 pyridaz.), 4.23 (s, 2H, NCH_2CO).

5.2.155 (±)-2-[5-Methyl-6-oxo-3-phenyl-5,6-dihydropyridazin-1(4H)-yl]acetic acid [(±)-52b]

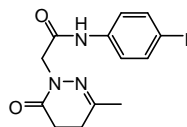


Yield ~ 100 %; mp = 87-89 °C (EtOH). $^1\text{H NMR}$ (CDCl_3) δ 1.31 (d, 3H, CH_2CHCH_3 , $J = 6.7$ Hz), 2.68-2.78 (m, 2H, CH_2CHCH_3), 3.04-3.16 (m, 1H, CH_2CHCH_3), 4.64 (s, 2H, NCH_2CO), 6.98 (exch br s, 1H, OH), 7.41-7.43 (m, 3H, Ar), 7.73-7.75 (m, 2H, Ar).

General procedure for 53a,(±)-53b-d. To a cooled (-5 °C) and stirred solution of the appropriate derivative **52** [**52a**,(±)-**52b**] (2.06 mmol) in anhydrous tetrahydrofuran (6 mL), Et_3N (7.21 mmol) was added. After 30 min, the mixture was allowed to warm up to 0 °C and ethyl chloroformate (2.27 mmol) was added. After 1 h, the appropriately substituted arylamine (4.12 mmol) was added. The reaction was carried out at room temperature for 12 h. The mixture was then concentrated in vacuo, diluted with cold water (20-30 mL) and extracted with CH_2Cl_2 (3 x 15 mL). The solvent was evaporated to afford final

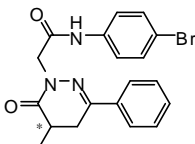
compounds **53a**,(\pm)-**53b-d**, which were purified by column chromatography using cyclohexane/ethyl acetate 1:3 (for compound **53a**), cyclohexane/ethyl acetate 2:1 (for compound (\pm)-**53b**) and *n*-hexane/ethyl acetate 3:2 (for compounds (\pm)-**53c,d**) as eluents.

5.2.156 *N*-(4-Iodophenyl)-2-[3-methyl-6-oxo-5,6-dihydropyridazin-1(4*H*)-yl]acetamide (**53a**)



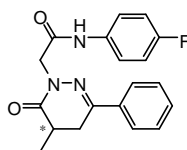
Yield = 98 %; mp = 174-76 °C (EtOH). ¹H NMR (CDCl₃) δ 2.11 (s, 3H, 3-CH₃), 2.55-2.60 (m, 4H, CH₂CH₂ pyridaz.), 4.52 (s, 2H, NCH₂CO), 7.31 (d, 2H, Ar, *J* = 8.8 Hz), 7.62 (d, 2H, Ar, *J* = 8.8 Hz), 8.11 (exch br s, 1H, NH).

5.2.157 (\pm)-*N*-(4-Bromophenyl)-2-[5-methyl-6-oxo-3-phenyl-5,6-dihydropyridazin-1(4*H*)-yl]acetamide [(\pm)-**53b**]



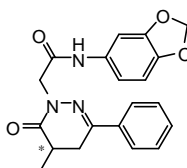
Yield = 23 %; mp = 148-149 °C (EtOH). ¹H NMR (CDCl₃) δ 1.37 (d, 3H, CH₂CHCH₃, *J* = 6.3 Hz), 2.74-2.81 (m, 2H, CH₂CHCH₃), 3.14-3.22 (quin, 1H, CH₂CHCH₃, *J* = 11.6 Hz), 4.68 (s, 2H, NCH₂CO), 7.28 (d, 2H, Ar, *J* = 10.1 Hz), 7.44 (t, 4H, Ar, *J* = 7.0 Hz), 7.60 (d, 1H, Ar, *J* = 3.9 Hz), 7.77-7.79 (m, 2H, Ar), 8.15 (exch, br, s, 1H, NH).

5.2.158 (\pm)-*N*-(4-Fluorophenyl)-2-[5-methyl-6-oxo-3-phenyl-5,6-dihydropyridazin-1(4*H*)-yl]acetamide [(\pm)-**53c**]



Yield = 61 %; mp = 164-165 °C (EtOH). ¹H NMR (CDCl₃) δ 1,35 (d, 3H, CH₂CHCH₃, *J* = 6.4 Hz), 2,69-2.80 (m, 2H, CH₂CHCH₃), 3,11-3,20 (m, 1H, CH₂CHCH₃), 4,68 (s, 2H, NCH₂CO), 6,98 (t, 2H, Ar, *J* = 8.8 Hz), 7,42-7.49 (m, 5H, Ar), 7,76-7.78 (m, 2H, Ar), 8.25 (exch, br, s, 1H, NH).

5.2.159 (\pm)-*N*-(1,3-Benzodioxol-5-yl)-2-[5-methyl-6-oxo-3-phenyl-5,6-dihydropyridazin-1(4*H*)-yl]acetamide [(\pm)-**53d**]

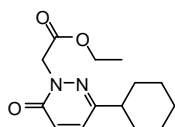


5. Experimental Chemistry

Yield = 88 %; mp = 170-171 °C (EtOH). $^1\text{H NMR}$ (CDCl_3) δ 1.35 (d, 3H, CH_2CHCH_3 , $J = 6.4$ Hz), 2.69-2.80 (m, 2H, CH_2CHCH_3), 3.16 (q, 1H, CH_2CHCH_3 , $J = 10.1$ Hz), 4.66 (s, 2H, NCH_2CO), 5.94 (s, 2H, OCH_2O), 6.72 (d, 1H, Ar, $J = 8.3$ Hz), 6.80 (dd, 1H, Ar, $J = 6.2$ Hz, $J = 2.1$ Hz), 7.24 (s, 1H, Ar), 7.44 (t, 3H, Ar, $J = 2.8$ Hz), 7.77-7.79 (m, 2H, Ar), 8.01 (exch, br, s, 1H, NH).

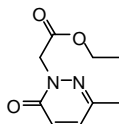
General procedure for 55a-c. A mixture of compound type **42** [**42c,d** and (\pm)-**42m**] (2.27 mmol), K_2CO_3 (4.54 mmol), and ethyl bromoacetate (3.41 mmol) in CH_3CN (3 mL) was refluxed under stirring for 2-3 h. The mixture was then concentrated in vacuo, diluted with cold water and extracted with CH_2Cl_2 (3 x 15 mL). The organic layer was evaporated in vacuo, and compounds **55a-c** were used for the following reactions without further purification.

5.2.160 Ethyl-2-[3-cyclohexyl-6-oxopyridazin-1(6H)-yl]acetate (**55a**)



Yield ~ 100 %; oil. $^1\text{H NMR}$ (CDCl_3) δ 1.28-1.46 (m, 8H, (2 x CH_2 + CH-*H*) cyclohexyl + CH_2CH_3), 1.71-1.86 (m, 5H, 2 x CH_2 + CH-*H* cyclohexyl), 2.51-2.60 (m, 1H, CH, cyclohexyl), 4.23 (dt, 2H, CH_2CH_3 , $J = 4.3$ Hz, $J = 1.4$ Hz), 4.83 (s, 2H, NCH_2CO), 6.90 (d, 1H, Ar, $J = 9.0$ Hz), 7.17 (d, 1H, Ar, $J = 9.6$ Hz).

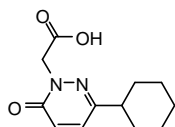
5.2.161 Ethyl-2-[3-methyl-6-oxopyridazin-1(6H)-yl]acetate (**55b**)



Yield ~ 100 %; oil. $^1\text{H NMR}$ (CDCl_3) δ 1.30 (t, 3H, CH_2CH_3 , $J = 7.1$ Hz), 2.37 (s, 3H, 3- CH_3), 4.26 (q, 2H, CH_2CH_3 , $J = 7.1$ Hz), 4.87 (s, 2H, NCH_2CO), 7.02 (d, 1H, Ar, $J = 9.4$ Hz), 7.20 (d, 1H, Ar, $J = 9.4$ Hz).

General procedure for 56a-c. A suspension of derivative **55** (**55a-c**) (0.91 mmol) in 6 N NaOH (4 mL) was stirred at rt to 80 °C for 2 h. The mixture was then diluted with cold water and acidified with 6 N HCl. Products **56a,c** were filtered off by suction and recrystallized from ethanol.

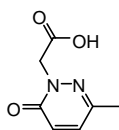
5.2.162 2-[3-Cyclohexyl-6-oxopyridazin-1(6H)-yl]acetic acid (**56a**)



Yield = 82 %; mp = 195-97 °C (EtOH). $^1\text{H NMR}$ (CDCl_3) δ 1.25-1.34 (m, 1H, CH-*H* cyclohexyl), 1.37-1.46 (m, 4H, 2 x CH_2 cyclohexyl), 1.76 (m, 1H, CH-*H* cyclohexyl), 1.79-1.93 (m, 4H, 2 x CH_2

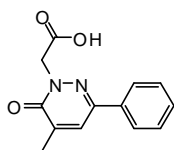
cyclohexyl), 2.50-2.60 (m, 1H, CH cyclohexyl), 4.94 (s, 2H, NCH₂CO), 6.99 (d, 1H, Ar, *J* = 9.5 Hz), 7.24 (d, 1H, Ar, *J* = 9.6 Hz).

5.2.163 2-[3-Methyl-6-oxopyridazin-1(6*H*)-yl]acetic acid (56b)



Yield = 72 %; mp = 247-49 °C (EtOH). ¹H NMR (CDCl₃) δ 2.37 (s, 3H, 3-CH₃), 4.94 (s, 2H, NCH₂CO), 6.97 (d, 1H, Ar, *J* = 9.5 Hz), 7.19 (d, 1H, Ar, *J* = 9.6 Hz).

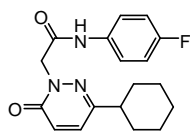
5.2.164 2-[5-Methyl-6-oxo-3-phenylpyridazin-1(6*H*)-yl]acetic acid (56c)



Yield = 90 %; mp = 92-94 °C (EtOH). ¹H NMR (CDCl₃) δ 2.34 (s, 3H, CH₃), 3.48 (exch br s, 1H, OH), 5.05 (s, 2H, CH₂COO), 7.45-7.50 (m, 3H, Ar), 7.63 (s, 1H, Ar), 7.78 (d, 2H, Ar, *J* = 4.5 Hz).

General procedure for 57a-f. To a cooled (-5 °C) and stirred solution of the appropriate compound **56** (**56a-c**) (0.59 mmol) in anhydrous tetrahydrofuran (3 mL), Et₃N (2.06 mmol) was added. After 30 min, the mixture was allowed to warm up to 0 °C and ethyl chloroformate (0.65 mmol) was added. After 1 h, the appropriately substituted arylamine (1.18 mmol) was added. The reaction was carried out at room temperature for 12 h. The mixture was then concentrated in vacuo, diluted with cold water (10-15 mL), and extracted with CH₂Cl₂ (3 x 15 mL). The solvent was evaporated to afford final compounds **57a-f**, which were purified by column chromatography using cyclohexane/ethyl acetate 1:1 (for compound **57a,d-f**), cyclohexane/ethyl acetate 1:2 (for compound **57b**) and CH₂Cl₂/CH₃OH 9.9:0.1 (for compound **57c**) as eluents.

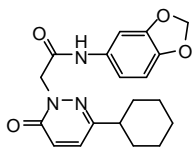
5.2.165 *N*-(4-Fluorophenyl)-2-[3-cyclohexyl-6-oxopyridazin-1(6*H*)-yl]acetamide (57a)



Yield = 98 %; mp = 149-51 °C (EtOH). ¹H NMR (CDCl₃) δ 1.21-1.30 (m, 1H, CH-*H* cyclohexyl), 1.39-1.48 (m, 4H, 2 x CH₂ cyclohexyl), 1.77 (d, 1H, CH-*H* cyclohexyl, *J* = 12.6 Hz), 1.85-1.93 (m, 4H, 2 x CH₂ cyclohexyl), 2.56-2.63 (m, 1H, CH cyclohexyl), 4.96 (s, 2H, NCH₂CO), 6.94-7.02 (m, 3H, Ar), 7.27 (d, 1H, Ar, *J* = 9.7 Hz), 7.46-7.49 (m, 2H, Ar), 9.10 (exch br s, 1H, NH).

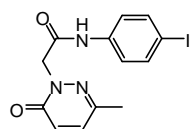
5. Experimental Chemistry

5.2.166 *N*-(1,3-Benzodioxol-5-yl)-2-[3-cyclohexyl-6-oxopyridazin-1(6*H*)-yl]acetamide (57b)



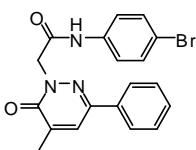
Yield ~ 100 %; mp = 185-87 °C (EtOH). ¹H NMR (CDCl₃) δ 1.20-1.28 (m, 1H, CH-*H* cyclohexyl), 1.30-1.48 (m, 4H, 2 x CH₂ cyclohexyl), 1.76 (d, 1H, CH-*H* cyclohexyl, *J* = 12.8 Hz), 1.85-1.93 (m, 4H, 2 x CH₂ cyclohexyl), 2.59-2.61 (m, 1H, CH cyclohexyl), 4.93 (s, 2H, NCH₂CO), 5.94 (s, 2H, OCH₂O), 6.72 (d, 1H, Ar, *J* = 8.4 Hz), 6.81 (dd, 1H, Ar, *J* = 6.3 Hz, *J* = 2.1 Hz), 7.00 (d, 1H, Ar, *J* = 9.5 Hz), 7.25-7.28 (m, 2H, Ar), 8.86 (exch br s, 1H, NH).

5.2.167 *N*-(4-Iodophenyl)-2-[3-methyl-6-oxopyridazin-1(6*H*)-yl]acetamide (57c)



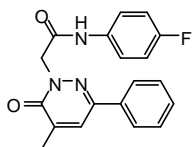
Yield ~ 100 %; mp = 160-61 °C (EtOH). ¹H NMR (CDCl₃) δ 2.39 (s, 3H, 3-CH₃), 4.96 (s, 2H, NCH₂CO), 6.97 (d, 1H, Ar, *J* = 9.5 Hz), 7.20-7.26 (m, 3H, Ar), 7.50 (dt, 2H, Ar, *J* = 5.2 Hz, *J* = 1.8 Hz), 9.27 (exch br s, 1H, NH).

5.2.168 *N*-(4-Bromophenyl)-2-[5-methyl-6-oxo-3-phenylpyridazin-1(6*H*)-yl]acetamide (57d)



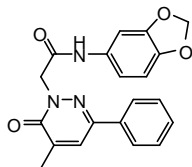
Yield = 38 %; mp = 149-51 °C (EtOH). ¹H NMR (CDCl₃) δ 2.37 (s, 3H, CH₃), 5.08 (s, 2H, CH₂CO), 7.40-7.49 (m, 7H, Ar), 7.68 (s, 1H, Ar), 7.82 (dd, 2H, Ar, *J* = 5.8 Hz, *J* = 1.4 Hz), 9.02 (exch br s, 1H, NH).

5.2.169 *N*-(4-Fluorophenyl)-2-[5-methyl-6-oxo-3-phenylpyridazin-1(6*H*)-yl]acetamide (57e)



Yield = 45 %; mp = 117-19 °C (EtOH). ¹H NMR (CDCl₃) δ 2.34 (s, 3H, CH₃), 5.11 (s, 2H, CH₂CO), 6.89-6.93 (td, 2H, Ar, *J* = 3.7 Hz, *J* = 2.1 Hz), 7.44-7.49 (m, 5H, Ar), 7.65 (s, 1H, Ar), 7.79-7.82 (dd, 2H, Ar, *J* = 3.1 Hz, *J* = 1.9 Hz), 9.21 (exch br s, 1H, NH).

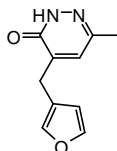
5.2.170 *N*-(1,3-Benzodioxol-5-yl)-2-[5-methyl-6-oxo-3-phenylpyridazin-1(6*H*)-yl]acetamide (**57f**)



Yield = 25 %; mp = 215-17 °C (EtOH). ¹H NMR (DMSO-*d*₆) δ 2.19 (s, 3H, CH₃), 4.95 (s, 2H, OCH₂O), 5.99 (s, 2H, CH₂CO), 6.87 (d, 1H, Ar, *J* = 8.3 Hz), 6.96 (d, 1H, Ar, *J* = 8.5 Hz), 7.29 (s, 1H, Ar), 7.49 (q, 3H, Ar, *J* = 7.5 Hz), 7.89 (d, 2H, Ar, *J* = 7.1 Hz), 8.04 (s, 1H, Ar), 10.26 (exch br s, 1H, NH).

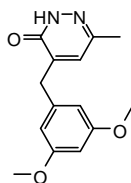
General Procedure for 58a-m. To 12 mL of KOH in absolute EtOH (5%, w/v), **42d** (4.46 mmol) and the appropriate substituted aromatic aldehyde (4.46 mmol) were added. The mixture was refluxed under stirring for 3-5 h. After cooling, it was concentrated in vacuo, diluted with ice-cold water (20-25 mL) and acidified with 2 N HCl. The suspension was extracted with CH₂Cl₂ (3 x 25 mL). Removal of the solvent afforded compounds **58a-m**, which were purified by crystallization in ethanol. For compound **58f** was necessary to perform an additional purification step by flash column chromatography using cyclohexane/ethyl acetate 2:1 as eluent.

5.2.171 **4-(Furan-3-ylmethyl)-6-methylpyridazin-3(2*H*)-one (58a)**



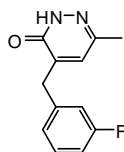
Yield = 24 %; mp = 137-39 °C (EtOH). ¹H NMR (CDCl₃) δ 2.29 (s, 3H, CH₃), 3.74 (s, 2H, CH₂), 6.33 (s, 1H, Ar), 6.86 (s, 1H, Ar), 7.39 (s, 1H, Ar), 7.46 (s, 1H, Ar).

5.2.172 **4-(3,5-Dimethoxybenzyl)-6-methylpyridazin-3(2*H*)-one (58f)**



Yield = 56 %; mp = 167-69 °C (EtOH). ¹H NMR (CDCl₃) δ 2.27 (s, 3H, CH₃), 3.81 (s, 6H, 2 x OCH₃), 3.85 (s, 2H, CH₂), 6.41 (s, 3H, Ar), 6.77 (s, 1H, Ar).

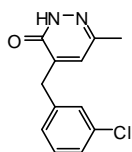
5.2.173 **4-(3-Fluorobenzyl)-6-methylpyridazin-3(2*H*)-one (58g)**



5. Experimental Chemistry

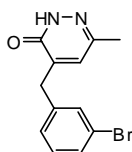
Yield = 95 %; mp = 114-16 °C (EtOH). ^1H NMR (CDCl_3) δ 2.28 (s, 3H, CH_3), 3.91 (s, 2H, CH_2), 6.75 (s, 1H, Ar), 6.98-7.07 (m, 3H, Ar), 7.30-7.36 (m, 1H, Ar), 11.31 (exch br s, 1H, NH).

5.2.174 4-(3-Chlorobenzyl)-6-methylpyridazin-3(2H)-one (58h)



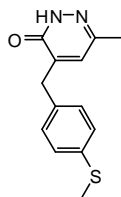
Yield = 81 %; mp = 124-26 °C (EtOH). ^1H NMR (CDCl_3) δ 2.28 (s, 3H, CH_3), 3.89 (s, 2H, CH_2), 6.75 (s, 1H, Ar), 7.16-7.18 (m, 1H, Ar), 7.26-7.31 (m, 3H, Ar), 11.09 (exch br s, 1H, NH).

5.2.175 4-(3-Bromobenzyl)-6-methylpyridazin-3(2H)-one (58j)



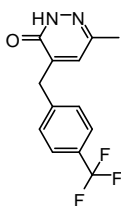
Yield = 28 %; mp = 147-49 °C (EtOH). ^1H NMR (CDCl_3) δ 2.28 (s, 3H, CH_3), 3.88 (s, 2H, CH_2), 6.75 (s, 1H, Ar), 7.24 (d, 2H, Ar, $J = 5.2$ Hz), 7.45 (d, 2H, Ar, $J = 9.1$ Hz), 10.82 (exch br s, 1H, NH).

5.2.176 6-Methyl-4-[4-(methylthio)benzyl]pyridazin-3(2H)-one (58k)



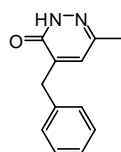
Yield = 46 %; mp = 151-53 °C (EtOH). ^1H NMR (CDCl_3) δ 2.26 (s, 3H, CH_3), 2.51 (s, 3H, SCH_3), 3.87 (s, 2H, CH_2), 6.71 (s, 1H, Ar), 7.18 (d, 2H, Ar, $J = 8.2$ Hz), 7.27 (dd, 3H, Ar, $J = 9.3$ Hz, $J = 1.8$ Hz).

5.2.177 6-Methyl-4-[4-(trifluoromethyl)benzyl]pyridazin-3(2H)-one (58l)



Yield = 94 %; mp = 153-55 °C (EtOH). ^1H NMR (CDCl_3) δ 2.29 (s, 3H, CH_3), 3.97 (s, 2H, CH_2), 6.77 (s, 1H, Ar), 7.40 (d, 2H, Ar, $J = 8.0$ Hz), 7.62 (d, 2H, Ar, $J = 8.1$ Hz), 11.19 (exch br s, 1H, NH).

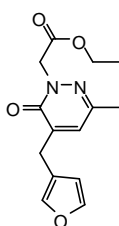
5.2.178 4-Benzyl-6-methylpyridazin-3(2H)-one (58m)



Yield ~ 100 %; mp = 113-15 °C (EtOH). ^1H NMR (CDCl_3) δ 2.26 (s, 3H, CH_3), 3.92 (s, 2H, CH_2), 6.73 (s, 1H, Ar), 7.26-7.33 (m, 3H, Ar), 7.28 (t, 2H, Ar, $J = 6.9$ Hz).

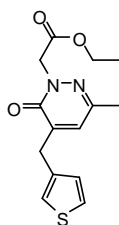
General Procedure for 59a-m. A mixture of the suitable intermediate type **58** (**58a-m**) (4.50 mmol), K_2CO_3 (9.00 mmol) and ethyl bromoacetate (6.75 mmol) in CH_3CN (10 mL) was refluxed under stirring for 2-4 h. The mixture was then concentrated in vacuo, diluted with cold water and extracted with CH_2Cl_2 (3 x 15 mL). The solvent was evaporated in vacuo and compounds **59a-m** were purified by crystallization from ethanol (compounds **59a,g,h,j,k**) or by flash column chromatography using cyclohexane/ethyl acetate 2:1 (for **59b-e**) and cyclohexane/ethyl acetate 1:1 (for **59f,i,l,m**) as eluents.

5.2.179 Ethyl-2-[5-(furan-3-ylmethyl)-3-methyl-6-oxopyridazin-1(6H)-yl]acetate (59a)



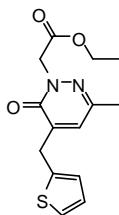
Yield = 69 %; mp = 61-67 °C (EtOH). ^1H NMR (CDCl_3) δ 1.31 (t, 3H, CH_2CH_3 , $J = 7.1$ Hz), 2.27 (s, 3H, 3- CH_3), 3.73 (s, 2H, CHCCH_2), 4.27 (q, 2H, OCH_2CH_3 , $J = 7.1$ Hz), 4.87 (s, 2H, NCH_2CO), 6.32 (s, 1H, Ar), 6.82 (s, 1H, Ar), 7.37 (s, 1H, Ar), 7.45 (s, 1H, Ar).

5.2.180 Ethyl-2-[3-methyl-6-oxo-5-(thiophen-3-ylmethyl)pyridazin-1(6H)-yl]acetate (59b)



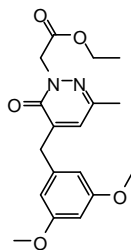
Yield = 91 %; oil. ^1H NMR (CDCl_3) δ 1.31 (t, 3H, CH_2CH_3 , $J = 7.1$ Hz), 2.25 (s, 3H, 3- CH_3), 3.93 (s, 2H, CHCCH_2), 4.25 (q, 2H, CH_2CH_3 , $J = 5.8$ Hz), 4.86 (s, 1H, NCH_2CO), 6.72 (s, 1H, Ar), 6.97 (dd, 1H, Ar, $J = 3.64$ Hz, $J = 1.2$ Hz), 7.11 (s, 1H, Ar), 7.33 (dd, 1H, Ar, $J = 2.0$ Hz, $J = 4.6$ Hz).

5.2.181 Ethyl-2-[3-methyl-6-oxo-5-(thiophen-2-ylmethyl)pyridazin-1(6H)-yl]acetate (59c)



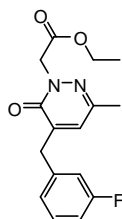
Yield ~ 100 %; oil. ^1H NMR (CDCl_3) δ 1.30 (t, 3H, CH_2CH_3 , $J = 7.1$ Hz), 2.26 (s, 3H, 3- CH_3), 4.11 (s, 2H, CHCCH_2), 4.25 (q, 2H, CH_2CH_3 , $J = 7.1$ Hz), 4.86 (s, 2H, NCH_2CO), 6.82 (s, 1H, Ar), 6.92 (d, 1H, Ar, $J = 3.3$ Hz), 7.00 (t, 1H, Ar, $J = 3.9$ Hz), 7.22 (d, 1H, Ar, $J = 5.1$ Hz).

5.2.182 Ethyl-2-[5-(3,5-dimethoxybenzyl)-3-methyl-6-oxopyridazin-1(6H)-yl]acetate (59f)



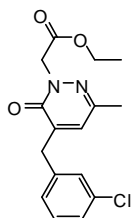
Yield = 95 %; brown oil. $^1\text{H NMR}$ (CDCl_3) δ 1.31 (t, 3H, CH_2CH_3), 2.24 (s, 3H, 3- CH_3), 3.79 (s, 6H, 2 x OCH_3), 3.84 (s, 2H, CHCCH_2), 4.24 (q, 2H, OCH_2CH_3 , $J = 7.1$ Hz), 4.86 (s, 2H, NCH_2CO), 6.39 (s, 3H, Ar), 6.70 (s, 1H, Ar).

5.2.183 Ethyl-2-[5-(3-fluorobenzyl)-3-methyl-6-oxopyridazin-1(6H)-yl]acetate (59g)



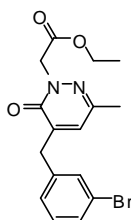
Yield = 89 %; mp = 74-76 °C (EtOH). $^1\text{H NMR}$ (CDCl_3) δ 1.31 (t, 3H, CH_2CH_3 , $J = 7.2$ Hz), 2.26 (s, 3H, 3- CH_3), 3.91 (s, 2H, CHCCH_2), 4.26 (q, 2H, OCH_2CH_3 , $J = 7.2$ Hz), 4.87 (s, 2H, NCH_2CO), 6.71 (s, 1H, Ar), 6.95-7.05 (m, 3H, Ar), 7.30 (q, 1H, Ar, $J = 6.5$ Hz).

5.2.184 Ethyl-2-[5-(3-chlorobenzyl)-3-methyl-6-oxopyridazin-1(6H)-yl]acetate (59h)

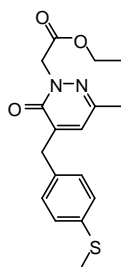


Yield ~ 100 %; mp = 89-91 °C (EtOH). $^1\text{H NMR}$ (CDCl_3) δ 1.31 (t, 3H, CH_2CH_3 , $J = 7.2$ Hz), 2.27 (s, 3H, 3- CH_3), 3.88 (s, 2H, CHCCH_2), 4.27 (q, 2H, OCH_2CH_3 , $J = 7.2$ Hz), 4.86 (s, 2H, NCH_2CO), 6.71 (s, 1H, Ar), 7.15 (dd, 1H, Ar, $J = 4.5$ Hz, $J = 1.8$ Hz), 7.24-7.30 (m, 3H, Ar).

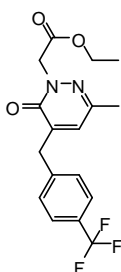
5.2.185 Ethyl-2-[5-(3-bromobenzyl)-3-methyl-6-oxopyridazin-1(6H)-yl]acetate (59j)



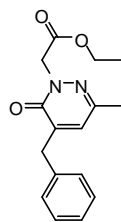
Yield = 82 %; mp = 98-100 °C (EtOH). $^1\text{H NMR}$ (CDCl_3) δ 1.31 (t, 3H, CH_2CH_3 , $J = 7.0$ Hz), 2.27 (s, 3H, 3- CH_3), 3.88 (s, 2H, CHCCH_2), 4.27 (q, 2H, OCH_2CH_3 , $J = 7.0$ Hz), 4.86 (s, 2H, NCH_2CO), 6.71 (s, 1H, Ar), 7.21-7.25 (m, 2H, Ar), 7.42 (d, 2H, Ar, $J = 11.9$ Hz).

5.2.186 Ethyl-2-{3-methyl-5-[4-(methylthio)benzyl]-6-oxopyridazin-1(6H)-yl}acetate (59k)

Yield ~ 100 %; mp = 129-31 °C (EtOH). $^1\text{H NMR}$ (CDCl_3) δ 1.31 (t, 3H, CH_2CH_3 , $J = 6.8$ Hz), 2.24 (s, 3H, 3- CH_3), 2.51 (s, 3H, SCH_3), 3.87 (s, 2H, CHCCH_2), 4.27 (q, 2H, OCH_2CH_3 , $J = 6.8$ Hz), 4.86 (s, 2H, NCH_2CO), 6.68 (s, 1H, Ar), 7.17 (d, 2H, Ar, $J = 7.3$ Hz), 7.25-7.29 (m, 2H, Ar).

5.2.187 Ethyl-2-{3-methyl-6-oxo-5-[4-(trifluoromethyl)benzyl]pyridazin-1(6H)-yl}acetate (59l)

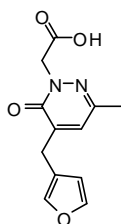
Yield ~ 100 %; brown oil. $^1\text{H NMR}$ (CDCl_3) δ 1.30 (t, 3H, CH_2CH_3 , $J = 7.0$ Hz), 2.27 (s, 3H, 3- CH_3), 3.96 (s, 2H, CHCCH_2), 4.26 (q, 2H, OCH_2CH_3 , $J = 7.1$ Hz), 4.86 (s, 2H, NCH_2CO), 6.73 (s, 1H, Ar), 7.38 (d, 2H, Ar, $J = 8.0$ Hz), 7.60 (d, 2H, Ar, $J = 8.0$ Hz).

5.2.188 Ethyl-2-[5-benzyl-3-methyl-6-oxopyridazin-1(6H)-yl]acetate (59m)

Yield = 98 %; oil. $^1\text{H NMR}$ (CDCl_3) δ 1.31 (t, 3H, CH_2CH_3 , $J = 7.1$ Hz), 2.22 (s, 3H, 3- CH_3), 3.90 (s, 2H, CHCCH_2), 4.24 (q, 2H, CH_2CH_3 , $J = 7.1$ Hz), 4.85 (s, 2H, NCH_2CO), 6.66 (s, 1H, Ar), 7.23-7.28 (m, 3H, Ar), 7.33-7.37 (m, 2H, Ar).

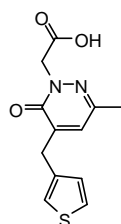
General Procedure for 60a-m. A suspension of the suitable intermediate type **59** (**59a-m**) (4.4 mmol) in 6 N NaOH (10 mL) was stirred at rt to 80 °C for 1-2 h. The mixture was firstly diluted with ice-cold water and then acidified with 6 N HCl. Products **60a-m** were filtered off by suction and recrystallized from ethanol.

5.2.189 2-[5-(Furan-3-ylmethyl)-3-methyl-6-oxopyridazin-1(6H)-yl]acetic acid (60a)



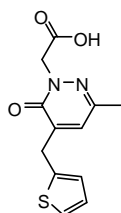
Yield = 69 %; mp = 62-64 °C (EtOH). ¹H NMR (CDCl₃) δ 2.29 (s, 3H, 3-CH₃), 3.46 (exch br s, 1H, OH), 3.75 (s, 2H, CHCCH₂), 4.93 (s, 2H, NCH₂CO), 6.31 (s, 1H, Ar), 6.86 (s, 1H, Ar), 7.37 (s, 1H, Ar), 7.45 (s, 1H, Ar).

5.2.190 2-[3-Methyl-6-oxo-5-(thiophen-3-ylmethyl)pyridazin-1(6H)-yl]acetic acid (60b)



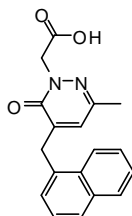
Yield ~ 100 %; mp = 123-25 °C (EtOH). ¹H NMR (CDCl₃) δ 2.27 (s, 3H, 3-CH₃), 3.95 (s, 2H, CHCCH₂), 4.93 (s, 2H, NCH₂CO), 5.21 (exch br s, 1H, OH), 6.76 (s, 1H, Ar), 6.97 (d, 1H, Ar, *J* = 4.8 Hz), 7.12 (s, 1H, Ar), 7.35 (t, 1H, Ar, *J* = 4.4 Hz).

5.2.191 2-[3-Methyl-6-oxo-5-(thiophen-2-ylmethyl)pyridazin-1(6H)-yl]acetic acid (60c)

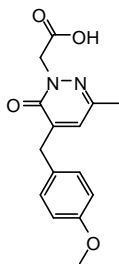


Yield = 88 %; mp = 123-25 °C (EtOH). ¹H NMR (CDCl₃) δ 2.28 (s, 3H, 3-CH₃), 4.13 (s, 2H, CHCCH₂), 4.93 (s, 2H, NCH₂CO), 6.85 (s, 1H, Ar), 6.94 (d, 1H, Ar, *J* = 3.4 Hz), 7.01 (dd, 1H, Ar, *J* = 1.6 Hz, *J* = 3.4 Hz), 7.24 (dd, 1H, Ar, *J* = 4.0 Hz, *J* = 1.0 Hz), 8.41 (exch br s, 1H, OH).

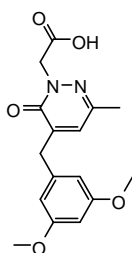
5.2.192 2-[3-Methyl-5-(naphthalen-1-ylmethyl)-6-oxopyridazin-1(6H)-yl]acetic acid (60d)



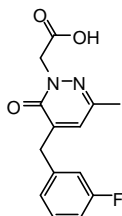
Yield = 98 %; mp = 198-200 °C (EtOH). ¹H NMR (CDCl₃) δ 2.11 (s, 3H, 3-CH₃), 4.39 (s, 2H, CHCCH₂), 5.01 (s, 2H, NCH₂CO), 5.83 (exch br s, 1H, OH), 6.42 (s, 1H, Ar), 7.41 (d, 1H, Ar, *J* = 6.8 Hz), 7.47-7.54 (m, 3H, Ar), 7.79 (d, 1H, Ar, *J* = 7.4 Hz), 7.86 (d, 1H, Ar, *J* = 8.2 Hz), 7.91 (d, 1H, Ar, *J* = 7.3 Hz).

5.2.193 2-[5-(4-Methoxybenzyl)-3-methyl-6-oxopyridazin-1(6H)-yl]acetic acid (60e)

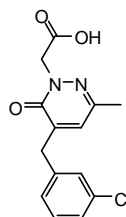
Yield = 96 %; mp = 144-45 °C (EtOH). $^1\text{H NMR}$ (CDCl_3) δ 2.26 (s, 3H, 3- CH_3), 3.84 (s, 3H, OCH_3), 3.87 (s, 2H, CHCCH_2), 4.93 (s, 2H, NCH_2CO), 6.69 (s, 1H, Ar), 6.91 (d, 2H, Ar, $J = 8.5$ Hz), 7.16 (d, 2H, Ar, $J = 8.5$ Hz).

5.2.194 2-[5-(3,5-Dimethoxybenzyl)-3-methyl-6-oxopyridazin-1(6H)-yl]acetic acid (60f)

Yield = 76 %; mp = 112-14 °C (EtOH). $^1\text{H NMR}$ (CDCl_3) δ 2.26 (s, 3H, 3- CH_3), 3.37 (exch br s, 1H, OH), 3.80 (s, 6H, 2 x OCH_3), 3.85 (s, 2H, CHCCH_2), 4.93 (s, 2H, NCH_2CO), 6.40 (s, 3H, Ar), 6.75 (s, 1H, Ar).

5.2.195 2-[5-(3-Fluorobenzyl)-3-methyl-6-oxopyridazin-1(6H)-yl]acetic acid (60g)

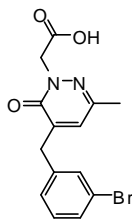
Yield = 82 %; mp = 124-26 °C (EtOH). $^1\text{H NMR}$ (CDCl_3) δ 2.27 (s, 3H, 3- CH_3), 3.92 (s, 2H, CHCCH_2), 4.92 (s, 2H, NCH_2CO), 6.35 (exch br s, 1H, OH), 6.72 (s, 1H, Ar), 6.95-7.04 (m, 3H, Ar), 7.30-7.36 (q, 1H, Ar, $J = 6.1$ Hz).

5.2.196 2-[5-(3-Chlorobenzyl)-3-methyl-6-oxopyridazin-1(6H)-yl]acetic acid (60h)

Yield = 75 %; mp = 162-64 °C (EtOH). $^1\text{H NMR}$ (CDCl_3) δ 2.28 (s, 3H, 3- CH_3), 3.90 (s, 2H, CHCCH_2), 4.93 (s, 2H, NCH_2CO), 6.72 (s, 1H, Ar), 7.14 (d, 1H, Ar, $J = 5.6$ Hz), 7.23-7.45 (m, 1H, Ar).

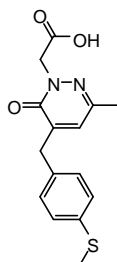
5. Experimental Chemistry

5.2.197 2-[5-(3-Bromobenzyl)-3-methyl-6-oxopyridazin-1(6H)-yl]acetic acid (60j)



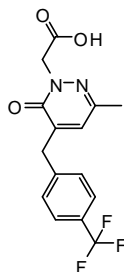
Yield = 89 %; mp = 173-75 °C (EtOH). $^1\text{H NMR}$ (CDCl_3) δ 2.29 (s, 3H, 3- CH_3), 3.90 (s, 2H, CHCCH_2), 4.92 (s, 2H, NCH_2CO), 6.74 (s, 1H, Ar), 7.19-7.26 (m, 2H, Ar), 7.43 (t, 2H, Ar, $J = 7.4$ Hz).

5.2.198 2-{3-Methyl-5-[4-(methylthio)benzyl]-6-oxopyridazin-1(6H)-yl}acetic acid (60k)



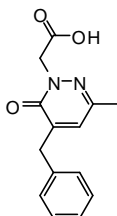
Yield ~ 100 %; mp = 87-89 °C (EtOH). $^1\text{H NMR}$ (CDCl_3) δ 2.25 (s, 3H, 3- CH_3), 2.51 (s, 3H, SCH_3), 3.87 (s, 2H, CHCCH_2), 4.91 (s, 2H, NCH_2CO), 6.69 (s, 1H, Ar), 7.16 (d, 2H, Ar, $J = 7.6$ Hz), 7.25 (d, 2H, Ar, $J = 7.6$ Hz).

5.2.199 2-{3-Methyl-6-oxo-5-[4-(trifluoromethyl)benzyl]pyridazin-1(6H)-yl}acetic acid (60l)



Yield = 82 %; mp = 127-29 °C (EtOH). $^1\text{H NMR}$ (CDCl_3) δ 2.28 (s, 3H, 3- CH_3), 3.98 (s, 2H, CHCCH_2), 4.93 (s, 2H, NCH_2CO), 6.74 (s, 1H, Ar), 7.37 (d, 2H, Ar, $J = 8.0$ Hz), 7.61 (d, 2H, Ar, $J = 8.0$ Hz).

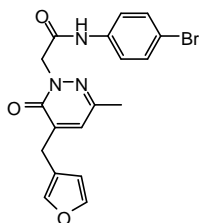
5.2.200 2-[5-Benzyl-3-methyl-6-oxopyridazin-1(6H)-yl]acetic acid (60m)



Yield = 92 %; mp = 120-22 °C (EtOH). $^1\text{H NMR}$ (CDCl_3) δ 2.25 (s, 3H, 3- CH_3), 3.93 (s, 2H, CHCCH_2), 4.94 (s, 2H, NCH_2CO), 5.50 (exch br s, 1H, OH), 6.70 (s, 1H, Ar), 7.24-7.32 (m, 3H, Ar), 7.35-7.39 (m, 2H, Ar).

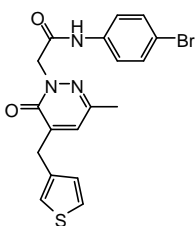
General Procedure for 61a-p. To a cooled (-5 °C) and stirred solution of the appropriate compound **60** (**60a-m**) (0.90 mmol), in anhydrous tetrahydrofuran (6 mL), Et₃N (3.15 mmol) was added. After 30 min, the mixture was allowed to warm up to 0 °C and ethyl chloroformate (0.99 mmol) was added. After 1 h, the appropriately substituted arylamine (1.80 mmol) was added. The reaction was carried out at room temperature for 12 h. The mixture was then concentrated in vacuo, diluted with cold water (10-15 mL), and extracted with CH₂Cl₂ (3 x 15 mL). The solvent was evaporated to afford final compounds **61a-p**, which were purified by column chromatography using cyclohexane/ethyl acetate 1:1 for compounds **61a,b,f,j,n,o**, CH₂Cl₂/CH₃OH 9.8:0.2 for compound **48c**, cyclohexane/ethyl acetate 2:1 for compounds **61d,g-i,l,m**, toluene/NH₄OH/EtOH/CH₂Cl₂/petroleum ether 7:0.05:0.30:2:0.65 for compound **61e** and cyclohexane/ethyl acetate 1:2 for compounds **61k,p**.

5.2.201 *N*-(4-Bromophenyl)-2-[5-(furan-3-ylmethyl)-3-methyl-6-oxo-pyridazin-1(6*H*)-yl]acetamide (**61a**)



Yield = 50 %; mp = 67-69 °C (EtOH). ¹H NMR (CDCl₃) δ 2.32 (s, 3H, 3-CH₃), 3.76 (s, 2H, CHCCH₂), 4.96 (s, 2H, NCH₂CO), 6.31 (s, 1H, Ar), 6.91 (s, 1H, Ar), 7.38-7.40 (m, 5H, Ar), 7.46 (s, 1H, Ar), 9.05 (exch br s, 1H, NH).

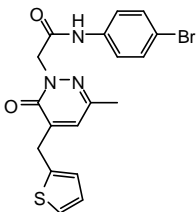
5.2.202 *N*-(4-Bromophenyl)-2-[3-methyl-6-oxo-5-(thiophen-3-ylmethyl)-pyridazin-1(6*H*)-yl]acetamide (**61b**)



Yield = 24 %; mp = 93-95 °C (EtOH). ¹H NMR (CDCl₃) δ 2.31 (s, 3H, 3-CH₃), 3.96 (s, 2H, CHCCH₂), 4.95 (s, 2H, NCH₂CO), 6.84 (s, 1H, Ar), 6.97 (d, 1H, Ar, *J* = 1.9 Hz), 7.12 (s, 1H, Ar), 7.35 (q, 1H, Ar, *J* = 4.8 Hz), 7.39 (s, 4H, Ar), 9.04 (exch br s, 1H, NH).

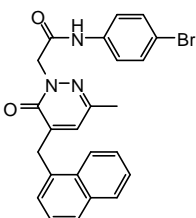
5. Experimental Chemistry

5.2.203 *N*-(4-Bromophenyl)-2-[3-methyl-6-oxo-5-(thiophen-2-ylmethyl)-pyridazin-1(6*H*)-yl]acetamide (61c)



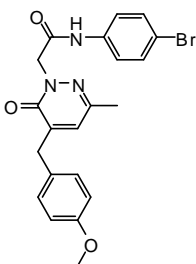
Yield = 80 %; colorless oil. $^1\text{H NMR}$ (CDCl_3) δ 2.32 (s, 3H, 3- CH_3), 4.14 (s, 2H, CHCCH_2), 4.97 (s, 2H, NCH_2CO), 6.93-6.95 (m, 2H, Ar), 6.99-7.01 (m, 1H, Ar), 7.24 (dd, 1H, Ar, $J = 4.0$ Hz, $J = 1.0$ Hz), 7.33 (q, 4H, Ar, $J = 4.2$ Hz), 9.25 (exch br s, 1H, NH).

5.2.204 *N*-(4-Bromophenyl)-2-[3-methyl-5-(naphthalen-1-ylmethyl)-6-oxo-pyridazin-1(6*H*)-yl]acetamide (61d)



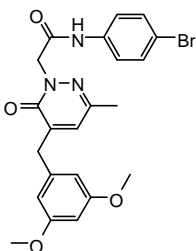
Yield = 77 %; mp = 208-09 °C (EtOH). $^1\text{H NMR}$ (CDCl_3) δ 2.16 (s, 3H, 3- CH_3), 4.39 (s, 2H, CHCCH_2), 5.04 (s, 2H, NCH_2CO), 6.54 (s, 1H, Ar), 7.33 (d, 2H, Ar, $J = 8.8$ Hz), 7.39 (d, 3H, Ar, $J = 9.2$ Hz), 7.45-7.54 (m, 3H, Ar), 7.80 (d, 1H, Ar, $J = 8.2$ Hz), 7.86 (d, 1H, Ar, $J = 8.2$ Hz), 7.92 (d, 1H, Ar, $J = 7.8$ Hz), 9.38 (exch br s, 1H, NH).

5.2.205 *N*-(4-Bromophenyl)-2-[5-(4-methoxybenzyl)-3-methyl-6-oxo-pyridazin-1(6*H*)-yl]acetamide (61e)



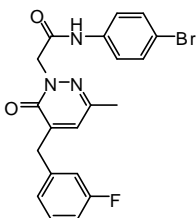
Yield = 73 %; mp = 139-141 °C (EtOH). IR (cm^{-1}) 3300 (NH), 1709 (CO), 1644 (CO). $^1\text{H NMR}$ (CDCl_3) δ 2.29 (s, 3H, 3- CH_3), 3.83 (s, 3H, OCH_3), 3.88 (s, 2H, $\text{CH}_2\text{-Ar}$), 4.94 (s, 2H, NCH_2CO), 6.78 (s, 1H, Ar), 6.90 (d, 2H, Ar, $J = 8.6$ Hz), 7.17 (d, 2H, Ar, $J = 8.6$ Hz), 7.40 (s, 4H, Ar), 9.01 (exch br s, 1H, NH). MS (ESI) calcd. For $\text{C}_{21}\text{H}_{20}\text{BrN}_3\text{O}_3$, 442,31. Found: m/z 442.08 [M] $^+$.

5.2.206 *N*-(4-Bromophenyl)-2-[5-(3,5-dimethoxybenzyl)-3-methyl-6-oxo-pyridazin-1(6*H*)-yl]acetamide (61f)



Yield = 62 %; mp = 87-89 °C (EtOH). ¹H NMR (CDCl₃) δ 2.29 (s, 3H, 3-CH₃), 3.77 (s, 6H, 2 x OCH₃), 3.83 (s, 2H, CHCCH₂), 4.94 (s, 2H, NCH₂CO), 6.37 (s, 3H, Ar), 6.85 (s, 1H, Ar), 7.27 (q, 4H, Ar, *J* = 11.4 Hz), 9.49 (exch br s, 1H, NH).

5.2.207 *N*-(4-Bromophenyl)-2-[5-(3-fluorobenzyl)-3-methyl-6-oxopyridazin-1(6*H*)-yl]acetamide (61g)



Yield = 47 %; mp = 88-89 °C (EtOH). ¹H NMR (CDCl₃) δ 2.32 (s, 3H, 3-CH₃), 3.93 (s, 2H, CHCCH₂), 4.95 (s, 2H, NCH₂CO), 6.85 (s, 1H, Ar), 6.97-7.05 (m, 3H, Ar), 7.28-7.34 (m, 5H, Ar), 9.14 (exch br s, 1H, NH).

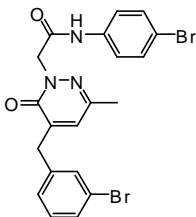
5.2.208 *N*-(4-Bromophenyl)-2-[5-(3-chlorobenzyl)-3-methyl-6-oxopyridazin-1(6*H*)-yl]acetamide (61h)



Yield = 26 %; mp = 185-187 °C (EtOH). ¹H NMR (CDCl₃) δ 2.33 (s, 3H, 3-CH₃), 3.89 (s, 2H, CHCCH₂), 4.94 (s, 2H, NCH₂CO), 6.86 (s, 1H, Ar), 7.14 (s, 1H, Ar), 7.28 (dd, 7H, Ar, *J* = 1.3 Hz, *J* = 5.4 Hz), 9.26 (exch br s, 1H, NH).

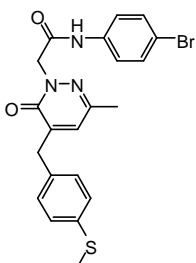
5. Experimental Chemistry

5.2.209 *N*-(4-Bromophenyl)-2-[5-(3-bromobenzyl)-3-methyl-6-oxopyridazin-1(6*H*)-yl]acetamide (61i)



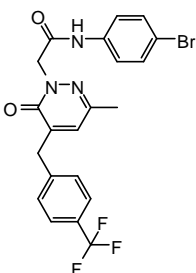
Yield = 47 %; mp = 99-101 °C (EtOH). ^1H NMR (CDCl_3) δ 2.33 (s, 3H, 3- CH_3), 3.90 (s, 2H, CHCCH_2), 4.94 (s, 2H, NCH_2CO), 6.85 (s, 1H, Ar), 7.19-7.23 (m, 2H, Ar), 7.35-7.40 (m, 4H, Ar), 7.43 (t, 2H, Ar, $J = 3.6$ Hz), 9.00 (exch br s, 1H, NH).

5.2.210 *N*-(4-Bromophenyl)-2-{3-methyl-5-[4-(methylthio)benzyl]-6-oxo-pyridazin-1(6*H*)-yl}acetamide (61j)

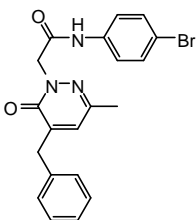


Yield = 10 %; mp = 97-99 °C (EtOH). ^1H NMR (CDCl_3) δ 2.30 (s, 3H, 3- CH_3), 2.50 (s, 3H, SCH_3), 3.89 (s, 2H, CHCCH_2), 4.94 (s, 2H, NCH_2CO), 6.80 (s, 1H, Ar), 7.17 (d, 2H, Ar, $J = 8.2$ Hz), 7.24 (d, 2H, Ar $J = 8.2$ Hz), 7.39 (dd, 4H, Ar, $J = 2.6$ Hz, $J = 5.7$ Hz), 9.01 (exch br s, 1H, NH).

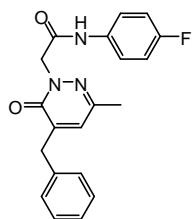
5.2.211 *N*-(4-Bromophenyl)-2-{3-methyl-6-oxo-5-[4-(trifluoromethyl) benzyl]pyridazin-1(6*H*)-yl}acetamide (61k)



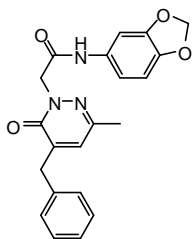
Yield = 44 %; mp = 81-83 °C (EtOH). ^1H NMR (CDCl_3) δ 2.32 (s, 3H, 3- CH_3), 3.99 (s, 2H, CHCCH_2), 4.94 (s, 2H, NCH_2CO), 6.84 (s, 1H, Ar), 7.32-7.40 (m, 6H, Ar), 7.61 (d, 2H, Ar, $J = 8.1$ Hz), 8.99 (exch br s, 1H, NH).

5.2.212 2-[5-Benzyl-3-methyl-6-oxopyridazin-1(6H)-yl]-N-(4-bromophenyl) acetamide (61 l)

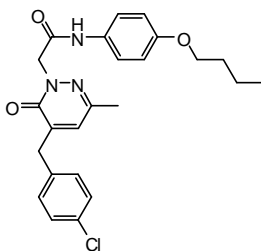
Yield = 47 %; colorless oil. $^1\text{H NMR}$ (CDCl_3) δ 2.30 (s, 3H, 3- CH_3), 3.93 (s, 2H, CHCCH_2), 4.94 (s, 2H, NCH_2CO), 6.82 (s, 1H, Ar), 7.24-7.28 (m, 2H, Ar), 7.30-7.38 (m, 7H, Ar), 9.18 (exch br s, 1H, NH).

5.2.213 N-(4-Fluorophenyl)-2-[5-benzyl-3-methyl-6-oxopyridazin-1(6H)-yl]acetamide (61m)

Yield = 53 %; mp = 175-76 °C (EtOH). $^1\text{H NMR}$ (CDCl_3) δ 2.29 (s, 3H, 3- CH_3), 3.94 (s, 2H, CHCCH_2), 4.95 (s, 2H, NCH_2CO), 6.80 (s, 1H, Ar), 6.97 (t, 2H, Ar, $J = 8.7$ Hz), 7.25-7.28 (m, 2H, Ar), 7.30-7.38 (m, 3H, Ar), 7.41-7.44 (m, 2H, Ar), 9.05 (exch br s, 1H, NH).

5.2.214 N-(1,3-Benzodioxol-5-yl)-2-[5-benzyl-3-methyl-6-oxopyridazin-1(6H)-yl]acetamide (61n)

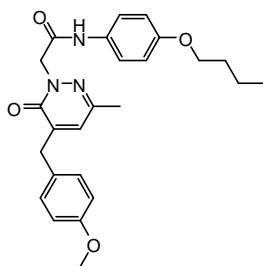
Yield = 26 %; mp = 63-65 °C (EtOH). $^1\text{H NMR}$ (CDCl_3) δ 2.22 (s, 3H, 3- CH_3), 3.80 (s, 2H, CHCCH_2), 4.79 (s, 2H, NCH_2CO), 5.99 (s, 2H, OCH_2O), 6.86 (d, 1H, Ar, $J = 8.4$ Hz), 6.93-6.95 (m, 1H, Ar), 7.08 (s, 1H, Ar), 7.22-7.34 (m, 7H, Ar), 10.19 (exch br s, 1H, NH).

5.2.215 N-(4-Butoxyphenyl)-2-[5-(4-chlorobenzyl)-3-methyl-6-oxopyridazin-1(6H)-yl]acetamide (61o)

5. Experimental Chemistry

Yield = 70 %. mp = 146-147 °C (EtOH). IR (cm⁻¹) 3298 (NH), 1708 (CO), 1642 (CO). ¹H NMR (CDCl₃) δ 0.99 (t, 3H, O(CH₂)₃CH₃, *J* = 7.4 Hz), 1.49 (sext, 2H, OCH₂CH₂CH₂CH₃, *J* = 7.5 Hz), 1.76 (quint, 2H, OCH₂CH₂CH₂CH₃, *J* = 7.0 Hz), 2.29 (s, 3H, 3-CH₃), 3.88 (s, 2H, CHCCH₂), 3.93 (t, 2H, OCH₂, *J* = 6.5 Hz), 4.94 (s, 2H, NCH₂CO), 6.76 (s, 1H, Ar), 6.81 (d, 2H, Ar, *J* = 9.0 Hz), 7.18 (d, 2H, Ar, *J* = 8.4 Hz), 7.32 (d, 2H, Ar, *J* = 8.4 Hz), 7.38 (d, 2H, Ar, *J* = 9.0 Hz), 8.69 (exch br s, 1H, NH). MS (ESI) calcd. For C₂₄H₂₆ClN₃O₃, 439.93. Found: *m/z* 440.17 [M + H]⁺.

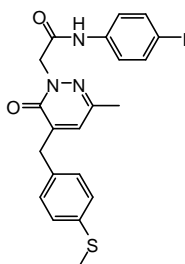
5.2.216 *N*-(4-Butoxyphenyl)-2-[5-(4-methoxybenzyl)-3-methyl-6-oxo-pyridazin-1(6*H*)-yl]acetamide (61p)



Yield = 60 %; mp = 160-161 °C (EtOH). IR (cm⁻¹) 3300 (NH), 1707 (CO), 1644 (CO). ¹H NMR (CDCl₃) δ 0.98 (t, 3H, O(CH₂)₃CH₃, *J* = 7.4 Hz), 1.45-1.54 (m, 2H, OCH₂CH₂CH₂CH₃), 1.77 (quint, 2H, OCH₂CH₂CH₂CH₃, *J* = 7.1 Hz), 2.28 (s, 3H, 3-CH₃), 3.83 (s, 3H, OCH₃), 3.88 (s, 2H, CHCCH₂), 3.94 (t, 2H, OCH₂, *J* = 6.5 Hz), 4.93 (s, 2H, NCH₂CO), 6.74 (s, 1H, Ar), 6.82 (d, 2H, Ar, *J* = 9.0 Hz), 6.90 (d, 2H, Ar, *J* = 8.6 Hz), 7.17 (d, 2H, Ar, *J* = 8.5 Hz), 7.39 (d, 2H, Ar, *J* = 9.0 Hz), 8.67 (exch br s, 1H, NH). MS (ESI) calcd. For C₂₅H₂₉N₃O₄, 435.52. Found: *m/z* 436.23 [M + H]⁺.

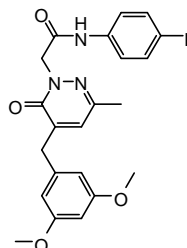
General Procedure for 62a-c. To 5 mL of KOH in absolute EtOH (5%, w/v), **53a** (0.13 mmol) and the appropriate substituted aromatic aldehyde (0.13 mmol) were added. The mixture was refluxed under stirring for 1-5 h. After cooling, the suspension was concentrated in vacuo, diluted with ice-cold water (5-10 mL), acidified with 2 N HCl and extracted with CH₂Cl₂ (3 x 25 mL). Removal of the solvent afforded compounds **62a-c**, which were purified by flash column chromatography using cyclohexane/ethyl acetate 2:1 (for **62a**) and cyclohexane/ethyl acetate 1:1 (for **62b,c**) as eluents.

5.2.217 *N*-(4-Iodophenyl)-2-[3-methyl-5-[4-(methylthio)benzyl]-6-oxo-pyridazin-1(6*H*)-yl]acetamide (62a)



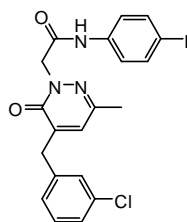
Yield = 46 %; mp = 68-70 °C (EtOH). $^1\text{H NMR}$ (CDCl_3) δ 2.30 (s, 3H, 3- CH_3), 2.51 (s, 3H, SCH_3), 3.89 (s, 2H, CHCCH_2), 4.93 (s, 2H, NCH_2CO), 6.80 (s, 1H, Ar), 7.18 (d, 2H, Ar, $J = 8.4$ Hz), 7.24-7.28 (m, 4H, Ar), 7.61 (d, 2H, Ar, $J = 8.8$ Hz), 8.92 (exch br s, 1H, NH).

5.2.218 *N*-(4-Iodophenyl)-2-[5-(3,5-dimethoxybenzyl)-3-methyl-6-oxo pyridazin-1(6*H*)-yl]- acetamide (**62b**)



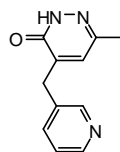
Yield = 30 %; mp = 63-65 °C (EtOH). $^1\text{H NMR}$ (CDCl_3) δ 2.30 (s, 3H, 3- CH_3), 3.79 (s, 6H, 2 x OCH_3), 3.87 (s, 2H, CHCCH_2), 4.94 (s, 2H, NCH_2CO), 6.40 (s, 3H, Ar), 6.82 (s, 1H, Ar), 7.28 (d, 2H, Ar, $J = 5.7$ Hz), 7.58 (d, 2H, Ar, $J = 8.6$ Hz), 9.01 (exch br s, 1H, NH).

5.2.219 *N*-(4-Iodophenyl)-2-[5-(3-chlorobenzyl)-3-methyl-6-oxopyridazin-1(6*H*)-yl]acetamide (**62c**)



Yield = 25 %; mp = 58-60 °C (EtOH). $^1\text{H NMR}$ (CDCl_3) δ 2.33 (s, 3H, 3- CH_3), 3.90 (s, 2H, CHCCH_2), 4.94 (s, 2H, NCH_2CO), 6.86 (s, 1H, Ar), 7.13-7.16 (m, 1H, Ar), 7.20 (d, 2H, Ar, $J = 7.0$ Hz), 7.28 (d, 3H, Ar, $J = 4.2$ Hz), 7.52 (d, 2H, Ar, $J = 8.7$ Hz), 9.14 (exch br s, 1H, NH).

5.2.220 6-Methyl-4-(pyridin-3-ylmethyl)pyridazin-3(2*H*)-one (**63**)

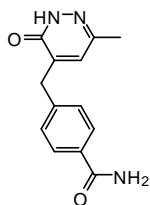


To 6 mL of KOH in absolute EtOH (5%, w/v), **42d** (1.78 mmol) and commercially available pyridine-3-carbaldehyde (1.78 mmol) were added. The mixture was refluxed under stirring for 5 h. After cooling, the suspension was concentrated in vacuo, diluted with ice-cold water (10 mL), acidified with 2 N HCl and extracted with CH_2Cl_2 (3 x 25 mL). Removal of the solvent afforded compound **63**, which was purified by flash column chromatography using $\text{NH}_4\text{OH}/\text{EtOH}/\text{CH}_2\text{Cl}_2/\text{petroleum ether}$ 4:25:150:50 as eluents. Yield = 53 %; mp = 181-183 °C (EtOH). $^1\text{H NMR}$ (CDCl_3) δ 2.28 (s, 3H, 6- CH_3), 3.93 (s, 2H, CHCCH_2),

5. Experimental Chemistry

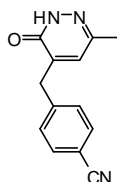
6.80 (s, 1H, Ar), 7.33 (dd, 1H, Ar, $J = 2.7$ Hz, $J = 5.0$ Hz), 7.70 (dd, 1H, Ar, $J = 6.1$ Hz, $J = 1.8$ Hz), 8.57 (s, 2H, Ar), 11.53 (exch br s, 1H, NH).

5.2.221 4-[(6-Methyl-3-oxo-2,3-dihydropyridazin-4-yl)methyl]benzamide (64)



To 6 mL of KOH in absolute EtOH (5%, w/v), **42d** (1.78 mmol) and commercially available 4-cyanobenzaldehyde (3.56 mmol) were added. The mixture was refluxed under stirring for 4 h. After cooling, the suspension was concentrated in vacuo, diluted with ice-cold water (10 mL) and acidified with 2 N HCl. After 1 h stirring in ice-bath, the precipitate was filtered off and purified by crystallization in ethanol. Yield = 70 %; mp = 164-166 °C (EtOH). IR (cm⁻¹) 3300 (NH), 3200 (NH₂), 1649 (CO), 1608 (CO). ¹H NMR (CDCl₃) δ 2.18 (s, 3H, 6-CH₃), 3.80 (s, 2H, CHCCH₂), 7.06 (s, 1H, Ar), 7.33 (d, 2H, Ar, $J = 8.2$ Hz), 7.80 (d, 2H, Ar, $J = 8.1$ Hz), 12.72 (exch br s, 1H, NH₂).

5.2.222 4-[(6-Methyl-3-oxo-2,3-dihydropyridazin-4-yl)methyl]benzonitrile (65)

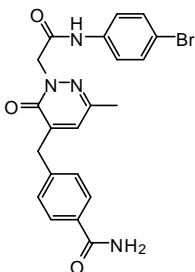


A suspension of **64** (0.82 mmol) in 5 mL of POCl₃ was stirred at 60 °C for 3 h. After cooling, the mixture was concentrated in vacuo, diluted with ice-cold water (10 mL) and extracted with CH₂Cl₂ (3 x 15 mL). The organic layer was dried (Na₂SO₄) and concentrated in vacuo, to afford a yellow solid which was purified by flash column chromatography using CH₂Cl₂/CH₃OH 7:3 as eluent. Yield = 60 %; mp = 213-215 °C (EtOH). IR (cm⁻¹) 2225 (CN), 1649 (CO), 1609 (CO). ¹H NMR (CDCl₃) δ 2.29 (s, 3H, 6-CH₃), 3.96 (s, 2H, CHCCH₂), 6.79 (s, 1H, Ar), 7.41 (d, 2H, Ar, $J = 7.0$ Hz), 7.65 (d, 2H, Ar, $J = 6.9$ Hz), 10.61 (exch br s, 1H, NH). MS (ESI) calcd. For C₂₅H₂₉N₃O₄, 435,52. Found: m/z 436.23 [M + H]⁺.

General Procedure for 66a-c. A mixture of compound **63**, **64** or **65** (0.79 mmol), K₂CO₃ (1.58 mmol) and *N*-(4-bromophenyl)-2-chloroacetamide **22** (1.19 mmol) in CH₃CN (2 mL), was refluxed under stirring for 2-3 h. The mixture was then concentrated in vacuo and diluted with cold water. After 1 h stirring in ice-bath, the precipitate was filtered off by suction and purified by flash column

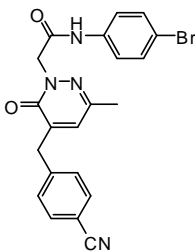
chromatography using alternatively CH₂Cl₂/CH₃OH 9.5:0.5 (for **66a**), CH₂Cl₂/CH₃OH 9.9:0.1 (for **66b**) or CH₂Cl₂/CH₃OH/NH₄OH 9.5:0.5:0.05 (for **66c**) as eluents.

5.2.223 **4-{2-[(4-Bromophenyl)carbamoyl]methyl}-6-methyl-3-oxo-2,3-dihydropyridazin-4-ylmethyl}benzamide (66a)**



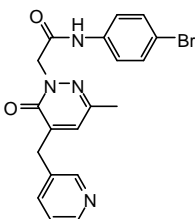
Yield = 59 %; mp = 168-171 °C (EtOH). IR (cm⁻¹) 3200 (NH₂), 1654 (CO), 1609 (CO). ¹H NMR (CDCl₃) δ 2.31 (s, 3H, 6-CH₃), 3.99 (s, 2H, CHCCH₂), 4.93 (s, 2H, NCH₂CO), 6.81 (s, 1H, Ar), 7.34-7.41 (m, 6H, Ar), 7.80 (d, 2H, Ar, *J* = 8.1 Hz), 8.89 (exch br s, 1H, NH).

5.2.224 ***N*-(4-Bromophenyl)-2-[5-(4-cyanobenzyl)-3-methyl-6-oxopyridazin-1(6*H*)-yl]acetamide (66b)**



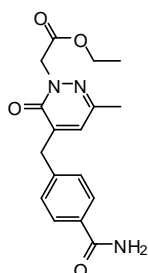
Yield = 19 %; mp = 210-211 °C (EtOH). IR (cm⁻¹) 2225 (CN), 1650 (CO), 1598 (CO). ¹H NMR (CDCl₃) δ 2.33 (s, 3H, 3-CH₃), 3.99 (s, 2H, CHCCH₂), 4.93 (s, 2H, NCH₂CO), 6.85 (s, 1H, Ar), 7.39 (q, 6H, Ar, *J* = 8.3 Hz), 7.65 (d, 2H, Ar, *J* = 8.2 Hz), 8.77 (exch br s, 1H, NH).

5.2.225 ***N*-(4-Bromophenyl)-2-[3-methyl-6-oxo-5-(pyridin-3-ylmethyl)-pyridazin-1(6*H*)-yl]acetamide (66c)**



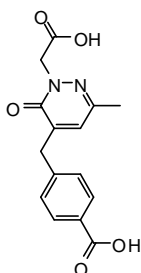
Yield = 61 %; mp = 216-218 °C (EtOH). ¹H NMR (CDCl₃) δ 2.30 (s, 3H, 3-CH₃), 3.92 (s, 2H, CHCCH₂), 4.93 (s, 2H, NCH₂CO), 6.86 (s, 1H, Ar), 7.27-7.33 (m, 5H, Ar), 7.61 (d, 1H, Ar, *J* = 7.8 Hz), 8.54 (d, 2H, Ar, *J* = 6.2 Hz), 9.29 (exch br s, 1H, NH).

5.2.226 Ethyl-2-[5-(4-carbamoylbenzyl)-3-methyl-6-oxopyridazin-1(6H)-yl]acetate (67)

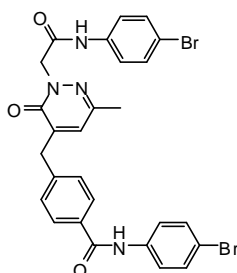


A mixture of compound **64** (1.56 mmol), K_2CO_3 (3.12 mmol) and ethyl bromoacetate (2.34 mmol) in CH_3CN (6 mL), was refluxed under stirring for 2 h. The mixture was then concentrated in vacuo and diluted with cold water. After 1h stirring in ice-bath, the yellow precipitate was filtered off by suction and purified by recrystallization in ethanol. Yield = 78 %; mp = 174-76 °C (EtOH). 1H NMR ($CDCl_3$) δ 1.31 (t, 3H, CH_2CH_3), 2.25 (s, 3H, 3- CH_3), 3.96 (s, 2H, $CHCCH_2$), 4.26 (q, 2H, CH_2CH_3 , $J = 7.2$ Hz), 4.86 (s, 2H, NCH_2CO), 6.70 (s, 1H, Ar), 7.34 (d, 2H, Ar, $J = 7.7$ Hz), 7.80 (d, 2H, Ar, $J = 7.7$ Hz).

5.2.227 4-{[2-(Carboxymethyl)-6-methyl-3-oxo-2,3-dihydropyridazin-4-yl]methyl} benzoic acid (68)

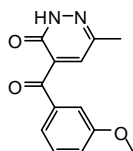


A suspension of the intermediate **67** (1.22 mmol) in 6 N NaOH (5 mL) was stirred at 60 °C for 2 h. The mixture was diluted with ice-cold water (3 mL), acidified with 6 N HCl and the final product **68** was then filtered off by suction and recrystallized from ethanol. Yield = 76 %; mp = 225-27 °C (EtOH). 1H NMR ($CDCl_3$) δ 2.22 (s, 3H, 6- CH_3), 3.87 (s, 2H, $CHCCH_2$), 4.69 (s, 2H, NCH_2CO), 7.15 (s, 1H, Ar), 7.39 (d, 2H, Ar, $J = 8.0$ Hz), 7.88 (d, 2H, Ar, $J = 8.0$ Hz), 13.01 (exch br s, 1H, OH).

5.2.228 *N*-(4-Bromophenyl)-4-{2-[(4-bromophenylcarbamoyl)methyl]-6-methyl-3-oxo-2,3-dihydropyridazin-4-ylmethyl}benzamide (69)

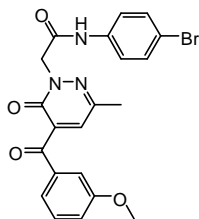
To a cooled (-5 °C) and stirred solution of compound **68** (0.93 mmol) in anhydrous tetrahydrofuran (7 mL), Et₃N (3.26 mmol) was added. After 30 min, the mixture was allowed to warm up to 0 °C and ethyl chloroformate (1.02 mmol) was added. After 1 h, 4-bromo aniline (1.86 mmol) was added. The reaction was carried out at room temperature for 12 h. The mixture was then concentrated in vacuo, diluted with cold water (15 mL) and extracted with CH₂Cl₂ (3 x 15 mL). After removal of the solvent, the residue was purified by column chromatography using CH₂Cl₂/CH₃OH/NH₄OH 9.5:0.5:0.05 as eluent. The analytical sample of compound **69** was obtained from a further purification through a silica gel preparative TLC (eluent: CH₂Cl₂/CH₃OH/NH₄OH 9.5:0.5:0.05). Yield = 10 %; mp = 226-228 °C (EtOH). ¹H NMR (CDCl₃) δ 2.31 (s, 3H, 6-CH₃), 4.00 (s, 2H, CHCCH₂), 4.93 (s, 2H, NCH₂CO), 6.83 (s, 1H, Ar), 7.40 (t, 6H, Ar, *J* = 8.4 Hz), 7.51 (d, 2H, Ar, *J* = 8.7 Hz), 7.57 (d, 2H, Ar, *J* = 8.9 Hz), 7.84 (d, 2H, Ar, *J* = 7.7 Hz), 8.67 (exch br s, 1H, NH). MS (ESI) calcd. For C₂₇H₂₂Br₂N₄O₃, 610.30. Found: *m/z* 609 [M - H]⁻, 611.2 [M + H]⁺.

5.2.229 4-(3-Methoxybenzoyl)-6-methylpyridazin-3(2H)-one (**70**)



To a stirred and heated (60 °C) suspension of compound **43** (2.39 mmol) in 15 mL of 50 % (v/v) acetic acid, Ce(NH₄)₂(NO₃)₆ (7.17 mmol) was slowly added over 0.5 h and the reaction is carried out at 60 °C for additional 1 h. The mixture was then diluted with ice-cold water (10 mL) and extracted with CH₂Cl₂ (15 mL). After washing with H₂O (3 x 10 mL), the organic layer was evaporated under vacuo and the residue was purified by CombyFlash[®] (eluent: cyclohexane/ethyl acetate, gradient 1:1 to 1:3). Yield = 17 %; oil. ¹H NMR (CDCl₃) δ 2.25 (s, 3H, 6-CH₃), 3.92 (s, 3H, OCH₃), 6.74-6.95 (m, 4H, Ar), 7.31 (t, 1H, Ar, *J* = 7.8 Hz), 11.32 (exch br s, 1H, NH).

5.2.230 *N*-(4-Bromophenyl)-2-[5-(3-methoxybenzoyl)-3-methyl-6-oxopyridazin-1(6H)-yl]acetamide (**71**)

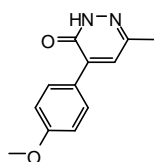


A mixture of intermediate **70** (0.41 mmol), K₂CO₃ (0.82 mmol) and *N*-(4-bromophenyl)-2-chloroacetamide **22** (0.61 mmol) in CH₃CN (5 mL), was refluxed under stirring for 6 h. The mixture was

5. Experimental Chemistry

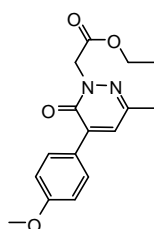
then concentrated in vacuo and extracted with CH_2Cl_2 (3 x 15 mL). After removal of the solvent under vacuo the residue was purified by flash column chromatography using $\text{NH}_4\text{OH}/\text{EtOH}/\text{CH}_2\text{Cl}_2/\text{petroleum ether}$ 4:25:150:269 as eluent. Yield = 10 %; mp = 176-177 °C (EtOH). $^1\text{H NMR}$ (CDCl_3) δ 2.32 (s, 3H, 3- CH_3), 3.82 (s, 3H, OCH_3), 4.92 (s, 2H, NCH_2CO), 6.62 (s, 1H, Ar), 6.69 (t, 1H, Ar, $J = 2.1$ Hz), 6.74 (d, 1H, Ar, $J = 7.5$ Hz), 6.85 (dd, 1H, Ar, $J = 6.3$ Hz, $J = 2.0$ Hz), 7.29 (t, 1H, Ar, $J = 8.2$ Hz), 7.38-7.46 (m, 4H, Ar), 9.10 (exch br s, 1H, NH). MS (ESI) calcd. For $\text{C}_{21}\text{H}_{18}\text{BrN}_3\text{O}_4$, 456,29. Found: m/z 457.20 [$\text{M} + \text{H}$] $^+$.

5.2.231 4-(4-Methoxyphenyl)-6-methylpyridazin-3(2H)-one (74)



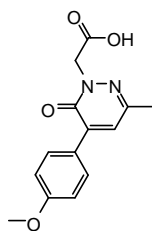
To an ice-cold solution of (*E*)-methyl 2-(4-methoxyphenyl)-4-oxopent-2-enoate **73** (0.34 mmol) in dry toluene (3 mL), hydrazine hydrate (0.68 mmol) was added drop-wise. The solution was stirred at reflux temperature for 2 h. The solvent was evaporated and ice-cold water (5 mL) was added to the residue. The aqueous layer was extracted with CH_2Cl_2 (3 x 15 mL) and the combined organic layers were dried over Na_2SO_4 and evaporated in vacuo. The crude product was purified by flash column chromatography (eluent: cyclohexane/ethyl acetate 1:3) to yield **74** as an amorphous white solid. Yield = 55 %; mp = 155-158 °C (EtOH). $^1\text{H NMR}$ (CDCl_3) δ 2.39 (s, 3H, 6- CH_3), 3.88 (s, 3H, OCH_3), 6.99 (d, 2H, Ar, $J = 8.9$ Hz), 7.24 (s, 1H, Ar), 7.86 (d, 2H, Ar, $J = 8.9$ Hz), 10.51 (exch br s, 1H, NH).

5.2.233 Ethyl-2-[5-(4-methoxyphenyl)-3-methyl-6-oxopyridazin-1(6H)-yl]acetate (75)

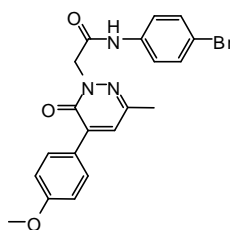


A mixture of the intermediate **74** (0.18 mmol), K_2CO_3 (0.36 mmol) and ethyl bromoacetate (0.28 mmol) in CH_3CN (2 mL), was refluxed under stirring for 1.5 h. The mixture was then concentrated in vacuo and extracted with CH_2Cl_2 (3 x 10 mL). After removal of the solvent under vacuo the residue was purified by flash column chromatography using cyclohexane/ethyl acetate 1:1 as eluent. Yield ~ 100 %; colorless oil. $^1\text{H NMR}$ (CDCl_3) δ 1.30 (t, 3H, CH_2CH_3 , $J = 7.0$ Hz), 2.37 (s, 3H, 3- CH_3), 3.92 (s, 3H, OCH_3), 4.23 (q, 2H, CH_2CH_3 , $J = 7.0$ Hz), 4.89 (s, 2H, NCH_2CO), 6.94 (d, 2H, Ar, $J = 8.8$ Hz), 7.21 (s, 1H, Ar), 7.81 (d, 2H, Ar, $J = 8.8$ Hz).

5.2.234 2-[5-(4-Methoxyphenyl)-3-methyl-6-oxopyridazin-1(6H)-yl]acetic acid (76)

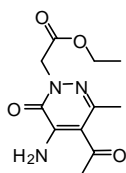


A suspension of the intermediate **75** (0.20 mmol) in 6 N NaOH (1.5 mL) was stirred at 60 °C for 0.5 h. The mixture was diluted with ice-cold water (1 mL), acidified with 6 N HCl and the final product **68** was then filtered off by suction and recrystallized from ethanol. Yield ~ 100 %; mp = 202-203 °C (EtOH). ¹H NMR (CDCl₃) δ 2.41 (s, 3H, 3-CH₃), 3.87 (s, 3H, OCH₃), 4.99 (s, 2H, NCH₂CO), 6.98 (d, 2H, Ar, *J* = 8.8 Hz), 7.26 (s, 1H, Ar), 7.82 (d, 2H, Ar, *J* = 8.8 Hz).

5.2.235 *N*-(4-Bromophenyl)-2-[5-(4-methoxyphenyl)-3-methyl-6-oxo-pyridazin-1(6H)-yl]acetamide (77)

To a cooled (-5 °C) and stirred solutions of compound **76** (0.20 mmol) in anhydrous tetrahydrofuran (2 mL), Et₃N (0.70 mmol) was added. After 30 min, the mixture was allowed to warm up to 0 °C and ethyl chloroformate (0.22 mmol) was added. After 1 h, 4-bromoaniline (0.40 mmol) was added and the reaction was carried out at room temperature for 12 h. The mixture was then concentrated in vacuo, diluted with cold water (5 mL) and extracted with CH₂Cl₂ (3 x 10 mL). After removal of the solvent, the residue was purified by column chromatography using cyclohexane/ethyl acetate 2:1 as eluent. Yield = 35 %; mp = 251-253 °C (EtOH). ¹H NMR (CDCl₃) δ 2.43 (s, 3H, 6-CH₃), 3.88 (s, 3H, OCH₃), 5.00 (s, 2H, NCH₂CO), 7.00 (d, 2H, Ar, *J* = 8.7 Hz), 7.27 (s, 1H, Ar), 7.40 (q, 4H, Ar, *J* = 9.2 Hz), 7.80 (d, 2H, Ar, *J* = 8.7 Hz), 9.07 (exch br s, 1H, NH).

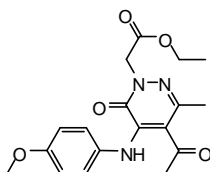
5.2.236 Ethyl-2-[4-acetyl-5-amino-3-methyl-6-oxopyridazin-1(6H)-yl]acetate (80)



5. Experimental Chemistry

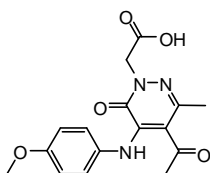
A mixture of the intermediate **79** (0.99 mmol), K_2CO_3 (1.98 mmol), and ethyl bromoacetate (1.34 mmol) in CH_3CN (3 mL) was refluxed under stirring for 3 h. The mixture was then concentrated in vacuo, diluted with cold water, and extracted with CH_2Cl_2 (3 x 15 mL). The solvent was evaporated in vacuo, and compound **80** was purified by recrystallization from ethanol. Yield = 44 %; mp = 145-46 °C (EtOH). 1H NMR ($CDCl_3$) δ 1.32 (t, 3H, CH_2CH_3 , $J = 7.2$ Hz), 2.53 (s, 3H, 3- CH_3), 2.60 (s, 3H, $COCH_3$), 4.27 (q, 2H, OCH_2CH_3 , $J = 7.1$ Hz), 4.83 (s, 2H, NCH_2CO), 7.75 (exch br s, 1H, NH).

5.2.237 Ethyl-2-[4-acetyl-5-(4-methoxyphenylamino)-3-methyl-6-oxopyridazin-1(6H)-yl]acetate (**81**)



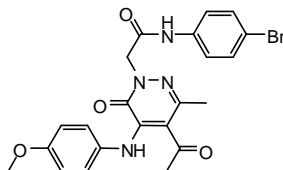
To the suspension of **80** (0.91 mmol), copper acetate (1.36 mmol) and 4-methoxyphenylboronic acid (1.82 mmol) in CH_2Cl_2 (4 mL), Et_3N (1.82 mmol) was added and the mixture was stirred at room temperature for 12 h. The suspension was extracted with 15% aqueous ammonia (3 x 10 mL), then the organic layer was washed with water (10 mL) and dried over Na_2SO_4 . After removal of the solvent in vacuo, the residue was purified by flash column chromatography using cyclohexane/ethyl acetate 1:3 as eluent. Yield = 61 %; mp = 115-17 °C (EtOH). 1H NMR ($CDCl_3$) δ 1.34 (t, 3H, CH_2CH_3 , $J = 7.2$ Hz), 1.88 (s, 3H, $COCH_3$), 2.14 (s, 3H, 3- CH_3), 3.81 (s, 3H, OCH_3), 4.29 (q, 2H, OCH_2CH_3 , $J = 7.2$ Hz), 4.88 (s, 2H, $COCH_2N$), 6.85 (d, 2H, Ar, $J = 6.7$ Hz), 7.04 (d, 2H, Ar, $J = 8.9$ Hz), 7.62 (exch br s, 1H, NH).

5.2.238 2-[4-Acetyl-5-(4-methoxyphenylamino)-3-methyl-6-oxopyridazin-1(6H)-yl]acetic acid (**82**)



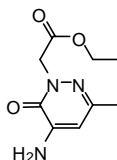
A suspension of the intermediate **81** (0.39 mmol) in 6 N NaOH (10 mL) was stirred at rt to 80 °C for 1.5 h. The mixture was diluted with cold water and acidified with 6 N HCl. After 1 h stirring in ice-bath, the product **82** was filtered off by suction and recrystallized from ethanol. Yield = 76 %; mp = 104-06 °C (EtOH). 1H NMR ($CDCl_3$) δ 1.88 (s, 3H, $COCH_3$), 2.10 (exch br s, 1H, OH), 2.16 (s, 3H, 3- CH_3), 3.82 (s, 3H, OCH_3), 4.95 (s, 2H, $COCH_2N$), 6.86 (d, 2H, Ar, $J = 8.6$ Hz), 7.05 (d, 2H, Ar, $J = 8.6$ Hz), 7.62 (exch br s, 1H, NH).

5.2.239 *N*-(4-Bromophenyl)-2-[4-acetyl-5-(4-methoxyphenylamino)-3-methyl-6-oxopyridazin-1(6*H*)-yl]acetamide (**83**)



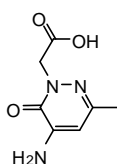
To a cooled (-5 °C) and stirred solution of **82** (0.30 mmol) in anhydrous tetrahydrofuran (3 mL), Et₃N (1.06 mmol) was added. After 30 min, the mixture was allowed to warm up to 0 °C and ethyl chloroformate (0.33 mmol) was added. After 1 h, 4-bromo aniline (0.60 mmol) was added and the reaction was carried out at room temperature for 12 h. The mixture was then concentrated in vacuo, diluted with cold water (10 mL), and extracted with CH₂Cl₂ (3 x 15 mL). The organic layer was dried over Na₂SO₄ and the solvent was evaporated to afford final compound **83**, which was purified by flash column chromatography using cyclohexane/ethyl acetate 1:1 as eluent. Yield = 62 %; mp = 210-11 °C (EtOH). ¹H NMR (CDCl₃) δ 1.88 (s, 3H, COCH₃), 2.19 (s, 3H, 3-CH₃), 3.83 (s, 3H, OCH₃), 4.97 (s, 2H, COCH₂N), 6.87 (d, 2H, Ar, *J* = 8.9 Hz), 7.05 (d, 2H, Ar, *J* = 8.9 Hz), 7.44 (td, 4H, Ar, *J* = 2.8 Hz, *J* = 6.5 Hz), 7.65 (exch br s, 1H, NH), 8.64 (exch br s, 1H, NH).

5.2.240 Ethyl-2-[5-amino-3-methyl-6-oxopyridazin-1(6*H*)-yl]acetate (**85**)



A mixture of **84** (0.80 mmol), K₂CO₃ (1.60 mmol) and ethyl bromoacetate (1.20 mmol) in CH₃CN (5 mL) was refluxed under stirring for 3 h. The solvent was removed under reduced pressure, then the crude mixture was diluted with cold water (10 mL) and extracted with CH₂Cl₂ (3 x 15 mL). The organic layer was dried over Na₂SO₄ and evaporated in vacuo; finally compound **85** was purified by column chromatography using CH₂Cl₂/CH₃OH 95:5 as eluent. Yield = 71 %; oil. ¹H NMR (CDCl₃) δ 1.30 (t, 3H, CH₂CH₃, *J* = 7.1 Hz), 2.22 (s, 3H, 3-CH₃), 4.25 (qd, 2H, OCH₂CH₃, *J* = 4.1 Hz, *J* = 3.0 Hz), 4.84 (s, 2H, NCH₂CO), 6.17 (s, 1H, Ar).

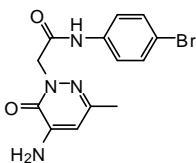
5.2.241 2-[5-Amino-3-methyl-6-oxopyridazin-1(6*H*)-yl]acetic acid (**86**)



5. Experimental Chemistry

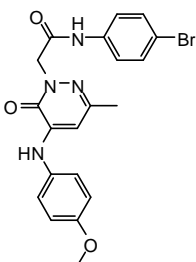
A suspension of compound **85** (0.28 mmol) in 6 NaOH (2 mL) was stirred at rt to 80 °C for 2 h. The mixture was diluted with ice-cold water (1 mL), acidified with 6 N HCl and the aqueous phase was evaporated in vacuo. The crude residue was dissolved in ethanol and the precipitate was filtered off. Finally, evaporation of the solvent afforded compound **86**, which was purified by crystallization from cyclohexane. Yield ~ 100 %; mp = 234-36 °C (cyclohexane). ¹H NMR (CDCl₃) δ 2.09 (s, 3H, 3-CH₃), 4.62 (s, 2H, NCH₂CO), 6.13 (s, 1H, Ar), 6.37 (exch br s, 2H, NH₂), 6.55 (exch br s, 1H, OH).

5.2.242 *N*-(4-Bromophenyl)-2-[5-amino-3-methyl-6-oxopyridazin-1(6*H*)-yl]acetamide (**87**)



To a cooled (-5 °C) and stirred solution of compound **86** (0.33 mmol), in anhydrous tetrahydrofuran (3 mL), Et₃N (1.15 mmol) was added. After 30 min, the mixture was allowed to warm up to 0 °C and ethyl chloroformate (0.36 mmol) was added. After 1 h 4-bromo aniline (0.66 mmol) was added and the reaction was carried out at room temperature for 12 h. The mixture was then concentrated in vacuo, diluted with ice-cold water (10 mL) and extracted with CH₂Cl₂ (3 x 15 mL). The solvent was evaporated to afford final compound **87**, which was purified by flash column chromatography using cyclohexane/ethyl acetate 1:1 as eluent. Yield = 50 %; mp = 244-45 °C (EtOH). ¹H NMR (CDCl₃) δ 2.27 (s, 3H, 3-CH₃), 4.93 (s, 2H, COCH₂N), 6.24 (s, 1H, Ar), 7.42 (s, 4H, Ar), 8.83 (exch br s, 1H, NH), 8.64 (exch br s, 1H, NH).

5.2.243 *N*-(4-Bromophenyl)-2-[5-(4-methoxyphenylamino)-3-methyl-6-oxopyridazin-1(6*H*)-yl]acetamide (**88**)

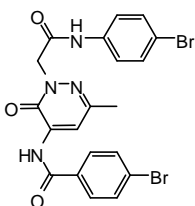


To a suspension of **87** (0.36 mmol), copper acetate (0.53 mmol) and 4-methoxyphenylboronic acid (0.36 mmol) in CH₂Cl₂ (3 mL), Et₃N (0.72 mmol) was added and the mixture was stirred at room temperature for 12 h. The suspension was extracted with 15% aqueous ammonia (3 x 10 mL), and the organic layer was washed with 10 mL of water and dried over Na₂SO₄. After removal of the solvent under reduced pressure, the residue was purified by flash column chromatography using CH₂Cl₂/CH₃OH 9.5:0.5 as eluent. The analytical sample of compound **88** was obtained from a further purification through a silica

gel preparative TLC (eluent: CH₂Cl₂/CH₃OH 9.5:0.5). Yield = 10 %; mp = 249-51 °C (EtOH). ¹H NMR (CDCl₃) δ 2.26 (s, 3H, 3-CH₃), 3.86 (s, 3H, OCH₃), 4.97 (s, 2H, COCH₂N), 6.38 (s, 1H, Ar), 6.97 (d, 2H, Ar, *J* = 8.9 Hz), 7.18 (d, 2H, Ar, *J* = 8.9 Hz), 7.35 (exch br s, 1H, NH), 7.44 (dd, 4H, Ar, *J* = 5.5 Hz, *J* = 9.1 Hz), 8.77 (exch br s, 1H, NH).

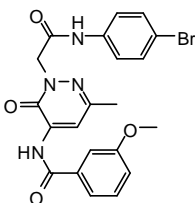
General Procedure for 89a,b. A solution of compound **87** (0.21 mmol), Et₃N (5 drops) and the appropriate substituted benzoyl chloride (0.25 mmol), in dry CH₂Cl₂ (5 mL), was stirred at 0 °C for 1 h. Extra benzoyl chloride (0.25 mmol) was added. The reaction was carried out always at 0 °C for additional 3 h and then, 12 h at room temperature. The mixture was extracted with 6 N NaOH (3 x 10 mL), then the organic layer was washed with water (10 mL) and dried over Na₂SO₄. After removal of the solvent in vacuo, compound **89a** was purified by two consecutive silica gel preparative TLC using in both cases cyclohexane/ethyl acetate 1:2 as eluent. Differently, in the case of compound **89b** the residue was purified by flash column chromatography using cyclohexane/ethyl acetate 1:3 as eluent.

5.2.244 4-Bromo-*N*-{2-[2-(4-bromophenylcarbamoyl)methyl]-6-methyl-3-oxo-2,3-dihydropyridazin-4-yl}benzamide (89a)



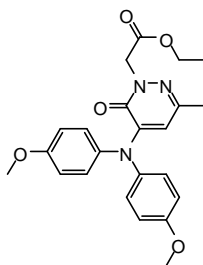
Yield = 10 %; colorless oil. ¹H NMR (CDCl₃) δ 2.43 (s, 3H, 6-CH₃), 4.98 (s, 2H, COCH₂N), 7.44 (s, 4H, Ar), 7.69 (d, 2H, Ar, *J* = 8.6 Hz), 7.82 (d, 2H, Ar, *J* = 8.6 Hz), 8.24 (s, 1H, Ar).

5.2.245 3-Methoxy-*N*-{2-[2-(4-bromophenylcarbamoyl)methyl]-6-methyl-3-oxo-2,3-dihydropyridazin-4-yl}benzamide (89b)



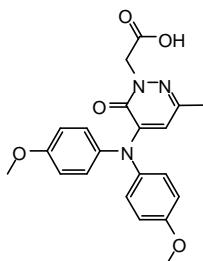
Yield = 13 %; mp = 226-28 °C (EtOH). ¹H NMR (CDCl₃) δ 2.27 (s, 3H, 6-CH₃), 3.89 (s, 3H, OCH₃), 4.93 (s, 2H, COCH₂N), 4.98 (exch br s, 1H, NH), 6.24 (s, 1H, Ar), 7.16-7.19 (m, 1H, Ar), 7.39-7.45 (m, 5H, Ar), 7.63 (t, 1H, Ar, *J* = 2.5 Hz), 7.73 (dd, 1H, Ar, *J* = 5.3 Hz, *J* = 1.0 Hz), 8.83 (exch br s, 1H, Ar).

5.2.246 Ethyl-2-{5-[bis(4-methoxyphenyl)amino]-3-methyl-6-oxopyridazin-1(6H)-yl}acetate (90)



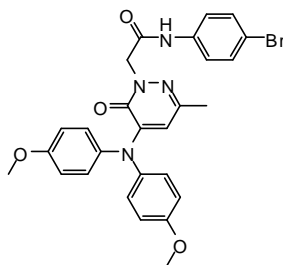
To a suspension of compound **85** (0.57 mmol), copper acetate (0.85 mmol) and 4-methoxyphenylboronic acid (1.14 mmol) in CH_2Cl_2 (3 mL), Et_3N (0.64 mmol) was added and the mixture was stirred at room temperature for 14 h. The mixture was extracted with 15% aqueous ammonia (3 x 10 mL) and the organic layer was washed with 10 mL of water and dried over Na_2SO_4 . After removal of the solvent in vacuo, the residue was purified by flash column chromatography using cyclohexane/ethyl acetate 1:3 as eluent. Yield = 21 %; colorless oil. $^1\text{H NMR}$ (CDCl_3) δ 1.28 (t, 3H, CH_2CH_3 , $J = 7.2$ Hz), 2.18 (s, 3H, 3- CH_3), 3.81 (s, 6H, 2 x OCH_3), 4.21 (q, 2H, CH_2CH_3 , $J = 7.2$ Hz), 4.83 (s, 2H, NCH_2CO), 6.32 (s, 1H, Ar), 6.86 (dd, 4H, Ar, $J = 3.4$ Hz, $J = 2.3$ Hz), 6.99 (dd, 4H, Ar, $J = 4.5$ Hz, $J = 2.3$ Hz).

5.2.247 2-{5-[Bis-(4-methoxyphenyl)amino]-3-methyl-6-oxopyridazin-1(6H)-yl}acetic acid (91)



A suspension of the intermediate **90** (0.12 mmol), 6 NaOH (10 mL) and EtOH (3 mL) was stirred at rt 12 h. After removal of the solvent under vacuo, the mixture was diluted with ice-cold water and acidified with 6 N HCl. After 1 h stirring in ice-bath, the product **91** was filtered off by suction and recrystallized from ethanol. Yield = 84 %; mp = 192-93 °C (EtOH). $^1\text{H NMR}$ (CDCl_3) δ 2.20 (s, 3H, 3- CH_3), 3.82 (s, 6H, 2 x OCH_3), 4.88 (s, 2H, NCH_2CO), 6.34 (s, 1H, Ar), 6.86 (d, 4H, Ar, $J = 8.8$ Hz), 6.99 (d, 4H, Ar, $J = 8.8$ Hz).

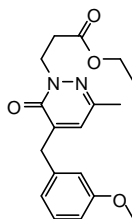
5.2.248 *N*-(4-Bromophenyl)-2- $\{5$ -[bis(4-methoxyphenyl)amino]-3-methyl-6-oxopyridazin-1(6*H*)-yl}acetamide (**92**)



To a cooled (-5 °C) and stirred solution of compound **91** (0.10 mmol) in anhydrous tetrahydrofuran (4 mL), Et₃N (0.35 mmol) was added. After 30 min, the mixture was allowed to warm up to 0 °C and ethyl chloroformate (0.11 mmol) was added. After 1 h 4-bromo aniline (0.20 mmol) was added and the reaction was carried out at room temperature for 12 h. The mixture was then concentrated in vacuo, diluted with cold water (10 mL) and extracted with CH₂Cl₂ (3 x 15 mL). The solvent was evaporated to afford final compound **92**, which was purified by flash column chromatography using cyclohexane/ethyl acetate 1:1 as eluent. Yield = 55 %; mp = 244-245 °C (EtOH). ¹H NMR (CDCl₃) δ 2.23 (s, 3H, 3-CH₃), 3.79 (s, 6H, 2 x OCH₃), 4.81 (s, 2H, NCH₂CO), 6.39 (s, 1H, Ar), 6.84 (dd, 4H, Ar, *J* = 4.6 Hz, *J* = 2.2 Hz), 6.99 (dd, 4H, Ar, *J* = 2.2 Hz, *J* = 3.4 Hz), 7.25-7.38 (m, 4H, Ar), 9.00 (exch br s, 1H, NH).

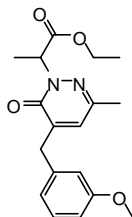
General Procedure for 93a,b. A mixture of **43** (1.13 mmol), K₂CO₃ (2.26 mmol), and the appropriate alkyl halide (1.70 mmol) in CH₃CN (3 mL) was refluxed under stirring for 6 h. The mixture was then concentrated in vacuo, diluted with cold water and extracted with CH₂Cl₂ (3 x 15 mL). The solvent was evaporated in vacuo and compounds **93a,b** were purified by column chromatography using cyclohexane/ethyl acetate 1:1 as eluent.

5.2.249 Ethyl-3-[5-(3-methoxybenzyl)-3-methyl-6-oxopyridazin-1(6*H*)-yl]propanoate (**93a**)



Yield = 86 %; oil. ¹H NMR (CDCl₃) δ 1.26 (t, 3H, OCH₂CH₃, *J* = 7.1 Hz), 2.22 (s, 3H, 3-CH₃), 2.84 (t, 2H, NCH₂CH₂CO, *J* = 7.2 Hz), 3.83 (s, 3H, OCH₃), 3.87 (s, 2H, CH₂-Ar), 4.17 (q, 2H, OCH₂CH₃, *J* = 7.1 Hz), 4.45 (t, 2H, NCH₂CH₂COO, *J* = 7.3 Hz), 6.64 (s, 1H, Ar), 6.80 (s, 1H, Ar), 6.83 (d, 2H, Ar, *J* = 7.9 Hz), 7.26-7.30 (m, 1H, Ar).

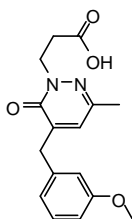
5.2.250 Ethyl-2-[5-(3-methoxybenzyl)-3-methyl-6-oxopyridazin-1(6H)-yl]propanoate (93b)



Yield = 85 %; oil. $^1\text{H NMR}$ (CDCl_3) δ 1.22 (t, 3H, OCH_2CH_3 , $J = 7.1$ Hz), 1.65 (d, 3H, CH_3CHN , $J = 7.2$ Hz), 2.21 (s, 3H, 3- CH_3), 3.78 (s, 3H, OCH_3), 3.84 (s, 2H, CH_2 -Ar), 4.19 (q, 2H, OCH_2CH_3 , $J = 6.7$ Hz), 5.51 (q, 1H, CH_3CHN , $J = 7.2$ Hz), 6.64 (s, 1H, Ar), 6.77-6.81 (m, 3H, Ar), 7.22-7.26 (m, 1H, Ar).

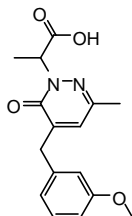
General Procedure for 94a,b. A suspension of the appropriate intermediate type **93** (**93a,b**) (0.5 mmol), and 6 N NaOH (6 mL) in ethanol (2 mL) was stirred at rt to 80 °C for 1 h. The mixture was then concentrated in vacuo, diluted with cold water and acidified with 6 N HCl. Compound **94a** was filtered off by suction and recrystallized from ethanol. For compound **94b** differently, after acidification with 6 N HCl, the mixture was extracted with CH_2Cl_2 (3 x 15 mL) and the solvent was evaporated in vacuo to give the pure compound as an oil.

5.2.251 3-[5-(3-Methoxybenzyl)-3-methyl-6-oxopyridazin-1(6H)-yl]propanoic acid (94a)



Yield = 96 %; mp = 86-88 °C (EtOH). $^1\text{H NMR}$ (CDCl_3) δ 2.22 (s, 3H, 3- CH_3), 2.89 (t, 2H, $\text{NCH}_2\text{CH}_2\text{CO}$, $J = 7.2$ Hz), 3.81 (s, 3H, OCH_3), 3.87 (s, 2H, CH_2 -Ar), 4.46 (t, 2H, $\text{NCH}_2\text{CH}_2\text{CO}$, $J = 7.2$ Hz), 6.66 (s, 1H, Ar), 6.78 (s, 1H, Ar), 6.81-6.85 (m, 2H, Ar), 7.25-7.29 (m, 1H, Ar), 9.99 (exch br s, 1H, OH).

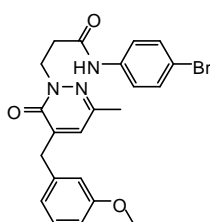
5.2.252 2-[5-(3-Methoxybenzyl)-3-methyl-6-oxopyridazin-1(6H)-yl]propanoic acid (94b)



Yield = 85 %; oil. $^1\text{H NMR}$ (CDCl_3) δ 1.71 (d, 3H, CH_3CHN , $J = 7.2$ Hz), 2.25 (s, 3H, 3- CH_3), 3.81 (s, 3H, OCH_3), 3.88 (s, 2H, CH_2 -Ar), 5.54 (q, 1H, CH_3CHN , $J = 7.2$ Hz), 6.67 (s, 1H, Ar), 6.79-6.85 (m, 3H, Ar), 7.26-7.29 (m, 1H, Ar).

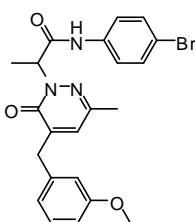
General Procedure for 95a,b. To a cooled (-5 °C) and stirred solution of compound **94a** or **94b** (0.35 mmol), in anhydrous tetrahydrofuran (3-5 mL), Et₃N (1.22 mmol) was added. After 30 min, the mixture was allowed to warm up to 0 °C and ethyl chloroformate (0.38 mmol) was added. After 1 h, 4-bromoaniline (0.7 mmol) was added and the reaction was carried out at room temperature for 12 h. The mixture was then concentrated in vacuo, diluted with cold water (20-30 mL) and extracted with CH₂Cl₂ (3 x 15 mL). The solvent was evaporated to afford the final compounds **95a,b**, which were purified by column chromatography using cyclohexane/ethyl acetate 1:2 as eluent for compound **95a**, cyclohexane/ethyl acetate 2:1 for compound **95b**.

5.2.253 *N*-(4-Bromophenyl)-3-[5-(3-methoxybenzyl)-3-methyl-6-oxo-pyridazin-1(6*H*)-yl]propanamide (**95a**)



Yield = 82 %; mp = 123-125 °C (EtOH). IR (cm⁻¹) 3297 (NH), 1710 (CO), 1644 (CO). ¹H NMR (CDCl₃) δ 2.27 (s, 3H, 3-CH₃), 3.00 (t, 2H, NCH₂CH₂CO, *J* = 6.3 Hz), 3.80 (s, 3H, OCH₃), 3.88 (s, 2H, CH₂-Ar), 4.54 (t, 2H, NCH₂CH₂COO, *J* = 6.3 Hz), 6.76-6.84 (m, 4H, Ar), 7.25 (t, 1H, Ar, *J* = 7.9 Hz), 7.40 (d, 2H, Ar, *J* = 8.8 Hz), 7.50 (d, 2H, Ar, *J* = 8.8 Hz), 9.29 (exch br s, 1H, NH). MS (ESI) calcd. For C₂₂H₂₂BrN₃O₃, 456.33. Found: *m/z* 456.09 [M]⁺.

5.2.254 (±)-*N*-(4-Bromophenyl)-2-[5-(3-methoxybenzyl)-3-methyl-6-oxo-pyridazin-1(6*H*)-yl]propanamide (**95b**)



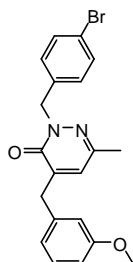
Yield = 53 %; oil; IR (cm⁻¹) 3300 (NH), 1709 (CO), 1643 (CO). ¹H NMR (CDCl₃) δ 1.71 (d, 3H, CH₃CHN, *J* = 7.1 Hz), 2.31 (s, 3H, 3-CH₃), 3.80 (s, 3H, OCH₃), 3.90 (s, 2H, CH₂-Ar), 5.71 (q, 1H, CH₃CHN, *J* = 7.0 Hz), 6.79-6.85 (m, 4H, Ar), 7.25-7.29 (m, 1H, Ar), 7.35-7.36 (m, 4H, Ar), 9.18 (exch br s, 1H, NH). MS (ESI) calcd. For C₂₂H₂₂BrN₃O₃, 456.33. Found: *m/z* 456.09 [M]⁺.

General Procedure for 96a,b. A mixture of **43** (1.13 mmol), K₂CO₃ (2.26 mmol), and appropriate alkyl halide (1.70 mmol) in CH₃CN (3 mL) was refluxed under stirring for 6 h. The mixture was then concentrated in vacuo, diluted with cold water and extracted with CH₂Cl₂ (3 x 15 mL). The

5. Experimental Chemistry

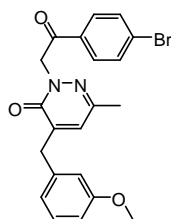
solvent was evaporated in vacuo and compounds **96a,b** were purified by column chromatography using cyclohexane/ethyl acetate 2:1 for **96a** and cyclohexane/ethyl acetate 1:1 for **96b** as eluents.

5.2.255 2-(4-Bromobenzyl)-4-(3-methoxybenzyl)-6-methyl-pyridazin-3(2H)-one (**96a**)



Yield = 68 %; mp = 112-114 °C (EtOH). IR (cm⁻¹) 1638 (CO). ¹H NMR (CDCl₃) δ 2.23 (s, 3H, 6-CH₃), 3.81 (s, 3H, OCH₃), 3.86 (s, 2H, CH₂-Ar), 5.25 (s, 2H, NCH₂Ar), 6.64 (s, 1H, Ar), 6.78-6.85 (m, 3H, Ar), 7.26-7.30 (m, 1H, Ar), 7.35 (d, 2H, Ar, *J* = 8.4 Hz), 7.45-7.47 (m, 2H, Ar). MS (ESI) calcd. For C₂₀H₁₉BrN₂O₂, 399.28. Found: *m/z* 399.07 [M]⁺.

5.2.256 2-[2-(4-Bromophenyl)-2-oxo-ethyl]-4-(3-methoxybenzyl)-6-methyl-pyridazin-3(2H)-one (**96b**)

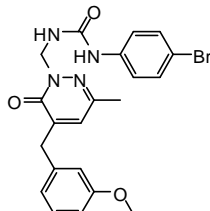


Yield = 95 %; oil. IR (cm⁻¹) 1715 (CO), 1644 (CO). ¹H NMR (CDCl₃) δ 2.25 (s, 3H, 6-CH₃), 3.83 (s, 3H, OCH₃), 3.89 (s, 2H, CH₂-Ar), 5.52 (s, 2H, NCH₂CO), 6.72 (s, 1H, Ar), 6.80 (s, 1H, Ar), 6.84 (d, 2H, Ar, *J* = 7.9 Hz), 7.27-7.31 (m, 1H, Ar), 7.66 (d, 2H, Ar, *J* = 8.6 Hz), 7.88 (d, 2H, Ar, *J* = 8.5 Hz). MS (ESI) calcd. For C₂₁H₁₉BrN₂O₃, 427.29. Found: *m/z* 427.07 [M]⁺.

General Procedure for 97a,b. A mixture of **43a** (0.32 mmol), 40% formaldehyde (3 mL) and 33% NH₃ (1.5 mL) in dioxane (1.5-2 mL) was heated at 50 °C for 1 h. The solvent was then evaporated in vacuo, and the residue was extracted with CH₂Cl₂ (3 x 15 mL). The organic layer was dried with Na₂SO₄ and evaporated to afford an oil. For compound **97a**, the residual oil was dissolved in 2 mL of anhydrous CH₂Cl₂ and 4-bromophenyl isocyanate (0.35 mmol) was added. The mixture was stirred at room temperature for 12 h, then the solid residue was filtered off and the solution was evaporated in vacuo to afford compound **97a**, which was purified by flash chromatography using cyclohexane/ethyl acetate 3:1 as eluent. For compound **97b**, the residual oil was dissolved in 3 mL of anhydrous CH₂Cl₂ and, after cooling (0 °C), 4-bromobenzoyl chloride (0.44 mmol) was added and the mixture was stirred at 0 °C for 6 h. Finally, the residue was washed with cold 0.5 N NaOH (3 x 10 mL) and with cold water (2 x 10 mL).

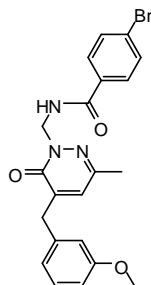
Evaporation of the organic layer afforded compound **97b**, which was purified by flash chromatography using cyclohexane/ethyl acetate 3:1 as eluent.

5.2.257 1-(4-Bromophenyl)-3-[5-(3-methoxybenzyl)-3-methyl-6-oxo-6H-pyridazin-1-ylmethyl]-urea (97a)



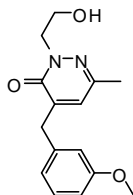
Yield = 27 %; mp = 112- 114 °C (EtOH). IR (cm⁻¹) 3270 (NH), 3265 (NH), 1708 (CO), 1630 (CO). ¹H NMR (CDCl₃) δ 2.25 (s, 3H, 3-CH₃), 3.82 (s, 3H, OCH₃), 3.88 (s, 2H, CH₂-Ar), 6.13 (s, 2H, NCH₂N), 6.68 (s, 1H, Ar), 6.78-6.81 (m, 1H, Ar), 6.83-6.86 (m, 2H, Ar), 6.99 (exch br s, 1H, NH), 7.27-7.31 (m, 3H, Ar), 7.41 (m, 2H, Ar, *J* = 8.8 Hz). MS (ESI) calcd. For C₂₁H₂₁BrN₄O₃, 457.32. Found: *m/z* 458.07 [M + H]⁺.

5.2.258 4-Bromo-N-[5-(3-methoxybenzyl)-3-methyl-6-oxo-6H-pyridazin-1-ylmethyl]-benzamide (97b)



Yield = 30 %; oil. IR (cm⁻¹) 3290 (NH), 1708 (CO), 1640 (CO). ¹H NMR (CDCl₃) δ 2.26 (s, 3H, 3-CH₃), 3.83 (s, 3H, OCH₃), 3.90 (s, 2H, CH₂-Ar), 6.29 (s, 2H, NCH₂N), 6.69 (s, 1H, Ar), 6.81-6.87 (m, 3H, Ar), 7.28-7.32 (m, 1H, Ar), 7.58 (d, 2H, Ar, *J* = 8.6 Hz), 7.94 (d, 2H, Ar, *J* = 8.6 Hz). MS (ESI) calcd. For C₂₁H₂₀BrN₃O₃, 442.31. Found: *m/z* 443.06 [M + H]⁺.

5.2.259 2-(2-Hydroxyethyl)-4-(3-methoxybenzyl)-6-methyl-pyridazin-3(2H)-one (98)

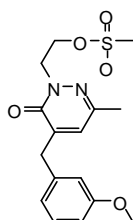


To a refluxed mixture of compound **44** (0.47 mmol) and NaBH₄ (2.64 mmol) in anhydrous THF (6 mL), CH₃OH (1.45 mL) was slowly added. After stirring for 1 h at 60 °C, the mixture was concentrated in vacuo, diluted with cold water (10-15 mL), and extracted with CH₂Cl₂ (3 x 15 mL). Evaporation of the

5. Experimental Chemistry

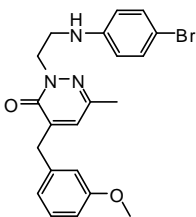
solvent afforded compound **98**. Yield = 95 %; oil. $^1\text{H NMR}$ (CDCl_3) δ 2.23 (s, 3H, 6- CH_3), 3.80 (s, 3H, OCH_3), 3.86 (s, 2H, $\text{CH}_2\text{-Ar}$), 4.00 (t, 2H, $\text{NCH}_2\text{CH}_2\text{OH}$, $J = 5.1$ Hz), 4.35 (t, 2H, $\text{NCH}_2\text{CH}_2\text{OH}$, $J = 5.0$ Hz), 4.66 (exch br s, 1H, OH), 6.68 (s, 1H, Ar), 6.78-6.84 (m, 3H, Ar), 7.25-7.29 (m, 1H, Ar).

5.2.260 Methanesulfonic acid 2-[5-(3-methoxybenzyl)-3-methyl-6-oxo-6H-pyridazin-1-yl]ethyl ester (**99**)



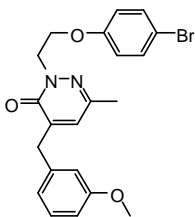
To a cooled (0 °C) and stirred solution of **98** (0.47 mmol) and pyridine (0.5 mmol) in anhydrous CH_2Cl_2 (2 mL), methanesulfonyl chloride (0.61 mmol) was added dropwise, and the mixture was stirred at room temperature for 4 h. Then ice cold water was added and the mixture was extracted with CH_2Cl_2 (3 x 15 mL): evaporation of the solvent afforded the desired compound. Yield = 85 %; oil. $^1\text{H NMR}$ (CDCl_3) δ 2.22 (s, 3H, 3- CH_3), 2.98 (s, 3H, CH_3SO_3), 3.80 (s, 3H, OCH_3), 3.86 (s, 2H, $\text{CH}_2\text{-Ar}$), 3.87-3.90 (m, 2H, $\text{NCH}_2\text{CH}_2\text{O}$), 4.45 (t, 2H, $\text{NCH}_2\text{CH}_2\text{O}$, $J = 6.6$ Hz), 6.66 (s, 1H, Ar), 6.78 (s, 1H, Ar), 6.82 (d, 2H, Ar, $J = 8.1$ Hz), 7.24-7.28 (m, 1H, Ar).

5.2.261 2-[2-(4-Bromophenylamino)-ethyl]-4-(3-methoxybenzyl)-6-methyl-pyridazin-3(2H)-one (**100**)



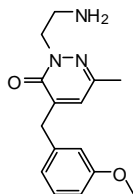
A solution of **99** (0.4 mmol) and 4-bromoaniline (0.8 mmol) in 2-propanol (2 mL) was heated under stirring for 6 h at 60 °C. Then, the mixture was concentrated in vacuo, cold water (30 mL) was added and the suspension was extracted with CH_2Cl_2 (3 x 15 mL). Evaporation of the solvent afforded the final compound **100**, which was purified by column chromatography using toluene/ethyl acetate 8:2 as eluent. Yield = 58 %; mp = 86-88 °C (EtOH). IR (cm^{-1}) 3350 (NH), 1643 (CO). $^1\text{H NMR}$ (CDCl_3) δ 2.24 (s, 3H, 6- CH_3), 3.58 (t, 2H, $\text{NCH}_2\text{CH}_2\text{NHAr}$, $J = 5.7$ Hz), 3.82 (s, 3H, OCH_3), 3.86 (s, 2H, $\text{CH}_2\text{-Ar}$), 4.46 (t, 2H, $\text{NCH}_2\text{CH}_2\text{NHAr}$, $J = 5.8$ Hz), 6.65-6.68 (m, 3H, Ar), 6.79-6.86 (m, 3H, Ar), 7.27-7.31 (m, 3H, Ar). MS (ESI) calcd. For $\text{C}_{21}\text{H}_{22}\text{BrN}_3\text{O}_2$, 428.32. Found: m/z 428.10 $[\text{M}]^+$.

5.2.262 **2-[2-(4-Bromophenoxy)-ethyl]-4-(3-methoxybenzyl)-6-methyl-pyridazin-3(2H)-one (101)**



To a suspension of **98** (0.55 mmol), copper acetate (0.82 mmol) and 4-bromophenylboronic acid (1.08 mmol) in CH_2Cl_2 (2 mL), Et_3N (1.08 mmol) was added and the mixture was stirred at room temperature for 12 h. The suspension was extracted with 15% aqueous ammonia (10 mL), then the organic layer was washed with water (10 mL) and dried over Na_2SO_4 . After removal of the solvent, the residue was purified by flash column chromatography using toluene/ethyl acetate 8:2 as eluent. Yield = 26 %; mp = 82-83 °C (EtOH). IR (cm^{-1}) 1643 (CO). ^1H NMR (CDCl_3) δ 2.24 (s, 3H, 6- CH_3), 3.82 (s, 3H, OCH_3), 3.87 (s, 2H, $\text{CH}_2\text{-Ar}$), 4.36 (t, 2H, $\text{NCH}_2\text{CH}_2\text{O}$, $J = 5.9$ Hz), 4.54 (t, 2H, $\text{NCH}_2\text{CH}_2\text{O}$, $J = 5.8$ Hz), 6.66 (s, 1H, Ar), 6.79-6.86 (m, 5H, Ar), 7.27-7.35 (m, 1H, Ar), 7.35-7.37 (m, 2H, Ar). MS (ESI) calcd. For $\text{C}_{21}\text{H}_{21}\text{BrN}_2\text{O}_3$, 429.31. Found: m/z 430.08 $[\text{M} + \text{H}]^+$.

5.2.263 **2-(2-Aminoethyl)-4-(3-methoxybenzyl)-6-methyl-pyridazin-3(2H)-one (102)**



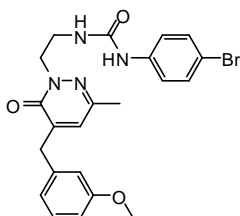
A mixture of **99** (0.43 mmol) and 33% NH_3 (3 mL) in isopropanol (2 mL) was stirred at 60 °C for 3 h. After concentration of the solvent and dilution with cold water (20 mL), the mixture was extracted with CH_2Cl_2 (3 x 15 mL). Evaporation of the solvent afforded desired compound **102**. Yield = 68 %; oil. ^1H NMR (CDCl_3) δ 2.25 (s, 3H, 6- CH_3), 3.82 (s, 3H, OCH_3), 3.88 (s, 2H, $\text{CH}_2\text{-Ar}$), 4.02-4.04 (m, 2H, $\text{NCH}_2\text{CH}_2\text{NH}_2$), 4.37 (t, 2H, $\text{NCH}_2\text{CH}_2\text{NH}_2$, $J = 4.9$ Hz), 5.38 (exch br s, 2H, NH_2), 6.69 (s, 1H, Ar), 6.79-6.85 (m, 3H, Ar), 7.26-7.30 (m, 1H, Ar).

General Procedure for 103a,b. Compounds **103a,b** were obtained starting from the intermediate **102**. For compound **103a**, to a cooled (0 °C) and stirred solution of compound **102** (0.35 mmol) in anhydrous CH_2Cl_2 (2 mL), 4-bromophenyl isocyanate (0.40 mmol) was added. The mixture was stirred at 0 °C to rt 6 h. Removal of the solvent gave a residue that was purified by column chromatography using cyclohexane/ethyl acetate 1:1 as eluent. For compound **103b**, Et_3N (1.8 mmol) and 4-bromobenzoyl chloride (1.43 mmol) were added to a cooled (0 °C) and stirred solution of **102** (0.73 mmol) in anhydrous

5. Experimental Chemistry

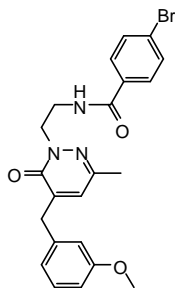
CH₂Cl₂ (2 mL) and the mixture was stirred at 0 °C for 6 h. The solid residue was filtered off and, in turn, the organic layer was washed with 6 N NaOH (3 x 10 mL) and with cold water (2 x 10 mL). The organic layer was dried with Na₂SO₄ and evaporated in vacuo to afford compound **103b**, which was purified by flash chromatography using CH₂Cl₂/CH₃OH 99:1 as eluent.

5.2.264 1-(4-Bromophenyl)-3-{2-[5-(3-methoxybenzyl)-3-methyl-6-oxo-6H-pyridazin-1-yl]-ethyl}-urea (103a)



Yield = 15 %; mp = 114-115 °C (EtOH). IR (cm⁻¹) 3270 (NH), 3265 (NH), 1705 (CO), 1630 (CO). ¹H NMR (CDCl₃) δ 2.23 (s, 3H, 3-CH₃), 3.81 (s, 3H, OCH₃), 3.87 (s, 2H, CH₂-Ar), 4.47 (t, 2H, NCH₂CH₂NH, *J* = 5.2 Hz), 4.57 (t, 2H, NCH₂CH₂NH, *J* = 5.1 Hz), 6.69 (s, 1H, Ar), 6.78-6.84 (m, 3H, Ar), 7.04 (exch br s, 1H, NH), 7.25-7.28 (m, 3H, Ar), 7.41 (d, 2H, Ar, *J* = 8.8 Hz). MS (ESI) calcd. For C₂₂H₂₃BrN₄O₃, 471.35. Found: *m/z* 472.08 [M + H]⁺.

5.2.265 4-Bromo-*N*-{2-[5-(3-methoxybenzyl)-3-methyl-6-oxo-6H-pyridazin-1-yl]-ethyl}-benzamide (103b)

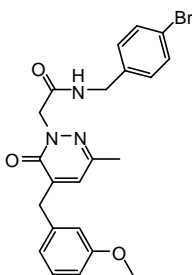


Yield = 13 %; oil. IR (cm⁻¹) 3300 (NH), 1707 (CO), 1643 (CO). ¹H NMR (CDCl₃) δ 2.18 (s, 3H, 3-CH₃), 3.82 (s, 3H, OCH₃), 3.87 (s, 2H, CH₂-Ar), 4.55 (t, 2H, NCH₂CH₂NH, *J* = 5.4 Hz), 4.70 (t, 2H, NCH₂CH₂NH, *J* = 5.4 Hz), 6.67 (s, 1H, Ar), 6.68-6.85 (m, 3H, Ar), 7.26 (d, 1H, Ar, *J* = 7.8 Hz), 7.56 (d, 2H, Ar, *J* = 8.5 Hz), 7.86 (d, 2H, Ar, *J* = 8.5 Hz). MS (ESI) calcd. For C₂₂H₂₂BrN₃O₃, 456.33. Found: *m/z* 457.08 [M + H]⁺.

General Procedure for 104a-c. To a cooled (-5 °C) and stirred solution of compound **45** (0.35 mmol) in anhydrous tetrahydrofuran (3-5 mL), Et₃N (1.22 mmol) was added. After 30 min, the mixture was allowed to warm up to 0 °C, and ethyl chloroformate (0.38 mmol) was added. After 1 h, the 4-Bromobenzylamine, 4-Bromophenol or 4-Bromo-*N*-methylaniline (0.7 mmol) were respectively added. The reaction was carried out at room temperature for 12 h. The mixture was then concentrated in vacuo,

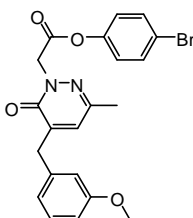
diluted with cold water (20-30 mL) and extracted with CH_2Cl_2 (3 x 15 mL). The solvent was evaporated to afford final compounds **104a-c**, which were purified by column chromatography using cyclohexane/ethyl acetate 1:2 for compounds **104a** and cyclohexane/ethyl acetate 2:1 for **104b,c** as eluents.

5.2.266 *N*-(4-Bromobenzyl)-2-[5-(3-methoxybenzyl)-3-methyl-6-oxo-6*H*-pyridazin-1-yl]acetamide (**104a**)



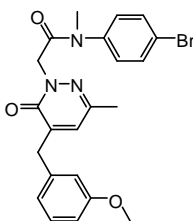
Yield = 97 %; mp = 184-185 °C (EtOH). IR (cm^{-1}) 3300 (NH), 1708 (CO), 1644 (CO). ^1H NMR (DMSO-d_6) δ 2.21 (s, 3H, 3- CH_3), 3.73 (s, 3H, OCH_3), 3.76 (s, 2H, CH_2NHCO), 4.27 (d, 2H, $\text{OCH}_3\text{-C}_6\text{H}_4\text{-CH}_2$), 4.68 (s, 2H, NCH_2CO), 6.80-6.86 (m, 3H, Ar), 7.05 (s, 1H, Ar), 7.23-7.26 (m, 3H, Ar), 7.51 (d, 2H, Ar, $J = 8.3$ Hz), 8.63 (exch br t, 1H, NH, $J = 5.8$ Hz). MS (ESI) calcd. For $\text{C}_{22}\text{H}_{22}\text{BrN}_3\text{O}_3$, 456.33. Found: m/z 456.09 $[\text{M}]^+$.

5.2.267 [5-(3-Methoxybenzyl)-3-methyl-6-oxo-6*H*-pyridazin-1-yl]acetic acid-(4-bromophenyl)ester (**104b**)



Yield = 97 %; mp = 111-112 °C (EtOH). IR (cm^{-1}) 3300 (NH), 1745 (CO), 1644 (CO). ^1H NMR (CDCl_3) δ 2.27 (s, 3H, 3- CH_3), 3.81 (s, 3H, OCH_3), 3.90 (s, 2H, $\text{CH}_2\text{-Ar}$), 5.10 (s, 2H, NCH_2COO), 6.73 (s, 1H, Ar), 6.80 (s, 1H, Ar), 6.83-6.86 (m, 2H, Ar), 7.05 (d, 2H, Ar, $J = 8.7$ Hz), 7.26-7.30 (m, 1H, Ar), 7.50 (d, 2H, Ar, $J = 8.7$ Hz). MS (ESI) calcd. For $\text{C}_{21}\text{H}_{19}\text{BrN}_2\text{O}_4$, 443.29. Found: m/z 443.06 $[\text{M}]^+$.

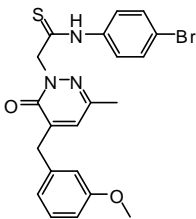
5.2.268 *N*-(4-Methoxyphenyl)-*N*-methyl-2-[5-(3-Methoxybenzyl)-3-methyl-6-oxo-6*H*-pyridazin-1-yl]acetamide (**104c**)



5. Experimental Chemistry

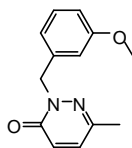
Yield = 45 %; mp = 125-127 °C (EtOH). IR (cm⁻¹) 1709 (CO), 1644 (CO). ¹H NMR (CDCl₃) δ 2.21 (s, 3H, 3-CH₃), 3.32 (s, 3H, CH₃N), 3.82 (s, 3H, OCH₃), 3.86 (s, 2H, CH₂-Ar), 4.64 (s, 2H, NCH₂CO), 6.62 (s, 1H, Ar), 6.77 (s, 1H, Ar), 6.80-6.85 (m, 2H, Ar), 7.26-7.30 (m, 3H, Ar), 7.60 (d, 2H, Ar, *J* = 8.4 Hz). MS (ESI) calcd. For C₂₂H₂₂BrN₃O₃, 456.33. Found: *m/z* 456.09 [M]⁺.

5.2.269 N-(4-Bromophenyl)-2-[5-(3-methoxybenzyl)-3-methyl-6-oxo-pyridazin-1(6H)-yl]ethanethioamide (105)

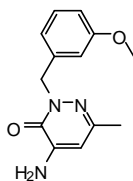


Lawesson's reagent (0.28 mmol) was slowly added to a stirred solution of compound **46a** (0.14 mmol) in toluene (3 mL) and the reaction was carried out at reflux for 3 h. The solvent was removed in vacuo and the mixture was diluted with ice-cold water and extracted with CH₂Cl₂ (3 x 10 mL). The crude product was finally purified by flash column chromatography using cyclohexane/ethyl acetate 1:1 as eluent, to yield **105** as an amorphous solid. Yield = 30 %; mp = 68-70 °C (EtOH). ¹H NMR (CDCl₃) δ 2.32 (s, 3H, 3-CH₃), 3.81 (s, 3H, OCH₃), 3.92 (s, 2H, CH₂-Ar), 5.37 (s, 2H, NCH₂CS), 6.81 (s, 1H, Ar), 6.83-6.87 (m, 3H, Ar), 7.28 (t, 1H, Ar, *J* = 5.0 Hz), 7.48 (d, 2H, Ar, *J* = 8.8 Hz), 7.74 (d, 2H, Ar, *J* = 8.8 Hz), 11.46 (exch br s, 1H, NH). MS (ESI) calcd. For C₂₂H₂₂BrN₃O₃, 458.37. Found: *m/z* 458.17 [M + H]⁺, 482.36 [M + Na]⁺, 378.45 [M - Br]⁺, 231.17 [M - C₈H₇BrNS]⁺.

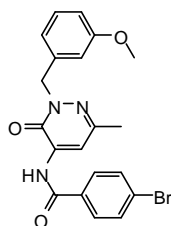
5.2.270 2-(3-Methoxybenzyl)-6-methylpyridazin-3(2H)-one (106)



A mixture of **54b** (1.13 mmol), K₂CO₃ (2.26 mmol) and 3-methoxybenzyl chloride (1.70 mmol) in CH₃CN (3 mL) was refluxed under stirring for 6 h. The mixture was then concentrated in vacuo, diluted with cold water and extracted with CH₂Cl₂ (3 x 15 mL). The solvent was evaporated in vacuo and compound **106** was purified by flash chromatography using CH₂Cl₂/CH₃OH 9.9:0.1 as eluent. Yield = 86 %; mp = 53-55 °C (cyclohexane). ¹H NMR (CDCl₃) δ 2.32 (s, 3H, 6-CH₃), 3.80 (s, 3H, OCH₃), 5.26 (s, 2H, NCH₂), 6.81-6.84 (m, 1H, Ar), 6.87 (d, 1H, Ar, *J* = 9.4 Hz), 6.97-7.05 (m, 2H, Ar), 7.07 (d, 1H, Ar, *J* = 9.4 Hz), 7.22-7.26 (m, 1H, Ar).

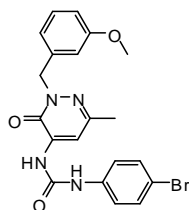
5.2.271 4-Amino-2-(3-methoxybenzyl)-6-methylpyridazin-3(2H)-one (**107**)

A suspension of **106** (0.78 mmol) and hydrazine hydrate (3.12 mmol) was stirred in a sealed tube at 180 °C for 12 h. After cooling, ice-cold water was added. The suspension was kept at 0 °C in ice-bath for 2 h and the precipitate was then filtered off to give a first batch of **107**. The solution was saturated with NH₄Cl and extracted with CH₂Cl₂ (3 x 25 mL). Removal of the solvent afforded a second batch of product. Yield = 89 %; mp = 96-98 °C (EtOH). ¹H NMR (CDCl₃) δ 2.23 (s, 3H, CH₃), 3.81 (s, 3H, OCH₃), 4.85 (exch br s, 2H, NH₂), 5.27 (s, 2H, CH₂), 6.16 (s, 1H, Ar), 6.81-6.85 (m, 1H, Ar), 6.97-7.02 (m, 2H, Ar), 7.23-7.28 (m, 1H, Ar).

5.2.272 4-Bromo-N-[2-(3-methoxybenzyl)-6-methyl-3-oxo-2,3-dihydro-pyridazin-4-yl]benzamide (**108**)

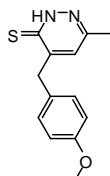
Et₃N (1.8 mmol) and 4-bromobenzoyl chloride (1.43 mmol) were added to a cooled (0 °C) and stirred solution of **107** (0.73 mmol) in anhydrous CH₂Cl₂ (2 mL), and the mixture was monitored under stirring at 0 °C for 10 h. The solid residue was removed by filtration. The organic layer was washed with 6 N NaOH (3 x 10 mL) and with cold water (2 x 10 mL). Drying with Na₂SO₄ and evaporation of the solvent in vacuo afforded compound **108**, which was purified by flash chromatography using cyclohexane/ethyl acetate 3:1 as eluent. Yield = 28 %; mp = 162-164 °C (EtOH). IR (cm⁻¹) 3300 (NH), 1709 (CO), 1644 (CO). ¹H NMR (CDCl₃) δ 2.40 (s, 3H, CH₃), 3.82 (s, 3H, OCH₃), 5.32 (s, 2H, CH₂), 6.84-6.87 (m, 1H, Ar), 6.98-7.02 (m, 2H, Ar), 7.26-7.30 (m, 1H, Ar), 7.66 (d, 1H, Ar, *J* = 8.7 Hz), 7.80 (d, 2H, Ar, *J* = 8.6 Hz), 8.14 (s, 1H, Ar), 9.37 (exch br s, 1H, NH). MS (ESI) calcd. For C₂₀H₁₈BrN₃O₃, 428.28. Found: *m/z* 428.06 [M]⁺.

5.2.273 1-(4-Bromophenyl)-3-[2-(3-methoxybenzyl)-6-methyl-3-oxo-2,3-dihydro pyridazin-4-yl]urea (109)



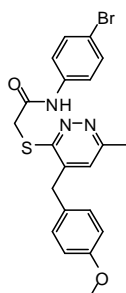
To a stirred solution of compound **107** (0.35 mmol) in anhydrous toluene (2 mL), 4-bromophenyl isocyanate (0.40 mmol) was added. The mixture was refluxed for 7 h and after cooling, the solvent was removed under reduced pressure. The mixture was diluted with ice-cold water and extracted with CH_2Cl_2 (3 x 15 mL). Evaporation of the solvent gave a crude product that was purified by column chromatography using firstly CH_2Cl_2 , to remove the 4-bromophenyl urea, and then cyclohexane/ethyl acetate 2:1 as eluent. Yield = 56 %; mp = 207-209 °C (EtOH). IR (cm^{-1}) 3270 (NH), 3265 (NH), 1705 (CO), 1630 (CO). ^1H NMR (CDCl_3) δ 2.12 (s, 3H, CH_3), 3.57 (s, 3H, OCH_3), 5.08 (s, 2H, CH_2), 6.51-6.58 (m, 3H, Ar), 6.97- 7.04 (m, 3H, Ar), 7.23 (d, 2H, Ar, $J = 8.7$ Hz), 7.86 (s, 1H, Ar), 8.70 (exch br s, 1H, NH), 8.94 (exch br s, 1H, NH). MS (ESI) calcd. For $\text{C}_{20}\text{H}_{19}\text{BrN}_4\text{O}_3$, 443.29. Found: m/z 443.07 [M] $^+$.

5.2.274 4-(4-methoxybenzyl)-6-methylpyridazine-3(2H)-thione (110)



Lawesson's reagent (0.87 mmol) was slowly added to a stirred solution of compound **58e** (0.87 mmol) in toluene (3 mL) and the reaction was carried out at reflux for 2 h. The mixture was cooled and after 1 h stirring in ice-bath the precipitate was filtered off and purified by recrystallization from ethanol. Yield = 47 %; mp = 191-93 °C (EtOH). ^1H NMR (CDCl_3) δ 2.30 (s, 3H, 3- CH_3), 3.85 (s, 3H, OCH_3), 4.11 (s, 2H, CH_2 -Ar), 6.57 (s, 1H, Ar), 6.93 (d, 2H, Ar, $J = 8.5$ Hz), 7.17 (d, 2H, Ar, $J = 8.5$ Hz), 12.12 (exch br s, 1H, SH).

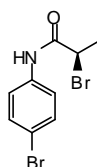
5.2.275 N-(4-Bromophenyl)-2-[4-(4-methoxybenzyl)-6-methylpyridazin-3-ylthio] acetamide (111)



A mixture of **110** (0.41 mmol), K_2CO_3 (0.82 mmol), and *N*-(4-bromophenyl)-2-chloro acetamide **22** (0.61 mmol) in CH_3CN (4 mL) was refluxed under stirring for 1.5 h. After cooling, the solvent was evaporated and the mixture was diluted with cold water. The precipitate was filtered off and purified by flash chromatography using cyclohexane/ethyl acetate 1:2 as eluent. Yield = 96 %; mp = 116-118 °C (EtOH). 1H NMR ($CDCl_3$) δ 2.62 (s, 3H, 6- CH_3), 3.84 (s, 3H, OCH_3), 3.87 (s, 2H, CH_2 -Ar), 4.08 (s, 2H, SCH_2CO), 6.84 (s, 1H, Ar), 6.92 (d, 2H, Ar, $J = 8.5$ Hz), 7.11 (d, 2H, Ar, $J = 8.5$ Hz), 7.38 (d, 2H, Ar, $J = 8.8$ Hz), 7.48 (d, 2H, Ar, $J = 8.8$ Hz), 10.26 (exch br s, 1H, NH).

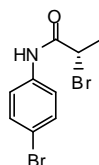
General Procedure for R-(+)-112 and S(-)-112. To a stirred solution of the suitable bromopropionic acid [R-(+)- or S(-)-] (1.31 mmol), in anhydrous CH_2Cl_2 (5 mL), $SOCl_2$ (7.86 mmol) was added dropwise and the reaction was carried out at 40 °C for 4 h. The mixture was allowed to cool down and then the solvent and the excess of $SOCl_2$ were removed in vacuo. The residue was dissolved in anhydrous THF (5 mL) and 4-bromoaniline (2.62 mmol) was added. The reaction was stirred for additional 4 h at room temperature. After removal of the solvent under reduced pressure, the mixture was dissolved in CH_2Cl_2 and washed, in turn, with 2 N HCl (3 x 15 mL), 2 N NaOH (3 x 15 mL) and with H_2O (15 mL). The organic layer was dried over Na_2SO_4 and evaporated under vacuo to give the crude products which were purified by flash column chromatography using toluene/ethyl acetate 6:1 as eluents.

5.2.276 R-(+)-2-Bromo-*N*-(4-bromophenyl)propanamide [R-(+)-112]



Yield = 12 %; mp = 150-51 °C (EtOH). $[\alpha]_D^{20} = + 25^\circ$ ($c = 1$, $CHCl_3$). e.e. > 99.9 % (determined by analytical chiral HPLC). 1H NMR ($CDCl_3$) δ 1.98 (d, 3H, $CHCH_3$, $J = 7.0$ Hz), 4.56 (q, 1H, $CHCH_3$, $J = 7.0$ Hz), 7.45-7.50 (dd, 4H, Ar, $J = 6.3$ Hz, $J = 2.9$ Hz), 8.09 (exch br s, 1H, NH).

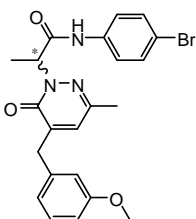
5.2.277 S(-)-2-Bromo-*N*-(4-bromophenyl)propanamide [S(-)-112]



Yield = 15 %; mp = 150-51 °C (EtOH). $[\alpha]_D^{20} = - 25^\circ$ ($c = 1$, $CHCl_3$). e.e. > 99.9 % (determined by analytical chiral HPLC). 1H NMR ($CDCl_3$) δ 1.99 (d, 3H, $CHCH_3$, $J = 7.0$ Hz), 4.56 (q, 1H, $CHCH_3$, $J = 7.0$ Hz), 7.46-7.50 (dd, 4H, Ar, $J = 3.7$ Hz, $J = 2.6$ Hz), 8.07 (exch br s, 1H, NH).

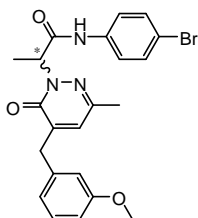
General procedure for (+)-113 [rac 70:30, from S-(-)-112] and (-)-113 [rac 60:40, from R-(+)-112]. A mixture of intermediate **43** (0.17 mmol), K_2CO_3 (0.34 mmol) and **R-(+)-112** or **S-(-)-112** (0.19 mmol) respectively, in CH_3CN (3 mL) were refluxed under stirring for 2 h. After cooling, the solvent was evaporated and the mixture was diluted with ice-cold water and extracted using CH_2Cl_2 (3 x 10 mL). The organic layer was collected, dried over Na_2SO_4 and evaporated in vacuo. The crude residues were purified by flash column chromatography using cyclohexane/ethyl acetate 2:1 as eluent.

5.2.278 (+)-N-(4-Bromophenyl)-2-[5-(3-methoxybenzyl)-3-methyl-6-oxopyridazin-1(6H)-yl]propanamide [(+)-113, rac 70:30]



Yield = 90 %; mp = 63-64 °C (*n*-hexane). $[\alpha]_D^{20} = + 35^\circ$ ($c = 1$, $CHCl_3$). e.e. = 70 % (of the (+)-enantiomer, determined by analytical chiral HPLC). 1H NMR ($CDCl_3$) δ 1.71 (d, 3H, $CHCH_3$, $J = 7.1$ Hz), 2.30 (s, 3H, 3- CH_3), 3.81 (s, 3H, OCH_3), 3.91 (s, 2H, CH_2 -Ar), 5.71 (q, 1H, $CHCH_3$, $J = 7.1$ Hz), 6.79 (d, 2H, Ar, $J = 7.6$ Hz), 6.84 (d, 2H, Ar, $J = 8.3$ Hz), 7.28 (t, 1H, Ar, $J = 9.1$ Hz), 7.38 (d, 4H, Ar, $J = 6.0$ Hz), 9.09 (exch br s, 1H, NH).

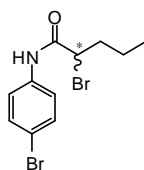
5.2.279 (-)-N-(4-Bromophenyl)-2-[5-(3-methoxybenzyl)-3-methyl-6-oxopyridazin-1(6H)-yl]propanamide [(-)-113, rac 60:40]



Yield = 93 %; mp = 63-64 °C (*n*-hexane). $[\alpha]_D^{20} = - 30^\circ$ ($c = 1$, $CHCl_3$). e.e. = 60 % (of the n (-)-enantiomer, determined by analytical chiral HPLC). 1H NMR ($CDCl_3$) δ 1.71 (d, 3H, $CHCH_3$, $J = 7.1$ Hz), 2.31 (s, 3H, 3- CH_3), 3.80 (s, 3H, OCH_3), 3.90 (s, 2H, CH_2 -Ar), 5.71 (q, 1H, $CHCH_3$, $J = 7.1$ Hz), 6.79 (q, 2H, Ar, $J = 1.0$ Hz), 6.84 (dd, 2H, Ar, $J = 6.0$ Hz, $J = 1.0$ Hz), 7.27 (t, 1H, Ar, $J = 8.2$ Hz), 7.36 (d, 4H, Ar, $J = 6.0$ Hz), 9.16 (exch br s, 1H, NH).

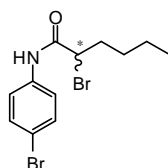
General Procedure for racemates (\pm)-115a-f and 116. Compounds (\pm)-115a-f and 116 were synthesized using the suitable carboxylic acid and following the same procedure exploited for **R-(+)-** and **S-(-)-112**.

5.2.280 (±)-2-Bromo-N-(4-bromophenyl)pentanamide [(±)-115b]



Yield = 10 %; mp = 94-96 °C (EtOH). $^1\text{H NMR}$ (CDCl_3) δ 1.00 (t, 3H, CH_2CH_3 , $J = 7.4$ Hz), 1.50-1.65 (m, 2H, $\text{CH}_2\text{CH}_2\text{CH}_2\text{CH}_3$), 2.05-2.16 (m, 1H, COCHCH-HCH_2), 2.20-2.25 (m, 1H, COCHCH-HCH_2), 4.47 (dd, 1H, COCHCH_2 , $J = 3.1$ Hz, $J = 5.2$ Hz), 7.43-7.50 (m, 4H, Ar), 8.10 (exch br s, 1H, NH).

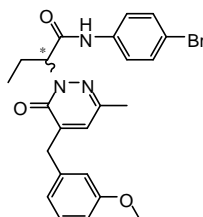
5.2.281 (±)-2-Bromo-N-(4-bromophenyl)hexanamide [(±)-115d]



Yield = 10 %; mp = 114-15 °C (EtOH). $^1\text{H NMR}$ (CDCl_3) δ 0.95 (t, 3H, CH_2CH_3 , $J = 7.2$ Hz), 1.37-1.44 (m, 2H, $\text{CH}_2\text{CH}_2\text{CH}_2\text{CH}_3$), 1.48-1.57 (m, 2H, $\text{CH}_2\text{CH}_2\text{CH}_2\text{CH}_3$), 2.06-2.14 (m, 1H, COCHCH-HCH_2), 2.20-2.29 (m, 1H, COCHCH-HCH_2), 4.45 (dd, 1H, COCHCH_2 , $J = 7.9$ Hz, $J = 5.2$ Hz), 7.44-7.50 (m, 4H, Ar), 8.07 (exch br s, 1H, NH).

General Procedure for racemates (±)-117a-f and 118. A mixture of compound **43** (0.13 mmol), K_2CO_3 (0.26 mmol) and the suitable intermediate type **115** [(±)-115a-f] or **116** (0.14 mmol), in CH_3CN (3 mL) was refluxed under stirring for 4-5 h. After cooling, the solvent was evaporated and ice-cold water was added to the mixture. For racemate (±)-117a, after 1 h stirring in ice-bath the precipitate was filtered off and purified by crystallization in cyclohexane. For racemates (±)-117b-f and compound **118**, differently, the mixture was extracted using CH_2Cl_2 (3 x 10 mL). The organic layer was collected, dried over Na_2SO_4 and evaporated in vacuo. The crude residue was purified by flash column chromatography using as eluent cyclohexane/ethyl acetate 2:1 for racemates (±)-117b-d, cyclohexane/ethyl acetate 1:3 for racemate (±)-117e and cyclohexane/ethyl acetate 1:1 for compounds (±)-117f and **118**.

5.2.282 (±)-N-(4-Bromophenyl)-2-[5-(3-methoxybenzyl)-3-methyl-6-oxopyridazin-1(6H)-yl]butanamide [(±)-117a]

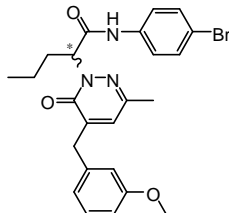


Yield = 98 %; mp = 79-81 °C (cyclohexane). $^1\text{H NMR}$ (CDCl_3) δ 0.95 (t, 3H, CHCH_3 , $J = 7.4$ Hz), 2.19-2.38 (m, 5H, 3- CH_3 + CH_2CH_3), 3.81 (s, 3H, OCH_3), 3.91 (s, 2H, CH_2 -Ar), 5.46 (dd, 1H, NCHCH_2 , $J =$

5. Experimental Chemistry

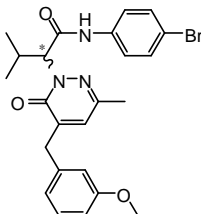
1.4 Hz, $J = 6.9$ Hz), 6.77-6.85 (m, 4H, Ar), 7.27 (t, 1H, Ar, $J = 7.9$ Hz), 7.30-7.44 (m, 4H, Ar), 9.13 (exch br s, 1H, NH).

5.2.283 (\pm)-*N*-(4-Bromophenyl)-2-[5-(3-methoxybenzyl)-3-methyl-6-oxopyridazin-1(6*H*)-yl]pentanamide [(\pm)-117b]



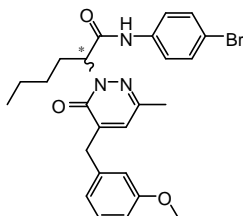
Yield = 94 %; colorless oil. ^1H NMR (CDCl_3) δ 0.98 (t, 3H, CHCH_3 , $J = 7.6$ Hz), 1.26-1.40 (m, 2H, $\text{CH}_2\text{CH}_2\text{CH}_3$), 2.17-2.28 (m, 2H, CHCH_2CH_2), 2.30 (s, 3H, 3- CH_3), 3.81 (s, 3H, OCH_3), 3.90 (s, 2H, CH_2 -Ar), 5.56 (t, 1H, NCHCH_2 , $J = 8.2$ Hz), 6.75 (s, 1H, Ar), 6.79 (s, 1H, Ar), 6.82-6.86 (m, 2H, Ar), 7.27 (t, 1H, Ar, $J = 7.8$ Hz), 7.38 (s, 4H, Ar), 9.03 (exch br s, 1H, NH).

5.2.284 (\pm)-*N*-(4-Bromophenyl)-2-[5-(3-methoxybenzyl)-3-methyl-6-oxopyridazin-1(6*H*)-yl]-3-methylbutanamide [(\pm)-117c]



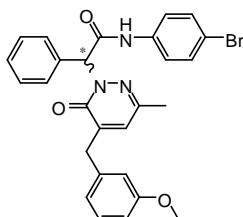
Yield = 80 %; mp = 161-62 °C (*n*-hexane). ^1H NMR (CDCl_3) δ 0.83 (d, 3H, CHCH_3 , $J = 6.6$ Hz), 1.16 (d, 3H, CHCH_3 , $J = 6.6$ Hz), 2.30 (s, 3H, 3- CH_3), 2.85-2.98 (m, 1H, CHCH_3), 3.81 (s, 3H, OCH_3), 3.90 (s, 2H, CH_2 -Ar), 5.14 (d, 1H, NCHCHCH , $J = 11.0$ Hz), 6.72 (s, 1H, Ar), 6.78-6.85 (m, 3H, Ar), 7.28 (t, 1H, Ar, $J = 7.8$ Hz), 7.39-7.44 (m, 4H, Ar), 9.06 (exch br s, 1H, NH).

5.2.285 (\pm)-*N*-(4-Bromophenyl)-2-[5-(3-methoxybenzyl)-3-methyl-6-oxopyridazin-1(6*H*)-yl]hexanamide [(\pm)-117d]



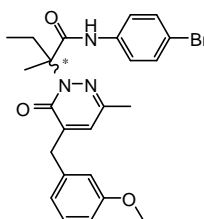
Yield = 93 %; colorless oil. ^1H NMR (CDCl_3) δ 0.92 (t, 3H, CHCH_3 , $J = 7.3$ Hz), 1.24-1.43 (m, 4H, $\text{CH}_2\text{CH}_2\text{CH}_2\text{CH}_3$), 2.22-2.30 (m, 5H, 3- CH_3 + $\text{CHCH}_2\text{CH}_2\text{CH}_2\text{CH}_3$), 3.81 (s, 3H, OCH_3), 3.91 (s, 2H, CH_2 -Ar), 5.53 (dd, 1H, NCHCH_2 , $J = 1.3$ Hz, $J = 6.9$ Hz), 6.74 (s, 1H, Ar), 6.80-6.86 (m, 3H, Ar), 7.28 (t, 1H, Ar, $J = 8.5$ Hz), 7.35-7.45 (m, 4H, Ar), 8.98 (exch br s, 1H, NH).

5.2.286 (\pm) -*N*-(4-Bromophenyl)-2-[5-(3-methoxybenzyl)-3-methyl-6-oxopyridazin-1(6*H*)-yl]-2-phenylacetamide [(\pm)-117e]



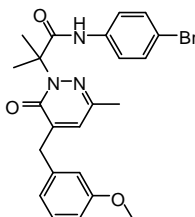
Yield = 42 %; mp = 117-19 °C (EtOH). ¹H NMR (CDCl₃) δ 2.26 (s, 3H, 3-CH₃), 3.81 (s, 3H, OCH₃), 3.89 (s, 2H, CH₂-Ar), 6.67 (s, 1H, Ar), 6.87-6.87 (m, 4H, NCHCO + 3 x Ar), 7.28 (t, 1H, Ar, *J* = 7.6 Hz), 7.36-7.45 (m, 7H, Ar), 7.56-7.59 (m, 2H, Ar), 8.33 (exch br s, 1H, NH).

5.2.287 (\pm) -*N*-(4-Bromophenyl)-2-[5-(3-methoxybenzyl)-3-methyl-6-oxopyridazin-1(6*H*)-yl]-2-methylbutanamide [(\pm)-117f]



Yield = 60 %; mp = 141-42 °C (*n*-hexane). ¹H NMR (CDCl₃) δ 0.90 (t, 3H, CH₂CH₃, *J* = 7.3 Hz), 1.83 (s, 3H, COCCH₃), 2.25 (sext, 1H, NCCH-HCH₃, *J* = 6.9 Hz), 2.38 (sext, 1H, NCCH-HCH₃, *J* = 7.4 Hz), 2.59 (s, 3H, 3-CH₃), 3.78 (s, 3H, OCH₃), 3.97 (qd, 2H, CH₂-Ar, *J* = 3.3 Hz, *J* = 16.2 Hz), 6.73 (s, 1H, Ar), 6.77 (d, 1H, Ar, *J* = 7.6 Hz), 6.85 (dd, 1H, Ar, *J* = 6.0 Hz, *J* = 1.9 Hz), 7.09 (s, 1H, Ar), 7.23 (d, 2H, Ar, *J* = 8.9 Hz), 7.29 (t, 1H, Ar, *J* = 8.0 Hz), 7.37 (d, 2H, Ar, *J* = 8.8 Hz), 8.15 (exch br s, 1H, NH).

5.2.288 *N*-(4-Bromophenyl)-2-[5-(3-methoxybenzyl)-3-methyl-6-oxopyridazin-1(6*H*)-yl]-2-methylpropanamide [(\pm)-118]



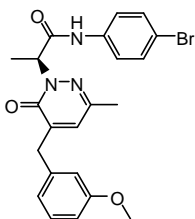
Yield = 65 %; mp = 58-60 °C (*n*-hexane). ¹H NMR (CDCl₃) δ 1.83 (s, 6H, 2 x NCCH₃), 2.61 (s, 3H, 3-CH₃), 3.80 (s, 3H, OCH₃), 3.97 (s, 2H, CH₂-Ar, *J* = 3.3 Hz), 6.76-6.88 (m, 3H, Ar), 7.11 (s, 1H, Ar), 7.27-7.32 (m, 3H, Ar), 7.37 (dd, 2H, Ar, *J* = 4.7 Hz, *J* = 2.0 Hz), 8.26 (exch br s, 1H, NH).

HPLC resolution of (\pm)-95b and (\pm)-117a by Chiral Phase HPLC. Both racemates were separated by chiral-phase HPLC with a Chiralcel OD[®] (250mm x 4.6mm I.D., 10 μm particle size) column. The eluent mixture *n*-hexane/IPA 95:5 was used in isocratic mode with the flow 1.2 mL/min at

5. Experimental Chemistry

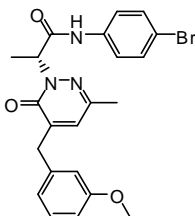
25 °C and the UV signal was followed at $\lambda = 250$ nm. Racemates were dissolved in ethanol (1 mg/mL solution) and 50 μ L were injected each time. In order to separate about 20 mg of racemic mixtures 600 injections were needed and it took about 200 h to obtain the resolved enantiomeric pairs **S-(+)-95b/R-(-)-95b** ($t_R = 19.2$, $t_R = 23.2$) and **S-(+)-117a/R-(-)-117a** ($t_R = 15.9$, $t_R = 17.9$) (see section 3.3.6.4 for the assignment of the absolute configuration).

5.2.289 S-(+)-N-(4-Bromophenyl)-2-[5-(3-methoxybenzyl)-3-methyl-6-oxopyridazin-1(6H)-yl]propanamide [**S-(+)-95b**]



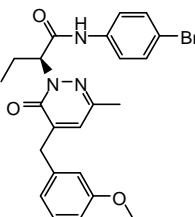
Light-yellow oil. $[\alpha]_D^{20} = +80^\circ$ ($c = 1$, CHCl_3). e.e. > 99.9 % (determined by analytical chiral HPLC). ^1H NMR (CDCl_3) δ 1.71 (d, 3H, CHCH_3 , $J = 7.0$ Hz), 2.29 (s, 3H, 3- CH_3), 3.82 (s, 3H, OCH_3), 3.91 (s, 2H, CH_2 -Ar), 5.71 (q, 1H, CHCH_3 , $J = 7.0$ Hz), 6.78 (s, 1H, Ar), 6.81 (s, 1H, Ar), 6.84 (d, 2H, Ar, $J = 7.4$ Hz), 7.28 (t, 1H, Ar, $J = 9.0$ Hz), 7.40 (d, 4H, Ar, $J = 4.9$ Hz), 8.99 (exch br s, 1H, NH).

5.2.290 R-(-)-N-(4-Bromophenyl)-2-[5-(3-methoxybenzyl)-3-methyl-6-oxopyridazin-1(6H)-yl]propanamide [**R-(-)-95b**]



Light-yellow oil. $[\alpha]_D^{20} = -78^\circ$ ($c = 1$, CHCl_3). e.e. = 97.4 % (determined by analytical chiral HPLC). ^1H NMR (CDCl_3) δ 1.71 (d, 3H, CHCH_3 , $J = 7.0$ Hz), 2.30 (s, 3H, 3- CH_3), 3.81 (s, 3H, OCH_3), 3.91 (s, 2H, CH_2 -Ar), 5.71 (q, 1H, CHCH_3 , $J = 7.0$ Hz), 6.78 (s, 1H, Ar), 6.81 (s, 1H, Ar), 6.84 (d, 2H, Ar, $J = 8.3$ Hz), 7.28 (t, 1H, Ar, $J = 8.8$ Hz), 7.40 (d, 4H, Ar, $J = 3.0$ Hz), 9.01 (exch br s, 1H, NH).

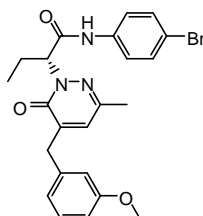
5.2.291 S-(+)-N-(4-Bromophenyl)-2-[5-(3-methoxybenzyl)-3-methyl-6-oxopyridazin-1(6H)-yl]butanamide [**S-(+)-117a**]



Light-yellow oil. $[\alpha]_D^{20} + 129^\circ$ ($c = 1$, CHCl_3). e.e. > 99.9 % (determined by analytical chiral HPLC). ^1H NMR (CDCl_3) δ 0.96 (t, 3H, CHCH_3 , $J = 7.4$ Hz), 2.18-2.39 (m, 5H, 3- CH_3 + CH_2CH_3), 3.81 (s, 3H,

OCH₃), 3.90 (s, 2H, CH₂-Ar), 5.47 (dd, 1H, NCHCH₂, $J = 1.5$ Hz, $J = 6.9$ Hz), 6.75 (s, 1H, Ar), 6.79 (d, 1H, Ar, $J = 1.9$ Hz), 6.82-6.86 (m, 2H, Ar), 7.28 (t, 1H, Ar, $J = 7.9$ Hz), 7.35-7.41 (m, 4H, Ar), 9.08 (exch br s, 1H, NH).

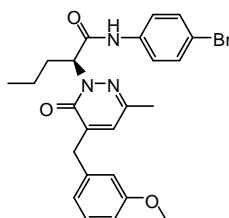
5.2.292 R-(-)-N-(4-Bromophenyl)-2-[5-(3-methoxybenzyl)-3-methyl-6-oxopyridazin-1(6H)-yl]butanamide [R-(-)-117a]



Light-yellow oil. $[\alpha]_D^{20} - 129^\circ$ ($c = 1$, CHCl₃). e.e. = 98.0 % (determined by analytical chiral HPLC). ¹H NMR (CDCl₃) δ 0.96 (t, 3H, CHCH₃, $J = 7.4$ Hz), 2.18-2.39 (m, 5H, 3-CH₃ + CH₂CH₃), 3.81 (s, 3H, OCH₃), 3.91 (s, 2H, CH₂-Ar), 5.47 (dd, 1H, NCHCH₂, $J = 1.2$ Hz, $J = 7.0$ Hz), 6.75 (s, 1H, Ar), 6.79 (s, 1H, Ar), 6.82-6.86 (m, 2H, Ar), 7.28 (t, 1H, Ar, $J = 8.1$ Hz), 7.36-7.41 (m, 4H, Ar), 9.08 (exch br s, 1H, NH).

HPLC resolution of (±)-117b-f by Chiral Phase HPLC. Racemates were separated by chiral-phase HPLC with a Lux Amylose-2[®] (250 mm x 4.6 mm I.D., 5 μ m particle size) column. The eluent mixture *n*-hexane/IPA 60:40 was used in isocratic mode with the flow 1.5 mL/min at 40 °C and the UV signal was followed at $\lambda = 250$ nm. Racemates were dissolved in ethanol (2 mg/mL solution), then 100 μ L of (±)-117b-e and 80 μ L of (±)-117f were injected each time. In order to separate about 20 mg of racemic mixtures 50 injections were needed and it took about 10 h to obtain the resolved enantiomeric pairs **S-(+)-117b/R-(-)-117b** ($t_R = 5.1$, $t_R = 9.4$), **S-(+)-117c/R-(-)-117c** ($t_R = 3.9$, $t_R = 10.1$), **S-(+)-117d/R-(-)-117d** ($t_R = 5.4$, $t_R = 9.7$), **R-(-)-117e/S-(+)-117e** ($t_R = 7.6$, $t_R = 12.3$) and **R-(-)-117f/S-(+)-117f** ($t_R = 6.7$, $t_R = 8.6$) (see section 3.3.6.4 for the assignment of the absolute configuration).

5.2.293 S-(+)-N-(4-Bromophenyl)-2-[5-(3-methoxybenzyl)-3-methyl-6-oxopyridazin-1(6H)-yl]pentanamide [S-(+)-117b]

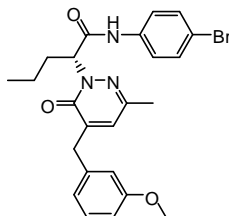


Light-yellow oil. $[\alpha]_D^{20} + 139^\circ$ ($c = 1$, CHCl₃). e.e. > 99.9 % (determined by analytical chiral HPLC). ¹H NMR (CDCl₃) δ 0.98 (t, 3H, CHCH₃, $J = 7.3$ Hz), 1.27-1.42 (m, 2H, CH₂CH₂CH₃), 2.15-2.28 (m, 2H, CHCH₂CH₂), 2.30 (s, 3H, 3-CH₃), 3.81 (s, 3H, OCH₃), 3.90 (s, 2H, CH₂-Ar), 5.56 (t, 1H, NCHCH₂, $J =$

5. Experimental Chemistry

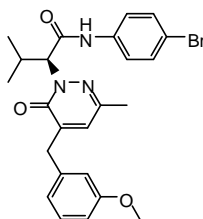
8.2 Hz), 6.75 (s, 1H, Ar), 6.79 (d, 1H, Ar, $J = 1.9$ Hz), 6.82-6.86 (m, 2H, Ar), 7.28 (t, 1H, Ar, $J = 9.0$ Hz), 7.39 (s, 4H, Ar), 9.02 (exch br s, 1H, NH).

5.2.294 R-(-)-N-(4-Bromophenyl)-2-[5-(3-methoxybenzyl)-3-methyl-6-oxopyridazin-1(6H)-yl]pentanamide [R-(-)-117b]



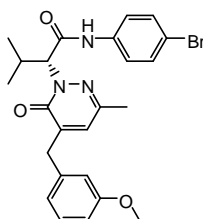
Light-yellow oil. $[\alpha]_D^{20} - 137^\circ$ ($c = 1$, CHCl_3). e.e. = 99.9 % (determined by analytical chiral HPLC). ^1H NMR (CDCl_3) δ 0.98 (t, 3H, CHCH_3 , $J = 7.4$ Hz), 1.28-1.40 (m, 2H, $\text{CH}_2\text{CH}_2\text{CH}_3$), 2.17-2.28 (m, 2H, CHCH_2CH_2), 2.30 (s, 3H, 6- CH_3), 3.81 (s, 3H, OCH_3), 3.90 (s, 2H, CH_2 -Ar), 5.56 (t, 1H, NCHCH_2 , $J = 7.2$ Hz), 6.75 (s, 1H, Ar), 6.79 (d, 1H, Ar, $J = 1.5$ Hz), 6.82-6.86 (m, 2H, Ar), 7.28 (t, 1H, Ar, $J = 9.0$ Hz), 7.39 (s, 4H, Ar), 9.14 (exch br s, 1H, NH).

5.2.295 S-(+)-N-(4-Bromophenyl)-2-[5-(3-methoxybenzyl)-3-methyl-6-oxopyridazin-1(6H)-yl]-3-methylbutanamide [S-(+)-117c]



mp 63-65 °C. $[\alpha]_D^{20} + 99^\circ$ ($c = 1$, CHCl_3). e.e. > 99.9 % (determined by analytical chiral HPLC). ^1H NMR (CDCl_3) δ 0.83 (d, 3H, CHCH_3 , $J = 6.6$ Hz), 1.16 (d, 3H, CHCH_3 , $J = 6.6$ Hz), 2.31 (s, 3H, 3- CH_3), 2.86-2.96 (m, 1H, CHCH_3), 3.81 (s, 3H, OCH_3), 3.90 (s, 2H, CH_2 -Ar), 5.14 (d, 1H, NCHCHCH , $J = 11.0$ Hz), 6.71 (s, 1H, Ar), 6.78 (s, 1H, Ar), 6.81-6.86 (m, 2H, Ar), 7.28 (t, 1H, Ar, $J = 7.5$ Hz), 7.38-7.44 (m, 4H, Ar), 9.06 (exch br s, 1H, NH).

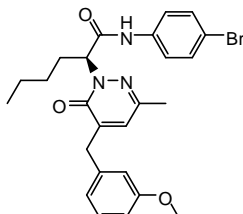
5.2.296 R-(-)-N-(4-Bromophenyl)-2-[5-(3-methoxybenzyl)-3-methyl-6-oxopyridazin-1(6H)-yl]-3-methylbutanamide [R-(-)-117c]



mp 63-65 °C. $[\alpha]_D^{20} - 97^\circ$ ($c = 1$, CHCl_3). e.e. = 99.9 % (determined by analytical chiral HPLC). ^1H NMR (CDCl_3) δ 0.83 (d, 3H, CHCH_3 , $J = 6.6$ Hz), 1.16 (d, 3H, CHCH_3 , $J = 6.6$ Hz), 2.30 (s, 3H, 3- CH_3), 2.86-2.96 (m, 1H, CHCH_3), 3.81 (s, 3H, OCH_3), 3.90 (s, 2H, CH_2 -Ar), 5.14 (d, 1H, NCHCHCH , $J = 11.0$ Hz),

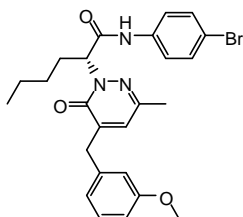
6.71 (s, 1H, Ar), 6.78 (s, 1H, Ar), 6.81-6.86 (m, 3H, Ar), 7.28 (t, 1H, Ar, $J = 7.8$ Hz), 7.38-7.44 (m, 4H, Ar), 9.06 (exch br s, 1H, NH).

5.2.297 S-(+)-N-(4-Bromophenyl)-2-[5-(3-methoxybenzyl)-3-methyl-6-oxopyridazin-1(6H)-yl]hexanamide [S-(+)-117d]



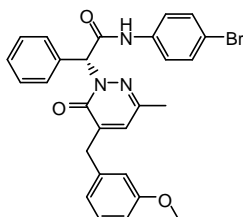
Light-yellow oil. $[\alpha]_D^{20} + 111^\circ$ ($c = 1$, CHCl_3). e.e. > 99.9 % (determined by analytical chiral HPLC). ^1H NMR (CDCl_3) δ 0.92 (t, 3H, CHCH_3 , $J = 7.3$ Hz), 1.17-1.46 (m, 4H, $\text{CH}_2\text{CH}_2\text{CH}_2\text{CH}_3$), 2.14-2.34 (m, 5H, 6- CH_3 + $\text{CHCH}_2\text{CH}_2\text{CH}_2\text{CH}_3$), 3.81 (s, 3H, OCH_3), 3.91 (s, 2H, CH_2 -Ar), 5.54 (dd, 1H, NCHCH_2 , $J = 1.3$ Hz, $J = 6.9$ Hz), 6.75 (d, 1H, Ar, $J = 1.1$ Hz), 6.79 (t, 1H, Ar, $J = 1.7$ Hz), 6.82-6.86 (m, 2H, Ar), 7.28 (t, 1H, Ar, $J = 9.4$ Hz), 7.38 (s, 4H, Ar), 9.04 (exch br s, 1H, NH).

5.2.298 R-(-)-N-(4-Bromophenyl)-2-[5-(3-methoxybenzyl)-3-methyl-6-oxopyridazin-1(6H)-yl]hexanamide [R-(-)-117d]



Light-yellow oil. $[\alpha]_D^{20} - 110^\circ$ ($c = 1$, CHCl_3). e.e. = 99.9 % (determined by analytical chiral HPLC). ^1H NMR (CDCl_3) δ 0.92 (t, 3H, CHCH_3 , $J = 7.3$ Hz), 1.17-1.46 (m, 4H, $\text{CH}_2\text{CH}_2\text{CH}_2\text{CH}_3$), 2.16-2.34 (m, 5H, 6- CH_3 + $\text{CHCH}_2\text{CH}_2\text{CH}_2\text{CH}_3$), 3.81 (s, 3H, OCH_3), 3.90 (s, 2H, CH_2 -Ar), 5.54 (dd, 1H, NCHCH_2 , $J = 1.2$ Hz, $J = 6.9$ Hz), 6.75 (s, 1H, Ar), 6.79 (d, 1H, Ar, $J = 2.0$ Hz), 6.82-6.86 (m, 2H, Ar), 7.28 (t, 1H, Ar, $J = 9.3$ Hz), 7.36-7.41 (s, 4H, Ar), 9.04 (exch br s, 1H, NH).

5.2.299 R-(-)-N-(4-Bromophenyl)-2-[5-(3-methoxybenzyl)-3-methyl-6-oxopyridazin-1(6H)-yl]-2-phenylacetamide [R-(-)-117e]

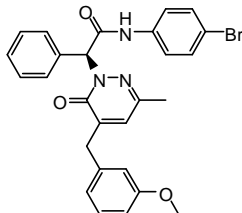


Light-yellow oil. $[\alpha]_D^{20} - 17^\circ$ ($c = 1$, CHCl_3). e.e. = 99.9 % (determined by analytical chiral HPLC). ^1H NMR (CDCl_3) δ 2.26 (s, 3H, 3- CH_3), 3.81 (s, 3H, OCH_3), 3.89 (s, 2H, CH_2 -Ar), 6.68 (s, 1H, Ar), 6.77 (s, 1H, Ar), 6.80-6.85 (m, 2H, Ar), 6.88 (s, 1H, NCHCO), 7.28 (t, 1H, Ar, $J = 7.6$ Hz), 7.36-7.45 (m, 7H,

5. Experimental Chemistry

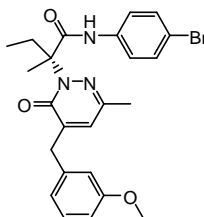
Ar), 7.56-7.59 (m, 2H, Ar), 8.33 (exch br s, 1H, NH). MS (ESI) calcd. For $C_{27}H_{24}BrN_3O_3$, 518.40. Found: m/z 519.10 $[M + H]^+$, 541.30 $[M + Na]^+$.

5.2.300 S-(-)-N-(4-Bromophenyl)-2-[5-(3-methoxybenzyl)-3-methyl-6-oxo pyridazin-1(6H)-yl]-2-phenylacetamide [S-(+)-117e]



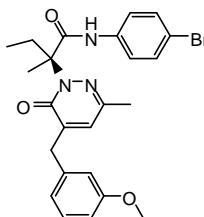
Light-yellow oil. $[\alpha]_D^{20} + 16^\circ$ ($c = 1$, $CHCl_3$). e.e. > 99.9 % (determined by analytical chiral HPLC). 1H NMR ($CDCl_3$) δ 2.26 (s, 3H, 3- CH_3), 3.80 (s, 3H, OCH_3), 3.89 (s, 2H, CH_2 -Ar), 6.68 (s, 1H, Ar), 6.77 (s, 1H, Ar), 6.80-6.85 (m, 2H, Ar), 6.88 (s, 1H, NCHCO), 7.28 (t, 1H, Ar, $J = 7.6$ Hz), 7.36-7.45 (m, 7H, Ar), 7.56-7.59 (m, 2H, Ar), 8.33 (exch br s, 1H, NH). MS (ESI) calcd. For $C_{27}H_{24}BrN_3O_3$, 518.40. Found: m/z 519.10 $[M + H]^+$, 541.30 $[M + Na]^+$.

5.2.301 R-(-)-N-(4-Bromophenyl)-2-[5-(3-methoxybenzyl)-3-methyl-6-oxo pyridazin-1(6H)-yl]-2-methylbutanamide [R-(-)-117f]



mp 108-09 °C. $[\alpha]_D^{20} - 18^\circ$ ($c = 1$, $CHCl_3$). e.e. > 99.9 % (determined by analytical chiral HPLC). 1H NMR ($CDCl_3$) δ 0.90 (t, 3H, CH_2CH_3 , $J = 7.4$ Hz), 1.83 (s, 3H, $NCCH_3$), 2.26 (sext, 1H, $NCCH-HCH_3$, $J = 7.4$ Hz), 2.39 (sext, 1H, $NCCH-HCH_3$, $J = 7.4$ Hz), 2.60 (s, 3H, 6- CH_3), 3.79 (s, 3H, OCH_3), 3.97 (d, 2H, CH_2 -Ar, $J = 3.0$ Hz, $J = 16.2$ Hz), 6.73 (s, 1H, Ar), 6.77 (d, 1H, Ar, $J = 7.6$ Hz), 6.85 (d, 1H, Ar, $J = 8.1$ Hz), 7.10 (s, 1H, Ar), 7.23 (d, 2H, Ar, $J = 8.8$ Hz), 7.30 (t, 1H, Ar, $J = 8.1$ Hz), 7.38 (d, 2H, Ar, $J = 8.7$ Hz), 8.13 (exch br s, 1H, NH).

5.2.302 S-(+)-N-(4-Bromophenyl)-2-[5-(3-methoxybenzyl)-3-methyl-6-oxo pyridazin-1(6H)-yl]-2-methylbutanamide [S-(+)-117f]

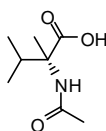


mp 108-09 °C. $[\alpha]_D^{20} + 17$ ($c = 1$, $CHCl_3$). e.e. = 99.3 % (determined by analytical chiral HPLC). 1H NMR ($CDCl_3$) δ 0.90 (t, 3H, CH_2CH_3 , $J = 7.4$ Hz), 1.83 (s, 3H, $NCCH_3$), 2.26 (sext, 1H, $NCCH-HCH_3$, J

= 7.4 Hz), 2.39 (sext, 1H, NCCH-*H*CH₃, *J* = 7.1 Hz), 2.60 (s, 3H, 6-CH₃), 3.79 (s, 3H, OCH₃), 3.97 (qd, 2H, CH₂-Ar, *J* = 3.0 Hz, *J* = 16.2 Hz), 6.73 (s, 1H, Ar), 6.77 (d, 1H, Ar, *J* = 7.5 Hz), 6.85 (dd, 1H, Ar, *J* = 6.3 Hz, *J* = 1.9 Hz), 7.10 (s, 1H, Ar), 7.23 (d, 2H, Ar, *J* = 8.7 Hz), 7.29 (t, 1H, Ar, *J* = 7.9 Hz), 7.38 (d, 2H, Ar, *J* = 8.7 Hz), 8.13 (exch br s, 1H, NH).

General Procedure for reference compounds R-(-)-119 and S-(-)-120. To an aqueous (75 mL) solution of R-(-)-2-phenylglycine or S-(-)- α -Methylvaline (99.33 mmol) respectively, acetic anhydride (0.75 mol) was added. The mixture was stirred for 0.5 h at 70 °C until all the amino acid was dissolved. When the reaction mixture was cooled to 5 °C, the crystallized amide was separated by filtration and the final products were purified by recrystallization from ethanol.

5.2.303 S-(-)-2-Acetamido-2,3-dimethylbutanoic acid [S-(-)-120]



Yield = 36 %; mp = 213-14 °C (EtOH). $[\alpha]_D^{20} = -1.4^\circ$ (*c* = 1, EtOH). e.e. > 99.9 % (determined by analytical chiral HPLC). ¹H NMR (DMSO-*d*₆) δ 0.84 (d, 3H, CHCH₃, *J* = 6.8 Hz), 0.91 (d, 3H, CHCH₃, *J* = 6.8 Hz), 1.25 (s, 3H, CHCCH₃), 1.81 (s, 3H, COCH₃), 1.91-1.99 (m, 1H, CCH(CH₃)₂), 7.07 (exch br s, 1H, NH), 12.08 (exch br s, 1H, OH).

6. BIOLOGICAL METHODS

6.1 Cell Culture

Human promyelocytic leukemia HL-60 cells stably transfected with FPR1 (HL-60-FPR1), FPR2 (HL-60-FPR2), or FPR3 (HL-60-FPR3) were cultured in RPMI 1640 medium supplemented with 10% heat-inactivated fetal calf serum, 10 mM HEPES, 100 µg/ml streptomycin, 100 U/ml penicillin, and G418 (1 mg/mL), as previously described.³¹⁵ Wild-type HL-60 cells were cultured under the same conditions, but without G418.

6.2 Isolation of Human Neutrophils

Blood was collected from healthy donors in accordance with a protocol approved by the Institutional Review Board at Montana State University. Neutrophils were purified from the blood using dextran sedimentation, followed by Histopaque 1077 gradient separation and hypotonic lysis of red blood cells, as previously described.²⁰⁴ Isolated neutrophils were washed twice and resuspended in HBSS without Ca^{2+} and Mg^{2+} (HBSS⁻). Neutrophil preparations were routinely > 95 % pure, as determined by light microscopy, and > 98 % viable, as determined by trypan blue exclusion.

6.3 Ca^{2+} Mobilization Assay

Changes in intracellular Ca^{2+} were measured with a FlexStation II scanning fluorometer using a FLIPR 3 calcium assay kit (Molecular Devices, Sunnyvale, CA) for human neutrophils and HL-60 cells. All active compounds were evaluated in parent (wild-type) HL-60 cells for supporting that the agonists are inactive in non-transfected cells. Human neutrophils or HL-60 cells, suspended in HBSS⁻ containing 10 mM HEPES, were loaded with Fluo-4 AM dye (Invitrogen) (1.25 µg/mL final concentration) and incubated for 30 min in the dark at 37 °C. After dye loading, the cells were washed with HBSS⁻ containing 10 mM HEPES, resuspended in HBSS containing 10 mM HEPES and Ca^{2+} and Mg^{2+} (HBSS⁺), and aliquotted into the wells of a flat-bottomed, half-area-well black microtiter plates (2×10^5 cells/well). The compound source plate contained dilutions of test compounds in HBSS⁺. Changes in fluorescence were monitored ($\lambda_{\text{ex}} = 485$ nm, $\lambda_{\text{em}} = 538$ nm) every 5 s for 240 s at room temperature after automated addition of compounds. Maximum change in fluorescence, expressed in arbitrary units over baseline, was used to determine agonist response. Responses were normalized to the response induced by 5 nM fMLF (Sigma Chemical Co., St. Louis, MO) for HL-60-FPR1 and neutrophils, or 5 nM WKYMVm (Calbiochem, San Diego, CA) for HL-60-FPR2 and HL-60-FPR3 cells, which were assigned a value of 100%. Curve fitting (5-6 points) and calculation of median effective concentration values (EC_{50}) were performed by nonlinear regression analysis of the dose-response curves generated using Prism 5 (GraphPad Software, Inc., San Diego, CA).

6. Biological Methods

6.4 Chemotaxis Assay

Neutrophils were suspended in HBSS⁺ containing 2% (v/v) fetal bovine serum (FBS) (2×10^6 cells/mL), and chemotaxis was analyzed in 96-well ChemoTx chemotaxis chambers (Neuroprobe, Gaithersburg, MD), as previously described.²⁰⁴ In brief, lower wells were loaded with 30 μ L of HBSS⁺ containing 2% (v/v) FBS and the indicated concentrations of test compound, DMSO (negative control), and 1 nM fMLF as a positive control. The number of migrated cells was determined by measuring ATP in lysates of transmigrated cells using a luminescence-based assay (CellTiter-Glo; Promega, Madison, WI), and luminescence measurements were converted to absolute cell numbers by comparison of the values with standard curves obtained with known numbers of neutrophils. The results are expressed as percentage of negative control and were calculated as follows: (number of cells migrating in response to test compounds/spontaneous cell migration in response to control medium) \times 100. EC₅₀ values were determined by nonlinear regression analysis of the dose-response curves generated using Prism 5 software.

7. BIBLIOGRAPHIC REFERENCES

- (1) Nauseef, W. M.; Clark, R. A. In *Basic Principles in the Diagnosis and Management of Infectious Diseases*. Mandel, G. L., Bennett, J. E., Dolin, R., Eds; Churchill Livingstone: New York, **2000**; vol. 1, pp. 89-112.
- (2) Bruno, O.; Brullo, C.; Bondavalli, F.; Schenone, S.; Ranise, A.; Arduino, N.; Bertolotto, M. B.; Montecucco, F.; Ottonello, L.; Dallegri, F.; Tognolini, M.; Ballabeni, V.; Bertoni, S.; Barocelli E. Synthesis and Biological Evaluation of *N*-Pyrazolyl-*N'*-alkyl/benzyl/phenylureas: a New Class of Potent Inhibitors of Interleukin 8-Induced Neutrophil Chemotaxis. *J. Med. Chem.* **2007**, *50*, 3618-3626.
- (3) Lee, H. Y.; Bae, Y. S. The Anti-infective Peptide, Innate Defense-Regulator Peptide, Stimulates Neutrophil Chemotaxis Via a Formyl Peptide Receptor. *Biochem. Biophys. Res. Commun.* **2008**, *369*, 573-578.
- (4) Gouin, J. P.; Hantsoo, L.; Kiekolt-Glaser, J. K. Immune Disregulation and Chronic Stress Among Older Adults: A Review. *Neuroimmunomod.* **2008**, *15*, 251-259.
- (5) Jones, R. N. Resistance Patterns Among Nosocomial Pathogens: Trends Over the Past Few Years. *Chest* **2001**, *119*, 397S-404S.
- (6) Gilroy, D. W.; Lawrence, T.; Perretti, P.; Rossi, A. G. Inflammatory Resolution: new opportunities for drug discovery. *Nat. Rev. Drug Discov.* **2004**, *3*, 401-416.
- (7) Zhang, L.; Falla, T. J. Host Defense Peptides for Use as Potential Therapeutics. *Curr. Opin. Invest. Drugs* **2009**, *10*, 164-171.
- (8) LaFleur-Brooks, M. In *Exploring Medical Language, 7th ed.: A Student-Directed Approach*. Mosby Elsevier: St. Louis, Missouri, **2008**; pp. 398.
- (9) Blumenreich, M. S. In *Clinical Methods, 3rd ed.: The History, Physical, and Laboratory Examinations. Chapter 153: The White Blood Cell and Differential Count*. Walker H. K., Hall W. D., Hurst J. W., Eds; Boston: Butterworths, **1990**; pp. 724-727.
- (10) Gartner, L. P.; Hiatt, J. L. In *Color Textbook of Histology, 3rd ed.* Saunders Elsevier: Philadelphia, **2007**; pp. 225.
- (11) Nathan, C. Neutrophils and immunity: challenges and opportunities. *Nat. Rev. Immunol.* **2006**, *6*, 173-182.
- (12) Klebanoff, S. J.; Clark, R. A. *The Neutrophil: Function and Clinical Disorders*. Elsevier/North-Holland: Amsterdam, **1978**.
- (13) Waugh, D. J.; Wilson C. The interleukin-8 pathway in cancer. *Clin. Cancer Res.* **2008**, *14*, 6735-6741.
- (14) De Larco, J. E.; Wuertz, B. R. K.; Furcht, L. T. The Potential Role of Neutrophils in Promoting the Metastatic Phenotype of Tumors Releasing Interleukin-8. *Clin. Cancer Res.* **2004**, *10*, 4895-4900.
- (15) Cohen, S. S.; Burns, R. C.; Eds. In *Pathways of the pulp, 8th ed.* Mosby Elsevier: St. Louis, Missouri, **2002**; pp. 465.
- (16) Witko-Sarsat, V.; Rieu, P.; Descamps-Latscha, B.; Lesavre, P.; Halbwachs-Mecarelli L. Neutrophils: molecules, functions and pathophysiological aspects. *Lab. Invest.* **2000**, *80*, 617-653.
- (17) Hickey, M. J.; Kubes, P. Intravascular immunity: the host-pathogen encounter in blood vessels. *Nat. Rev. Immunol.* **2009**, *9*, 364-375.
- (18) Ear, T.; McDonald, P. P. Cytokine generation, promoter activation, and oxidant-independent NF- κ B activation in a transfectable human neutrophilic cellular model. *BMC Immunol.* **2008**, *9*, 14.
- (19) Voehringer, D. The role of basophils in helminth infection. *Trends in Parasitol.* **2009**, *25*, 551-556.
- (20) Janeway, C. A., Jr.; Travers, P.; Walport, M.; Shlomchik, M. J.; et al. *Immunobiology, 5th ed.* (electronic full text via NCBI Bookshelf). Garland Publishing: New York and London, **2001**.
- (21) Schroeder, J. T. Basophils beyond effector cells of allergic inflammation. *Adv. Immunol.* **2009**, *101*, 123-161.

7. Bibliographic References

- (22) Young, B.; Lowe, J. S.; Stevens, A.; Heath, J. W.; et al. *Wheater's Functional Histology, 5th ed.: a Text and Colour Atlas*. Elsevier Limited: Philadelphia, **2006**.
- (23) Rothenberg, M. E.; Hogan, S. P. The eosinophil. *Annu. Rev. Immunol.* **2006**, *24*, 147-174.
- (24) Yamaguchi, Y.; Suda, T.; Suda, J.; Eguchi, M.; Miura, Y.; Harad, N.; Tominaga, A.; Takatsu, K. Purified interleukin-5 supports the terminal differentiation and proliferation of murine eosinophilic precursors. *J. Exp. Med.* **1988**, *167*, 43-56.
- (25) Trulsson, A.; Byström, J.; Engström, A.; Larsson, R.; Venge, P. The functional heterogeneity of eosinophil cationic protein is determined by a gene polymorphism and post-translational modifications. *Clin. Exp. Allergy* **2007**, *37*, 208-218.
- (26) Gleich, G.; Adolphson, C. The eosinophilic leukocyte: structure and function. *Adv. Immunol.* **1986**, *39*, 177-253.
- (27) **Bandeira-Melo, C.**; Bozza, P. T.; Weller P. F. The cellular biology of eosinophil eicosanoid formation and function. *J. Allergy Clin. Immunol.* **2002**, *109*, **393-400**.
- (28) Kato, Y.; Fujisawa, T.; Nishimori, H.; Katsumata, H.; Atsuta, J.; Iguchi, K.; Kamiya, H. Leukotriene D4 induces production of transforming growth factor-beta1 by eosinophils. *Int. Arch. Allergy Immunol.* **2005**, *137* (Suppl 1), 17-20.
- (29) Horiuchi, T.; Weller, P. F. Expression of vascular endothelial growth factor by human eosinophils: upregulation by granulocyte macrophage colony-stimulating factor and interleukin-5. *Am. J. Respir. Cell Mol. Biol.* **1997**, *17*, 70-77.
- (30) Abbas A. K.; Lichtman A. H. *Cellular and Molecular Immunology, 5th ed.* Saunders Elsevier: Philadelphia, **2003**.
- (31) Kumar, V.; Abbas, A. K.; Fausto, N. *Rpbbons & Cotran Pathologic Basis of Disease, 7th ed.* Saunders Elsevier: Philadelphia, **2005**.
- (32) Pantaleo, G.; Demarest, J. F.; Soudeyins, H.; Graziosi, C.; Denis, F.; Adelsberger, J. W.; Borrow, P.; Saag, M. S.; Shaw, G. M.; Sekaly, R. P.; Fauci A. S. Major expansion of CD8+ T cells with a predominant V beta usage during the primary immune response to HIV. *Nature* **1994**, *370*, 463-467.
- (33) Swirski, F. K.; Nahrendorf, M.; Etzrodt, M.; Wildgruber, M.; Cortez-Retamozo, V.; Panizzi, P.; Figueiredo, J.-L.; Kohler, R. H.; Chudnovskiy, A.; Waterman, P.; Aikawa, E.; Mempel, T. R.; Libby, P.; Weissleder R.; Pittet, M. J. Identification of Splenic Reservoir Monocytes and Their Deployment to Inflammatory Sites. *Science* **2009**, *325*, 612-616.
- (34) Ziegler-Heitbrock, H. W. L. The CD14+ CD16+ blood monocytes: their role in infection and inflammation. *J. Leukoc. Biol.* **2007**, *81*, 584-592.
- (35) Fingerle, G.; Pforte, A.; Passlick, B.; Blumenstein, M.; Strobel, M.; Ziegler-Heitbrock, H. W. L. The Novel Subset of CD14+/CD16+ Blood Monocytes Is Expanded in Sepsis Patients. *Blood* **1993**, *82*, 3170-3176.
- (36) McKenna, K.; Beignon, A.; Bhardwaj, N. Plasmacytoid dendritic cells: linking innate and adaptive immunity. *J. Virol.* **2005**, *79*, 17-27.
- (37) Steinman, R. M.; Cohn, Z. A. Identification of a novel cell type in peripheral lymphoid organs of mice. I. Morphology, quantitation, tissue distribution. *J. Exp. Med.* **1973**, *137*, 1142-1162.
- (38) Sallusto F, Lanzavecchia A. The instructive role of dendritic cells on T-cell responses. *Arthritis Res.* **2002**, *4* (Suppl 3), S127-132.
- (39) Beutler, B. Innate immunity: An overview. *Mol. Immunol.* **2004**, *40*, 845-859.
- (40) Le, Y.; Murphy P. M.; Wang J. M. Formyl-peptide receptors revisited. *Trends Immunol* **2002**, *23*, 541-548.
- (41) Le, Y.; Ye, R. D.; Gong, W.; Li, J.; Iribarren, P.; Wang J. M. Identification of functional domains in the formyl peptide receptor-like 1 for agonist-induced cell chemotaxis. *FEBS Journal* **2005**, *272*, 769-778.
- (42) Snyderman, R.; Uhing R. J. In *Inflammation: Basic Principles and Clinical*, 2nd ed. Gallin, J. I., Goldstein, I. M. and Snyderman, R., Eds.; Raven Press: New York, **1992**, pp. 421-439.

- (43) Beutler, B.; Hoebe, K.; Du, X.; Ulevitch, R. J. How we detect microbes and respond to them: the Toll-like receptors and their transducers. *J. Leukoc. Biol.* **2003**, *74*, 479-485.
- (44) Guo, R. F.; Ward, P. A. Role of C5a in inflammatory responses. *Annu. Rev. Immunol.* **2005**, *23*, 821-852.
- (45) Sun, R.; Iribarren, P.; Zhang, N.; Zhou, Y.; Gong, W.; Cho, E. H.; Lockett, S.; Chertov, O.; Bednar, F.; Rogers, T. J.; Oppenheim, J. J.; Wang, J. M. Identification of Neutrophil Granule Protein Cathepsin G as a Novel Chemotactic Agonist for the G Protein-coupled Formyl Peptide Receptor. *J. Immunol.* **2004**, *173*, 428-436.
- (46) Kobayashi, S. D.; Voyich, J. M.; De Leo, F. R. Regulation of the neutrophil-mediated inflammatory response to infection. *Microbes Infect.* **2003**, *5*, 1337-1344.
- (47) Delves, P. J.; Roitt, I. M. The immune system. Second of two parts. *N. Engl. J. Med.* **2000**, *343*, 108-117.
- (48) Migeotte, I.; Communi, D.; Parmentier, M.; Formyl peptide receptors: a promiscuous subfamily of G protein-coupled receptors controlling immune responses. *Cytok. Growth Factor Rev.* **2006**, *17*, 501-519.
- (49) Ye, R. D.; Boulay, F.; Wang, J. M.; Dahlgren, C.; Gerard, C.; Parmentier, M.; Serhan, C. N.; Murphy, P. M. International Union of Basic and Clinical Pharmacology. LXXIII. Nomenclature for the formyl peptide receptor (FPR) family. *Pharmacol. Rev.* **2009**, *61*, 119-161.
- (50) Bokoch, G. M.; Gilman, A. G. Inhibition of Receptor-Mediated Release of Arachidonic Acid by Pertussis Toxin. *Cell* **1984**, *39*, 301-308.
- (51) Simon, M. I.; Strathmann, M. P.; Gautam, N. Diversity of G proteins in signal transduction. *Science* **1991**, *252*, 802-808.
- (52) Bokoch, G. M.; Katada, T.; Northup, J. K.; Ui, M.; Gilman, A. G. Purification and properties of the inhibitory guanine nucleotide-binding regulatory component of adenylate cyclase. *J. Biol. Chem.* **1984**, *259*, 3560-3567.
- (53) Gierschik, P.; Sidiropoulos, D.; Jakobs, K. H. Two distinct Gi-proteins mediate formyl peptide receptor signal transduction in human leukemia (HL-60) cells. *J. Biol. Chem.* **1989**, *264*, 21470-21473.
- (54) Schiffmann, E.; Showell, H. V.; Corcoran, B. A.; Ward, P. A.; Smith, E.; Becker, E. L. The isolation and partial characterization of neutrophil chemotactic factors from *Escherichia coli*. *J. Immunol.* **1975**, *114*, 1831-1837.
- (55) Schiffmann, E.; Corcoran, B. A.; Wahl, S. M. N-formylmethionyl peptides as chemoattractants for leucocytes. *Proc. Natl. Acad. Sci. USA* **1975**, *72*, 1059-1062.
- (56) Freer, R. J.; Day, A. R.; Radding, J. A.; Schiffmann, E.; Aswanikumar, S.; Showell, H. J.; Becker, E. L. Further studies on the structural requirements for synthetic peptide chemoattractants. *Biochemistry* **1980**, *19*, 2404-10.
- (57) Showell, H. J.; Freer, R. J.; Zigmond, S. H.; Schiffmann, E.; Aswanikumar, S.; Corcoran, B.; Becker, E. L. The structure-activity relations of synthetic peptides as chemotactic factors and inducers of lysosomal secretion for neutrophils. *J. Exp. Med.* **1976**, *143*, 1154-1169.
- (58) Prossnitz ER and Ye RD (1997) *Pharmacol Ther* **74**:73-102;
- (59) Mills, J. S.; Miettinen, H. M.; Jesaitis A.J. In *Molecular Biology of Inflammation: The N-formyl peptide receptor: Structure, signaling and disease*. Serhan, C. N. and Ward, P. A., Eds); Humana Press: Totowa, NJ, **1999**; pp.215-245.
- (60) Gao, J. L.; Lee, E. J.; Murphy, P. M. Impaired antibacterial host defense in mice lacking the N-formylpeptide receptor. *J. Exp. Med.* **1999**, *189*, 657-662.
- (61) Nanamori, M.; Cheng, X.; Mei, J.; Sang, H.; Xuan, Y.; Zhou, C.; Wang, M. W.; Ye, R. D. A Novel Nonpeptide Ligand for Formyl Peptide Receptor-Like 1. *Mol. Pharmacol.* **2004**, *66*, 1213-1222.

7. Bibliographic References

- (62) Yang, D.; Chen, Q.; Gertz, B.; He, R.; Phulsuksombati, M.; Ye, R. D.; Oppenheim, J. J. Human dendritic cells express functional formyl peptide receptor-like-2 (FPRL2) throughout maturation. *J. Leukoc. Biol.* **2002**, *72*, 598-607.
- (63) Yang, D.; Chen, Q.; Le, Y.; Wang, J. M.; Oppenheim, J. J. Differential regulation of formyl peptide receptor-like 1 expression during the differentiation of monocytes to dendritic cells and macrophages. *J. Immunol.* **2001**, *166*, 4092-4098.
- (64) Allen, R. A.; Jesaitis, A. J.; Cochrane, C. G. In *Cellular and Molecular Mechanisms of Inflammation*. Academic Press, San Diego, CA, **1990**; Vol. 1, pp. 83-112
- (65) Boulay, F.; Tardif, M.; Brouchon, L.; Vignais, P. Synthesis and use of a novel N-formyl peptide derivative to isolate a human N-formyl peptide receptor cDNA. *Biochem. Biophys. Res. Commun.* **1990**, *168*, 1103-1109.
- (66) Boulay, F.; Tardif, M.; Brouchon, L.; Vignais, P. The human N-formylpeptide receptor. Characterization of two cDNA isolates and evidence for a new subfamily of G-protein-coupled receptors. *Biochemistry* **1990**, *29*, 11123-11133.
- (67) Quehenberger, O.; Prossnitz, E. R.; Cavanagh, S. L.; Cochrane, C. G.; Ye, R. D. Multiple domains of the N-formyl peptide receptor are required for high-affinity ligand binding. Construction and analysis of chimeric N-formyl peptide receptors. *J. Biol. Chem.* **1993**, *268*, 18167-18175.
- (68) Ye, R. D.; Quehenberger, O.; Thomas, K. M.; Navarro, J.; Cavanagh, S. L.; Prossnitz, E. R.; Cochrane, C. G. The rabbit neutrophil N-formyl peptide receptor. cDNA cloning, expression, and structure/function implications. *J. Immunol.* **1993**, *150*, 1383-1394.
- (69) Kirpotina, L. N.; Khlebnikov, A. I.; Schepetkin, I. A.; Ye, R. D.; Rabiet, M. J.; Jutila, M. A.; Quinn, M. T. Identification of novel small-molecule agonists for human formyl peptide receptors and pharmacophore models of their recognition. *Mol. Pharmacol.* **2010**, *77*, 159-170.
- (70) Becker, E. L.; Forouhar, F. A.; Grunnet, M. L.; Boulay, F.; Tardif, M.; Bormann, B. J.; Sodja, D.; Ye, R. D.; Woska, J. R. Jr, Murphy, P. M. Broad immunocytochemical localization of the formylpeptide receptor in human organs, tissues, and cells. *Cell Tissue Res.* **1998**, *292*, 129-35.
- (71) Murphy, P. M.; Ozçelik, T.; Kenney, R. T.; Tiffany, H. L.; McDermott, D.; Franche, U. A structural homologue of the N-formyl peptide receptor. Characterization and chromosome mapping of a peptide chemoattractant receptor family. *J. Biol. Chem.* **1992**, *267*, 7637-7643.
- (72) Perez, H. D.; Holmes, R.; Kelly, E.; McClary, J.; Andrews, W. H. Cloning of a cDNA encoding a receptor related to the formyl peptide receptor of human neutrophils. *Gene* **1992**, *118*, 303-304.
- (73) Ye, R. D.; Cavanagh, S. L.; Quehenberger, O.; Prossnitz, E. R.; Cochrane, C. G. Isolation of a cDNA that encodes a novel granulocyte N-formyl peptide receptor. *Biochem. Biophys. Res. Commun.* **1992**, *184*, 582-589.
- (74) Bao, L.; Gerard, N. P.; Eddy, R. L. Jr; Shows, T. B.; Gerard, C. Mapping of genes for the human C5a receptor (C5AR), human FMLP receptor (FPR), and two FMLP receptor homologue orphan receptors (FPRH1, FPRH2) to chromosome 19. *Genomics* **1992**, *13*, 437-440.
- (75) Nomura, H.; Nielsen, B. W.; Matsushima, K. Molecular cloning of cDNAs encoding a LD78 receptor and putative leukocyte chemotactic peptide receptors. *Int. Immunol.* **1993**, *5*, 1239-1249.
- (76) Perretti, M.; Chiang, N.; La, M.; Fierro, I. M.; Marullo, S.; Gettino, S. J.; Solito, E.; Serhan, C. N. Endogenous lipid- and peptide-derived anti-inflammatory pathways generated with glucocorticoid and aspirin treatment activate the lipoxin A4 receptor. *Nat. Med.* **2002**, *8*, 1296-1302.
- (77) Resnati, M.; Pallavicini, I.; Wang, J. M.; Oppenheim, J.; Serhan, C. N.; Romano, M.; Blasi, F. The fibrinolytic receptor for urokinase activates the G protein-coupled chemotactic receptor FPRL1/LXA4R. *Proc. Natl. Acad. Sci. USA* **2002**, *99*, 1359-1364.
- (78) Fiore, S.; Maddox, J. F.; Perez, H. D.; Serhan, C. N. Identification of a human cDNA encoding a functional high affinity lipoxin A4 receptor. *J. Exp. Med.* **1994**, *180*, 253-260.
- (79) Chiang, N.; Serhan, C. N.; Dahlén, S. E.; Drazen, J. M.; Hay, D. W.; Rovati, G. E.; Shimizu, T.; Yokomizo, T.; Brink, C. The lipoxin receptor ALX: potent ligand-specific and stereoselective actions in vivo. *Pharmacol. Rev.* **2006**, *58*, 463-487.

- (80) Le, Y.; Oppenheim, J. J.; Wang, J. M. Pleiotropic roles of formyl peptide receptors. *Cytok. Growth Factor Rev.* **2001**, *12*, 91-105.
- (81) Brink, C.; Dahlén, S. E.; Drazen, J.; Evans, J. F.; Hay, D. W.; Nicosia, S.; Serhan, C. N.; Shimizu, T.; Yokomizo, T. International Union of Pharmacology XXXVII. Nomenclature for leukotriene and lipoxin receptors. *Pharmacol. Rev.* **2003**, *55*, 195-227.
- (82) Rabiet, M. J.; Huet, E.; Boulay, F. Human mitochondria-derived N-formylated peptides are novel agonists equally active on FPR and FPRL1, while *Listeria monocytogenes*-derived peptides preferentially activate FPR. *Eur. J. Immunol.* **2005**, *35*, 2486-2495.
- (83) Durstin, M.; Gao, J. L.; Tiffany, H. L.; McDermott, D.; Murphy, P. M. Differential expression of members of the N-formylpeptide receptor gene cluster in human phagocytes. *Biochem. Biophys. Res. Commun.* **1994**, *201*, 174-179.
- (84) Christophe, T.; Karlsson, A.; Dugave, C.; Rabiet, M. J.; Boulay, F.; Dahlgren, C. The synthetic peptide Trp-Lys-Tyr-Met-Val-Met-NH₂ specifically activates neutrophils through FPRL1/lipoxin A4 receptors and is an agonist for the orphan monocyte-expressed chemoattractant receptor FPRL2. *J. Biol. Chem.* **2001**, *276*, 21585-21593.
- (85) Betten, A.; Bylund, J.; Christophe, T.; Cristophe, T.; Boulay, F.; Romero, A.; Hellstrand, K.; Dahlgren, C. A proinflammatory peptide from *Helicobacter pylori* activates monocytes to induce lymphocyte dysfunction and apoptosis. *J. Clin. Invest.* **2001**, *108*, 1221-1228.
- (86) Migeotte, I.; Riboldi, E.; Franssen, J. D.; Grégoire, F.; Loison, C.; Wittamer, V.; Detheux, M.; Robberecht, P.; Costagliola, S.; Vassart, G.; Sozzani, S.; Parmentier, M.; Communi, D. Identification and characterization of an endogenous chemotactic ligand specific for FPRL2. *J. Exp. Med.* **2005**, *201*, 83-93.
- (87) Dufton, N.; Perretti, M. Therapeutic anti-inflammatory potential of formyl-peptide receptor agonists. *Pharmacol. Ther.* **2010**, *127*, 175-188.
- (88) Rabiet, M. J., Huet, E.; Boulay, F. The N-formyl peptide receptors and the anaphylatoxin C5a receptors: an overview. *Biochimie* **2007**, *89*, 1089-1106.
- (89) Partida-Sánchez, S.; Iribarren, P.; Moreno-García, M. E.; Gao, J. L.; Murphy, P. M.; Oppenheimer, N.; Wang, J. M.; Lund, F. E. Chemotaxis and calcium responses of phagocytes to formyl peptide receptor ligands is differentially regulated by cyclic ADP ribose. *J. Immunol.* **2004**, *172*, 1896-1906.
- (90) Katanaev, V. L. Signal transduction in neutrophil chemotaxis. *Biochemistry* **2001**, *66*, 351-368.
- (91) Hanahan, D. J. Platelet activating factor: A biologically active phosphoglyceride. *Annu. Rev. Biochem.* **1986**, *55*, 483-509.
- (92) Crooks, S. W.; Stockley, R. A. Leukotriene B4. *Int. J. Biochem. Cell Biol.* **1998**, *30*, 173-178.
- (93) Gerard, C.; Gerard, N. P. C5a anaphylatoxin and its seven transmembrane-segment receptor. *Annu. Rev. Immunol.* **1994**, *12*, 775-808.
- (94) Baggiolini, M. Chemokines and leukocyte traffic. *Nature* **1998**, *392*, 565-568.
- (95) Ali, H.; Richardson, R. M.; Haribabu, B.; Snyderman, R. Chemoattractant receptor cross-desensitization. *J. Biol. Chem.* **1999**, *274*, 6027-6030.
- (96) Panaro, M. A.; Mitolo, V. Cellular responses to FMLP challenging: A mini-review. *Immunopharmacol. Immunotoxicol.* **1999**, *21*, 397-419.
- (97) Selvatici, R.; Falzarano, S.; Mollica, A.; Spisani, S. Signal transduction pathways triggered by selective formylpeptide analogues in human neutrophils. *Eur. J. Pharmacol.* **2006**, *534*, 1-11.
- (98) Campbell, J. J.; Foxman, E. F.; Butcher, E. C. Chemoattractant receptor cross talk as a regulatory mechanism in leukocyte adhesion and migration. *Eur. J. Immunol.* **1997**, *27*, 2571-2578.
- (99) Foxman, E. F.; Campbell, J. J.; Butcher, E. C. Multistep navigation and the combinatorial control of leukocyte chemotaxis. *J. Cell Biol.* **1997**, *139*, 1349-1360.
- (100) Foxman, E. F.; Kunkel, E. J.; Butcher, E. C. Integrating conflicting chemotactic signals. The role of memory in leukocyte navigation. *J. Cell Biol.* **1999**, *147*, 577-588.

7. Bibliographic References

- (101) Heit, B.; Robbins, S. M.; Downey, C. M.; Guan, Z.; Colarusso, P.; Miller, B. J.; Jirik, F. R.; Kubes, P. PTEN functions to 'prioritize' chemotactic cues and prevent 'distraction' in migrating neutrophils. *Nat. Immunol.* **2008**, *9*, 743-752.
- (102) Heit, B.; Tavener, S.; Raharjo, E.; Kubes, P. An intracellular signalling hierarchy determines direction of migration in opposing chemotactic gradients. *J. Cell Biol.* **2002**, *159*, 91-102.
- (103) Boxer, L. A.; Yoder, M.; Bonsib, S.; Schmidt, M.; Ho, P.; Jersild, R.; Baehner, R. L. Effects of a chemotactic factor, N-formylmethionyl peptide, on adherence, superoxide anion generation, phagocytosis, and microtubule assembly of human polymorphonuclear leukocytes. *J. Lab. Clin. Med.* **1979**, *93*, 506-514.
- (104) Lehmeyer, J. E.; Snyderman, R.; Johnston, R. B. Jr. Stimulation of neutrophil oxidative metabolism by chemotactic peptides: influence of calcium ion concentration and cytochalasin B and comparison with stimulation by phorbol myristate acetate. *Blood* **1979**, *54*, 35-45.
- (105) Babior, B. M.; Lambeth, J. D.; Nauseef, W. The neutrophil NADPH oxidase. *Arch. Biochem. Biophys.* **2002**, *397*, 342-344.
- (106) Karnad, A. B.; Hartshorn, K. L.; Wright, J.; Myers, J. B.; Schwartz, J. H.; Tauber, A. I. Priming of human neutrophils with N-formyl-methionyl-leucyl-phenylalanine by a calcium-independent, pertussis toxin-insensitive pathway. *Blood* **1989**, *74*, 2519-2526.
- (107) Bentwood, B. J.; Henson, P. M. The sequential release of granule constituents from human neutrophils. *J. Immunol.* **1980**, *124*, 855-862.
- (108) Nauseef, W. M. How human neutrophils kill and degrade microbes: an integrated view. *Immunol. Rev.* **2007**, *219*, 88-102.
- (109) Sengeløv, H.; Boulay, F.; Kjeldsen, L.; Borregaard, N. Subcellular localization and translocation of the receptor for N-formylmethionyl-leucyl-phenylalanine in human neutrophils. *Biochem. J.* **1994**, *299*, 473-479.
- (110) Bylund, J.; Karlsson, A.; Boulay, F.; Dahlgren, C. Lipopolysaccharide-induced granule mobilization and priming of the neutrophil response to *Helicobacter pylori* peptide Hp(2-20), which activates formyl peptide receptor-like 1. *Infect. Immun.* **2002**, *70*, 2908-2914.
- (111) Smith, R. J.; Sam, L. M.; Justen, J. M. Diacylglycerols modulate human polymorphonuclear neutrophil responsiveness: effects on intracellular calcium mobilization, granule exocytosis, and superoxide anion production. *J. Leukoc. Biol.* **1998**, *43*, 411-419.
- (112) Sengeløv, H.; Kjeldsen, L.; Borregaard, N. Control of exocytosis in early neutrophil activation. *J. Immunol.* **1993**, *150*, 1535-1543.
- (113) Lloyd, A. R.; Oppenheim, J. J. Poly's lament: the neglected role of the polymorphonuclear neutrophil in the afferent limb of the immune response. *Immunol. Today* **1992**, *13*, 169-172.
- (114) Cassatella, M. A.; Bazzoni, F.; Ceska, M.; Ferro, I.; Baggiolini, M.; Berton, G. IL-8 production by human polymorphonuclear leukocytes. The chemoattractant formylmethionyl-leucyl-phenylalanine induces the gene expression and release of IL-8 through a pertussis toxin-sensitive pathway. *J. Immunol.* **1992**, *148*, 3216-3220.
- (115) McDonald, P. P.; Bald, A.; Cassatella, M. A. Activation of the NF-kappaB pathway by inflammatory stimuli in human neutrophils. *Blood* **1997**, *89*, 3421-3433.
- (116) He, R.; Sang, H.; Ye, R. D. Serum amyloid A induces IL-8 secretion through a G protein-coupled receptor, FPRL1/LXA₄R. *Blood* **2003**, *101*, 1572-1581.
- (117) Ye, R. D. Regulation of nuclear factor kappaB activation by G-protein-coupled receptors. *J. Leukoc. Biol.* **2001**, *70*, 839-848.
- (118) Perretti, M. The annexin 1 receptor(s): is the plot unravelling? *Trends Pharmacol. Sci.* **2003**, *24*, 574-579.
- (119) József, L.; Zouki, C.; Petasis, N. A.; Serhan, C. N.; Filep, J. G. Lipoxin A₄ and aspirin-triggered 15-epi-lipoxin A₄ inhibit peroxynitrite formation, NF-kappa B and AP-1 activation, and IL-8 gene expression in human leukocytes. *Proc. Natl. Acad. Sci. USA* **2002**, *99*, 13266-13271.

- (120) Damian, M.; Mary, S.; Martin, A.; Pin, J. P.; Banères, J. L. G protein activation by the leukotriene B4 receptor dimer. Evidence for an absence of trans-activation. *J. Biol. Chem.* **2008**, *283*, 21084-21092.
- (121) Su, S. B.; Gong, W.; Gao, J. L.; Shen, W.; Murphy, P. M.; Oppenheim, J. J.; Wang, J. M. A seven-transmembrane, G protein-coupled receptor, FPRL1, mediates the chemotactic activity of serum amyloid A for human phagocytic cells. *J. Exp. Med.* **1999**, *189*, 395-402.
- (122) Bae, Y. S.; Park, J. C.; He, R.; Ye, R. D.; Kwak, J. Y.; Suh, P. G.; Ho Ryu S. Differential signaling of formyl peptide receptor-like 1 by Trp-Lys-Tyr-Met-Val-Met-CONH₂ or lipoxin A4 in human neutrophils. *Mol. Pharmacol.* **2003**, *64*, 721-730.
- (123) Prat, C.; Bestebroer, J.; de Haas, C. J.; van Strijp, J. A.; van Kessel, K. P. A new staphylococcal anti-inflammatory protein that antagonizes the formyl peptide receptor-like 1. *J. Immunol.* **2006**, *177*, 8017-8026.
- (124) Maddox, J. F.; Hachicha, M.; Takano, T.; Petasis, N. A.; Fokin, V. V.; Serhan, C. N. Lipoxin A4 stable analogs are potent mimetics that stimulate human monocytes and THP-1 cells via a G-protein-linked lipoxin A4 receptor. *J. Biol. Chem.* **1997**, *272*, 6972-6978.
- (125) Savill, J. Apoptosis in resolution of inflammation. *J. Leukoc. Biol.* **1997**, *61*, 375-380.
- (126) Colotta, F.; Re, F.; Polentarutti, N.; Sozzani, S.; Mantovani, A. Modulation of granulocyte survival and programmed cell death by cytokines and bacterial products. *Blood* **1992**, *80*, 2012-2020.
- (127) Kettritz, R.; Falk, R. J.; Jennette, J. C.; Gaido, M. L. Neutrophil superoxide release is required for spontaneous and FMLP-mediated but not for TNF alphamediated apoptosis. *J. Am. Soc. Nephrol.* **1997**, *8*, 1091-1100.
- (128) Cui, Y.; Le, Y.; Yazawa, H.; Gong, W.; Wang, J. M. Potential role of the formyl peptide receptor-like 1 (FPRL1) in inflammatory aspects of Alzheimer's disease. *J. Leukoc. Biol.* **2002**, *72*, 628-635.
- (129) Arterburn, J. B.; Oprea, T. I.; Prossnitz, E. R.; Edwards, B. S.; Sklar, L. A. Discovery of selective probes and antagonists for G-protein-coupled receptors FPR/FPRL1 and GPR30. *Curr. Top. Med. Chem.* **2009**, *9*, 1227-1236.
- (130) Tsuruky, T.; Takahata, K.; Yoshikawa, M. Mechanism of protective effect of intraperitoneally administered agonists for Formyl Peptide Receptors against Chemotherapy induced alopecia, *Biosci. Biotheol. Biochem.* **2007**, *71*, 1198-1202.
- (131) Zhou, H.; Zhou, X.; Kouadir, M.; Zhang, Z.; Yin, X.; Yang, L.; Zhao, D. Induction of macrophage migration by neurotoxic prion protein fragment. *J. Neurosci. Methods* **2009**, *181*, 1-5.
- (132) Wild, C.; Dubay, J. W.; Greenwell, T.; Baird, T. Jr; Oas, T. G.; McDanal, C.; Hunter, E.; Matthews, T. Propensity for a leucine zipper-like domain of human immunodeficiency virus type 1 gp41 to form oligomers correlates with a role in virus-induced fusion rather than assembly of the glycoprotein complex. *Proc. Natl. Acad. Sci. USA* **1994**, *91*, 12676-12680.
- (133) Kilby, J. M.; Hopkins, S.; Venetta, T. M.; Di Massimo, B.; Cloud, G. A.; Lee, J. Y.; Alldredge, L.; Hunter, E.; Lambertm D.; Bolognesi, D.; Matthews, T.; Johnson, M. R.; Nowak, M. A.; Shaw, G. M.; Saag, M. S. Potent suppression of HIV-1 replication in humans by T-20, a peptide inhibitor of gp41-mediated virus entry. *Nat. Med.* **1998**, *4*, 1302-1307.
- (134) Walther, A.; Riehemann, K.; Gerke, V. A novel ligand of the formyl peptide receptor: annexin I regulates neutrophil extravasation by interacting with the FPR. *Mol Cell.* **2000**, *5*, 831-840.
- (135) de Paulis, A.; Florio, G.; Prevete, N.; Triggiani, M.; Fiorentino, I.; Genovese, A.; Marone, G. HIV-1 Envelope gp41 Peptides Promote Migration of Human FcεRI⁺ Cells and Inhibit IL-13 Synthesis Through Interaction with Formyl Peptide Receptors. *J. Immunol.* **2002**, *169*, 4559-4567.
- (136) de Paulis, A.; Montuori, N.; Prevete, N.; Fiorentino, I.; Rossi, F. W.; Visconte, V.; Rossi, G.; Marone, G.; Ragno, P. Urokinase induces basophil chemotaxis through a urokinase receptor epitope that is an endogenous ligand for formyl peptide receptor-like 1 and -like 2. *J. Immunol.* **2004**, *173*, 5739-5748.

7. Bibliographic References

- (137) de Paulis, A.; Prevede, N.; Fiorentino, I.; Walls, A. F.; Curto, M.; Petraroli, A.; Castaldo, V.; Ceppa, P.; Fiocca, R.; Marone, G. Basophils infiltrate human gastric mucosa at sites of *Helicobacter pylori* infection, and exhibit chemotaxis in response to *H. pylori*-derived peptide Hp(2–20). *J. Immunol.* **2004**, *172*, 7734-7743.
- (138) Pieretti, S.; Di Giannuario, A.; De Felice, M.; Perretti, M.; Cirino, G. Stimulus-dependent specificity for annexin 1 inhibition of the inflammatory nociceptive response: the involvement of the receptor for formylated peptides. *Pain* **2004**, *109*, 52-63.
- (139) Edwards, B. S.; Bologna, C.; Young, S. M.; Balakin, K. V.; Prossnitz, E. R.; Savchuck, N. P.; Sklar, L. A.; Oprea, T. I. Integration of virtual screening with high-throughput flow cytometry to identify novel small molecule formylpeptide receptor antagonists. *Mol. Pharmacol.* **2005**, *68*, 1301-1310.
- (140) Medzhitov, R.; Janeway, C. Jr. Innate immune recognition: mechanisms and pathways. *Immunol. Rev.* **2000**, *173*, 89-97.
- (141) Gulden, P. H.; Fischer, P. 3rd; Sherman, N. E.; Wang, W.; Engelhard, V. H.; Shabanowitz, J.; Hunt, D. F.; Pamer, E. G. A *Listeria monocytogenes* pentapeptide is presented to cytolytic T lymphocytes by the H2–M3 MHC class Ib molecule. *Immunity* **1996**, *5*, 73-79.
- (142) Chen, J.; Bernstein, H. S.; Chen, M.; Wang, L.; Ishii, M.; Turck, C. W.; Coughlin, S. R. Tethered ligand library for discovery of peptide agonists. *J. Biol. Chem.* **1995**, *270*, 23398-23401.
- (143) Hashimoto, Y.; Niikura, T.; Ito, Y.; Sudo, H.; Hata, M.; Arakawa, E.; Abe, Y.; Kita, Y.; Nishimoto, I. Detailed characterization of neuroprotection by a rescue factor humanin against various Alzheimer's disease-relevant insults. *J. Neurosci.* **2001**, *21*, 9235-9245.
- (144) Ying, G.; Iribarren, P.; Zhou, Y.; Gong, W.; Zhang, N.; Yu, Z. X.; Le, Y.; Cui, Y.; Wang, J. M. Humanin, a newly identified neuroprotective factor, uses the G protein-coupled formylpeptide receptor-like-1 as a functional receptor. *J. Immunol.* **2004**, *172*, 7078-7085.
- (145) Harada, M.; Habata, Y.; Hosoya, M.; Nishi, K.; Fujii, R.; Kobayashi, M.; Hinuma, S. N-Formylated humanin activates both formyl peptide receptor-like 1 and 2. *Biochem. Biophys. Res. Commun.* **2004**, *324*, 255-261.
- (146) Mills, J. S.; Miettinen, H. M.; Barnidge, D.; Vlases, M. J.; Wimer-Mackin, S.; Dratz, E. A.; Sunner, J.; Jesaitis, A. J. Identification of a ligand binding site in the human neutrophil formyl peptide receptor using a site-specific fluorescent photoaffinity label and mass spectrometry. *J. Biol. Chem.* **1998**, *273*, 10428-10435.
- (147) Su, S. B.; Gao, J.; Gong, W.; Dunlop, N. M.; Murphy, P. M.; Oppenheim, J. J.; Wang, J. M. T21/DP107, A synthetic leucine zipper-like domain of the HIV-1 envelope gp41, attracts and activates human phagocytes by using G-protein-coupled Formyl peptide receptors. *J. Immunol.* **1999**, *162*, 5924-5930.
- (148) Su, S. B.; Gong, W. H.; Gao, J. L.; Shen, W. P.; Grimm, M. C.; Deng, X.; Murphy, P. M.; Oppenheim, J. J.; Wang, J. M. T20/DP178, an ectodomain peptide of human immunodeficiency virus type 1 gp41, is an activator of human phagocyte N-formyl peptide receptor. *Blood* **1999**, *93*, 3885-3892.
- (149) Le, Y.; Jiang, S.; Hu, J.; Gong, W.; Su, S.; Dunlop, N. M.; Shen, W.; Li, B.; Wang, J. M. N36, a synthetic N-terminal heptad repeat domain of the HIV-1 envelope protein gp41, is an activator of human phagocytes. *Clin. Immunol.* **2000**, *96*, 236-242.
- (150) Hartt, J. K.; Liang, T.; Sahagun-Ruiz, A.; Wang, J. M.; Gao, J. L.; Murphy, P. M. The HIV-1 cell entry inhibitor T-20 potently chemoattracts neutrophils by specifically activating the N-formylpeptide receptor. *Biochem. Biophys. Res. Commun.* **2000**, *272*, 699-704.
- (151) Shen, W.; Proost, P.; Li, B.; Gong, W.; Le, Y.; Sargeant, R.; Murphy, P. M.; Van Damme, J.; Wang, J. M. Activation of the chemotactic peptide receptor FPRL1 in monocytes phosphorylates the chemokine receptor CCR5 and attenuates cell responses to selected chemokines. *Biochem. Biophys. Res. Commun.* **2000**, *272*, 276-283.

- (152) Bellner, L.; Thorén, F.; Nygren, E.; Liljeqvist, J. A.; Karlsson, A.; Eriksson, K. A proinflammatory peptide from herpes simplex virus type 2 glycoprotein G affects neutrophil, monocyte, and NK cell functions. *J. Immunol.* **2005**, *174*, 2235-2241.
- (153) Mills, J. S. Peptides derived from HIV-1, HIV-2, Ebola virus, SARS coronavirus and coronavirus 229E exhibit high affinity binding to the formyl peptide receptor. *Biochim. Biophys. Acta* **2006**, *1762*, 693-703.
- (154) Kushner, I.; Rzewnicki, D. *Acute phase response*, In *Inflammation: Basic Principles and Clinical Correlates*. Gallin, J. I. and Snyderman, R. Eds. Lippincott Williams & Wilkins: Philadelphia, **1999**; pp. 317-329.
- (155) Lee, H. Y.; Kim, M. K.; Park, K. S.; Shin, E. H.; Jo, S. H.; Kim, S. D.; Jo, E. J.; Lee, Y. N.; Lee, C.; Baek, S. H.; Bae, Y. S. Serum amyloid A induces contrary immune responses via formyl peptide receptor-like 1 in human monocytes. *Mol. Pharmacol.* **2006**, *70*, 241-248.
- (156) O'Hara, R.; Murphy, E. P.; Whitehead, A. S.; FitzGerald, O.; Bresnihan, B. Local expression of the serum amyloid A and formyl peptide receptor-like 1 genes in synovial tissue is associated with matrix metalloproteinase production in patients with inflammatory arthritis. *Arthritis Rheum.* **2004**, *50*, 1788-1799.
- (157) Sodin-Semrl, S.; Spagnolo, A.; Mikus, R.; Barbaro, B.; Varga, J.; Fiore, S. Opposing regulation of interleukin-8 and NF-kappaB responses by lipoxin A4 and serum amyloid A via the common lipoxin A receptor. *Int. J. Immunopathol. Pharmacol.* **2004**, *17*, 145-156.
- (158) Lee, M. S.; Yoo, S. A.; Cho, C. S.; Suh, P. G.; Kim, W. U.; Ryu, S. H. Serum amyloid A binding to formyl peptide receptor-like 1 induces synovial hyperplasia and angiogenesis. *J. Immunol.* **2006**, *177*, 5585-5594.
- (159) Björkman, L.; Karlsson, J.; Karlsson, A.; Rabet, M. J.; Boulay, F.; Fu, H.; Bylund, J.; Dahlgren, C. Serum amyloid A mediates human neutrophil production of reactive oxygen species through a receptor independent of formyl peptide receptor like-1. *J. Leukoc. Biol.* **2008**, *83*, 245-253.
- (160) Le, Y.; Gong, W.; Tiffany, H. L.; Tumanov, A.; Nedospasov, S.; Shen, W.; Dunlop, N. M.; Gao, J. L.; Murphy, P. M.; Oppenheim, J. J.; Wang, J. M. Amyloid (beta)42 activates a G-protein-coupled chemoattractant receptor, FPR-like-1. *J. Neurosci.* **2001**, *21*, RC123.
- (161) Tiffany, H. L.; Lavigne, M. C.; Cui, Y. H.; Wang, J. M.; Leto, T. L.; Gao, J. L.; Murphy, P. M. Amyloid-beta induces chemotaxis and oxidant stress by acting at formyl peptide receptor 2, a G protein-coupled receptor expressed in phagocytes and brain. *J. Biol. Chem.* **2001**, *276*, 23645-23652.
- (162) Le, Y.; Yazawa, H.; Gong, W.; Yu, Z.; Ferrans, V. J.; Murphy, P. M.; Wang, J. M. The neurotoxic prion peptide fragment PrP(106-126) is a chemotactic agonist for the G protein-coupled receptor formyl peptide receptor-like 1. *J. Immunol.* **2001**, *166*, 1448-1451.
- (163) Chen, K.; Iribarren, P.; Hu, J.; Chen, J.; Gong, W.; Cho, E. H.; Lockett, S.; Dunlop, N M.; Wang, J. M. Activation of Toll-like receptor 2 on microglia promotes cell uptake of Alzheimer disease-associated amyloid beta peptide. *J. Biol. Chem.* **2006**, *281*, 3651-3659.
- (164) Yazawa, H.; Yu, Z. X.; Takeda, L. Y.; Gong, W.; Ferrans, V. J.; Oppenheim, J. J.; Li, C. C.; Wang, J. M. Beta amyloid peptide (Abeta42) is internalized via the G-protein coupled receptor FPRL1 and forms fibrillar aggregates in macrophages. *Faseb J.* **2001**, *15*, 2454-2462.
- (165) Hashimoto, Y.; Niikura, T.; Ito, Y.; Sudo, H.; Hata, M.; Arakawa, E.; Abe, Y.; Kita, Y.; Nishimoto, I. Detailed characterization of neuroprotection by a rescue factor humanin against various Alzheimer's disease-relevant insults. *J. Neurosci.* **2001**, *21*, 9235-9245.
- (166) Harada, M.; Habata, Y.; Hosoya, M.; Nishi, K.; Fujii, R.; Kobayashi, M.; Hinuma, S. N-Formylated humanin activates both formyl peptide receptor-like 1 and 2. *Biochem Biophys. Res. Commun.* **2004**, *324*, 255-261.
- (167) Ying, G.; Iribarren, P.; Zhou, Y.; Gong, W.; Zhang, N.; Yu, Z. X.; Le, Y.; Cui, Y.; Wang, J. M. Humanin, a newly identified neuroprotective factor, uses the G protein-coupled formylpeptide receptor-like-1 as a functional receptor. *J. Immunol.* **2004**, *172*, 7078-7085.

7. Bibliographic References

- (168) Gargiulo, L.; Longanesi-Cattani, I.; Bifulco, K.; Franco, P.; Raiola, R.; Campiglia, P.; Grieco, P.; Peluso, G.; Stoppelli, M. P.; Carriero M. V. Cross-talk between fMLP and vitronectin receptors triggered by urokinase receptor-derived SRSRY peptide. *J. Biol. Chem.* **2005**, *280*, 25225-25232.
- (169) Furlan, F.; Orlando, S.; Laudanna, C.; Resnati, M.; Basso, V.; Blasi, F.; Mondino, A. The soluble D2D3(88–274) fragment of the urokinase receptor inhibits monocyte chemotaxis and integrin-dependent cell adhesion. *J. Cell. Sci.* **2004**, *117*, 2909-2916.
- (170) Yang, D.; Chen, Q.; Schmidt, A. P.; Anderson, G. M.; Wang, J. M.; Wooters, J.; Oppenheim, J. J.; Chertov, O. LL-37, the neutrophil granule- and epithelial cell-derived cathelicidin, utilizes formyl peptide receptor-like 1 (FPRL1) as a receptor to chemoattract human peripheral blood neutrophils, monocytes, and T cells. *J. Exp. Med.* **2000**, *192*, 1069-1074.
- (171) Koczulla, R.; von Degenfeld, G.; Kupatt, C.; Krötz, F.; Zahler, S.; Gloe, T.; Issbrücker, K.; Unterberger, P.; Zaiou, M.; Lebherz, C.; Karl, A.; Raake, P.; Pfosser, A.; Boekstegers, P.; Welsch, U.; Hiemstra, P. S.; Vogelmeier, C.; Gallo, R. L.; Clauss, M.; Bals, R. An angiogenic role for the human peptide antibiotic LL-37/hCAP-18. *J. Clin. Invest.* **2003**, *111*, 1665-1672.
- (172) Sun, R.; Iribarren, P.; Zhang, N.; Zhou, Y.; Gong, W.; Cho, E. H.; Lockett, S.; Chertov, O.; Bednar, F.; Rogers, T. J.; Oppenheim, J. J.; Wang, J. M. Identification of neutrophil granule protein cathepsin G as a novel chemotactic agonist for the G protein-coupled formyl peptide receptor. *J. Immunol.* **2004**, *173*, 428-436.
- (173) Ernst, S.; Lange, C.; Wilbers, A.; Goebeler, V.; Gerke, V.; Rescher, U. An annexin 1 N-terminal peptide activates leukocytes by triggering different members of the formyl peptide receptor family. *J. Immunol.* **2004**, *172*, 7669-7676.
- (174) Karlsson, J.; Fu, H.; Boulay, F.; Dahlgren, C.; Hellstrand, K.; Movitz, C. Neutrophil NADPH-oxidase activation by an annexin AI peptide is transduced by the formyl peptide receptor (FPR), whereas an inhibitory signal is generated independently of the FPR family receptors. *J. Leukoc. Biol.* **2005**, *78*, 762-771.
- (175) Serhan, C. N.; Maddox, J. F.; Petasis, N. A.; Akritopoulou-Zanze, I.; Papayianni, A.; Brady, H. R.; Colgan, S. P.; Madara, J. L. Design of lipoxin A4 stable analogs that block transmigration and adhesion of human neutrophils. *Biochemistry* **1995**, *34*, 14609-14615.
- (176) Serhan, C. N. Resolution phase of inflammation: novel endogenous anti-inflammatory and proresolving lipid mediators and pathways. *Annu. Rev. Immunol.* **2007**, *25*, 101-137.
- (177) Fiore, S.; Ryeom, S. W.; Weller, P. F.; Serhan, C. N. Lipoxin recognition sites. Specific binding of labeled lipoxin A4 with human neutrophils. *J. Biol. Chem.* **1992**, *267*, 16168-16176.
- (178) Nigam, S.; Fiore, S.; Lusinskas, F. W.; Serhan, C. N. Lipoxin A4 and lipoxin B4 stimulate the release but not the oxygenation of arachidonic acid in human neutrophils: dissociation between lipid remodeling and adhesion. *J. Cell. Physiol.* **1990**, *143*, 512-523.
- (179) Fiore, S.; Romano, M.; Reardon, E. M.; Serhan, C. N. Induction of functional lipoxin A4 receptors in HL-60 cells. *Blood* **1993**, *81*, 3395-3403.
- (180) Serhan, C. N. Lipoxins and aspirin-triggered 15-epi-lipoxins are the first lipid mediators of endogenous anti-inflammation and resolution. *Prostaglandins Leukot Essent. Fatty Acids* **2005**, *73*, 141-162.
- (181) O'Meara, S. J.; Rodgers, K.; Godson, C. Lipoxins: update and impact of endogenous pro-resolution lipid mediators. *Rev. Physiol. Biochem. Pharmacol.* **2008**, *160*, 47-70.
- (182) Takano, T.; Clish, C. B.; Gronert, K.; Petasis, N.; Serhan, C. N. Neutrophil-mediated changes in vascular permeability are inhibited by topical application of aspirin-triggered 15-epi-lipoxin A4 and novel lipoxin B4 stable analogues. *J. Clin. Invest.* **1998**, *101*, 819-826.
- (183) Takano, T.; Fiore, S.; Maddox, J. F.; Brady, H. R.; Petasis, N. A.; Serhan, C. N. Aspirin-triggered 15-epi-lipoxin A4 (LXA4) and LXA4 stable analogues are potent inhibitors of acute inflammation: evidence for anti-inflammatory receptors. *J. Exp. Med.* **1997**, *185*, 1693-1704.

- (184) Hachicha, M.; Pouliot, M.; Petasis, N. A.; Serhan, C. N. Lipoxin (LX)A4 and aspirin-triggered 15-epi-LXA4 inhibit tumor necrosis factor 1 α -initiated neutrophil responses and trafficking: regulators of a cytokine-chemokine axis. *J. Exp. Med.* **1999**, *189*, 1923-1930.
- (185) Colgan, S. P.; Serhan, C. N.; Parkos, C. A.; Delp-Archer, C.; Madara, J. L. Lipoxin A4 modulates transmigration of human neutrophils across intestinal epithelial monolayers. *J. Clin. Invest.* **1993**, *92*, 75-82.
- (186) Kucharzik, T.; Gewirtz, A. T.; Merlin, D.; Madara, J. L.; Williams, I. R. Lateral membrane LXA4 receptors mediate LXA4's anti-inflammatory actions on intestinal epithelium. *Am. J. Physiol. Cell Physiol.* **2003**, *284*, C888-896.
- (187) Paul-Clark, M. J.; Van Cao, T.; Moradi-Bidhendi, N.; Cooper, D.; Gilroy, D. W. 15-epi-lipoxin A4-mediated induction of nitric oxide explains how aspirin inhibits acute inflammation. *J. Exp. Med.* **2004**, *200*, 69-78.
- (188) Wu, S. H.; Lu, C.; Dong, L.; Zhou, G. P.; He, Z. G.; Chen, Z. Q. Lipoxin A4 inhibits TNF- α -induced production of interleukins and proliferation of rat mesangial cells. *Kidney Int.* **2005**, *68*, 35-46.
- (189) Bonnans, C.; Gras, D.; Chavis, C.; Mainprice, B.; Vachier, I.; Godard, P.; Chanez, P. Synthesis and anti-inflammatory effect of lipoxins in human airway epithelial cells. *Biomed. Pharmacother.* **2007**, *61*, 261-267.
- (190) Wu, S. H.; Liao, P. Y.; Dong, L.; Chen, Z. Q. Signal pathway involved in inhibition by lipoxin A(4) of production of interleukins induced in endothelial cells by lipopolysaccharide. *Inflamm. Res.* **2008**, *57*, 430-437.
- (191) Aliberti, J.; Hieny, S.; Reis, C.; Sousa, C.; Serhan, C. N.; Sher, A. Lipoxin-mediated inhibition of IL-12 production by DCs: a mechanism for regulation of microbial immunity. *Nat. Immunol.* **2002**, *3*, 76-82.
- (192) Aliberti, J.; Serhan, C.; Sher, A. Parasite-induced lipoxin A4 is an endogenous regulator of IL-12 production and immunopathology in *Toxoplasma gondii* infection. *J. Exp. Med.* **2002**, *196*, 1253-1262.
- (193) Svensson, C. I.; Zattoni, M.; Serhan, C. N. Lipoxins and aspirin-triggered lipoxin inhibit inflammatory pain processing. *J. Exp. Med.* **2007**, *204*, 245-252.
- (194) Godson, C.; Mitchell, S.; Harvey, K.; Petasis, N. A.; Hogg, N.; Brady, H. R. Cutting edge: lipoxins rapidly stimulate nonphlogistic phagocytosis of apoptotic neutrophils by monocyte-derived macrophages. *J. Immunol.* **2002**, *164*, 1663-1667.
- (195) Baek, S. H.; Seo, J. K.; Chae, C. B.; Suh, P. G.; Ryu, S. H. Identification of the peptides that stimulate the phosphoinositide hydrolysis in lymphocyte cell lines from peptide libraries. *J. Biol. Chem.* **1996**, *271*, 8170-8175.
- (196) Le, Y.; Gong, W.; Li, B.; Dunlop, N. M.; Shen, W.; Su, S. B.; Ye, R. D.; Wang, J. M. Utilization of two seven-transmembrane, G protein-coupled receptors, formyl peptide receptor-like 1 and formyl peptide receptor, by the synthetic hexapeptide WKYMVm for human phagocyte activation. *J. Immunol.* **1999**, *163*, 6777-6784.
- (197) Kang, H. K.; Lee, H. Y.; Kim, M. K.; Park, K. S.; Park, Y. M.; Kwak, J. Y.; Bae, Y. S. The synthetic peptide Trp-Lys-Tyr-Met-Val-D-Met inhibits human monocyte-derived dendritic cell maturation via formyl peptide receptor and formyl peptide receptorlike 2. *J. Immunol.* **2005**, *175*, 685-692.
- (198) Karlsson, J.; Fu, H.; Boulay, F.; Bylund, J.; Dahlgren, C. The peptide Trp-Lys-Tyr-Met-Val-D-Met activates neutrophils through the formyl peptide receptor only when signaling through the formylpeptide receptor like 1 is blocked. A receptor switch with implications for signal transduction studies with inhibitors and receptor antagonists. *Biochem. Pharmacol.* **2006**, *71*, 1488-1496.

7. Bibliographic References

- (199) Klein, C.; Paul, J. I.; Sauv , K.; Schmidt, M. M.; Arcangeli, L.; Ransom, J.; Trueheart, J.; Manfredi, J. P.; Broach, J. R.; Murphy, A. J. Identification of surrogate agonists for the human FPRL-1 receptor by autocrine selection in yeast. *Nat. Biotechnol.* **1998**, *16*, 1334-1337.
- (200) Hu, J. Y.; Le, Y.; Gong, W.; Dunlop, N. M.; Gao, J.L.; Murphy, P. M.; Wang, J. M. Synthetic peptide MMK-1 is a highly specific chemotactic agonist for leukocyte FPRL1. *J. Leukoc. Biol.* **2001**, *70*, 155-161.
- (201) Chen, J.; Bernstein, H. S.; Chen, M.; Wang, L.; Ishii, M.; Turck, C. W.; Coughlin, S. R. Tethered ligand library for discovery of peptide agonists. *J. Biol. Chem.* **1995**, *270*, 23398-23401.
- (202) B rli, R. W.; Xu, H.; Zou, X.; Muller, K.; Golden, J.; Frohn, M.; Adlam, M.; Plant, M. H.; Wong, M.; McElvain, M.; Regal, K.; Viswanadhan, V. N.; Tagari, P.; Hungate, R. Potent hFPRL1 (ALXR) agonists as potential anti-inflammatory agents. *Bioorg. Med. Chem. Lett.* **2006**, *16*, 3713-3718.
- (203) Frohn, M.; Xu, H.; Zou, X.; Chang, C.; McElvain, M.; Plant, M. H.; Wong, M.; Tagari, P.; Hungate, R.; B rli R. W. New 'chemical probes' to examine the role of the hFPRL1 (or ALXR) receptor in inflammation. *Bioorg. Med. Chem. Lett.* **2007**, *17*, 6633-6637.
- (204) Schepetkin, I. A.; Kirpotina, L. N.; Khlebnikov, A. I.; Quinn, M. T. Highthroughput screening for small-molecule activators of neutrophils: identification of novel *N*-formyl peptide receptor agonists. *Mol. Pharmacol.* **2007**, *71*, 1061-1074.
- (205) Schepetkin I. A.; Kirpotina, L. N.; Tian, J.; Khlebnikov, A. I.; Ye, R. D.; Quinn, M. T. Identification of novel formyl peptide receptor-like 1 agonists that induce macrophage tumor necrosis factor alpha production. *Mol. Pharmacol.* **2008**, *74*, 392-402.
- (206) Kirpotina, L. N.; Khlebnikov, A. I.; Schepetkin, I. A.; Ye, R. D.; Rabiet, M. J.; Jutila, M. A.; Quinn, M. T. Identification of Novel Small-Molecule Agonists for Human Formyl Peptide Receptors and Pharmacophore Models of Their Recognition. *Mol. Pharmacol.* **2010**, *77*, 159-170.
- (207) Khlebnikov, A. I.; Schepetkin, I. A.; Quinn, M. T. Computational structure-activity relationship analysis of small-molecule agonists for human Formyl peptide receptors. *Europ. J. Med. Chem.* **2010**, *45*, 5406-5419.
- (208) Gavins, F. N.; Yona, S.; Kamal, A. M.; Flower, R. J.; Perretti, M. Leukocyte antiadhesive actions of annexin 1: ALXR- and FPR-related anti-inflammatory mechanisms. *Blood* **2003**, *101*, 4140-4147.
- (209) Machado, F. S.; Johndrow, J. E.; Esper, L.; Dias, A.; Bafica, A.; Serhan, C. N.; Aliberti, J. Anti-inflammatory actions of lipoxin A4 and aspirin-triggered lipoxin are SOCS-2 dependent. *Nat. Med.* **2006**, *12*, 330-334.
- (210) Stenfeldt, A. L.; Karlsson, J.; Wenner s, C.; Bylund, J.; Fu, H.; Dahlgren, C. Cyclosporin H, Boc-MLF and Boc-FLFLF are antagonists that preferentially inhibit activity triggered through the formyl peptide receptor. *Inflammation* **2007**, *30*, 224-229.
- (211) Wenzel-Seifert, K.; Gr nbaum, L.; Seifert, R. Differential inhibition of human neutrophil activation by cyclosporins A, D, and H. Cyclosporin H is a potent and effective inhibitor of formyl peptide-induced superoxide formation. *J. Immunol.* **1991**, *147*, 1940-1946.
- (212) Wenzel-Seifert, K.; Seifert, R. Cyclosporin H is a potent and selective Formyl peptide receptor antagonist. Comparison with *N*-*t*-butoxycarbonyl-L-phenylalanyl-L-leucyl-L-phenylalanyl-L-leucyl-L-phenylalanine and cyclosporins A, B, C, D, and E. *J. Immunol.* **1993**, *150*, 4591-4599.
- (213) Wenzel-Seifert, K.; Hurt, C. M.; Seifert, R. High constitutive activity of the human formyl peptide receptor. *J. Biol. Chem.* **1998**, *273*, 24181-24189.
- (214) Yamamoto, Y.; Kanazawa, T.; Shimamura, M.; Ueki, M.; Hazato, T. Inhibitory effects of spinorphin, a novel endogenous regulator, on chemotaxis, O₂⁻ generation, and exocytosis by *N*-formylmethionyl-leucyl-phenylalanine (FMLP)-stimulated neutrophils. *Biochem. Pharmacol.* **1997**, *54*, 695-701.

- (215) Liang, T. S.; Gao, J. L.; Fatemi, O.; Lavigne, M.; Leto, T. L.; Murphy, P. M. The endogenous opioid spinorphin blocks fMet-Leu-Phe-induced neutrophil chemotaxis by acting as a specific antagonist at the N-formylpeptide receptor subtype FPR. *J. Immunol.* **2001**, *167*, 6609-6614.
- (216) Chen, X.; Mellon, R. D.; Yang, L.; Dong, H.; Oppenheim, J. J.; Howard, O. M. Regulatory effects of deoxycholic acid, a component of the anti-inflammatory traditional Chinese medicine Niu Huang, on human leukocyte response to chemoattractants. *Biochem. Pharmacol.* **2002**, *63*, 533-541.
- (217) Chen, X.; Yang, D.; Shen, W.; Dong, H. F.; Wang, J. M.; Oppenheim, J. J.; Howard, M. Z. Characterization of chenodeoxycholic acid as an endogenous antagonist of the G-coupled formyl peptide receptors. *Inflamm. Res.* **2000**, *49*, 744-755.
- (218) Haas, P. J.; de Haas, C. J.; Kleibeuker, W.; Poppelier, M. J.; van Kessel, K. P.; Kruijtzter, J. A.; Liskamp, R. M.; van Strijp, J. A. N-terminal residues of the chemotaxis inhibitory protein of *Staphylococcus aureus* are essential for blocking formylated peptide receptor but not C5a receptor. *J. Immunol.* **2004**, *173*, 5704-5711.
- (219) Zhou, C.; Zhang, S.; Nanamori, M.; Zhang, Y.; Liu, Q.; Li, N.; Sun, M.; Tian, J.; Ye, P. P.; Cheng, N.; Ye, R. D.; Wang, M. W. Pharmacological characterization of a novel nonpeptide antagonist for formyl peptide receptor-like 1. *Mol. Pharmacol.* **2007**, *72*, 976-983.
- (220) Dal Piaz, V.; Giovannoni, M. P.; Castellana, C.; Palacios, J. M.; Beleta, J.; Doménech, T.; Segarra, V. Novel heterocyclic-fused pyridazinones as potent and selective phosphodiesterase IV inhibitors. *J. Med. Chem.* **1997**, *40*, 1417-1421.
- (221) Azzolina, O.; Dal Piaz, V.; Collina, S.; Giovannoni, M. P.; Tadini, C. Chiral resolution and absolute configuration of the enantiomers of 5-acetyl-2-methyl-4-methylsulfinyl-6-phenyl-3(2H)-pyridazinone and evaluation of their platelet aggregation inhibitory activity. *Chirality* **1997**, *9*, 681-685.
- (222) Barlocco, D.; Cignarella, G.; Vinello, P.; Dal Piaz, V.; Giovannoni, M. P.; Malandrino, S.; Barocelli, E.; Chiavarini, M.; Impicciatore, M. Indenopyridazinone derivatives as potential antisecretory and antiulcer agents. *Drug Des. Discov.* **1997**, *15*, 95-103.
- (223) Costantino, L.; Rastelli, G.; Gamberoni, M. C.; Giovannoni, M. P.; Dal Piaz, V.; Vinello, P.; Barlocco, D. Isoxazolo-[3,4-d]-pyridazin-7-(6H)-one as a potential substrate for new aldose reductase inhibitors. *J. Med. Chem.* **1999**, *42*, 1894-900.
- (224) Dal Piaz, V.; Giovannoni, M. P. Phosphodiesterase 4 inhibitors, structurally unrelated to rolipram, as promising agents for the treatment of asthma and other pathologies. *Eur J. Med. Chem.* **2000**, *35*, 463-480.
- (225) Dal Piaz, V.; Castellana, M. C.; Vergelli, C.; Giovannoni, M. P.; Gavaldà, A.; Segarra, V.; Belata, J.; Ryder, H.; Palacios, J. M. Synthesis and evaluation of some pyrazolo[3,4-d]pyridazinones and analogues as PDE 5 inhibitors potentially useful as peripheral vasodilator agents. *J. Enz. Inhib. Med. Chem.* **2002**, *17*, 227-233.
- (226) Dal Piaz, V.; Rascón, A.; Dubra, M. E.; Giovannoni, M. P.; Vergelli, C.; Castellana, M. C. Isoxazolo[3,4-d]pyridazinones and analogues as *Leishmania mexicana* PDE inhibitors. *Farmaco* **2002**, *57*, 89-96.
- (227) Feixas, J.; Giovannoni, M. P.; Vergelli, C.; Gavaldà, A.; Cesari, N.; Graziano, A.; Dal Piaz, V. New pyrazolo[1',5':1,6]pyrimido[4,5-d]pyridazin-4(3H)-ones as potent and selective PDE5 inhibitors. *Bioorg. Med. Chem. Lett.* **2005**, *15*, 2381-2384.
- (228) Giovannoni, M. P.; Vergelli, C.; Biancalani, C.; Cesari, N.; Graziano, A.; Biagini, P.; Gracia, J.; Gavaldà, A.; Dal Piaz, V. Novel pyrazolopyrimidopyridazinones with potent and selective phosphodiesterase 5 (PDE5) inhibitory activity as potential agents for treatment of erectile dysfunction. *J. Med. Chem.* **2006**, *49*, 5363-5371.
- (229) Vergelli, C.; Giovannoni, M. P.; Pieretti, S.; Di Giannuario, A.; Dal Piaz, V.; Biagini, P.; Biancalani, C.; Graziano, A.; Cesari, N. 4-Amino-5-vinyl-3(2H)-pyridazinones and analogues as

7. Bibliographic References

- potent antinociceptive agents: Synthesis, SARs, and preliminary studies on the mechanism of action. *Bioorg. Med. Chem.* **2007**, *15*, 5563-5575.
- (230) Giovannoni, M. P.; Cesari, N.; Vergelli, C.; Graziano, A.; Biancalani, C.; Biagini, P.; Ghelardini, C.; Vivoli, E.; Dal Piaz, V. 4-amino-5-substituted-3(2H)-pyridazinones as orally active antinociceptive agents: synthesis and studies on the mechanism of action. *J. Med. Chem.* **2007**, *50*, 3945-3953.
- (231) Biancalani, C.; Giovannoni, M. P.; Pieretti, S.; Cesari, N.; Graziano, A.; Vergelli, C.; Cilibrizzi, A.; Di Gianuario, A.; Colucci, M.; Mangano, G.; Garrone, B.; Polenzani, L.; Dal Piaz, V. Further studies on arylpiperazinyl alkyl pyridazinones: discovery of an exceptionally potent, orally active, antinociceptive agent in thermally induced pain. *J. Med. Chem.* **2009**, *52*, 7397-7409.
- (232) Giovannoni, M. P.; Vergelli, C.; Cilibrizzi, A.; Crocetti, L.; Biancalani, C.; Graziano, A.; Dal Piaz, V.; Loza, M. I.; Cadavid, M. I.; Díaz, J. L.; Gavaldà, A. Pyrazolo- [1',5':1,6]pyrimido[4,5-d]pyridazin-4(3H)-ones as selective human A₁ adenosine receptor ligands. *Bioorg. Med. Chem.* **2010**, *18*, 7890-7899.
- (233) Cilibrizzi, A.; Quinn, M. T.; Kirpotina, L. N.; Schepetkin, I. A.; Holderness, J.; Ye, R. D.; Rabiet, M. J.; Biancalani, C.; Cesari, N.; Graziano, A.; Vergelli, C.; Pieretti, S.; Dal Piaz, V.; Giovannoni, M. P. 6-methyl-2,4-disubstituted pyridazin-3(2H)-ones: a novel class of small-molecule agonists for formyl peptide receptors. *J. Med. Chem.* **2009**, *52*, 5044-5057.
- (234) El-Gendy, A. A.; Osman, A. N.; Khalifa, M. Synthesis of 3-Indoleacetyl Derivatives of Certain Amino and Phenolic Compounds Likely to Possess Antiinflammatory Activity. *Pharmazie* **1982**, *37*, 481-482.
- (235) Hermeecz, I.; Mészáros, Z.; Vasvári-Debreczy, L.; Horváth, A.; Horváth, G.; Pongor-Csákvári M. Nitrogen bridgehead compounds. Part 4. 1 → 3 N→C-acyl migration. Part 2. *J. Chem. Soc., Perkin Trans. 1* **1977**, 789-795.
- (236) Adams, R.; Pachter, I. J. Ultraviolet Spectra and Structures of the Pyrido [1,2-a]pyrimidones. *J. Amer. Chem. Soc.* **1952**, *74*, 5491-5497.
- (237) Kato, T.; Katagiri, N.; Wagai, A. Synthesis of methylpyridine derivatives-XXXIII Chem. Pharm. Bull. *25*, 203 (1977): Phosphonylation and chlorination of methylpyridine and 3-nitromethylpyridine derivatives. *Tetrahedron* **1978**, *34*, 3445-3449.
- (238) Takahashi, K.; Mitsuhashi, K. Conversion of the carboxyl group to the corresponding trichloromethyl group in the quinoline series. *J. Heterocycl. Chem.* **1977**, *14*, 881-884.
- (239) Conrad, M.; Limpach, L. Beiträge zur Kenntniss des γ -Oxychinaldins. *Berichte* **1888**, *21*, 1965-1984.
- (240) Kato, T.; Katagiri, N.; Wagai, A. Trichloromethylquinolines: Synthesis and Reaction with Trimethyl Phosphite. *Chem. Pharm. Bull.* **1981**, *29*, 1069-1075.
- (241) Baraldi, P. G.; Preti, D.; Tabrizi, M. A.; Fruttarolo, F.; Saponaro, G.; Baraldi, S.; Romagnoli, R.; Moorman, A. R.; Gessi, S.; Varani, K.; Borea, P. A. N₆-[(Hetero)aryl/(cyclo)alkyl-carbamoyl-methoxy-phenyl]-(2-chloro)-5'-N-Ethylcarbox-amido-adenosines: The first example of adenosine-related structures with potent agonist activity at the human A_{2B} adenosine receptor. *Bioorg. Med. Chem.* **2007**, *15*, 2514-2527.
- (242) Galin, F. Z.; Sakhautdinov, I. M.; Tukhvatullin, O.R. Synthesis of pyrrolo[2,1-a]phthalazine-2,6-dione derivative from dioxophthalazine-containing sulfur ylide. *Russ. Chem. Bull.* **2007**, *56*, 2305-2307.
- (243) Choi, W. Y.; Cho, S. D.; Kim, S. K.; Yoon, Y. J. Synthesis and reactions of 1-(2-oxopropyl)pyridazin-6-ones. *J. Heterocycl. Chem.* **1997**, *34*, 1307-1313.
- (244) Lee, S. G.; Kweon, D. H.; Yoon, Y. J. Synthesis of Novel Pyridazine Nucleosides. *J. Hetrocycl. Chem.* **2001**, *38*, 1179-1183.
- (245) Gong, Y.; He, W. A Direct Approach to the Synthesis of 5-Aryl-4-chloropyridazinone: From Microwave Assisted Catalyst Screen to Room Temperature Regio- and Chemoselective Suzuki Arylation. *Heterocycles* **2004**, *62*, 851-856.

- (246) Sotelo, E. Pyridazines. Part 37: Facile solution phase combinatorial synthesis of highly substituted pyridazin-3-ones. *Mol. Divers.* **2004**, *8*, 159-163.
- (247) Mátyus, P.; Maes, B. U. W.; Riedl, Z.; Hajós, G.; Lemièrre, G. L. F.; Tapolcsányi, P.; Monsieurs, K.; Éliás, O.; Dommissie, R. A.; Krajsovsky, G. New Pathways Towards Pyridazino-Fused Ring Systems. *Synlett.* **2004**, *7*, 1123-1139.
- (248) Renzi, G.; Dal Piaz, V. Investigation on some 4,5-disubstituted-3-ethoxycarbonyl isoxaloles. *Gazz. Chim. Ital.* **1965**, *95*, 1478-1491.
- (249) Renzi, G.; Pinzauti, S. New derivatives of the isoxazolo-(3,4-d)-pyridazin-7-one system. *Gazz. Chim. Ital.* **1968**, *98*, 656-668.
- (250) Renzi, G.; Pinzauti, S. New derivatives of the isoxazolo-(3,4-d)-pyridazin-7-one system. *Farmaco Sci.* **1969**, *24*, 885-892.
- (251) Overend, W. G.; Wiggins, L. F. The conversion of sucrose into pyridazine derivatives. Part II. 4-Amino-2-phenyl-6-methyl-3-pyridazinone, 4-Amino-2-(p-nitrophenyl)-6-methyl-3-pyridazine, and their sulfalinamido-derivatives. *J. Chem. Soc.* **1947**, 549-554.
- (252) Reddy, R. S.; Saravanan, K.; Kumar, P. An efficient approach to γ -alkylidene γ -butyrolactones: Application to the syntheses of pyridazinones and diazocinones. *Tetrahedron* **1998**, *54*, 6553-6564.
- (253) Meng, Q.; Hesse, M. N-N Bond Cleavage: A Route to Macrocyclic Dilactams. *Synlett* **1990**, *3*, 148-150.
- (254) Druey, J. Pyridazine in der Arzneimittelsynthese. *Angew. Chem.* **1958**, *70*, 5-13.
- (255) Barberis, M.; Pérez-Prieto, J. Enantioselective synthesis of sabina ketone. *Tetrahedron Lett.* **2003**, *44*, 6683-6685.
- (256) Shinkai, H.; Ozeki, H.; Motomura, T.; Ohta, T.; Furukawa, N.; Uchida, I. 4-(trans-4-Methylcyclohexyl)-4-Oxobutyric Acid (JTT-608). A New Class of Antidiabetic Agent. *J. Med. Chem.*, **1998**, *41*, 5420-5428.
- (257) Singh, S.; Verma, M.; Singh, K. N. Superoxide ion induced oxidation of γ -lactones to γ -ketocarboxylic acids in aprotic medium. *Synthetic Commun.* **2004**, *34*, 4471-4475.
- (258) Grundmann, C. Über Sulfanilamido-pyridazine (Heterocyclische Sulfonamide, I. Mitteil). *Chem. Ber.* **1948**, *81*, 1-11.
- (259) Gouault, N.; Cupif, J. F.; Picard, S.; Lecat, A.; David, M. Synthesis of diverse 4,5-dihydro-3(2H)-pyridazinones on Wang resin. *J. Pharm. Pharmacol.* **2001**, *53*, 981-985.
- (260) Banerjee, P. S.; Sharma, P. K.; Nema, R. K. Synthesis and Anticonvulsant Activity of Pyridazinone Derivatives. *Int. J. ChemTech Res.* **2009**, *1*, 522-525.
- (261) Steiner, G.; Gries, J.; Lenke, D. Synthesis and antihypertensive activity of new 6-heteroaryl-3-hydrazinopyridazine derivatives. *J. Med. Chem.* **1981**, *24*, 59-63.
- (262) Kaupp, G.; Schmeyers, J. Solid-state reactivity of the hydrazine-hydroquinone complex. *J. Phys. Org. Chem.* **2000**, *13*, 388-394.
- (263) Hu, W.; Ralay Ranaivo, H.; Roy, S. M.; Behanna, H. A.; Wing, L. K.; Munoz, L.; Guo, L.; Van Eldik, L. J.; Watterson, D. M. Development of a novel therapeutic suppressor of brain proinflammatory cytokine up-regulation that attenuates synaptic dysfunction and behavioral deficits. *Bioorg. Med. Chem. Lett.* **2007**, *17*, 414-418.
- (264) Steck, E. A.; Brundage, R. P.; Fletcher, L. T. Pyridazine Derivatives. I. Some Amebocidal 3-Pyridazines. *J. Am. Chem. Soc.* **1953**, *75*, 1117-1119.
- (265) Castleman, E. R.; Wiselogle, F. Y. Studies in the Pyridazine Series. The Absorption Spectrum of Pyridazine. *J. Am. Chem. Soc.* **1945**, *67*, 60-62.
- (266) Kaddah, A. M.; Khalil, A. M. Reactions of 3-pyridazinones with aldehydes and Grignard reagents. *Indian J. Chem.* **1977**, *15B*, 1025-1028.
- (267) Overend, W. G.; Wiggins, L. F. The conversion of sucrose into pyridazine derivatives. Part I. 3-Sulfanilamido-6-methylpyridazine. *J. Chem. Soc.* **1947**, 239-244.

7. Bibliographic References

- (268) Sotelo, E.; Fraiz, N.; Yáñez, M.; Terrades, V.; Laguna, R.; Cano, E.; Raviña, E. Pyridazines. Part XXIX: synthesis and platelet aggregation inhibition activity of 5-substituted-6-phenyl-3(2H)-pyridazinones. Novel aspects of their biological actions. *Bioorg. Med. Chem.* **2002**, *10*, 2873-1882.
- (269) Wermuth, C. G.; Leclerc, G. Pyridazine derivatives of therapeutic interest. VI. Synthesis of 2-morpholinoethyl-4-methyl-6-phenyl-3-pyridazone (Ag 246) analogs modified in the aminoalkyl side chain. *Chim. Ther.* **1970**, *5*, 243-246.
- (270) Ismail, M. F.; El Khamry, A. A.; Shams, N. A.; El Sawy, O. M. Base-catalyzed condensation of aromatic aldehydes with 4,5-dihydro-6-methylpyridazin-3(2H)-one. *Indian J. Chem.* **1980**, *19B*, 203-205.
- (271) Ismail, M. F.; Shams, N. A.; El Sawy, O. M. Synthesis of some 3-mercaptopyridazine derivatives. *Synthesis* **1980**, *5*, 410-412.
- (272) Kandile, N. G.; Ahmed, E. A. Synthesis of some new pyridazinones. *Acta Chim. Hung.* **1990**, *127*, 829-835.
- (273) Powell, P.; Sosabowski, M. H. Preparation and reactions of some 2-thienyl- and 3-thienylpyridazinones and -pyridazines. *J. Chem. Res. (S)* **1995**, *8*, 306-307.
- (274) Ismail, M. F.; Shams, N. A.; El Sawy, O. M. Some reactions with 4-(arylmethyl)-6-methylpyridazin-3(2H)-ones. *Egypt. J. Chem.* **1982**, *24*, 223-226.
- (275) Nakanishi, M.; Bolm, C. Iron-catalyzed benzylic oxidation with aqueous tert-butyl hydroperoxide. *Adv. Synth. Cat.* **2007**, *349*, 861-864.
- (276) Ma, M.; Li, C.; Peng, L.; Xie, F.; Zhang, X.; Wang, J. An efficient synthesis of aryl α -keto esters. *Tetrahedron Lett.* **2005**, *46*, 3927-3929.
- (277) Romo, D.; Romine, J. L.; Midura, W.; Meyers, A. I. Diastereoselective cyclopropanations of chiral bicyclic lactams leading to enantiomerically pure cyclopropanes. Application to the total synthesis of CIS-(1S, 3R)-deltamethrinic acid and R-(-)- dictyopterene C. *Tetrahedron* **1990**, *46*, 4951-4994.
- (278) Collomb, D.; Chantegrel, B.; Deshayes C. D. Chemoselectivity in the rhodium(II) acetate catalysed decomposition of α -diazo- β -keto- γ,δ -alkenyl- δ -aryl compounds: Aromatic C-H insertion reaction or wolff rearrangement-electrocyclization. *Tetrahedron* **1996**, *52*, 10455-10472.
- (279) Lerche, H.; Koenig, D.; Severin, T. Reactions with nitroenamines. XII. Reaction of esters and lactones with nitroenamines. *Chem. Ber.* **1974**, *107*, 1509-1517.
- (280) Giovannoni, M. P.; Vergelli, C.; Ghelardini, C.; Galeotti, N.; Bartolini, A.; Dal Piaz, V. [(3-Chlorophenyl)piperazinylpropyl]pyridazinones and Analogues as Potent Antinociceptive Agents. *J. Med. Chem.* **2003**, *46*, 1055-1059.
- (281) Coates, W. J.; McKillop, A. Preparation of 4-amino-3(2H)-pyridazinones by direct amination of 3(2H)-pyridazinones with hydrazine. *Heterocycles* **1989**, *29*, 1077-1090.
- (282) Youssef, A. S. A.; Marzouk, M. I.; Madkour, H. M. F.; El-Soll, A. M. A.; El-Hashash, M. A. Synthesis of some heterocyclic systems of anticipated biological activities via 6-aryl-4-pyrazol-1-ylpyridazin-3-one. *Can. J. Chem.* **2005**, *83*, 251-259.
- (283) Guandalini, L.; Martini, E.; Dei, S.; Manetti, D.; Scapecchi, S.; Teodori, E.; Romanelli, M. N.; Varani, K.; Greco, G.; Spadola, L.; Novellino, E. Design of novel nicotinic ligands through 3D database searching. *Bioorg. Med. Chem.* **2005**, *13*, 799-807.
- (284) Jesberger, M.; Davis, T. P.; Barner, L. Applications of Lawesson's reagent in organic and organometallic syntheses. *Synthesis* **2003**, *13*, 1929-1958.
- (285) Ammazalorso, A.; Amoroso, R.; Bettoni, G.; De Filippis, B. Synthesis of diastereomerically enriched 2-bromoesters and their reaction with nucleophiles. *Chirality* **2001**, *13*, 102-108.
- (286) Tanasova, M.; Yang, Q.; Olmsted, C. C.; Vasileiou, C.; Li, X.; Anyika, M.; Borhan, B. An Unusual Conformation of α -Haloamides Due to Cooperative Binding with Zincated Porphyrins. *Eur. J. Org. Chem.* **2009**, *25*, 4242-4253.

- (287) Bergman, J.; Brynolf, A. Synthesis of chrysogine, a metabolite of *Penicillium chrysogenum* and some related 2-substituted 4-(3H)-quinazolinones. *Tetrahedron* **1990**, *46*, 1295-1310.
- (288) Maes, B.; Lemière, G. Pyridazines and their benzo derivatives. In: *Six-membered rings with two heteroatoms, and their fused carbocyclic derivatives*. Aitken, R. A., Eds.; Elsevier: Amsterdam, **2008**, pp. 1-116.
- (289) Wermuth, C. G.; Leclerc, G.; Schreiber, J. Pyridazine derivatives of therapeutic interest. VII. Synthesis of 2-morpholinoethyl-4-methyl-6-phenyl-3-pyridazone (Ag 246) analogs modified on carbon atoms 4 and 5. *Chim. Ther.* **1971**, *6*, 109-115.
- (290) Laborit, H.; Wermuth, C. G.; Weber, B. P.; Delbarre, B.; Chekler, Cl.; Baron, C.; Rosengarten, H. A psychotropic compound with central and peripheral effect showing anesthetic, anticonvulsant, antiinflammatory, and antiparkinsonian activity and no ventilatory depressive effects. 2-Morpholinoethyl-4-methyl-6-phenyl-3-pyridazone hydrochloride. *Agressologie* **1965**, *6*, 415-460.
- (291) Eloy, F.; Deryckere, A. Thienopyridines. *Bull. SOC. Chim. Belg.* **1970**, *79*, 301-311.
- (292) Robba, M.; Lecomte, J. M.; Cugnon de Sevrécourt, M. Thienopyrimidines. V. Thieno[2,3-d]pyrimidones. *Bull. SOC. Chim. Fr.* **1975**, *3/4*, 587-591.
- (293) Tornøe, C. W.; Davis, P.; Porreca, F.; Meldal, M. α -Azido acids for direct use in solid-phase peptide synthesis. *J. Peptide Sci.* **2000**, *6*, 594-602.
- (294) Freund, H. E.; Arndt, F.; Rusch, R. Selective herbicides. EP, DE 1189312 19650318, **1965**.
- (295) Kozlov, N. S.; Pak, V. D.; Mashevskii, V. V. 1,3-Diaryl-2,2-dihaloethylenimines. *Tr. Perm. Sel'skokhoz. Inst.* **1971**, *79*, 35-40.
- (296) Mashevskii, V. V.; Pak, V. D.; Zalesov, V. S.; Karavaeva, E. G. Products of 1,2-diaryl-3,3-dihaloethylenimine hydrolysis and the study of their physiological action. *Tr. Perm. Sel'skokhoz. Inst.* **1975**, *112*, 51-54.
- (297) Maran, F.; Vianello, E. Electrogenerated carbanions and self-protonation. *Bull. Electrochem.* **1990**, *6*, 276-277.
- (298) Maran, F.; Roffia, S.; Severin, Maria, G.; Vianello, E. Study on a proton transfer reaction between electrogenerated carbon bases and parent nitrogen acids. *Electrochim. Acta* **1990**, *35*, 81-88.
- (299) Okamoto, M. Reversal of elution order during the chiral separation in high performance liquid chromatography. *J. Pharm. Biom. Anal.* **2002**, *27*, 401-407.
- (300) Roussel, C.; Vanthuyne, N.; Serradeil-Albalat, M.; Vallejos, J. C. True or apparent reversal of elution order during chiral high-performance liquid chromatography monitored by a polarimetric detector under different mobile phase conditions. *J. Chromatogr. A* **2003**, *995*, 79-85.
- (301) Collina, S.; Loddo, G.; Urbano, M.; Rossi, D.; Mamolo, M. G.; Zampieri, D.; Alcaro, S.; Gallelli, A.; Azzolina, O. Enantioselective chromatography and absolute configuration of N,N-dimethyl-3-(naphthalen-2-yl)-butan-1-amines: potential sigma1 ligands. *Chirality* **2006**, *18*, 245-253.
- (302) Comini, M.; Pozzoli, C.; Incerti, M.; Rossi, D.; Collina, S.; Azzolina, O.; Di Vittorio, E.; Morini, G.; Poli, E. Stereospecific effects of benzo[d]isothiazolyloxy-propanolamine derivatives at beta-adrenoceptors: synthesis, chiral resolution, and biological activity in vitro. *Chirality* **2009**, *21*, 284-291.
- (303) Azzolina, O.; Collina, S.; Brusotti, G.; Rossi, D.; Callegari, A.; Linati, L.; Barbieri, A.; Ghislandi, V. Chemical and biological profile of racemic and optically active dialkyl-aminoalkylnaphthalenes with analgesic activity. *Tetrahedron: Asym.* **2002**, *13*, 1073-1081.
- (304) Azzolina, O.; Collina, S.; Urbano, M.; Fata, E.; Loddo, G.; Linati, L.; Lanza, E.; Barbieri, A. Highly diastereoselective synthesis of enantiopure naphthyl amino alcohols with analgesic properties. *Chirality* **2006**, *18*, 841-848.
- (305) Cirilli, R.; Ferretti, R.; Gallinella, B.; Turchetto, L.; Bolasco, A.; Secci, D.; Chimenti, P.; Pierini, M.; Fares, V.; Befani, O.; La Torre, F. Enantiomers of C5-chiral 1-acetyl-3,5-diphenyl-4,5-dihydro-(1H)-pyrazole derivatives: Analytical and semipreparative HPLC separation, chiroptical properties, absolute configuration, and inhibitory activity against monoamine oxidase. *Chirality* **2004**, *16*, 625-636.

7. Bibliographic References

- (306) Scapecchi, S.; Nesi, M.; Matucci, R.; Bellucci, C.; Buccioni, M.; Dei, S.; Guandalini, L.; Manetti, D.; Martelli, C.; Martini, E.; Marucci, G.; Orlandi, F.; Romanelli, M. N.; Teodori, E.; Cirilli, R. Synthesis, Affinity Profile and Functional Activity of Potent Chiral Muscarinic Antagonists with a Pyrrolidinylfuran Structure. *J. Med. Chem.* **2010**, *53*, 201-207.
- (307) Qiu, Y. L.; Hempel, A.; Camerman, N.; Camerman, A.; Geiser, F.; Ptak, R. G.; Breitenbach, J. M.; Kira, T.; Li, L.; Gullen, E.; Cheng, Y. C.; Drach, J. C.; Zemlicka, J. (R)-(-)- and (S)-(+)-Synadenol: Synthesis, Absolute Configuration, and Enantioselectivity of Antiviral Effect. *J. Med. Chem.* **1998**, *41*, 5257-5264.
- (308) Ahmadian, H.; Nielsen, B.; Braeuner-Osborne, H.; Johansen, T. N.; Stensbol, T. B.; Slok, F. A.; Sekiyama, N.; Nakanishi, S.; Krogsgaard-Larsen, P.; Madsen, U. (S)-Homo-AMPA, a Specific Agonist at the mGlu6 Subtype of Metabotropic Glutamic Acid Receptors. *J. Med. Chem.* **1997**, *40*, 3700-3705.
- (309) Salas-Coronado, R.; Vasquez-Badillo, A.; Medina-Garcia, M.; Garcia-Colon, J. G.; Noth, H.; Contreras, R.; Flores-Parra, A. Hydrogen bonds and preferred conformation of optically active amides. *J. Mol. Struct. THEOCHEM* **2001**, *543*, 259-275.
- (310) Fadnavis, N. W.; Reddy, N. P.; Bhalerao, U. T. Reverse micelles, an alternative to aqueous medium for microbial reactions: yeast mediated resolution of α -amino acids in reverse micelles. *J. Org. Chem.* **1989**, *54*, 3218-3221.
- (311) Beller, M.; Moradi, W. A.; Eckert, M.; Neumann, H. A new improved palladium-catalyzed amidocarbonylation. *Tetrahedron Lett.* **1999**, *40*, 4523-4526.
- (312) Adam, W.; Roschmann, K. J.; Saha-Moller, C. R. Catalytic asymmetric aziridination of enol derivatives in the presence of chiral copper complexes to give optically active α -amino ketones. *Eur. J. Org. Chem.* **2000**, *3*, 557-561.
- (313) Didsbury, J. R.; Uhing, R. J.; Tomhave, E.; Gerard, C.; Gerard, N.; Snyderman, R. Functional high efficiency expression of cloned leukocyte chemoattractant receptor cDNAs. *FEBS Lett* **1992**, *297*, 275-279.
- (314) Prossnitz, E. R.; Quehenberger, O.; Cochrane, C. G.; Ye, R. D. Transmembrane signalling by the N-formyl peptide receptor in stably transfected fibroblasts. *Biochem. Biophys. Res. Commun.* **1991**, *179*, 471-476.
- (315) Christophe, T.; Karlsson, A.; Rabiet, M. J.; Boulay, F.; Dahlgren, C. Phagocyte Activation by Trp-Lys-Tyr-Met-Val-Met, Acting Through FPRL1/LXA4R, Is Not Affected by Lipoxin A4. *Scand. J. Immunol.* **2002**, *56*, 470-476.

8. SUPPLEMENT :

Solid-Phase Synthesis of Transition State Mimetics in the Quorum Sensing System of Staphylococcus Aureus to Develop Catalytic Antibodies

7-months training period at Chemistry Department of the
University of Cambridge

Supervisor: Dr. David R. Spring

Tutor: Dr. Albert Isidro-Llobet

8.1 INTRODUCTION

8.1.1 Antibiotics today: an overview

The development of antibacterial agents is arguably one of the greatest successes of the 20th century medicine.¹ Antibiotic drugs have played an essential role in the global increase in life expectancy and quality that has occurred over the last century.² However, since the “glory days” of antibiotic discovery in the 1960s and 1970s, there has been a sharp decline in investment for new antibacterial interventions by the large pharmaceutical companies. Concomitantly, the incidence of resistance among clinical isolates against conventional antibiotics is on the increase.³ Indeed, bacteria have quickly become resistant to the most commonly prescribed antibiotics.⁴ As a result, we are left with a legacy of relatively few efficacious drugs and,¹ unfortunately, pathogens continue to adapt faster than new antimicrobial agents can be developed to control them.⁵ Thus, bacterial infection, particularly from multi-drug resistant strains, remains a serious threat to human lives.^{1,4} Indeed, the scarcity of new antibiotic products has prompted some commentators to refer to an impending “pharmageddon” and to an impending return to the “pre-antibiotic” era, at least for the treatment of some bacterial organisms. Consequently, the development of novel therapies for the treatment of human bacterial infections is of paramount importance.⁶

Existing antibiotics generally inhibit bacterial cellular processes that are essential for microbial survival.^{7,8} An inherent problem with this approach is that it creates a selection pressure for drug-resistant mutations.^{9,10} Antivirulence therapies seek to address this issue.^{7,8} These methods aim to target bacterial systems associated with virulence rather than essential cellular process and the hope is that such strategies will reduce selective survival pressures and slow the development of resistance.¹¹

Over the last decade, the work of many groups has shown that systems associated with virulence in bacteria are valid targets for the development of new antibacterial agents. Although virulence is a multi-factorial phenotype, in many clinically-relevant bacteria the trait is controlled by a relatively small number of signalling pathways.^{12,13} Crucially for the current proposal, small molecules are often found at the apex of these signalling pathways, so that theoretically by eliminating these compounds from the growth medium, the virulence of the organism in question should be reduced. Indeed, disruption of these signalling pathways, either through mutation or through chemical intervention, is a proven way of diminishing the pathogenicity of a number of organisms and facilitating their immune clearance from the infected host. In addition, to reduce the selection pressure for drug-resistant mutations, non-lethal alternatives to antibiotic interventions are an attractive therapeutic strategy as well because, by specifically targeting virulence, it is possible to decrease the potential negative impact of treatment on the patient.¹² Recent years have witnessed a growing realisation that antivirulence therapies represent a

8. Supplement

potentially valuable alternative to traditional antibiotic methods for the treatment of bacterial infections. In this context, bacterial quorum sensing (QS) systems offer an attractive target.^{14,15}

8.1.2 Quorum sensing (QS)

QS is a method of intercellular communication employed by many species of bacteria. This signalling process is used by bacterial colonies to coordinate gene expression in a cell density-dependent manner.¹⁶⁻¹⁸ Several clinically relevant pathogens use quorum-sensing systems to regulate processes associated with virulence.¹⁹ However, quorum sensing is not directly involved in biological processes that are essential for bacterial survival.^{20,21} Thus, selective disruption of QS (so-called “*quorum quenching*”) using non-native small molecule entities represents a strategy to attenuate bacterial pathogenicity without imposing an intense selective pressure for the development of resistant mutants,^{22,23} compared to existing antibiotic treatments.²⁴

Quorum sensing is mediated by small diffusible molecules termed *autoinducers*. These small molecule entities are synthesized intracellularly (throughout the growth of the bacteria) and released into the surrounding growth medium. The extracellular concentration of the small molecules led to an increase of the cell density. In fact, when this concentration exceeds a certain value, the accumulated signal molecules are sensed by specific receptors on the bacterial.²⁵ The binding of the autoinducers to the receptors occurs and starting from this, a signal transduction cascade leads to a change in gene expression.^{15,26,27} In this way, the bacterial population reaches a critical “threshold” cell density which is of primary importance for its virulence.

In the case of pathogens, QS-controlled genes often encode virulence factors.²⁸ Indeed, virulence factor production in several clinically relevant pathogenic bacteria including *Staphylococcus aureus*, *Clostridium difficile* and *Pseudomonas aeruginosa* is known to be regulated by QS systems. In this scenario, at low cell densities, the cells do not produce virulence factors and therefore appear “innocent” to the host. However, once the population becomes quorate, the QS system simultaneously stimulates virulence factor production, ensuring that the population as a whole produces a welter of tissue-damaging proteins in a highly coordinated and cooperative manner.²⁹⁻³² Nature is known to have evolved quorum-quenching enzyme that are capable of hydrolyzing quorum sensing QS molecules and,^{23,33-35} recently, the concept of quorum quenching using the catalytic antibody technology directed towards the development of functionally equivalent “unnatural” enzymes, has been introduced.³⁶⁻³⁸ This approach uses small molecules as haptens to elicit antibodies capable of catalyzing QS molecules hydrolysis and thus inhibit quorum sensing. The hypothesis underpinning this aim is that by selectively depleting these small molecules from the site of bacterial infection, the invading organism will be made less aggressive

allowing the host immune system a better chance of clearing the infection before the bacteria cause too much tissue damage.

8.1.3 Catalytic antibodies through Transition State (TS) mimetics

Catalytic antibodies or “abzymes” are essentially tailor-made biological catalysts capable of accelerating the rate of a specific chemical reaction by preferentially stabilizing the transition state of the intended “natural” substrate to product conversion,³⁷ following the same way of enzymes. Although several abzymes, that catalyze a variety of chemical transformations, have been generated, the most active antibodies have usually been found to provide rate enhancements for reactions with intrinsically low activation energy barriers.³⁶ That is, abzymes generally catalyze reactions that happen at a slow, but measurable rate under ambient conditions. The procurement of catalytic antibodies for a specific reaction typically requires the use of a molecule which has been designed to be a stable mimic of the transition state structure associated with the reaction.³⁹ The aim is to obtain antibodies that bind to this transition state analogue with high affinity; such antibodies should therefore be able to bind tightly to, and preferentially stabilise, the transition state of the reaction of interest thus decreasing the activation energy barrier to the process (**figure 8.1**).⁴⁰⁻⁴³ Since abzymes are far more structurally-constrained than their enzyme counterparts, their catalytic activity is often relatively poor in comparison with the latter. However, they still provide rate enhancements of 10^4 or more over the uncatalyzed reaction and they have proven therapeutic potential in the treatment of drug addiction.⁴⁴

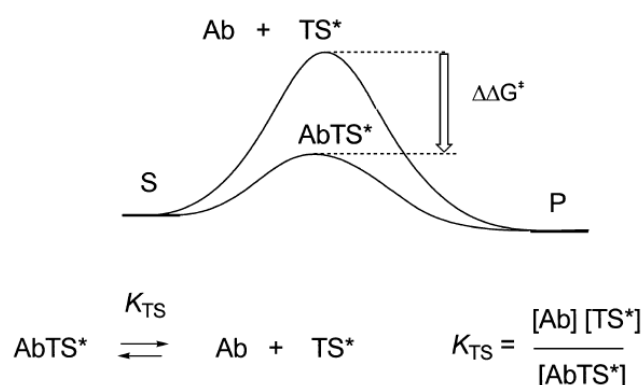


Figure 8.1. Energy diagram for an antibody-catalyzed and uncatalyzed transformation of a substrate S to a product P proceeding via a transition state (TS^*) or an antibody-bound transition state (Ab.TS^*). The catalytic effect of the antibody is given by $\Delta\Delta G^*$, which corresponds to the transition state dissociation constant K_{TS} . Adapted from Reymond (2002).⁴⁴

The improved pharmacological potential of many abzymes (compared to non host-derived enzymes) comes from the fact that, as in much of the proposed work, they can be based around a human antibody framework and are therefore not targets for immune clearance. A more recent work has shown that the

8. Supplement

kinetic parameters of abzymes can be improved through targeted design strategies, and it is now clear that in some cases, residues in the substrate-binding site can also make additional catalytic contributions through, for example, acid-base catalysis.⁴⁵

8.1.4 Transition state mimetics and *quorum quenching*

In principle, if stable small molecules that mimic the transition states associated with possible decomposition pathways of autoinducers can be synthesized, it should be possible to use these molecules to generate catalytic antibodies capable of degrading said autoinducers (“*quorum quenching*”), thereby interfering with the quorum sensing process. Since different species of bacteria generally use different autoinducer molecules, the nature of the transition state mimics required to elicit catalytic antibodies is species-dependent. In this work we focused upon quorum sensing in the Gram positive bacterium *Staphylococcus aureus* where stable structural moieties that mimic the transition states associated with the degradation reaction of the autoinducers need to be identified.⁵

8.1.5 Quorum sensing in *Staphylococcus aureus*

Staphylococcus aureus is a prevalent and highly adaptable Gram-positive bacterium responsible for numerous clinical infections.⁴⁶ It is one of the most dreaded pathogens in hospitals and causes more nosocomial infections than any other Gram-positive bacterium. Methicillin-resistant strains of *S. aureus* (MRSA) represent an important problem, since infections can advance so rapidly that they become life-threatening before clinical intervention can be realised. The treatment issue is compounded by the fact that MRSA strains are resistant to most clinically-used β -lactam antibiotics, so vancomycin, “*the antibiotic of last resort*”, is often the necessary choice of treatment. Worryingly, vancomycin-resistant *S. aureus* strains are now also appearing in hospitals, reinforcing the need for new anti-staphylococcal interventions. The emergence of antibiotic resistance in this and other species has become a serious concern in the medical community.⁶

Various aspects of virulence in *S. aureus* are known to be regulated by a quorum sensing system which employs small autoinducing (oligo)peptides (AIPs), comprised of 7-10 amino acid residues, as the signalling molecules. AIPs function as extracellular signalling molecules that allow individual cells to sense the surrounding population density. Once a “*quorum*” of cells has been achieved, the bacteria modulate their gene expression to facilitate cooperative behaviours that confer survivability to the developing colony.⁴⁷ The discovery of this global regulatory system for virulence in *S. aureus* has provided an avenue for interrupting these defenses.^{48,49} AIP mimics that perturb this system would be useful chemical probes and could potentially be developed for therapeutic applications.⁵

8.1.6 Autoinducing (oligo)peptides (AIPs)

The quorum sensing circuit outlined in **figure 8.2** represent the basic paradigm for AIP-mediated signalling in *S. aureus*. QS in *S. aureus* is encoded by the accessory gene regulator (*agr*) locus.⁵⁰ Each bacterium secretes AIPs that accumulate in the extracellular environment. Once these ligands reach a threshold concentration, they will bind productively to a cognate receptor protein located on the cell exterior named AgrC. AIP binding activates a two-component intracellular signalling system that up-regulates the production of virulence determinant-encoding genes (including genes that encode toxins, host cell-adhesion factors and extracellular hemolytic/proteolytic enzymes) and also up-regulates production of the four *agr* proteins (AgrA-D).

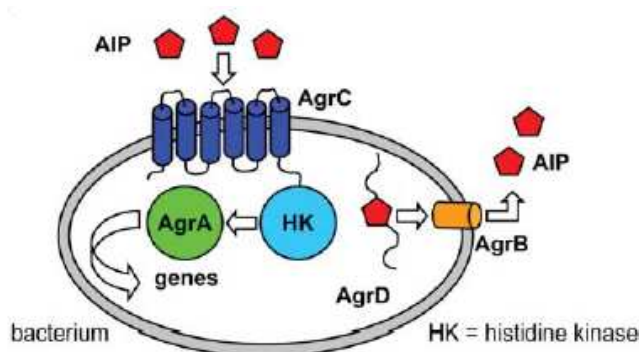


Figure 8.2. Proposed mechanism of the two-component *agr* autoinduction system in *S. aureus*. AgrB processes the propeptide AgrD to generate an AIP and secretes it into the extracellular environment. The AIPs bind to the AgrC receptor, a histidine-kinase that phosphorylates the intracellular response regulator AgrA. This second signalling component then promotes gene transcription that induces virulence and produces the *agr* proteins, completing the autoinduction circuit. Adapted from Gorske and Blackwell (2006).⁵

The *agr*-mediated QS systems in *S. aureus* have evolutionarily diverged into four different sub-groups (AIP-I/IV) (**figure 8.3**).

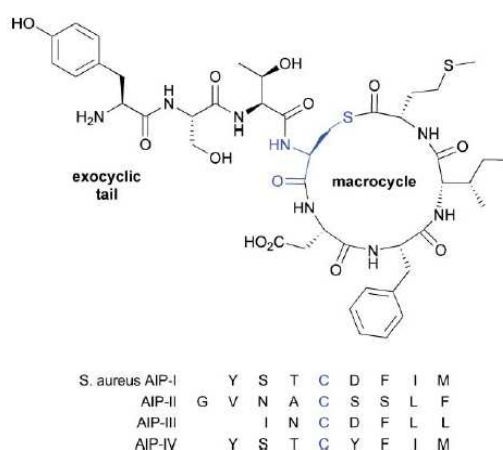


Figure 8.3. Chemical structure of AIP-I and peptide sequences of AIPs I through IV. The cysteine residue that forms the thiolactone is highlighted in blue. Adapted from Gorske and Blackwell (2006).⁵

Each sub-group is associated with a distinct AIP. However, in all cases, the AIPs have a similar core structure; they all comprise a macrocyclic thiolactone and a conjoined linear tail moiety. The macrocycle

appears to be the main determinant required for molecular recognition by the membrane receptor AgrC, while the exocyclic peptide moiety is required for receptor activation. The conserved thiolactone is labile and it is known that cleavage of this ring abolishes agonistic activity in the AIPs. Thus the thiolactone ring moiety is an excellent target for the development of catalytic antibodies. If stable small molecules that mimic possible transition states associated with the rate determining steps of thiolactone ring hydrolysis can be identified, in theory, these could be used to elicit antibodies that are capable of catalysing this hydrolysis step, thereby inhibiting QS in *S. aureus* and thus attenuating its virulence.^{5,51}

8.2 BACKGROUND AND AIMS OF THE PROJECT

The main goal of the proposed study is the synthesis of transition state (TS) mimetics of the degradation reaction of the AIPs, that could potentially be used to elicit catalytic antibodies capable to attenuate the expression of virulence determinants in the Gram positive bacterium *S. aureus*. To achieve this aim, our primary experimental objective was the synthesis of macrocyclic phosphopeptides as new structural peptidomimetic analogues that mimic the *transition state* associated with the degradation of AIPs involved in the population cell density-control of *S. aureus*. This approach will hopefully reduce or abolish the expression of virulence determinants associated with the AIPs and allow the establishment of structure-activity relationships (SARs) in these systems, to better understand quorum sensing signalling pathway and be able to develop new peptidomimetic inhibitors.

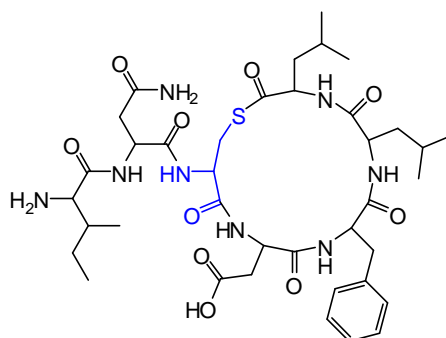


Figure 8.4. Structure of the natural autoinducing (oligo)peptide **AIP-III**. The cysteine residue that forms the thiolactone is highlighted in blue.

AIP-III (**figure 8.4**) was chosen as the reference peptide, because it is the substrate of EMRSA-16, an important Methicillin-resistant *S. aureus* strain available at the Biochemistry Department of the University of Cambridge and because all the AIP peptides have a similar core structure being the macrocycle the main determinant required for the activity. Therefore, one of the aims of the project was the total synthesis of the natural substrate (**AIP-III**),⁵² to use it as reference in the biological tests, following a Fmoc/*t*-Bu solid-phase synthesis.⁵¹ The thioester group (**figure 8.4**), as previously mentioned, is an excellent target to develop catalytic antibodies since cleavage of the thiolactone ring

abolishes agonistic activity of the AIPs. As phosphate derivatives are structurally similar to thioester bonds, the most important aim of this project is the synthesis, using a Fmoc/*t*-Bu solid-phase strategy, of two phosphorus **AIP-III** analogues as potential TS mimetics (**figure 8.5**).⁵³

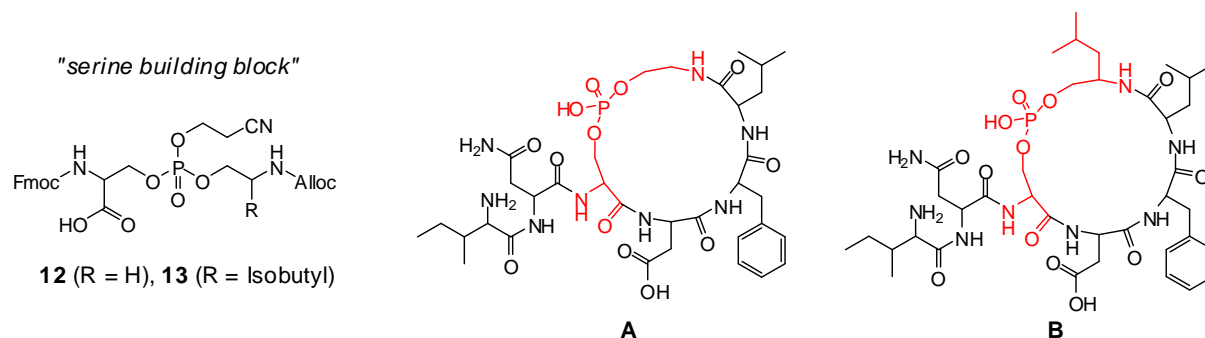


Figure 8.5. Structures of the “serine building blocks” and the two **AIP-III** analogues designed (**A** and **B**). The phosphodipeptide inserted in the macrocycle is highlighted in red. The structure **A** is reported as **23** in the **section 8.3.2.2** (**scheme S.5**).

In these new molecules the thioester group is replaced by a phosphate group, previously built in a “serine building block” (**figure 8.5**). It should be noted that the two new macrocycles, compared to the natural peptide, have two members more, one O and one CH₂ but the size of the cycle does not seem to be crucial for the activity.⁵²

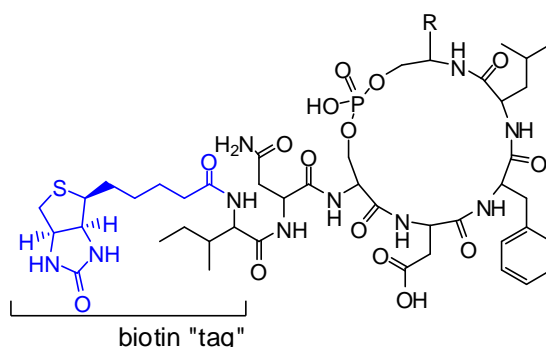


Figure 8.6. The biotinylated variants of the **AIP-III** analogue designed.

The transition state mimetics will be tested to evaluate their activity as quorum quenching agents and later on will be attached to a biotin-tag (**figure 8.6**) for phage library screening.²³

8.3 CHEMISTRY

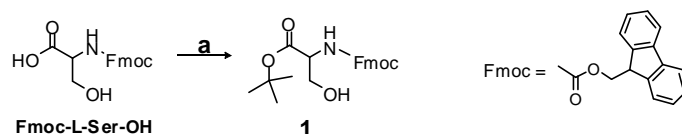
The chemistry of this project is divided in 3 parts: synthesis of the “serine building blocks” (**section 8.3.1**), synthesis of the phosphorus cyclic peptides (**section 8.3.2**), synthesis of the natural substrate (**AIP-III**) (**section 8.3.3**).

8.3.1 Synthesis of the “serine building blocks”

The two “serine building blocks” (**figure 8.5**) which will be incorporated in the phosphorus cyclic peptides were prepared following the synthetic pathways depicted in **schemes S.1-S.3**.

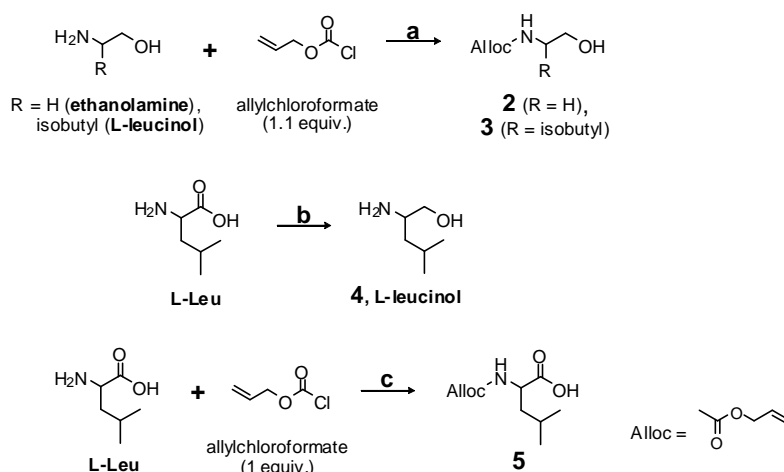
8.3.1.1 Protection of the starting amino acids and amino alcohols

N- α -Fmoc-serine-*t*-butyl ester **1** (**scheme S.1**) was readily obtained in quantitative yield following the literature.⁵⁴



Scheme S.1. Reagents and conditions: a) *t*-Butyl-trichloroacetimidate (4 equiv), CHX/EtOAc, rt, o/n.

On the other hand, reaction of the amino alcohols, ethanolamine and L-leucinol (obtained in quantitative yield by reduction of L-leucine,⁵⁵ **scheme S.2**), with allyl chloroformate yielded the corresponding Alloc protected ethanolamine (**2**) and L-leucinol (**3**) with 97% and 86% yield respectively after purification by flash chromatography (**scheme S.2**).⁵⁶ The Alloc group was chosen because its Pd catalyzed removal is compatible with Fmoc/*t*-Bu solid-phase strategy that will be used in the phosphopeptides synthesis.⁵⁷



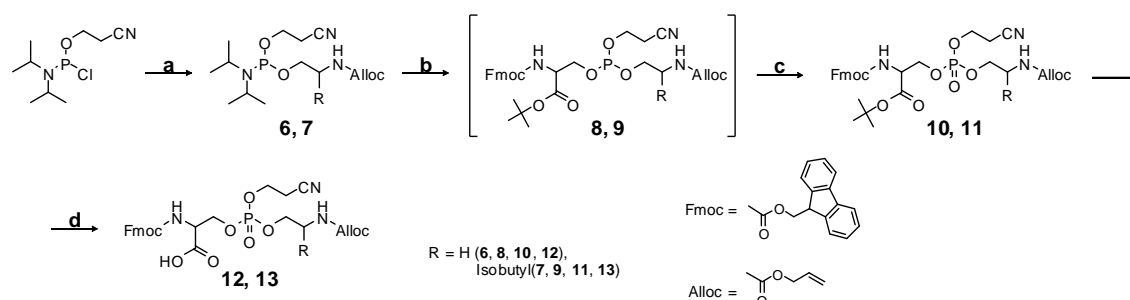
Scheme S.2. Reagents and conditions: a) NaHCO₃ (1.1 equiv), dioxane/water (1:1), 0 °C → rt, 3 h, b) LiBH₄ (2 equiv), trimethylsilyl chloride (4 equiv), THF anhydrous, 0 °C → rt, 16 h, c) NaN₃ (1.5 equiv), dioxane/water, Na₂CO₃ 1% in water, rt, 1 d (10% Na₂CO₃ in water is added to keep the pH between 8-10).

Another necessary building block for the phosphopeptide synthesis was Alloc-L-Leu-OH, which was obtained in 77% yield by reaction of in situ generated allyl carbonazidate with L-leucine (**scheme S.2**).⁵⁸

8.3.1.2 Phosphorus couplings

The desired “*serine building blocks*” were obtained in 4 synthetic steps (**scheme S.3**) using the commercially available 2-cyanoethyl-*N,N*-diisopropyl-chlorophosphoramidite as the phosphorus source.⁵⁹⁻⁶¹ The first reaction is a coupling of the Alloc-ethanolamine (**2**) or Alloc-L-leucinol (**3**) on the 2-cyanoethyl-*N,N*-diisopropyl-chlorophosphoramidite (**scheme S.3**).^{62,63} The purified products must be stored under N₂ at -20 °C, since they decompose to complex mixtures after few days at room temperature.

The following reaction of of *N*- α -Fmoc-serine-*t*-butyl ester **1** with compounds **6** and **7** (scheme S.3) was performed in the presence of tetrazole.^{64,65}



Scheme S.3. Reagents and conditions: **a)** Alloc-ethanolamine (**2**) or Alloc-L-leucinol (**3**) (0.7 equiv), DIPEA (4.7 equiv), CH_2Cl_2 anhydrous, N_2 , rt, 2-3 h; **b)** Fmoc-L-Ser-*t*-Bu ester (**1**) (1 equiv), tetrazole (1.2 equiv), THF anhydrous, N_2 , rt, o/n; **c)** *t*-BuOOH, THF anhydrous, N_2 , rt, 3-4 h; **d)** TFA (20 equiv), CH_2Cl_2 , rt, 2-3h.

When explosive tetrazole was replaced by 4,5-dicyanoimidazole, the crude product obtained was much less pure both by ^1H NMR and TLC.⁶⁶ The obtained phosphite intermediates **8** and **9** are unstable trivalent phosphorus species which could be isolated by flash chromatography on silica gel, but it is more convenient to oxidize them straight away to afford the more stable pentavalent species **10** and **11** (scheme S.3).^{61,67} *m*-CPBA was initially used as an oxidizing agent but the yields were very low. In contrast, when *tert*-butyl hydroperoxide was used, fully protected phospho-amino acids **10** (R = H) and **11** (R = Isobutyl) were obtained in 57 and 20% yield respectively over two steps (scheme S.3). Subsequent treatment of **10** and **11** with 50% trifluoroacetic acid afforded the free acids **12** (R = H) and **13** (R = Isobutyl). It is important to note that compounds **10**, **11** and the corresponding free carboxylic acids (**12** and **13**) were obtained as diastereomeric mixtures because the chiral centre on the phosphorus was present in its 2 configurations. These diastereomeric mixtures were inseparable by flash chromatography or HPLC and made the ^1H NMR analysis more complex. However, once the cyanoethyl group was removed during the treatment with piperidine to remove the Fmoc group, performed in the phosphopeptide synthesis (scheme S.4), the phosphorus center is no longer chiral, leading to only one stereoisomer of the desired phosphopeptide.

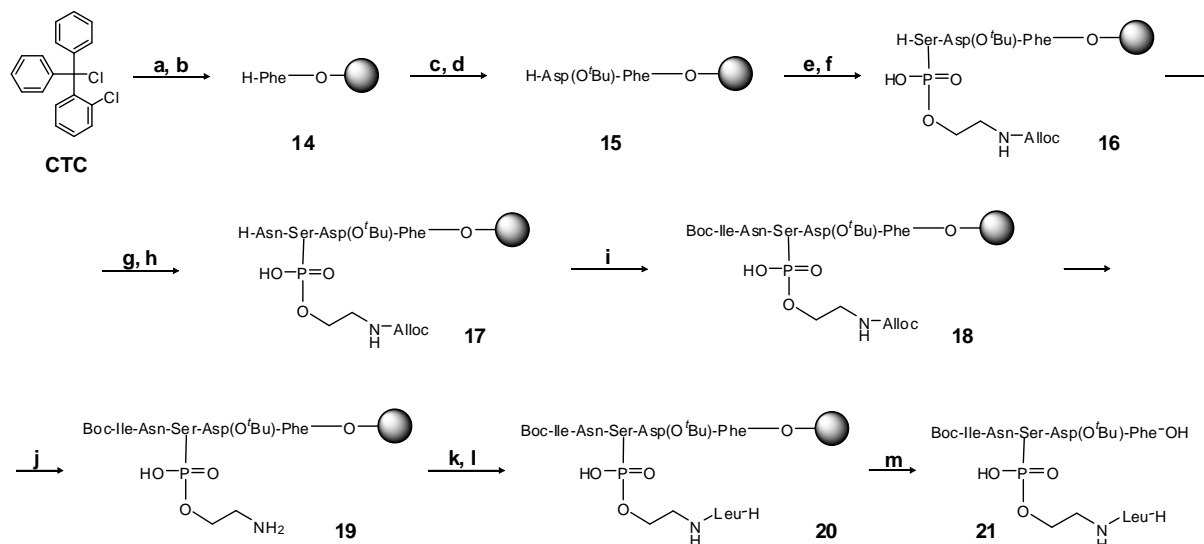
8.3.2 Synthesis of the phosphorus cyclic peptides

Linear and branched solid-phase syntheses of AIPs analogues using different orthogonal protecting schemes have been described in literature.^{51,68} In most of them the cyclization and final deprotection are performed in solution.^{5,51,52} We decided to adapt these strategies to the synthesis of phosphorus analogues of **AIP-III**. Our strategy is divided in two main parts: 1) Fmoc/*t*-Bu solid-phase synthesis of branched peptides (scheme S.4); 2) Cyclization and final deprotection in solution (scheme S.5). In the latter case,

the final cyclization is carried out through the formation of an amide bond between L-leucine and L-phenylalanine and there is no risk of a five-member ring formation.

8.3.2.1 Fmoc/*t*-Bu solid-phase synthesis of the branched peptides

Solid-phase synthesis of protected peptides requires a resin that facilitates the cleavage of the peptide without removing the side-chain protecting groups.^{69,70} The resin of choice was the commercially available super-acid-labile chlorotriptyl chloride polystyrene (CTC) resin (**scheme S.4**) which allows the release of peptides with 1-2 % of TFA in CH₂Cl₂ or even with trifluoroethanol solutions.^{71,72} An additional advantage of the CTC resin is that its hindered structure minimizes the formation of diketopiperazines (DKP) during removal of the temporary protecting group of the second amino acid.^{73,74} The Fmoc/*t*-Bu solid-phase strategy involves the use of the base labile Fmoc group for α -amino protection and *t*-Bu-based protecting groups for side chain protection. *t*-Bu-based protecting groups are highly convenient because they are removed with high concentrations of trifluoroacetic acid (TFA) in the presence of scavengers, being stable to piperidine, used to remove the Fmoc group, and to low concentrations of TFA, used to cleave the peptide from the CTC resin. In addition, they are also stable to the Pd(0) treatment required to remove the Alloc group. The branched approach depicted in **scheme S.4** was chosen in order to avoid the risk of cyclization on the free phosphate group which would lead to a stable five-member ring.



Scheme S.4. Reagents and conditions: **a)** Fmoc-L-Phe-OH (0.7 equiv), DIPEA (2.1 + 4.2 equiv), CH₂Cl₂, rt, 45 min; **b)** **Fmoc-removal:** piperidine-DMF (2:8, v/v) (1 x 2 min, 2 x 10 min); **c)** Fmoc-L-Asp-(O-*t*-Bu) (4 equiv), ethylcyanoglyoxylate-2-oxime (4 equiv), DIC (4 equiv), DMF, rt, 1.5 h; **d)** Fmoc-removal; **e)** **12** (3 equiv), PyAOP (3 equiv), DIPEA (3 + 6 equiv), DMF, rt, 2 h; **f)** Fmoc-removal; **g)** Fmoc-L-Asn-OH (4 equiv), ethylcyano-glyoxylate-2-oxime (4 equiv), DIC (4 equiv), DMF, rt, 1.5 h; **h)** Fmoc-removal; **i)** Boc-L-Ile-OH (4 equiv), ethylcyanoglyoxylate-2-oxime (4 equiv), DIC (4 equiv), DMF, rt, 1.5 h; **j)** **Alloc-removal:** Pd(PPh₃)₄ (0.1 equiv), PhSiH₃ (10 equiv), CH₂Cl₂ (3 x 15 min); **k)** Alloc-L-Leu-OH (**5**) (4 equiv), ethylcyanoglyoxylate-2-oxime (4 equiv), DIC (4 equiv), DMF, rt, 1.5 h; **l)** Alloc-removal; **m)** TFA:Et₃SiH:CH₂Cl₂ (1:1:98), rt, 1h.

The first coupling of Fmoc-L-Phe-OH on the resin was carried out using DIPEA as a base. The following amino acid-couplings were performed using diisopropylcarbodiimide (DIC), to activate the carboxylic group, and ethylcyanoglyoxylate-2-oxime, to minimize the epimerization. This new “*anti-epimerization agent*” has recently been reported to be a more efficient non-explosive alternative to the commonly used HOBt or HOAt.⁷⁵

The couplings of the phosphorus building blocks **12** and **13** (**scheme S.3**) were performed using PyAOP and DIPEA (**scheme S.4**). Phosphonium derivatives such as PyAOP are more convenient for slow couplings compared with aminium/uronium reagents such as HATU, since this latter can terminate the peptide chain through a guanidination reaction.⁷⁶ Furthermore, PyAOP contains HOAt, which is the most reactive benzotriazole.⁷⁷ Unfortunately, the coupling reaction worked fine only for building block **12** but not for the more hindered **13**.

The Chloranil test for detection of primary and secondary amines was performed after each coupling to confirm the coupling completion.⁷⁸⁻⁸⁰ When the test was negative (absence of free amines) the Fmoc group was removed with piperidine-DMF (2:8, v/v). Otherwise the corresponding Fmoc-amino acid was re-coupled in the same conditions. It should be noted that the phosphate only loses the β -cyanoethyl protecting group (**scheme S.3** and **S.4**) after the piperidine-induced Fmoc removal.^{66,81} This α -elimination removal of the cyanoethyl group allowed the solid phase synthesis of the remaining phosphoserine peptide using Fmoc-based chemistry.⁸²⁻⁸⁴ Washings between deprotection, coupling and again deprotection steps were performed with DMF and CH₂Cl₂. The Alloc group was removed by Pd(0), using a catalytic amount of Tetrakis(triphenylphosphine)-palladium(0), in rather neutral conditions and in the presence of phenylsilane as a scavenger of the allyl carbocations (**scheme S.4**).^{85,86} Washings after deprotection steps were performed using CH₂Cl₂, DMF and a solution 0.02 M of sodium diethyldithiocarbamate in DMF. Peptide synthesis transformations and washings were always done at 25 °C. Synthesis carried out on solid-phase were controlled by HPLC of the intermediates obtained after cleaving an aliquot (approximately 2 mg) of the peptidyl-resin with TFA/Et₃SiH/CH₂Cl₂ (1:1:98) for 1 hour (**scheme S.4**). The required polymer-bound branched protected peptide **22** obtained via standard Fmoc/*t*-Bu solid-phase peptide assembly was subsequently treated with TFA/Et₃SiH/CH₂Cl₂ (1:1:98 v/v) for 1 hour. This step resulted in the chemoselective acidolysis of the 2-chlorotrityl ester resin linkage and afforded the partially protected heptapeptide **21** in typically quantitative yields. Partial purification of **21** was accomplished by filtration of the acidolytic resin suspension into pyridine-methanol (1.5:75 v/v) and evaporation of the filtrate to dryness in vacuo. A small fraction of the dried partially protected peptide **21** was exposed to TFA/H₂O/Et₃SiH (90:5:5) for 1 h to remove the protecting groups, followed by HPLC-UV analysis, which revealed a peptide purity >80%.

8.3.2.2 Macrocyclization

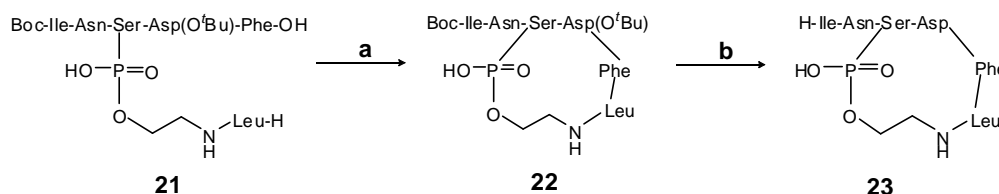
The cyclization of the branched peptide **21** was the limiting step of this synthetic strategy. As shown in **table 8.1**, several macrocyclization conditions were screened. Even when the desired cyclic product was detected, it was part of very complex mixtures.

	Coupling reagents	solvent	time	work up	HPLC-UV-MS results
1	<i>N</i> -polystyrene methyl- <i>N'</i> -cyclohexylcarbo-diimide (e equiv), DMAP (0.1 equiv), HOAt (5 equiv)	CHCl ₃	2 d	filtration and evaporation	CM*. No branched (SM [§]) and no cyclic peptide (22)
2	<i>N</i> -polystyrene methyl- <i>N'</i> -cyclohexylcarbo-diimide (5 equiv), DMAP (0.1 equiv), Ethylcyanoglyoxylate-2-oxime (5 equiv)	CHCl ₃	2 d	filtration and evaporation	CM. No branched peptide (SM). The peak of 22 is too weak.
3	<i>N</i> -polystyrene methyl- <i>N'</i> -cyclohexylcarbo-diimide (5 equiv), DMAP (0.1 equiv)	CHCl ₃	3d	filtration and evaporation	CM. No branched peptide (SM). The peak (+ Na) of 22 is big enough to be detected.
4	<i>N</i> -polystyrene methyl- <i>N'</i> -cyclohexylcarbo-diimide (5 equiv), DMAP (0.1 equiv), HOAt(5 equiv)	CH ₂ Cl ₂	1 d	filtration and evaporation	CM. No cyclic peptide (22). The SM is still in a high amount.
5	<i>N</i> -polystyrene methyl- <i>N'</i> -cyclohexylcarbo-diimide (5 equiv), DMAP (0.1 equiv)	CH ₂ Cl ₂	1 d	filtration and evaporation	CM. No branched (SM) and no cyclic peptide (22)
6	<i>N</i> -polystyrene methyl- <i>N'</i> -cyclohexylcarbo-diimide (5 equiv), HOAt (5 equiv)	CH ₂ Cl ₂	1 d	filtration and evaporation	CM. No branched (SM) and no cyclic peptide (22)
7	EDC (5 equiv), DMAP (0.1 equiv), HOAt (5 equiv)	CH ₂ Cl ₂	1 d	Extraction with citric acid and H ₂ O, evaporation	CM. The SM is still in a high amount.
8	EDC (5 equiv), DMAP (0.1 equiv)	CH ₂ Cl ₂	1 d	Extraction with citric acid and H ₂ O, evaporation	CM. No branched (SM) and no cyclic peptide (22)
9	EDC (5 equiv), DMAP (0.1 equiv)	CHCl ₃	2 d	Extraction with citric acid and H ₂ O, evaporation	CM. No branched (SM) and no cyclic peptide (22)
10	PyAOP (1 + 1 equiv), DIEA (2 equiv)	CH ₂ Cl ₂	1 d	Extraction with H ₂ O, evaporation	CM. No branched (SM) and no cyclic peptide (22)
11	DIC (5 equiv), HOAt (5 equiv)	CH ₂ Cl ₂	1 d	evaporation	CM. The peak of 22 is big enough to be detected.

Table 8.1. Macrocyclization conditions screened for the synthesis of transition state mimetic **23** [* CM = complex mixture; [§] SM = starting material (**21**)].

On the basis of the screening, we concluded that the methods based on *N*-polystyrene methyl-*N'*-cyclohexylcarbodiimide/DMAP (**entry 3, table 8.1**) or DIC/HOAt (**entry 11, table 8.1**) as coupling reagents gave better results because, although we had always a very complex crude mixture to purify, it was possible to detect the peak of the right cyclic peptide, after hydrolysis of the protecting groups (Boc and *t*-Bu), by UV and mass spectrometry HPLC analysis. Therefore, for the purpose of the this dissertation, only these cyclization conditions will be described in detail. In the first case, macrocyclization was achieved by exposing a dilute solution of **21** in CHCl₃ (2 mM) to *N*-polystyrene methyl-*N'*-cyclohexylcarbodiimide, a commercially available polymer-supported carbodiimide analogue

of *N*-polystyrene methyl-*N'*-isopropylcarbodiimide,^{87,88} in the presence of 4-dimethylaminopyridine (DMAP) for 3 days at room temperature (**scheme S.5**). In the second case macrocyclization was carried out always by exposing a dilute solution of **21** in CH₂Cl₂ to DIC in the presence of 7-aza-1-hydroxybenzotriazole (HOAt) (**scheme S.5**).⁸⁹

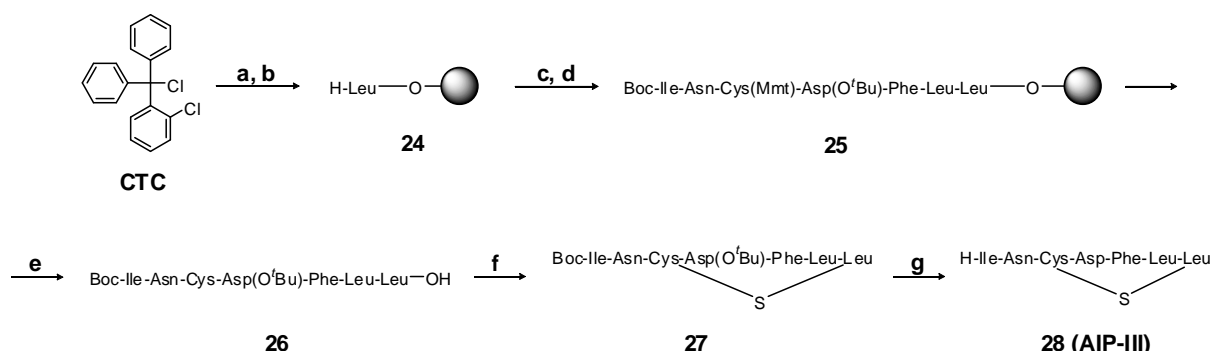


Scheme S.5. Reagents and conditions: a) see **table 8.1**; b) TFA:Et₃SiH:H₂O (90:5:5), rt, 1-1.5 h.

In both cyclization reactions, after a standard workup, 90% TFA-mediated acidolytic treatment of the crude protected macrocyclic peptide **22** afforded a complex mixture containing the desired phosphorus-peptide analogue **23**. Significantly, HPLC analysis showed virtually absence of the starting branched peptide. Unfortunately, after purification by semi-preparative HPLC the cyclic heptapeptide **23** was not obtained as a pure compound.

8.3.3 Total synthesis of the AIP-III

The natural substrate **AIP-III**, involved in the quorum sensing system of *S. aureus*, had been already obtained through different synthetic strategies based on either Fmoc/*t*-Bu or Boc/Bn chemistry.^{5,52,68} We used a synthetic pathway described in literature for a similar peptide,⁵¹ based on the Fmoc/*t*-Bu solid-phase synthesis of a linear peptide followed by macrocyclization in solution.⁹⁰⁻⁹³ For this linear approach the macrocyclization was carried out through the formation of a thioester bond between the L-Cys sulfhydryl and the C-terminus carboxyl group of the L-Leu (**scheme S.6**).⁹⁴⁻⁹⁶



Scheme S.6. Reagents and conditions: a) Fmoc-L-Leu-OH (0.7 equiv), DIPEA (2.1 + 4.2 equiv), CH₂Cl₂, rt, 45 min; b) **Fmoc-removal:** piperidine-DMF (2:8, v/v) (1 x 2 min, 2 x 10 min); c) Fmoc-L-aa-OH or Boc-L-Ile-OH (4 equiv), ethylcyano glyoxylate-2-oxime (4 equiv), DIC (4 equiv), DMF, rt, 1.5-2 h; d) Fmoc-removal (for deprotection of all the aa used with the exception of Boc-L-Ile-OH); e) TFA:Et₃SiH:CH₂Cl₂ (1:1:98), rt, 1h; f) see **table 8.2**; g) TFA:Et₃SiH:H₂O (90:5:5), rt, 1.5 h.

Solid-phase synthesis was undertaken using a *tetra-orthogonal protecting scheme* similar to that previously used to obtain the phosphorus cyclic peptide **23** (**scheme S.4** and **S.5**) and it was performed in

8. Supplement

polypropylene syringes (12 mL) fitted with a polyethylene porous disc. Solvents and soluble reagents were removed by suction. CTC, protected Fmoc amino acids and all the coupling reagents used during the synthesis are commercially available. After the first coupling of Fmoc-L-leucine on the CTC, carried out using DIEA as a base, all the following amino acid couplings were performed using diisopropylcarbodiimide, to activate the carboxylic group, and ethylcyanoglyoxylate-2-oxime to prevent or minimize epimerization. After each coupling the reaction was checked always by the previous mentioned Chloranil test,⁷⁸⁻⁸⁰ and the Fmoc group was removed using a piperidine/DMF solution (2:8 v/v). The following treatment of the resin-bonded peptide **25** with TFA/Et₃SiH/CH₂Cl₂ (1:1:98, v/v), raise concomitantly chemoselective unmasking of the Cys sulfhydryl group and release from the solid support. Partial purification of **26** was accomplished by filtration of the acidolytic resin suspension into pyridine-methanol (1.5:75 v/v) and evaporation of the filtrate to dryness in vacuo. After trituration of the residue with ice-water and filtration, the dried partially protected peptide **26** was macrocyclized using a commercially available dialkylcarbodiimide reagent, followed by TFA-mediated global deprotection to afford the desired thiolactone peptide **28** (AIP-III). As shown in **table 8.2**, we tried the cyclization of the partially protected peptide screening several coupling methods. A range of results were obtained depending on the carbodiimide involved in the reaction.

	Coupling reagents	solvent	time	work up	HPLC-UV-MS results
1	<i>N</i> -polystyrene methyl- <i>N</i> '-cyclohexylcarbo-diimide (5 equiv), DMAP (0.1 equiv), HOAt (5 equiv)	CHCl ₃	3 d	filtration and evaporation	CM. No linear peptide (SM). The peak of 27 is too weak.
2	<i>N</i> -polystyrene methyl- <i>N</i> '-cyclohexylcarbo-diimide (5 equiv), DMAP (0.1 equiv), ethylcyano-glyoxylate-2-oxime (5 equiv)	CHCl ₃	3 d	filtration and evaporation	CM. No linear peptide (SM). The peak of 27 is too weak.
3	<i>N</i> -polystyrene methyl- <i>N</i> '-cyclohexylcarbo-diimide (5 equiv), DMAP (0.1 equiv)	CHCl ₃	4 d	filtration and evaporation	CM. The SM is still in a high amount. It is possible to detect the peak of 27
4	EDC (5 equiv), DMAP (0.1 equiv), ethylcyano-glyoxylate-2-oxime (5 equiv)	CHCl ₃	1 d	extraction with citric acid and H ₂ O, evaporation	CM. No linear (SM) and no cyclic peptide (27)
5	EDC (5 equiv), DMAP (0.1 equiv)	CHCl ₃	4 d	extraction with citric acid and H ₂ O, evaporation	CM. No linear peptide (SM). The peak of 27 is detected in a relatively high amount.
6	DCC (5 equiv), DMAP (0.1 equiv)	CHCl ₃	4 d	filtration and evaporation	CM. The SM is still in a high amount. It is possible to detect the peak of 27

Table 8.2. Coupling methods screened to carry out the cyclization for the synthesis of the AIP-III (**28**).

On the basis of this screening, considering the conversion of the linear peptide **26** in the cyclic one **27**, we concluded that the method based on EDC and DMAP gave the best results (**entry 5, table 8.2**) in terms of

yields and purity, estimated from the absence of side-products in the HPLC chromatograms. Therefore, a new macrocyclization was carried out following the **entry 5** in **table 8.2** conditions: a dilute solution of **26** in chloroform (2 mM solution) was treated with EDC, in the presence of DMAP for 3 days at room temperature. The crude mixture was washed with a 5 % citric acid solution and water, to remove the excess of carbodiimide and of urea formed during the reaction. The crude protected macrocyclic peptide **27** was treated with TFA/H₂O/Et₃SiH (90:5:5) to afford the desired natural cyclic peptide **28** (**AIP-III**) in a complex mixture (**scheme S.6**). Significantly, HPLC analysis showed virtually absence of the starting linear peptide. After purification by semi-preparative HPLC, the thiolacton heptapeptide **28** was obtained with 10-15% yield, as stated in literature.^{50,58,62}

8.4 RESULTS AND CONCLUSIONS

The initial aim of this project was the synthesis of two transition state mimetics of the natural oligopeptide **AIP-III** involved in quorum sensing-system of *S. aureus*. The synthetic strategy involved the use of a Fmoc/*t*-Bu solid-phase methodology and serine phosphodiester **12** and **13** as the key building-blocks. This required the development of an efficient synthetic route for **12** and **13** (**scheme S.3**), which was achieved after preliminary protection of the starting amino acids and aminoalcohols (**schemes S.1** and **S.2**). The synthetic route outlined in **section 8.3.1** is relatively simple and high-yielding and has been proven to be suitable for scaling-up. The availability of these building blocks is of vital importance to allow us the synthesis of a peptide sequence using standard Fmoc-based chemistry. Unexpectedly, during the solid phase synthesis of the branched peptide (**scheme S.4**) it was possible to introduce in the peptide sequence just the “*serine building block*” **12**. In contrast, the coupling reaction of phosphodiester **13** in the peptide chain didn't work, probably because **13** is more sterically hindered than **12**. However, our data show that the Fmoc/*t*-Bu solid-phase strategy is an efficient way to obtain the branched phosphopeptide **21** (**scheme S.4**) in good yield. The cyclization process was much more difficult to understand. Several coupling methods were screened and different coupling reagents were used (**table 8.1**) to obtain the phosphorus cyclic peptide. Even if the cyclization reaction involved simply the formation of an amide bond (**scheme S.5**), some coupling reagents resulted quite inefficient and when the cyclic product was present, it was part of a complex mixture. On the basis of the screening, *N*-polystyrene methyl-*N'*-cyclohexylcarbodiimide or DIC gave better results as coupling reagent. Although very complex mixtures were always obtained, it was possible to detect the peak of the right cyclic peptide by UV and mass spectrometry. In addition, HPLC analysis showed virtually absence of the starting branched peptide **21**. The main problems for the cyclization were obviously the side reactions and the instability of the

8. Supplement

phosphate group. One of the most frequent fragment and two possible side products that could occur during the cyclization, confirmed by mass spectrometry analysis, are shown in the **figure 8.7**.

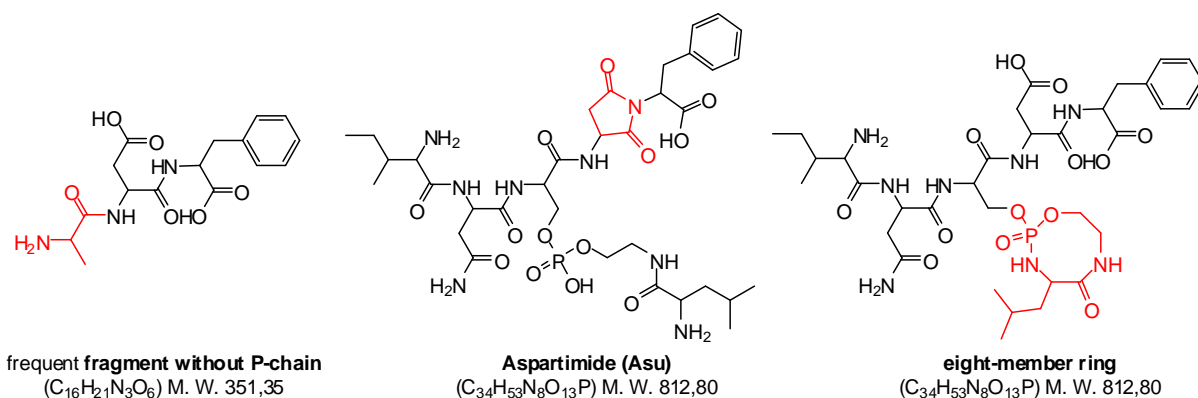


Figure 8.7. A frequent fragment detected by mass spectrometry due to the instability of the phosphate group and two possible side products that could occur during the cyclization.

It is not completely sure that the two presumed side products (**figure 8.7**) could be formed during the reaction. Considering a difficult event the formation of an eight-member ring, perhaps the aspartimide or aminosuccinimide (3-amino-pyrrolidine-2,5-dione, Asu) formation is a more realistic hypothesis.⁹⁷ In fact it is the first step of the well-known degradation, at alkaline, neutral and acidic pH, of peptides and proteins containing aspartic acids/ asparagines.⁹⁸⁻¹⁰⁰ The reaction results in a variety of rearranged and racemized products and it is especially problematic in Fmoc/*t*-Bu SPPS because strong base, such as piperidine, promotes Asu formation.¹⁰¹ Semi-preparative HPLC did not afford the cyclic heptapeptide **23** (**scheme S.4**) as a pure compound due to the high complexity of the crude mixture. Work is underway to better understand the reasons of this evident degradation and formation of side products. The imminent future work will involve a previous purification of the branched peptide **21** by semipreparative HPLC, in order to obtain a crude mixture less complex and easier to purify after cyclization. Moreover, alternative coupling reagents and conditions will be screened in order to improve the yield of the final cyclization for the achievement of **23**.

The total synthesis of the **AIP-III** was the ultimate goal of this project. On the basis of the literature results, the Fmoc/*t*-Bu solid-phase strategy was always the selected methodology for the synthesis of the linear peptide. After cyclization carried out in solution, the **AIP-III** (**28**) has been obtained and it will be useful as reference compound in the biological tests.

In conclusion, this work presents a facile and efficient synthesis of caged phospho-amino acids suitable for Fmoc-based SPPS. Moreover, the total synthesis of the natural substrate **AIP-III** had been successfully carried out and the transition state mimetic analogue **23** had been obtained, but its yield and purity must be improved in order to start the biological assays.

8.5 EXPERIMENTAL CHEMISTRY

8.5.1 Materials and Methods

Reactions were performed using oven-dried glassware apparatus (130 °C) under an atmosphere of nitrogen with anhydrous, freshly distilled solvents unless otherwise stated. Anhydrous reactions were carried out under nitrogen atmosphere. Solvents were distilled prior to use. Reagents/solvents for anhydrous reactions were dried as follows: THF was dried over wire Na and distilled from a mixture of CaH₂ and LiAlH₄ with triphenylmethane as indicator; diethyl ether was distilled over a mixture of CaH₂ and LiAlH₄; petroleum ether was distilled before use and refers to the fraction between 30-40 °C; dichloromethane, methanol, *n*-hexane, acetonitrile and toluene were distilled from CaH₂. All other reagents were purified in accordance with the instructions in “Purification of Laboratory Chemicals”,¹⁰² or obtained from commercial sources.

Room temperature (rt) refers to ambient temperature. Temperatures of 0 °C were maintained using an ice-water bath.

Yields refer to chromatographically and spectroscopically pure compounds. All reactions were monitored by thin layer chromatography (TLC) using glass plates precoated with Merck silica gel 60 F254 or aluminum oxide 60 F254. Visualization was performed by the quenching of UV fluorescence ($\lambda_{\text{max}} = 254$ nm) or by staining with ceric ammonium molybdate or potassium permanganate or Dragendorff's reagent (0.08% w/v bismuth subnitrate and 2% w/v KI in 3M aq. AcOH). Flash column chromatography was performed using slurry-packed Merck 9325 Kieselgel 60 silica gel (230-400 mesh) unless otherwise stated, eluting with distilled solvents as described.

Melting points were obtained using a Reichert hot plate microscope with a digital thermometer attachment and are uncorrected.

Proton magnetic resonance (¹H NMR) spectra were recorded using an internal deuterium lock at ambient probe temperatures (unless otherwise stated) on the following instruments: Bruker DPX-400 (400 MHz), Bruker Avance 400 QNP (400 MHz), Bruker Avance 500 BB ATM (500 MHz) and Bruker Avance 500 Cryo Ultrashield (500 MHz), Bruker Avance 700 MHz Fourier transform spectrometers in deuteriochloroform or deuterodimethyl sulfoxide operating at 400, 500 and 700 MHz respectively and using an internal deuterium lock at ambient probe temperatures (unless otherwise stated). Chemical shifts (δ) are quoted in ppm, to the nearest 0.01 ppm and are referred to the residual non-deuterated solvent peak. Coupling constants (*J* values) are given in Hz and were calculated using ‘Mestre-C 2.3a’ software rounded to the nearest 0.5 Hz.¹⁰³ Data are reported as follows: chemical shift, multiplicity [exch, exchange; br, broad; s, singlet; d, doublet; t, triplet; q, quartet; quin, quintet; sept, septet; m, multiplet; or as a combination of these (e.g. dd, dt *etc.*)], integration, assignment and coupling constant(s). The

8. Supplement

numbering/lettering on selected structures does not follow the IUPAC naming system and is used for the assignment of the ^1H NMR. Proton assignments were determined either on the basis of unambiguous chemical shift or coupling pattern, by analogy to fully interpreted spectra for related compounds. Diastereotopic protons are assigned as H and *H*.

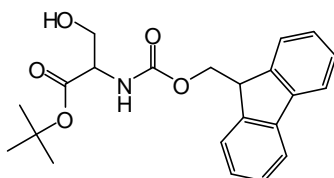
Analytical LC-MS spectra were recorded on an HP/Agilent MSD LC-MS APCI 120-1000 full gradient ACq T = 1 min 1 μ L. High resolution mass measurements were made using a Micromass Quadrupole-Time of Flight (Q-ToF) spectrometer and reported mass values are within the error limits of ± 5 ppm mass units. The ionisation technique used is indicated by the following abbreviations: CI = chemical ionisation; EI = electron ionisation; ESI = electrospray ionisation; FAB (LSIMIS) = fast atom bombardment (liquid secondary ion mass spectrometry); MALDI = matrix-assisted laser desorption /ionisation.

Semi-preparative HPLC purifications were performed on an Agilent HP 1100 series chromatograph (Supelco ABZ+PLUS, 10cm x 2.1mm, 5 μ m) attached to a HP MSD mass spectrometer with a multimode ESI/APCI ionisation source in ESI/APCI mode. Elution was carried out at a flow rate of 1.0 mL/min using a reverse phase gradient of acetonitrile and water containing 0.1 % formic acid and detection was with diode array detection (λ = 195, 210, 215, 220 and 254 nm). Retention times (in min) are reported below as t_R . MALDI-TOF and MS (ESI) analysis of peptide samples were performed in a PerSeptive Biosystems Voyager DE RP, using ACH matrix, and in a Waters Micromass ZQ spectrometer and in an Agilent Ion Trap 1100 Series LC/MSDTrap.

The “&” symbol is used in the nomenclature for cyclic peptides and precursors.¹⁰⁴ The appearance of “&” in a given position of the one-line formula indicates the location of one end of a chemical bond and the second “&” the point to which this bond is attached. Thus, “&” represents the start or the end of a chemical bond, which is ‘cut’ with the aim to facilitate the view of a complex formula. In this way, two “&” symbols indicate one chemical bond.

8.5.2 Protection of amino acids and amino alcohols

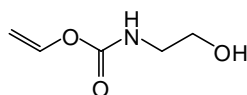
8.5.2.1 *tert*-Butyl-2-[[*(9H*-fluoren-9-yl)methoxy]carbonylamino]-3-hydroxy propanoate, “Fmoc-Ser-O-*t*-Bu” (1)



To a solution of Fmoc-Ser-OH (1.0 g, 3.10 mmol, 1 equiv) in EtOAc (30 ml), a solution of *t*-Butyltrichloro-acetimidate (2.6 g, 12.20 mmol, 4 equiv) in CHX (10 ml) was added at rt. The mixture was stirred at rt until TLC analysis (Hex/EtOAc 2:1) showed absence of Fmoc-L-Ser-OH (12 h). The solvents

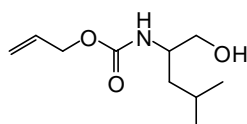
were removed under reduced pressure and the crude residue was purified by flash column chromatography (Hex/EtOAc 2:1) to afford the desired compound as a white solid (1.1 g, 2.88 mmol, 94 % yield). mp = 102-04 °C. ^1H NMR (CDCl_3) δ 7.78 (d, 2H, Ar, $J = 7.5$ Hz), 7.62 (d, 2H, Ar, $J = 7.5$ Hz), 7.42 (t, 2H, Ar, $J = 7.5$ Hz), 7.33 (t, 2H, Ar, $J = 7.5$ Hz), 6.37-6.68 (exch br s, 1H, OH) 5.79 (exch br d, 2H, NH, $J = 6.5$ Hz), 4.43 (d, 2H, CH_2OCO , $J = 7.0$ Hz), 4.32-4.38 (m, 1H, CHCH_2OCO), 4.24 (t, 1H, CHCH_2OH , $J = 7.0$ Hz), 3.92-3.98 (m, 2H, CH_2OH), 1.51 (s, 9H, 3 CH_3 *t*-Bu).

8.5.2.2 Allyl 2-hydroxyethylcarbamate, "Alloc-ethanolamine" (2)



A solution of ethanolamine (1.0 ml, 16.40 mmol, 1 equiv) in dioxane/ H_2O (1:1, 25.0 ml) was cooled to 0 °C. NaHCO_3 (1.5 g, 18.00 mmol, 1.1 equiv) and allylchloroformate (1.9 ml, 18.00 mmol, 1.1 equiv) were added. The mixture was allowed to warm to rt and stirred until TLC analysis (Hex/EtOAc, 1:2) showed absence of ethanolamine (3 h). The organic solvent was removed under reduced pressure and the aqueous phase was extracted with EtOAc (3 times). The organic layers were then collected, dried (MgSO_4) and concentrated under reduced pressure. The resulting oil was purified by flash column chromatography (Hex/EtOAc, 1:2) to yield **2** as a colourless oil (2.3 g, 15.70 mmol, 96 % yield). ^1H NMR (CDCl_3) δ 5.80-5.90 (m, 1H, CHCH_2O), 5.23 (dq, 1H, CH-HCHCH_2 allyl, $J = 12.5$ Hz, $J = 1.5$ Hz), 5.14 (dt, 1H, CH-HCHCH_2 allyl, $J = 1.5$ Hz, $J = 1.0$ Hz), 4.51 (d, 2H, CH_2OCO , $J = 5.5$ Hz), 3.65 (t, 2H, CH_2OH , $J = 6.0$ Hz), 3.28 (t, 2H, CH_2NH , $J = 6.0$ Hz).

8.5.2.3 Allyl 1-hydroxy-4-methylpentan-2-ylcarbamate, "Alloc-L-leucinol" (3)

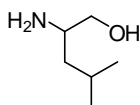


A solution of L-leucinol (**4**) (0.9 mg, 7.60 mmol, 1 equiv) in dioxane/ H_2O (1:1, 25.0 ml) was cooled to 0 °C. NaHCO_3 (0.7 mg, 8.40 mmol, 1.1 equiv) and allylchloroformate (0.9 ml, 8.40 mmol, 1.1 equiv) were added. The mixture was allowed to warm to rt and stirred until TLC analysis (Hex/EtOAc, 1:2) showed absence of L-leucinol (3 h). The organic solvent was removed under reduced pressure and the aqueous phase was extracted with EtOAc (3 times). The organic layers were then collected, dried (MgSO_4) and concentrated under reduced pressure. The resulting colourless oil was purified by flash column chromatography (Hex/EtOAc 1:2) to yield **3** as a colourless oil (1.3 g, 6.56 mmol, 86 % yield). ^1H NMR (CDCl_3) δ 5.80-5.90 (m, 1H, CHCH_2O), 5.24 (dt, 1H, CH-HCHCH_2 allyl, $J = 12.5$ Hz, $J = 1.5$ Hz), 5.14 (dd, 1H, CH-HCHCH_2 allyl, $J = 9.0$ Hz, $J = 1.5$ Hz), 4.80 (exch br d, 1H, NH, $J = 8.0$ Hz), 4.49 (d, 2H, CH_2OCO , $J = 5.0$ Hz), 3.66-3.75 (m, 1H, CHNH), 3.59-3.63 (m, 1H, CH-HOH), 3.44-3.48 (m, 1H, CH-

8. Supplement

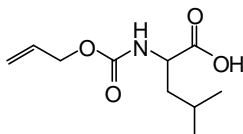
HOH), 2.41 (exch br s, 1H, OH), 1.57-1.64 (m, 1H, $CH(CH_3)_2$), 1.17-1.34 (m, 2H, $CH_2CH(CH_3)_2$), 0.87 (dd, 6H, 2 CH_3 , $J = 5.0$ Hz, $J = 1.5$ Hz).

8.5.2.4 2-Amino-4-methylpentan-1-ol, "L-leucinol" (4)



Trimethylsilylchloride (3.9 ml, 30.50 mmol, 4 equiv) was added to a cold (0 °C) solution of lithium borohydride (0.3 mg, 15.30 mmol, 2 equiv) in 3 ml of anhydrous THF under N_2 . The cooling ice/water bath was removed and the mixture was stirred at rt for 15 min. The mixture was cooled to 0 °C and a solution of L-Leu (1.0 g, 7.62 mmol, 1 equiv) in 3 ml of anhydrous THF was added. The cooling bath was removed and the reaction mixture was stirred at rt for 16 h. The mixture was cooled again to 0 °C and methanol (7.5 ml) was added dropwise followed by NaOH (4.1 ml, 2.5 N aqueous solution). The organic solvents were removed under reduced pressure and the resulting residue was extracted with chloroform (3 times). The combined organic extracts were dried ($MgSO_4$) and concentrated under reduced pressure to furnish **4** as a colourless oil (0.9 g, 7.59 mmol, quantitative yield). The product was analytically pure and was used in subsequent reactions without further purification. 1H NMR ($CDCl_3$) δ 3.88 (dd, 1H, CH-HOH, $J = 8.0$ Hz, $J = 3.0$ Hz), 3.41-3.47 (m, 1H, CH-HOH), 3.30 (exch br s, 1H, OH), 3.11-3.16 (m, 1H, $CHNH_2$), 2.47 (exch br s, 2H, NH_2), 1.43-1.60 (m, 1H, $CH(CH_3)_2$), 1.05-1.15 (m, 2H, $CH_2CH(CH_3)_2$), 0.75-0.81 (m, 6H, 2 CH_3).

8.5.2.5 2-(Allyloxycarbonylamino)-4-methylpentanoic acid, "Alloc-L-Leu-OH" (5)

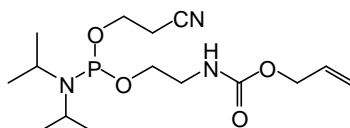


Allyl-chloroformate (0.7 ml, 6.35 mmol, 1 equiv) was dissolved in dioxane (4.0 ml) and a solution of NaN_3 (0.6 g, 9.52 mmol, 1.5 equiv) in H_2O (3.0 ml) was added at rt. The reaction mixture was stirred at rt for 1 h whereupon a solution of L-Leu (1.0 g, 7.62 mmol, 1.2 equiv) in 1% aqueous Na_2CO_3 /dioxane 1:1 (20.0 ml) was added. The pH of the reaction was monitored periodically and 10% aqueous Na_2CO_3 was added when necessary to keep the pH between 8-10. The reaction was stirred at rt until TLC analysis (Hex/EtOAc, 1:4) showed absence of the allyl-chloroformate (24 h). Then the mixture was poured into water (100.0 mL), 10% aqueous Na_2CO_3 was added to keep the pH between 9 and 10 and the aqueous phase was extracted several times with *tert*-butyl methyl ether to remove the by-products (e.g. azidoformate, protected dipeptides). The aqueous solution was acidified to pH 2.0 with 2 N aqueous HCl and extracted with EtOAc (3 times). The organic phase was dried ($MgSO_4$) and concentrated under reduced pressure to yield a colourless oil (1.1 g, 4.8 mmol, 77% yield). The purity of the colorless oil was measured by NMR and it was > 95 %. The product was used for the synthesis of **20** without further

purification. ^1H NMR (CDCl_3) δ 10.34 (exch br s, 1H, OH), 5.88-6.02 (m, 1H, CHCH_2O), 5.32 (dd, 1H, CH-HCHCH_2 allyl, $J = 17.0$ Hz, $J = 1.0$ Hz), 5.23 (dd, 1H, CH-HCHCH_2 allyl, $J = 9.0$ Hz, $J = 1.29$ Hz), 5.19 (exch br s, 1H, NH), 4.60 (d, 2H, CH_2OCO , $J = 5.5$ Hz), 4.37-4.44 (m, 1H, CHNH), 1.68-1.81 (m, 2H, $\text{CH}_2\text{CH}(\text{CH}_3)_2$), 1.53-1.62 (m, 1H, $\text{CH}(\text{CH}_3)_2$), 0.98 (d, 6H, 2 CH_3 , $J = 6.5$ Hz).

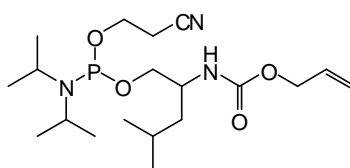
8.5.3 Phosphorus couplings

8.5.3.1 Allyl-2-(2-cyanoethoxydiisopropylaminophosphinoxy)ethyl carbamate (6)



To a solution of **2** (0.3 g, 1.80 mmol, 1 equiv) in anhydrous CH_2Cl_2 (8.0 ml) under N_2 , DIPEA (2.1 ml, 12.60 mmol, 7 equiv) and 2-cyanoethyl-*N,N*-diisopropyl-chloro-phosphoramidite (0.6 ml, 2.70 mmol, 1.5 equiv) were added at rt. The reaction mixture was stirred at rt until TLC analysis (Hex/EtOAc 1:1) showed absence of **2** (1.5 h). The solvent was removed under reduced pressure. The residue was then dissolved in EtOAc and washed with brine (3 times). The organic phase was dried (MgSO_4) and concentrated under reduce pressure. The resulting colourless oil was purified by flash column chromatography (Hex/EtOAc 1:1) to furnish **6** as a colourless oil (0.5 g, 1.49 mmol, 83 %). ^1H NMR (CDCl_3) δ 5.81-5.90 (m, 1H, CHCH_2O), 5.23 (dd, 1H, CH-HCHCH_2 allyl, $J = 5.5$ Hz, $J = 1.5$ Hz), 5.14 (dd, 1H, CH-HCHCH_2 allyl, $J = 10.45$ Hz, $J = 1.5$ Hz), 5.09 (exch br s, 1H, NH), 4.50 (d, 2H, CH_2OCO , $J = 5.0$ Hz), 3.49-3.83 (m, 6H, $\text{CH}_2\text{CH}_2\text{CN} + \text{CH}_2\text{CH}_2\text{NH}$), 3.33 (q, 2H, 2 $\text{CH}(\text{CH}_3)_2$, $J = 10.5$ Hz), 2.58 (t, 2H, CH_2CN , $J = 6.5$ Hz), 1.12 (dd, 6H, 2 CH_3 , $J = 6.5$ Hz, $J = 5.5$ Hz).

8.5.3.2 Allyl-1-(2-cyanoethoxydiisopropylaminophosphinoxy)-4-methyl pentan-2-yl-carbamate (7)

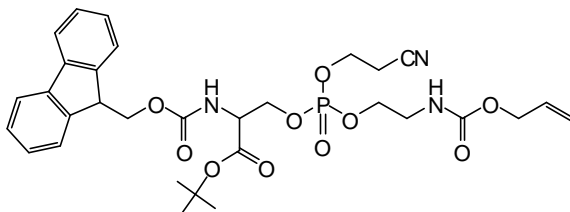


To a solution of **3** (0.6 g, 2.82 mmol, 1 equiv) in anhydrous CH_2Cl_2 (10.0 ml) under N_2 , DIPEA (3.3 ml, 19.76 mmol, 7 equiv) and 2-cyanoethyl-*N,N*-diisopropyl-chlorophosphoramidite (0.9 ml, 4.23 mmol, 1.5 equiv) were added at rt. The reaction mixture was stirred at rt until TLC analysis (Hex/EtOAc 1:1) showed absence of **3** (1.5 h). The solvent was removed under reduced pressure. The residue was then dissolved in EtOAc and washed with brine (3 times). The organic phase was dried (MgSO_4) and concentrated under reduce pressure. The resulting colourless oil was purified by flash column chromatography (Hex/EtOAc 1:1) to furnish **7** as a colourless oil (1.0 g, 2.55 mmol, 90 % yield). ^1H NMR (CDCl_3) δ 9.19 (exch br s, 1H, NH), 5.80-5.96 (m, 1H, CHCH_2O), 5.23 (dq, 1H, CH-HCHCH_2

8. Supplement

allyl, $J = 12.5$ Hz, $J = 1.5$ Hz), 5.17-5.12 (m, 1H, CH-*HCHCH*₂ allyl), 4.47-4.53 (m, 2H, CH₂OCO), 4.21-4.27 (m, 1H, CHNH), 3.96-4.12 (m, 2H, CH₂CH₂CN), 3.71-3.89 (m, 2H, CH₂CHNH), 3.50-3.57 (m, 2H, 2 CH(CH₃)₂), 2.63-2.72 (m, 1H, CH-H-CN), 2.53-2.60 (m, 1H, CH-H-CN), 1.54-1.66 (m, 1H, CH₂CH(CH₃)₂), 1.17-1.19 (m, 2H, CHCH₂CH), 1.11 (dd, 12H, 2 x (CH₃)₂CHN, $J = 4.0$ Hz, $J = 3.0$ Hz), 0.86 (dt, 6H, 2 x CH₃CHCH₂, $J = 3.5$ Hz, $J = 3.0$ Hz).

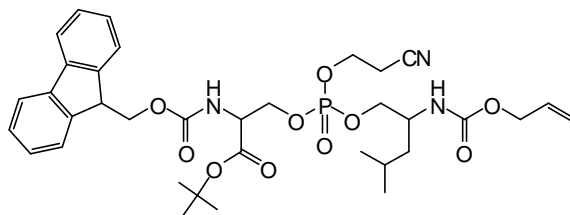
8.5.3.3 *tert*-Butyl-8-(2-cyanoethoxy)-1-(9*H*-fluoren-9-yl)-3,13-dioxo-2,7,9,14-tetraoxa-4,12-diaza-8-phosphoryloxyheptadec-16-ene-5-carboxylate (**10**)



To a solution of **6** (500.0 mg, 1.50 mmol, 1 equiv) in anhydrous THF (6.0 ml) under N₂, a solution of tetrazole (130.0 mg, 1.80 mmol, 1.2 equiv) in anhydrous THF (6.0 ml) was added at rt. The solution was stirred at rt for 15 min and then added dropwise to a previously prepared solution of **1** (580.0 g, 1.50 mmol, 1 equiv) in anhydrous THF (8.0 ml) under N₂ at rt. The mixture was stirred at rt until TLC analysis (Hex/EtOAc 1:3) showed absence of **6** (15 h). The solvent was then removed under reduced pressure and the resulting residue was dissolved in EtOAc and washed with 10 % aqueous NaHCO₃ (2 times) and brine. The organic layer was dried (MgSO₄) and concentrated under reduced pressure to yield the corresponding unstable phosphite **8** (940.0 mg, 1.50 mmol, quantitative yield).

To a solution of **8** (940.0 g, 1.50 mmol, 1 equiv) in anhydrous THF (15.0 ml) under N₂, *t*-butylhydroperoxide (0.3 ml, 3.00 mmol, 2 equiv) was added at rt. The reaction was stirred at rt until TLC analysis (Hex/EtOAc 1:3) showed absence of the phosphite (2 h). The solvent was then removed under reduced pressure. The residue was dissolved in EtOAc and washed with 10% aqueous NaHCO₃ (2 times) and brine. The organic layer was dried (MgSO₄) and concentrated under reduced pressure. The resulting colourless oil was then purified by flash column chromatography (Hex/EtOAc gradient 1:1 to 1:3) to afford **10** as a clear oil (540 mg, 0.84 mmol, 57 % yield over 2 steps from **6**). ¹H NMR (CDCl₃) δ 7.69 (d, 2H, Ar, $J = 7.5$ Hz), 7.55 (t, 2H, Ar, $J = 6.0$ Hz), 7.33 (t, 2H, Ar, $J = 7.5$ Hz), 7.24 (t, 2H, Ar, $J = 11.0$ Hz), 5.77-5.89 (m, 1H, CHCH₂O allyl), 5.32 (exch br s, 1H, NH), 5.20 (d, 1H, CH-*HCHCH*₂ allyl, $J = 17.0$ Hz), 5.11 (d, 1H, CH-*HCHCH*₂ allyl, $J = 10.5$ Hz), 4.48 (d, 2H, CH₂OCO allyl, $J = 4.5$ Hz), 4.30-4.42 (m, 4H, CHCH₂OCO + CH₂CHCOO), 4.10-4.18 (m, 4H, CH₂CH₂CN + CH₂CH₂NH), 4.02-4.08 (m, 3H, CH₂CH₂NH + CHCH₂OCO), 3.38 (d, 1H, CH₂CHCOO, $J = 5.0$ Hz), 2.63 (t, 2H, CH₂CH₂CN, $J = 6.0$ Hz), 1.42 (s, 9H, 3 CH₃-CO). MS (ESI) calcd. For C₃₁H₃₈N₃O₁₀P, 643.621. Found: m/z 644.13 [M + H]⁺, 588.50 [M + H - *t*-Bu]⁺.

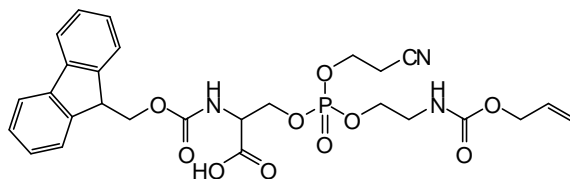
8.5.3.4 tert-Butyl-8-(2-cyanoethoxy)-1-(9H-fluoren-9-yl)-11-isobutyl-3,13-dioxo-2,7,9,14-tetraoxa-4,12-diaza-8-phosphoryloxyheptadec-16-ene-5-carboxylate (11)



To a solution of **7** (1.0 g, 2.54 mmol, 1 equiv) in anhydrous THF (8.0 ml) under N₂, a solution of tetrazole (0.2 g, 3.05 mmol, 1.2 equiv) in anhydrous THF (8.0 ml) was added at rt. The solution was stirred at rt for 15 min and then added dropwise to a previously prepared solution of **1** (1.0 g, 2.54 mmol, 1 equiv) in anhydrous THF (9.0 ml) under N₂ at rt. The mixture was stirred at rt until TLC analysis (Hex/EtOAc 1:3) showed absence of **7** (15 h). The solvent was then removed under reduced pressure and the resultant residue was dissolved in EtOAc and washed with 10 % aqueous NaHCO₃ (2 times) and brine. The organic layer was dried (MgSO₄) and concentrated under reduced pressure. The crude mixture of the phosphite **9** was directly used without purification for the following oxidation reaction to get the compound **11**, as already seen for the analogue unstable compound **8** (1.7 g, 2.54 mmol, quantitative yield).

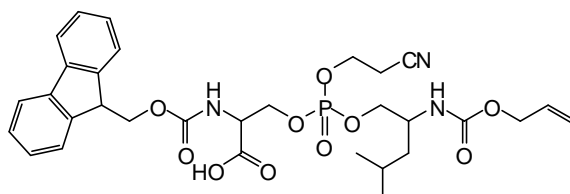
To a solution of **9** (1.7 g, 2.54 mmol, 1 equiv) in anhydrous THF (15.0 ml) under N₂, *t*-butylhydroperoxide (0.5 ml, 5.08 mmol, 2 equiv) was added at rt. The reaction was stirred at rt until TLC analysis (Hex/EtOAc 1:2) showed absence of the phosphite (2.5 h). The solvent was then removed under reduced pressure. The residue was dissolved in EtOAc and washed with 10% aqueous NaHCO₃ (2 times) and brine. The organic layer was dried (MgSO₄) and concentrated under reduced pressure. The resulting colourless oil was then purified by flash column chromatography (Hex/EtOAc gradient 1:1 to 1:2) to afford **11** as a clear oil (350.0 mg, 0.50 mmol, 20 % yield over 2 steps from **7**). ¹H NMR (CDCl₃) δ 8.62 (exch br s, 1H, NH), 7.78 (d, 2H, Ar, *J* = 7.5 Hz), 7.64 (d, 2H, Ar, *J* = 7.0 Hz), 7.42 (t, 2H, Ar, *J* = 7.5 Hz), 7.33 (t, 2H, Ar, *J* = 7.5 Hz), 5.88-5.99 (m, 1H, CHCH₂O allyl), 5.30 (dq, 1H, CH-HCHCH₂ allyl, *J* = 5.5 Hz, *J* = 1.5 Hz), 5.18-5.24 (m, 1H, CH-HCHCH₂ allyl), 4.56 (d, 2H, CH₂OCO allyl, *J* = 5.0 Hz), 4.37-4.45 (m, 2H, CH₂CHCOO), 4.15-4.29 (m, 2H, CHCH₂CO), 4.10-4.16 (m, 2H, CH₂CH₂CN), 3.96 (d, 2H, CH₂CHNH, *J* = 5.5 Hz), 3.88-3.97 (m, 1H, CHCH₂OCO), 3.74-3.77 (m, 1H, CH₂CHCOO), 3.39-3.51 (m, 1H, CH₂CHNH), 2.61 (t, 2H, CH₂CH₂CN, *J* = 6.0 Hz), 1.65-1.72 (m, 1H, CHCH₃), 1.52 (s, 9H, 3 CH₃-CO), 1.33-1.44 (m, 2H, CHCH₂CH), 0.95 (d, 6H, 2 CH₃CH, *J* = 6.5 Hz). MS (ESI) calcd. For C₃₅H₄₆N₃O₁₀P, 699.73. Found: *m/z* 700.17 [M + H]⁺, 644.50 [M + H - *t*-Bu]⁺, 616.16 [M + H - Alloc]⁺.

8.5.3.5 8-(2-Cyanoethoxy)-1-(9H-fluoren-9-yl)-3,13-dioxo-2,7,9,14-tetraoxa-4,12-diaza-8-phosphoryloxyheptadec-16-ene-5-carboxylic acid (12)



TFA (1.3 ml, 16.93 mmol, 20 equiv) was added to a solution of **10** (540 mg, 0.85 mmol, 1 equiv) in CH_2Cl_2 (1.3 ml) at rt. The reaction was stirred at rt until TLC analysis (Hex/EtOAc 1:3) showed absence of **10** (2.5 h). The excess TFA was removed by co-evaporation with CH_2Cl_2 under reduced pressure (5 times). The residue was dried in a vacuum desiccator o/n to yield **12** as a colourless oil (480.0 mg, 0.82 mmol, 97 %). The compound was used in subsequent SPPS without further purification. ^1H NMR (CDCl_3) δ 8.20 (exch br s, 1H, NH), 7.69 (d, 2H, Ar, $J = 7.5$ Hz), 7.52 (d, 2H, Ar, $J = 4.5$ Hz), 7.33 (t, 2H, Ar, $J = 7.5$ Hz), 7.24 (t, 2H, Ar, $J = 7.0$ Hz), 5.80-5.84 (m, 1H, CHCH_2O allyl), 5.23 (d, 1H, CH-HCHCH_2 allyl, $J = 5.0$ Hz), 5.13 (d, 1H, CH-HCHCH_2 allyl, $J = 4.0$ Hz), 4.50-4.57 (m, 4H, CH_2OCO allyl, CHCH_2OCO), 4.32-4.38 (m, 3H, $\text{CH}_2\text{CH}_2\text{CN} + \text{CHCH}_2\text{OCO}$), 4.04-4.16 (m, 6H, + $\text{CH}_2\text{CHCOO} + \text{CH}_2\text{CH}_2\text{NH}$), 3.28-3.43 (m, 1H, CH_2CHCOO), 2.65 (t, 2H, $\text{CH}_2\text{CH}_2\text{CN}$, $J = 5.5$ Hz). MS (ESI) calcd. For $\text{C}_{27}\text{H}_{30}\text{N}_3\text{O}_{10}\text{P}$, 587.51. Found: m/z 588.06 $[\text{M} + \text{H}]^+$.

8.5.3.6 8-(2-Cyanoethoxy)-1-(9H-fluoren-9-yl)-11-isobutyl-3,13-dioxo-2,7,9,14-tetraoxa-4,12-diaza-8-phosphoryloxyheptadec-16-ene-5-carboxylic acid (13)



TFA (0.7 ml, 9.66 mmol, 20 equiv) was added to a solution of **11** (0.3 g, 0.48 mmol, 1 equiv) in CH_2Cl_2 (0.7 ml) at rt. The reaction was stirred at rt until TLC analysis (Hex/EtOAc 1:3) showed absence of **11** (2.5 h). The excess TFA was removed by co-evaporation with CH_2Cl_2 under reduced pressure (5 times). The residue was dried in a vacuum desiccator o/n to yield **13** as a colourless oil (0.3 g, 0.47 mmol, 97 %). The compound was used in subsequent SPPS without further purification. ^1H NMR (CDCl_3) δ 7.99 (exch br s, 1H, NH), 7.69 (d, 2H, Ar, $J = 7.5$ Hz), 7.56 (t, 2H, Ar, $J = 6.0$ Hz), 7.33 (t, 2H, Ar, $J = 7.5$ Hz), 7.24 (t, 2H, Ar, $J = 14.0$ Hz), 5.79-5.88 (m, 1H, CHCH_2O allyl), 5.23 (d, 1H, CH-HCHCH_2 allyl, $J = 17.0$ Hz), 5.13 (d, 1H, CH-HCHCH_2 allyl, $J = 10.0$ Hz), 4.47-4.58 (m, 3H, CH_2OCO allyl + CHCH_2OCO), 4.26-4.35 (m, 2H, CH_2CHCOO), 4.10-4.19 (m, 2H, CHCH_2CO), 4.00-4.08 (m, 1H, CH_2CHCOO), 3.77-3.96 (m, 4H, $\text{CH}_2\text{CHNH} + \text{CH}_2\text{CH}_2\text{CN}$), 3.34-3.43 (m, 1H, CH_2CHNH), 2.63-2.70 (m, 2H, $\text{CH}_2\text{CH}_2\text{CN}$),

1.58-1.64 (m, 1H, $CHCH_3$), 1.28 (t, 2H, $CHCH_2CH$, $J = 2.0$ Hz), 0.87 (d, 6H, 2 CH_3CH , $J = 6.5$ Hz). MS (ESI) calcd. For $C_{31}H_{38}N_3O_{10}P$, 643.62. Found: m/z 644.14 $[M + H]^+$.

8.5.4 Total synthesis of the TS mimetic

8.5.4.1 H-Phe-O-CTC (14)

Cl-TrtCl-resin (0.2 g, 1.01 mmol/g) was placed in a 20 ml polypropylene syringe fitted with a polyethylene filter disk. The resin was then washed with CH_2Cl_2 (5 x 0.5 min) and a solution of Fmoc-L-Phe-OH (54.2 mg, 0.14 mmol, 0.7 equiv) and DIPEA (70.0 μ L, 0.42 mmol, 2.1 equiv) in CH_2Cl_2 (2.5 ml) was added. The mixture was then stirred for 15 min. Extra DIPEA (140.0 μ L, 0.85 mmol, 4.2 equiv) was added and the mixture was stirred for an additional 45 min. The reaction was stopped by adding MeOH (320.0 μ l) and stirred for 10 min. The aim of this procedure was to obtain a resin loading of 0.7 mmol/g. The Fmoc-L-Phe-O-TrtCl-resin was subjected to the following washings/treatments with CH_2Cl_2 (3 x 0.5 min), DMF (3 x 0.5 min) and piperidine-DMF solution to remove the Fmoc as indicated in the following General Procedure for Fmoc-removal (section 8.5.4.2).

8.5.4.2 General Procedure for Fmoc-removal: the Fmoc group was removed by treatment with piperidine/DMF (2:8, v/v) (1 x 2 min, 2 x 10 min). Washings between deprotection, coupling, and again deprotection steps were performed with DMF (5 x 0.5 min) and CH_2Cl_2 (5 x 0.5 min) using 10.0 ml solvent/g resin each time.

8.5.4.3 H-Asp(O-*t*-Bu)-Phe-O-CTC (15)

Fmoc-L-Asp(O-*t*-Bu)-OH (230.4 mg, 0.56 mmol, 4 equiv), DIC (86.8 μ L, 0.56 mmol, 4 equiv) and Ethylcyanoglyoxylate-2-oxime (79.6 mg, 0.56 mmol, 4 equiv) in DMF (2.5 ml) were added to the above obtained H-Phe-O-CTC (14). After 90 min of coupling, the chloranil test was negative. Removal of Fmoc group and washings were performed as described in General Procedures for Fmoc-removal (section 8.5.4.2).

8.5.4.4 H-Ser[P(OC₂H₄-NH-Alloc)O₂H]-Asp(O-*t*-Bu)-Phe-O-CTC (16)

Fmoc-Ser[P(OC₂H₄CN)(OC₂H₄-NH-Alloc)O₂H] (12) (246.8 mg, 0.42 mmol, 3 equiv), PyAOP (218.9 mg, 2.5 mmol, 3 equiv) and DIPEA (308.2 μ L, 1.86 mmol, 9 equiv) were added to the above obtained H-Asp(O-*t*-Bu)-Phe-O-CTC (15). After 2 h, the peptidyl-resin was subjected to the following washings/treatments with CH_2Cl_2 (3 x 0.5 min), DMF (3 x 0.5 min). Before the piperidine treatment for Fmoc-removal, an aliquot of the peptidyl-resin was treated with TFA/Et₃SiH/ CH_2Cl_2 (1:1:98) and TFA/Et₃SiH/H₂O (90:5:5). The HPLC analysis ($t_R = 4.34$ min) of the crude obtained after evaporation showed a purity of > 95%. MS (ESI) calcd. For $C_{44}H_{51}N_4O_{15}P$, 906.87. Found: m/z 850.11 $[M - t-Bu]^+$. Removal of Fmoc group and washings were performed as described in General Procedures for Fmoc-removal (section 8.5.4.2).

8.5.4.5 H-Asn-Ser[P(OC₂H₄-NH-Alloc)O₂H]-Asp(O-*t*-Bu)-Phe-O-CTC (17)

Fmoc-L-Asn-OH (198.4 mg, 0.56 mmol, 4 equiv) was added to the above obtained H-Ser[P(OC₂H₄-NH-Alloc)O₂H]-Asp(O-*t*-Bu)-Phe-O-CTC (**16**) using DIC (86.8 μ L, 0.56 mmol, 4 equiv) and Ethylcyanoglyoxylate-2-oxime (79.6 mg, 0.56 mmol, 4 equiv) in DMF (2.5 ml). After 90 min of coupling, the chloranil test was negative. Removal of Fmoc group and washings were performed as described in General Procedures for Fmoc-removal (section 8.5.4.2).

8.5.4.6 Boc-Ile-Asn-Ser[P(OC₂H₄-NH-Alloc)O₂H]-Asp(O-*t*-Bu)-Phe-O-CTC (18)

Boc-L-Ile-OH (129.4 mg, 0.56 mmol, 4 equiv) was added to the above obtained H-Asn-Ser[P(OC₂H₄-NH-Alloc)O₂H]-Asp(O-*t*-Bu)-Phe-O-CTC (**17**) using DIC (86.8 μ L, 0.56 mmol, 4 equiv) and ethylcyanoglyoxylate-2-oxime (79.6 mg, 0.56 mmol, 4 equiv) in DMF (2.5 ml). After 90 min of coupling, the chloranil test was positive and the coupling was repeated again in the same conditions. An aliquot of the peptidyl-resin was treated with TFA/Et₃SiH/CH₂Cl₂ (1:1:98) and TFA/Et₃SiH/H₂O (90:5:5). The HPLC analysis (t_R = 3.27 min) of the crude obtained after evaporation showed a purity of > 90 %. MS (ESI) calcd. For C₄₀H₅₉N₆O₁₈P, 942,90. Found: m/z 801.11 [M - H - Boc and *t*-Bu].

8.5.4.6 General procedure for Alloc-removal: Boc-Ile-Asn-Ser[P(OC₂H₄-NH₂)O₂H]-Asp(O-*t*-Bu)-Phe-O-CTC (19). The Alloc group of the peptide resin (**18**) was removed with Pd(PPh₃)₄ (16.2 mg, 0.04 mmol, 0.1 equiv) in the presence of PhSiH₃ (520. μ L, 4.21 mmol, 10 equiv) and the resin was washed with CH₂Cl₂ (3 x 0.5 min), DMF (3 x 0.5 min), 0.02 M sodium diethyldithiocarbamate in DMF (3 x 15 min) and DMF (3 X 0.5 min).

8.5.4.7 Boc-Ile-Asn-Ser[P(OC₂H₄-NH-Leu)O₂H]-Asp(O-*t*-Bu)-Phe-O-CTC (20)

Alloc-L-Leu-OH (120.5 mg, 0.56 mmol, 4 equiv) was coupled to the above obtained Boc-Ile-Asn-Ser[P(OC₂H₄-NH₂)O₂H]-Asp(O-*t*-Bu)-Phe-O-CTC (**19**) using DIC (86.8 μ L, 0.56 mmol, 4 equiv) and ethylcyanoglyoxylate-2-oxime (79.6 mg, 0.56 mmol, 4 equiv) in DMF (2.5 ml). After 90 min of coupling, the chloranil test was negative. The peptidyl-resin was subjected to the following washings/treatments with CH₂Cl₂ (3 x 0.5 min) and DMF (3 x 0.5 min). Removal of Alloc group and washings were performed as already described in General Procedures for Alloc-removal (section 8.5.4.6).

8.5.4.8 Boc-Ile-Asn-Ser[P(OC₂H₄-NH-Leu-NH₂)O₂H]-Asp(O-*t*-Bu)-Phe-OH (21)

The protected and branched polymer-bound peptide (**20**) was cleaved from the resin by treatment with TFA/Et₃SiH/CH₂Cl₂ (1:1:98, 2.0 ml) for 1 h. Partial purification of **21** was accomplished by filtration of the acidic resin suspension in 4.5 ml of pyridine-methanol (1.5:75 v/v) solution and evaporation of the filtrate to dryness in vacuo. A small title of the dried partially protected peptide **21** was exposed to TFA/H₂O/Et₃SiH (90:5:5) for 1 h to remove the protecting groups and the HPLC (t_R = 11.35 min) of the crude obtained after evaporation showed a purity of > 80%. MS (ESI) calcd. For C₄₂H₆₇N₈O₁₆P, 971,00.

Found: m/z 830.18 [M - Boc and *t*-Bu]⁺. MS (MALDI) calcd. for C₄₂H₆₇N₈O₁₆P, 971,00. Found: m/z 831.30 [M + 1 - Boc and *t*-Bu]⁺. The product was used without further purification.

8.5.4.9 Boc-Ile-Asn-Ser{P[OC₂H₄-NH-Leu(&)]O₂H}-Asp(O-*t*-Bu)-Phe(&) (22)

Procedure A (entry 3 in table 8.1, section 8.3.2.2): The protected peptide (**21**) (90.0 mg, 0.09 mmol, 1 equiv) was dissolved in CHCl₃ (45.6 ml, 2 mM solution) and *N*-polystyrene methyl-*N'*-cyclohexylcarbodiimide (197.8 mg, 2.3 mmol/g, 5 equiv) and DMAP (1.10 mg, 0.01 mmol, 0.1 equiv) were added. The mixture was stirred for 3 d and the course of the cyclization was checked by HPLC (t_R = 9.34 min). The solid supported carbodiimide was then filtered and the solvent was removed by evaporation in vacuo.

Procedure B (entry 11 in table 8.1, section 8.3.2.2): The protected peptide (**21**) (25.0 mg, 0.02 mmol, 1 equiv) was dissolved in CH₂Cl₂ (9.0 mL, 2 mM solution) and DIC (15.8 μ l, 0.10 mmol, 5 equiv) and HOAt (17.0 mg, 0.12 mmol, 0.1 equiv) were added. The mixture was stirred for 1 d. The course of the cyclization was checked by HPLC (t_R = 9.34 min) and the solvent was removed by evaporation under reduced pressure.

8.5.4.10 H-Ile-Asn-Ser{P[OC₂H₄-NH-Leu(&)]O₂H}-Asp-Phe(&) (23)

In both cyclization reactions the protected cyclic peptide (**22**) (87.0 mg, 0.09 mmol, 1 equiv) was exposed to TFA-mediated acidolytic treatment for 1.5 h with TFA/H₂O/Et₃SiH (90:5:5, 4 ml). The HPLC (t_R = 13.75 min) of the crude obtained after evaporation showed a purity of < 5 %. MS (ESI) calcd. For C₃₄H₅₃N₈O₁₃P, 812,80. Found: m/z 813.28 [M + 1]⁺, 825.50 [M + Na]⁺. MS (MALDI) calcd. for C₃₄H₅₃N₈O₁₃P, 812,80. Found: m/z 813.29 [M + 1]⁺. After semipreparative HPLC (t_R = 11.04 min) the product **23** was not pure enough for the biological tests.

8.5.5 Total synthesis of the AIP-III

8.5.5.1 H-Leu-O-CTC (24)

Cl-TrtCl-resin (0.2 g, 1.01 mmol/g) was placed in a 20.0 ml polypropylene syringe fitted with a polyethylene filter disk. The resin was then washed with CH₂Cl₂ (5 x 0.5 min), and a solution of Fmoc-L-Leu-OH (49.4 mg, 0.14 mmol, 0.7 equiv) and DIPEA (70.0 μ l, 0.42 mmol, 2.1 equiv) in CH₂Cl₂ (2.5 ml) was added. The mixture was then stirred for 15 min. Extra DIPEA (140.0 μ L, 0.85 mmol, 4.2 equiv) was added and the mixture was stirred for an additional 45 min. The reaction was stopped by adding MeOH (320.0 μ l) and stirred for 10 min. The aim of this procedure was obtaining a resin loading of 0.7 mmol/g. The Fmoc-L-Leu-O-TrtCl-resin was subjected to the following washings/treatments with CH₂Cl₂ (3 x 0.5 min), DMF (3 x 0.5 min), piperidine-DMF solution to remove the Fmoc as indicated in the General Procedure for Fmoc-removal (section 8.5.4.2).

8.5.5.2 Boc-Ile-Asn-Cys(Mmt)-Asp(O-*t*-Bu)-Phe-Leu-Leu-O-CTC (25)

Fmoc-L-Leu-OH (198.00 mg, 0.56 mmol, 4 equiv), Fmoc-L-Phe-OH (217.00 mg, 0.56 mmol, 4 equiv), Fmoc-L-Asp(O-*t*-Bu)-OH (230.40 mg, 0.56 mmol, 4 equiv), Fmoc-L-Cys(Mmt)-OH (344.80 mg, 0.56 mmol, 4 equiv), Fmoc-L-Asn-OH (198.40 mg, 0.56 mmol, 4 equiv) and Boc-L-Ile-OH (129.40 mg, 0.56 mmol, 4 equiv) were added sequentially to the above obtained H-Leu-O-TrtCl-resin (**24**) using DIC (86.80 μ L, 0.56 mmol, 4 equiv) and ethylcyanoglyoxylate-2-oxime (79.60 mg, 0.56 mmol, 4 equiv) in DMF (2.5 mL). After 90 min shaking, with the exception for Fmoc-L-Cys(Mmt)-OH (2 h), the chloranil test was negative for all the amino acids coupled. After each coupling removal of Fmoc group and washings were performed as described in General Procedures for Fmoc-removal (**section 8.5.4.2**), with the exception of Boc-L-Ile-OH coupling.

8.5.5.3 Boc-Ile-Asn-Cys-Asp(O-*t*-Bu)-Phe-Leu-Leu-OH (26)

The protected linear polymer-bound peptide (**25**) was cleaved from the resin by treatment with TFA/Et₃SiH/CH₂Cl₂ (1:1:98, 3 ml) for 40 min. Partial purification of **26** was accomplished by filtration of the acidolytic resin suspension in 4.5 ml of pyridine-methanol (1.5:75 v/v). After evaporation of the solvents, the residue was triturated with ice-water, filtrated and dried under reduced pressure. A small title of the dried partially protected peptide **26** was exposed to TFA/H₂O/Et₃SiH (90:5:5) for 1 h to remove the protecting groups and HPLC analysis ($t_R = 3.69$ min) of the crude obtained after evaporation showed a purity of > 90%. MS (ESI) calcd. For C₄₇H₇₆N₈O₁₃S, 993,22. Found: m/z 837.27 [M - Boc and *t*-Bu]⁺. The product was used without further purification.

8.5.5.4 Boc-Ile-Asn-Cys(&)-Asp(O-*t*-Bu)-Phe-Leu-Leu(&) (27)

The protected peptide (**26**) (80.00 mg, 0.08 mmol, 1 equiv) was dissolved in CHCl₃ (40.28 mL, 2 mM solution) and EDC (76.70 mg, 0.40 mmol, 5 equiv) and DMAP (1.00 mg, 0.008 mmol, 0.1 equiv) were added. The mixture was stirred for 3 d. The course of the cyclization was checked by HPLC ($t_R = 3.88$ min). The residue was then extracted twice with 5% citric acid solution to remove the excess of carbodiimide and washed with water. The organic phase was concentrated by evaporation under reduced pressure.

8.5.5.5 H-Ile-Asn-Cys(&)-Asp-Phe-Leu-Leu(&) (28) (AIP-III)

The protected cyclic peptide (**27**) (78.00 mg, 0.08 mmol, 1 equiv) was exposed to TFA-mediated acidolytic treatment for 1.5 h with TFA:H₂O:Et₃SiH (90:5:5, 4 ml). The crude obtained was dissolved in 5 ml of water and washed with CHCl₃. After evaporation under reduced pressure of the aqueous phase, the crude residue was purified by semi-preparative HPLC ($t_R = 3.97$ min) and obtained with 10-15% yield. Following HPLC analysis showed a purity between 80 and 90 %. MS (ESI) calcd. For C₃₈H₅₈N₈O₁₀S, 818,98. Found: m/z 819.30 [M + 1]⁺.

8.6 BIBLIOGRAPHIC REFERENCES

- (1) Hancock, R. E. The End of an Era. *Nat. Rev. Drug Discov.* **2007**, *6*, 28.
- (2) Walsh, C.; Wright, G. Introduction: antibiotic resistance. *Chem. Rev.* **2005**, *105*, 391-394.
- (3) Palumbi, S. R. Humans as the world's greatest evolutionary force. *Science* **2001**, *293*, 1786-1790.
- (4) Brown, E. D.; Wright, G. D. New targets and screening approaches in antimicrobial drug discovery. *Chem. Rev.* **2005**, *105*, 759-774.
- (5) Gorske, B. C.; Blackwell, H. E. Interception of quorum sensing in *Staphylococcus aureus*: a new niche for peptidomimetics. *Org. Biomol. Chem.* **2006**, *4*, 1441-1445.
- (6) Andersson, D. I. Persistence of antibiotic resistant bacteria. *Curr. Opin. Microbiol.* **2003**, *6*, 452-456.
- (7) Marra, A. Can virulence factors be viable antibacterial targets? *Expert Rev. Anti Infect. Ther.* **2004**, *2*, 61-72.
- (8) Cegelski, L.; Marshall, G. R.; Eldridge, G. R.; Hultgren, S. J. The biology and future prospects of antivirulence therapies. *Nat. Rev. Microbiol.* **2008**, *6*, 17-27.
- (9) Von Nussbaum, F.; Brands, M.; Hinzen, B. Antibacterial natural products in medicinal chemistry – exodus or revival? *Angew. Chem. Int. Ed.* **2006**, *45*, 5072-5129.
- (10) Everts, S. Bacterial conversations. *Chem. Eng. News* **2006**, *84*, 17-26.
- (11) Hentzer, M.; Givskov, M. Pharmacological inhibition of quorum sensing for the treatment of chronic bacterial infections. *J. Clin. Invest.* **2003**, *112*, 1300-1307.
- (12) Payne, D. J.; Gwynn, M. N.; Holmes, D. J.; Pompliano, D. L. Drugs for bad bugs: confronting the challenges of antibacterial discovery. *Nat. Rev. Drug Discov.* **2007**, *6*, 29-40.
- (13) Clatworthy, A. E.; Pierson, E.; Hung, D. T. Targeting virulence: a new paradigm for antimicrobial therapy. *Nat. Chem. Biol.* **2007**, *3*, 541-548.
- (14) Amer, F. A.; El-Behedy, E. M.; Mohtady, H. A. New targets for antibacterial agents. *Biotechnol. Mol. Biol. Rev.* **2008**, *3*, 46-57.
- (15) Hentzer, M.; Wu, H.; Andersen, J. B.; Riedel, K.; Rasmussen, T. B.; Bagge, N.; Kumar, N.; Schembri, M. A.; Song, Z.; Kristoffersen, P.; Manefield, M.; Costerton, J. W.; Molin, S.; Eberl, L.; Steinberg, P.; Kjelleberg, S.; Høiby, N.; Givskov, M. Attenuation of *Pseudomonas aeruginosa* virulence by quorum sensing inhibitors. *EMBO J.* **2003**, *22*, 3803-3815.
- (16) Fuqua, W. C.; Winans, S. C.; Greenberg, E. P. Quorum sensing in bacteria: the LuxR-LuxI family of cell density-responsive transcriptional regulators. *J. Bacteriol.* **1994**, *176*, 269-275.
- (17) Bassler, B. L.; Losick, R. Bacterially speaking. *Cell* **2006**, *125*, 237-46.
- (18) Fuqua, C.; Parsek, M. R.; Greenberg, E. P. Regulation of gene expression by cell-to-cell communication. *Annu. Rev. Genet.* **2001**, *35*, 439-468.
- (19) Smith, D.; Wang, J. H.; Swatton, J. E.; Davenport, P.; Price, B.; Mikkelsen, H.; Stickland, H.; Nishikawa, K.; Gardiol, N.; Spring, D. R.; Welch, M. Variations on a theme: diverse N-acyl homoserine lactone-mediated quorum sensing mechanisms in gram-negative bacteria. *Sci. Prog.* **2006**, *89*, 167-211.
- (20) Rasmussen, T. B.; Givskov, M. Quorum sensing inhibitors: a bargain of effects. *Microbiology* **2006**, *152*, 895-904.
- (21) Galloway, W. R. J. D.; Hodgkinson, J. T.; Welch, M.; Spring, D. R. Mastering the chemical language of bacteria. *Chem. Biol.* **2009**, *16*, 913-914.
- (22) Amer, F. A. A.; El-Behedy, E. M.; Mohtady, H. A. New Targets for Antibacterial Agents. *Biotechnol. Mol. Biol. Rev.* **2008**, *3*, 46-57.
- (23) Kapadnis, P. B.; Hall, E.; Ramstedt, M.; Galloway, W. R. J. D.; Welch, M.; Spring, D. R. Towards quorum-quenching catalytic antibodies. *Chem. Commun.* **2009**, *5*, 538-540.
- (24) Suga, H.; Smith, K. M. Molecular mechanisms of bacterial quorum sensing as a new drug target. *Curr. Opin. Chem. Biol.* **2003**, *7*, 586-591.

- (25) Schuster, M.; Lostroh, C. P.; Ogi, T.; Greenberg, E. P. Identification, timing, and signal specificity of *Pseudomonas aeruginosa* quorum-controlled genes: a transcriptome analysis. *J. Bacteriol.* **2003**, *185*, 2066-2079.
- (26) Welch, M.; Todd, D. E.; Whitehead, N. A.; McGowan, S. J.; Bycroft, B. W.; Salmond, G. P. C. N-acyl homoserine lactone binding to the CarR receptor determines quorum-sensing specificity in *Erwinia*. *EMBO J.* **2000**, *19*, 631-641.
- (27) Wagner, V. E.; Bushnell, D.; Passador, L.; Brooks, A. I.; Iglewski, B. H. Microarray analysis of *Pseudomonas aeruginosa* quorum-sensing regulons: effects of growth phase and environment. *J. Bacteriol.* **2003**, *185*, 2080-2095.
- (28) Wagner, V. E.; Gillis, R. J.; Iglewski, B. H. Transcriptome analysis of quorum-sensing regulation and virulence factor expression in *Pseudomonas aeruginosa*. *Vaccine* **2004**, *22*, S 15-20.
- (29) Williams, P.; Camara, M.; Hardman, A.; Swift, S.; Milton, D.; Hope, V. J.; Winzer, K.; Middleton, B.; Pritchard, D. I.; Bycroft, B. W. *Philos. Trans. R. Soc. London B* **2000**, *355*, 667-680.
- (30) Miller, M. B.; Bassler, B. L. Quorum sensing in bacteria. *Annu. Rev. Microbiol.* **2001**, *55*, 165-199.
- (31) Winzer, K.; Hardie, K. R.; Williams, P. Bacterial cell-to-cell communication: sorry, can't talk now – gone to lunch! *Curr. Opin. Microbiol.* **2002**, *5*, 216-222.
- (32) Lyon, G. J.; Muir, T. W. Chemical Signaling among Bacteria and Its Inhibition. *Chem. Biol.* **2003**, *10*, 1007-1010.
- (33) Lin, Y. H.; Xu, J. L.; Hu, J.; Wang, L. H.; Ong, S. L.; Leadbetter, J. R.; Zhang, L. H. Acyl-homoserine lactone acylase from *Ralstonia* *Ralstonia* str. XJ12B represents a novel and potent class of quorum quenching enzymes. *Mol. Microbiol.* **2003**, *47*, 849-860.
- (34) Dong, Y. H.; Xu, J. L.; Li, X. Z.; Zhang, L. H. AiiA, an enzyme that inactivates the acylhomoserine lactone quorum-sensing signal and attenuates the virulence of *Erwinia carotovora*. *Proc. Natl. Acad. Sci. USA* **2000**, *97*, 3526-3531.
- (35) Teiber J. F.; Horke, S.; Haines, D. C.; Chowdhary, P. K.; Xiao, J.; Kramer, G. L.; Haley, R. W.; Draganov, D. I. Dominant Role of Paraoxonases in Inactivation of the *Pseudomonas aeruginosa* Quorum-Sensing Signal *N*-(3-Oxododecanoyl)-L-Homoserine Lactone *Infect. Immun.* **2008**, *76*, 2512-2519.
- (36) Schultz, P. G. Catalytic Antibodies. *Angew. Chem. Int. Ed. Engl.* **1989**, *28*, 1283-1295.
- (37) Janda, K. D. Catalytic antibodies and enzyme inhibitors. *Pure Appl. Chem.* **1994**, *66*, 703-708.
- (38) Marin, S. D.; Xu, Y.; Meijler, M. M.; Janda K. D. Antibody catalyzed hydrolysis of a quorum sensing signal found in Gram-negative bacteria. *Bioorg. Med. Chem. Lett.* **2007**, *17*, 1549-1552.
- (39) Wentworth, P. Active immunization with a glycolipid transition state analogue protects against endotoxic shock. *Science* **2002**, *296*, 2247-2249.
- (40) Gao, C.; Lavey, B. J.; Lo, C. H. L.; Datta, A.; Wentworth, P. Jr.; Janda, K. D. Direct Selection for Catalysis from Combinatorial Antibody Libraries Using a Boronic Acid Probe: Primary Amide Bond Hydrolysis. *J. Am. Chem. Soc.* **1998**, *120*, 2211-2217.
- (41) Nevinsky, G. A.; Buneva, V. N. Catalytic antibodies in healthy humans and patients with autoimmune and viral diseases. *J. Cell. Mol. Med.* **2003**, *7*, 265-276.
- (42) Shokat, K. M.; Ko, M. K.; Scanlan, T. S.; Kochersperger, L.; Yonkovich, S.; Thaisrivongs, S.; Schultz, P. G. Catalytic Antibodies: A New Class of Transition-State Analogues Used to Elicit Hydrolytic Antibodies. *Angew. Chem. Int. Ed. Engl.* **1990**, *29*, 1296-1303.
- (43) Stewart, J. D.; Benkovich, S. J. Transition-state stabilization as a measure of the efficiency of antibody catalysis. *Nature* **1995**, *375*, 388-391.
- (44) Reymond, J. L. Detection strategies for catalytic antibodies. *J. Immunol. Methods* **2002**, *269*, 125-131.
- (45) Xu, Y.; Yamamoto, N.; Janda, K. D. Catalytic antibodies: hapten design strategies and screening methods. *Bioorg. Med. Chem.* **2004**, *12*, 5247-5268.

- (46) Fluit, A. C.; Wielders, C. L. C.; Verhoef, J.; Schmitz, F. J. Epidemiology and susceptibility of 3,051 *Staphylococcus aureus* isolates from 25 university hospitals participating in the European SENTRY study. *J. Clin. Microbiol.* **2001**, *39*, 3727-3732.
- (47) Recsei, P.; Kreiswirth, B.; O'Reilly, M.; Schlievert, P.; Gruss, A.; Novick, R. P. Regulation of exoprotein gene expression in *Staphylococcus aureus* by agr. *Mol. Gen. Genet.* **1986**, *202*, 58-61.
- (48) Ji, G.; Beavis, R. C.; Novick, R. P. Cell density control of staphylococcal virulence mediated by an octapeptide pheromone. *Proc. Natl. Acad. Sci. USA* **1995**, *92*, 12055-12059.
- (49) Balaban, N.; Goldkorn, T.; Nhan, R. T.; Dang, L. B.; Scott, S.; Ridgley, R. M.; Rasooly, A.; Wright, S. C.; Larrick, J. W.; Rasooly, R.; Carlson, J. R. Autoinducer of virulence as a target for vaccine and therapy against *Staphylococcus aureus*. *Science* **1998**, *280*, 438-440.
- (50) Lyon, G. J.; Wright, J. S.; Muir, T. W.; Novick, R. P. Key Determinants of Receptor Activation in the agr Autoinducing Peptides of *Staphylococcus aureus*. *Biochemistry* **2002**, *41*, 10095-10104.
- (51) Scott, R. J.; Lian, L. Y.; Muharram, S. H.; Cockayne, A.; Wood, S. J.; Bycroft, B. W.; Williams, P.; Chan, W. C. Side-chain-to-tail thiolactone peptide inhibitors of the staphylococcal quorum-sensing system. *Bioorg. Med. Chem. Lett.* **2003**, *13*, 2449-2453.
- (52) McDowell, P.; Affas, Z.; Reynolds, C.; Golden, M. T. G.; Wood, S. J.; Saint, S.; Cockayne, A.; Hill, P. J.; Dodd, C. E. R.; Bycroft, B. W.; Chan, W. C.; Williams, P. Structure, activity and evolution of the group I thiolactone peptide quorum-sensing system of *Staphylococcus aureus*. *Mol. Microbiol.* **2001**, *41*, 503-512.
- (53) Schowen, R. L. The elicitation of carboxylesterase activity in antibodies by reactive immunization with labile organophosphorus antigens: a role for flexibility. *J. Immunol. Meth.* **2002**, *269*, 59-65.
- (54) Le Corre, L.; Gravier-Pelletier, C.; Le Merrer, Y. Towards New MraY Inhibitors: A Serine Template for Uracil and 5-Amino-5-deoxyribosyl Scaffolding. *Eur. J. Org. Chem.* **2007**, *32*, 5386-5394.
- (55) Isidro-Llobet A.; Álvarez, M.; Albericio F. Amino acid-protecting groups. *Chem. Rev.* **2009**, *109*, 2455-2504.
- (56) Townsend, C. A.; Basak, A. Experiments and speculations on the role of oxidative cyclization chemistry in natural product biosynthesis. *Tetrahedron* **1991**, *47*, 2591-2602.
- (57) Organ, M. G.; Bilokin, Y. V.; Bratovanov, S. Approach toward the Total Synthesis of Orevactaene. 2. Convergent and Stereoselective Synthesis of the C18-C31 Domain of Orevactaene. Evidence for the Relative Configuration of the Side Chain. *J. Org. Chem.* **2002**, *67*, 5176-5183.
- (58) Cruz, L. J.; Beteta, N. G.; Ewenson, A.; Albericio, F. "One-Pot" Preparation of N-Carbamate Protected Amino Acids via the Azide. *Org. Process Res. Dev.* **2004**, *8*, 920-924.
- (59) McMurray, J. S.; Coleman, D. R.; Wang, W.; Campbell, M. L. The Synthesis of Phosphopeptides. *Biopolymers* **2001**, *60*, 3-31.
- (60) Sinha, N. D.; Biernat, J.; Köster, H. β -Cyanoethyl N,N-dialkylamino/N-morpholino-monochloro phosphoramidites, new phosphitylating agents facilitating ease of deprotection and work-up of synthesized oligonucleotides. *Tetrahedron Lett.* **1983**, *24*, 5843-5846.
- (61) Kupihár, Z.; Váradi, G.; Monostori, E.; Tóth, G. K. Preparation of an asymmetrically protected phosphoramidite and its application in solid-phase synthesis of phosphopeptides. *Tetrahedron Lett.* **2000**, *41*, 4457-4461.
- (62) Morales, J. C.; Reina, J. J.; Díaz, I.; Aviñó, A.; Nieto, P. M.; Eritja, R. Experimental measurement of carbohydrate aromatic stacking in water using a dangling-ended DNA model system. *Chem. Eur. J.* **2008**, *14*, 7828-7835.
- (63) Rothman, D. M.; Vazquez, M. E.; Vogel, E. M.; Imperiali, B. General method for the synthesis of caged phosphopeptides: Tools for the exploration of signal transduction pathways. *Org. Lett.* **2002**, *4*, 2865-2868.
- (64) Tetzlaff, C. N.; Richert, C. Synthesis and hydrolytic stability of 5'-aminoacylated oligouridylic acids, *Tetrahedron Lett.* **2001**, *42*, 5681-5684.

- (65) Nicolaou, K. C.; Flörke, H.; Egan, M. G.; Barth, T.; Estevez, V. A. Carbonucleotoids and carbopeptoids: New carbohydrate oligomers. *Tetrahedron Lett.* **1995**, *36*, 1775-1778.
- (66) Rothman, D. M.; Vazquez, M. E.; Vogel, E. M.; Imperiali, B. Caged phospho-amino acid building blocks for solid-phase peptide synthesis. *J. Org. Chem.* **2003**, *68*, 6795-6798.
- (67) Bhandari, R.; Saiardi, A.; Ahmadibeni, Y.; Snowman, A. M.; Resnick, A. C.; Kristiansen, T. Z.; Molina, H.; Pandey, A.; Werner, J. K. Jr; Juluri, K. R.; Xu, Y.; Prestwich, G. D.; Parang, K.; Snyder, S. H. Protein pyrophosphorylation by inositol pyrophosphates is a posttranslational event. *Proc. Natl. Acad. Sci. USA* **2007**, *104*, 15305-15310.
- (68) Chan, W. C.; Coyle, B.; Williams, P. Virulence regulation and quorum sensing in staphylococcal infections: competitive AgrC antagonists as quorum sensing inhibitors. *J. Med. Chem.* **2004**, *47*, 4633-4641.
- (69) Lloyd-Williams, P.; Albericio, F.; Giralt E. Convergent solid-phase peptide synthesis. *Tetrahedron* **1993**, *49*, 11065-11133.
- (70) Benz, H. The role of solid-phase fragment condensation (SPFC) in peptide synthesis. *Synthesis* **1994**, *4*, 337-358.
- (71) Barlos, K.; Gatos, D.; Schäfer, W. Synthesis of Prothymosin α (ProT α)-a Protein Consisting of 109 Amino Acid Residues. *Angew. Chem. Int. Ed. Engl.* **1991**, *30*, 590-593.
- (72) Barlos, K.; Chatzi, O.; Gatos, D.; Stavropoulos, G. 2-Chlorotriyl chloride resin: studies on anchoring of Fmoc-amino acids and peptide cleavage. *Int. J. Pept. Protein Res.* **1991**, *37*, 513-520.
- (73) Rovero, P.; Viganò, S.; Pegoraro, S.; Quartana, L. Synthesis of the bradykinin B1 antagonist [desArg10]HOE 140 on 2-chlorotriyl resin. *Lett. Pept. Sci.* **1996**, *2*, 319-323.
- (74) Chiva, C.; Vilaseca, M.; Giralt, E.; Albericio, F. An HPLC-ESMS study on the solid-phase assembly of C-terminal proline peptides. *J. Pept. Sci.* **1999**, *5*, 131-140.
- (75) Subirós-Funosas, R.; Prohens, R.; Barbas, R.; El-Faham, A.; Albericio, F. Oxyma: an efficient additive for peptide synthesis to replace the benzotriazole-based HOBt and HOAt with a lower risk of explosion. *Chem. Eur. J.* **2009**, *15*, 9394-9403.
- (76) Albericio, F.; Bofill, J. M.; El-Faham, A.; Kates, S. A. Use of Onium Salt-Based Coupling Reagents in Peptide Synthesis. *J. Org. Chem.* **1998**, *63*, 9678-9683.
- (77) Carpino, L. A.; El-Faham, A.; Minor, C. A.; Albericio, F. Advantageous applications of azabenzotriazole (triazolopyridine)-based coupling reagents to solid-phase peptide synthesis. *Chem. Commun.* **1994**, 201-203.
- (78) Christensen, T. Qualitative test for monitoring coupling completeness in solid phase peptide synthesis using chloranil. *Acta Chem. Scand. Ser. B* **1979**, *33*, 763-766.
- (79) Vojkovsky, T. Detection of secondary amine on solid phase. *Peptide Res.* **1995**, *8*, 236-237.
- (80) Vázquez, J.; Qushair, G.; Albericio, F. Qualitative Colorimetric Tests for Solid Phase Synthesis. *Meth. Enzymol.*, **2003**, *369*, 21-35.
- (81) Gegnas, L. D.; Waddell, S. T.; Chabin, R. M.; Reddy, S.; Wong, K. K. Inhibitors of the bacterial cell wall biosynthesis enzyme MurD. *Bioorg. Med. Chem.* **1998**, *8*, 1643-1648.
- (82) Wakamiya, T.; Saruta, K.; Yasuoka, J.; Kusumoto, S. An efficient procedure for solid-phase synthesis of phosphopeptides by the Fmoc strategy. *Chem. Lett.* **1994**, *23*, 1099-1102.
- (83) Wang, Q.; Dechert, U.; Jirik, F.; Withers, S. G. Suicide inactivation of human prostatic acid phosphatase and a phosphotyrosine phosphatase. *Biochem. Biophys. Res. Commun.* **1994**, *200*, 577-583.
- (84) Letsinger, R. I.; Finnan, J. L.; Heavner, G. A.; Lunsford, W. B. Nucleotide chemistry. XX. Phosphite coupling procedure for generating internucleotide links. *J. Am. Chem. Soc.* **1975**, *97*, 3278-3279.
- (85) Allylic protecting groups and their use in a complex environment part I: Allylic protection of alcohols. *Tetrahedron* **1997**, *53*, 13509-13556.

- (86) Guibé, F. Allylic protecting groups and their use in a complex environment part II: Allylic protecting groups and their removal through catalytic palladium π -allyl methodology. *Tetrahedron* **1998**, *54*, 2967-3042.
- (87) Weinshenker, N. M.; Shen, C. M. Polymeric reagents I. Synthesis of an insoluble polymeric carbodiimide. *Tetrahedron Lett.* **1972**, *32*, 3281-3284.
- (88) Weinshenker, N. M.; Shen, C. M.; Wong, J. Y. Polymeric carbodiimide preparation. *Org. Synth.* **1977**, *56*, 95-98.
- (89) Carpino, L. A. 1-Hydroxy-7-azabenzotriazole. An efficient peptide coupling additive. *J. Am. Chem. Soc.* **1993**, *115*, 4397-4398.
- (90) White, P. D.; Chan, W. C. In *Fmoc solid phase peptide synthesis*. Chan, W. C., White, P. D., Eds; Oxford University Press: Oxford, **2000**.
- (91) Otto, M.; Süßmuth, R.; Jung, G.; Götz, F. Structure of the pheromone peptide of the *Staphylococcus epidermidis* agr system. *FEBS Lett.* **1998**, *424*, 89-94.
- (92) Otto, M.; Süßmuth, R.; Vuong, C.; Jung, G.; Götz, F. Inhibition of virulence factor expression in *Staphylococcus aureus* by the *Staphylococcus epidermidis* agr pheromone and derivatives. *FEBS Lett.* **1999**, *450*, 257-262.
- (93) Otto, M.; Echner, H.; Voelter, W.; Gotz, F. Pheromone cross-inhibition between *Staphylococcus aureus* and *Staphylococcus epidermidis*. *Infect. Immun.* **2001**, *69*, 1957-1960.
- (94) Alsina, J.; Yokum, T. S.; Albericio, F.; Barany, G. Backbone Amide Linker (BAL) Strategy for N(α)-9-Fluorenylmethoxycarbonyl (Fmoc) Solid-Phase Synthesis of Unprotected Peptide p-Nitroanilides and Thioesters. *J. Org. Chem.* **1999**, *64*, 8761-8769.
- (95) Sewing, A.; Hilvert, D. Fmoc-Compatible Solid-Phase Peptide Synthesis of Long C-Terminal Peptide Thioesters. *Angew. Chem. Int. Ed.* **2001**, *40*, 3395-3396.
- (96) Von Eggelkraut-Gottanka, R.; Klose, A.; Beck-Sickinger, A. G.; Beyermann, M. Peptide α -thioester formation using standard Fmoc-chemistry. *Tetrahedron Lett.* **2003**, *44*, 3551-3554.
- (97) Barany, G.; Merrifield, R. B. In *The Peptides: Analysis, Synthesis and Biology*. Gross, E., Meienhofer, J., Eds.; Academic Press: New York, **1980**; vol. 2, pp. 190-208.
- (98) Radkiewicz, J. L.; Zipse, H.; Clarke, S.; Houk, K. N. Neighboring Side Chain Effects on Asparaginyl and Aspartyl Degradation: An Ab Initio Study of the Relationship between Peptide Conformation and Backbone NH Acidity. *J. Am. Chem. Soc.* **2001**, *123*, 3499-3506.
- (99) Clarke, S. Aging as war between chemical and biochemical processes: Protein methylation and the recognition of age-damaged proteins for repair. *Ageing Res. Rev.* **2003**, *2*, 263-285.
- (100) Robinson, N. E.; Robinson, A. B. In *Peptides and Proteins*. Althouse Press: Cave Junction, OR, **2004**; pp. 1-443.
- (101) Zahariev, S.; Guarnaccia, C.; Pongor, C. I.; Quaroni, L.; Čemažar, M.; Pongor, S. Synthesis of 'difficult' peptides free of aspartimide and related products, using peptoid methodology. *Tetrahedron Lett.* **2006**, *47*, 4121-4124.
- (102) Perrin, D. D.; Chai, C.; Armarego, W. L. F.; Perrin, D. R. *Purification of Laboratory Chemicals*, 5th edition. Butterworth-Heinemann, **2003**.
- (103) Mestre-C 2.3a software.
- (104) Spengler, J.; Jiménez, J. C.; Burger, K.; Giralt, E.; Albericio, F. Abbreviated nomenclature for cyclic and branched homo- and hetero-detic peptides. *J. Pept. Res.* **2005**, *65*, 550-555.